



CCCR2019

REPORT

Canada's Changing Climate Report



Government
of Canada

Gouvernement
du Canada

Canada



Canada's Changing Climate Report

CHAPTER 1	About This Report	7
CHAPTER 2	Global Observed Climate Change	24
CHAPTER 3	Modelling Future Climate Change	73
CHAPTER 4	Changes in Temperature and Precipitation Across Canada	112
CHAPTER 5	Changes in Snow, Ice, and Permafrost Across Canada	194
CHAPTER 6	Changes in Freshwater Availability Across Canada	261
CHAPTER 7	Changes in Oceans Surrounding Canada	343
CHAPTER 8	Changes in Canada's Regions in a National and Global Context	424



Edited by

Elizabeth Bush, Climate Research Division, Environment and Climate Change Canada

Donald S. Lemmen, Climate Change Impacts and Adaptation Division, Natural Resources Canada

Recommended Citation: Bush, E. and Lemmen, D.S., editors (2019): Canada's Changing Climate Report; Government of Canada, Ottawa, ON. 444 p.

The digital interactive version of the report is available at www.ChangingClimate.ca/CCCR2019. The report is also available at: adaptation.nrcan.gc.ca

Aussi disponible en français sous le titre : Rapport sur le climate changeant du Canada

Unless otherwise specified, you may not reproduce materials in this publication, in whole or in part, for the purposes of commercial redistribution without prior written permission from Environment and Climate Change Canada's copyright administrator. To obtain permission to reproduce Government of Canada materials for commercial purposes, apply for Crown Copyright Clearance by contacting:

ENVIRONMENT AND CLIMATE CHANGE CANADA

Public Inquiries Centre
12th Floor, Fontaine Building
200 Sacré-Coeur Boulevard
Gatineau QC K1A 0H3
Telephone: 819-938-3860
Toll Free: 1-800-668-6767 (in Canada only)
Email: ec.enviroinfo.ec@canada.ca

Cat. No.: En4-368/2019E-PDF (Online)

ISBN: 978-0-660-30222-5

Photos: © Shutterstock and Unsplash

© Her Majesty the Queen in Right of Canada, represented by the Minister of Environment and Climate Change, 2019

This report is part of *Canada in a Changing Climate: Advancing our Knowledge for Action*, the national assessment of how and why Canada's climate is changing; the impacts of these changes on our communities, environment, and economy; and how we are adapting. To find out more, please visit: <https://www.nrcan.gc.ca/environment/impacts-adaptation/19918>





Acknowledgements

We gratefully acknowledge the following people for taking the time to provide critical, expert reviews of one of more chapters of the report:

Louise Aubin
 Kevin Behan
 Ross Brown
 Andy Bush
 Jim Buttle
 Alex Cannon
 Hélène Côté
 Liese Coulter
 Stephen Dery
 Allan Douglas
 Paddy Enright
 Laura Fagherazzi
 Katja Fennel
 John Fyfe
 Stephen Gruber
 Katie Hayes
 Denise Joy
 Richard Kelly
 Slava Kharin
 Thomas Knutson

Ken Kunkel
 Paul Kushner
 Shawn Marshall
 Kerry Mazurek
 Dan McKenney
 Glenn Milne
 Adam Monahan
 Trevor Murdock
 Edna Murphy
 Paul Myers
 Mohammad Reza Najafi
 Kim Olson
 Dominique Paquin
 Dennis Paradine
 David Pearson
 Jackie Richter-Menge
 Stephen Ruddy
 Randy Scharien
 John Scinocca
 Nancy Shakell

Martin Sharp
 Marjorie Shepherd
 Murray Smith
 Emily Smits
 Chris Spence
 Sandy Steffen
 Rebecca Stranberg
 Neil Swart
 Tim Taylor
 Felix Vogel
 John WalshZeliang Wang
 Andrew Wilson
 Christopher Woodworth-Lynas
 Garth van der Kamp
 Knut von Salzen
 Anna Yusa
 Glen Zachary
 Francis Zwiers

We would also like to acknowledge the valuable guidance and input of the National Assessment Advisory Committee.

We would also like to recognize the contributions, hard work and commitment of the National Assessment Secretariat.

We would also like to recognize the following students for their helpful contributions:

Aurelie Ieroncig
 Kacie Conrad
 Arashdeep Panesar





Headline Statements

These headline statements tell a concise story about Canada's changing climate based on the findings of this report. The statements are cross-referenced to specific sections in chapters of the main report, where supporting evidence is found. There is *high confidence* or more associated with these statements, which are consistent with, and draw on, the Chapter Key Messages.



Canada's climate has warmed and will warm further in the future, driven by human influence. Global emissions of carbon dioxide from human activity will largely determine how much warming Canada and the world will experience in the future, and this warming is effectively irreversible. {2.3, 3.3, 3.4, 4.2}

Both past and future warming in Canada is, on average, about double the magnitude of global warming. Northern Canada has warmed and will continue to warm at more than double the global rate. {2.2, 3.3, 4.2}

Oceans surrounding Canada have warmed, become more acidic, and less oxygenated, consistent with observed global ocean changes over the past century. Ocean warming and loss of oxygen will intensify with further emissions of all greenhouse gases, whereas ocean acidification will increase in response to additional carbon dioxide emissions. These changes threaten the health of marine ecosystems. {2.2, 7.2, 7.6}

The effects of widespread warming are evident in many parts of Canada and are projected to intensify in the future. In Canada, these effects include more extreme heat, less extreme cold, longer growing seasons, shorter snow and ice cover seasons, earlier spring peak streamflow, thinning glaciers, thawing permafrost, and rising sea level. Because some further warming is unavoidable, these trends will continue. {4.2, 5.2, 5.3, 5.4, 5.5, 5.6, 6.2, 7.5}

Precipitation is projected to increase for most of Canada, on average, although summer rainfall may decrease in some areas. Precipitation has increased in many parts of Canada, and there has been a shift toward less snowfall and more rainfall. Annual and winter precipitation is projected to increase everywhere in Canada over the 21st century. However, reductions in summer rainfall are projected for parts of southern Canada under a high emission scenario toward the late century. {4.3}

The seasonal availability of freshwater is changing, with an increased risk of water supply shortages in summer. Warmer winters and earlier snowmelt will combine to produce higher winter streamflows, while smaller snowpacks and loss of glacier ice during this century will combine to produce lower summer streamflows. Warmer summers will increase evaporation of surface water and contribute to reduced summer water availability in the future despite more precipitation in some places. {4.2, 4.3, 5.2, 5.4, 6.2, 6.3, 6.4}

A warmer climate will intensify some weather extremes in the future. Extreme hot temperatures will become more frequent and more intense. This will increase the severity of heatwaves, and contribute to increased drought and wildfire risks. While inland flooding results from multiple factors, more intense rainfalls will increase urban flood risks. It is uncertain how warmer temperatures and smaller snowpacks will combine to affect the frequency and magnitude of snowmelt-related flooding. {4.2, 4.3, 4.4, 5.2, 6.2}



Canadian areas of the Arctic and Atlantic Oceans have experienced longer and more widespread sea-ice-free conditions. Canadian Arctic marine areas, including the Beaufort Sea and Baffin Bay, are projected to have extensive ice-free periods during summer by mid-century. The last area in the entire Arctic with summer sea ice is projected to be north of the Canadian Arctic Archipelago. This area will be an important refuge for ice-dependent species and an ongoing source of potentially hazardous ice, which will drift into Canadian waters. {5.3}

Coastal flooding is expected to increase in many areas of Canada due to local sea level rise. Changes in local sea-level are a combination of global sea level rise and local land subsidence or uplift. Local sea level is projected to rise, and increase flooding, along most of the Atlantic and Pacific coasts of Canada and the Beaufort coast in the Arctic where the land is subsiding or slowly uplifting. The loss of sea ice in Arctic and Atlantic Canada further increases the risk of damage to coastal infrastructure and ecosystems as a result of larger storm surges and waves. {7.5}

The rate and magnitude of climate change under high versus low emission scenarios project two very different futures for Canada. Scenarios with large and rapid warming illustrate the profound effects on Canadian climate of continued growth in greenhouse gas emissions. Scenarios with limited warming will only occur if Canada and the rest of the world reduce carbon emissions to near zero early in the second half of the century and reduce emissions of other greenhouse gases substantially. Projections based on a range of emission scenarios are needed to inform impact assessment, climate risk management, and policy development. {all chapters}

To view the full online version of the report visit www.ChangingClimate.ca/CCCR2019.



CHAPTER 1

**About this
Report**

CANADA'S CHANGING CLIMATE REPORT



Government
of Canada

Gouvernement
du Canada

Canada



Authors

Elizabeth Bush, Environment and Climate Change Canada

Greg Flato, Environment and Climate Change Canada

Recommended Citation: Bush, E. and Flato, G. (2019): About this report; Chapter 1 in Canada's Changing Climate Report, (ed.) E. Bush and D.S. Lemmen; Government of Canada, Ottawa, Ontario, p. 7–23.



Chapter Table Of Contents

1.1: Introduction

Box 1.1: The Intergovernmental Panel on Climate Change

Box 1.2: Responding to Climate Change: Mitigation and Adaptation

1.2: Purpose and scope

1.3: Sources of information and process of development

1.3.1: Sources of information

1.3.2: Process of development

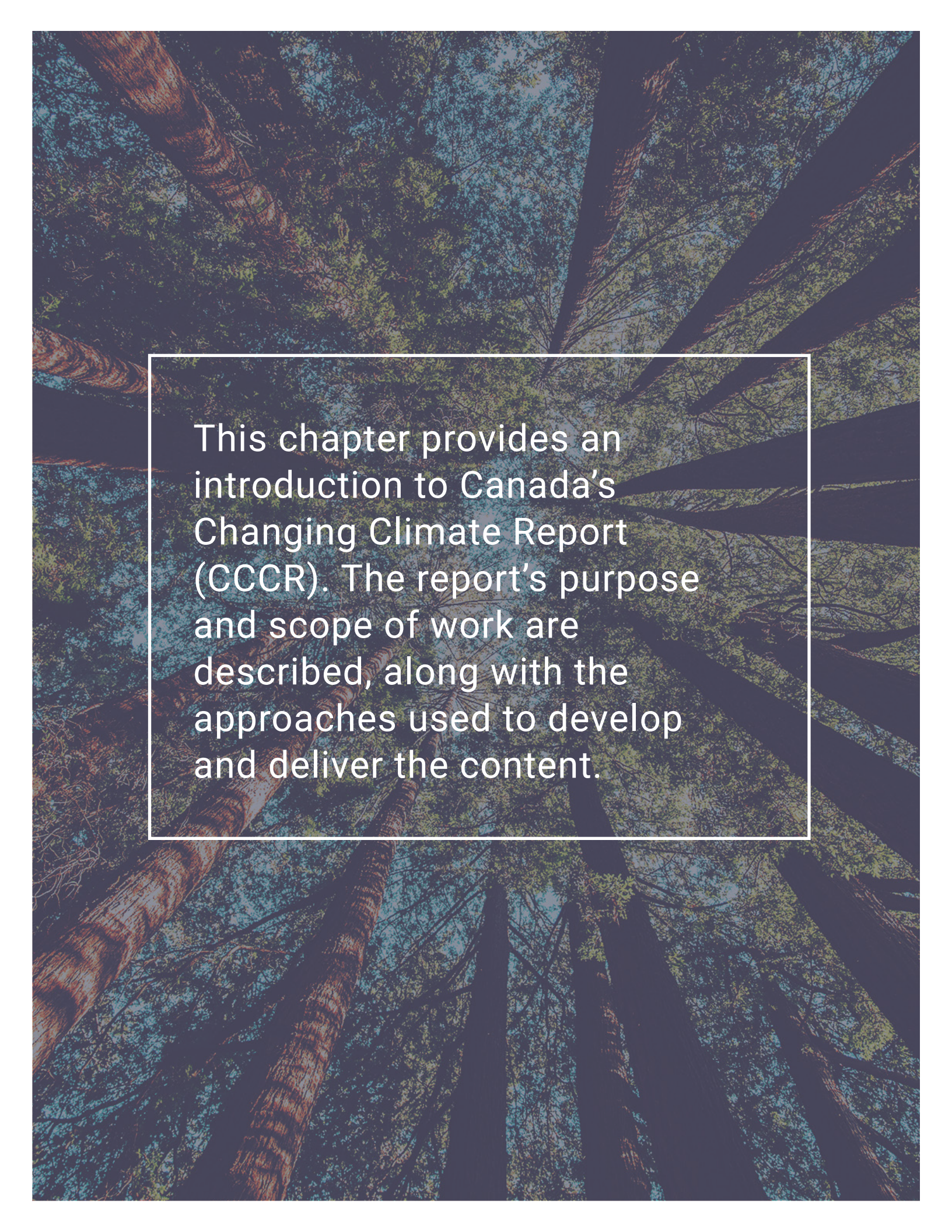
1.4: Guide to the report

1.4.1: Key messages and use of calibrated uncertainty language

1.4.2: Time frames and time periods of analysis

1.4.3: Chapter guide

REFERENCES



This chapter provides an introduction to Canada's Changing Climate Report (CCCR). The report's purpose and scope of work are described, along with the approaches used to develop and deliver the content.



1.1: Introduction

Climate change is one of the defining challenges of the 21st century. It is a global problem, and tackling it requires global action. Governments around the world have committed to work together to limit global warming, recognizing that climate-related risks grow with the magnitude of warming and associated changes in climate. The Paris Agreement under the United Nations Framework Convention on Climate Change, which entered into force on November 4, 2016,¹ established a goal of holding the increase in global temperature to 1.5°C–2°C above pre-industrial levels, as well as a commitment to engage in adaptation planning and implementation. Collective action in pursuit of the global temperature goal is being implemented; however, it is recognized that this goal will only reduce and not eliminate the risks and impacts of climate change. Governments and citizens need to understand how climate change might impact them, in order to plan and prepare for the challenges that climate change brings.

Understanding climate change and its consequences draws from the physical, biological, and social sciences. Ongoing research in these fields is leading to an ever-growing body of published scientific literature related to climate change. Assessing this growing knowledge base, and communicating how understanding of climate change has grown, is challenging, especially as there is a wide audience for this information. The impacts of climate change are a concern for individuals, communities, business sectors, and governments, from local and regional to national and international scales. “Science assessments” provide a way to critically analyze and synthesize existing knowledge on a topic, including an evaluation of confidence in our understanding and of remaining uncertainties. In so doing, science assessments can serve as a source of robust information for answering the questions and concerns of a wide audience. Global-scale scientific assessments of climate change have been conducted by the Intergovernmental Panel on Climate Change (IPCC) (see Box 1.1) regularly since 1990 and have been pivotal in providing the global community with a knowledge base to inform decision-making. National-scale climate change science assessments speak more directly to national audiences.

Box 1.1: The Intergovernmental Panel on Climate Change

The Intergovernmental Panel on Climate Change (IPCC) is an international body responsible for assessing the science related to climate change. It was set up in 1988 by the World Meteorological Organization (WMO) and the United Nations Environment Programme (UNEP) to provide decision-makers with regular assessments of the scientific basis of climate change, its impacts and future risks, and options for adaptation and mitigation. The assessments are undertaken and presented in a way that is relevant to policy but not prescriptive of any specific policy.

1 Canada ratified the Paris Agreement on Oct 5, 2016 (https://treaties.un.org/Pages/ViewDetails.aspx?s-rc=TREATY&mtdsg_no=XXVII-7-d&chapter=27&clang=en).



The IPCC is both scientific and governmental in nature. Participation in the IPCC is open to all member countries of the WMO and the United Nations. The Panel, made up of representatives of member states, makes major decisions at plenary sessions. The IPCC Bureau, elected by member governments, provides guidance to the Panel on the scientific and technical aspects of the Panel's work and advises the Panel on management and strategic issues. IPCC assessments are written by scientists who volunteer their time and expertise as authors of these reports. IPCC reports undergo multiple rounds of drafting and are reviewed by both scientific experts and governments to ensure they are comprehensive and objective, and are produced in an open and transparent way.

Canada is an active participant in the IPCC, and Canadian scientists contribute to IPCC assessments. More information on Canada's contribution to the IPCC is available here:

<https://www.canada.ca/en/environment-climate-change/services/climate-change/science-research-data/contribution-intergovernmental-panel.html>

SOURCE: IPCC FACTSHEET: WHAT IS THE IPCC? AVAILABLE FROM [HTTP://WWW.IPCC.CH/](http://www.ipcc.ch/)

Over the past two decades, Canada has produced three broad, national climate change assessments (Maxwell et al., 1997; Lemmen et al., 2008; Warren and Lemmen, 2014), as well as sector- or region-specific assessments on human health (Séguin, 2008), transportation (Palko and Lemmen, 2017), and marine coasts (Lemmen et al., 2016). These reports communicated to Canadians the risks and opportunities climate change presents and focused on assessing our readiness to adapt to potential impacts. National climate change assessments help citizens and stakeholders become better informed and engage in discussions about how to respond to the challenges of climate change in Canada through both mitigation and adaptation (see Box 1.2). While all of these assessments included high-level overviews of observed and projected changes in Canada's climate, only one report had a full chapter dedicated to changes in physical climate (Bush et al., 2014).

The current National Assessment, *Canada in a Changing Climate: Advancing our Knowledge for Action*, was launched in 2017 (<https://www.nrcan.gc.ca/environment/impacts-adaptation/19918>). As part of this process, a more comprehensive assessment of changes in Canada's climate has been carried out than in past assessments. The assessment as a whole will examine how Canada's climate is changing, the impacts of these changes, and how we are adapting to reduce risk. A series of authoritative reports will be completed between 2018 and 2021 as part of the National Assessment process. Canada's Changing Climate Report (CCCR) is the first major product of the current National Assessment, and it focuses on answering the questions: how has Canada's climate changed to date, why, and what changes are projected for the future? A National Issues report will focus on climate change impacts and adaptation issues that are of national importance or that would benefit from an integrated, cross-Canada perspective. A Regional Perspectives report will provide a picture of climate change impacts and adaptation in six regions of Canada. Health of Canadians in a Changing Climate will provide an assessment of the risks of climate change to the health of Canadians and to the health care system. An Enhanced Synthesis will be produced in 2021.

Box 1.2: Responding to climate change: mitigation and adaptation

Mitigation, in the context of climate change, is defined as a human intervention to reduce the sources or enhance the sinks of greenhouse gases (IPCC, 2013), since greenhouse gases (GHGs) have climate warming effects. A source is any process, activity, or mechanism that releases GHGs to the atmosphere. Both natural processes and human activities release GHGs. A sink is any process, activity, or mechanism that removes GHGs from the atmosphere. In addition to GHGs, mitigation also applies to reducing emissions of other substances that have a warming effect on the climate.

Adaptation is the process of adjustment to actual or expected climate and its effects. In human systems, adaptation seeks to moderate or avoid harm or exploit beneficial opportunities. In some natural systems, human intervention may facilitate adjustment to expected climate and its effects.

Climate change is a global phenomenon, and Canada's national climate change assessments build on a foundation provided by the global-scale science assessments of the IPCC, which have been produced every five to seven years since 1990. These assessments are widely recognized as the most authoritative reference documents on the state of knowledge on climate change, its potential consequences, and response options. Conclusions of successive IPCC assessments are considered to represent the most recent consensus of the international science community, based on publicly available knowledge up to that time. In this report, the most recent (Fifth) IPCC assessment (IPCC, 2013) is referred to heavily, especially in Chapters 2 and 3, which provide a synopsis of observed and future global-scale climate changes (see Section 1.4). A Sixth IPCC Assessment is currently underway, and a series of assessment reports will be released from October 2018 to spring 2022 (<http://www.ipcc.ch/>). A large volume of scientific papers have been published since the body of literature assessed in the IPCC Fifth Assessment. This report does not comprehensively assess this new literature, as doing so would duplicate the IPCC process. Rather, this report focuses on assessing new literature that advances understanding of climate change in Canada.

1.2: Purpose and scope

The objectives of the National Assessment process and its associated reports and other products are to:

- enhance understanding of climate change impacts and adaptation in Canada and provide the evidence base for responding;
- increase awareness of the relevance of climate change to Canadians and the need for timely action;
- expand engagement in the assessment process;
- equip and empower amplifier organizations to share findings with their audiences and create targeted products; and
- document progress made on advancing adaptation action in Canada.



The purpose of this report is to provide a climate science foundation for the other National Assessment products. Its objectives are to assess current knowledge about how Canada's climate is changing and why, and what changes are projected for the future, to help inform mitigation and adaptation decision-making, and to help raise public awareness and understanding of Canada's changing climate. The CCCR is therefore written for a broad range of professionals who are familiar with the topic of climate change but who may not have expertise in the physical sciences. The assessment process plans to engage intermediary (or amplifier) organizations to help raise awareness and understanding among the broader public of how Canada's climate is changing.

A climate science assessment, such as this report, is based on published scientific literature. It provides an overview and synthesis of that literature and an evaluation of the confidence in our understanding and of remaining uncertainties, based on the expert judgment of the authors. A climate science assessment can help inform decision-making but cannot provide detailed climate information to directly support local planning or decision-making – this is the role of climate services. Regional climate services in Canada have been available for more than a decade through institutions such as [Ouranos](#) and the [Pacific Climate Impacts Consortium](#) and are now being established at a national scale. Persons engaged in climate impact assessments or adaptation planning can make use of this assessment to provide an authoritative overview of climate science relevant to climate change in Canada but will need to identify sources of information that are best suited to their particular application. The Canadian Centre for Climate Services (CCCS) [Library of Climate Resources](#) is a collection of links to climate datasets, tools, guidance, and other related resources. The [Climate Services Support Desk](#) will assist Canadians in finding, understanding, and using climate data, information, and tools in their planning and adaptation decision-making.

The scope of the CCCR is limited to physical climate science and is aligned with the scope of assessments of the physical science basis of global-scale climate change by the IPCC's Working Group I. IPCC Working Group I reports (e.g., IPCC, 2013) cover climate drivers, observed changes in the global climate system and their causes, and projection of future global-scale changes. The scope of the CCCR is similar but focuses on observed and projected changes in climate for Canada's land area and surrounding oceans. Changes in freshwater availability, a topic considered by IPCC Working Group II (Impacts, Adaptation and Vulnerability) (IPCC, 2014), is included in the CCCR to maintain a close link to the underlying evidence base in terms of changes in physical drivers.

While the aim is to provide an assessment of changes for Canada as a whole, information on regional-scale changes is also included, where possible. Some dedicated regional climate analyses were undertaken in support of the National Assessment, using political boundaries to define the regions, consistent with regional definitions of previous national assessments (see Figure 1.1). These results are provided in Chapter 4. For some topics – such as changes in oceans surrounding Canada; changes in glaciers, sea ice, and permafrost; and changes in freshwater availability – regional perspectives are provided based on natural boundaries of the systems of concern. These results are in relevant chapters of this report (see Section 1.4). To note, in some places in this report, a geographical boundary for assessment of changes in northern Canada is used, defined as the region north of 60° latitude and rather than by political boundaries, as in Figure 1.1. Therefore, where “the North” is used, this refers to the three territories; where “northern Canada” is used, this refers to the region north of 60° latitude.

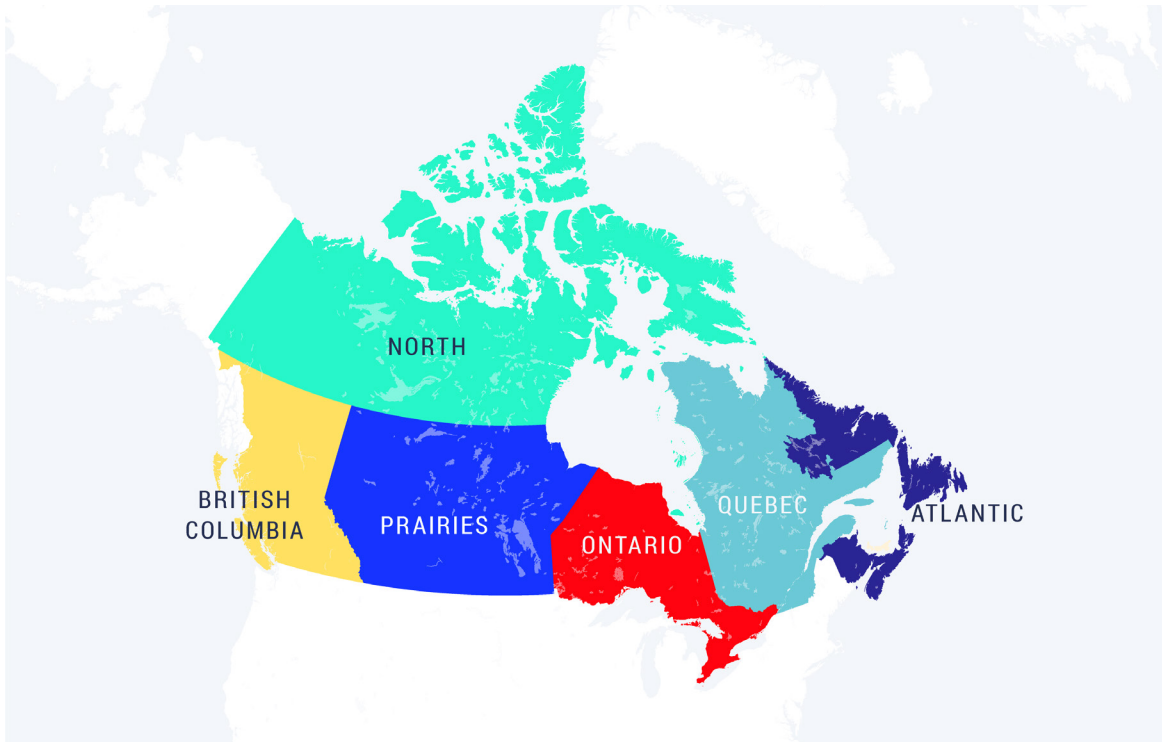


Figure 1.1: Regions used for specific climate analyses in the CCCR in support of the National Assessment

Figure caption: These six regions are defined by the political boundaries of the provinces and territories of Canada and match the regions analyzed in Canada's Third National Assessment. The North region includes Yukon, Northwest Territories, and Nunavut. The Prairie region includes the provinces of Alberta, Saskatchewan, and Manitoba. The Atlantic region includes the provinces of New Brunswick, Nova Scotia, Prince Edward Island, and Newfoundland and Labrador. The remaining three regions encompass single provinces only (British Columbia, Ontario, and Quebec).

Assessment of biogeochemical cycles, including carbon-cycle changes, and related information on Canadian sources and sinks of greenhouse gases, is beyond the scope of this report. Information on nationally reported anthropogenic emissions for Canada is available through [Canada's national GHG inventory \(https://www.canada.ca/en/environment-climate-change/services/climate-change/greenhouse-gas-emissions/inventory.html\)](https://www.canada.ca/en/environment-climate-change/services/climate-change/greenhouse-gas-emissions/inventory.html). Information on the state of the North American carbon cycle can be found in the [Second State of the Carbon Cycle Report](https://www.carboncyclescience.us/state-carbon-cycle-report-soccr), currently in development with a planned publication date in the fall of 2018 (<https://www.carboncyclescience.us/state-carbon-cycle-report-soccr>).

1.3: Sources of information and process of development

1.3.1: Sources of information

The CCCR draws primarily from existing sources of information that have been peer-reviewed and are publicly available. Exceptions include updates to published results, which were deemed acceptable as long as the method used to update data was citable. In addition, projections of future climate change for Canada, for some variables, are directly available as output from climate models. In this case, the projections specific to Canada have not always been published, although the models used to produce these projections have been comprehensively evaluated and documented in the peer-reviewed literature. Where relevant, quantitative information that has not been through external peer review was considered for inclusion; authors were required to judge the quality and reliability of the information and to maintain a copy of it. All chapters of this report underwent external peer review (see Section 1.3.2).

It is recognized that Indigenous observations and knowledge systems contribute significantly to our understanding of changing climate. This knowledge is incorporated in other reports of this assessment, where the holistic perspective of Indigenous knowledge systems contributes to a fuller understanding of climate change impacts and of the ability of human and natural systems to adapt.

1.3.2: Process of development

Environment and Climate Change Canada, as the focal point for climate science expertise in the federal government, led the development of the CCCR. Authors with recognized expertise were invited to lead individual chapters of the CCCR. The lead author team, assessment coordinators, and representative stakeholders came together for an initial scoping meeting in February 2017 to discuss the overall aims and scope of the CCCR and to develop initial chapter outlines. Lead authors then formed chapter author teams with the required expertise to comprehensively assess chapter topics. Discussions at the scoping meeting with a panel of stakeholders provided key input to developing the CCCR to be effective and relevant.

External review of the report included both a targeted review by invited reviewers with specific subject-matter expertise and an open review involving other experts who registered through the National Assessment portal (<https://www.nrcan.gc.ca/environment/impacts-adaptation/19924>). In addition, members of the National Assessment Advisory Committee, National Adaptation Platform, and the Atmosphere-Related Research in Canadian Universities (ARRCU) working group were invited to participate in the external review.

1.4: Guide to the report

1.4.1: Key messages and use of calibrated uncertainty language

Each chapter of the CCCR begins with a set of key messages: those findings the authors felt are most relevant to the target audiences. The key messages include quantitative information about how various components of the climate system – such as the atmosphere and cryosphere – have changed over specified periods of time and projections of additional change this century. These quantitative results emerge from the body of evidence assessed within each chapter of the CCCR. As a science assessment involves critically analyzing the knowledge base and deciding on the level of confidence in results (see Section 1.1), conveying the degree of certainty and uncertainty about results is important. In the CCCR, authors have done this for key messages by adopting the calibrated uncertainty language of the IPCC (Mastrandea et al., 2010). This allows authors and audiences to distinguish between what is well known and widely accepted and what is not well known or not agreed upon.

Two metrics are used to communicate the degree of certainty about key messages (see Figure 1.2):

Confidence in the validity of a result based on the type, amount, quality, and consistency of evidence (e.g., mechanistic understanding, theory, data, models, and expert judgment) and the degree of agreement. Confidence is expressed qualitatively.

Likelihood of a result occurring based on quantified measures of uncertainty expressed probabilistically (based on statistical analysis of observations or model results, or expert judgment). Likelihood is expressed quantitatively.

When a quantified measure of uncertainty (i.e., likelihood) is provided but no confidence level is given, a high or **very high confidence** level is implied. Calibrated uncertainty language is italicized where used in the CCCR (e.g., *likely* or *very likely*), and definitions are provided in Figure 1.2 and at the first use of one of these terms in each chapter. Confidence statements are used more frequently in this report than are likelihood statements because the requirements for an assessment of likelihood – quantified estimates of uncertainty – were not available in the supporting literature in many cases.

Some Key Messages include statements that are expressed without a confidence level. These are not to be construed as “no confidence” statements. In fact, the opposite is true; these are factual statements. For example, a Key Message from Chapter 7 includes the statement “Relative sea level in different parts of Canada is projected to rise or fall, depending on local vertical land motion.” By definition, relative sea level is expressed as the mean sea level relative to a local reference land level; therefore, this statement is a fact. In another example in Chapter 4, the following statement is part of a Key Message: “Annual and seasonal mean temperature is projected to increase everywhere, with much larger changes in northern Canada in winter.” This is a conditional statement of fact. Based on the assumptions driving the climate model, the output is as described. In other cases, factual statements represent assessed findings for which evidence and under-

standing are overwhelming. There is an example of this in Chapter 2, where the first key message includes the statement “Warming of the climate system during the Industrial Era is unequivocal, based on robust evidence from a suite of indicators.”

The application of calibrated uncertainty language is an important feature of the scientific assessments undertaken by the IPCC, and the same approach is adopted here. In essence, the author teams identify relevant scientific literature, data, or model outputs; evaluate the amount of evidence and the level of agreement (or disagreement); and then apply their collective expert judgment to make an assessment of confidence, or where possible, likelihood. The wording of each key message is a collective effort of the chapter author team, aimed at providing clear and concise messages that are underpinned by the literature cited in the body of the chapters. Summary statements are included in each chapter to provide a traceable account of the authors’ assessment of the supporting evidence for key messages.

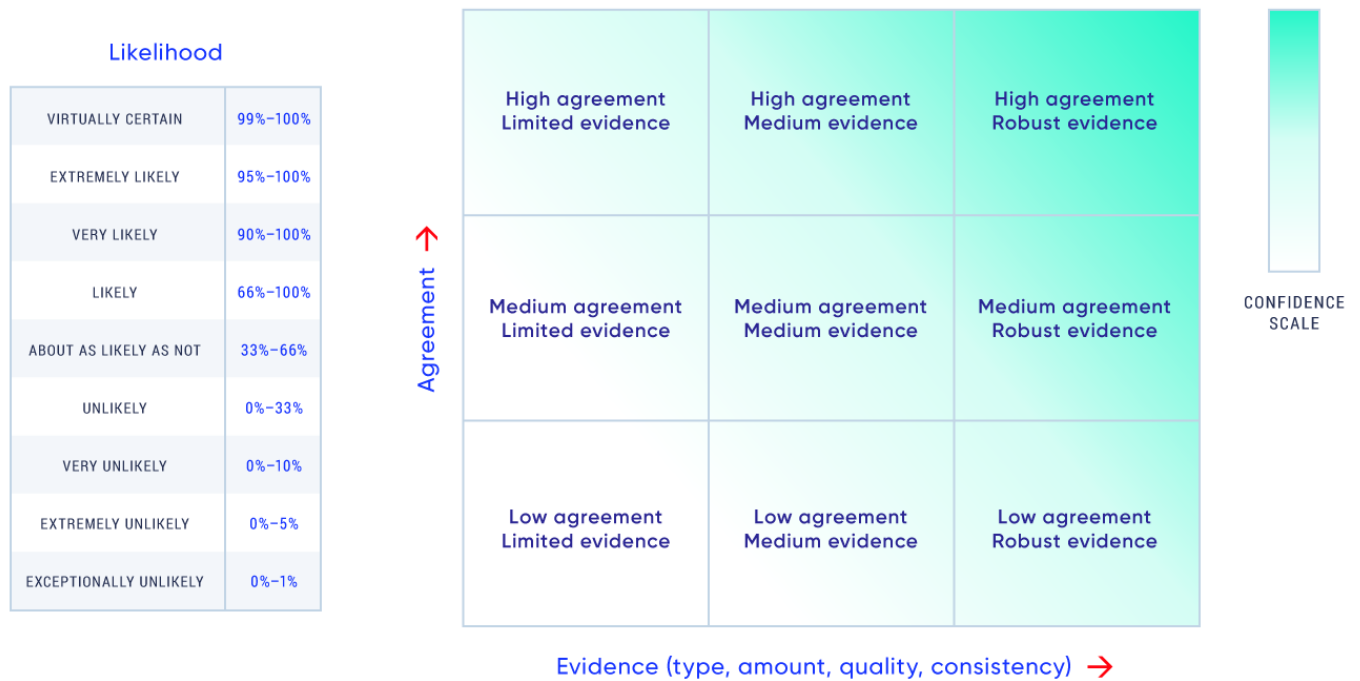


Figure 1.2: Confidence levels and likelihood statements used in this report

Figure caption: The confidence levels and likelihood statements used in this report are the same as those used in the IPCC Fifth Assessment Report (IPCC, 2013). Generally, evidence is most robust when there are multiple, consistent independent lines of high-quality evidence. A level of confidence is expressed using five qualifiers: very high, high, medium, low, and very low. The figure depicts summary statements about evidence and agreement and their relationship to the confidence scale. The relationship is flexible, with “fuzzy boundaries” between difference confidence levels. The categories of likelihood are also considered to have fuzzy boundaries. For example, a statement that a result is likely means that the probability of its occurrence ranges from over 66% to 100%. This corresponds to a chance of the event occurring of two-thirds or more.

1.4.2: Time frames and time periods of analysis

This report assesses observed and projected changes in climate for Canada. Therefore, it refers to both past and future time periods. Past changes are assessed over periods of time for which there are sufficient data records, either based on direct measurements (observations) and/or satellite data. This means that observed changes are described almost exclusively for time periods beginning sometime in the 20th century. The CCCR does not assess changes in current climate relative to conditions that existed in the distant past (paleoclimate) but does provide information on levels of greenhouse gases in the atmosphere going back to the mid-18th century using values directly measured from ice cores (see Chapter 2, Section 2.3).

To assess past changes in the climate, sufficiently long climate data records are needed for a detectable change to emerge from the natural fluctuations in the climate system. In general, estimates of change have smaller uncertainty with longer records. In the CCCR, different time periods for describing observed changes in climate are reported, reflecting the length of the available data record as well as the time when the work was completed. Some of these records extend back to the early 20th century, many begin after the mid-20th century, and satellite-based records start in the late 1970s at the earliest.

There are also no standard time periods for assessing and discussing future changes in climate. Time periods of interest depend on the needs and concerns of the user of the information; for some, near-term changes and impacts are of most concern, whereas, for others, their interest demands a longer-term view. In the CCCR, assessment of future climate changes is based primarily on results from coordinated experiments to model global climate (see Chapter 3, Box 3.1). These experiments have designated time periods describing near-term, mid-21st century, and late 21st century conditions. The near-term time period has, naturally, shifted forward in time while the mid-21st century (2046–2065) and late 21st century (2081–2100) time periods remained the same. In the CCCR, we consider 2031–2050, about 10–30 years from now, as the near-term period. Where changes in climate are discussed relative to the end-of-the-century, this should be understood to mean by the year 2100. The near-term and late-century time periods are used in Chapter 4 to provide projections of future changes for Canada for various indicators and indices related to temperature and precipitation. Elsewhere in the report, results from the fifth phase of the Coupled Model Intercomparison Project (CMIP5, see Chapter 3, Box 3.1) may be discussed with respect to the CMIP5 defined near-term time period (2016–2035). Climate models project future changes relative to a reference period. In the CMIP5 experiments, the reference period was 1986–2005, which was representative of “current climate” at the time the experimental set-up was established.

1.4.3: Chapter guide

The core content of the CCCR is contained within Chapters 2 to 7. Chapters 2 and 3 focus on global-scale climate changes, and Chapters 4 to 7 focus on changes in climate across Canada. The global context presented in Chapters 2 and 3 is useful for understanding changes in Canada, recognizing the interconnectedness between changes occurring within a country or region and those occurring throughout the world. Chapter 2 provides a historical perspective on global-scale changes, summarizing observations of change throughout the Earth's climate system and current understanding of the causes of these observed changes. Chapter 3 looks at future global-scale changes, describing the Earth system models used to project future climate change as well as the various emission scenarios – alternative plausible futures – used to drive these models. In addition to background on the methods of projecting future climate change, a synopsis of future changes at the global scale is presented, focusing on changes in temperature and precipitation, along with a discussion of how future global temperature change is related to the total amount of human emissions of carbon dioxide over time.

Chapters 4 to 7 each cover observed changes, understanding of causes of change (specifically, the contributions of human influences and natural climate variability), and future changes, for different components of the climate system in Canada. Chapter 4 assesses past and future changes in temperature and precipitation for Canada, including changes in temperature and precipitation extremes, and presents analyses of some recent individual extreme events and their causes. Chapter 5 covers the cryosphere – those parts of Canada with frozen water, including snow, sea ice, land ice (glaciers and ice caps), freshwater ice (lake and river ice), and permafrost. Chapter 6 assesses past and future climate-related changes to Canada's freshwater availability through key components of the water cycle, including streamflow, surface water levels (lakes and wetlands), soil moisture, drought, and groundwater. Chapter 7 looks at changes occurring in the three oceans surrounding Canada, including physical and chemical changes.

The final chapter of this report (Chapter 8) provides a short synopsis of changes for Canada as a whole and then a synthesis of changes assessed in Chapters 4 to 7 for northern Canada and for the five regions of southern Canada. This chapter may be useful for readers who prefer an overview of changes by geographical region before reading in-depth about changes in different components of the climate system in the core chapters. This chapter also helps transition to subsequent reports being prepared as part of the National Assessment (see Section 1.1).



References

Bush, E.J., Loder, J.W., James, T.S., Mortsch, L.D. and Cohen, S.J. (2014): An Overview of Canada's Changing Climate; in *Canada in a Changing Climate: Sector Perspectives on Impacts and Adaptation*, (ed.) F.J. Warren and D.S. Lemmen; Government of Canada, Ottawa, Ontario, p. 23–64.

IPCC [Intergovernmental Panel on Climate Change] (2013): *Climate Change 2013: The Physical Science Basis (Contribution of Working Group I to the Fifth Assessment Report of the Intergovernmental Panel on Climate Change)*; (ed.) T.F. Stocker, D. Qin, G.-K. Plattner, M. Tignor, S.K. Allen, J. Boschung, A. Nauels, Y. Xia, V. Bex and P.M. Midgley; Cambridge University Press, Cambridge, United Kingdom and New York, NY, USA, 1535 p. doi:10.1017/CBO9781107415324

IPCC (2014): *Climate Change 2014: Impacts, Adaptation, and Vulnerability. Part A: Global and Sectoral Aspects (Contribution of Working Group II to the Fifth Assessment Report of the Intergovernmental Panel on Climate Change)*; (ed.) C.B. Field, V.R. Barros, D.J. Dokken, K.J. Mach, M.D. Mastrandrea, T.E. Bilir, M. Chatterjee, K.L. Ebi, Y.O. Estrada, R.C. Genova, B. Girma, E.S. Kissel, A.N. Levy, S. MacCracken, P.R. Mastrandrea and L.L. White; Cambridge University Press, Cambridge, United Kingdom and New York, NY, USA, 1132 p.

Lemmen, D.S., Warren, F.J., James, T.S. and Mercer Clarke, C.S.L. (ed.) (2016): *Canada's Marine Coasts in a Changing Climate*; Government of Canada, Ottawa, Ontario, 274 p. http://www.nrcan.gc.ca/sites/www.nrcan.gc.ca/files/earthsciences/files/pdf/NRCAN_fullBook%20%20accessible.pdf [22 August 2018]

Lemmen, D.S., Warren, F.J., Lacroix, J. and Bush, E. (ed.) (2008): *From Impacts to Adaptation: Canada in a Changing Climate 2007*; Government of Canada, Ottawa, Ontario, 448 p. http://www.nrcan.gc.ca/sites/www.nrcan.gc.ca/files/earthsciences/pdf/assess/2007/full-complet_e.pdf [22 August 2018]

Mastrandrea, M.D., Field, C.B., Stocker, T.F., Edenhofer, O., Ebi, K.L., Frame, D.J., Held, H., Kriegler, E., Mach, K.J., Matschoss, P.R., Plattner G.-K., Yohe, G.W. and Zwiers, F.W. (2010): *Guidance note for lead authors of the IPCC Fifth Assessment Report on consistent treatment of uncertainties*. IPCC cross-Working Group meeting on consistent treatment of uncertainties. 6–7 July, 2010. <http://www.ipcc.ch/publications_and_data/publications_and_data_supporting_material.shtml?search=1>

Maxwell, B., Mayer, N. and Street, R. (ed.) (1997): *Canada Country Study: Climate Impacts and Adaptation*. National summary for policy makers; Environment Canada, Ottawa, Canada. <<http://publications.gc.ca/collections/Collection/En56-119-8-1997-1E.pdf>>

Palko, K. and Lemmen, D.S. (ed.) (2017): *Climate Risks and Adaptation Practices for the Canadian Transportation Sector 2016*; Government of Canada, Ottawa, Ontario, 309 p.



Séguin, J. (ed.) (2008): Human Health in a Changing Climate: a Canadian Assessment of Vulnerabilities and Adaptive Capacity; Health Canada, Ottawa, Ontario, 484 p.

Warren, F.J. and Lemmen, D.S. (2014): Canada in a Changing Climate: Sector Perspectives on Impacts and Adaptation; Government of Canada, Ottawa, Ontario, 286 p.





CHAPTER 2

Understanding Observed Global Climate Change

CANADA'S CHANGING CLIMATE REPORT



Government
of Canada

Gouvernement
du Canada

Canada



Authors

Elizabeth Bush, Environment and Climate Change Canada

Nathan Gillett, Environment and Climate Change Canada

Emma Watson, Environment and Climate Change Canada

John Fyfe, Environment and Climate Change Canada

Felix Vogel, Environment and Climate Change Canada

Neil Swart, Environment and Climate Change Canada

Recommended citation: Bush, E., Gillett, N., Watson, E., Fyfe, J., Vogel, F. and Swart, N. (2019): Understanding Observed Global Climate Change; Chapter 2 in Canada's Changing Climate Report, (ed.) E. Bush and D.S. Lemmen; Government of Canada, Ottawa, Ontario, p. 24–72.



Chapter Table Of Contents

CHAPTER KEY MESSAGES

SUMMARY

2.1: Introduction

2.2: Observed changes in the global climate system

2.2.1: Global annual and extreme temperature changes

2.2.2: Global annual and extreme precipitation and related hydrological changes

2.2.3: Ocean changes

2.2.4: Changes in the cryosphere

2.3: Understanding the causes of observed global climate change

2.3.1: Factors determining global climate

Box 2.1: The greenhouse effect and drivers of climate change

Box 2.2: Sources of the main greenhouse gases

Box 2.3: Positive feedbacks that amplify climate change

2.3.2: Changes in greenhouse gases and radiative forcing over the Industrial Era

2.3.2.1: Changes in greenhouse gas concentrations over the Industrial Era

FAQ 2.1: Are humans responsible for the observed rise in atmospheric carbon dioxide?

Box 2.4: Canadian atmospheric greenhouse gas monitoring

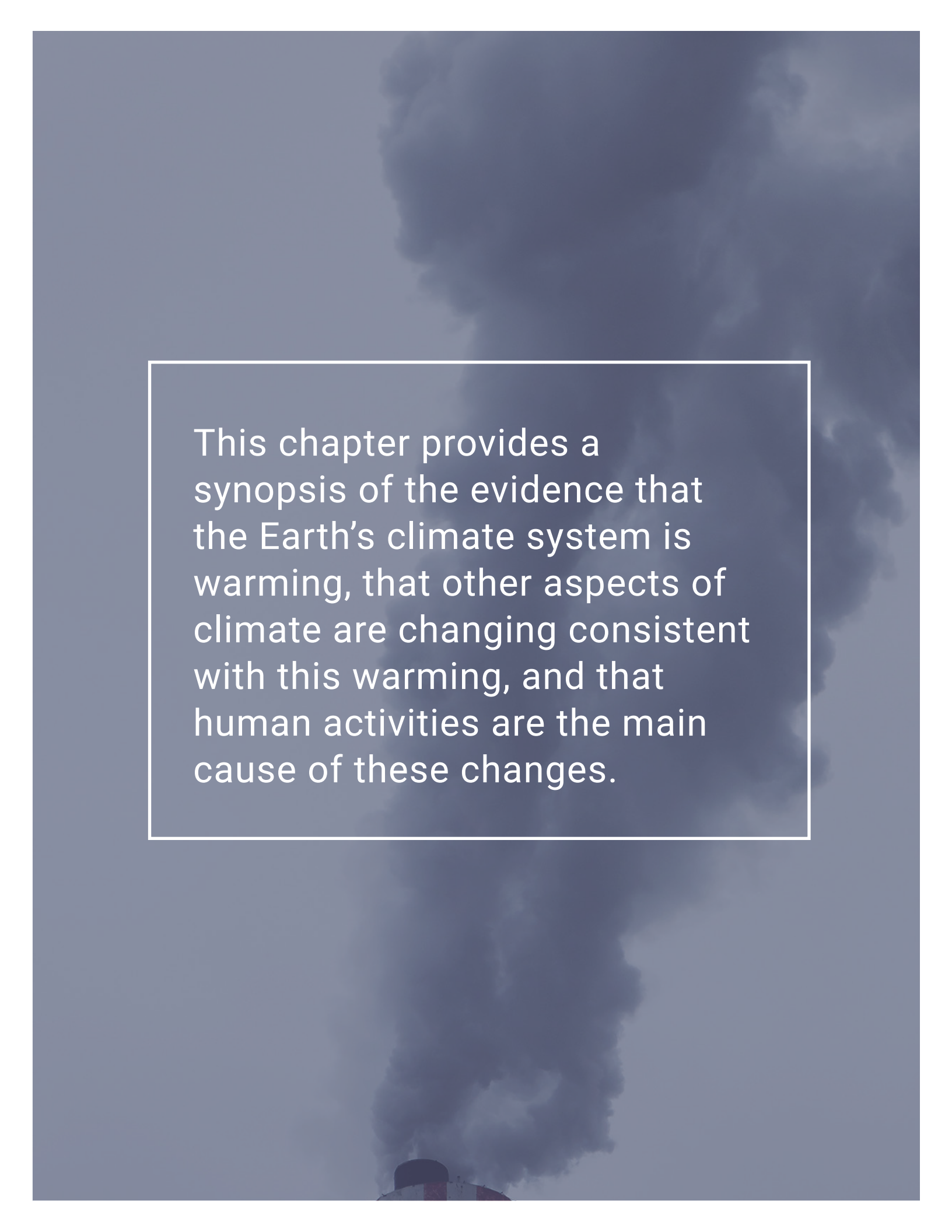
2.3.2.2: Changes in radiative forcing over the Industrial Era

2.3.3: Natural climate variability

Box 2.5: Modes of climate variability

2.3.4: Detection and attribution of observed changes

REFERENCES



This chapter provides a synopsis of the evidence that the Earth's climate system is warming, that other aspects of climate are changing consistent with this warming, and that human activities are the main cause of these changes.



Chapter Key Messages

2.2: Observed Changes In The Global Climate System

Warming of the climate system during the Industrial Era is unequivocal, based on robust evidence from a suite of indicators. Global average temperature has increased, as have atmospheric water vapour and ocean heat content. Land ice has melted and thinned, contributing to sea level rise, and Arctic sea ice has been much reduced.

2.3: Understanding The Causes Of Observed Global Change

Warming has not been steady over time, as natural climate variability has either added to or subtracted from human-induced warming. Periods of enhanced or reduced warming on decadal timescales are expected, and the factors causing the early 21st century warming slowdown are now better understood. In the last several years, global average temperature has warmed substantially, suggesting that the warming slowdown is now over.

The heat-trapping effect of atmospheric greenhouse gases is well-established. It is *extremely likely*² that human activities, especially emissions of greenhouse gases, are the main cause of observed warming since the mid-20th century. Natural factors cannot explain this observed warming. Evidence is widespread of a human influence on many other changes in climate as well.

2 This report uses the same calibrated uncertainty language as in the IPCC's Fifth Assessment Report. The following five terms are used to express assessed levels of confidence in findings based on the availability, quality and level of agreement of the evidence: very low, low, medium, high, very high. The following terms are used to express assessed likelihoods of results: virtually certain (99%–100% probability), extremely likely (95%–100% probability), very likely (90%–100% probability), likely (66%–100% probability), about as likely as not (33%–66% probability), unlikely (0%–33% probability), very unlikely (0%–10% probability), extremely unlikely (0%–5% probability), exceptionally unlikely (0%–1% probability). These terms are typeset in italics in the text. See chapter 1 for additional explanation.

Summary

The Earth's climate system comprises interacting physical components — the atmosphere, the hydrosphere (liquid water on Earth), the cryosphere (frozen elements), the land surface, and the biosphere, which encompasses all living things on land and in water. Measurements of variables within all of these systems provide independent lines of evidence that the global climate system is warming. The consistency of the signals across multiple components of the climate system provides a compelling story of unequivocal change.

The best-known indicator for tracking climate change is global mean surface temperature (GMST), estimated as the average (or mean) temperature for the world from measurements of sea surface temperatures and of near-surface air temperatures above the land. This measure has risen an estimated 0.85°C (90% uncertainty range between 0.65°C and 1.06°C) over the period 1880–2012. Each of the last three full decades (1980s, 1990s, and 2000s) has broken successive records for average 10-year temperatures. A warming slowdown occurred in the early 21st century, even though decadal temperature for the 2000s was higher than that for the 1990s. Natural climate variability influences GMST on a variety of timescales; therefore, periods of reduced or enhanced warming on decadal timescales are expected. The causes of the early 21st century warming slowdown are now better understood, and it appears to have ended, with the years 2015, 2016, and 2017 being the warmest on record, with GMST more than 1°C above the pre-industrial average level.

Signals of climate warming are also evident in other components of the climate system. The shift toward a warmer global climate on average has been accompanied by an increase in warm extremes and a decrease in cold extremes. The amount of water vapour (atmospheric humidity) in the atmosphere has *very likely* increased, consistent with the capacity of warmer air to hold more moisture. Not only has the ocean warmed at the surface, it is *virtually certain* that the whole upper ocean (to a depth of 700 m) has warmed. Global mean sea level has risen an estimated 0.19 m over the period 1901–2010 (90% uncertainty range between 0.17 m and 0.21 m) as a consequence of the expansion of ocean waters due to warming (warmer water takes up more volume) and the addition of new meltwater from shrinking glaciers and ice sheets worldwide. The extent of Arctic sea ice has also been shrinking in all seasons, with declines most evident in summer and autumn.

Understanding how much human activity has contributed to the observed warming of the climate system also draws from multiple lines of evidence. This includes evidence from observations, from improved understanding of processes and feedbacks within the system that determine how the climate system responds to both natural and human-induced perturbations, and from climate models (see Chapter 3.3.1).

The ability of greenhouse gases (GHGs) in Earth's atmosphere to absorb heat energy radiated from the Earth is well understood. Emissions of GHGs from human activities have led to a build-up of atmospheric GHG levels. This rise in atmospheric GHG levels, predominantly carbon dioxide, has been the main driver of climate warming during the Industrial Era. The strong warming effect of increases in GHGs has been offset to some extent by increases in levels of atmospheric aerosols, which have climate-cooling effects. Variations in the brightness of the sun during the Industrial Era have had a warming effect on climate that is at least 10 times smaller than that from human activity and cannot explain the observed rise in global temperature. Volcanic eruptions have cooling effects on global climate that can last several years but cannot explain the observed long-term change in global temperature.



Determining how much of the observed climate warming and other climatic changes are due to these drivers is a complex task, as the climate system does not respond to these drivers in a straightforward way. To accomplish this task, climate (or Earth system) models are essential tools for identifying the causes of observed climate changes. Experiments with these models simulate how the climate system responds to real-world changes, including the impacts of human activities, and compare this with idealized experiments without human interference. On the basis of analysis of observations and such experiments, it is *extremely likely* that human influences, primarily emissions of GHGs, have been the dominant cause of the observed global warming since the mid-20th century. Studies have confirmed that there is a human contribution to observed changes in the lower atmosphere, the cryosphere, and the ocean, on a global scale.

2.1: Introduction

The oscillation between cold ice ages and warm interglacial periods over the past two million years on Earth is a testament to the effect on Earth's climate of changes in global average temperature on the order of 5°C (Jansen et al., 2007; Masson-Delmotte et al., 2013). In modern times, on century timescales, the globe has warmed by about 1°C since the beginning of the Industrial Era (see Section 2.2.1), and additional warming is unavoidable in this century. The Paris Agreement under the United Nations Framework Convention on Climate Change³ has a stated goal of holding the increase in global average temperature to well below 2°C above pre-industrial levels and pursuing efforts to limit the temperature increase to 1.5°C. Given that historic warming has already moved us close to this goal, it is important to understand how and why climate is changing. This chapter provides a summary of that understanding, based primarily on the evidence presented in multiple chapters of the Intergovernmental Panel on Climate Change (IPCC) Working Group 1 Fifth Assessment Report (AR5) (IPCC, 2013a).

This is one of two chapters of this report that examine global-scale climate change. Together, Chapters 2 and 3 provide context and background information for the assessment of past and future climate change in Canada found in Chapters 4 to 7. This context allows the report to provide a complete narrative to Canadian audiences about how changes in Canada are a manifestation of global-scale climate change. The background information on climate change and climate variability in this chapter is referred to in subsequent chapters of the report. While drawing primarily from the IPCC AR5, this chapter also includes some recent studies to update trends for key indicators of global climate change and to highlight areas where scientific understanding has advanced significantly since 2013. This chapter focuses on contemporary climate change, covering recent periods in the past (from multi-decade to century timescales) for which instrumental records are available. For a recent assessment of changes in past climate over longer timescales (from multi-century to multi-millennia timescales) and their causes, readers are referred to chapter 5 in the IPCC AR5 (Masson-Delmotte et al., 2013).

This chapter first presents the evidence from observations of global-scale climate changes (see Section 2.2) and then addresses the causes of contemporary climate change. The chain of evidence that enables scientists to be confident that human activities have played the dominant role in observed climate change over the past century or so is presented in Section 2.3. This chapter assesses studies using models of the climate system. Such models are required to comprehensively evaluate the causes of observed climate change, because they incorporate the complex processes and feedbacks that determine the climate system's response to both human-caused and natural factors. Descriptions of how climate models are constructed, evaluated, and used to project future changes in climate are presented in Chapter 3, Section 3.3.

3 <https://unfccc.int/process-and-meetings/the-paris-agreement/the-paris-agreement>

2.2: Observed changes in the global climate system

Key Message

Warming of the climate system during the Industrial Era is unequivocal, based on robust evidence from a suite of indicators. Global average temperature has increased, as have atmospheric water vapour and ocean heat content. Land ice has melted and thinned, contributing to sea level rise, and Arctic sea ice has been much reduced.

The global climate system comprises a number of interacting components, encompassing the atmosphere, hydrosphere (liquid water in oceans, lakes, rivers, etc.), cryosphere (snow, ice, and frozen ground), biosphere (all living things on land and in water), and the land surface. Long-term changes that are consistent with an overall warming of the climate system can be observed throughout the various components of the system. In this section, observed changes in global mean surface temperature (GMST), precipitation, the cryosphere, and oceans are reviewed. These changes are summarized from Chapters 2, 3, and 4 of the IPCC AR5 (Hartmann et al., 2013; Rhein et al., 2013; Vaughan et al., 2013). More recent observations indicate a general continuation of warming and related changes, with short-term year-to-year variability evident, as it is in the earlier record (Blunden and Arndt, 2017; USGCRP, 2017).

“Climate” can be considered the average, or expected, weather and related atmospheric, land, and marine conditions for a particular location. Climate statistics are commonly calculated for 30-year periods, as recommended by the World Meteorological Organization. “Climate change” refers to a persistent, long-term change in the state of the climate, measured by changes in the mean state and/or its variability (IPCC, 2013c). Measuring climate change therefore requires long-term observations of climate parameters so that long-term trends can be distinguished from shorter-term variations (see Section 2.3.3).

Changes in the frequency, intensity, and duration of climate and weather extremes⁴ are expected to accompany a changing climate. These changes can have large impacts on human and natural systems. For some types of extremes (e.g., hot and cold days/nights), changes in frequency are a natural consequence of a shift toward a warmer climate on average. For other extremes, the factors underlying expected changes are more complicated and can involve changes in the water cycle, ocean temperatures, atmosphere-ocean circulation, and other factors.

Quantifying changes in many extremes of climate and weather is more challenging than quantifying changes in mean climate conditions, for several reasons (IPCC, 2012). By definition, extremes occur infrequently. Therefore, observational data spanning many decades or longer are needed to derive adequate statistics about the historical occurrence rate of extremes, but these are often lacking.

⁴ Weather extremes occur over shorter timescales (e.g., short-duration heavy precipitation event) than climate extremes (e.g., drought). For further details on differentiating weather and climate extremes, refer to IPCC (2012).

2.2.1: Global annual and extreme temperature changes

Global-scale records of surface temperatures, based on thermometer observations of surface air temperatures over land and measurements of sea surface temperatures, are available from the late 19th century onwards. From these observations, various research groups have developed global temperature datasets (see Figure 2.1) using different procedures for processing the available raw data, such as the treatment of gaps in observations (see Section 2.3.3). Based on these independently produced global temperature datasets, a best estimate of GMST has been calculated, which represents changes over both land and ocean. This estimate shows that GMST rose 0.85°C over the period 1880–2012 (based on a linear trend, with a 90% uncertainty range between 0.65°C and 1.06°C) (Hartmann et al., 2013). The last three full decades (1980–2010) have been the warmest on record, with the longest dataset extending back to 1850 (see Figure 2.1) (Hartmann et al., 2013). Global temperatures in the last three years with complete records (2015, 2016, and 2017) are the three warmest years on record for the globe on average (WMO, 2018), at more than 1°C above pre-industrial average levels (Blunden and Arndt, 2016, 2017; WMO, 2017, 2018; Hawkins et al., 2017).

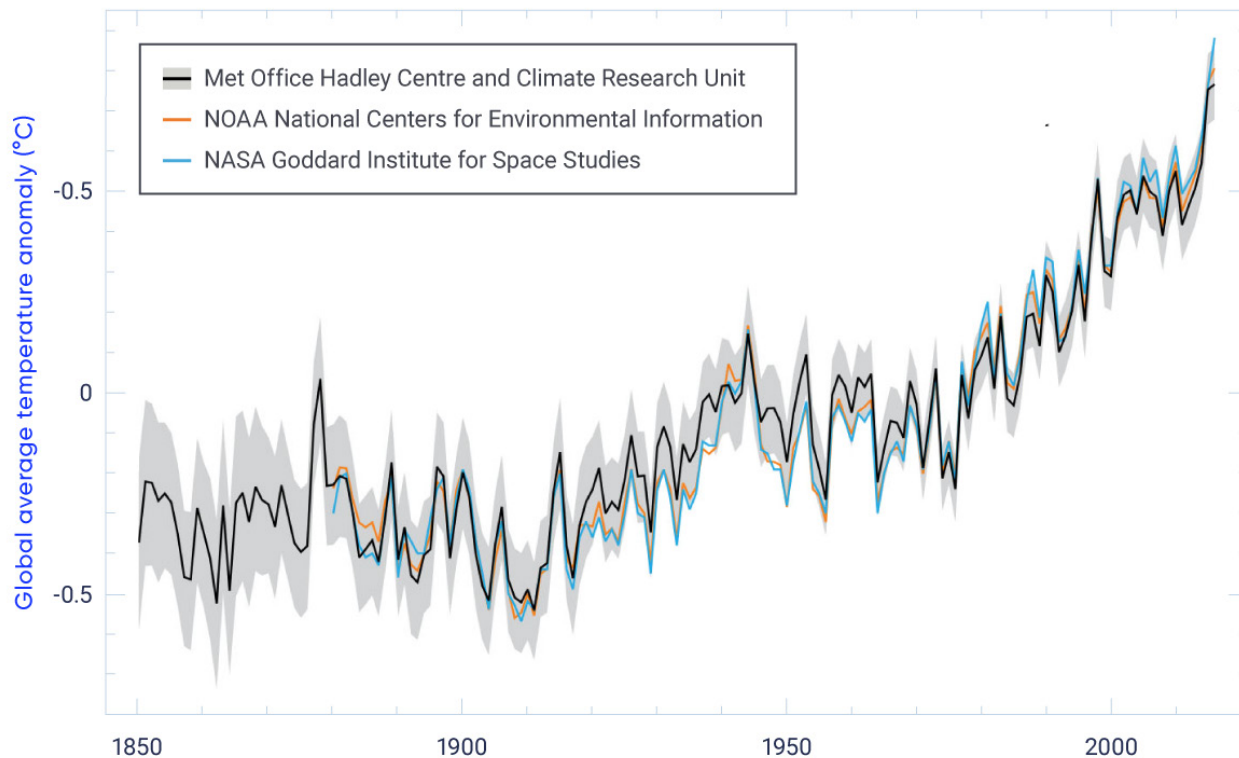


Figure 2.1: Observed global mean annual surface temperatures anomalies, 1850–2016

Figure caption: Departure (anomaly) of global mean annual surface temperature from the average over the 1961–1990 reference period, from three datasets. The grey shading indicates the uncertainty in the dataset produced by the Met Office Hadley Centre and the Climatic Research Unit at the University of East Anglia, UK (HadCRU).

Annual GMST has not increased in a steady linear progression since the late 19th century (see Figure 2.1). During several periods, warming was more pronounced (e.g., 1900–1940 and 1970 onwards) or less pronounced (e.g., 1940–1970). These fluctuations arise from natural variations within the climate system (internal climate variability) and outside (external) forces, including human factors (see Section 2.3.3).

Almost the entire globe experienced warming on a century scale (1901–2012). This warming was not uniform from one region of the Earth to another, owing to a range of factors, including internal climate variability, and regional variations in climate feedbacks and heat uptake (Hartman et al., 2013). In general, warming has been strongest at high northern latitudes and stronger over land than oceans. Since Canada has a large land mass, much of which is located at high northern latitudes, warming across Canada has been about twice the global average (see Chapter 4, Section 4.2.1).

Cold and warm extremes of temperature can have large impacts on human and natural systems. Based on multi-decadal observational datasets and rigorous statistical analysis, the IPCC AR5 reports that, for global land area as a whole, the number of warm days and nights⁵ *very likely* increased and the number of cold days and nights *very likely* decreased over the period 1951–2010. Robust statistical assessment of heat waves and warm spells is more challenging. The IPCC AR5 assesses with *medium confidence* that, since the mid-20th century, the length and frequency of warm spells, including heatwaves,⁶ has increased for global land areas as a whole (Hartmann et al., 2013). At the continental scale, it is *likely* that heatwave frequency has increased in some regions of Europe, Asia, and Australia over this period. For North America and Central America, there is *medium confidence* that more regions have experienced increases in heatwaves and warm spells than have experienced decreases (Hartmann et al., 2013).

2.2.2: Global annual and extreme precipitation and related hydrological changes

Increasing global temperatures have impacts on the hydrological (water) cycle. The amount of moisture the atmosphere can hold increases with rising temperatures (about 7% per degree Celsius of warming). It is *very likely* that global specific humidity — a measure of the amount of water vapour in the air — near the surface and in the troposphere⁷ (see Figure 2.2) has increased since the 1970s, consistent with the observed temperature increase over this period (Hartmann et al., 2013).

5 Warm days and nights and cold days and nights are defined from daily temperatures as days when daily maximum (daytime) and minimum (nighttime) temperatures are above the 90th (warm) or below the 10th (cold) percentile.

6 Heatwaves and warm spells are defined variously throughout the literature but refer to multi-day periods with high temperature extremes.

7 The troposphere is the lowest layer of the Earth's atmosphere, extending from the surface to an average altitude of 10 km in the mid-latitudes (this altitude varies by season and location).

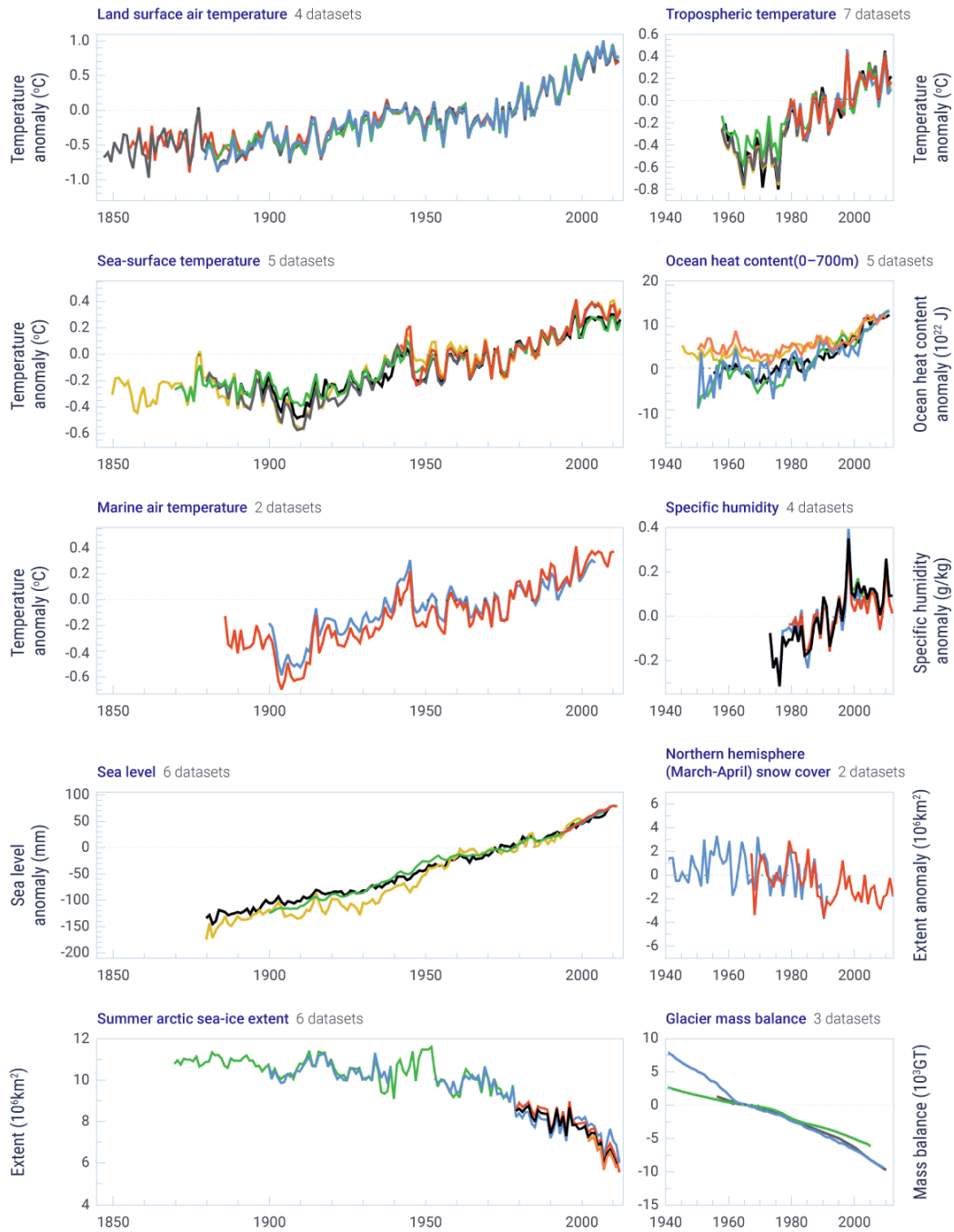


Figure 2.2: Multiple independent indicators of a changing global climate

Figure caption: Multiple indicators of a changing global climate from independently derived estimates. Datasets in each panel have been normalized to a common period of record.

FIGURE SOURCE: HARTMAN ET AL., 2013, FAQ 2.1, FIGURE 2. DATASETS ARE FOUND IN HARTMAN ET AL., 2013, SUPPLEMENTARY MATERIAL SECTION 2.SM.5.

The effects of increasing atmospheric concentrations of greenhouse gases (GHGs) on the hydrological cycle and precipitation are more complex than for temperature. Precipitation varies substantially over time and space, to a greater extent than does temperature. Long-term precipitation trends are smaller, compared to the range of precipitation variability, than are temperature trends relative to the range of temperature variability. Therefore, a greater density of monitoring stations with long records of precipitation is required for robust assessment of precipitation trends than is the case for temperature. Owing to a lack of data, there is *low confidence* in estimates of precipitation changes over land at the global scale before 1951 and *medium confidence* thereafter. Annual average precipitation for global land areas increased slightly over the period 1901–2008, and different datasets vary in the magnitude of observed changes (Hartmann et al., 2013). It remains a challenge to determine long-term trends in precipitation for the global oceans. At the regional scale, average annual precipitation for the mid-latitude land area in the Northern Hemisphere shows a *likely* overall increase since 1901, with *medium confidence* before 1951 and *high confidence* after that date (Hartmann et al., 2013). The changes in precipitation across Canada are discussed in Chapter 4.

As climate warming has made more moisture available in the atmosphere, this additional atmospheric moisture can lead to increased intensity of extreme precipitation events that varies by location. Observed changes in extreme precipitation are generally larger than those in total annual precipitation. At the global scale, extreme rainfall over land, measured as the number of heavy precipitation events, has *likely* increased in more regions than it has decreased since the 1950s. There is large variability among regions and between seasons, but the highest confidence in observed results is for central North America, where there was *very likely* a trend toward heavier precipitation events since the 1950s (Harman et al., 2013).

While changes in precipitation patterns may be expected to contribute to changes in drought and floods, there is *low confidence* in global-scale trends for both of these hazards (Hartmann et al., 2013). However, regional-scale trends are evident in some areas, with a *likely* increase in frequency and intensity of drought in the Mediterranean and West Africa and a *likely* decrease in central North America (mainly central United States but including parts of southern Canada) since 1950. Perspectives on changes in the frequency and magnitude of droughts and floods in a Canadian context are provided in Chapter 6 (see also Chapter 4, Section 4.4 for a discussion of the 2013 Alberta flood).

2.2.3: Ocean changes

A number of changes observed over the past century provide evidence of a warming global ocean (Rhein et al., 2013) (see Figure 2.2). Comprehensive estimates of global mean temperatures in the upper ocean (to a depth of 700 m) reveal that warming since the early 1970s is *virtually certain*. The global average warming for the upper 75 m of the ocean over the period 1971–2010 was an estimated 0.11°C (90% uncertainty range from 0.09°C to 0.13°C) per decade. There is greater uncertainty in measurements of ocean temperatures before 1971 due, in part, to the scarcity of observations, but the IPCC AR5 reports that global average ocean warming (0–700 m) from the 1870s to 1971 was *likely*. Warming has also been observed deeper in the oceans, although the trends are not as strong. The IPCC AR5 reports that the increasing ocean heat content (absorbed heat that has been stored in the ocean; see Figure 2.2) accounts for roughly 90% of the energy ac-

cumulated globally over the period 1971–2010 (*high confidence*). This accumulation of energy in the ocean is strong evidence of excess energy in the Earth system, with less energy leaving the Earth system than entering (see Section 2.3.1; Rhein et al., 2013). In addition to absorbing excess heat, the Earth's oceans have also been absorbing excess carbon dioxide (CO₂) from the atmosphere, increasing their acidity (See Chapter 7, Section 7.6.1).

Global sea level rises primarily as a result of the expansion of ocean waters due to warming (thermal expansion) and the addition of water to the ocean from land ice (glacier and ice sheets) that is delivered to the oceans by melting and increased ice discharge. Tide-gauge records from around the world and, more recently, satellite altimeter data, indicate that the global mean sea level has been rising since the late 19th century (see Figure 2.2). The level has risen by an estimated 0.19 m (90% uncertainty range from 0.17 m to 0.21 m), based on a linear trend over the period 1901–2010, and the rate of this sea level rise has *likely* increased since the early 20th century (Rhein et al., 2013).

Both rising global sea level and increasing ocean heat content are strong evidence of a warming world. Influences of these global changes on the oceans surrounding Canada are detailed in Chapter 7.

2.2.4: Changes in the cryosphere

The cryosphere refers to portions of the Earth with sufficiently cold temperatures for water to freeze, and includes snow, sea ice, land ice (glaciers and ice caps), freshwater ice (lake and river ice), permafrost, and seasonally frozen ground. The IPCC AR5 assessed changes in the cryosphere around the globe and found, with *very high confidence*, that almost all glaciers worldwide have continued to shrink and that the Greenland (*very high confidence*) and Antarctic (*high confidence*) ice sheets have lost mass (based on two decades of data) (Vaughan et al., 2013). The IPCC AR5 reported that, over the period 2003–2009, the greatest losses of glacier ice were from glaciers in Alaska, the Southern Andes, Asian mountains, the periphery of the Greenland ice sheet, and the Canadian Arctic (Vaughan et al., 2013).

There is *very high confidence* that the extent of Arctic sea ice (both newly formed annual ice and multi-year ice) declined over the period 1979–2012, and that declines occurred in all seasons but were most pronounced in summer and autumn (*high confidence*). Annual mean sea ice extent in the Arctic *very likely* declined at a rate of 3.5%–4.1% per decade over this period. Antarctic sea ice extent *very likely* increased over the same period at a rate of 1.2%–1.8% per decade. The causes of variations in Antarctic sea ice properties and trends remain less well known than those for the Arctic, and the World Meteorological Association (2018) reports that, since the increase was reported in 2013, Antarctic sea ice extent was at or near record low levels throughout 2017. There is also *very high confidence* that snow cover extent has declined in the Northern Hemisphere (especially in spring) and *high confidence* that permafrost temperatures have increased in most regions since the 1980s, which is related to regional warming. Overall, the net loss in mass of ice from the global cryosphere (due to changes in glaciers, ice sheets, snow cover, sea ice extent, melt period, and ice thickness) is evidence of strong warming at high latitudes (see Figure 2.2) (Vaughan et al., 2013). Further details on these changes and implications from a Canadian perspective are found in Chapter 5.



Section summary

In summary, these changes documented in the atmosphere, oceans, and cryosphere since the late 19th century (see Figure 2.2), as well as additional changes documented in the IPCC AR5, provide a strong, coherent picture of a warming planet based on multiple, independent lines of evidence. For this reason, warming of the climate system is robustly demonstrated; that is, it is found to be unequivocal.

2.3: Understanding the causes of observed global climate change

Key Message

Warming has not been steady over time, as natural climate variability has either added to or subtracted from human-induced warming. Periods of enhanced or reduced warming on decadal timescales are expected, and the factors causing the early 21st century warming slowdown are now better understood. In the last several years, global average temperature has warmed substantially, suggesting that the warming slowdown is now over.

Key Message

The heat-trapping effect of atmospheric greenhouse gases is well-established. It is *extremely likely* that human activities, especially emissions of greenhouse gases, are the main cause of observed warming since the mid-20th century. Natural factors cannot explain this observed warming. Evidence is widespread of a human influence on many other changes in climate as well.

2.3.1: Factors determining global climate

Scientists have understood the basic workings of Earth's climate for almost 200 years. Studies in the 19th century had already identified the key role of Earth's atmosphere and of CO₂ in raising the temperature of the planet (Fourier, 1827; Tyndall, 1859; Arrhenius, 1896). The fundamentals of the climate system, including factors that determine climate and that can drive climate change, have been included in every major IPCC assessment as foundational background information (IPCC, 1990, 1996, 2001, 2007, 2013a).

Earth's long-term climate and average temperature are regulated by a balance between energy arriving from the sun (in the form of shortwave radiation) and energy leaving the Earth (in the form of longwave radiation) (see Box 2.1). When this balance is disrupted in a persistent way, global temperature rises or falls. Factors that disrupt this balance are called "climate drivers" or "climate forcing agents," evoking their influence in forcing climate toward warmer or cooler conditions. Their effect on Earth's energy balance is called "radiative forcing," which is defined as the net change in the energy balance of the Earth system due to an external perturbation. The strength of radiative forcing is measured in units of watts per square metre (W/m²). Positive

radiative forcing indicates excess energy is being retained in the climate system — less energy is leaving than is entering the system — leading to a warmer climate, whereas negative radiative forcing indicates more energy is leaving the climate system than entering it, leading to a cooler climate (Le Treut et al., 2007; Cubasch et al., 2013). Radiative forcing provides a useful means of comparing and/or ranking the influence of different climate drivers.

Climate drivers can be either natural or anthropogenic — resulting from human activities. The fact that Earth's average temperature and climate have varied significantly over geologic time indicates that natural factors have varied in the past. On shorter timescales of decades to centuries, the main climate drivers are changes in solar irradiance, volcanic eruptions, changes in atmospheric composition, and changes to the land surface. The latter two are influenced by human activities. How changes in these climate drivers influence incoming or outgoing radiation is described below.

Box 2.1: The greenhouse effect and drivers of climate change

The Earth's climate system is powered by energy from the sun reaching the Earth in the form of sunlight. Some of the incoming solar radiation is reflected back to space, but the rest is absorbed by the atmosphere and at the Earth's surface, which warms the planet. The Earth cools down by emitting radiation back to space at a rate that depends on the temperature of Earth. Since the Earth is much colder than the sun, it emits infrared radiation in the lower-energy, longwave part of the energy spectrum (infrared radiation, invisible to the human eye), whereas the sun emits mainly high-energy, shortwave radiation (visible and ultraviolet light).

The Earth's average temperature is determined by the overall balance between the amount of absorbed incoming energy (as light) from the sun and the amount of outgoing energy (as infrared radiation) from Earth to space. Only a portion of the incoming energy from the sun is used to warm the Earth, as some of it is reflected by the Earth's atmosphere and surface. About two-thirds of the incoming solar energy (about 240 W/m²) is absorbed and used to warm the planet (Hartman et al., 2013). Some of the outgoing infrared radiation (heat radiation) is absorbed and then re-emitted by clouds and GHGs in the lower atmosphere. This process is known as the greenhouse effect, and it leads to heat being trapped in the lower atmosphere, which warms the Earth's surface. Naturally occurring GHGs in the atmosphere — mainly water vapour and CO₂ from natural sources — produce a natural greenhouse effect that raises the Earth's mean surface temperature from about -16°C to about +15°C (Lacis et al., 2010). This higher temperature creates conditions favourable for life on Earth and also increases the flow of heat from Earth to space (to about 240 W/m²) so that it balances the flow of incoming solar energy.

In a stable climate, global average temperature remains roughly constant because of this balance between incoming and outgoing energy. However, the Earth's energy balance can be perturbed. Factors that disrupt this balance and cause climate warming or cooling are called climate drivers or climate forcing agents. Climate drivers can be either natural or human-caused. They can disrupt the Earth's energy balance by 1) changing the amount of incoming solar radiation; 2) changing the Earth's albedo, that is, how much incoming solar radiation is reflected from the Earth's surface and atmosphere; and 3) changing the amount of outgoing infrared radiation by changing the composition of the atmosphere (see Figure 2.3).

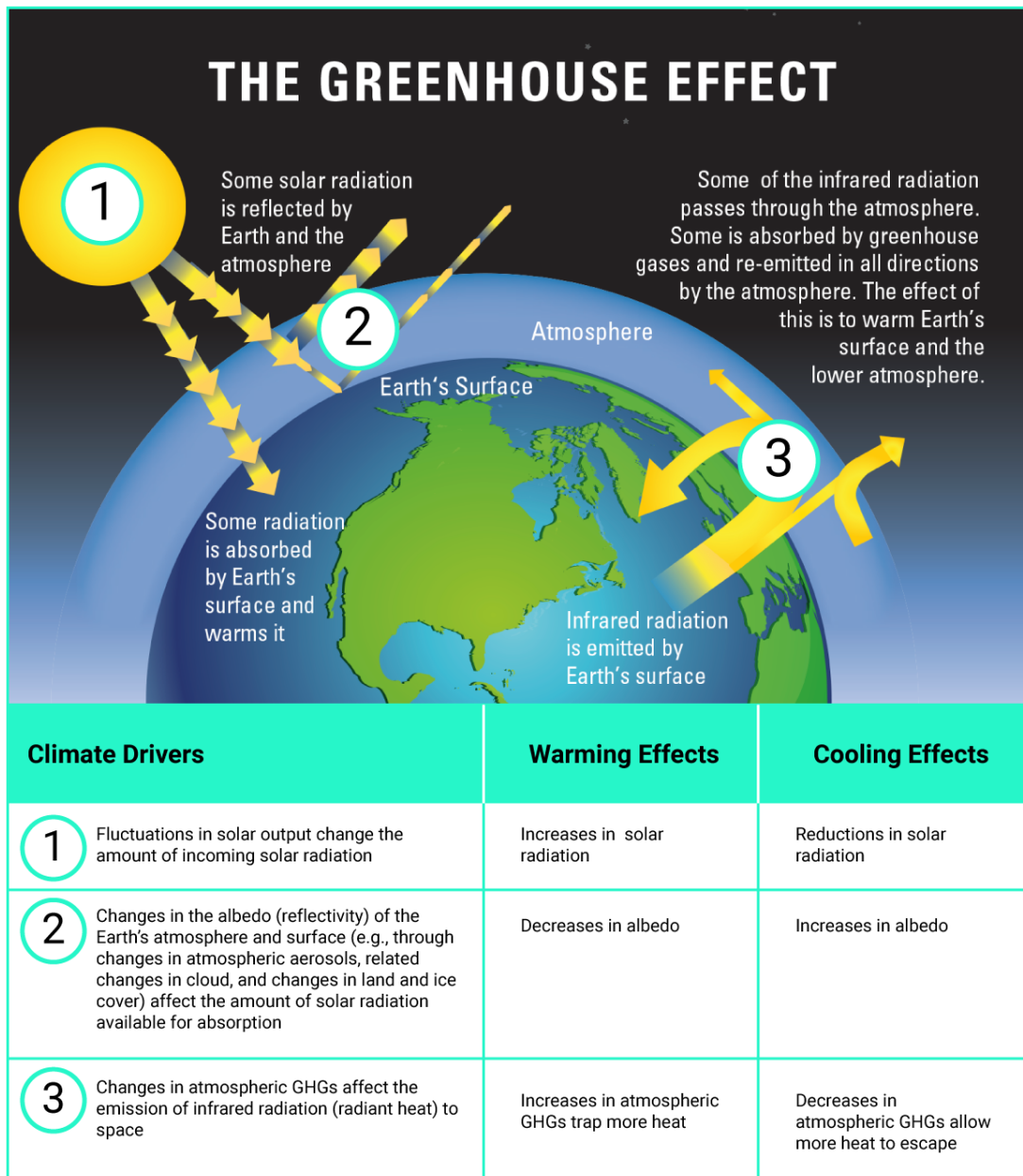


Figure 2.3: The greenhouse effect and key drivers of climate change

Figure caption: The sun is the source of energy for Earth (1). Some of the sun's energy is reflected back to space (2), but the rest is absorbed by the atmosphere, land, and ocean and re-emitted as longwave radiation (radiant heat). Some of this radiant heat is absorbed and then re-emitted by greenhouse gases in the lower atmosphere, trapping heat in the lower atmosphere and reducing how much is radiated to outer space. This process is known as the greenhouse effect (3). Changes to the amount of incoming solar radiation (1), the amount of reflected sunlight (2), and the heat-trapping capacity of the atmosphere (3) cause climate warming or cooling. Factors that drive such changes are called climate drivers or climate forcing agents.

FIGURE SOURCE: UPPER PANEL: NATIONAL ACADEMY OF SCIENCES AND THE ROYAL SOCIETY (2014).

Solar irradiance, the strength of solar radiation received at the Earth's surface, fluctuates by a small amount over a solar cycle of approximately 11 years, and these fluctuations can explain global temperature variations of up to approximately 0.1°C between the strongest and weakest parts of the cycle. Small, multi-decadal trends (increasing and decreasing) in solar irradiance can also occur, with similarly small effects on global climate (Masson-Delmotte et al., 2013).

Volcanic eruptions periodically eject large volumes of gases and dust into the stratosphere (upper atmosphere). Sulphate aerosols (tiny airborne particles) that form from these gases reflect solar radiation and thereby induce a cooling effect.⁸ Since volcanic eruptions are episodic, and sulphate aerosols remain in the stratosphere for only a few years, the cooling effects are short-lived. The global cooling effect of large volcanic eruptions, such as the eruption of Mount Pinatubo in the Philippines in 1991, is clearly evident in the global temperature record (see Section 2.3.3 and Figure 2.9).

Human activities affect Earth's reflectivity (albedo) by changing the atmospheric composition and the land surface. For example, the combustion of fossil fuels emits a variety of pollutants, in addition to GHGs, into the lower atmosphere, where they form aerosols of various chemical compositions. These aerosols may either reflect or absorb solar radiation and are important drivers of climate change. Aerosols in the lower atmosphere also serve as particles on which water vapour can condense to form clouds (cloud condensation nuclei). Changes in aerosol concentrations can therefore induce changes in cloud properties which, in turn, can affect Earth's albedo. While the interactions between aerosols and clouds are complex and involve a number of different processes, an increase in aerosol concentration is known to produce brighter clouds, which reflect more solar radiation, inducing a cooling effect. Human alterations of the land surface also tend to increase albedo. When forested lands are cleared for cultivation this tends to produce more reflective land surfaces (Le Treut et al., 2007; Cubasch et al., 2013).

Changes in solar irradiance, volcanic eruptions, and changes in albedo affect Earth's energy balance by altering the amount of incoming energy available to heat the Earth, but the primary driver of the amount of heat leaving the Earth is changes to the chemical composition of the atmosphere. While the two most abundant gases in Earth's atmosphere – nitrogen (78%) and oxygen (21%) – are transparent to outgoing longwave radiation, allowing this heat to escape to space, some trace gases absorb longwave radiation, creating the greenhouse effect, and are referred to as GHGs (see Box 2.1). GHGs have both natural and human sources. The main GHGs are water vapour, CO₂, methane (CH₄), ozone (O₃), nitrous oxide (N₂O), and groups of synthetic chemicals referred to as halocarbons (see Box 2.2). Changes to the atmospheric concentrations of GHGs affect the transparency of the atmosphere to outgoing heat. Individual GHGs differ in their capacity to trap heat, and most are more powerful GHGs than CO₂. However, CO₂ is by far the most abundant GHG (Myhre et al., 2013) aside from water vapour. The build-up of atmospheric GHGs has reduced heat loss to space and is therefore a positive radiative forcing, with a warming effect on the climate system (Le Treut et al., 2007; Cubasch et al., 2013).

⁸ Volcanoes also emit CO₂, a GHG, but the climate effect of volcanic CO₂ emissions is small (Myhre et al., 2013).

Box 2.2: Sources of the main greenhouse gases

The main greenhouse gases (GHGs) have both natural sources and anthropogenic sources – from human activity – with the exception of the group of GHGs referred to as halocarbons, which are human-made. Since anthropogenic sources add emissions to the atmosphere at a rate greater than natural processes can remove them from the atmosphere, atmospheric levels of GHGs are building up.

Carbon dioxide

Carbon dioxide (CO_2), along with methane (CH_4), is part of Earth's carbon cycle, which involves the movement of carbon among the atmosphere, the land, the ocean, and living things. CO_2 enters the atmosphere from a variety of natural sources, most notably as a result of plant and animal respiration, and is removed from the atmosphere through the photosynthesis of plants and uptake by the ocean. The main anthropogenic sources of CO_2 are the burning of carbon-containing fossil fuels (coal, oil, and natural gas) and deforestation / land clearing. Land clearing can involve either burning trees and other vegetation, which releases CO_2 immediately, or allowing cut vegetation to decay, which releases CO_2 slowly. The manufacture of cement is another important source, as it involves heating limestone (calcium carbonate), the main component of cement, in a process that releases CO_2 .

Methane

The main sources of CH_4 – a carbon-containing GHG – are from decomposition of organic matter by micro-organisms under low-oxygen conditions. Wetlands are by far the largest natural source of CH_4 . Anthropogenic sources include rice paddies, landfills, and sewage; fermentation in the gut of ruminant animals; and artificial wetlands. Along with other pollutants, CH_4 is also produced when fossil fuels and trees are burned with insufficient oxygen for combustion to be complete. It also leaks or is vented to the atmosphere from geological sources, mainly during the extraction, processing, and transportation of fossil fuels, although natural leaks also occur.

Nitrous oxide

Nitrous oxide (N_2O) is part of Earth's nitrogen cycle. Anthropogenic sources are mainly related to the use of nitrogen-based synthetic fertilizers and manure to improve crop productivity, and the cultivation of certain crops that enhance biological nitrogen fixation. These sources have added significant amounts of reactive nitrogen to Earth's ecosystems, some of which is converted to N_2O and released to the atmosphere. Some N_2O is also released to the atmosphere during the combustion of fossil fuels and biomass (e.g., trees or wood-based fuels) and from some industrial sources.

Halocarbons

Halocarbons are a group of synthetic chemicals containing a halogen (e.g., fluorine, chlorine, and bromine) and carbon. There are a variety of industrial sources.

Water vapour

Water vapour is the most important naturally occurring GHG. Human activities do not directly influence the amount of water vapour in the atmosphere to any significant degree. However, the amount of water vapour in the atmosphere changes with temperature, and changes in water vapour are considered a feedback in the climate system (see Box 2.3).

Determining the relative contribution of different forcing agents perturbing the Earth's energy balance provides a useful first-order assessment of the causes of observed climate change (see Section 2.2). However, the climate system does not respond in a straightforward way to changes in radiative forcing. An initial perturbation can trigger feedbacks in the climate system that alter the response. These climate feedbacks either amplify the effect of the initial forcing (positive feedback) or dampen it (negative feedback). Therefore, positive feedbacks in the climate system are cause for concern because they amplify the warming from an initial positive forcing, such as increases in atmospheric concentrations of GHGs.

There are a number of feedbacks in the climate system, operating on a wide range of timescales, from hours to centuries (Cubasch et al., 2013; see, in particular, Fig 1.2 and associated text in this reference). Important positive feedbacks that have contributed to warming over the Industrial Era include the water vapour feedback (water vapour, a strong GHG, increases with climate warming) and the snow/ice albedo feedback (snow and ice diminish with climate warming, decreasing surface albedo) (see Box 2.3). There is **very high confidence** that the net feedback – that is, the sum of the important feedbacks operating on century timescales – is positive, amplifying global warming (Flato et al., 2013; Fahey et al., 2017). Some feedbacks are expected to become increasingly important as climate warming continues this century and beyond. These include feedbacks that change how rapidly the land and ocean can remove CO₂ from the atmosphere and those that may lead to additional emissions of CO₂ and other GHGs, such as from thawing permafrost (Ciais et al., 2013; Fahey et al., 2017) (see Chapter 5, Section 5.6).

Box 2.3: Positive feedbacks that amplify climate change

The water vapour feedback

Water vapour is a greenhouse gas (GHG), as it absorbs outgoing longwave radiation (heat radiation) from Earth. Unlike other GHGs such as carbon dioxide (CO₂) and methane, water vapour levels in the atmosphere cannot be controlled or altered directly by human activity. Instead, the amount of water vapour in the atmosphere is a function of the temperature of the atmosphere. There is a physical limit to how much water vapour air can hold at a given temperature, with warmer air able to hold more moisture than cooler air. For every additional degree Celsius in air temperature, the atmosphere can hold about 7% more water vapour. When air becomes saturated with water vapour, the water vapour condenses and falls as rain or snow, which means that water vapour does not reside for long in the atmosphere. When an external forcing agent, such as increases in atmospheric CO₂, causes climate warming, the rise in temperature both increases the evaporation of water from the surface of the Earth and increases the atmospheric water vapour concentrations. This increased water vapour, in turn, amplifies the warming from the initial CO₂-induced forcing. Therefore, water vapour provides a strong positive climate feedback in response to changes initiated by human emissions of other GHGs (Boucher et al., 2013).

The snow/ice albedo feedback

Snow and ice are bright, highly reflective surfaces. While open water reflects only about 6% of incoming solar radiation and absorbs the rest, snow-covered sea ice reflects as much as 90% of incoming radiation. This value decreases to 40%–70% during the melt season, due to melt ponds on the ice surface (see Figure 2.4; Perovich et al., 1998; Perovich et al., 2007). Climate warming decreases the amount of snow and ice cover on Earth, reducing the Earth's albedo (reflectivity). Darker land and water surfaces exposed by melting snow and ice absorb more incoming solar radiation, adding more heat to the climate system and amplifying the initial warming, in turn causing further melting of snow and ice. Increased absorption of solar energy over the ocean is particularly important, as this additional heat must be dissipated in the autumn before ice can form again, thereby delaying the date of freeze-up. This positive climate feedback is particularly important in the Northern Hemisphere, where declines in Arctic Ocean sea ice and snow cover have been strong (see Chapter 5, Sections 5.2 and 5.3). In combination with other feedbacks involving the ocean, atmosphere, and clouds, the snow/ice albedo feedback explains why temperatures across the Arctic have warmed at approximately twice the rate of the rest of planet (Overland et al., 2017; Pithan and Mauritsen, 2014; Serreze and Barry, 2011).

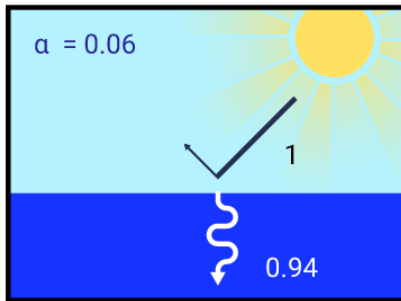
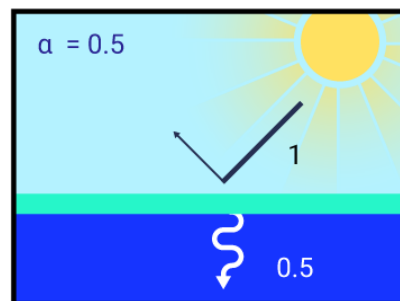
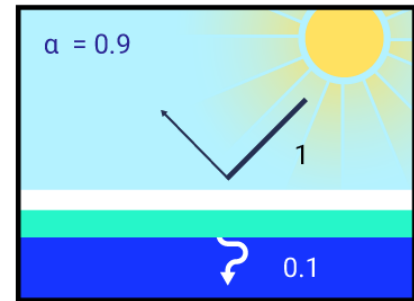
I. Open ocean**II. Bare ice****III. Ice with snow**

Figure 2.4: Snow and ice change Earth's albedo

Figure caption: Albedo is a unitless quantity that indicates how well a surface reflects solar energy. Albedo (α) ranges from 0 to 1, with 0 representing a black surface that absorbs 100% of energy and 1 representing a white surface that reflects 100% of energy. The presence of ice, and to a greater extent snow-covered ice, on dark surfaces (such as the ocean) increase albedo.

FIGURE SOURCE: NATIONAL SNOW AND ICE DATA CENTER. THERMODYNAMICS: ALBEDO; IN ALL ABOUT SEA ICE; NATIONAL SNOW AND ICE DATA CENTER. [HTTPS://NSIDC.ORG/CRYOSPHERE/SEAICE/PROCESSES/ALBEDO.HTML](https://nsidc.org/cryosphere/seaice/processes/albedo.html) [10 JULY 2018]

Section summary

In summary, the fundamental drivers of Earth's climate are therefore well known, as are the radiative properties and heat-trapping effect of GHGs in Earth's atmosphere. The very first scientific assessment by the IPCC's Working Group I (IPCC, 1990) began with the statement that "we are certain there is a natural greenhouse effect, which already keeps the Earth warmer than it would otherwise be" and "we are certain that emissions resulting from human activities are substantially increasing the atmospheric concentrations of GHGs and these increases will enhance the greenhouse effect, resulting on average in an additional warming of the Earth's surface." The body of scientific knowledge has grown enormously in the years since that assessment, as scientists continue to deepen their understanding of the myriad of processes within components of the climate system, and interactions among these components, that affect the climate system's response to changes in climate drivers. However, the fundamental relationship between increases in GHGs and climate warming is well established.

2.3.2: Changes in greenhouse gases and radiative forcing over the Industrial Era

The Industrial Era refers to the period in history, beginning around the mid-18th century and continuing today, marked by a rapid increase in industrial activity powered by the combustion of fossil fuels. Burning these carbon-based fuels releases CO₂, as well as other gases and pollutants, to the atmosphere. The Industrial Era is recognized as the period when human activity has substantially affected the chemical composition of the atmosphere by increasing the concentration of trace gases, including GHGs (Steffen et al., 2007).

2.3.2.1: Changes in greenhouse gas concentrations over the Industrial Era

GHGs are emitted to the atmosphere from both natural and human sources (see Box 2.2) and are also removed from the atmosphere, primarily through natural processes referred to as natural “sinks.” Atmospheric concentrations of GHGs increase when the rate of emission to the atmosphere exceeds the rate of removal. Even a small annual imbalance, in which emissions exceed removals, can lead to a large build-up of the gas in the atmosphere over time (in the same way that a small annual deficit in a financial budget can lead to a large accumulation of debt over time). Sinks and imbalances differ for different GHGs. CH₄ is removed from the atmosphere primarily through photochemical reactions that destroy it chemically. These reactions remove almost as much CH₄ each year as is emitted from both natural and human sources, leaving a small annual excess of emissions (Ciais et al., 2013; Saunio et al., 2016). In contrast, only about half of the CO₂ emitted from human activities each year is removed from the atmosphere through land sinks (mainly uptake by plants during photosynthesis) and ocean sinks (mainly through CO₂ dissolving into the ocean) (Ciais et al., 2013; Le Quéré et al., 2016). The ongoing annual excess of human-emitted CO₂ is the cause of the observed rise in atmospheric CO₂ concentrations (see FAQ 2.1).

FAQ 2.1: Are humans responsible for the observed rise in atmospheric carbon dioxide?

Multiple independent lines of evidence show with *high confidence* that human activities are responsible for the observed rise in atmospheric carbon dioxide (CO₂) since 1750, and that this rise is inconsistent with natural sources.

The carbon cycle involves the movement of carbon between different reservoirs on Earth – the atmosphere, oceans, terrestrial biosphere, and the solid Earth, including fossil-fuel reserves. While carbon naturally moves among these reservoirs, the total amount of carbon on Earth remains essentially constant. Over the 10,000 years preceding the Industrial Era, this natural carbon cycle was roughly balanced, with atmospheric CO₂

concentrations remaining nearly stable. Since the start of the Industrial Era, CO₂ in the atmosphere has rapidly increased. Over 1750–2011, the atmospheric increase was 240 Pg⁹ (90% uncertainty range from 230 to 250 Pg) of carbon (C), as shown by air samples from ice cores and by direct measurements of atmospheric CO₂ concentrations since 1958. How do we know that this measured increase was due to human activities rather than to changes in the natural carbon cycle?

From our records, we know that humans emitted 375 Pg C (90% uncertainty range from 345 to 405 Pg C) into the atmosphere from burning fossil fuels and manufacturing cement, and we can estimate that human-induced land use change (including deforestation and reforestation) contributed a further 180 Pg C (90% uncertainty range from 100 to 260 Pg C) to the atmosphere over the period 1750–2011. Together, these human emissions totalled 555 Pg C (90% uncertainty range from 470 to 640 Pg C). Since we know that the increase in atmospheric CO₂ (240 Pg C) was less than that amount, it follows directly that the natural system must have been a net sink of carbon over this period. This is known as the “bookkeeping method,” and it is a strong piece of evidence that human emissions, rather than natural sources, are responsible for the observed increase in atmospheric CO₂. There is also direct evidence that individual natural reservoirs have acted as sinks for atmospheric carbon. For example, the measured carbon in the oceans is estimated to have increased by 155 Pg C (90% uncertainty range from 125 to 185 Pg C), leading to ocean acidification (see Chapter 7, Section 7.6.1).

Independent geochemical evidence confirms that the increase in atmospheric CO₂ was primarily driven by fossil-fuel consumption and did not arise from natural sources (see Figure 2.5). Direct measurements starting in the 1990s show a small decrease in atmospheric oxygen (O₂) concentrations, consistent with fossil-fuel burning (as O₂ is consumed during combustion), but inconsistent with a non-oxidative natural source of CO₂, such as the oceans or volcanoes. Second, plants and fossil fuels (derived from ancient plants) have lower 13C/12C stable isotope ratios than the atmosphere, meaning these sources are relatively depleted in the isotope 13C. Burning fossil fuels and plants emits carbon (primarily as CO₂) to the atmosphere with depleted levels of 13C. This reduces the 13C/12C ratio of atmospheric CO₂. Measurements confirm that this is what is occurring. The observed atmospheric CO₂ increase, O₂ decline, and 13C/12C decrease are larger in the Northern Hemisphere, consistent with the major emissions source of fossil fuels. Together, these lines of evidence produce *high confidence* that observed atmospheric CO₂ increases are due to human activity (Ciais et al., 2013).

⁹ 1 petagram (Pg) = 10¹⁵ grams. 1 petagram is equivalent to 1 billion metric tonnes (1 gigatonne). In the atmosphere, the mass of carbon is directly related to the abundance of CO₂ per unit volume, measured in parts per million (ppm).

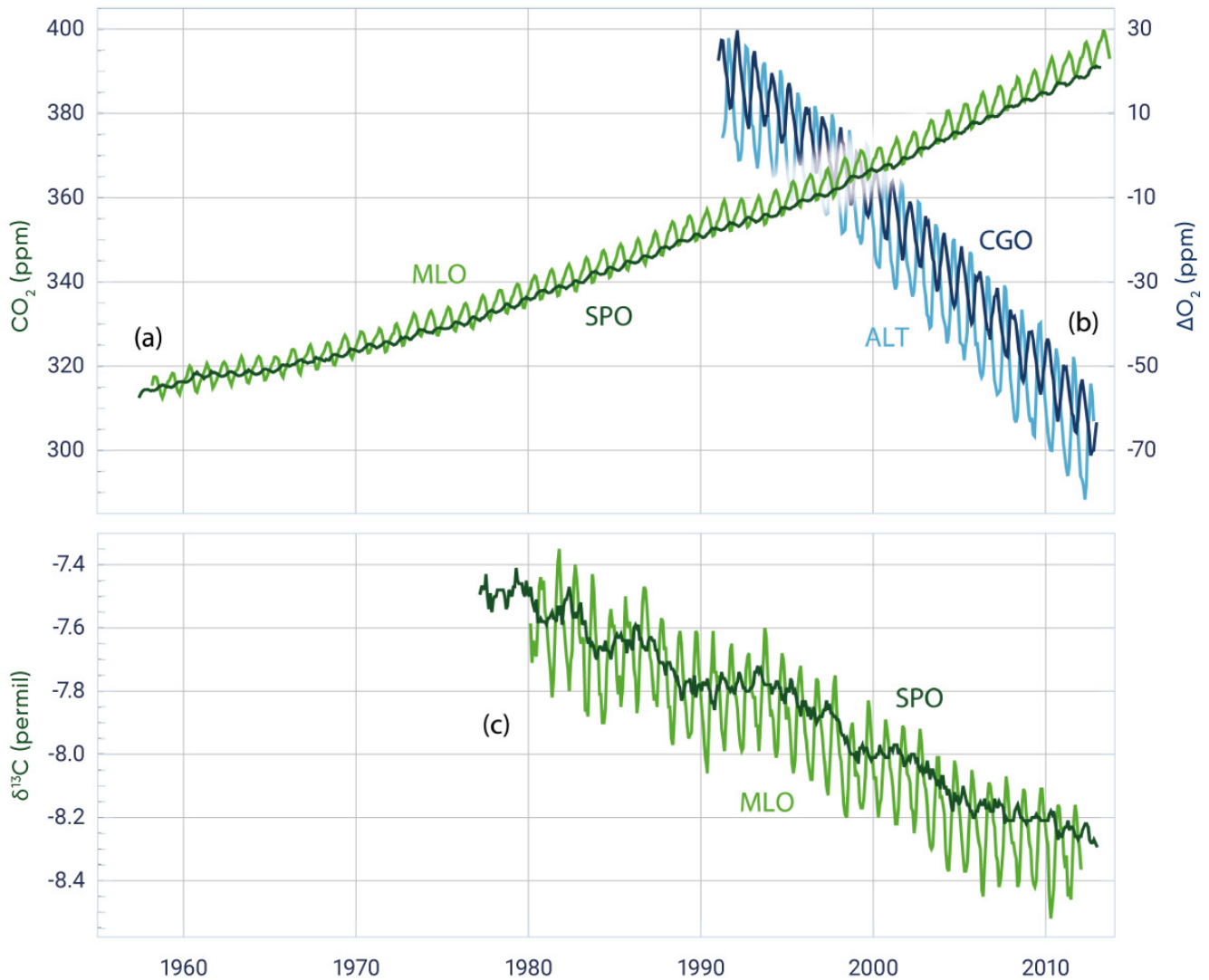


Figure 2.5: Changes in atmospheric composition indicating a human origin for the rise in carbon dioxide

Figure caption: Atmospheric concentration of carbon dioxide (CO₂), oxygen (O₂), and 13C/12C stable isotope ratio in CO₂ recorded over the last decades at representative stations. Top panel: CO₂ (green line) from Mauna Loa Northern Hemisphere (MLO) and South Pole Southern Hemisphere (SPO) atmospheric stations, and O₂ (blue line) from Alert Northern Hemisphere (ALT) and Cape Grim Southern Hemisphere (CGO). Lower panel: δ¹³C in CO₂ from MLO and SPO. The ratio of the 13C to 12C isotopes, relative to a standard, is measured by δ¹³C (delta C 13), which is defined as $\delta^{13}\text{C} = \left[\frac{(13\text{C}/12\text{C})_{\text{sample}}}{(13\text{C}/12\text{C})_{\text{standard}}} - 1 \right] \times 1000$ and has units of permil. Samples with a larger value of δ¹³C are said to be enriched, while samples with a lower δ¹³C are said to be depleted.

FIGURE SOURCE: CIAIS ET AL., 2013. FIG. 6-3 MODIFIED TO INCLUDE ONLY THE TOP TWO PANELS.

Well-mixed GHGs are those that persist in the atmosphere for a sufficiently long time for concentrations to become relatively uniform throughout the atmosphere. For such substances, emissions anywhere affect atmospheric concentrations everywhere. Global average concentrations of well-mixed GHGs can be determined from measurements taken at only a few monitoring locations around the globe. Canada monitors GHG concentrations at a number of locations, and these data are used, along with those from other monitoring stations, to determine global average GHG concentrations (see Box 2.4).

Box 2.4: Canadian atmospheric greenhouse gas monitoring

The Canadian Greenhouse Gas Measurement Program operates stations that precisely monitor atmospheric levels of greenhouse gases (GHGs) carbon dioxide (CO_2), methane (CH_4), and nitrous oxide (N_2O) in all regions of the country. The most remote site, at Alert, Nunavut, contributes measurements to the Global Atmosphere Watch Programme of the World Meteorological Organization, which tracks changes in global GHG concentrations. Northern Hemisphere GHG concentrations, such as those observed at Canadian sites, are slightly higher than the global average because of larger sources of emissions in the Northern Hemisphere. The long-term trends from all Canadian sites closely track the increasing global CO_2 concentration trend, while also showing clear seasonal cycles of CO_2 concentration due to photosynthesis (plants remove CO_2 from the atmosphere) and biogenic respiration (plants and animals breathe out CO_2) (see Figure 2.6).

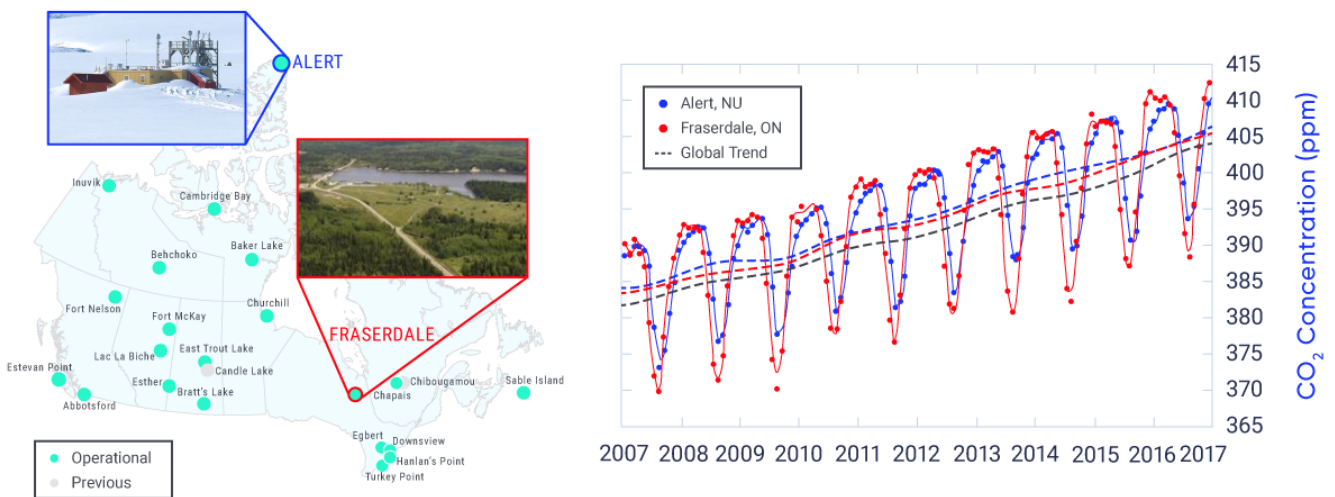


Figure 2.6: Canada's greenhouse gas monitoring network

Figure caption: Canada's greenhouse gas (GHG) monitoring network (map) and example observations for carbon dioxide (plot) from Alert, Nunavut (upper photo) and Fraserdale, Ontario (lower photo).



Canadian monitoring sites are also used to track changes in regional GHG emissions and removals due to the impact of the changing climate on vulnerable ecosystems, such as the tundra and boreal forest. The vast Canadian boreal forest (2.7 million km²) typically takes up a net 28 megatonnes of carbon from the atmosphere per year (Kurz et al., 2013). Fraserdale, situated close to the boreal forest, is influenced quite strongly by forest processes that affect atmospheric CO₂ levels. Lower concentrations of CO₂ are evident in summer (dominated by photosynthesis) and higher concentrations are evident in winter (dominated by respiration) compared with the more distant site at Alert that is not surrounded by significant vegetation. Research has found that the net amount of carbon taken up in the Canadian boreal forest has increased in warmer years (Chen et al., 2006). In contrast, studies in Scandinavian boreal forests have found that the net uptake of carbon has decreased in recent years (i.e., 1999–2013) (Hadden and Grelle, 2016). This highlights the value of performing specific atmospheric observations in the Canadian boreal forest. Furthermore, atmospheric observations of CH₄ in the Arctic could detect any rapid changes in emissions due to thawing of permafrost.

In summary, atmospheric observations play a key role in tracking global trends in GHG concentrations, in monitoring changes resulting from global GHG mitigation efforts, and in understanding the climate feedback of Canadian ecosystems.

Long-term records of changes in atmospheric concentrations of the three main well-mixed GHGs – CO₂, CH₄, and N₂O – are compiled from direct atmospheric measurements (beginning in the late 1950s for CO₂ and in the late 1970s for CH₄ and N₂O) and from ice-core measurements, which extend the time period of analysis back hundreds of thousands of years. The evidence clearly shows that the concentrations of these GHGs have increased substantially over the Industrial Era, by 40% for CO₂, 150% for CH₄, and 20% for N₂O (Hartman et al., 2013) (see Figure 2.7). Global concentrations of the main GHGs in 2015 were about 400 parts per million for CO₂, 1845 parts per billion for CH₄, and 328 parts per billion for N₂O (WMO, 2016). These concentrations exceed the highest concentrations during the past 800,000 years recorded in ice cores (Masson-Delmotte et al., 2013).

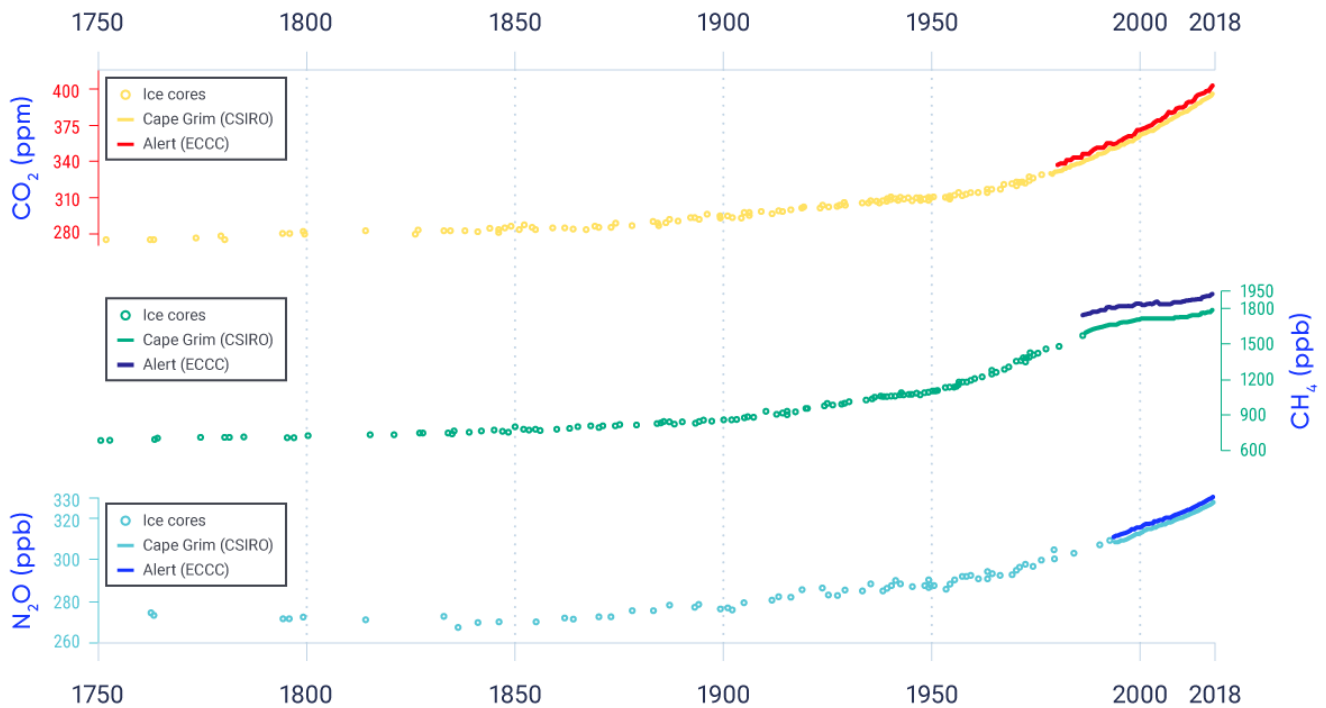


Figure 2.7: Increases in global greenhouse gas concentrations during the Industrial Era

Figure caption: Global mean atmospheric concentrations of carbon dioxide (CO₂) (magenta and red), methane (CH₄) (light and dark green), and nitrous oxide (N₂O) (light and dark blue), based on data from ice cores (dots) and direct atmospheric measurements from the Cape Grim Observatory, Australia (light lines) and from the Canadian greenhouse gas monitoring site at Alert, Nunavut (dark lines).

FIGURE SOURCE: CLIMATE RESEARCH DIVISION, ENVIRONMENT AND CLIMATE CHANGE CANADA.

2.3.2.2: Changes in radiative forcing over the Industrial Era

As discussed in Section 2.3, changes in atmospheric concentrations of GHGs produce a radiative forcing. The current understanding of the radiative forcing effects of all important climate forcing agents over the

Industrial Era is synthesized in Figure 2.8.¹⁰ The following discussion highlights major features of Figure 2.8, beginning with those agents causing warming effects, followed by those agents causing cooling effects, and concluding with a summary about the net forcing effects from human activity.

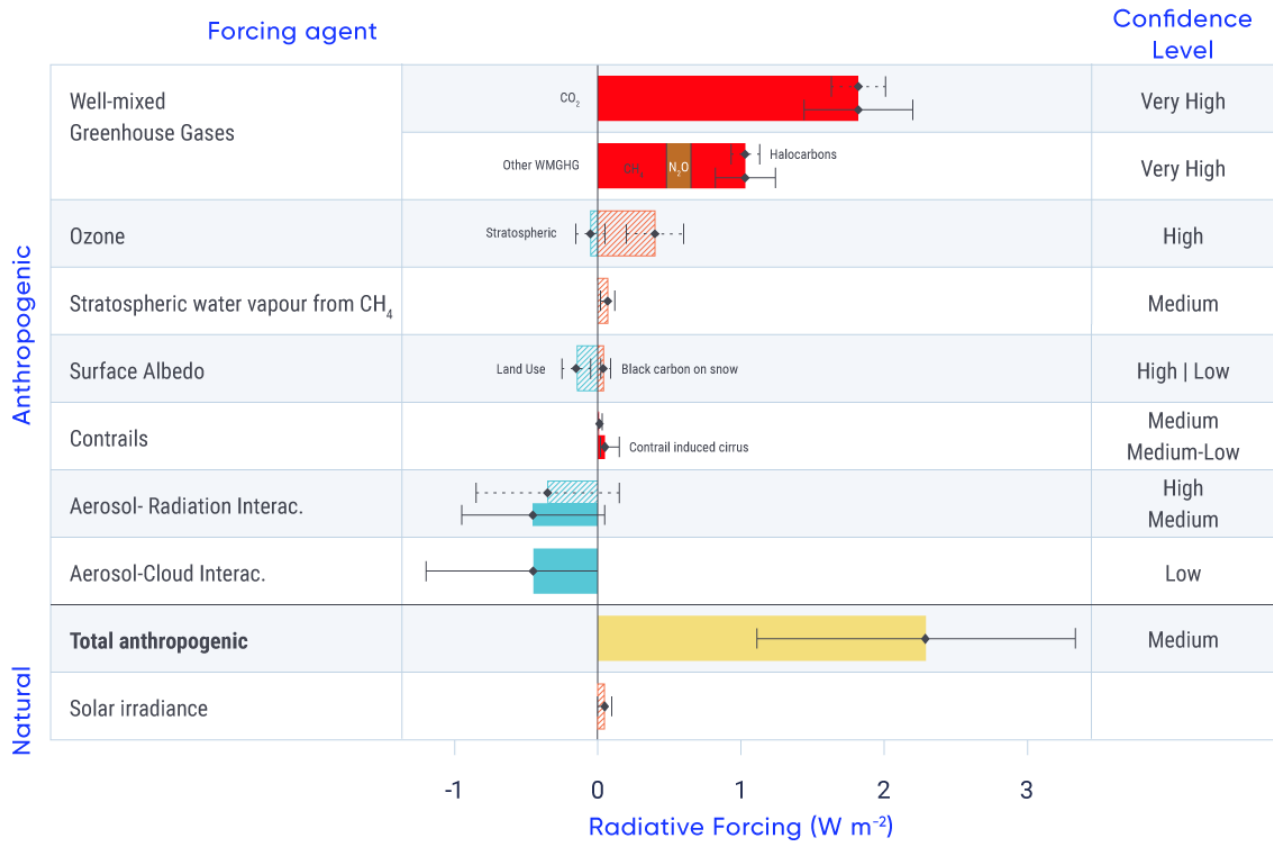


Figure 2.8: Natural and anthropogenic forcing of climate, 1750–2011

Figure caption: Radiative forcing (RF; the net change in the energy balance of the Earth system due to an external perturbation), based on changes in concentrations of forcing agents, between 1750 and 2011 (Myhre et al., 2013), in units of watts per square metre (W/m²). Hatched bars are radiative forcing (RF), and solid bars are effective radiative forcing (ERF), the RF once rapid adjustments in atmospheric temperatures, water vapour, and clouds to the initial perturbation are accounted for. Uncertainties (5%–95% uncertainty range) are given for ERF (solid horizontal lines [whiskers]) and for RF (dotted whiskers). The total anthropogenic forcing is the sum of the anthropogenic forcing contributions. See description in Section 2.2.

FIGURE SOURCE : BASED ON MYHRE ET AL., 2013, FIGURE 8.15; AND IPCC, 2013A, FIGURE TS.6.

10 The term “effective radiative forcing” was introduced in the IPCC Fifth Assessment Report to better quantify the impact of forcing agents by accounting for rapid adjustments in the climate system to an initial radiative forcing (Myhre et al., 2013). For well-mixed GHGs, radiative forcing (RF) and effective radiative forcing (ERF) values are similar, whereas for aerosols from human activity, these values are significantly different, and ERF is considered the better indicator. In this section, we use the term RF, but these terms are differentiated in Figure 2.8, on which the text is based.

The main warming agents, as indicated by bars extending to the right in Figure 2.8, are CO₂, CH₄, N₂O, and tropospheric ozone, with a few other gases contributing small warming effects globally. These other gases include halocarbons – synthetic industrial chemicals composed of carbon and a halogen, such as chlorofluorocarbons. Together, GHGs have been by far the dominant positive forcing agents over the Industrial Era. CO₂ alone accounts for two-thirds of the forcing (1.82 W/m² [90% uncertainty range from 1.63 W/m² to 2.01 W/m²]) from all well-mixed GHGs (2.83 W/m² [90% uncertainty range from 2.54 W/m² to 3.12 W/m²]). Increases in CH₄ concentrations have been the second largest contributor to positive forcing (0.48 W/m² [90% uncertainty range from 0.43 W/m² to 0.53 W/m²]). There is **very high confidence** in these values, because the radiative properties of well-mixed GHGs are well known and because historical concentrations of well-mixed GHGs are also well known from ice cores and direct measurements.

Ozone is not directly emitted but is formed in the lower atmosphere (troposphere) as a result of both natural processes and emissions of air pollutant gases, including CH₄. The warming effect of increases in tropospheric ozone is sizeable and known with **high confidence**. Ozone also forms naturally in the upper atmosphere (stratosphere) as a result of chemical reactions involving ultraviolet radiation and oxygen molecules. Stratospheric ozone levels have decreased as a result of human emissions of ozone-depleting substances such as refrigerants. The resulting cooling effect has slightly offset the warming effect of increases in tropospheric ozone (Myhre et al., 2013).

Cooling effects (as indicated by bars to the left in Figure 2.8) have been driven by human emissions that have increased the levels of aerosols in the atmosphere and by human changes to the land surface that have increased Earth's surface albedo. Aerosol forcing is divided into two components: direct effects, mainly from absorbing or scattering incoming solar radiation, and indirect effects from aerosol interactions with clouds. Most aerosols (e.g., sulphate and nitrate aerosols) predominantly scatter (reflect) radiation. In contrast, black carbon, an aerosol that is emitted as a result of the incomplete combustion of carbon-based fuels, absorbs radiation. Black carbon is a strong warming agent, although calculating the net effect of black carbon emission sources needs to consider the warming and cooling effects of the other aerosols and gases emitted with it during combustion (Bond et al., 2013; see Chapter 3, Box 3.3). The direct effect of aerosols is therefore composed of a negative forcing (cooling) from most aerosols and a positive forcing (warming) from black carbon, for a net negative forcing of 0.45 W/m² (90% uncertainty range from a negative forcing of 0.95 W/m² to a positive forcing of 0.05 W/m²)¹¹ (**medium confidence**). The total aerosol effect in the atmosphere, including aerosol–cloud interactions, is a strongly negative forcing, estimated with **medium confidence** to be 0.9 W/m² (90% uncertainty range from 1.9 W/m² to 0.1 W/m²). Although there continue to be large uncertainties associated with the magnitude of aerosol forcing, overall there is **high confidence** that the cooling effect of aerosol forcing has offset a substantial portion of the warming effect of GHG forcing.

There is also **high confidence** that human-caused land use changes (such as deforestation and conversion of other natural landscapes to managed lands) have had a cooling effect by increasing Earth's albedo, with a negative forcing of 0.15 W/m² (90% uncertainty range from 0.25 W/m² to 0.05 W/m²). However, this has been partially offset by decreases in Earth's albedo due to black carbon being deposited on snow and ice, darkening the surface and thereby increasing the absorption of solar radiation. Black carbon deposition on snow is

11 This value is the effective radiative forcing (ERF) from direct effects of aerosols, accounting for rapid adjustments of the climate system (see Figure 2.8).

estimated to have exerted a small warming effect of 0.04 W/m^2 (90% uncertainty range from 0.02 W/m^2 to 0.09 W/m^2) (*low confidence*) (Myhre et al., 2013).

The best estimate of total radiative forcing due to human activities is a warming effect of 2.3 W/m^2 (90% uncertainty range from 1.1 W/m^2 to 3.3 W/m^2) over the Industrial Era, composed of a strong positive forcing component from changes in atmospheric concentrations of GHGs, which is partially offset by a negative forcing (cooling effect) from aerosols and land use change. Forcing by CO_2 is the single largest contributor to human-caused forcing during the Industrial Era.

This total forcing from human activities can be compared with natural forcing from changes in volcanic eruptions and solar irradiance. During the Industrial Era, irregular volcanic eruptions have had brief cooling effects on global climate. The episodic nature of volcanic eruptions makes a comparison with other forcing agents difficult on a century timescale. Volcanic forcing is, however, well understood to be negative (climate-cooling effect) with the strongest forcing occurring over a limited period of about two years following eruptions (Myhre et al., 2013; see Section 2.3.3). Changes in total solar irradiance over the Industrial Era have caused a small positive forcing of 0.05 W/m^2 (90% uncertainty range from 0.00 to 0.10 W/m^2) (*medium confidence*). Consequently, there is *very high confidence* that, over the Industrial Era, natural forcing accounts for only a small fraction of forcing changes, amounting to less than 10% of the effects of human-caused forcing.

Section summary

In summary, as concluded by the IPCC (IPCC, 2013b), total radiative forcing is positive and has led to an uptake of energy by the climate system. The largest contribution to total radiative forcing is caused by the increase in the atmospheric concentration of CO_2 since the beginning of the Industrial Era. This factor is the dominant driver of global warming and climate change over this period. Natural forcing from solar irradiance changes and volcanic aerosols made only a small contribution throughout the last century, except for brief periods following volcanic eruptions.

2.3.3: Natural climate variability

Even when a strong anthropogenic forcing drives climate change (see Section 2.3.2), signals of climate change may be difficult to detect against a backdrop of a climate system that is naturally chaotic – “noisy”. This chaotic behaviour is due to internal climate variability and natural external forcings, which can be large over short periods (for example, forcing by volcanic eruptions). Internal climate variability, such as El Niño–Southern Oscillation (ENSO) (see Box 2.5), is variability that arises within the climate system, independent of variations in external forcing.

Box 2.5: Modes of climate variability

“Modes of climate variability” are distinct and robust features of variability in the climate system with identifiable characteristics, affecting particular regions over certain time periods. Generally, these features alternate or “oscillate” between one set of patterns and an alternate set. A familiar example is the El Niño–Southern Oscillation (ENSO), but there are other modes of variability also discussed in this report.

El Niño–Southern Oscillation and Indian Ocean Dipole

ENSO is a quasi-periodic variation in sea surface temperature and other related variables, such as surface pressure and surface wind, lasting about three to five years and situated mainly over the tropical eastern Pacific Ocean. ENSO affects much of the tropics and subtropics, but also influences the mid-latitudes of both hemispheres, including Canada. The warm phase of ENSO is known as El Niño (warm waters in the tropical eastern Pacific Ocean) and the cool phase as La Niña (cool waters in the tropical eastern Pacific Ocean). The warm phase tends to be associated with warmer winter air temperatures and drier conditions over much of Canada. The opposite is true during La Niña. Related to ENSO is the Indian Ocean Dipole (IOD), a variation in sea surface temperature centred in the Indian Ocean, with a typical timescale of about two years.

Pacific Decadal Oscillation and Interdecadal Pacific Oscillation

The Pacific Decadal Oscillation (PDO) is a recurring pattern of sea surface temperature variability centred over the northern mid-latitude Pacific Ocean. The PDO has varied irregularly, with a characteristic timescale ranging from as short as a few years to as long as several decades. As with ENSO, the warm (positive) phase of the PDO tends to be associated with warmer winter air temperatures over much of Canada (Shabbar and Yu, 2012). At times over the past century, this mode of variability has exerted a strong influence on continental surface air temperature and precipitation, from California to Alaska. The Interdecadal Pacific Oscillation (IPO) is related to the PDO, but with a much wider geographic range of influence (Salinger et al., 2001).

Arctic Oscillation and North Atlantic Oscillation

The Arctic Oscillation (AO), sometimes referred to as the Northern Annular Mode, is the dominant pattern of variability of sea level pressure and atmospheric pressure north of about 20° north latitude. If the pressures are high over the Arctic, they are low over the mid-latitudes, and vice versa. The AO varies over time, with no particular periodicity. The positive phase of the AO tends to be associated in winter with warmer air temperatures over western Canada, and colder temperatures in the north and east. The North Atlantic Oscillation (NAO) is related to the AO but is centred over the North Atlantic Ocean rather than the whole of the Northern Hemisphere. The NAO has a strong influence on the strength and direction of westerly winds and the location of the storm track over the North Atlantic Ocean. The positive phase of the NAO is also associated with warm winter temperatures over much of western Canada, and cold winter temperatures over eastern Canada.

Atlantic Multi-decadal Oscillation

The Atlantic Multi-decadal Oscillation (AMO) is a recurring pattern of sea surface temperature of the North Atlantic Ocean (north of the equator and south of about 80° north latitude), with a characteristic timescale of 60 to 80 years. The AMO has been known to influence hurricane activity, as well as rainfall patterns and intensity, across the North Atlantic Ocean.

Global mean surface temperature (GMST), as calculated by a linear trend, has increased significantly since the 1880s, especially since the 1950s (see Section 2.2.1). However, the changes in GMST have been far from uniform, with substantial variability among years, decades, and periods spanning several decades. These short-term fluctuations are superimposed on an underlying externally forced trend (see Figure 2.9) (Morice et al., 2012; Karl et al., 2015; Hansen et al., 2010).

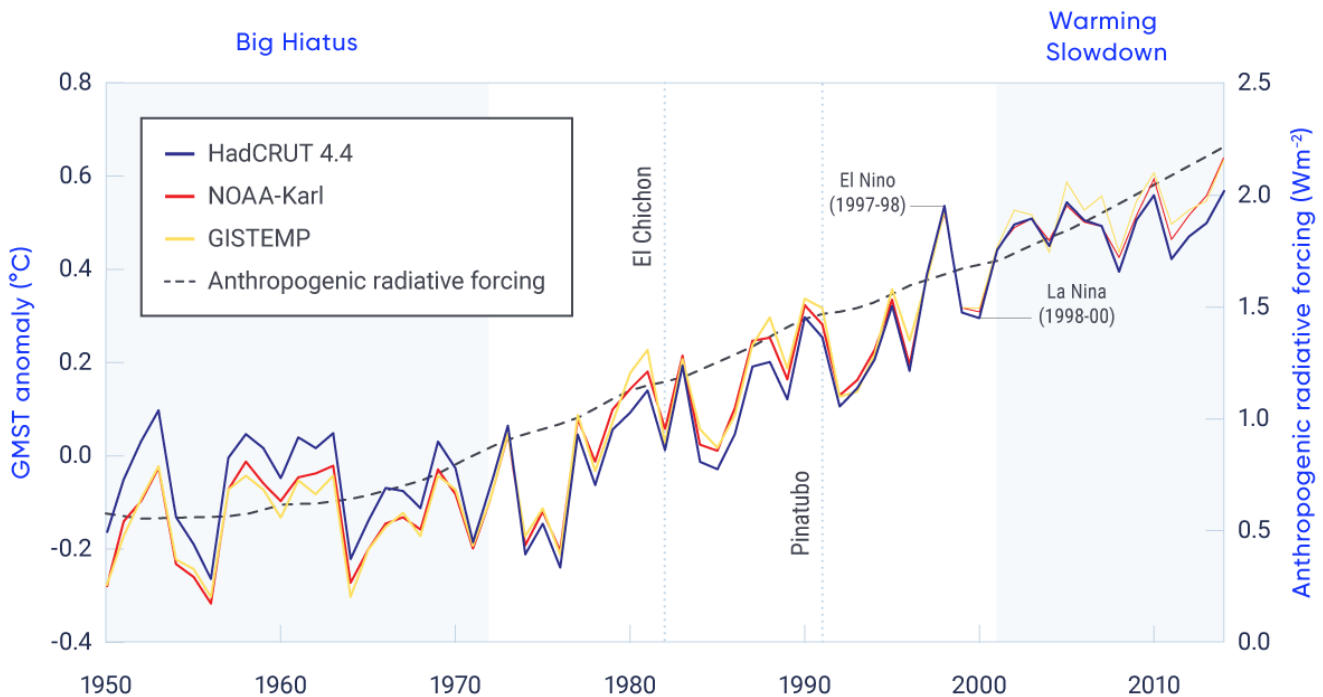


Figure 2.9: Annual global mean surface temperature and anthropogenic radiative forcing

Figure caption: Differences in annual global mean surface temperature (relative to 1961–1990) from three datasets. Radiative forcing due to human activities is shown by the black dashed line.

FIGURE SOURCE: ADAPTED FROM FYFE ET AL., 2016.

To analyze the causes of the short-term fluctuations in GMST, we first need to be confident that the observed variability is real and not an artifact, an error introduced by the way the data were collected or analyzed. Long-term GMST time series have been produced by a small number of scientific teams using data collected from around the world. Values are reported as an anomaly: a departure from the average over a reference period (1961–1990 for Figure 2.9). Differences among the estimates are due mainly to differing choices made in processing the underlying raw observations. For example, one estimate (HadCRUT4.4) is an average for only those grid cells where observations exist, whereas the other estimates (NOAA-Karl and GISTEMP) use infilling; if observations are missing for certain locations, they are estimated based on values for neighbouring locations. These estimates of GMST, and others, are routinely updated as errors are identified and adjusted (see Box 4.1). Correcting and updating long-term datasets with new observations as these become available is imperative for tracking global change from year-to-year, decade-to-decade, and century-to-century.

Some of the ups and downs over time shown in Figure 2.9 are associated with the ENSO, the fairly periodic internal variation in sea surface temperatures over the tropical eastern Pacific Ocean, affecting much of the tropics, subtropics, and some areas outside the tropics, including Canada (Box 2.6). The warming phase is known as El Niño and the cooling phase as La Niña. ENSO events can be powerful enough to be recorded as significant signals in GMST. The 1997/1998 El Niño was regarded as one of the most powerful El Niño events in recorded history, resulting in widespread droughts, flooding, and other natural disasters across the globe (Trenberth, 2002). It terminated abruptly in mid-1998 and was followed by a moderate-to-strong La Niña, which lasted until the end of 2000 (Shabbar and Yu, 2009).

Some other ups and downs shown in Figure 2.9 are associated with natural external forcing agents, such as large volcanic eruptions. The 1991 eruption of Mount Pinatubo, in the Philippines, was the second largest terrestrial eruption of the 20th century. It ejected a massive amount of particulate matter into the stratosphere and produced a global layer of sulphuric acid haze. GMST dropped significantly in 1991–1993 (McCormick et al., 1995). Similarly, the 1982 eruption of El Chichón, the largest volcanic eruption in modern Mexican history, ejected a large amount of sulphate aerosols into the stratosphere (Robock and Matson, 1983). The cooling impact of the El Chichón eruption on GMST from 1982 to 1984 was partly offset by global warming associated with a very strong El Niño event during this time (Robock, 2013).

Naturally occurring variations in GMST, whether internally generated or externally forced, should be viewed in the context of global mean radiative forcing caused by human activities (Fyfe et al., 2016). The combined radiative forcing from human activities has increased over time (see Figure 2.9) (Meinshausen et al., 2011). The periods in Figure 2.9 labelled “big hiatus” and “warming slowdown” correspond to times when the dominant mode of internal decadal variability in the Pacific – the Interdecadal Pacific Oscillation (IPO) – was in its negative (cold) phase. In addition, during the “big hiatus” period, radiative forcing increased relatively slowly, owing to cooling contributions from increasing tropospheric aerosols, as well as stratospheric aerosols from the Mount Agung eruption in 1963 (e.g., Fyfe et al. 2016). In the intervening period, the IPO was in its positive (warm) phase. A given phase, warm or cold, of the IPO typically lasts from 20 to 30 years, much longer than the timescale associated with ENSO. Recent computer models (Meehl et al., 2013; Kosaka and Xie, 2013; England et al., 2014) and studies based on observations (Steinman et al., 2015; Dai et al., 2015) indicate that the IPO plays an important role in changes in GMST over time.

Finally, the “warming slowdown” — a slowdown in the rate of increase of GMST observed over the early 2000s — has been much debated (Karl et al., 2015; Lewandowsky et al., 2015; Rajaratnam et al., 2015). Observations indicate that the rate of global mean surface warming from 2001 to 2015 was significantly less than the rate over the previous 30 years (Fyfe et al., 2016). It is now understood that both internal variability and external forcing contributed to the warming slowdown (Flato et al., 2013; Fyfe et al., 2016; Santer et al., 2017). The contribution from external forcing has been ascribed to: 1) a succession of moderate volcanic eruptions in the early 21st-century (Solomon et al., 2011; Vernier, 2011; Fyfe et al., 2013; Santer et al., 2014; Ridley et al., 2014; Santer et al., 2015); 2) a long and anomalously low solar minimum during the last solar cycle (Kopp and Lean, 2011; Schmidt et al., 2014); 3) increased atmospheric burdens of sulphate aerosols from human activity (Smith et al., 2016); and 4) a decrease in stratospheric water vapour (Solomon et al., 2010). In the last several years, GMST has warmed substantially (e.g., Hu and Fedorov, 2017), with an exceptionally strong ENSO in 2015/2016, suggesting that the warming slowdown is now over.

Section summary

In summary, multiple independent time series of historical GMST, model simulations of historical variability and change, projections of future change, and physical understanding of natural climate variability together indicate that, on decadal timescales, the rates of warming can differ, and periods of reduced or enhanced warming are expected. The IPCC AR5 concluded that both internal variability and external forcing contributed to the warming slowdown, and subsequent research confirms this conclusion and provides improved understanding of the contributions of various factors.

2.3.4: Detection and attribution of observed changes

Establishing the causes of observed changes in climate involves both “detection” and “attribution.” Specifically, “detection” means demonstrating that an observed change is inconsistent with internal climate variability; in effect, this is a task of detecting a signal from the “noise” of background climate variability. “Attribution” means identifying the causes of an observed change in terms of different forcings (Bindoff et al., 2013). The IPCC AR5 included a chapter (Bindoff et al., 2013) assessing the evidence for attributing global and regional changes in a range of variables to GHG increases and other forcings. Understanding the causes of climate change on the global scale is important for understanding the causes of regional climate change discussed in Chapters 4 to 7 of this report. In this subsection, we summarize relevant findings from the IPCC AR5 assessment and more recent findings on global-scale attribution. The relatively new science of attribution of individual events, as opposed to longer-term changes, is discussed in Chapter 4, Section 4.4.

Detection and attribution studies compare observed climate changes with simulations from different types of climate-model experiments: 1) simulations of the response to external forcings of interest; and 2) simulations

with no variations in external forcing that show the effect of internal climate variability. Confidence in such analyses is increased by using simulations from multiple climate models developed in centres around the world, and by validating simulated internal variability by comparison with observations. If an observed change is inconsistent with simulated internal variability alone, then a response to external forcing is detected. If the observed change is consistent with model simulations including a particular forcing, such as GHGs, and inconsistent with simulations omitting it, then the observed change is attributed, in part, to that forcing. Since more than one forcing drives trends in climate, an observed change is generally not wholly attributable to variations in one forcing. The sections below summarize attribution of observed changes in each component of the climate system.

Atmosphere and surface

The IPCC AR5 assessed contributions of greenhouse gases, other anthropogenic forcings (mainly aerosols), and natural forcings to the observed trend in GMST that increased approximately 0.6°C from 1951 to 2010, based on several studies that had assessed these trends quantitatively using detection and attribution methods. The trend attributable to combined forcings from human activities (mainly changes in GHGs and aerosols) is *likely* between 0.6°C and 0.8°C (see Figure 2.10) and *extremely likely* more than half of the observed increase (Bindoff et al., 2013). Note that, as expected, IPCC AR5 assigned a lower likelihood level to the narrower confidence interval (0.6°C to 0.8°C) and a higher likelihood level to the broader one (greater than half the observed warming). However, when the GMST response to forcings is separated into contributions from GHG forcing and aerosol forcing, uncertainties are larger due to several factors: large uncertainties in aerosol forcing, differences in the simulated responses to these forcings among models, and difficulties in separating the response to GHG increases from the response to aerosol changes. Nonetheless, more than half of the observed increase in GMST was *very likely* due to the observed human-caused increase in GHG concentrations. The combined effect of aerosols from volcanic eruptions and variations in solar irradiance made only a small contribution to observed trends over this period (statistically, the contribution was not significantly different from zero). Similarly, internal variability made only a small contribution to trends over this period. Warming was also observed over the first half of the 20th century, and this warming was *very unlikely* to have been due to internal variability alone, but it remains difficult to quantify the contributions of internal variability, anthropogenic forcing, and natural forcing to this warming (Bindoff et al., 2013).

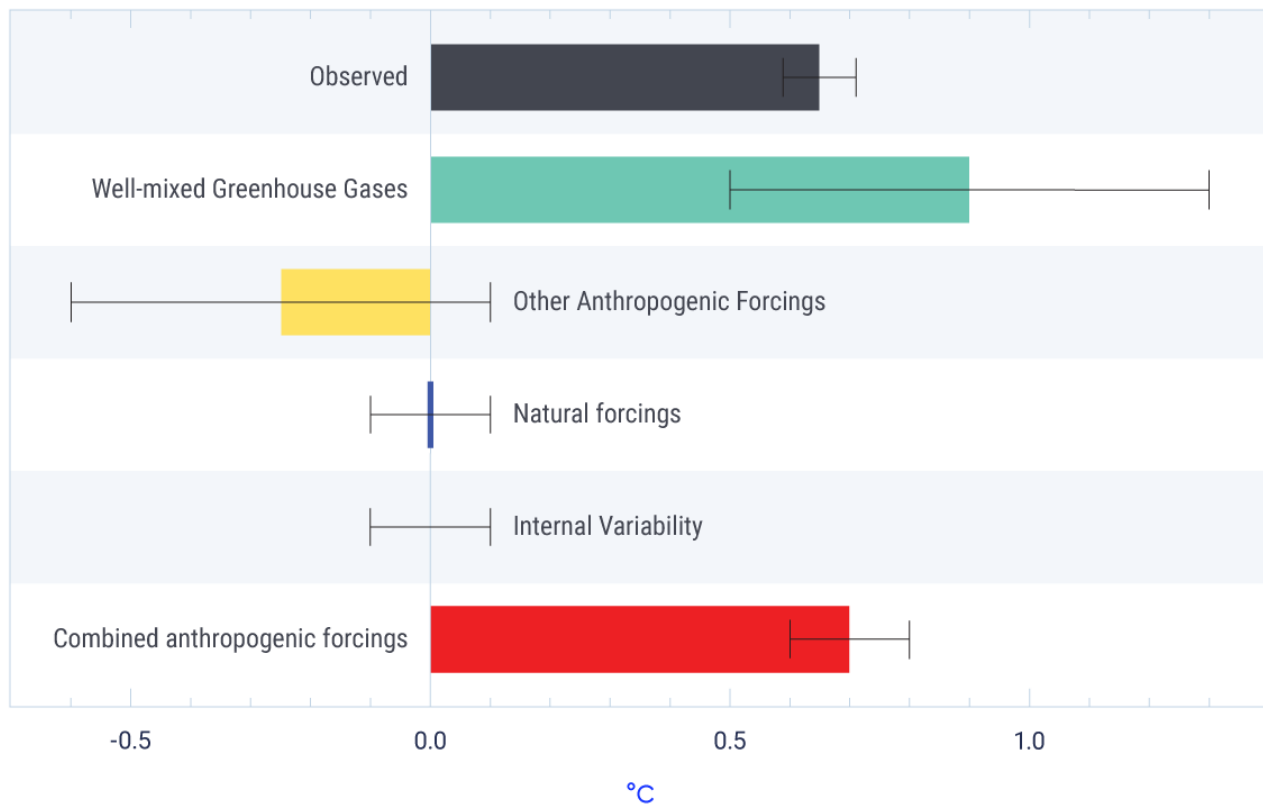


Figure 2.10: Forcings to which global mean warming has been attributed, 1951–2010

Figure caption: IPCC AR5 assessed *likely* ranges (horizontal lines [whiskers]) and their mid-points (bars) for forcings to which global mean warming over the 1951–2010 period can be attributed: well-mixed greenhouse gases, other anthropogenic forcings (dominated by aerosols), combined anthropogenic forcings, natural forcings, and internal variability. The black bar shows the observed temperature trend (HadCRUT4 dataset) and the associated 5% to 95% uncertainty range (whiskers). Bars to the left of 0.0°C indicate an attributable cooling; bars to the right indicate an attributable warming.

FIGURE SOURCE: BINDOFF ET AL., 2013, FIGURE 10.5.

Since the publication of the IPCC AR5, studies have shed further light on aspects of detection and attribution. For example, the influence of observational uncertainty on estimates of the GMST trend attributable to GHGs was found to be small relative to other sources of uncertainty (Jones and Kennedy, 2017). Another study found that considerable differences remain among models in the simulated response to forcings from human activity, particularly to non-GHG forcing (Jones et al., 2016). However, the conclusions of these studies remain consistent with the IPCC AR5 (Bindoff et al., 2013). Even when using a novel approach to detection and attribution (Ribes et al., 2017), the assessed range for the contribution to observed warming trends from human activities remains consistent with the range in the IPCC AR5 (Bindoff et al., 2013).

The IPCC AR5 also assessed that it was *likely* that forcings from human activity have contributed to warming of the lower atmosphere (troposphere) since 1961 (Bindoff et al., 2013). Recent research continues to sup-

port this assessment. A new study found that apparent differences between the rate of warming of the lower atmosphere in climate models and in satellite observations since 1979 are smaller than previously reported (Santer et al., 2017).

There is *medium confidence* that human activities have contributed to observed increases in atmospheric specific humidity and to global-scale changes in precipitation over land since 1950, including increases in the Northern Hemisphere at mid- to high latitudes (Bindoff et al., 2013). Large uncertainties in observations and models, and large internal variability in precipitation, precluded greater confidence. Research since the IPCC AR5 (e.g., Hegerl et al., 2015; Polson et al., 2016) has examined sources of uncertainty in more detail, but the overall conclusions remain consistent with those of IPCC AR5 (Bindoff et al., 2013).

Ocean

Several aspects of observed global-scale change in the oceans have been attributed to human activity. In particular, it is *very likely* that human-caused forcing made a substantial contribution to upper ocean warming since 1970 and to a rise in global mean sea level since the 1970s (Bindoff et al., 2013). It is *very likely* that human-caused increases in CO₂ have driven acidification of ocean surface waters, through uptake of CO₂ from the atmosphere, decreasing pH by 0.0014 to 0.0024 per year (see Chapter 7, Section 7.6.1). Recent research continues to support the attribution of ocean warming and sea level rise to human influence (e.g., Slangen et al., 2014; Weller et al., 2016), with new estimates of the heat content of the upper ocean showing a larger warming trend than that assessed in the IPCC AR5 (Durack et al., 2014).

Cryosphere

It is *very likely* that human-caused forcings have contributed to Arctic sea ice loss since 1979 (Bindoff et al., 2013). This conclusion was based on model simulations, which were able to reproduce the observed decline only when including human-caused forcings. There is *low confidence* in the understanding of an observed increase in the extent of Antarctic sea ice. However, since that assessment was made in 2013, Antarctic sea ice extent has decreased, with September 2017 sea ice extent being the second lowest on record (NOAA, 2017). It is *likely* that human-caused forcing contributed to the observed surface melting of the Greenland Ice Sheet since 1993 and to the observed retreat of glaciers since the 1960s, but there is *low confidence* in attribution of the causes of mass loss from the Antarctic Ice Sheet. There was *likely* a contribution of human activity to observed reductions in Northern Hemisphere snow cover since 1970 (Bindoff et al., 2013). New research strengthens the evidence for attribution of the decrease in Arctic sea ice extent (e.g., Kirchmeier-Young et al., 2017), and Northern Hemisphere snow cover (e.g., Najafi et al., 2016) to human influence.

Extremes

On the global scale, it is *very likely* that human-caused forcing has contributed to observed changes in the frequency of daily temperature extremes since 1950, including increases in hot extremes and decreases in cold extremes (Bindoff et al., 2013). For regions with sufficient observations, there is *medium confidence* that human-caused forcing has contributed to increased intensity of heavy precipitation events since 1950. New



research further strengthens the evidence for attribution of changes in temperature and precipitation extremes to human influence (Zhang et al., 2013; Kim et al., 2016; Fischer and Knutti, 2015; Christidis and Stott, 2016).

Section summary

In summary, the IPCC AR5 assessment (Bindoff et al., 2013) that it is *extremely likely* that human activities are the main cause of the observed warming since the mid-20th century was supported by robust evidence from multiple studies, and has been further supported by additional studies since 2013. Evidence for detectable human influence on other climate variables in the atmosphere, ocean, and cryosphere was very strong at the time of the publication of the IPCC AR5 (Bindoff et al., 2013), and evidence has continued to accumulate since then.

References

Arrhenius, S. (1896): On the influence of carbonic acid in the air on the temperature upon the temperature of the ground; *The London, Edinburgh and Dublin Philosophical Magazine and Journal of Science*, v. 4, p. 237–276.

Bindoff, N.L., Stott, P.A., AchutaRao, K.M., Allen, M.R., Gillett, N., Gutzler, D., Hansingo, K., Hegerl, G., Hu, Y., Jain, S., Mokhov, I.I., Overland, J., Perlwitz, J., Sebbari, R. and Zhang, X. (2013): Detection and Attribution of Climate Change: from Global to Regional; in *Climate Change 2013: The Physical Science Basis (Contribution of Working Group I to the Fifth Assessment Report of the Intergovernmental Panel on Climate Change)*, (ed.) T.F. Stocker, D. Qin, G.-K. Plattner, M. Tignor, S.K. Allen, J. Boschung, A. Nauels, Y. Xia, V. Bex and P.M. Midgley; Cambridge University Press, Cambridge, United Kingdom and New York, NY, USA, pp. 867–952. doi:10.1017/CBO9781107415324.022

Blunden, J. and Arndt, D.S. (ed.) (2016): *State of the Climate in 2015*; *Bulletin of the American Meteorological Society*, v. 97, p. S1–S275. doi:10.1175/2016BAMSStateoftheClimate.1

Blunden, J. and Arndt, D.S. (ed.) (2017): *State of the Climate in 2016*; *Bulletin of the American Meteorological Society*, v. 98, p. Si–S277. doi:10.1175/2017BAMSStateoftheClimate.1

Bond, T.C., Doherty, S.J., Fahey, D.W., Forster, P.M., Bernsten, T., DeAngelo, B.J., Flanner, M.G., Ghan, S., Kärcher, B., Koch, D., Kinne, S., Kondo, Y., Quinn, P.K., Sarofim, M. C., Schultz, M.G., Schulz, M., Venkataraman, C., Zhang, H., Zhang, S., Bellouin, N., Guttikunda, S.K., Hopke, P.K., Jacobson, M.Z., Kaiser, J.W., Klimont, Z., Lohmann, U., Schwarz, J.P., Shindell, D., Storelvmo, T., Warren, S.G. and Zender, C.S. (2013): Bounding the role of black carbon in the climate system: A scientific assessment; *Journal of Geophysical Research: Atmosphere*, v. 118, p. 5380–5552. doi:10.1002/jgrd.50171

Boucher, O., Randall, D., Artaxo, P., Bretherton, C., Feingold, G., Forster, P., Kerminen, V.-M., Kondo, Y., Liao, H., Lohmann, U., Rasch, P., Satheesh, S.K., Sherwood, S., Stevens, B. and Zhang, X.Y. (2013): Clouds and Aerosols; in *Climate Change 2013: The Physical Science Basis (Contribution of Working Group I to the Fifth Assessment Report of the Intergovernmental Panel on Climate Change)*, (ed.) T.F. Stocker, D. Qin, G.-K. Plattner, M. Tignor, S.K. Allen, J. Boschung, A. Nauels, Y. Xia, V. Bex and P.M. Midgley; Cambridge University Press, Cambridge, United Kingdom and New York, NY, USA, p. 571–658. doi:10.1017/CBO9781107415324.016

Chen, J.M., Chen, B., Higuchi, K., Liu, J. Chan, D., Worthy, D., Tans, P. and Black, A. (2006): Boreal ecosystems sequestered more carbon in warmer years; *Geophysical Research Letters*, v. 33. doi:10.1029/2006GL025919

Christidis, N. and Stott, P. (2016): Attribution analyses of temperature extremes using a set of 16 indices; *Weather and Climate Extremes*, v. 14, p. 24–35. doi:10.1016/j.wace.2016.10.003

Ciais, P., Sabine, C., Bala, G., Bopp, L., Brovkin, V., Canadell, J., Chhabra, A., DeFries, R., Galloway, J., Heimann, M., Jones, C., Le Quéré, C., Myneni, R.B., Piao, S. and Thornton, P. (2013): Carbon and Other Biogeochemical



Cycles; in *Climate Change 2013: The Physical Science Basis* (Contribution of Working Group I to the Fifth Assessment Report of the Intergovernmental Panel on Climate Change), (ed.) T.F. Stocker, D. Qin, G.-K. Plattner, M. Tignor, S.K. Allen, J. Boschung, A. Nauels, Y. Xia, V. Bex and P.M. Midgley; Cambridge University Press, Cambridge, United Kingdom and New York, NY, USA, p. 465–570. doi:10.1017/CBO9781107415324.015

Cubasch, U., Wuebbles, D., Chen, D., Facchini, M.C., Frame, D., Mahowald, N. and Winther, J.-G. (2013): Introduction; in *Climate Change 2013: The Physical Science Basis* (Contribution of Working Group I to the Fifth Assessment Report of the Intergovernmental Panel on Climate Change), (ed.) T.F. Stocker, D. Qin, G.-K. Plattner, M. Tignor, S.K. Allen, J. Boschung, A. Nauels, Y. Xia, V. Bex and P.M. Midgley; Cambridge University Press, Cambridge, United Kingdom and New York, NY, USA, p. 119–158. doi:10.1017/CBO9781107415324.007

Dai, A., Fyfe, J.C., Xie, S.-P. and Dai, X. (2015): Decadal modulation of global surface temperature by internal climate variability; *Nature Climate Change*, v. 5, p. 555–559.

Durack, P.J., Gleckler, P.J., Landerer, F.W. and Taylor, K.E. (2014): Quantifying underestimates of long-term upper-ocean warming; *Nature Climate Change*, v. 4, p. 999–1005.

England, M.H., McGregor, S., Spence, P., Meehl, G.A., Timmermann, A., Cai, W., Sen Gupta, A., McPhaden, M.J., Purich, A. and Santoso, A. (2014): Recent intensification of wind-driven circulation in the Pacific and the ongoing warming hiatus; *Nature Climate Change*, v. 4, p. 222–227.

Fahey, D.W., Doherty, S.J., Hibbard, K.A., Romanou, A. and Taylor, P.C. (2017): Physical drivers of climate change; in *Climate Science Special Report: Fourth National Climate Assessment, Volume 1*, (ed.) D.J. Wuebbles, D.W. Fahey, K.A. Hibbard, D.J. Dokken, B.C. Stewart, T.K. Maycock; U.S. Global Change Research Program, Washington, DC, USA, p. 73–113. doi:10.7930/J0513WC

Fischer, E.M. and Knutti, R. (2015): Anthropogenic contribution to global occurrence of heavy-precipitation and high-temperature extremes; *Nature Climate Change*, v. 5, p. 560–564.

Flato, G., Marotzke, J., Abiodun, B., Braconnot, P., Chou, S.C., Collins, W., Cox, P., Driouech, F., Emori, S., Eyring, V., Forest, C., Gleckler, P., Guilyardi, E., Jakob, C., Kattsov, V., Reason, C. and Rummukainen, M. (2013): Evaluation of Climate Models; in *Climate Change 2013: The Physical Science Basis* (Contribution of Working Group I to the Fifth Assessment Report of the Intergovernmental Panel on Climate Change), (ed.) T.F. Stocker, D. Qin, G.-K. Plattner, M. Tignor, S.K. Allen, J. Boschung, A. Nauels, Y. Xia, V. Bex and P.M. Midgley; Cambridge University Press, Cambridge, United Kingdom and New York, NY, USA, p. 741–866.

Fourier, J.-B. J. (1827): Mémoires sur les températures du globe terrestre et des espace planétaires [On the temperatures of the terrestrial sphere and interplanetary space] (trans. 2004); R.T. Pierrehumbert, <<https://geosci.uchicago.edu/~rtp1/papers/Fourier1827Trans.pdf>> [February 2018].

Fyfe, J.C., Meehl, G.A., England, M.H., Mann, M.E., Santer, B.D., Flato, G.M., Hawkins, E., Gillett, N.P., Xie, S.-P., Kosaka, Y. and Swart, N.C. (2016): Making sense of the early-2000s global warming slowdown; *Nature Climate Change*, v. 6, p. 224–228.



Fyfe, J.C., von Salzen, K., Cole, J.N.S., Gillett, N.P. and Vernier, J-P. (2013): Surface response to stratospheric aerosol changes in a coupled atmosphere–ocean model; *Geophysical Research Letters*, v. 40, p. 584–588.

Hadden, D. and Grelle, D. (2016): Changing temperature response of respiration turns boreal forest from carbon sink into carbon source; *Agricultural and Forest Meteorology*, v. 223, p. 30–38.

Hansen, J., Ruedy, R., Sato, M. and Lo, K. (2010): Global surface temperature change; *Review of Geophysics*, v. 48. doi:10.1029/2010RG000345

Hartmann, D.L., Klein Tank, A.M.G., Rusticucci, M., Alexander, L.V., Brönnimann, S., Charabi, Y., Dentener, F.J., Dlugokencky, E.J., Easterling, D.R., Kaplan, A., Soden, B.J., Thorne, P.W., Wild, M. and Zhai, P.M. (2013): Observations: Atmosphere and Surface; in *Climate Change 2013: The Physical Science Basis (Contribution of Working Group I to the Fifth Assessment Report of the Intergovernmental Panel on Climate Change)*, (ed.) T.F. Stocker, D. Qin, G.-K. Plattner, M. Tignor, S.K. Allen, J. Boschung, A. Nauels, Y. Xia, V. Bex and P.M. Midgley; Cambridge University Press, Cambridge, United Kingdom and New York, NY, USA, p. 159–254. doi:10.1017/CBO9781107415324.008

Hawkins, E., Ortega, P., Suckling, E., Schurer, A., Hergel, G., Jones, P., Joshi, M., Osborn, T.J., Masson-Delmotte, V., Mignot, J., Thorne, P. and Van Oldenborgh, G.J. (2017): Estimating changes in global temperature since the pre-industrial period; *Bulletin of the American Meteorological Society*, v. 98, p. 1841–1856. doi:10.1175/BAMS-D-16-0007.1

Hegerl, G.C., Black, E., Allan, R.P., Ingram, W.J., Polson, D., Trenberth, K.E., Chadwick, R.S., Arkin, P.A., Sarojini, B.B., Becker, A., Dai, A., Durack, P.J., Easterling, D., Fowler, H.J., Kendon, E.J., Huffman, G.J., Liu, C., Marsh, R., New, M., Osborn, T.J., Skliris, N., Stott, P.A., Vidale, P., Wijffels, S.E., Wilcox, L.J., Willett, K.M., and Zhang, X. (2015): Challenges in quantifying changes in the global water cycle; *Bulletin of the American Meteorological Society*, v. 96, p. 1097–1115.

Hu, A. and Fedorov, A.V. (2017): The extreme El Niño of 2015–2016 and the end of global warming hiatus; *Geophysical Research Letters*, v. 44, p. 3816–3824.

IPCC [Intergovernmental Panel on Climate Change] (1990): *Climate Change: The IPCC Scientific Assessment (1990) (Report prepared for Intergovernmental Panel on Climate Change by Working Group I)*, (ed.) J.T. Houghton, G.J. Jenkins and J.J. Ephraums; Cambridge University Press, Cambridge, United Kingdom, New York, NY, USA and Melbourne, Australia, 410 p.

IPCC [Intergovernmental Panel on Climate Change] (1996): *Climate Change 1995: The Science of Climate Change (Contribution of Working Group I to the Second Assessment Report of the Intergovernmental Panel on Climate Change)*, (ed.) J.T. Houghton, L.G. Meira Filho, B.A. Callander, N. Harris, A. Kattenberg, and K. Maskell; Cambridge University Press, Cambridge, United Kingdom and New York, NY, USA.

IPCC [Intergovernmental Panel on Climate Change] (2001): *Climate Change 2001: The Scientific Basis (Contribution of Working Group I to the Third Assessment Report of the Intergovernmental Panel on Climate Change)*, (ed.) J.T. Houghton, Y. Ding, D.J. Griggs, M. Noguer, P.J. van der Linden, X. Dai, K. Maskell and C.A. Johnson; Cambridge University Press, Cambridge, United Kingdom and New York, NY, USA, 881 p.



IPCC [Intergovernmental Panel on Climate Change] (2007): Climate Change 2007: The Physical Science Basis (Contribution of Working Group I to the Fourth Assessment Report of the Intergovernmental Panel on Climate Change), (ed.) S. Solomon, D. Qin, M. Manning, Z. Chen, M. Marquis, K.B. Averyt, M. Tignor and H.L. Miller; Cambridge University Press, Cambridge, United Kingdom and New York, NY, USA, 996 p.

IPCC [Intergovernmental Panel on Climate Change] (2012): Managing the Risks of Extreme Events and Disasters to Advance Climate Change Adaptation (A Special Report of Working Groups I and II of the Intergovernmental Panel on Climate Change), (ed.) C.B. Field, V. Barros, T.F. Stocker, D. Qin, D.J. Dokken, K.L. Ebi, M.D. Mastrandrea, K.J. Mach, G.-K. Plattner, S.K. Allen, M. Tignor, and P.M. Midgley; Cambridge University Press, Cambridge, United Kingdom, 582 p.

IPCC [Intergovernmental Panel on Climate Change] (2013a): Climate Change 2013: The Physical Science Basis (Contribution of Working Group I to the Fifth Assessment Report of the Intergovernmental Panel on Climate Change), (ed.) T.F. Stocker, D. Qin, G.-K. Plattner, M. Tignor, S.K. Allen, J. Boschung, A. Nauels, Y. Xia, V. Bex and P.M. Midgley; Cambridge University Press, Cambridge, United Kingdom and New York, NY, USA, 1535 p. doi:10.1017/CBO9781107415324

IPCC [Intergovernmental Panel on Climate Change] (2013b): Summary for Policymakers; in Climate Change 2013: The Physical Science Basis (Contribution of Working Group I to the Fifth Assessment Report of the Intergovernmental Panel on Climate Change), (ed.) T.F. Stocker, D. Qin, G.-K. Plattner, M. Tignor, S.K. Allen, J. Boschung, A. Nauels, Y. Xia, V. Bex and P.M. Midgley; Cambridge University Press, Cambridge, United Kingdom and New York, NY, USA, p. 1–30. doi:10.1017/CBO9781107415324.004

IPCC [Intergovernmental Panel on Climate Change] (2013c): Annex III: Glossary, (ed.) Planton, S.; in Climate Change 2013: The Physical Science Basis (Contribution of Working Group I to the Fifth Assessment Report of the Intergovernmental Panel on Climate Change), (ed.) T.F. Stocker, D. Qin, G.-K. Plattner, M. Tignor, S.K. Allen, J. Boschung, A. Nauels, Y. Xia, V. Bex and P.M. Midgley; Cambridge University Press, Cambridge, United Kingdom and New York, NY, USA, p. 1–30. doi:10.1017/CBO9781107415324.004

Jansen, E., Overpeck, J., Briffa, K.R., Duplessy, J.-C., Joos, F., Masson-Delmotte, V., Olago, D., Otto-Bliesner, B., Peltier, W.R., Rahmstorf, S., Ramesh, R., Raynaud, D., Rind, D., Solomina, O., Villalba R. and Zhang, D. (2007): Palaeoclimate; in Climate Change 2007: The Physical Science Basis (Contribution of Working Group I to the Fourth Assessment Report of the Intergovernmental Panel on Climate Change), (ed.) S. Solomon, D. Qin, M. Manning, Z. Chen, M. Marquis, K.B. Averyt, M. Tignor and H.L. Miller; Cambridge University Press, Cambridge, United Kingdom and New York, NY, USA, 996 p.

Jones, G.S. and Kennedy, J.J. (2017): Sensitivity of attribution of anthropogenic near-surface warming to observational uncertainty; *Journal of Climate*, v. 30, p. 4677–4691.

Jones, G.S., Stott, P.A. and Mitchell, J.F. (2016): Uncertainties in the attribution of greenhouse gas warming and implications for climate prediction; *Journal of Geophysical Research: Atmospheres*, v. 121, p. 6969–6992.



Karl, T.R., Arguez, A., Huang, B., Lawrimore, J.H., McMahon, J.R., Menne, M.J., Peterson, T.C., Vose, R.S. and Zhang, H.-M. (2015): Possible artifacts of data biases in the recent global surface warming hiatus; *Science*, v. 348, p. 1469–1472.

Kim, Y.H., Min, S.K., Zhang, X., Zwiers, F., Alexander, L.V., Donat, M.G. and Tung, Y.S. (2016): Attribution of extreme temperature changes during 1951–2010; *Climate Dynamics*, v. 46, p. 1769–1782.

Kirchmeier-Young, M.C., Zwiers, F.W. and Gillett, N.P. (2017): Attribution of extreme events in Arctic Sea ice extent; *Journal of Climate*, v. 30, p. 553–571.

Kopp, G. and Lean, J.L. (2011): A new, lower value of total solar irradiance: evidence and climate significance; *Geophysical Research Letters*, v. 38.

Kosaka, Y. and Xie, S.-P. (2013): Recent global-warming hiatus tied to equatorial Pacific surface cooling; *Nature*, v. 501, p. 403–407.

Kurz, W.A., Shaw, C.H., Boisvenue, C., Stinson, G., Metsaranta, J., Leckie, D., Dyk, A., Smyth, C., Neilson, E.T. (2013): Carbon in Canada's boreal forest – a synthesis; *Environmental Reviews*, v. 21, p. 260–292.

Lacis, A., Schmidt, G., Rind, D. and Ruedy, R. (2010): Atmospheric CO₂: principal control knob governing Earth's temperature; *Science*, v. 330, p. 356–359.

Le Quéré, C.L., Andrew, R.M., Canadell, J.G., Sitch, S., Korsbakken, J.I., Peters, G.P., Manning, A.C., Boden, T.A., Tans, P.P., Houghton, R.A., Keeling, R.F., Alin, S., Andrews, O.D., Anthoni, P., Barbero, L., Bopp, L., Chevallier, F., Chini, L.P., Ciais, P., Currie, K., Delire, C., Doney, S.C., Friedlingstein, P., Gkritzalis, T., Harris, I., Hauck, J., Haverd, V., Hoppema, M., Klein Goldewijk, K., Jain, A.K., Kato, E., Körtzinger, A., Landschützer, P., Lefèvre, N., Lenton, A., Lienert, S., Lombardozi, D., Melton, J.R., Metzl, N., Millero, F., Monteiro, P.M.S., Munro, D.R., Nabel, J.E.M.S., Nakaoka, S.-I., O'Brien, K., Olsen, A., Omar, A.M., Ono, T., Pierrot, D., Poulter, B., Rödenbeck, B., Salisbury, J., Schuster, U., Schwinger, J., Séférian, R., Skjelvan, I., Stocker, B.D., Sutton, A.J., Takahashi, T., Tian, H., Tilbrook, B., van der Laan-Luijkx, I.T., van der Werf, G.R., Viovy, N., Walker, A.P., Wiltshire, A.J. and Zaehle, S. (2016): Global carbon budget 2016; *Earth System Science Data*, v. 8, p. 605–649.

Le Treut, H., Somerville, R., Cubasch, U., Ding, Y., Mauritzen, C., Mokssit, A., Peterson, T. and Prather, M. (2007): Historical Overview of Climate Change; in *Climate Change 2007: The Physical Science Basis (Contribution of Working Group I to the Fourth Assessment Report of the Intergovernmental Panel on Climate Change)*, (ed.) S. Solomon, D. Qin, M. Manning, Z. Chen, M. Marquis, K.B. Averyt, M. Tignor and H.L. Miller; Cambridge University Press, Cambridge, United Kingdom and New York, NY, USA, p. 93–127.

Lewandowsky, S., Risbey, J.S. and Oreskes, N. (2015): On the definition and identifiability of the alleged "hiatus" in global warming; *Scientific Reports*, v.5, article number: 16784. doi:10.1038/srep16784



Masson-Delmotte, V., Schulz, M., Abe-Ouchi, A., Beer, J., Ganopolski, A., González Rouco, J.F., Jansen, E., Lambeck, K., Luterbacher, J., Naish, T., Osborn, T., Otto-Bliesner, B., Quinn, T., Ramesh, R., Rojas, M., Shao, X. and Timmermann, A. (2013): Information from Paleoclimate Archives; in *Climate Change 2013: The Physical Science Basis (Contribution of Working Group I to the Fifth Assessment Report of the Intergovernmental Panel on Climate Change)*, (ed.) T.F. Stocker, D. Qin, G.-K. Plattner, M. Tignor, S.K. Allen, J. Boschung, A. Nauels, Y. Xia, V. Bex and P.M. Midgley; Cambridge University Press, Cambridge, United Kingdom and New York, NY, USA, p. 383–464. doi:10.1017/CBO9781107415324.013

McCormick, L.M.P. Thomason, W. and Trepte, C.R. (1995): Atmospheric effects of the Mt Pinatubo eruption; *Nature*, v. 373, p. 399–404.

Meehl, G.A., Hu, A., Arblaster, J.M., Fasullo, J. and Trenberth, K.E. (2013): Externally forced and internally generated decadal climate variability associated with the Interdecadal Pacific Oscillation; *Journal of Climate*, v. 26, p. 7298–7301, doi:10.1175/JCLI-D-12-00548.1.

Meinshausen, M., Smith, S.J., Calvin, K., Daniel, J.S., Kainuma, M.L.T., Lamarque, J-F., Matsumoto K., Montzka, S.A., Raper, S.C.B., Riahi, K., Thomson, A., Velders, G.J.M., van Vuuren, D.P.P. (2011): The RCP greenhouse gas concentrations and their extensions from 1765 to 2300; *Climatic Change*, v. 109, p. 213–241, doi:10.1007/s10584-011-0156-z.

Morice, C.P., Kennedy, J.J., Rayner, N.A. and Jones, P.D. (2012): Quantifying uncertainties in global and regional temperature change using an ensemble of observational estimates: The HadCRUT4 dataset; *Journal of Geophysical Research Atmospheres*, v. 117. doi:10.1029/2011JD017187

Myhre, G., Shindell, D., Bréon, F.-M., Collins, W., Fuglestedt, J., Huang, J., Koch, D., Lamarque, J.-F., Lee, D., Mendoza, D., Nakajima, T., Robock, A., Stephens, G., Takemura, T. and Zhang, H. (2013): Anthropogenic and Natural Radiative Forcing; in *Climate Change 2013: The Physical Science Basis (Contribution of Working Group I to the Fifth Assessment Report of the Intergovernmental Panel on Climate Change)*, (ed.) T.F. Stocker, D. Qin, G.-K. Plattner, M. Tignor, S.K. Allen, J. Boschung, A. Nauels, Y. Xia, V. Bex and P.M. Midgley; Cambridge University Press, Cambridge, United Kingdom and New York, NY, USA, p. 659–740. doi:10.1017/CBO9781107415324.018

Najafi, M.R., Zwiers, F.W. and Gillett, N.P. (2016): Attribution of the spring snow cover extent decline in the Northern Hemisphere, Eurasia and North America to anthropogenic influence; *Climatic Change*, v. 136, p. 571–586.

National Academy of Sciences and the Royal Society (2014): *Climate Change: Evidence and Causes*; Washington, DC, The National Academies Press. doi:10.17226/18730

NOAA [National Centers for Environmental Information] (2017): *State of the Climate: Global Snow and Ice for September 2017*; National Oceanic and Atmospheric Administration (NOAA), <<https://www.ncdc.noaa.gov/sotc/global-snow/201709>> [January 2018].

Overland, J., Walsh, J. and Kattsov, V. (2017). Trends and Feedbacks; in *Snow, Water, Ice and Permafrost in the Arctic (SWIPA)*; Arctic Monitoring and Assessment Programme (AMAP), Oslo, Norway, p. 9–24.



Perovich, D.K., Nghiem, S.V., Markus, T. and Schweiger, A. (2007): Seasonal evolution and interannual variability of the local solar energy absorbed by the Arctic sea ice-ocean system; *Journal of Geophysical Research*, v. 112.

Perovich, D.K., Roesler, C.S., and Pegau, W.S. (1998): Variability in Arctic sea ice optical properties; *Journal of Geophysical Research*, v. 103, p. 1193–1208.

Pithan, F. and Mauritsen, T. (2014): Arctic amplification dominated by temperature feedbacks in contemporary climate models; *Nature Geoscience*, v. 7, p. 181–184.

Polson, D., Hegerl, G.C. and Solomon, S. (2016): Precipitation sensitivity to warming estimated from long island records; *Environmental Research Letters*, v. 11.

Rajaratnam, B., Romano, J., Tsiang, M. and Diffenbaugh, N.S. (2015): Debunking the climate hiatus; *Climatic Change*, v. 133, p. 129–140.

Rhein, M., Rintoul, S.R., Aoki, S., Campos, E., Chambers, D., Feely, R.A., Gulev, S., Johnson, G.C., Josey, S.A., Kostianoy, A., Mauritzen, C., Roemmich, D., Talley, L.D. and Wang, F. (2013): Observations: Ocean; in *Climate Change 2013: The Physical Science Basis (Contribution of Working Group I to the Fifth Assessment Report of the Intergovernmental Panel on Climate Change)*, (ed.) T.F. Stocker, D. Qin, G.-K. Plattner, M. Tignor, S.K. Allen, J. Boschung, A. Nauels, Y. Xia, V. Bex and P.M. Midgley; Cambridge University Press, Cambridge, United Kingdom and New York, NY, USA, p. 255–316. doi:10.1017/CBO9781107415324.010

Ribes, A., Zwiers, F.W., Azais, J.M. and Naveau, P. (2017): A new statistical approach to climate change detection and attribution; *Climate Dynamics*, v. 48, p. 367–386.

Ridley, D.A., Solomon, S., Barnes, J. E., Burlakov, V.D., Deshler, T., Dolgii, S.I., Herber, A.B., Nagai, T., Neely III, R.R., Nevzorov, A.V., Ritter, C., Sakai, T., Santer, B.D., Sato, M., Schmidt, A., Uchino, O., Vernier, J.P. (2014): Total volcanic stratospheric aerosol optical depths and implications for global climate change; *Geophysical Research Letters*, v. 41, p. 7763–7769. doi:10.1002/2014GL061541.

Robock, A. (2013): Climate model simulations of the effects of the El Chichón eruption; *Geofísica Internacional*, v. 23, p. 403–414.

Robock, A. and Matson, M. (1983): Circumglobal transport of the El Chichón volcanic dust cloud; *Science*, v. 221, p. 195–197.

Salinger, M.J., Renwick, J.A. and Mullan, A.B. (2001): Interdecadal Pacific Oscillation and South Pacific Climate; *International Journal of Climatology*, v. 21, p. 1705–1721.

Santer, B.D., Fyfe, J.C., Pallotta, G., Flato, G.M., Meehl, G.A., England, M.H., Hawkins, E., Mann, M.E., Painter, J.F., Bonfils, C. and Cvijanovic, I. (2017): Causes of differences in model and satellite tropospheric warming rates; *Nature Geoscience*, v. 10, p. 478–485.

Santer, B.D., Solomon, S., Bonfils, C., Zelinka, M.D., Painter, J.F., Beltran, F., Fyfe, J.C., Johannesson, G., Mears, C., Ridley, D.A., Vernier, J.-P. and Wentz, F.J. (2014): Volcanic contribution to decadal changes in tropospheric temperature; *Nature Geoscience*, v. 7, p. 185–189.



Santer, B. D., Solomon, S., Bonfils, C., Zelinka, M.D., Painter, J.F., Beltran, F., Fyfe, J.C., Johannesson, G., Mears, C., Ridley, D.A., Vernier, J.-P., Wentz, F.J. (2015): Observed multivariable signals of late 20th and early 21st century volcanic activity; *Geophysical Research Letters*, v. 42, p. 500–509.

Saunio, M., Bousquet, P., Poulter, B., Peregon, A., Ciais, P., Canadell, J.G., Dlugokencky, E.J., Etiope, G., Bastviken, D., Houweling, S., Janssens-Maenhout, G., Tubiello, F.N., Castaldi, S., Jackson, R.B., Alexe, M., Arora, V.K., Beerling, D.J., Bergamaschi, P., Blake, D.R., Brailsford, G., Brovkin, V., Bruhwiler, L., Crevoisier, C., Crill, P., Covey, K., Curry, C., Frankenberg, C., Gedney, N., Höglund-Isaksson, L., Ishizawa, M., Ito, A., Joos, F., Kim, H.-S., Kleinen, T., Krummel, P., Lamarque, J.-F., Langenfelds, R., Locatelli, R., Machida, T., Maksyutov, S., McDonald, K.C., Marshall, J., Melton, J.R., Morino, I., Naik, V., O'Doherty, S., Parmentier, F.-J.W., Patra, P.K., Peng, C., Peng S., Peters, G.P., Pison, I., Prigent, C., Prinn, R., Ramonet, M., Riley, W.J., Saito, M., Santini, M., Schroeder, R., Simpson, I.J., Spahni, R., Steele, P., Takizawa, A., Thornton, B.F., Tian, H., Tohjima, Y., Viovy, N., Voulgarakis, A., van Weele, M., van der Werf, G.R., Weiss, R., Wiedinmyer, C., Wilton, D.J., Wiltshire, A., Worthy, D., Wunch, D., Xu, X., Yoshida, Y., Zhang, B., Zhang, Z. and Zhu, Q. (2016): The global methane budget 2000–2012; *Earth System Science Data*, v. 8, p. 697–751.

Schmidt, G.A., Shindell, D.T. and Tsigaridis, K. (2014): Reconciling warming trends; *Nature Geoscience*, v. 7, p. 1–3.

Serreze, M. and Barry, R.G. (2011): Processes and impacts of Arctic Amplification: A research synthesis; *Global Planetary Change*, v. 77, p. 85–96.

Shabbar, A. and Yu, B. (2009): The 1998–2000 La Niña in the context of historically strong La Niña events; *Journal of Geophysical Research: Atmospheres*, v. 114.

Shabbar, A., and Yu, B. (2012): Intraseasonal Canadian winter temperature responses to interannual and interdecadal Pacific SST modulations. *Atmosphere–Ocean*, v. 50, p. 109–121. doi:10.1080/07055900.2012.657154.

Slangen, A., Church, J.A., Zhang, X. and Monselesan, D. (2014): Detection and attribution of global mean thermosteric sea level change; *Geophysical Research Letters*, v. 41, p. 5951–5959.

Smith, D.M., Booth, B.B.B., Dunstone, N.J., Eade, R., Hermanson, L., Jones, G.S., Scaife, A.A., Sheen, K.L. and Thompson, V. (2016): Role of volcanic and anthropogenic aerosols in the recent global surface warming slowdown; *Nature Climate Change*, v. 6, p. 936–940.

Solomon, S., Daniel, J.S., Neely III, R.R., Vernier J.-P., Dutton, E.G., and Thomason, L.W. (2011): The persistently variable “background” stratospheric aerosol layer and global climate change; *Science*, v. 333, p. 866–870.

Solomon, S., Rosenlof, K.H., Portmann, R.W., Daniel, J.S., Davis, S.M., Sanford, T.J. and Plattner, G.-K. (2010): Contributions of stratospheric water vapor to decadal changes in the rate of global warming; *Science*, v. 327, p. 1219–1223.



Steffen, W., Crutzen, P.J. and McNeill, J.R. (2007): The Anthropocene: Are Humans Now Overwhelming the Great Forces of Nature?; *Ambio*, v. 36, p. 614–621.

Steinman, B.A., Mann, M.E. and Miller, S.K. (2015): Atlantic and Pacific multidecadal oscillations and Northern Hemisphere temperatures; *Science*, v. 347, p. 988–991.

Trenberth, K.E. (2002): Evolution of El Niño–Southern Oscillation and global atmospheric surface temperatures; *Journal of Geophysical Research*, v. 107.

Tyndall, J. (1859): On the transmission of heat of different qualities through gases of different kinds; *Proceedings of the Royal Institution*, v. 3, p. 155–158; cited in Hulme, M. (2009): On the origin of 'the greenhouse effect': John Tyndall's 1859 interrogation of nature; *Weather, Magazine of the Royal Meteorological Society*, v. 64, p. 121–123.

USGCRP [United States Global Change Research Program] (2017): Climate Science Special Report: Fourth National Climate Assessment, Volume I, (ed.) D.J. Wuebbles, D.W. Fahey, K.A. Hibbard, D.J. Dokken, B.C. Stewart, and T.K. Maycock; U.S. Global Change Research Program, Washington, DC, USA, 470 p. doi:10.7930/J0J964J6

Vaughan, D.G., Comiso, J.C., Allison, I., Carrasco, J., Kaser, G., Kwok, R., Mote, P., Murray, T., Paul, F., Ren, J., Rignot, E., Solomina, O., Steffen, K. and Zhang, T. (2013): Observations: Cryosphere; in *Climate Change 2013: The Physical Science Basis (Contribution of Working Group I to the Fifth Assessment Report of the Intergovernmental Panel on Climate Change)*, (ed.) T.F. Stocker, D. Qin, G.-K. Plattner, M. Tignor, S.K. Allen, J. Boschung, A. Nauels, Y. Xia, V. Bex and P.M. Midgley; Cambridge University Press, Cambridge, United Kingdom, and New York, NY, USA, p. 317–382. doi:10.1017/CBO9781107415324.012

Vernier, J.-P. (2011): Major influence of tropical volcanic eruptions on the stratospheric aerosol layer during the last decade; *Geophysical Research Letters*, v. 38.

Weller, E., Min, S.K., Palmer, M. D., Lee, D., Yim, B. Y. and Yeh, S.W. (2016): Multi-model attribution of upper-ocean temperature changes using an isothermal approach; *Scientific reports*, v. 6.

WMO [World Meteorological Organization] (2016): WMO Greenhouse Gas Bulletin: The State of Greenhouse Gases in the Atmosphere Based on Observations Through 2015; WMO, No. 12.

WMO [World Meteorological Organization] (2017): WMO Statement on the State of the Global Climate in 2016; WMO, No. 1189.

WMO [World Meteorological Organization] (2018): WMO Statement on the State of the Global Climate in 2017; WMO, No. 1212.

Zhang, X., Wan, H., Zwiers, F.W., Hegerl, G.C. and Min, S.K. (2013): Attributing intensification of precipitation extremes to human influence; *Geophysical Research Letters*, v. 40, p. 5252–5257.





CHAPTER 3

Modelling Future Climate Change

CANADA'S CHANGING CLIMATE REPORT



Government
of Canada

Gouvernement
du Canada

Canada



Authors

Greg Flato, Environment and Climate Change Canada

Nathan Gillett, Environment and Climate Change Canada

Vivek Arora, Environment and Climate Change Canada

Alex Cannon, Environment and Climate Change Canada

James Anstey, Environment and Climate Change Canada

Recommended citation: Flato, G., Gillett, N., Arora, V., Cannon, A. and Anstey, J. (2019): Modelling Future Climate Change; Chapter 3 in Canada's Changing Climate Report, (ed.) E. Bush and D.S. Lemmen; Government of Canada, Ottawa, Ontario, p. 74–111.



Chapter Table Of Contents

CHAPTER KEY MESSAGES

SUMMARY

3.1: Introduction

3.2: Future change and climate forcing

3.3: Modelling the response of the climate system to external forcing

3.3.1: Earth system models

FAQ 3.1: Why is Canada warming faster than the world as a whole?

Box 3.1: The Coupled Model Intercomparison Project

3.3.2: Sources of confidence and uncertainty

3.3.3: Global-scale climate projections

Box 3.2: Model projections and weighting

3.3.4: Compatible emissions

3.4: Cumulative carbon dioxide and global temperature change

3.4.1: The climate response to cumulative carbon dioxide emissions

3.4.2: Irreversibility of climate change

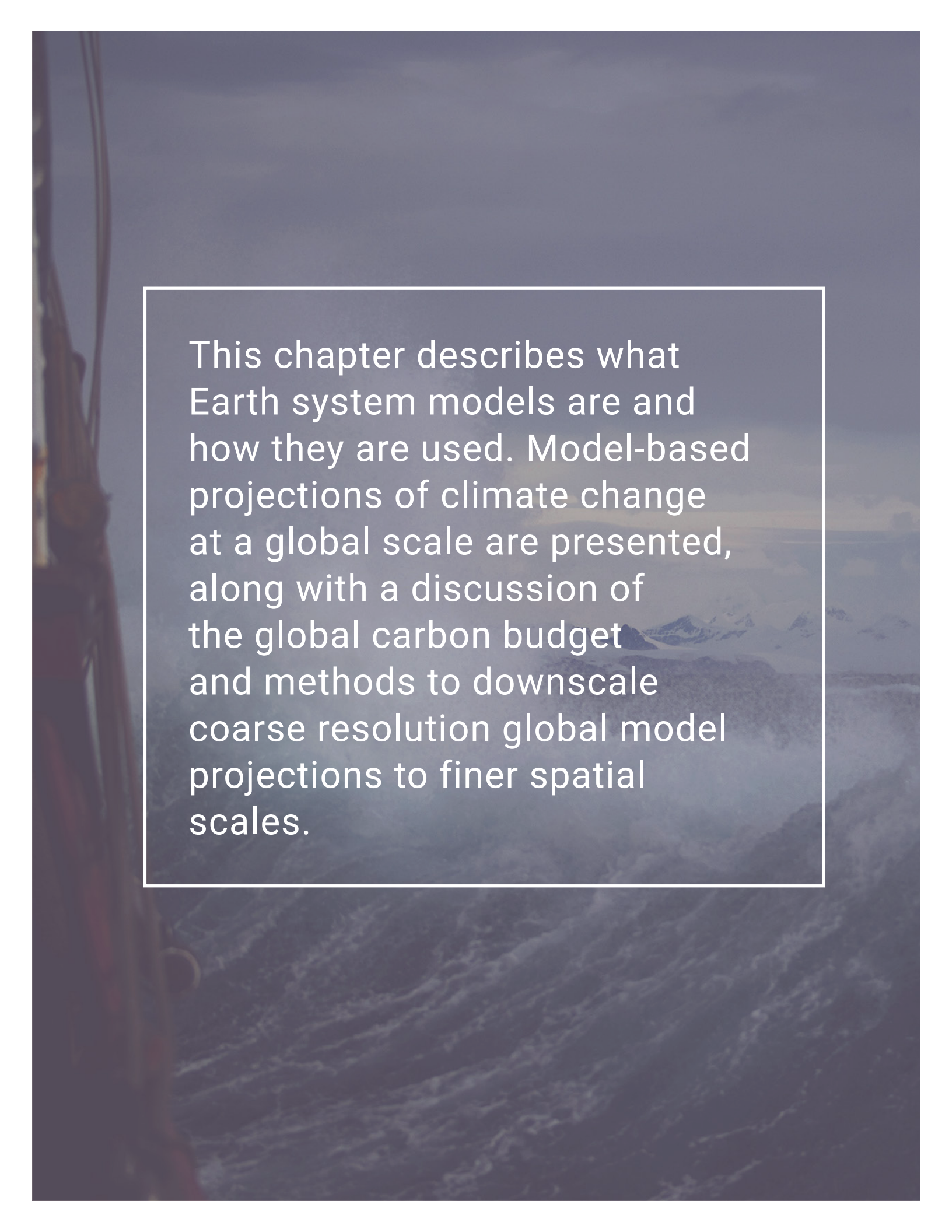
Box 3.3: Short-lived climate forcing agents

3.5: Regional downscaling

3.5.1: Downscaling strategies

3.5.2: Downscaling results for North America and Canada

REFERENCES



This chapter describes what Earth system models are and how they are used. Model-based projections of climate change at a global scale are presented, along with a discussion of the global carbon budget and methods to downscale coarse resolution global model projections to finer spatial scales.

Chapter Key Messages

3.2: Future Change and Climate Forcing

Emissions of greenhouse gases from human activity, particularly carbon dioxide, will largely determine the magnitude of climate change over the next century. Therefore, reducing human emissions will reduce future climate change.

3.3: Modelling the Response of the Climate System to External Forcing

In the near term (to approximately 2040), projected warming will be similar under all emission pathways. But by the late 21st century, the differences between possible emission pathways will have a considerable effect. Available estimates indicate that the global climate will warm by an additional 1°C (for a low emission scenario) to 3.7°C (for a high emission scenario). Scenarios that would limit warming to an additional 1°C or less require rapid and deep emission reductions.

3.4: Cumulative Carbon and Global Temperature Change

Global temperature change is effectively irreversible on multi-century timescales. This is because the total amount of carbon dioxide emitted over time is the main determinant of global temperature change and because carbon dioxide has a long (century-scale) lifetime in the atmosphere.

3.5: Regional Downscaling

Climate projections are based on computer models that represent the global climate system at coarse resolution. Understanding the effects of climate change for specific regions benefits from methods to downscale these projections. However, uncertainty in climate projections is larger as one goes from global to regional to local scale.

Summary

This chapter provides an overview of Earth system models and how they are used to simulate historical climate and to make projections of future climate. Historical simulations allow models to be evaluated via comparison with observations, and these show that models are able to reproduce many aspects of observed climate change and variability. They also allow experiments to be conducted in which human and natural causes of climate change can be identified and quantified. In order to make future projections, it is necessary to specify future emissions, or concentrations of greenhouse gases and aerosols, as well as future land-use change. Owing to uncertainty regarding future human activity (in particular, the extent to which ambitious emission reductions will be implemented), a range of future scenarios must be used. Results from future climate projections are discussed, along with sources of confidence and uncertainty. On average, the models project a future global mean temperature change (relative to the 1986–2005 reference period) of about 1°C for the low emission scenario (Representative Concentration Pathway [RCP] 2.6) and 3.7°C for the high emission scenario (RCP 8.5) by the late 21st century, with individual model results ranging about 1°C above or below the multi-model average. This change is over and above the 0.6°C change that had already occurred from 1850 to the reference period. The low emission scenario (RCP2.6) is consistent with limiting the global temperature increase to roughly 2°C and is therefore roughly compatible with the global temperature goal agreed to in the Paris Agreement. This scenario requires global carbon emissions to peak almost immediately and reduce to near zero well before the end of the century.

Regardless of the global mean surface temperature level attained when emissions become net zero, temperature will remain at about that level for centuries. In other words, global temperature change is effectively irreversible on multi-century timescales. The relationship between cumulative emissions of carbon dioxide (CO₂) and global mean surface temperature provides a simple means of connecting emissions from fossil fuels – the main source of anthropogenic CO₂ – to climate change. It also leads to the concept of a carbon emissions budget – the amount of carbon that can be emitted before temperatures exceed a certain value. The Intergovernmental Panel on Climate Change (IPCC, 2014) has assessed that, to have a 50% chance of keeping global warming to less than 2°C above the pre-industrial value, CO₂ emissions from 2011 onward would have to remain below 1300 billion tonnes of CO₂ (GtCO₂), roughly equal to what has already been emitted since the beginning of the Industrial Era. For a 50% chance of keeping the temperature increase to less than 1.5°C, emissions from 2011 onward would have to be limited to 550 GtCO₂. It must be noted that estimation of carbon budgets, especially for low temperature targets, is a rapidly developing area of research, and updated budgets will be assessed in the near future.

The chapter concludes with a discussion of downscaling methods, that is, methods to transform global Earth system model results into more detailed, local information better suited to impact studies. Downscaled results are often used in impact studies, but users must keep in mind that the enhanced detail provided does not necessarily mean added value, and that uncertainty is larger at smaller spatial scales.

3.1: Introduction

Future climate change will be driven primarily by human emissions of greenhouse gases (GHGs). Emissions of aerosols (airborne particles) collectively cool the climate and so offset some climate warming, but this effect is projected to decrease in the future as aerosol emissions decline. To understand the effects of these drivers on the climate, scientists use models – complex computer simulations of the climate system. Models are used to make projections of future climate, based on future scenarios of GHG and aerosol forcing. These models are developed and used at climate research institutions around the world, and results from multiple models allow us to estimate uncertainty and overall confidence in future projections. While Earth system models can simulate the climate system's response to human emissions of GHGs, they cannot predict future human activities. Therefore, projections are made using various scenarios, or pathways, of future GHG concentrations, aerosol loading and land-use change (climate forcing agents; see Chapter 2, Section 2.3.1). These pathways are described in Section 3.2. In Section 3.3, Earth system models are briefly described, along with global-scale projections of future climate and sources of uncertainty in such projections. While all forcing agents affect climate, carbon dioxide (CO₂) is the main determinant of long-term global temperature change. Section 3.4 describes the relationship between CO₂ emissions and global temperature change – a relationship that is important in developing policies on temperature targets and on global emission reductions. This section also discusses why climate change is irreversible, due to the long lifetime of CO₂ in the climate system. Finally, Section 3.5 discusses how global model results can be “downscaled” to provide more detailed regional information more suitable for impact assessment and adaptation planning.

3.2: Future climate change and climate forcing

Key Message

Emissions of greenhouse gases from human activity, particularly carbon dioxide, will largely determine the magnitude of climate change over the next century. Therefore, reducing human emissions will reduce future climate change.

Projections of future climate change require projections of future climate forcing – the external drivers of change such as GHGs and aerosols. These projections, in turn, arise from scenarios of future GHG and aerosol emissions, which are based on varying assumptions about how human activities, such as fossil fuel consumption and land use, will change. Future emission scenarios are typically developed using integrated assessment models, which combine economic, demographic, and policy modelling with simplified physical climate models to make projections of population growth, economic development, land use, and the implications of different policy options on climate-relevant emissions. As there is large uncertainty in the social and economic aspects of such projections, a range of scenarios is generally provided, ranging from those in which emissions are aggressively reduced to those with limited actions taken to mitigate emissions.

The projections described in the IPCC Fifth Assessment (see Chapter 1) were based on a suite of future forcing scenarios called Representative Concentration Pathways (RCPs) that cover the period from 2006 onward (van Vuuren et al., 2011). The RCPs are identified by a number indicating the change in radiative forcing – the imbalance between the solar radiation entering the climate system and the infrared (longwave) radiation leaving it caused by greenhouse gases and other external drivers (see Chapter 2, Section 2.3.1) – by the end of the 21st century. RCP2.6 represents a low emission pathway with a change in radiative forcing of roughly 2.6 W/m², RCP4.5 and RCP6 represent intermediate emission pathways, and RCP8.5 represents a pathway with continued growth in GHG emissions, leading to a radiative forcing of roughly 8.5 W/m² at the end of the century. In this report, we will refer to climate scenarios based on RCP2.6 as “low emission scenarios,” those based on RCP4.5 and RCP6 as “medium emission scenarios,” and those based on RCP8.5 as “high emission scenarios.” For each RCP, the integrated assessment models provide a comprehensive time series of emissions and concentrations of individual GHGs (CO₂, methane [CH₄], nitrous oxide [N₂O], chlorofluorocarbons, etc.), along with aerosol emissions and land-use change. All of these forcings are inputs to Earth system models, which then simulate the future response of the climate system, including biogeochemical feedbacks, to these external forcing scenarios.

The RCPs supersede the so-called “SRES scenarios” (Nakicenovic et al., 2000), which served as the basis for model runs reported in the IPCC Fourth Assessment Report. Although there are differences in detail, the SRES A2 forcing scenario is roughly comparable to RCP8.5, the SRES A1B scenario is roughly midway between RCP6 and RCP8.5, and SRES B1 is roughly comparable to RCP4.5 (e.g., Burkett et al., 2014). There was no SRES forcing scenario comparable to RCP2.6. These forcing scenarios are updated every few years, and new shared socioeconomic pathways (building upon the RCPs) will be used in model runs that will feed into the upcoming IPCC Sixth Assessment (e.g., Riahi et al., 2017).

In all cases, CO₂ is the largest contributor to the historical and projected change radiative forcing, followed by CH₄ and N₂O (Myhre et al., 2013; Collins et al., 2013). This means that future changes in human emissions of CO₂ will largely determine future climate.

An illustration of aspects of the RCPs is shown in Figure 3.1. It is important to note that no likelihoods are ascribed to these future forcing scenarios – they are all deemed plausible, although, as emissions continue to increase, low emission pathways become more difficult to achieve (e.g., Millar et al., 2017). The spread across the RCPs represents some measure of our uncertainty about how socioeconomic factors may change in the future, especially how aggressively humans will pursue emission mitigation, and therefore the pace at which humans will continue to drive climate change. The low emission (RCP2.6) scenario is consistent with limiting global temperature increase to roughly 2°C above the pre-industrial value (see Section 3.3.3) and is therefore roughly compatible with the global temperature goal agreed to in the Paris Agreement (UNFCCC, 2015). This scenario requires global CO₂ emissions to peak almost immediately and reduce to near zero well before the end of the century. Global annual CO₂ emissions reached about 10 Gt of carbon (about 37 GtCO₂) in 2017 (Le Quéré et al., 2017)

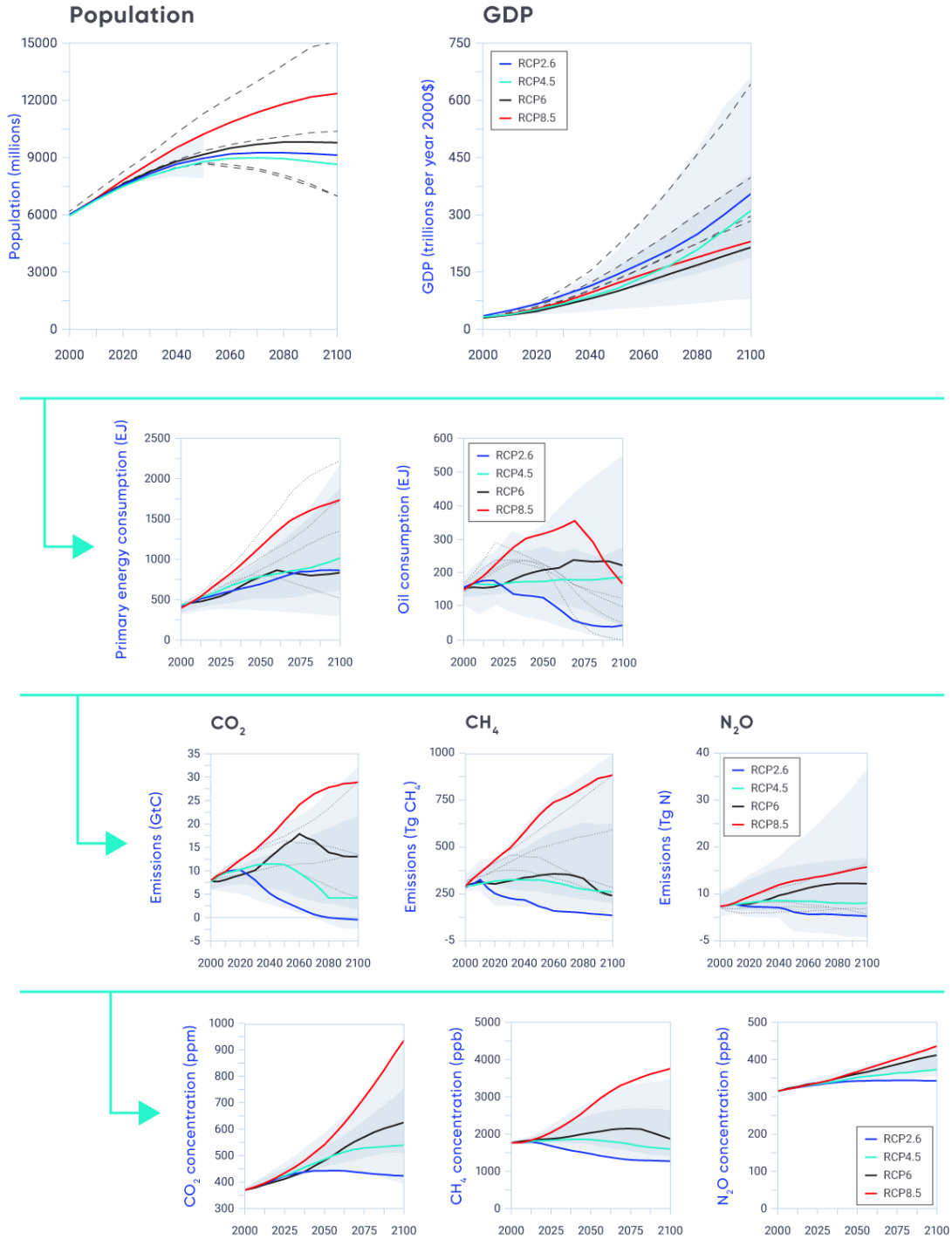


Figure 3.1: Underlying features of the Representative Concentration Pathways

Figure caption: Socioeconomic (top row), energy intensity (second row), greenhouse gas emissions (third row), and ultimately greenhouse gas concentration (bottom row) scenarios underlying the Representative Concentration Pathways (RCPs) used to drive future climate projections. The light grey shading indicates the 98th percentile and the dark grey shading the 90th percentile of the underlying databases.

FIGURE SOURCE: REPRODUCED FROM VAN VUUREN ET AL. (2011), WHERE FURTHER DETAILS ARE PROVIDED.

Section summary

In summary, projections of future climate require projections of future forcing from GHGs, aerosols, and land-use change, which in turn depend on projections of future population and energy consumption. CO₂ is the largest contributor to human-induced climate forcing, and so CO₂ emissions and the extent to which they grow or decline will largely determine future climate.

3.3: Modelling the response of the climate system to external forcing

Key Message

In the near term (to approximately 2040), projected warming will be similar under all emission pathways. But by the late 21st century, the differences between possible emissions pathways will have a considerable effect. Available estimates indicate that the global climate will warm by an additional 1°C (for a low emission scenario) to 3.7°C (for a high emission scenario). Scenarios that would limit warming to an additional 1°C or less require rapid and deep emission reductions.

3.3.1: Earth system models

Earth system models are based on a mathematical representation of the behaviour of the atmosphere, ocean, land surface, and cryosphere. They simulate a virtual planet using powerful supercomputers, allowing scientists to probe the connections between various physical and biogeochemical processes, e.g., how the ocean takes up heat and carbon, stores and then redistributes it. Two main ways such models are used are (1) to compare simulations with and without historical forcings to determine human versus natural forcing effects, and (2) to simulate future climate in response to various forcing scenarios.

Earth system models have some features in common with global weather-prediction models (used to make daily weather forecasts) but do not depend on the use of observations as inputs and typically operate at somewhat lower spatial resolution (i.e., the level of spatial detail is often limited to features with scales of a hundred kilometres or larger). The lower resolution is necessitated by the computing demand of the long simulations that are required. Simulations begin with the historical period (from 1850 to present), driven by observationally based climate forcing (e.g., historical changes in GHG concentrations), and then continue into the future, using different forcing scenarios (such as those described in the previous section) out to year 2100 or further (Figure 3.2).

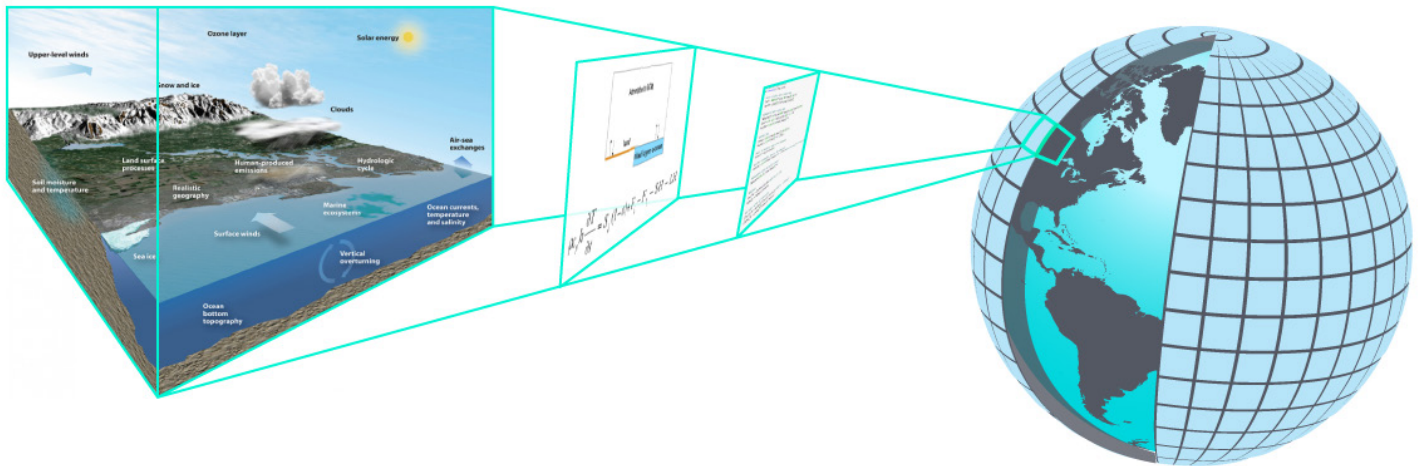


Figure 3.2: Building an Earth system model

Figure caption: Schematic illustration of the processes included in an Earth system model, and the way in which mathematical equations describing physical processes are solved on a three-dimensional grid.

FIGURE SOURCE: CLIMATE RESEARCH DIVISION, ENVIRONMENT AND CLIMATE CHANGE CANADA.

Earth system models represent an evolution from earlier physical climate models (representing the coupled atmosphere, ocean, land, and sea ice components of the climate system) to models that go beyond this with explicit representation of the carbon cycle (Flato, 2011; Flato et al., 2013). Including carbon and other biogeochemical cycles in the models allows simulation of global interactions among ecosystems, carbon, and climate, as well as several terrestrial processes that occur at high latitudes. Changes to snow and sea ice can cause positive (amplifying) snow/ice albedo feedbacks in the climate system (Euskirchen et al., 2016; Kashiyase et al., 2017; see Chapter 2, Box 2.4). As temperatures increase, the spatial extent of snow and sea ice declines, reducing the reflectivity of land and oceans, allowing more solar radiation to be absorbed, and hence further increasing temperatures. This feedback makes an important contribution to the higher rate of warming in the Arctic region, called Arctic amplification (FAQ 3.1; see Section 3.3.3). The models can also simulate



increased growth of vegetation at northern high latitudes in response to a warming climate, an effect that may reduce the land surface albedo and affect the exchange of energy and water between the land and the atmosphere (Forkel et al., 2016). Changes in permafrost in response to changing climate – leading to changes in hydrological conditions and CH₄ release (Schuur et al., 2008) – are also now included in some models.

FAQ 3.1: Why is Canada warming faster than the world as a whole?

Short answer

The response of the climate system to increasing greenhouse gases varies from one region to another. As a result, the rates of warming around the world are not the same. These variations are a result of climate processes and feedbacks that depend on local conditions. For example, in Canada, loss of snow and sea ice is reducing the reflectivity (or albedo, see Chapter 2, Box 2.3) of the surface, which is increasing the absorption of solar radiation. This causes larger surface warming than in more southerly regions. Because of this and other mechanisms, Canada is warming faster than the world as a whole – at more than twice the global rate – and the Canadian Arctic is warming even faster – at about three times the global rate.

Long answer

Canada's rate of surface warming is more than twice the global rate (Figure 3.3). The difference is even more dramatic for the Canadian Arctic, where the rate of warming is about three times the global rate. Enhanced warming for Canada as a whole and for the Canadian Arctic in particular is part of a climate phenomenon known as "Arctic amplification."

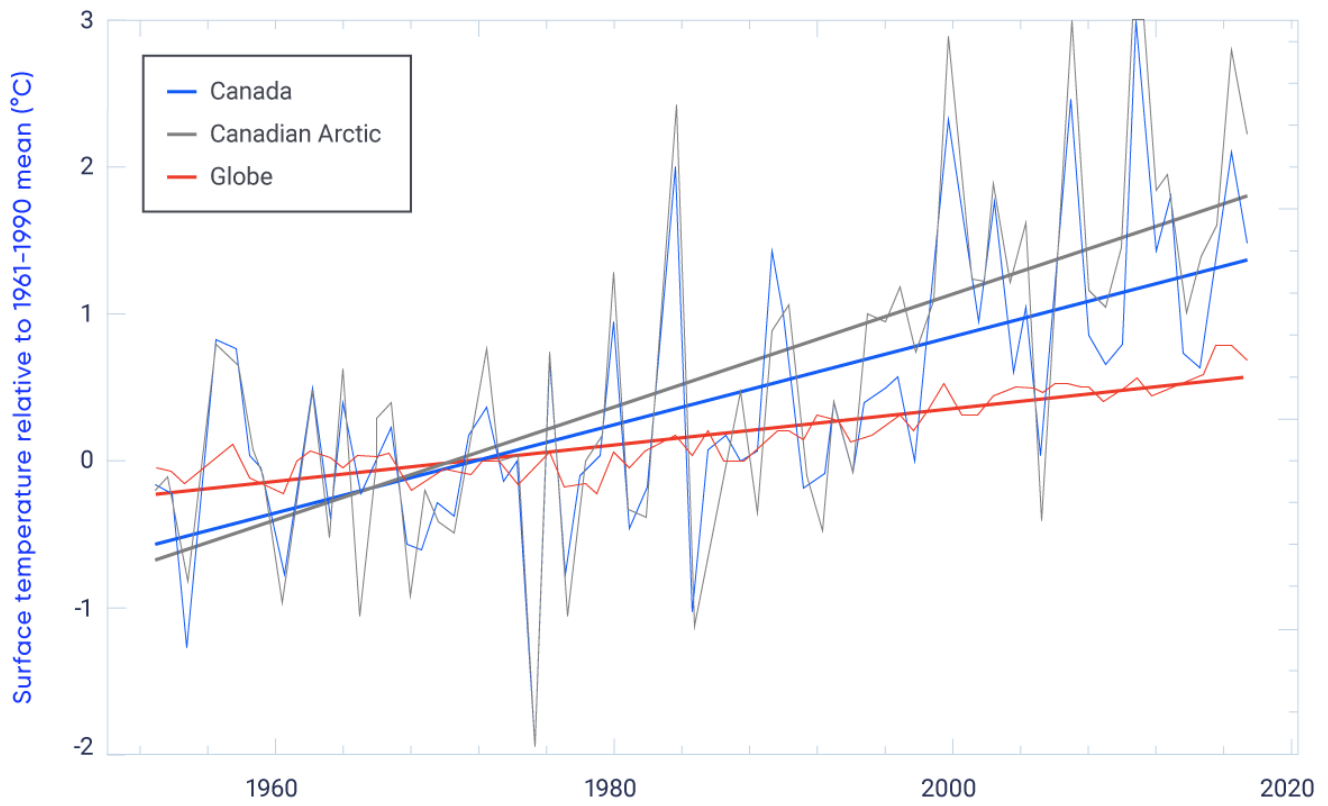


Figure 3.3: Rates of warming for Canada, the Canadian Arctic and the world

Historical observations of annual mean surface temperature show that the rate of surface warming for Canada (slope of the blue line) is more than twice the rate of surface warming for the globe (slope of the red line). The rate of warming for the Canadian Arctic (slope of the grey line) is about three times the global rate. Canadian results are based on the Adjusted and Homogenized Canadian climate data (Vincent et al., 2015). The global result is based on the HadCRUT data set (Morice et al., 2012).

FIGURE SOURCE: ENVIRONMENT CANADA CLIMATE RESEARCH DIVISION.

In all regions of the world, the climate response to radiative forcing¹² (see Chapter 2, Section 2.3) from greenhouse gases is determined by subsequent processes and feedbacks within the climate system. To understand Arctic amplification, we can use climate models to estimate the contributions to temperature change from different physical mechanisms. These estimates for the Arctic can then be compared with estimates for other regions of the world. This approach has shown that that enhanced warming over high-northern latitudes is due to contributions from five well-known climate feedbacks. These are, in decreasing order of importance,

12 Radiative forcing is the net change in the energy balance of the earth system due to an external perturbation. A positive radiative forcing, such as that from the increase in atmospheric greenhouse gases, causes climate warming, whereas a negative radiative forcing causes climate cooling.

lapse-rate feedback, snow/ice albedo feedback, Planck feedback, cloud feedback, and water vapour feedback (Figure 2). In the Arctic, each of these is a positive (amplifying) feedback –these feedbacks enhance the warming from greenhouse gas forcing. These feedbacks operate elsewhere as well, but their strength and direction vary from one region to another, and most are stronger in the Arctic (Figure 3.4)

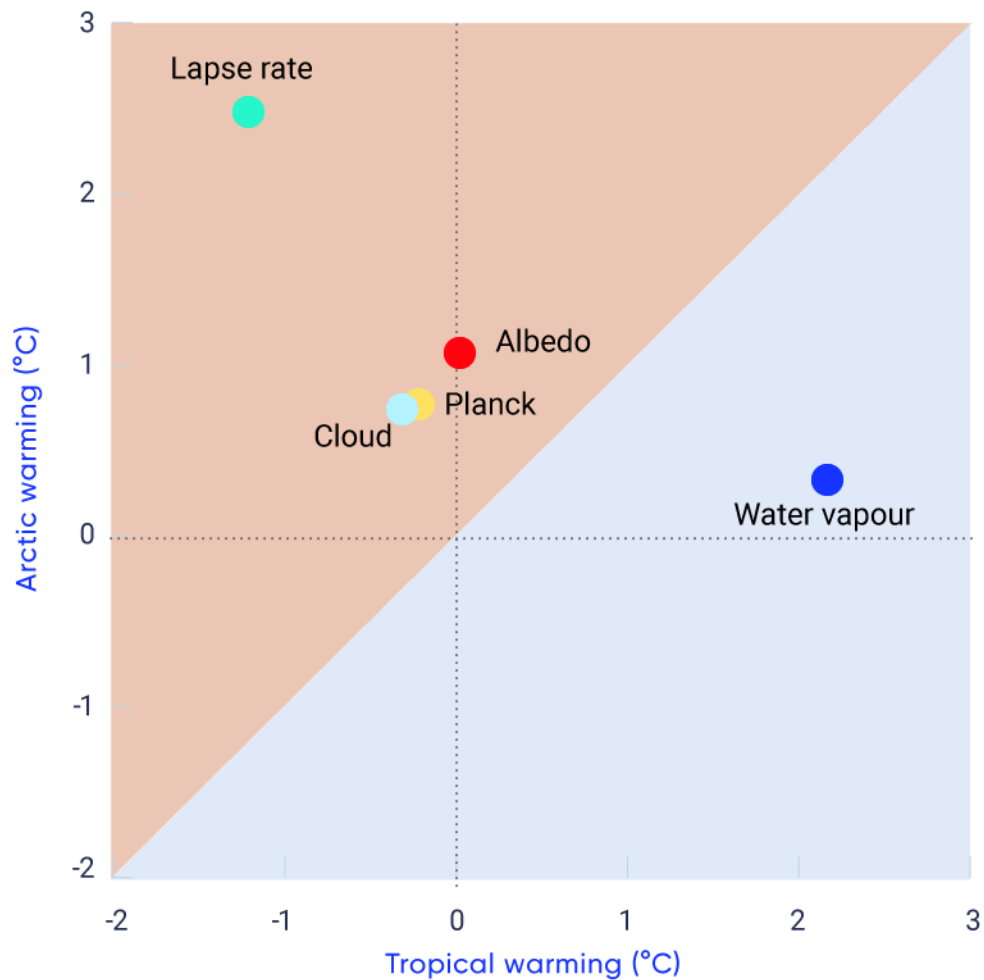


Figure 3.4: Contributions to warming of various feedback mechanisms for the Arctic and the Tropics

Feedback mechanisms make different contributions to warming, depending on the region of the world. The contributions of lapse-rate, snow/ice albedo, Planck, cloud, and water vapour feedbacks to warming for the Arctic and for the Tropics are shown for a modelled climate state in which carbon dioxide concentrations are quadrupled from their pre-industrial levels. Feedbacks in the red-shaded area of the figure contribute to enhanced warming in the Arctic relative to the Tropics, whereas feedbacks in the blue-shaded area contribute to enhance warming in the Tropics relative to the Arctic.

FIGURE SOURCE: ADAPTED FROM STUECKER ET AL. (2018).

LAPSE-RATE FEEDBACK: The lapse rate is how much the temperature in Earth's atmosphere decreases as altitude increases. Differences in the lapse rate in different parts of the world affect the response to increasing greenhouse gas amounts. In the Arctic, for example, warming due to greenhouse gas forcing is largest near the surface. The opposite is true in the Tropics, where warming due to greenhouse gas forcing is largest higher up in the atmosphere, allowing radiant heat from Earth to more easily escape to space, and hence cool the climate.

SNOW/ICE ALBEDO FEEDBACK: Snow and ice reflect considerable solar energy back to space (see Chapter 2, Figure 2.4). Warming melts snow and ice, causing the now darker surface to absorb more solar radiation and heat further. Of course, this feedback only applies to regions where ice and snow are found. Thus, its contribution to warming is substantial in the Arctic and negligible in the Tropics.

PLANCK FEEDBACK: The higher the temperature of any body (such as the Earth), the more energy it radiates, creating a cooling effect. This is a negative feedback that, ultimately, limits warming on a global scale. However, this cooling effect is weaker in the Arctic than in the Tropics, and therefore allows for a relatively larger warming response at high latitudes.

CLOUD FEEDBACK: In climate models, greenhouse gas forcing generally results in more cloudiness in high latitudes and less in low latitudes. In the Arctic, the increase in clouds enhances warming by trapping heat near the surface.

WATER VAPOR FEEDBACK: Water vapor, like carbon dioxide, is a greenhouse gas. As the atmosphere warms, it is able to hold more water vapor and so warming is enhanced. The Arctic atmosphere is very dry and for this reason the contribution of the water vapor feedback to warming is small as compared to the Tropics, where the atmosphere is moist.

In summary, warming caused by increasing greenhouse gas concentrations varies from place to place, largely due to differing feedbacks at play from one region of the world to the next. Enhanced rates of warming over Canada and the Canadian Arctic are due to a unique combination of such feedback mechanisms.

How do we know that models are accurately projecting future climate? One method of measuring whether models can realistically represent the complex interconnections among climate processes is to gauge their ability to reproduce past changes. Simulations using observationally based historical forcing from 1850 onward provide the opportunity to directly compare model results to observations. The IPCC Assessment Reports have traditionally included a chapter devoted to this type of model evaluation (e.g., Flato et al., 2013), and these provide a synthesis of the large number of scientific papers on model performance. Figure 3.5 provides one example of model evaluation, comparing the annual global mean surface air temperature from several different sources with simulations from 36 different models that participated in the fifth phase of the Coupled Model Intercomparison Project (CMIP5; see Box 3.1). As the figure shows, Earth system models are

able to reproduce the observed long-term increase in temperature (heavy black lines), along with the sporadic cooling that follows large explosive volcanic eruptions. The magnitude of natural year-to-year variability is also well simulated (thin lines), although one does not expect individual ups and downs to coincide (as each model simulates its own internal variability). The heavy red line in the figure shows the multi-model average, which is an approximation of the response of the climate system to external forcing (changing GHG concentrations and aerosol amount, land-use change, variations in solar irradiance, and volcanic aerosol), upon which internal variability is superimposed. The difference between observed temperature and the multi-model average from roughly 2000 onward has been extensively analyzed (e.g., Fyfe et al., 2016) and is due to a combination of small errors in the observational record, decadal timescale internal variability, and incomplete early 21st century volcanic forcing in the models (see Chapter 2, Section 2.3.3).

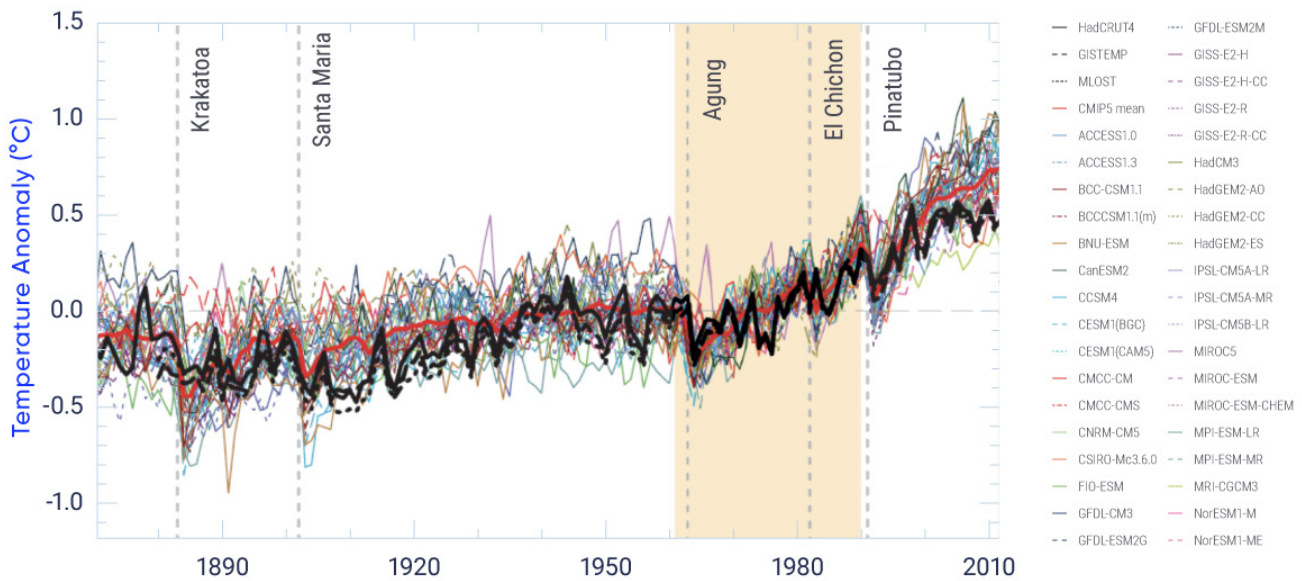


Figure 3.5: Evaluating model performance against observations

Figure caption: Global annual mean surface air temperature anomalies from 1850 to 2012 (anomalies are computed relative to the 1961–1990 average shown by yellow shading). The heavy black lines represent three different reconstructions of temperature based on observations. Each of the thin coloured lines represents a simulation from one of 36 climate models. The heavy red line indicates the multi-model average. The overall warming trend is evident in both observations and simulations, particularly since about 1960, and both show cooling following large volcanic eruptions (vertical dashed lines).

FIGURE SOURCE: FLATO ET AL. (2013).

Box 3.1: The Coupled Model Intercomparison Project

All models used to project climate have some uncertainty associated with them, owing to approximations that must be made in representing certain physical processes. To understand the uncertainty in models, scientists compare them with other models and evaluate how much the models differ in their projections. To determine this, an ensemble of models is needed, allowing a range of simulations and projections to be analyzed and compared. The World Climate Research Programme has established the Coupled Model Intercomparison Project (CMIP) specifically for this purpose. An agreed-upon suite of historical simulations and future climate projections are performed using the same external forcing (changing GHGs, land-use, etc.). The outputs from the models are archived in a common format for analysis by the climate research community (Taylor et al., 2012). Previous versions of CMIP have provided model results assessed in earlier IPCC Assessment Reports. The most recent, fifth phase of this project, CMIP5, provided climate model results that were assessed in the IPCC Fifth Assessment Report (IPCC, 2013), and many of these results are available from the [Canadian Climate Data and Scenarios](#) website. Future climate projections in CMIP5 used the Representative Concentration Pathways emission scenarios (see Section 3.2) (van Vuuren et al., 2011). A new version, CMIP6, is currently underway and will serve as input to the IPCC Sixth Assessment.

3.3.2: Sources of confidence and uncertainty

Confidence in climate model projections arises from many sources. First, climate models are solidly based on physical laws and scientific understanding of physical processes. Second, climate model results are evaluated in detail by comparing model output to observations, as described in Section 3.3.1. The model evaluation chapter in the most recent IPCC Assessment report provides many examples (Flato et al., 2013). Third, some of the models used to make climate projections are also used to make seasonal climate predictions whose skill is routinely evaluated (e.g., Kirtman et al., 2013; Merryfield et al., 2013; Sigmond et al., 2013; Kharin et al., 2017).

There are, however, uncertainties that have to be considered when using model projections. These uncertainties stem from the fact that models cannot simulate all physical processes exactly (and therefore must make approximations), and from internal variability in both the simulated and the real climate system (see Chapter 2, Box 2.5). The uncertainty due to approximations of physical processes can be reduced, in principle, and models continue to improve in this regard (Flato et al., 2013). However, it is impossible to reduce the uncertainty from internal variability that is superimposed on the underlying forced climate change. In addition, there is uncertainty about what future climate forcing (e.g., future GHG emissions) will be, which is accounted for by making projections with a range of forcing scenarios. These sources of uncertainty vary in importance depending on the time and space scale under consideration – generally, uncertainties diminish at larger spatial scales as internal variability “averages out” to a certain degree when one considers larger regions (e.g., Haw-

kins and Sutton, 2009). This also means that uncertainty is larger when one looks at small regions or specific locations. In addition, at longer time scales (say, by the end of the 21st century), uncertainty is dominated by differences in the forcing scenarios and internal variability is, by comparison, much smaller.

3.3.3: Global-scale climate projections

As described in Section 3.2, climate projections are a result of driving climate models with different future forcing scenarios (RCPs, in the case of CMIP5). These projections include the response of the climate system to external forcing (e.g., changing GHG concentrations), internal variability, and uncertainties associated with differences between models. These effects can be separated, to some extent, by drawing upon projections from multiple models (e.g., Collins et al., 2013). The multi-model average provides an estimate of the response of the climate system to forcing, since internal variability and model differences are “averaged out” to a large extent (see Box 3.2). The upper panel of Figure 3.6 shows the change over time in global mean surface air temperature, as simulated by the CMIP5 models, spanning the period from 1950 to 2100. The heavy lines indicate the multi-model average, and the shaded band represents the range of model results around this average. Within this shaded band, each individual model result would look like one of the individual coloured lines in Figure 3.5, but for clarity this collection of individual lines is shown as a shaded band. The high emission scenario (RCP8.5) results are shown by the red line and the orange shaded band, whereas the low emission scenario (RCP2.6) results are shown by the blue line and the blue shaded band.

Box 3.2: Model projections and weighting

Climate change projections are generally based on an ensemble of climate models representing the state-of-the-art in understanding and modelling climate. The reason for using an ensemble of models is that no single model can be considered the best, since different models exhibit varying levels of realism in simulating climate, depending on the region and variable of interest. Even if a single best model could be determined, there is no guarantee that its present-day performance would cause it to give more reliable projections of future climate.

Climate change projections differ from weather forecasts in several crucial respects. One important difference is that, while we learn the accuracy of weather forecasts in the next few days, the true performance of future climate projections will remain unknown until many decades from now (Weigel et al., 2010). In the absence of a consensus on which models are the best, common practice has been to rely on “model democracy,” whereby each model in a multi-model ensemble is treated equally. This equal-weighting method assumes that each model is different and yet equally plausible.

In recent years, however, there is increasing evidence in the scientific literature that model democracy has some drawbacks. Accurate present-day model performance may not guarantee future performance, but poor

performance clearly does not inspire confidence (for example, models that severely underestimate current Arctic sea ice coverage may not be reliable in projecting future changes in sea ice coverage). As a result, there is a growing appreciation that some performance-based weighting of model projections may be appropriate. Indeed, the IPCC Fifth Assessment illustrated this for the case of Arctic sea ice (Collins et al., 2013). However, a clear consensus on to how to weight models has not yet emerged.

A further drawback of model democracy is that it assumes each model is independent. However, climate models often share common features because one model may use computer code adopted from another model with minor adjustments, or two models may have been developed from a common earlier model. Although schemes to account for model performance and independence are being developed and tested (e.g., Sanderson et al., 2017; Knutti et al., 2017), this is still an emerging area of research. Initial exploration of weighting approaches suggests that differences between weighted and unweighted projections for Canada are small, and so traditional, unweighted multi-model projections are presented in this report.

There are two key points illustrated in the upper panel of Figure 3.6. First, when looking at projected climate change, the spread across models (the vertical extent of the shaded bands) is smaller in the near term (to around 2040) than it is toward the end of the 21st century, indicating that model uncertainty has a larger effect further into the future. (Internal variability also contributes to the width of the shaded bands, as described previously, but the size of this contribution is not expected to change significantly in the future.) Second, the differences among forcing scenarios are small in the near term, but become large toward the end of the 21st century (as illustrated by the growing separation between results for the low emission scenario [RCP2.6] and high emission scenario [RCP8.5]). For simplicity, the medium emission scenarios (RCP4.5 and RCP6.0) are not shown in the main part of the figure, but their end-of-century results are shown on the right-hand side of the top panel for comparison.

The spatial patterns of projected temperature and precipitation change are shown in the bottom panel of Figure 3.6. The large difference in mean change between the high and low emission scenarios is clearly evident in the maps (darker colours indicate larger change), but there is a marked similarity in pattern. For temperature, changes are larger over land than over the adjacent ocean, and are larger at high latitudes, particularly over the Arctic, an illustration of Arctic amplification. As a result, projected warming in Canada is roughly double the global mean. For precipitation, the pattern of change is more complex, with the polar and equatorial regions projected to have increased annual precipitation, whereas precipitation decreases are projected for much of the subtropics (roughly 24° to 35° north and south latitude). For southern Canada, the projected change in precipitation is rather small, but projected increases are larger further north. (Changes in annual mean precipitation do not translate directly into changes in seasonal snow cover or water availability, as discussed in Chapter 5 and Chapter 6.)

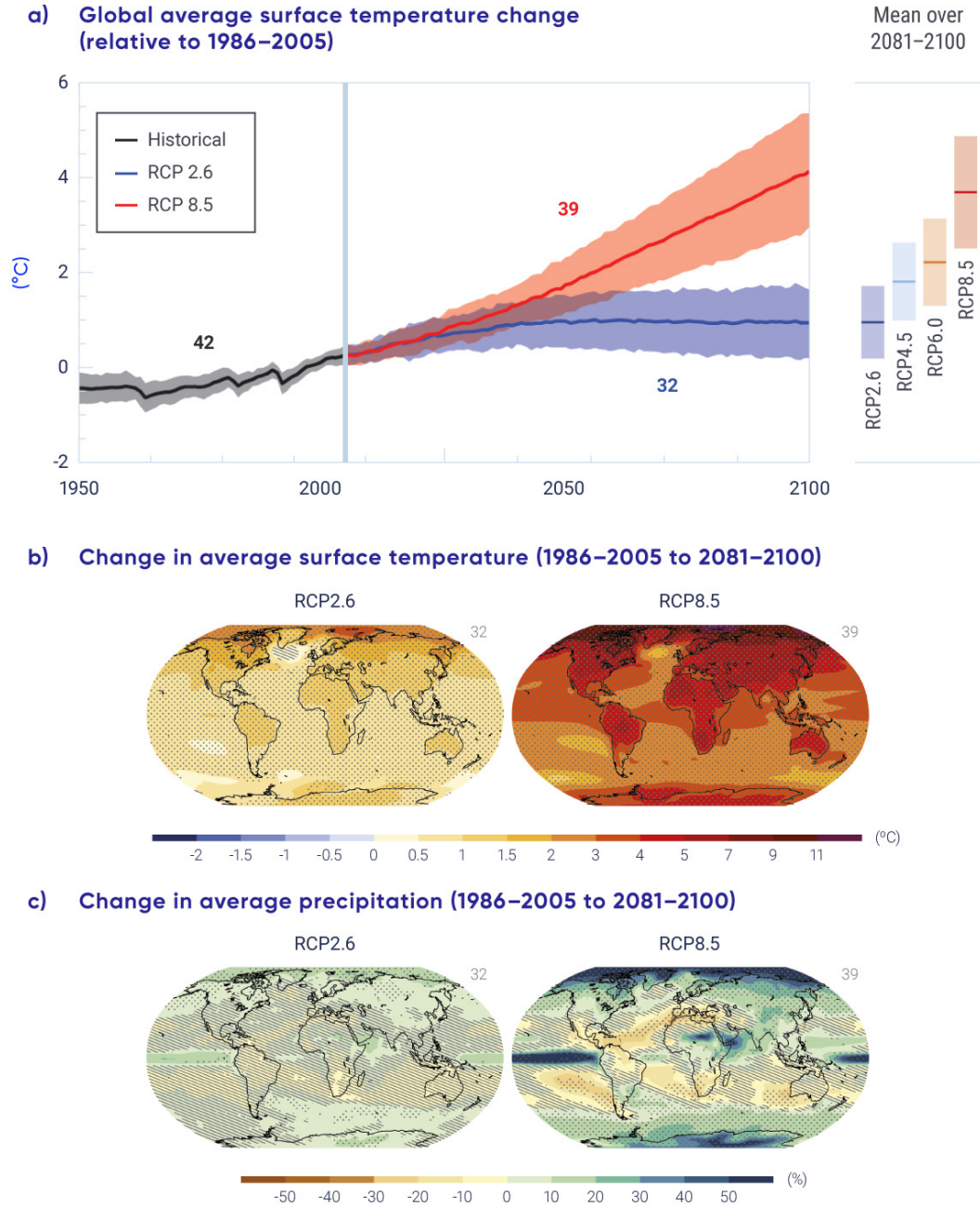


Figure 3.6: Global climate projections

Figure caption: The upper panel shows the multi-model annual global mean surface temperature change relative to a historical reference period (1986–2005) for a range of emission scenarios. The shaded bands indicate the 5%–95% spread across the multi-model ensemble. The lower panels show the multi-model mean projected change by late century (the 2081–2100 average minus the 1986–2005 average) for annual (a) mean surface air temperature and (b) precipitation for the low emission scenario (RCP2.6) and the high emission scenario (RCP8.5).

FIGURE SOURCE: COLLINS ET AL. (2013).

On average, the models project a future global mean temperature change (relative to the 1986–2005 reference period) of about 1°C for the low emission scenario (RCP2.6) and 3.7°C for the high emission scenario (RCP 8.5) by the late 21st century, with a 5%–95% range of about 1°C above and below the multi-model average. This change is over and above the 0.6°C change that had already occurred from 1850 to the reference period. Therefore, the average projected change under the low emission scenario is consistent with the global temperature target in the Paris Agreement of limiting global warming to between 1.5°C and 2.0°C, although the projected range from all models extends both below and above this target. The low emission (RCP2.6) scenario requires emissions of CO₂ to peak almost immediately and reduce to near zero before the end of the century. Recent studies (e.g., Millar et al., 2017) provide more detailed analysis of scenarios that will limit warming to 1.5°C, and these also involve very rapid and deep emission reductions.

More details regarding future projections, with a focus on Canada, are provided in other chapters of this report. Confidence in climate change projections varies by region and by climate variable. So, for example, confidence in temperature change is higher than confidence in precipitation change. This is in large part because temperature change is a direct consequence of radiative forcing, whereas precipitation change is affected by a number of complex interactions, including changes in the water-holding capacity of a warming atmosphere, in global atmospheric circulation, in evaporation, and in other factors (e.g., Shepherd, 2014) (see Chapter 4). Changes in snow and ice are a consequence of changes in both temperature and precipitation and are discussed in more detail in Chapter 5. Freshwater availability (see Chapter 6) and ocean changes (see Chapter 7) are also affected by changes in temperature and precipitation, as well as by other factors.

3.3.4: Compatible emissions

Earth system models can be run in two different ways: one in which GHG concentrations are set and another in which GHG emissions are set (both are available as part of the RCP datasets). Concentration-driven simulations allow scientists to assess the difference, from one model to another, in how the climate responds to identical changes in GHG concentrations in the atmosphere. This helps separate the response of the climate system to a change in forcing (e.g., change in GHG concentrations) from the effect of carbon-cycle feedbacks involving the terrestrial and oceanic biospheres. The response of these natural carbon sinks to atmospheric CO₂ levels and to climate change will influence anthropogenic emissions compatible with a given CO₂ pathway. Therefore, an interesting aspect of these concentration-forced simulations is that global anthropogenic emissions can be computed – emissions that are compatible with the prescribed concentration pathway (e.g., Jones et al., 2013). The range in compatible CO₂ emissions between different models provides a measure of the uncertainty inherent in representing carbon-cycle feedbacks in models. Figure 3.7 illustrates results from compatible emission calculations and shows that, while there is some variation, this group of models is consistent. For the RCP 2.6 scenario in which temperature is stabilized below about 2°C, the models have compatible emissions that start reducing immediately and reach near zero well before the end of the century.

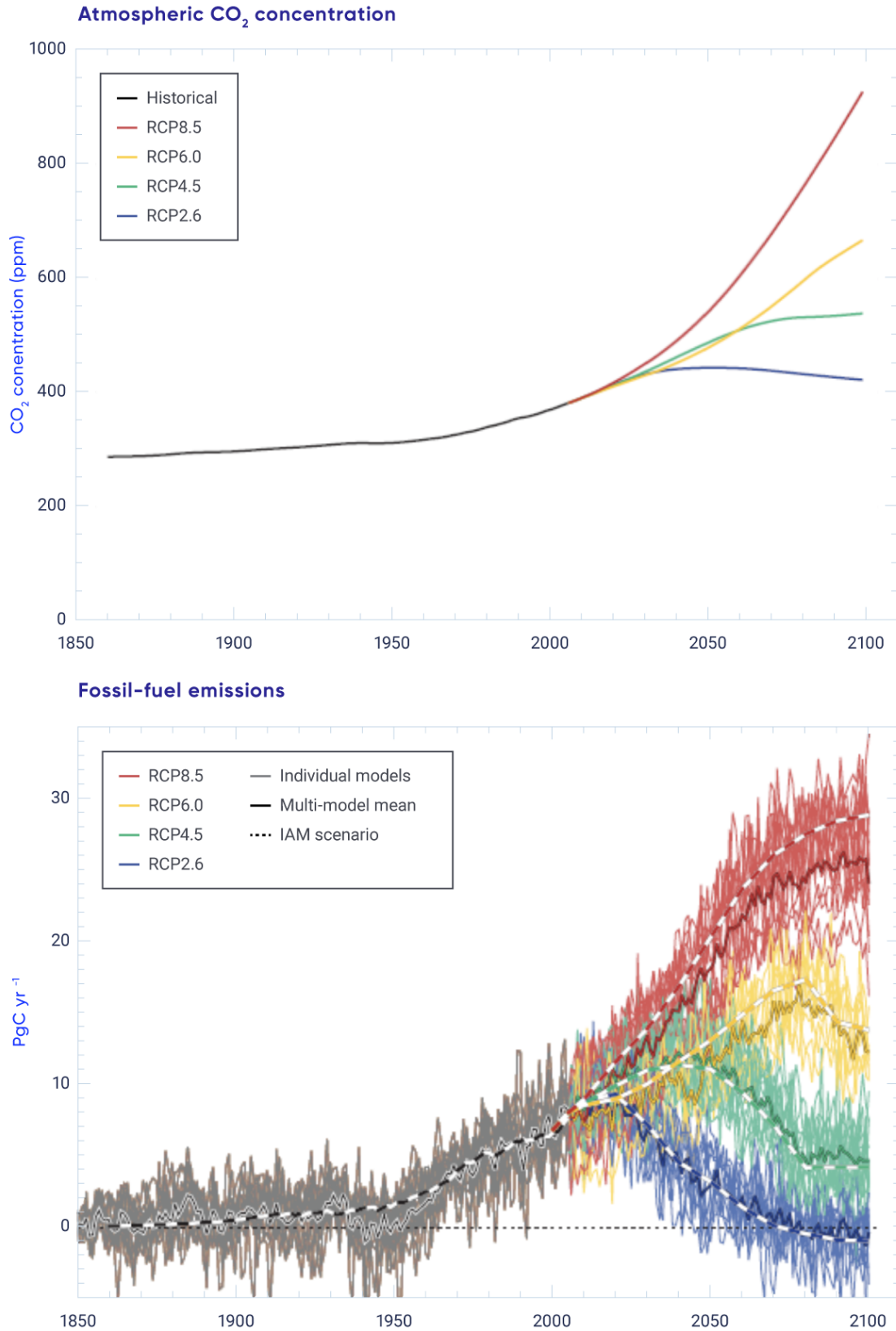


Figure 3.7: Carbon dioxide concentrations and compatible emissions under the four Representative Concentration Pathways

Figure caption: Carbon dioxide concentrations for four different Representative Concentration Pathways (RCPs; upper panel) and the corresponding compatible emissions (lower panel) based on simulations from five different Earth system models (Jones et al., 2013). The high emission scenario (RCP8.5) corresponds to emissions that are more than double those today by the end of the century, whereas the low emission scenario (consistent with temperature stabilization below 2°C) requires emissions to be rapidly reduced to near zero, or even negative, levels well before the end of the century. Note that the IAM scenario curves indicate the emissions obtained from the integrated assessment models that provide the RCP concentrations (see Figure 3.1).

FIGURE SOURCE: JONES ET AL., 2013.

Section summary

In summary, many Earth system models have been developed and used to make projections of future climate. Uncertainty in these projections arises from internal climate variability, from shortcomings in the models themselves, and from differences between plausible future forcing scenarios. Analysis of the entire collection of model results allows the first two sources of uncertainty to be reduced (though not eliminated), as model errors and internal variability are reduced by averaging across models. In the near term, to about 2040, the differences between forcing scenarios is not large. By the end of the 21st century, however, the global mean temperature increase projected for a low emission scenario is roughly 1°C, while for a high emission scenario it is roughly 4°C. The lower emission scenarios require rapid cuts in human emissions.

3.4: Cumulative carbon dioxide and global temperature change

Key Message

Global temperature change is effectively irreversible on multi-century timescales. This is because the total amount of carbon dioxide emitted over time is the main determinant of global temperature change and because carbon dioxide has a long (century-scale) lifetime in the atmosphere.

CO₂ is the largest contributor to anthropogenic radiative forcing and hence the dominant driver of anthropogenic climate change (Myhre et al., 2013) (see Chapter 2, Section 2.3.2). It also has a very long atmospheric lifetime (see Box 3.3). These properties mean that CO₂ emissions are the dominant control on future climate change. Traditionally, the focus has been on annual average emissions and their changes over time. However, recent research has found that the accumulation of CO₂ emissions over time are what determine global warming. From this research has emerged the concept of a level of cumulative emissions (called a cumulative carbon emissions budget) that must not be exceeded in order to limit temperature increases to a certain threshold.

3.4.1: The climate response to cumulative carbon dioxide emissions

The IPCC Fifth Assessment Report found that warming induced by CO₂ at any point in time since the beginning of the Industrial Era is proportional to the total amount of CO₂ emitted up to that time (cumulative CO₂ emissions; IPCC, 2013). This relationship has been seen in a range of climate models, across a range of emissions pathways, and even at high levels of cumulative emissions (Tokarska et al., 2016). Figure 3.8 shows that average warming is closely proportional to cumulative CO₂ emissions for the CMIP5 models' simulation of a CO₂ increase of 1% per year (thin black line). In this idealized simulation, atmospheric CO₂ concentration increases from its 1850 value of around 285 ppm by 1% per year until its concentration quadruples in 140 years to about 1140 ppm. The relationship between cumulative emissions of CO₂ and global mean surface temperature (GMST) is altered somewhat by the effects of other climate forcing agents (such as CH₄, N₂O, and various aerosols) that are included in the RCP scenarios, as shown by the divergence of the coloured lines in Figure 3.8 from the thin black CO₂-only line. Yet the total warming (due to CO₂ and other climate forcing agents) is approximately the same, as a function of cumulative emissions, across the four RCP scenarios shown in Figure 3.8. There is uncertainty in the relationship between warming and cumulative emissions, indicated by the shaded bands in the figure, and this must be taken into account when interpreting the results.

This relationship between cumulative CO₂ emissions and the increase in GMST can be used to estimate the maximum amount of CO₂ that can be emitted while limiting the temperature increase to a certain level. So, for example, in order to limit global warming to less than 2°C, as agreed in the Paris Agreement (UNFCCC, 2015), cumulative emissions of CO₂ must stay below a given level. Because of the uncertainty in this relationship, a likelihood must be attached to this level. Hence, the IPCC (2013) assessed that, to have a 50% chance of keeping global warming to less than 2°C, CO₂ emissions from 2011 onward would have to remain below 1300 billion tonnes of CO₂ (GtCO₂), roughly equal to what has already been emitted since the beginning of the Industrial Era. For a 50% chance of keeping the temperature increase to less than 1.5°C, emissions from 2011 onward would have to be limited to 550 GtCO₂. Similar carbon emissions budgets were obtained using an integrated assessment model driven by a broader range of scenarios, an approach that may be more robust (Rogelj et al., 2016). The median IPCC (2014) 1.5°C emissions budget of 550 GtCO₂ relative to 2011 is only 13.8 years of CO₂ emissions at current levels of approximately 40 Gt CO₂ per year, and we have already used about six years of this. However, several recent studies calculated this budget using an alternative approach, based on an estimate of human-caused global warming from pre-industrial times to 2015 of approximately 0.9°C (e.g., Millar et al., 2017). This leaves room for an additional approximately 0.6°C of warming to be consistent with a 1.5°C target. From this, cumulative carbon emissions budgets consistent with limiting warming to 0.6°C relative to 2010–2019 with 50% or more chance were estimated to be 760–850 GtCO₂ (Millar et al., 2017; Goodwin et al., 2018; Tokarska and Gillett, 2018), substantially more than the 390 GtCO₂ (from 2015) assessed by IPCC (2014). Conversely, accounting for carbon-cycle feedbacks involving permafrost, which were not included in the models assessed by IPCC (2014), would somewhat increase the warming for a given level of CO₂ emissions and hence somewhat reduce the emissions budgets, particularly at higher warming levels (MacDougall et al., 2015). The upcoming IPCC Special Report on Global Warming of 1.5°C will comprehensively assess these emissions budgets and give an updated estimate of the remaining allowable emissions to meet the global temperature target under the Paris Agreement.

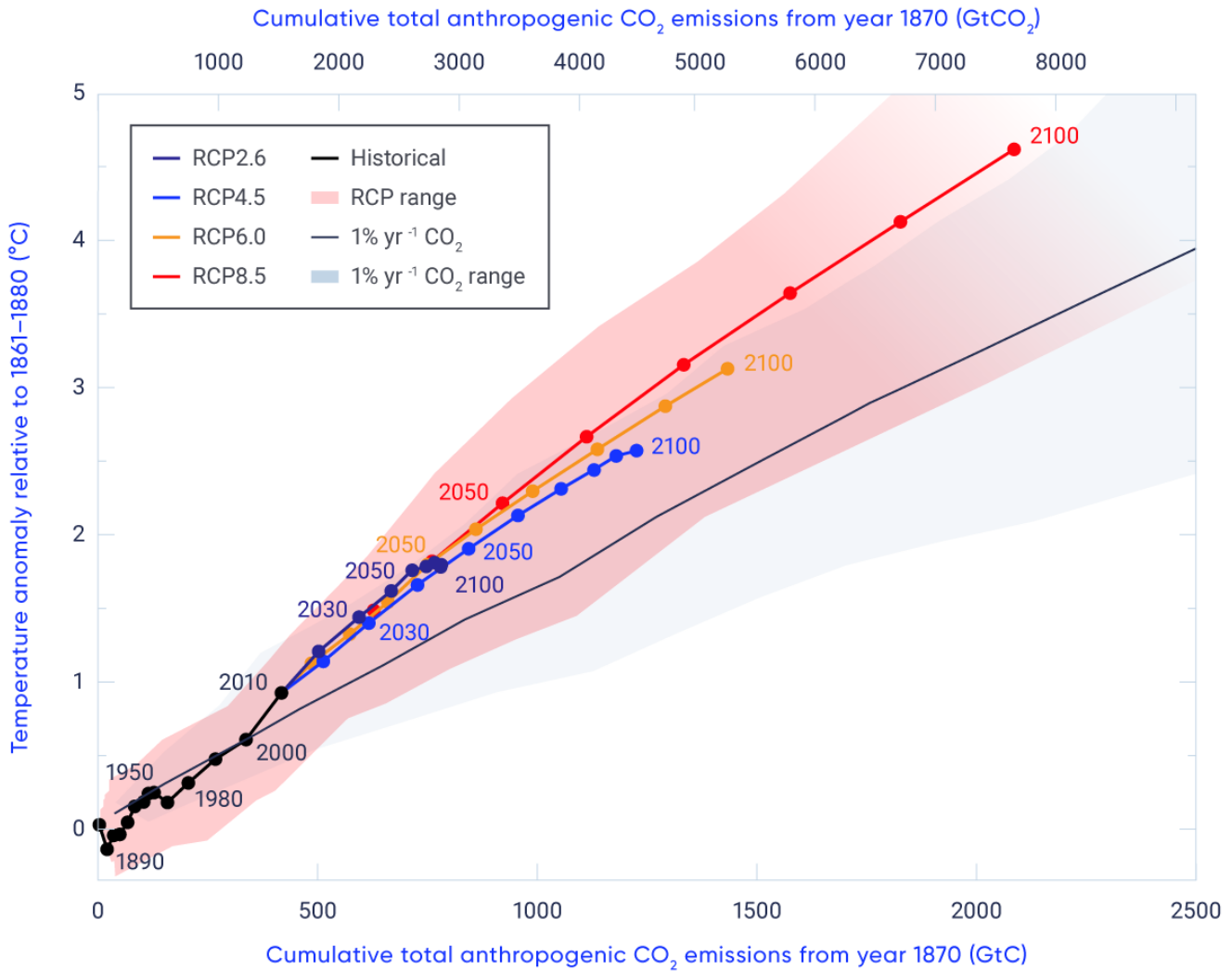


Figure 3.8: Relationship between global temperature and cumulative carbon dioxide emissions

Figure caption: Increases in global mean surface temperature with increasing cumulative carbon dioxide (CO₂) emissions (lower axis label refers to emissions in gigatonnes of carbon, upper axis label in gigatonnes of CO₂). Coloured lines show multi-model average results from the Climate Model Intercomparison Project (CMIP5) for each Representative Concentration Pathway (RCP) until 2100, and dots show decadal means. Model results over the historical period (1860 to 2010) are indicated in black. The coloured plume illustrates the multi-model spread over the historical and four RCP scenarios. The thin black line and grey area indicate the multi-model mean (line) and range (area) simulated by CMIP5 models resulting from a CO₂ increase of 1% per year.

FIGURE SOURCE: IPCC (2013).

3.4.2: Irreversibility of climate change

Earth system model simulations of the response to CO₂ emissions show that GMST remains approximately constant for many centuries following a cessation of emissions (Collins et al., 2013). For example, GMST remains high in two simulations of Environment and Climate Change Canada's first-generation Earth system model, CanESM1, under a scenario in which CO₂ emissions increase and subsequently cease, being reduced to zero in 2100 or in 2100 (Figure 3.9; Gillett et al., 2011). Similar results are obtained using other models (e.g., Matsuno et al., 2012; Matthews and Caldeira, 2008; Frölicher and Joos, 2010). Thus, regardless of when emissions cease, GMST remains approximately constant for the subsequent millennium.

Ceasing emissions of aerosols, which are short-lived and that largely exert climate-cooling effects (see Box 3.3) would lead to rapid warming, whereas ceasing short-lived GHG emissions would cause cooling (Collins et al., 2013). The response to a cessation of emissions of other long-lived GHGs is qualitatively similar to that to CO₂ (Smith et al., 2012), taking a very long time to reduce temperature. While GMST is expected to remain constant after emissions cease, other aspects of the climate system are expected to continue to change. Vegetation, ice sheet volume, deep ocean temperature, ocean acidity, and sea level are projected to change for centuries after stabilization of GMST (Collins et al., 2013).

Box 3.3: Short-lived climate forcers

Climate forcers, also referred to as climate forcing agents, act directly to change climate and include both natural and human contributors. They are often distinguished as short- or long-lived, according to their lifetime in the atmosphere. For example, carbon dioxide (CO₂), the largest climate forcer from human activity, is considered long-lived. Although often described as having a lifetime of a century or more, a single lifetime value is not strictly applicable (owing to its complex interactions with the Earth system), but an estimated 15%–40% of CO₂ emitted by the year 2100 will remain in the atmosphere, and continue to exert a climate warming effect, for more than 1000 years (Ciais et al., 2013). Short-lived climate forcers are those with a lifetime of a few days to a few decades and include sulphate aerosols and black carbon (soot) with lifetimes of a few days; tropospheric ozone and various hydrofluorocarbons, with a lifetime of a few weeks; and methane, with a lifetime of a decade or so. Reducing emissions of short-lived substances leads to lower atmospheric concentrations of these substances shortly thereafter. Many of these short-lived species contribute to poor air quality. Those that have a climate warming effect are also referred to as short-lived climate pollutants (<http://www.ccacoalition.org/en/science-resources>) and include black carbon, methane, and tropospheric ozone. In some cases, aerosols that have a cooling effect are co-emitted with short-lived warming agents (Arctic Council, 2011), complicating estimates of the near-term effectiveness of emission reductions. Short-lived climate forcers are important in climate policy discussions because targeted mitigation of those with warming effects can both slow global temperature increase and improve human health by improving air quality.

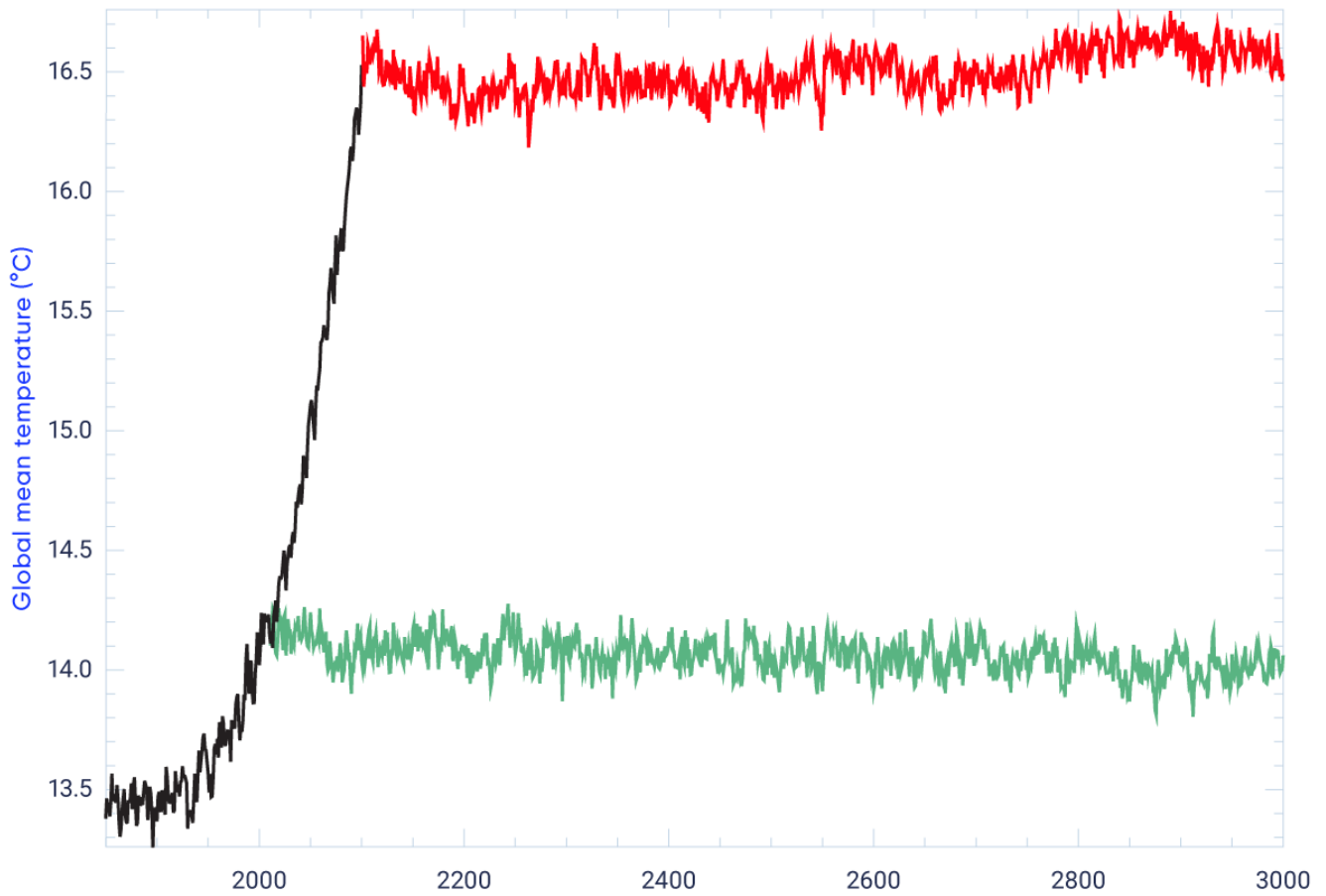


Figure 3.9: Persistent elevation of global temperature after cessation of emissions

Figure caption: Global mean surface temperature simulated by the CanESM1 model under a scenario of increasing CO₂ emissions (black), followed by a cessation of emissions in 2010 (green) and 2100 (red).

FIGURE SOURCE: GILLETT ET AL. (2011).

Section summary

In summary, many aspects of climate change are irreversible on multi-century timescales. CO₂ persisting for a century or more in the atmosphere is the main determinant of global mean temperature change, and global temperature will remain elevated even after emissions cease. GMST could be reduced only if human intervention could remove CO₂ from the atmosphere over a sustained period.

3.5: Regional downscaling

Key Message

Climate projections are based on computer models that represent the global climate system at coarse resolution. Understanding the effects of climate change for specific regions benefits from methods to downscale these projections. However, uncertainty in climate projections is larger as one goes from global to regional to local scale.

3.5.1: Downscaling strategies

Climate projections must be made using global models because many of the processes and feedbacks that shape the response of the climate system to external forcing operate at the global scale. For many applications, where only the change in some climate quantity is needed, global model projections can be used directly. This is because climate change normally applies over a much larger area than the climate itself, which can vary markedly over short distances in some regions. This is particularly the case for projected change in temperature, which has a very broad spatial structure, although local temperature may differ between, for example, the bottom of a valley and the surrounding hillsides.

However, for other applications, global climate model projections are not adequate, as they typically have horizontal spatial resolution, or grid spacing, of 100 km or coarser (see Figure 3.2 for explanation of model characteristics) (e.g., Charon, 2014). As an example, when using climate projections to drive a detailed hydrological model at the scale of a drainage basin, one needs values of future climate variables at a scale that respects local topographic, coastal, and other features, and represents high-frequency variability and extremes. Users of climate projections must therefore first evaluate whether they really need high-resolution climate

scenarios or whether they could make effective use of lower-resolution climate change scenarios. Higher resolution, in and of itself, does not necessarily indicate higher-quality or more valuable climate information. But, for many applications, higher resolution may be necessary, and can also facilitate better understanding among, and communication to, users. A caution, however, is that internal climate variability is reduced by averaging results over large areas, and so as one goes from global to regional to local scale, internal variability becomes larger, leading to larger uncertainty in projections at the local scale, relative to that at regional or global scale (Hawkins and Sutton, 2009).

When climate information at a higher spatial- or temporal-resolution is needed, there are several approaches available to take global climate model projections and “downscale” them to higher resolution for a region of interest (or even a single location). These generally fall into two categories: statistical and dynamical downscaling.

Statistical downscaling is a form of climate model “post-processing” that combines climate model projections with local or regional observations to provide climate information with more spatial detail (Maraun et al., 2010; Hewitson et al., 2014). Statistical post-processing methods typically downscale to higher resolution and correct systematic model biases. A simple example is the so-called “delta method,” in which the change in some climate quantity, obtained from a climate model projection, is added to the observed historical value of that quantity. This allows projected changes from different climate models to be used in a consistent manner, since each model’s climatological bias is eliminated. Bias correction is particularly important when using downscaled climate information to drive impact models that depend on crossing absolute thresholds. For example, snow accumulation is sensitive to whether temperature is above or below freezing.

Simple techniques like the delta method may be suitable for some quantities, such as mean temperature, but not for others, such as daily precipitation, for which biases may be manifested differently, in variability, extremes, or dry/wet spells (Maraun et al., 2010). More complex statistical downscaling approaches are required in such cases, making use of detailed high-resolution observational datasets that reflect local topographic influences. These high-resolution data are used to interpolate low-resolution climate change projections to much higher resolution. In some cases, bias correction and other refinements are applied to correct statistical properties such as variances (Werner and Cannon, 2016). Yet other statistical downscaling methods take advantage of observed relationships between large-scale atmospheric circulation patterns, which are often well simulated by climate models, and local variables. By assuming that these statistical relationships remain fixed under a changing climate, climate model projections of circulation patterns can be used to make projections of future climate at a particular location. The statistical relationships introduce some aspects of local climate that may not be well represented in the driving global model (e.g., local topography and proximity to a lake). Fundamentally, all statistical downscaling methods assume that relationships between a model’s historical simulation and observations do not change over time, and that the information provided by the climate model and historical observations at their respective spatial scales is credible. Thus, the quality of statistical downscaling is directly related to the quality and availability of observational data. Recent critical reviews provide more information on the strengths and weaknesses of statistical downscaling and bias correction methods (Hewitson et al., 2014; Maraun, 2016).

Dynamical downscaling involves the use of a regional climate model, which is a physically based climate

model (of the same level of complexity as a global model) that operates at high resolution over a limited area. Regional climate models incorporate much the same physical processes and scientific understanding as global climate models and indeed often share much of the same computer code. The important distinction is that regional climate models are driven at their lateral boundaries by output from a global climate model, as shown in Figure 3.10. The regional model also inherits errors and biases that may be present in the global model whose results are provided at the boundaries. The main advantage of dynamical downscaling is that, due to its limited area, a regional model can simulate climate on a much higher resolution than is possible with a global model, using a similar amount of computing effort. This additional detail is often desirable, particularly where the regional model output is used to drive another model (e.g., a hydrological model in which detailed basin geometry, high-frequency precipitation and extremes, and other small-scale features are essential). However, it remains an ongoing research topic to determine whether, and under what conditions, regional models add value relative to the original global model results that are being downscaled. There are no agreed-upon measures for added value (Di Luca et al., 2015; 2016; Scinocca et al., 2016), although the evidence available at the time of the IPCC Fifth Assessment indicated that there is added value in some locations owing to the better representation of topography, land/water boundaries, and certain physical processes, and that extremes are better simulated in high-resolution regional models (e.g., Flato et al., 2013).

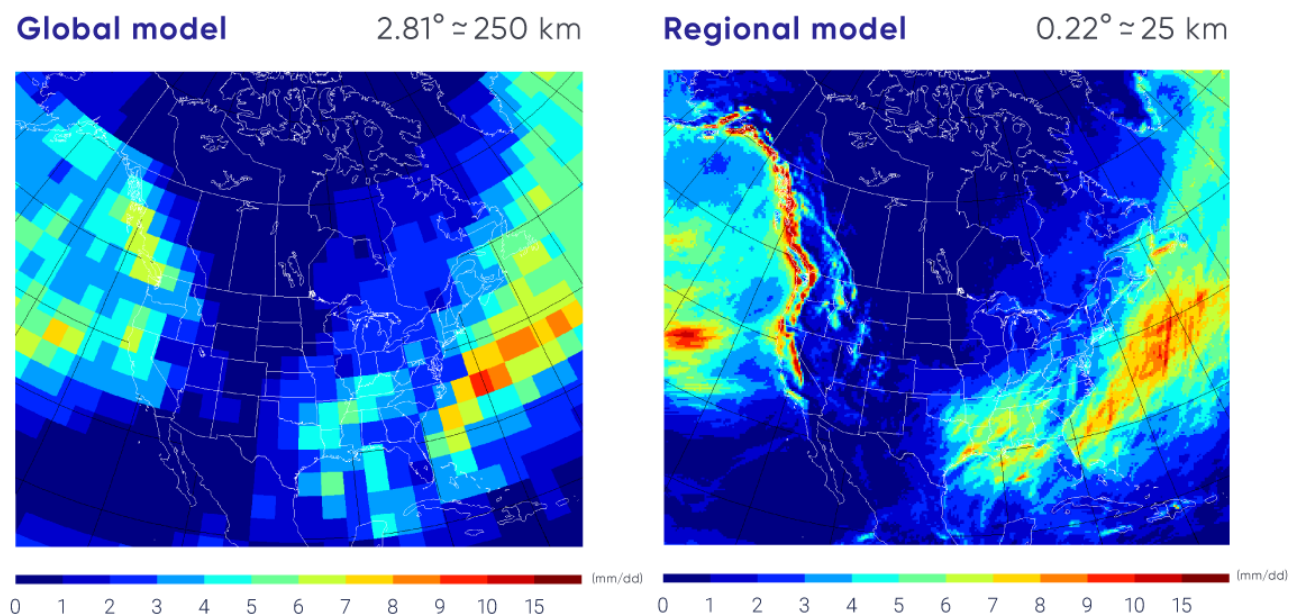


Figure 3.10: Comparative resolution of global and regional climate models

Figure caption: Monthly precipitation simulated by the global model (left) and regional model (right) based on simulations described by Scinocca et al. (2016). The global model results are provided to the regional model along its boundaries, and the regional model recomputes climate in the interior of that limited area domain. The higher-resolution regional model provides more detail, as seen in the simulated precipitation patterns.

FIGURE SOURCE: BASED ON SIMULATIONS DESCRIBED BY SCINOCCA ET AL. (2016).

An additional advantage of dynamical over statistical downscaling is that physical relationships between different climate variables (such as temperature and precipitation) are maintained. For very high-resolution dynamical downscaling (at model resolution of a few kilometres), physical processes such as convection can be resolved explicitly and can lead to improved simulation of climate variables such as precipitation extremes. Several recent studies indicate added value, including a dynamical downscaling system that includes a detailed representation of the Great Lakes (Gula and Peltier, 2012), the potential for added value near well-resolved coastlines (Di Luca et al., 2013), and evidence for improved simulation of temperature and precipitation extremes (Curry et al., 2016a,b; Erler and Peltier, 2016).

3.5.2: Downscaling results for North America and Canada

Both statistical and dynamical downscaling approaches have been applied and evaluated in many areas of the world. For North America, coordinated dynamical downscaling comparisons have been undertaken as part of the North American Regional Climate Change Assessment Program (NARCCAP: <http://www.narccap.ucar.edu/>) and the Coordinated Regional Downscaling Experiment (CORDEX: <https://na-cordex.org/>). For CORDEX, simulations were run at resolutions of approximately 25 km and 50 km. In both NARCCAP and CORDEX, Canadian models are represented. Coordinated experiments like these provide results from different regional climate models, driven at their boundaries by output from different global climate models. They also allow scientists to determine whether regional differences in projected climate change are related to the differences in the global driving models or to differences in the regional downscaling models. However, the CORDEX ensemble is considerably smaller than the CMIP global model ensemble, and studies using the CORDEX ensemble tends to focus on sub-regions rather than on Canada as a whole.

For Canada, regional climate models with smaller domains and higher resolution are being used, particularly by the Ouranos consortium and the Centre pour l'étude et la simulation du climat à l'échelle régionale (ESCER) at the Université du Québec à Montréal. Some of these simulations provide results at 15 km resolution (e.g., <https://www.ouranos.ca/en/program/climate-simulation-and-analysis/>). Statistical downscaling results are also readily available for Canada (<https://www.pacificclimate.org/data/statistically-downscaled-climate-scenarios>), with daily temperature and precipitation data at approximately 10 km resolution. These state-of-the-art downscaling approaches (Werner and Cannon, 2016) are driven by multiple global climate model projections. In addition to the more detailed spatial structure, sophisticated statistical downscaling approaches can also provide estimates of future changes in climate extremes and other indices (such as frequency of hot days, growing season length, and drought indices) that are particularly important for certain impact studies (see Chapter 4). Downscaled results can also be used as inputs to impacts models – such as hydrological, crop, and ecosystem models – that are sensitive to variability on small spatial scales and to biases in climate models (Wood et al., 2004).



Section summary

In summary, global Earth system models are necessarily limited in the level of fine spatial detail they can resolve. Techniques such as statistical or dynamical downscaling allow transformation of these large-scale projections to a level of detail better suited to the climate information needs of many local and regional impact studies. It must be noted, however, that uncertainty due to internal climate variability is reduced by area averaging (e.g., averaging over Canada or the globe), and so uncertainty in climate projections is larger as one goes from global to regional to local scale.

References

- Arctic Council (2011): Arctic Council Task Force on short-lived climate forcers: progress report and recommendations for ministers; 12 p., <https://oaarchive.arctic-council.org/bitstream/handle/11374/79/3-0a_TF_SPM_recommendations_2May11_final%20%281%29.pdf?sequence=1&isAllowed=y> [17 August 2018].
- Burkett, V.R., Suarez, A.G., Bindi, M., Conde, C., Mukerji, R., Prather, M.J., St. Clair, A.L. and Yohe, G.W. (2014): Point of departure; in *Climate Change 2014: Impacts, Adaptation, and Vulnerability; Part A: Global and Sectoral Aspects (Contribution of Working Group II to the Fifth Assessment Report of the Intergovernmental Panel on Climate Change)*, (ed.) C.B. Field, V.R. Barros, D.J. Dokken, K.J. Mach, M.D. Mastrandrea, T.E. Bilir, M. Chatterjee, K.L. Ebi, Y.O. Estrada, R.C. Genova, B. Girma, E.S. Kissel, A.N. Levy, S. MacCracken, P.R. Mastrandrea and L.L. White; Cambridge University Press, Cambridge, United Kingdom and New York, NY, USA, p. 169–194.
- Charron, I. (2014): *A guidebook on climate scenarios: using climate information to guide adaptation research and decisions*; Consortium on regional climatology and adaptation to climate change, Ouranos, Montreal, QC, Canada, 86 p.
- Ciais, P., Sabine, C., Bala, G., Bopp, L., Brovkin, V., Canadell, J., Chhabra, A., DeFries, R., Galloway, J., Heimann, M., Jones, C., Le Quééré, C., Myneni, R.B., Piao S., and Thornton, P. (2013): Carbon and other biogeochemical cycles; in *Climate Change 2013: The Physical Science Basis (Contribution of Working Group I to the Fifth Assessment Report of the Intergovernmental Panel on Climate Change)*, (ed.) T.F. Stocker, D. Qin, G.-K. Plattner, M. Tignor, S.K. Allen, J. Boschung, A. Nauels, Y. Xia, V. Bex and P.M. Midgley; Cambridge University Press, Cambridge, United Kingdom and New York, NY, USA, p. 465–570.
- Collins, M., Knutti, R., Arblaster, J., Dufresne, J.-L., Fichetef, T., Friedlingstein, P., Gao, X., Gutowski, W.J., Johns, T., Krinner, G., Shongwe, M., Tebaldi, C., Weaver, A.J. and Wehner, M. (2013): Long-term climate change: projections, commitments and irreversibility; in *Climate Change 2013: The Physical Science Basis (Contribution of Working Group I to the Fifth Assessment Report of the Intergovernmental Panel on Climate Change)*, (ed.) T.F. Stocker, D. Qin, G.-K. Plattner, M. Tignor, S.K. Allen, J. Boschung, A. Nauels, Y. Xia, V. Bex and P.M. Midgley; Cambridge University Press, Cambridge, United Kingdom and New York, NY, USA, p. 1029–1136.
- Curry, C.L., Tencer, B., Whan, K., Weaver, A.J. and Giguère, M. (2016a): Searching for added value in simulating climate extremes with a high-resolution regional climate model over western Canada; *Atmosphere-Ocean*, v. 54., p. 364–384. doi:10.1080/07055900.2016.1158146
- Curry, C.L., Tencer, B., Whan, K., Weaver, A.J., Giguère, M. and Wiebe, E. (2016b): Searching for added value in simulating climate extremes with a high-resolution regional climate model over western Canada. II: Basin-Scale Results; *Atmosphere-Ocean*, v. 54, p. 385–402.
- Di Luca, A., Argüeso, D., Evans, J.P., de Elía, R. and Laprise, R. (2016): Quantifying the overall added value of dynamical downscaling and the contribution from different spatial scales; *Journal of Geophysical Research Atmospheres*, v. 121, p. 1575–1590. doi:10.1002/2015JD024009.



Di Luca, A., de Elía, R. and Laprise, R. (2013): Potential added value of RCM's downscaled climate change signal; *Climate Dynamics*, v. 40, p. 601–618. doi:10.1007/s00382-012-1415-z

Di Luca, A., de Elía, R. and Laprise, R. (2015): Challenges in the quest for added value of regional climate dynamical down-scaling; *Current Climate Change Report*, v. 1, p. 10–21. doi:10.1007/s40641-015-0003-9

Erler, A.R. and Peltier, W.R. (2016): Projected changes in precipitation extremes for western Canada based on high-resolution regional climate simulations; *Journal of Climate*, v. 29, p. 8841–8863. doi:10.1175/JCLI-D-15-0530.1

Euskirchen, E.S., Bennett, A.P., Breen, A.L., Genet, H., Lindgren, M.A., Kurkowski, T.A., McGuire, A.D. and Rupp, T.S. (2016): Consequences of changes in vegetation and snow cover for climate feedbacks in Alaska and northwest Canada; *Environmental Research Letters*, v. 11, 19 p. doi:10.1088/1748-9326/11/10/105003

Flato, G.M. (2011): Earth system models: An overview. *WIREs Climate Change*, v. 2, p. 783–800. doi:10.1002/wcc.148

Flato, G., Marotzke, J., Abiodun, B., Braconnot, P., Chou, S.C., Collins, W., Cox, P., Driouech, F., Emori, S., Eyring, V., Forest, C., Gleckler, P., Guilyardi, E., Jakob, C., Kattsov, V., Reason C. and Rummukainen M. (2013): Evaluation of climate models; in *Climate Change 2013: The Physical Science Basis (Contribution of Working Group I to the Fifth Assessment Report of the Intergovernmental Panel on Climate Change)*, (ed.) T.F. Stocker, D. Qin, G.-K. Plattner, M. Tignor, S.K. Allen, J. Boschung, A. Nauels, Y. Xia, V. Bex and P.M. Midgley; Cambridge University Press, Cambridge, United Kingdom and New York, NY, USA, p. 741–866.

Forkel, M., Carvalhais, N., Rödenbeck, C., Keeling, R., Heimann, M., Thonicke, K., Zaehle, S. and Reichstein, M. (2016): Enhanced seasonal CO₂ exchange caused by amplified plant productivity in northern ecosystems; *Science*, v. 351, p. 696–699.

Frölicher, T.L. and Joos, F. (2010): Reversible and irreversible impacts of greenhouse gas emissions in multi-century projections with the NCAR global coupled carbon cycle-climate model; *Climate Dynamics*, v. 35, p. 1439–1459.

Fyfe, J.C., Meehl, G.A., England, M.H., Mann, M.E., Santer, B.D., Flato, G.M., Hawkins, E., Gillett, N.P., Xie, S.-P., Kosaka, Y. and Swart, N.C. (2016): Making sense of the early-2000s global warming slowdown; *Nature Climate Change*, v. 6, p. 224–228.

Gillett, N.P., Arora V.K., Zickfeld K., Marshall S.J., Merryfield W.J. (2011): Ongoing climate change following a complete cessation of carbon dioxide emissions; *Nature Geoscience*, v. 4, p. 83–87.

Goodwin, P., Katavouta, A., Roussenov, V.M., Foster, G.L., Rohling, E.J. and Williams, G. (2018): Pathways to 1.5 °C and 2 °C warming based on observational and geological constraints; *Nature Geoscience*, v. 11, p. 102–107. doi:10.1038/s41561-017-0054-8

Gula, J. and Peltier, W.R. (2012): Dynamical downscaling over the Great Lakes Basin of North America using the WRF regional climate model: The impact of the Great Lakes System on regional greenhouse warming; *Journal of Climate*, v. 25, p. 7723–7742. doi.org/10.1175/JCLI-D-11-00388.1



Hawkins, E. and Sutton, R. (2009): The potential to narrow uncertainty in regional climate predictions; *Bulletin of the American Meteorological Society*, v. 90, p. 1095–1107. doi:10.1175/2009BAMS2607.1

Hewitson, B.C., Daron, J., Crane, R.G., Zermoglio, M.F. and Jack, C. (2014): Interrogating empirical-statistical downscaling; *Climatic Change*, v. 122, p. 539–554.

IPCC [Intergovernmental Panel on Climate Change] (2013): Summary for Policymakers; in *Climate Change 2013: The Physical Science Basis (Contribution of Working Group I to the Fifth Assessment Report of the Intergovernmental Panel on Climate Change)*, (ed.) T.F. Stocker, D. Qin, G.-K. Plattner, M. Tignor, S.K. Allen, J. Boschung, A. Nauels, Y. Xia, V. Bex and P.M. Midgley; Cambridge University Press, Cambridge, United Kingdom and New York, NY, USA, p. 3–29.

IPCC [Intergovernmental Panel on Climate Change] (2014): *Climate Change 2014: Synthesis Report (Contribution of Working Groups I, II and III to the Fifth Assessment Report of the Intergovernmental Panel on Climate Change)*, (ed.) Core Writing Team, R.K. Pachauri and L.A. Meyer; IPCC, Geneva, Switzerland, 151 p.

Jones, C., Robertson, E., Arora, V., Friedlingstein, P., Shevliakova, E., Bopp, L., Brovkin, V., Hajima, T., Kato, E., Kawamiya, M., Liddicoat, S., Lindsay, K., Reick, C.H., Roelandt, C., Segschneider, J. and Tjiputra, J. (2013): Twenty-first-century compatible CO₂ emissions and airborne fraction simulated by CMIP5 earth system models under four Representative Concentration Pathways; *Journal of Climate*, v. 26, p. 4398–4413.

Kashiwase, H., Ohshima, K.I., Nihashi, S. and Eicken, H. (2017): Evidence for ice-ocean albedo feedback in the Arctic Ocean shifting to a seasonal ice zone; *Scientific Reports*, v. 7, 10 p. doi:10.1038/s41598-017-08467-z

Kharin, V.V., Merryfield, W.J., Boer, G.J. and Lee, W.-S. (2017): A postprocessing method for seasonal forecasts using temporally and spatially smoothed statistics; *Monthly Weather Review*, v. 145, p. 3545–3561. doi.org/10.1175/MWR-D-16-0337.1

Kirtman, B., Power, S.B., Adedoyin, J.A., Boer, G.J., Bojariu, R., Camilloni, I., Doblas-Reyes, F.J., Fiore, A.M., Kimoto, M., Meehl, G.A., Prather, M., Sarr, A., Schär, C., Sutton, R., van Oldenborgh, G.J., Vecchi, G. and Wang, H.J. (2013): Near-term climate change: projections and predictability; in *Climate Change 2013: The Physical Science Basis (Contribution of Working Group I to the Fifth Assessment Report of the Intergovernmental Panel on Climate Change)*, (ed.) T.F. Stocker, D. Qin, G.-K. Plattner, M. Tignor, S.K. Allen, J. Boschung, A. Nauels, Y. Xia, V. Bex and P.M. Midgley; Cambridge University Press, Cambridge, United Kingdom and New York, NY, USA, p. 953–1028. doi:10.1017/CBO9781107415324.023

Knutti, R., Sedláček, J., Sanderson, B.M., Lorenz, R., Fischer, E.M. and Eyring, V. (2017): A climate model projection weighting scheme accounting for performance and interdependence; *Geophysical Research Letters*, v. 44, p. 1909–1918. doi:10.1002/2016GL072012



Le Quéré, C., Andrew, R.M., Friedlingstein, P., Sitch, S., Pongratz, J., Manning, A.C., Korsbakken, J.I., Peters, G.P., Canadell, J.G., Jackson, R.B., Boden, T.A., Tans, P.P., Andrews, O.D., Arora, V.K., Bakker, D.C.E., Barbero, L., Becker, M., Betts, R.A., Bopp, L., Chevallier, F., Chini, L.P., Ciais, P., Cosca, C.E., Cross, J., Currie, K., Gasser, T., Harris, I., Hauck, J., Haverd, V., Houghton, R.A., Hunt, C.W., Hurtt, G., Ilyina, T., Jain, A.K., Kato, E., Kautz, M., Keeling, R.F., Goldewijk, K.K., Körtzinger, A., Landschützer, P., Lefèvre, N., Lenton, A., Lienert, S., Lima, I., Lombardozzi, D., Metzl, N., Millero, F., Monteiro, P.M.S., Munro, D.R., Nabel, J.E.M.S., Nakaoka, S.-I., Nojiri, Y., Padín, A.X., Peregon, A., Pfeil, B., Pierrot, D., Poulter, B., Rehder, G., Reimer, J., Rödenbeck, C., Schwinger, J., Séférian, R., Skjelvan, I., Stocker, B.D., Tian, H., Tilbrook, B., van der Laan-Luijkx, I.T., van der Werf, G.R., van Heuven, S., Viovy, N., Vuichard, N., Walker, A.P., Watson, A.J., Wiltshire, A.J., Zaehle, S. and Zhu, D. (2017): Global carbon budget 2017; *Earth System Science Data Discussions*, v. 10, p. 405–448. doi:10.5194/essdd-2017-123

MacDougall, A.H., Zickfeld, K., Knutti, R. and Matthews, D. (2015): Sensitivity of carbon budgets to permafrost carbon feedbacks and non-CO₂ forcings; *Environmental Research Letters*, v. 10, 10 p. doi:10.1088/1748-9326/10/12/125003

Maraun, D. (2016): Bias correcting climate change simulations – a critical review; *Current Climate Change Reports*, v. 2, p. 211–220.

Maraun, D., Wetterhall, F., Ireson, A.M., Chandler, R. E., Kendon, E.J., Widmann, M., Brienen, S., Rust, H. W., Sauter, T., Themeßl, M., Venema, V.K.C., Chun, K.P., Goodess, C.M., Jones, R.G., Onof, C., Vrac, M. and Thiele-Eich, I. (2010): Precipitation downscaling under climate change: Recent developments to bridge the gap between dynamical models and the end user; *Reviews of Geophysics*, v. 48, 34 p. doi:10.1029/2009RG000314

Matsuno, T., Maruyama, K. and Tsutsui, J. (2012): Stabilization of atmospheric carbon dioxide via zero emissions – an alternative way to a stable global environment. Part 1: examination of the traditional stabilization concept; *Proceedings Japan Academic Series B Physical Biological Science*, v. 88, p. 368–384.

Matthews, H.D. and Caldeira, K. (2008): Stabilizing climate requires near-zero emissions; *Geophysical Research Letters*, v. 35, 5 p. doi:10.1029/2007GL032388

Merryfield, W.J., Lee, W.-S., Wang, W., Chen, M. and Kumar, A. (2013): Multi-system seasonal predictions of Arctic sea ice, *Geophysical Research Letters*, v. 40, p. 1551–1556. doi:10.1002/grl.50317

Millar, R., Fuglestedt, J., Friedlingstein, P., Rogelj, J., Grubb, M., Matthews, H.D., Skeie, R.B., Forster, P.M., Frame, D.J. and Allen, M.R. (2017): Emission budgets and pathways consistent with limiting warming to 1.5° C; *Nature Geoscience*, v. 10, p. 741–747.



Myhre, G., Shindell, D., Bréon, F.-M., Collins, W., Fuglestedt, J., Huang, J., Koch, D., Lamarque, J.-F., Lee, D., Mendoza, B., Nakajima, T., Robock, A., Stephens, G., Takemura, T. and Zhang, H. (2013): Anthropogenic and natural radiative forcing; in *Climate Change 2013: The Physical Science Basis (Contribution of Working Group I to the Fifth Assessment Report of the Intergovernmental Panel on Climate Change)*, (ed.) T.F. Stocker, D. Qin, G.-K. Plattner, M. Tignor, S.K. Allen, J. Boschung, A. Nauels, Y. Xia, V. Bex and P.M. Midgley; Cambridge University Press, Cambridge, United Kingdom and New York, NY, USA, p. 659–740. doi:10.1017/CBO9781107415324.018

Nakicenovic, N., Alcamo, J., Davis, G., de Vries, B., Fenhann, J., Gaffin, S., Gregory, K., Grübler, A., Jung, T.Y., Kram, T., La Rovere, E.L., Michaelis, L., Mori, S., Morita, T., Pepper, W., Pitcher, H., Price, L., Riahi, K., Roehrl, A., Rogner, H.-H., Sankovski, A., Schlesinger, M., Shukla, P., Smith, S., Swart, R., van Rooijen, S., Victor, N. and Dadi, Z. (2000): Special report on emissions scenarios (Contribution of Working Group III to the Fifth Assessment Report of the Intergovernmental Panel on Climate Change); Cambridge University Press, Cambridge, United Kingdom and New York, NY, USA, 599 p.

Riahi, K., van Vuuren, D.P., Kriegler, E., Edmonds, J., O'Neil, B.C., Fujimori, S., Bauer, N., Calvin, K., Dellink, R., Fricko, O., Lutz, W., Popp, A., Cuaresma, J.C., KC, S., Leimbach, M., Jiang, L., Kram, T., Rao, S., Emmerling, J., Ebi, K., Hasegawa, T., Havlik, P., Humpenöder, F., Da Silva, L.A., Smith, S., Stehfest, E., Bosetti, V., Eom, J., Gernaat, D., Masui, T., Rogelj, J., Strefler, J., Drouet, L., Krey, V., Luderer, G., Harmsen, M., Takahashi, K., Baumsark, L., Doelman, J.C., Kainuma, M., Klimont, Z., Marangoni, G., Lotze-Campen, H., Obersteiner, M., Tabeau, A. and Tavoni, M. (2017): The shared socioeconomic pathways and their energy, land use, and greenhouse gas emissions implications: An overview; *Global Environmental Change*, v. 42, p. 153–168. doi.org/10.1016/j.gloenvcha.2016.05.009

Rogelj, J., Schaeffer, M., Friedlingstein, P., Gillett, N.P., Van Vuuren, D.P., Riahi, K., Allen, M. and Knutti, R. (2016): Differences between carbon budget estimates unravelled; *Nature Climate Change*, v. 6, p. 245–252.

Sanderson, B.M., Wehner, M. and Knutti, R. (2017): Skill and independence weighting for multi-model assessments; *Geoscientific Model Development*, v. 10, p. 2379–2395. doi:10.5194/gmd-10-2379-2017

Schuur, E.A.G., Bockheim, J., Canadell, J.G., Euskirchen, E., Field, C.B., Goryachkin, S.V., Hagemann, S., Kuhry, P., Lafleur, P.M., Mazhitova, H.L.G., Nelson, F.E., Rinke, A., Romanovsky, V.E., Shiklomanov, N., Tarnocai, C., Venevsky, S., Vogel, J.G. and Zimov, S.A. (2008): Vulnerability of permafrost carbon to climate change: implications for the global carbon cycle; *BioScience*, v. 58, p. 701–714. doi:10.1641/B580807

Scinocca, J.F., Kharin, V.V., Jian, Y., Qian, M.W., Lazare, M., Solheim, L. and Flato, G.M. (2016): Coordinated global and regional climate modelling; *Journal of Climate*, v. 29, p. 17–35. doi:10.1175/JCLI-D-15-0161.1

Shepherd, T.G. (2014): Atmospheric circulation as a source of uncertainty in climate change projections; *Nature Geoscience*, v. 7, p. 703–708. doi:10.1038/ngeo2253



- Sigmond, M., Fyfe, J.C., Flato, G.M., Kharin, V.V. and Merryfield, W.J. (2013): Seasonal forecast skill of Arctic sea ice area in a dynamical forecast system; *Geophysical Research Letters*, v. 40, p. 529–534. doi:10.1002/grl.50129
- Smith, S.M., Lowe, J.A., Bowerman, N.H., Gohar, L.K., Huntingford, C. and Allen, M.R. (2012): Equivalence of greenhouse-gas emissions for peak temperature limits; *Nature Climate Change*, v. 2, p. 535–538.
- Stuecker, M.F., Bitz, C.M., Armour, K.C., Proistosescu, C., Kang, S.M., Xie, S-P., Kim, D., McGregor, S., Zhang, W., Zhao, S., Cai, W., Dong, Y., Jin, F-F. (2018): Polar amplification dominated by local forcing and feedbacks. *Nature Climate Change*, v. 8, p. 1076-1081.
- Taylor, K.E., Stouffer, R.J. and Meehl, G.A. (2012): An overview of CMIP5 and the experimental design; *Bulletin American Meteorological Society*, v. 93, p. 485–498. doi:10.1175/BAMS-D-11-00094.1
- Tokarska K.B. and Gillett, N.P. (2018): Cumulative carbon emissions budgets consistent with 1.5 °C global warming; *Nature Climate Change*, v. 8, p. 269–299.
- Tokarska, K.B., Gillett, N.P., Weaver, A.J., Arora, V.K. and Eby, M. (2016): The climate response to five trillion tonnes of carbon; *Nature Climate Change*, v. 6, p. 851–855.
- UNFCCC [United Nations Framework Convention on Climate Change] (2015): The Paris Agreement; United Nations Framework Convention on Climate Change.
- van Vuuren, D.P., Edmonds, J., Kainuma, M., Riahi, K., Thomson, A., Hibbard, K., Hurtt, G.C., Kram, T., Krey, V., Lamarque, J.-F., Masui, T., Meinshausen, M., Nakicenovic, N., Smith, S.J. and Rose, S.K. (2011): The representative concentration pathways: An overview; *Climatic Change*, v. 109, p. 5–31.
- Weigel, A.P., Knutti, R., Liniger, M.A. and Appenzeller, C. (2010): Risks of model weighting in multimodel climate projections; *Journal of Climate*, v. 23, p. 4175–4191. doi: 10.1175/2010JCLI3594.1
- Werner, A.T. and Cannon, A.J. (2016): Hydrologic extremes: An intercomparison of multiple gridded statistical downscaling methods; *Hydrology and Earth System Sciences*, v. 20, p. 1483–1508. doi:10.5194/hess-20-1483-2016
- Wood, A.W., Leung, L.R., Sridhar, V. and Lettenmaier, D.P. (2004): Hydrologic implications of dynamical and statistical approaches to downscaling climate model outputs; *Climatic Change*, v. 62, p. 189–216.





CHAPTER 4

Temperature and Precipitation Across Canada

CANADA'S CHANGING CLIMATE REPORT



Government
of Canada

Gouvernement
du Canada

Canada



Authors

Xuebin Zhang, Environment and Climate Change Canada

Greg Flato, Environment and Climate Change Canada

Megan Kirchmeier-Young, Environment and Climate Change Canada

Lucie Vincent, Environment and Climate Change Canada

Hui Wan, Environment and Climate Change Canada

Xiaolan Wang, Environment and Climate Change Canada

Robin Rong, Environment and Climate Change Canada

John Fyfe, Environment and Climate Change Canada

Guilong Li, Environment and Climate Change Canada

Viatchelsav V. Kharin, Environment and Climate Change Canada

Recommended citation: Zhang, X., Flato, G., Kirchmeier-Young, M., Vincent, L., Wan, H., Wang, X., Rong, R., Fyfe, J., Li, G., Kharin, V.V. (2019): Changes in Temperature and Precipitation Across Canada; Chapter 4 *in* Bush, E. and Lemmen, D.S. (Eds.) Canada's Changing Climate Report. Government of Canada, Ottawa, Ontario, pp 112-193.



Chapter Table Of Contents

CHAPTER KEY FINDINGS (BY SECTION)

SUMMARY

4.1 Introduction

4.2: Temperature

Box 4.1: An example of climate data inhomogeneity

4.2.1: Mean temperature

4.2.1.1: Observed changes

4.2.1.2: Causes of observed changes

4.2.1.3: Projected changes and uncertainties

4.2.2: Temperature extremes and other indices

4.2.2.1 Observed changes

4.2.2.2 Causes of observed changes

4.2.2.3 Projected changes and uncertainties

4.3: Precipitation

4.3.1: Mean precipitation

4.3.1.1: Observed changes

4.3.1.2: Causes of observed changes

4.3.1.3: Projected changes and uncertainties

4.3.2: Extreme precipitation

4.3.2.1: Observed changes

4.3.2.2: Projected changes and uncertainties

Box 4.2: The impact of combined changes in temperature and precipitation on observed and projected changes in fire weather

4.4: Attribution of extreme events


Box 4.3: Methods for event attribution

4.4.1: Attribution of two recent events

4.4.1.1: 2013 Southern Alberta flood

4.4.1.2: 2016 Fort McMurray wildfire

REFERENCES

A dramatic landscape photograph featuring a lightning storm over a field of tall, golden-brown grass. The sky is dark and filled with heavy, grey clouds, with several bright, jagged lightning bolts striking down. The foreground is dominated by the dense, textured grass, which is illuminated by a low sun, creating a warm, golden glow. A dirt path or road winds through the center of the field, leading the eye towards the horizon. The overall mood is intense and powerful, capturing a moment of extreme weather.

This chapter assesses observed and projected changes in temperature and precipitation for Canada, and it presents analyses of some recent extreme events and their causes.

Chapter Key Findings

4.2: Temperature

It is *virtually certain* that Canada's climate has warmed and that it will warm further in the future. Both the observed and projected increases in mean temperature in Canada are about twice the corresponding increases in the global mean temperature, regardless of emission scenario.

Annual and seasonal mean temperatures across Canada have increased, with the greatest warming occurring in winter. Between 1948 and 2016, the best estimate of mean annual temperature increase is 1.7°C for Canada as a whole and 2.3°C for northern Canada.

While both human activities and natural variations in the climate have contributed to the observed warming in Canada, the human factor is dominant. It is *likely*¹³ that more than half of the observed warming in Canada is due to the influence of human activities.

Annual and seasonal mean temperature is projected to increase everywhere, with much larger changes in northern Canada in winter. Averaged over the country, warming projected in a low emission scenario is about 2°C higher than the 1986–2005 reference period, remaining relatively steady after 2050, whereas in a high emission scenario, temperature increases will continue, reaching more than 6°C by the late 21st century.

Future warming will be accompanied by a longer growing season, fewer heating degree days, and more cooling degree days.

Extreme temperature changes, both in observations and future projections, are consistent with warming. Extreme warm temperatures have become hotter, while extreme cold temperatures have become less cold. Such changes are projected to continue in the future, with the magnitude of change proportional to the magnitude of mean temperature change.

13 This report uses the same calibrated uncertainty language as in the IPCC's Fifth Assessment Report. The following five terms are used to express assessed levels of confidence in findings based on the availability, quality and level of agreement of the evidence: very low, low, medium, high, very high. The following terms are used to express assessed likelihoods of results: virtually certain (99%–100% probability), extremely likely (95%–100% probability), very likely (90%–100% probability), likely (66%–100% probability), about as likely as not (33%–66% probability), unlikely (0%–33% probability), very unlikely (0%–10% probability), extremely unlikely (0%–5% probability), exceptionally unlikely (0%–1% probability). These terms are typeset in italics in the text. See chapter 1 for additional explanation.

4.3: Precipitation

There is *medium confidence* that annual mean precipitation has increased, on average, in Canada, with larger percentage increases in northern Canada. Such increases are consistent with model simulations of anthropogenic climate change.

Annual and winter precipitation is projected to increase everywhere in Canada over the 21st century, with larger percentage changes in northern Canada. Summer precipitation is projected to decrease over southern Canada under a high emission scenario toward the end of the 21st century, but only small changes are projected under a low emission scenario.

For Canada as a whole, observational evidence of changes in extreme precipitation amounts, accumulated over periods of a day or less, is lacking. However, in the future, daily extreme precipitation is projected to increase (*high confidence*).

4.4: Attribution Of Extreme Events

Anthropogenic climate change has increased the likelihood of some types of extreme events, such as the 2016 Fort McMurray wildfire (*medium confidence*) and the extreme precipitation that produced the 2013 southern Alberta flood (*low confidence*).

Summary

Temperature and precipitation are fundamental climate quantities that directly affect human and natural systems. They are routinely measured as part of the meteorological observing system that provides current and historical data on changes across Canada. Changes in the observing system, such as changes in instruments or changes in location of the measurement site, must be accounted for in the analysis of the long-term historical record. The observing system is also unevenly distributed across Canada, with much of northern Canada having a very sparse network that has been in place for only about 70 years. There is **very high confidence**¹ that temperature datasets are sufficiently reliable for computing regional averages of temperature for southern Canada¹⁴ from 1900 to present and for northern Canada² from 1948 to present. There is **medium confidence** that precipitation datasets are sufficiently reliable for computing regional averages of normalized precipitation anomalies (departure from a baseline mean divided by the baseline mean) for southern Canada from 1900 to present but only **low confidence** for northern Canada from 1948 to present.

These datasets show that temperature in Canada has increased at roughly double the global mean rate, with Canada's mean annual temperature having risen about 1.7°C (**likely** range 1.1°C – 2.3°C) over the 1948–2016 period. Temperatures have increased more in northern Canada than in southern Canada, and more in winter than in summer. Annual mean temperature over northern Canada increased by 2.3°C (**likely** range 1.7°C–3.0°C) from 1948 to 2016, or roughly three times the global mean warming rate. More than half of the warming can be attributed to human-caused emissions of greenhouse gases. Climate models project similar patterns of change in the future, with the amount of warming dependent on future greenhouse gas emissions. A low emission scenario (RCP2.6), generally compatible with the global temperature goal in the Paris Agreement, will increase annual mean temperature in Canada by a further 1.8°C¹⁵ by mid-century, remaining roughly constant thereafter. A high emission scenario (RCP8.5), under which only limited emission reductions are realized, would see Canada's annual mean temperature increase by more than 6°C¹⁵ by the late 21st century. In all cases, northern Canada is projected to warm more than southern Canada, and winter temperatures are projected to increase more than summer temperatures. There will be progressively more growing degree days (a measure of the growing season, which is important for agriculture) and fewer freezing degree days (a measure of winter severity), in lock-step with the change in mean temperature.

There is **medium confidence**, given the available observing network across Canada, that annual mean precipitation has increased, on average, in Canada, with larger relative increases over northern Canada. Climate models project further precipitation increases, with annual mean precipitation projected to increase by about 7%¹⁵ under the low emission scenario (RCP2.6) and 24%¹⁵ under the high emission scenario (RCP8.5) by the late 21st century. As temperatures increase, there will continue to be a shift from snow to rain in the spring and fall seasons.

14 For simplicity, southern and northern Canada are defined according to geographical location in this report: southern Canada is defined as the region south of 60° north latitude, while the region north of this latitude is defined as northern Canada. The phrase “the North,” is used to refer to the three northern territories, based on their political boundaries (see Chapter 1, Figure 1.1).

15 The values presented in this Summary are median projections based on multiple climate models. Some models project larger increases, while others project smaller increases.

While, in general, precipitation is projected to increase in the future, summer precipitation in parts of southern Canada is projected to decrease by the late 21st century under a high emission scenario. However, there is lower confidence in this projected summer decrease than in the projected increase in annual precipitation. There is *high confidence* in the latter because different generations of models produce consistent projections, and because increased atmospheric water vapour in this part of the world should translate into more precipitation, according to our understanding of physical processes. The lower confidence for summer decreases in southern Canada is because this region is at the northern tip of the region in the continental interior of North America where precipitation is projected to decrease, and at the transition to a region where precipitation is projected to increase. The atmospheric circulation-controlled pattern is uncertain at its edge, and different models do not agree on the location of the northern boundary of this pattern.

The most serious impacts of climate change are often related to changes in climate extremes. There have been more extreme hot days and fewer extreme cold days — a trend that is projected to continue in the future. Higher temperatures in the future will contribute to increased fire potential (“fire weather”). Extreme precipitation is also projected to increase in the future, although the observational record has not yet shown evidence of consistent changes in short-duration precipitation extremes across the country.

The changing frequency of temperature and precipitation extremes can be expected to lead to a change in the likelihood of events such as wildfires, droughts, and floods. The emerging field of “event attribution” provides insights about how climate change may have affected the likelihood of events such as the 2013 flood in southern Alberta or the 2016 Fort McMurray wildfire. In both cases, human-caused greenhouse gas emissions may have increased the risk of such extreme events relative to their risk in a pre-industrial climate.

4.1: Introduction

Temperature and precipitation have a critical influence on both human society and natural systems. They influence decisions about the most suitable crops to grow in a region, building heating and cooling requirements, and the size of a street storm drain. Temperature and precipitation are also the best monitored and most heavily studied climate variables. This chapter focuses on changes in mean and extreme temperature and precipitation across Canada. It assesses past changes, our understanding of the causes of these changes, as well as future projections. In addition, we evaluate climate indices derived from temperature and precipitation data that are relevant to impacts or planning, such as heating, cooling, and growing degree days. This report also assesses changes to the physical environment that are driven mainly by the combination of temperature and precipitation, such as fire weather (see Box 4.2); snow and ice conditions (see Chapter 5); and river runoff, flood, and drought (see Chapter 6). Other climate variables, such as mean and extreme wind speeds, are not assessed in this report owing to limited analyses of available observations and limited research on the mechanisms and causes of observed and projected changes in Canada, although they are highly relevant to issues such as wind-energy production and building codes.

Extreme climate events frequently result in costly climate impacts. A single event, such as the 2013 flood in southern Alberta, can result in damage valued at billions of dollars. To better understand whether climate change has contributed to the occurrence of a particular extreme event, we assess the extent to which human influence on the climate may have played a role in such catastrophic events. As the science of event attribution is still emerging, we provide a general description of event attribution, along with two examples: the 2013 flood in southern Alberta and the 2016 Fort McMurray wildfire.

Canadian climate is wide ranging, varying from one region to another. It also naturally fluctuates from one year to another and from one decade to another, on the backdrop of human-induced changes in the climate. As we will see, natural internal climate variability¹⁶ is an important contributor to some of the observed changes discussed in this chapter. Natural internal climate variability refers to the short-term fluctuations around the mean climate at a location or over a region. Some aspects of natural variability are associated with large-scale “modes of variability,” which are robust features in the climate system with identifiable spatial and temporal characteristics (see Chapter 2, Box 2.5). For example, the positive (warm) phase of El Niño–Southern Oscillation (ENSO), known as El Niño, tends to be associated in winter with warmer air temperatures and drier conditions across much of Canada. The opposite is true during the negative (cold) phase of ENSO, known as La Niña. Other common modes of variability are also characterized by positive (warm) or negative (cold) phases that tend to be associated with warmer or cooler seasonal temperatures for all or parts of Canada (see Chapter 2, Box 2.5).

16 There are two types of variability in the climate not caused by human activities. One is a result of the chaotic nature of the climate system, referred to as natural internal climate variability. The other is a response to natural forcing external to the climate system, such as those caused by solar or volcanic activities (see Chapter 2).



4.2: Temperature

Key Message

It is *virtually certain* that Canada's climate has warmed and that it will warm further in the future. Both the observed and projected increases in mean temperature in Canada are about twice the corresponding increases in the global mean temperature, regardless of emission scenario.

Key Message

Annual and seasonal mean temperatures across Canada have increased, with the greatest warming occurring in winter. Between 1948 and 2016, the best estimate of mean annual temperature increase is 1.7°C for Canada as a whole and 2.3°C for northern Canada.

Key Message

While both human activities and natural variations in the climate have contributed to the observed warming in Canada, the human factor is dominant. It is *likely* that more than half of the observed warming in Canada is due to the influence of human activities.

Key Message

Annual and seasonal mean temperature is projected to increase everywhere, with much larger changes in northern Canada in winter. Averaged over the country, warming projected in a low emission scenario is about 2°C higher than the 1986–2005 reference period, remaining relatively steady after 2050, whereas in a high emission scenario, temperature increases will continue, reaching more than 6°C by late the 21st century.

Key Message

Future warming will be accompanied by a longer growing season, fewer heating degree days, and more cooling degree days.

Key Message

Extreme temperature changes, both in observations and future projections, are consistent with warming. Extreme warm temperatures have become hotter while extreme cold temperatures have become less cold. Such changes are projected to continue in the future, with the magnitude of change proportional to the magnitude of mean temperature change.

Temperatures referred to in this chapter are surface air temperatures, typically measured 2 m above the ground, which have an immediate effect on human comfort and health, play an important role in determining the types of crops a farmer can grow, and influence the functioning of local ecosystems. Temperatures in Canada vary widely across the country. The lowest temperature on record is -63°C , observed at Snag, Yukon, on February 3, 1947. The highest temperature on record is 45°C , observed at Midale and Yellow Grass, Saskatchewan, on July 5, 1937. Annual mean temperature provides a simple measure of the overall warmth of a region: it varies from about 10°C in some southern regions to about -20°C in the far north. Seasonally, this variability is even more pronounced. Winter averages range from -5°C in the south to about -35°C in the far north, while summer averages vary from about 22°C in the south to 2°C in the far north (Gullett and Skinner, 1992).

In some locations in Canada, temperatures have been observed for a long time. For example, an observing site in Toronto has provided continuous daily temperature records since 1840. Multiple sites have temperature records that date back a century or longer. However, the availability of temperature data is unevenly distributed across the country or over different time periods. Observation sites are relatively densely distributed in the populated portion of southern Canada, while, for much of Canada, especially northern Canada, observations are sparse (see Figure 4.1), and very few observation sites predate 1948. As a result, the analysis of past changes in temperature for Canada as a whole is limited to the period since 1948, while 1900 can be used as a starting point for records in southern Canada (Vincent et al., 2015; DeBeer et al., 2016).

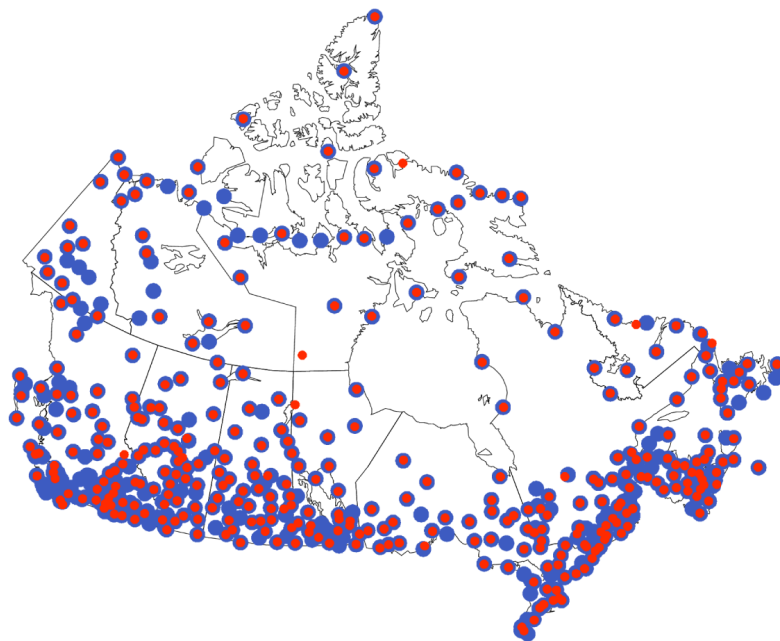


Figure 4.1: Observing stations for precipitation and temperature in Canada

Figure caption: Location of stations for which long-term precipitation (blue) and temperature (red) observations exist and for which the data have been homogenized (for temperature) and adjusted (for changes in the instruments for precipitation). Over the past two decades, monitoring technology has evolved and the climate observing network has transitioned from manual to automated observations. Procedures are currently under develop-

ment for joining and adjusting past manual and current automated climate observations in order to preserve continuity for climate monitoring and trend analysis (Milewska et al. 2018; Vincent et al. 2018).

FIGURE SOURCE: CLIMATE RESEARCH DIVISION, ENVIRONMENT AND CLIMATE CHANGE CANADA.

Temperature is also a key indicator of the climate response to human emissions of greenhouse gases (GHGs), as increasing GHG concentrations result in warming of the lower atmosphere (see Chapter 2, Section 2.3). While the original purpose of historical observations was to monitor daily to seasonal climate variability and support weather prediction, today these observations also support climate change impact studies and climate services. Monitoring instruments, observational sites, and their surrounding environment, as well as observation procedures, have undergone changes over the past century to meet new needs and to introduce new technology. These changes also introduce non-climatic changes, referred to as “data inhomogeneities,” in data records. Inhomogeneities affect the reliability of long-term trend assessment if not accounted for (Milewska and Vincent, 2016; Vincent et al., 2012, see Box 4.1). In particular, the reduction in the number of manned observational sites, with many being converted to automatic stations, has necessitated the integration of data from these different sources, which has proven challenging. Changes identified in the historical data archive reflect changes in both climate and data inhomogeneity (Vincent et al., 2012). Techniques for removing climate data inhomogeneity (“climate data homogenization”) have been developed to identify such artifacts in climate records and remove them (see Box 4.1; Vincent et al., 2002, 2012, 2017; Wang et al., 2007, 2010).

Box 4.1: An example of climate data inhomogeneity

The record of observed temperature at Amos, Quebec, shows how changes in sites and their surrounding environment can affect the estimation of long-term changes in the climate. Between 1927 and 1963, the Stevenson screen at the Amos station was located at the bottom of a hill (see Figure 4.2a) and was moved after 1963 (see Figure 4.2b) to level ground several metres away from its original place. The site was sheltered by trees and a building between 1927 and 1963, which could have prevented the cold air from draining freely during nighttime. The current site has an open exposure and is more representative of its surrounding region. Careful comparison of the temperature data at this site with those at a nearby station revealed two step-changes, one of -0.8°C in 1927 and another of 1.3°C in 1963 (see Figure 4.2c). The station history files do not provide information on the cause of the first step, but it is possible that the screen was also relocated at that time. These differences resulted in the original temperature data showing an increasing trend of 2.4°C for 1951–1995 (see Figure 4.2d), whereas, after the artifact in temperature reading was removed, a warming of only 0.8°C was shown.

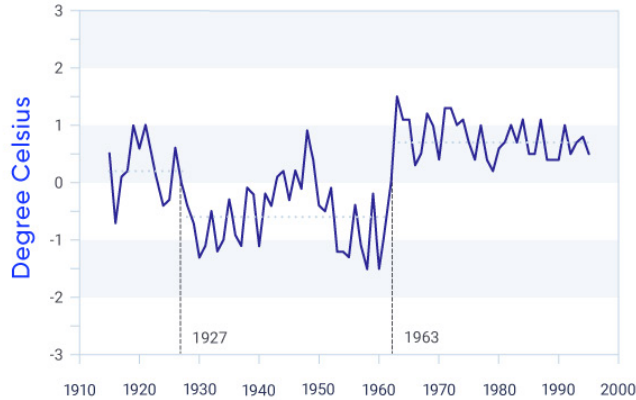
a) Amos, Quebec site before 1963



b) Amos, Quebec site after 1963



c) Difference between Amos, QC and reference station



d) Temperature prior to and after adjustment

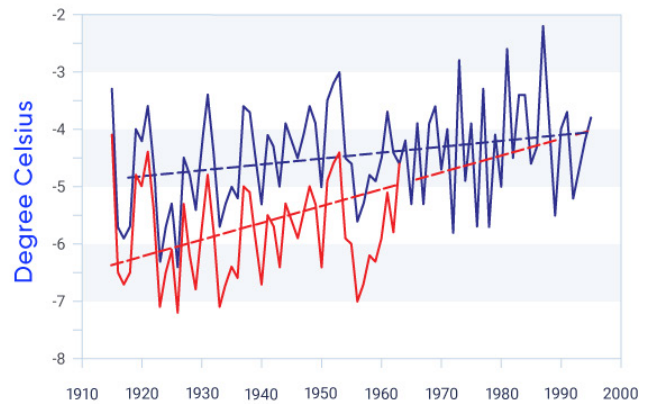


Figure 4.2: How artifacts in instrument data can affect temperature change estimates

Figure caption: Photos of the observing site Amos, Quebec, taken by inspectors showing the site before 1963 (a) and after 1963 (b). (c) Time series of the difference in the annual mean of the daily minimum temperatures between Amos and a reference station shows a decreasing step in 1927 and an increasing step in 1963, (d) The original (red line) and adjusted (blue line) time series of the annual mean of the daily minimum temperatures. The red dashed line shows an increasing trend of 2.4°C for 1915–1995 in the original series, while the blue dashed line shows an increasing trend of 0.8°C for 1915–1995 in the homogenized data.

FIGURE SOURCE: CLIMATE RESEARCH DIVISION, ENVIRONMENT AND CLIMATE CHANGE CANADA.

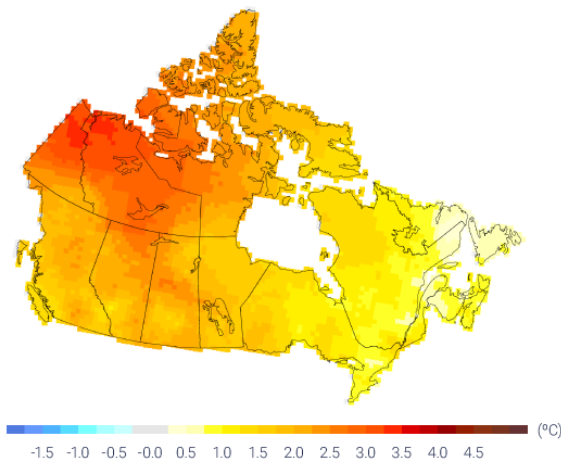
4.2.1: Mean temperature

4.2.1.1: Observed changes

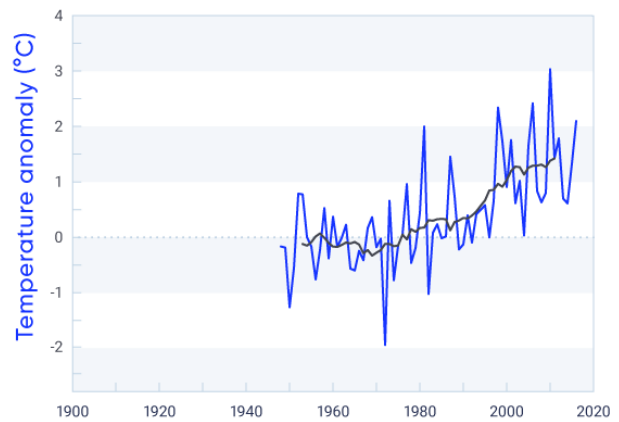
The annual average temperature in Canada increased by 1.7°C (*likely* range 1.1°C –2.3°C¹⁷) between 1948 and 2016 (updated from Vincent et al., 2015; Figure 4.3 and Table 4.1), roughly twice the increase observed for the Earth as a whole (0.8°C for 1948–2016 according to the global mean surface temperature dataset produced by the Met Office Hadley Centre and the Climatic Research Unit at the University of East Anglia, UK, HadCRUT4 [Osborn and Jones, 2014]). Warming was not uniform across seasons, with considerably more warming in winter than in summer. The mean temperature increased by 3.3°C in winter, 1.7°C in spring, 1.5°C in summer, and 1.7°C in autumn between 1948 and 2016 (see Figure 4.4 and Table 4.1). The changes in temperatures are significant at the 5% level (i.e., there is only a 5% possibility that such changes are due to chance). As well, warming was unevenly distributed across the country. The largest increases in the annual mean temperature were in the northwest, where it increased by more than 3°C in some areas. Annual mean temperature over northern Canada increased by 2.3°C (*likely* range 1.7 °C–3.0°C) from 1948 to 2016, or roughly three times the global mean warming rate. Warming was much weaker in the southeast of Canada, where average temperature increased by less than 1°C in some maritime areas. Winter warming was predominant in northern British Columbia and Alberta, Yukon, Northwest Territories, and western Nunavut, ranging from 4°C to 6°C over the 1948–2016 period. Spring had a similar warming pattern, but with smaller magnitude. Summer warming was much weaker than that in winter and spring, but the magnitude of the warming was generally more uniform across the country than during other seasons. During autumn, most of the warming was observed in the northeast regions of Canada (mainly in northern Northwest Territories, Nunavut, and northern Quebec). In addition to higher temperatures, the reduction in snow cover (see Chapter 5) and earlier snowmelt (see Chapter 6) also indicate Canada has warmed.

17 The 95% uncertainty range of the trend estimate based on the annual temperature is 1.1 °C–2.3°C. Here and elsewhere, in this chapter, computed 90% and 95% uncertainty ranges are referred to as the likely range (nominally representing 66% likelihood). This is done to account for other sources of uncertainty, such as data quantity and spatial/temporal coverage.

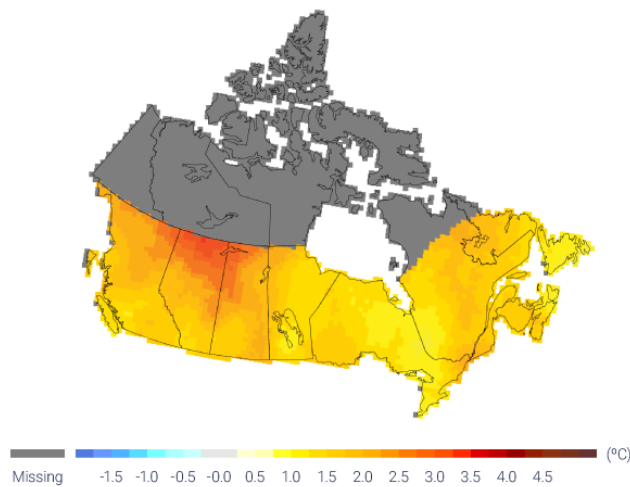
a) 1948–2016



b) 1948–2016



c) 1900–2016



d) 1900–2016

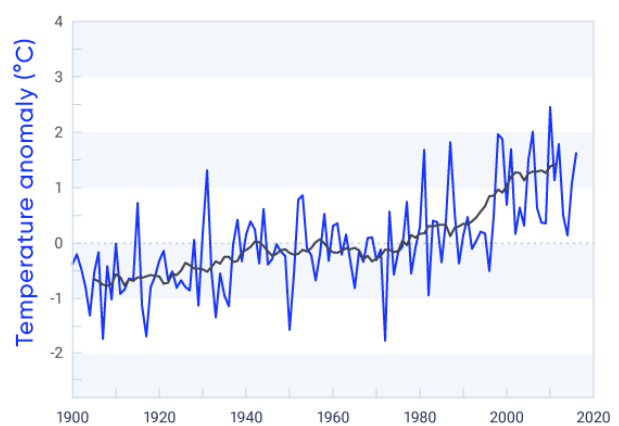


Figure 4.3: Trends in annual temperatures across Canada

Figure caption: Observed changes (°C) in annual temperature between (a) 1948 and 2016 and (c) 1900 and 2016. Changes are computed based on linear trends over the respective periods. Annual temperature anomalies (departures from baseline means) are expressed relative to the mean for the period 1961–1990 (b) for Canada as a whole and (d) for southern Canada (south of 60° north latitude); the black lines are 11-year running means. Estimates are derived from the gridded station data. There are insufficient data in northern Canada to confidently calculate warming trends from 1900 to 2016.

FIGURE SOURCE: UPDATED FROM FIGURE 2 OF VINCENT ET AL., 2015.

Table 4.1: Observed changes in annual and seasonal mean temperature between 1948 and 2016 for six regions and for all Canadian land area^a

REGION	CHANGE IN TEMPERATURE, °C				
	Annual	Winter	Spring	Summer	Autumn
British Columbia	1.9	3.7	1.9	1.4	0.7
Prairies	1.9	3.1	2.0	1.8	1.1
Ontario	1.3	2.0	1.5	1.1	1.0
Quebec	1.1	1.4	0.7	1.5	1.5
Atlantic	0.7	0.5	0.8	1.3	1.1
Northern Canada	2.3	4.3	2.0	1.6	2.3
Canada	1.7	3.3	1.7	1.5	1.7

^a Changes are represented by linear trends over the period. Estimates are derived from the gridded station data. There is a lack of data for northern Canada (see Figure 4.1).

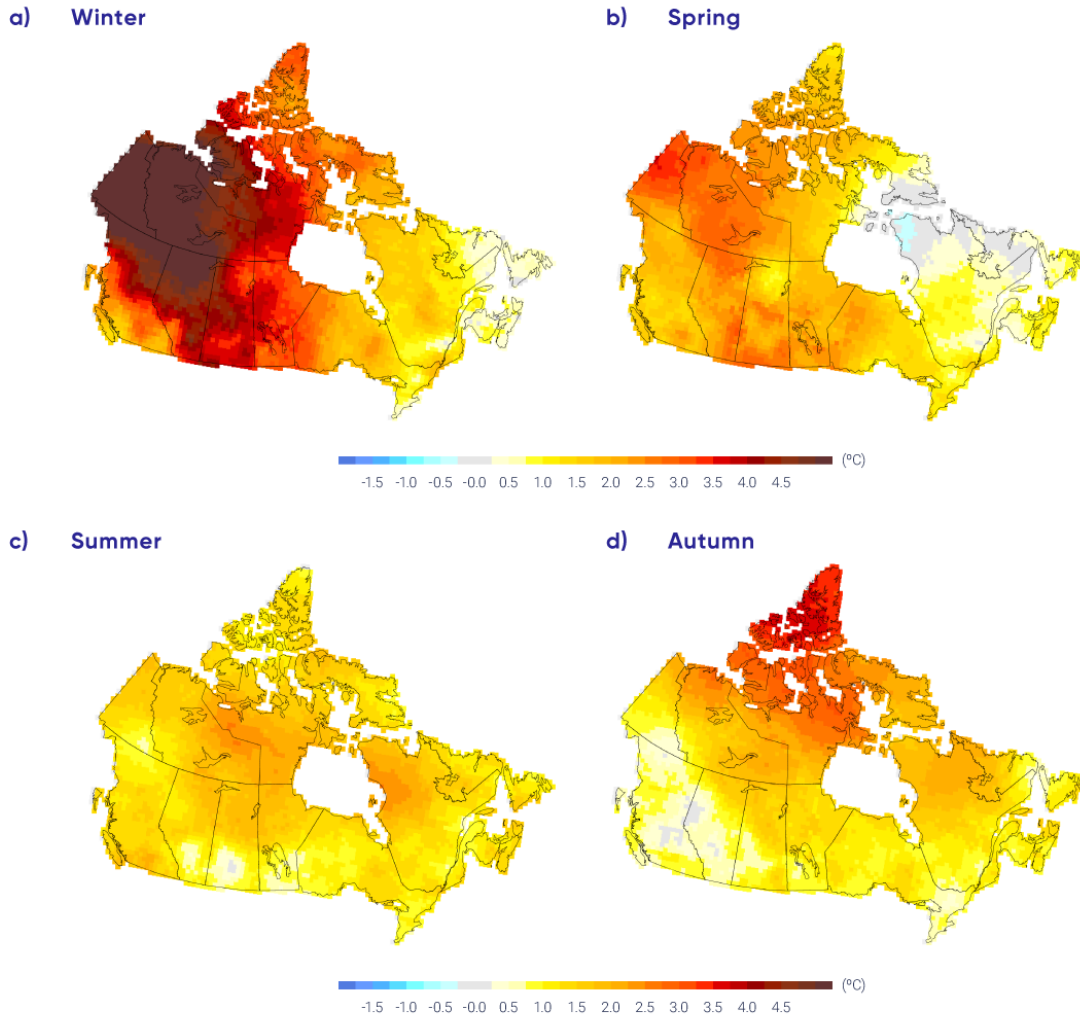


Figure 4.4: Trends in seasonal temperatures across Canada

Figure caption: Observed changes (°C) in seasonal mean temperatures between 1948 and 2016 for the four seasons. Estimates are derived based on linear trends in the gridded station data.

FIGURE SOURCE: UPDATED FROM FIGURE 3 OF VINCENT ET AL., 2015.

In southern Canada, annual mean temperature increased by 1.9°C between 1900 and 2016 (updated from Vincent et al., 2015). This warming is significant at the 5% level. This temperature did not rise steadily over time. Temperature increased until about the 1940s, decreased slightly until 1970, and then increased rapidly through 2016. This long-term behaviour of temperature is consistent with that observed globally (see Chapter 2, Section 2.2.1; Hartmann et al., 2013), but the magnitude of warming in Canada is larger. Mean temperature in southern Canada increased by 2.8°C in winter, 2.2°C in spring, 1.7°C in summer, and 1.6°C in autumn during the same period.

4.2.1.2: Causes of observed changes

It is *extremely likely* that human activities have caused more than half of the observed increase in global mean surface temperature from 1951 to 2010 (Bindoff et al., 2013). This causal effect was established through detection and attribution analysis, comparing the observed changes with the natural internal climate variability and with the expected climate responses to human activities (see Chapter 2, Section 2.3.4). Changes in the climate become detectable if they are large when compared with natural internal climate variability, and the change is attributed to human activity if it is (1) consistent with the expected “fingerprint” of human-caused change, as simulated by climate models (see Chapter 3); and (2) inconsistent with other plausible causes. For Canada and the Arctic, where natural internal variability of temperature is high, attribution of observed warming is more difficult than it is on a global scale. Nevertheless, evidence of anthropogenic influence on Canadian temperature has emerged (Gillett et al., 2004; Zhang et al., 2006; Wan et al., 2018), with a detectable contribution to warming in annual and seasonal temperatures and in extreme temperatures.

Two modes of natural internal climate variability that affect temperatures in Canada are the Pacific Decadal Oscillation (PDO) and the North Atlantic Oscillation (NAO) (see Chapter 2, Box 2.5). About 0.5°C of the observed warming of 1.7°C over the 1948–2012 period can be explained by a linear relationship between the PDO and the NAO. Assuming this is completely due to natural climate variability, roughly 1.1°C (*likely* range 0.6°C–1.5°C) of the observed 1.7°C increase in annual mean temperature in Canada from 1948–2012 can be attributed to human influence (see Figure 4.5; Wan et al., 2018). There is a 33% probability that anthropogenic influence increased Canadian temperature by at least 0.9°C. It is *likely* that more than half of the observed warming in Canada is due to human influence. The effects of natural internal climate variability on Canadian temperature trends differ in different parts of Canada, enhancing the warming trend in the western Canada and reducing the warming trend in eastern Canada over the past half of the 20th century (Vincent et al., 2015). The detection of anthropogenic influence on Canadian temperature is also corroborated by other independent evidence, including the attribution of Arctic temperature change to the influence of GHGs and aerosols (Najafi et al., 2015). The reduction in spring snow pack and the ensuing reduction in summer streamflow in British Columbia have been attributed to anthropogenic climate change (Najafi et al. 2017a, 2017b; see Chapter 6, Section 6.2.1). Anthropogenic warming has also increased fire risk in Alberta (Kirchmeier-Young et al., 2017a; see Section 4.4.1.2).

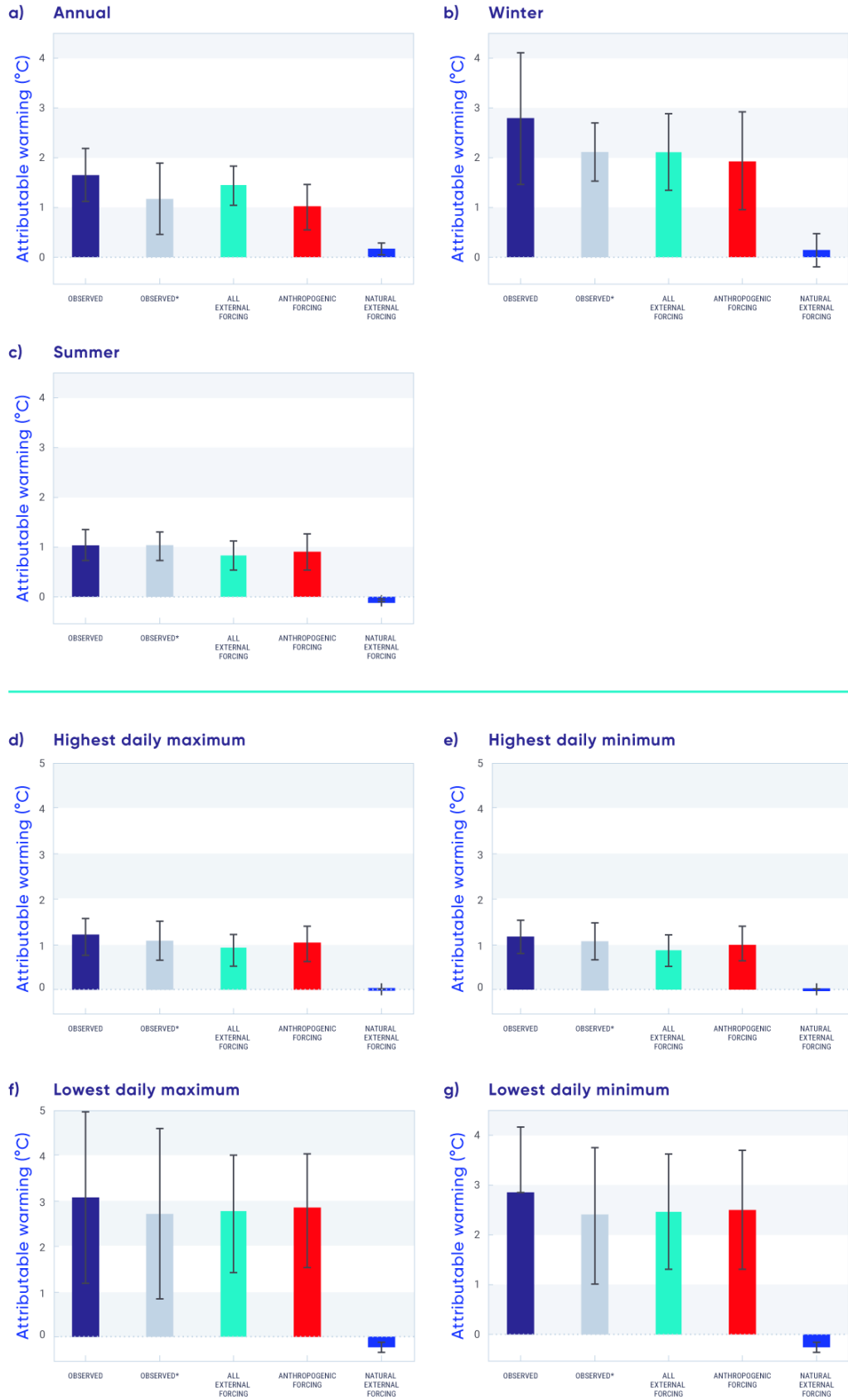


Figure 4.5: Attribution of causes to temperature change in Canada, 1948–2012

Figure caption: Changes in the observations (Observed, navy) and in the observed data removing the effects of the Pacific Decadal Oscillation and the North Atlantic Oscillation (Observed*, grey), along with the estimated contribution of all external forcing, anthropogenic forcing, and natural external forcing (effects of solar and volcanic activities) to observed changes in mean (a, b, c) and extreme (d, e, f, g) temperatures for Canada as a whole over the 1948–2012 period. The top panels show the estimations of attributable warming for (a) annual, (b) winter, and (c) summer mean temperatures. The bottom panels show estimates of attributable warming for extreme temperatures, including (d) annual highest daily maximum temperature, (e) annual highest daily minimum temperature, (f) annual lowest daily maximum temperature, and (g) annual lowest daily minimum temperature. The thin black bars indicate the 5%–95% uncertainty range.

FIGURE SOURCE: ADAPTED FROM FIGURE 7 OF WAN ET AL., 2018

4.2.1.3: Projected changes and uncertainties

Earth system models or global climate models provide projections of future climate change based on a range of future scenarios incorporating GHGs, aerosols, and land-use change (see Chapter 3, Section 3.3.1). The fifth phase of the Coupled Model Intercomparison Project (CMIP5, see Chapter 3, Box 3.1) was an internationally coordinated effort that produced a multi-model ensemble of climate projections. Results from this ensemble specific to Canada have been generated using output from 29 CMIP5 models, based on three scenarios: a low emission scenario (RCP2.6), a medium emission scenario (RCP4.5), and a high emission scenario (RCP8.5). Results for a fourth scenario that was part of the CMIP5 protocol (RCP6.0) are also available, but from fewer models. These multi-model results are described by Environment and Climate Change Canada (ECCC, 2016) and are available for download from the [Canadian Climate Data and Scenarios website](http://climate-scenarios.canada.ca/?page=download-intro) (<<http://climate-scenarios.canada.ca/?page=download-intro>>).

In the following, multi-model climate change projections for 2031–2050 and 2081–2100 (relative to a 1986–2005 reference period) are shown for Canada for a low emission scenario (RCP2.6) and a high emission scenario (RCP8.5), spanning the range of available scenarios. The low emission scenario assumes rapid and deep emission reductions and near-zero emissions this century, whereas the high emission scenario assumes continued growth in emissions this century. The two time periods were chosen to provide information for the near term (2031–2050), when differences in emission scenarios are modest, and for the late century (2081–2100), when climatic responses to the low and high emission scenarios will have diverged considerably. This latter difference illustrates the long-term climate benefit associated with aggressive mitigation efforts. The multi-model median change is shown in map form, along with time series of the average from individual models, which is computed for all Canadian land area. The box and whisker symbols at the right side of the time series provide an indication of the spread across models for 2081–2100. Values for different regions in Canada are provided in Table 4.2.

Table 4.2: Projected change in annual mean surface air temperature for six regions and for all Canadian land area, relative to 1986–2005^a

REGION ^b	SCENARIO; PERIOD; MEDIAN TEMPERATURE (25TH, 75TH PERCENTILE), °C			
	RCP2.6		RCP8.5	
	2031–2050	2081–2100	2031–2050	2081–2100
British Columbia	1.3 (0.8, 1.9)	1.6 (1.1, 2.1)	1.9 (1.4, 2.5)	5.2 (4.3, 6.2)
Prairies	1.5 (1.1, 2.1)	1.9 (1.2, 2.2)	2.3 (1.7, 3.0)	6.5 (5.2, 7.0)
Ontario	1.5 (1.1, 2.1)	1.7 (1.0, 2.1)	2.3 (1.7, 2.9)	6.3 (5.3, 6.9)
Quebec	1.5 (1.0, 2.1)	1.7 (1.0, 2.2)	2.3 (1.7, 2.9)	6.3 (5.3, 6.9)
Atlantic	1.3 (0.9, 1.8)	1.5 (0.9, 2.0)	1.9 (1.5, 2.4)	5.2 (4.5, 6.1)
North	1.8 (1.2, 2.5)	2.1 (1.3, 2.5)	2.7 (2.0, 3.5)	7.8 (6.2, 8.4)
Canada	1.5 (1.0, 2.1)	1.8 (1.1, 2.5)	2.3 (1.7, 2.9)	6.3 (5.6, 7.7)

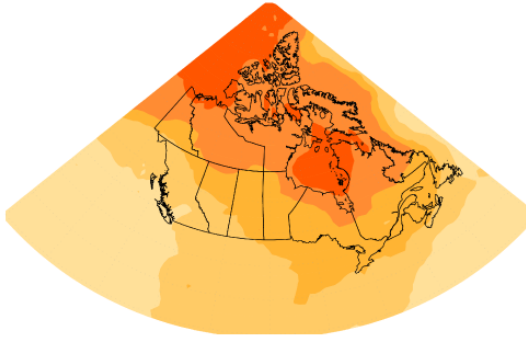
^a The median or 50th percentile value is based on the CMIP5 multi-model ensemble. The 25th percentile value indicates that 25% of the CMIP5 model projections have a change smaller than this value. The 75th percentile value indicates 25% of CMIP5 model projections have a change larger than this value.

^b The linear warming trend from 1948 (start date for climate trend analysis for all of Canada based on historical observations) to 1996 (mid-point of 1986–2005) is calculated to be 1.2°C. ^c Regions are defined by political boundaries; “North” includes the three territories (see Figure 1.1).

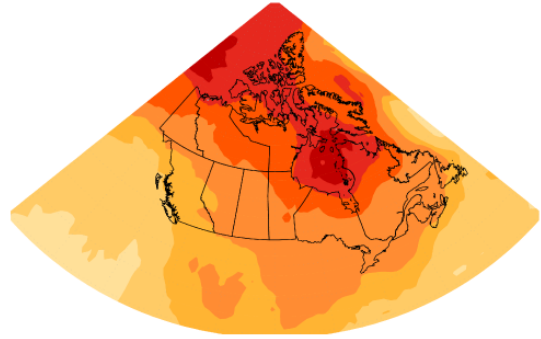
Projected temperature changes for winter (December–February average), summer (June–August average), and annual mean are shown in Figures 4.6, 4.7, and 4.8, respectively. Enhanced warming at higher latitudes is evident in the winter and annual mean. This is a robust feature of climate projections, both for Canada and the Earth, and is due to a combination of factors, including reductions in snow and ice (and thus a reduction in albedo) and increased heat transport from southern latitudes (see Chapter 3). This high-latitude amplification is not apparent in the summer maps because, over the Arctic Ocean, summer temperatures remain near 0°C – the melting temperature of snow and sea ice. In the near term (2031–2050), the differences in pattern and magnitude between the low emission scenario (RCP2.6) and the high emission scenario (RCP8.5) are modest (on the order of 0.5°C to 1°C). However, for the late century (2081–2100), the differences become very large. Under the high emission scenario, projected temperature increases are roughly 4°C higher, when averaged for Canada as a whole, than under the low emission scenario. The differences are even greater in northern Canada and the Arctic in winter. In southern Canada, projected winter temperature change is larger in the east than in the west, with British Columbia projected to warm slightly less than elsewhere in Canada. The projected summer change is more uniform across the country.

a) Temperature change RCP2.6 (2031–2050)

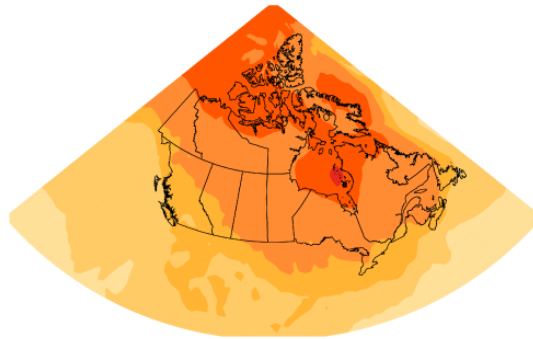
December–February

**b) Temperature change RCP8.5 (2031–2050)**

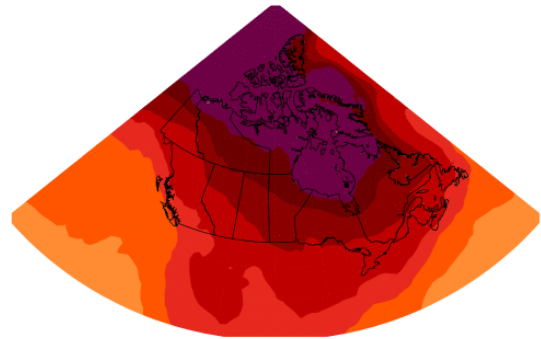
December–February

**c) Temperature change RCP2.6 (2081–2100)**

December–February

**d) Temperature change RCP8.5 (2081–2100)**

December–February



-2 -1.5 -1 -0.5 0 0.5 1 1.5 2 3 4 5 7 9 11 (°C)

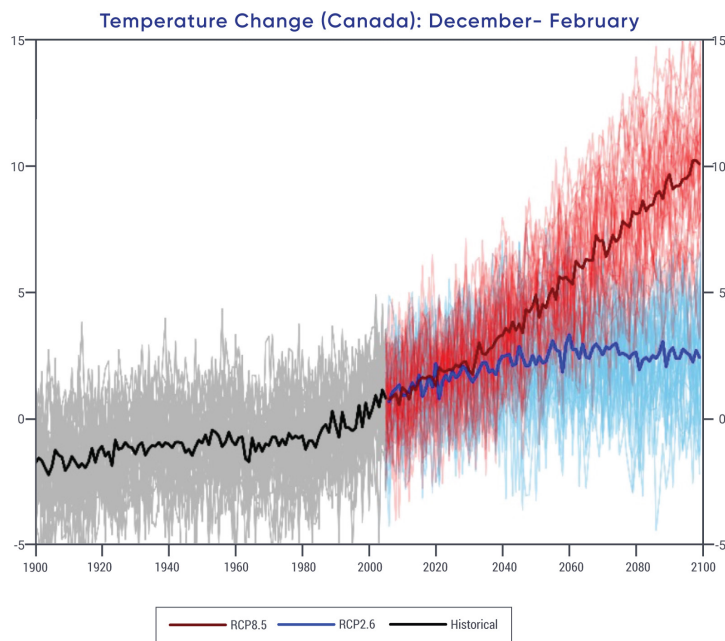


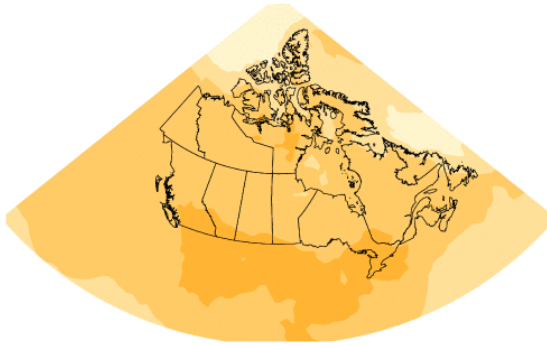
Figure 4.6: Projected temperature changes for winter season



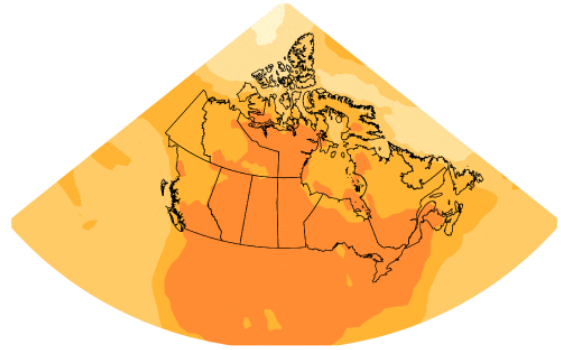
Figure caption: Maps and time series of projected temperature change (°C) for December, January, and February, as represented by the median of the CMIP5 multi-model ensemble. Changes are relative to the 1986–2005 period. The upper maps show temperature change for the 2031–2050 period and the lower maps, for the 2081–2100 period. The left-hand maps show changes resulting from the low emission scenario (RCP2.6), whereas the right-hand maps show changes from the high emission scenario (RCP8.5). The time series at the bottom of the figure shows the temperature change averaged for the Canadian land area over the 1900–2100 period. The thin lines show results from the individual CMIP5 models, and the heavy line is the multi-model mean. The spread among models, evident in the thin lines, is quantified by the box and whisker plots to the right of each panel. They show, for the 2081–2100 period, the 5th, 25th, 50th (median), 75th, and 95th percentile values.

FIGURE SOURCE: CLIMATE RESEARCH DIVISION, ENVIRONMENT AND CLIMATE CHANGE CANADA.

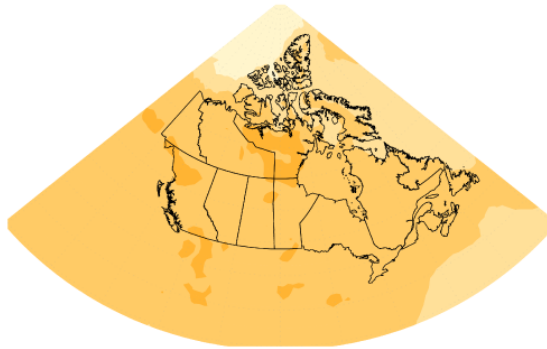
a) **Temperature change RCP2.6 (2031–2050)**
June–August



b) **Temperature change RCP8.5 (2031–2050)**
June–August



c) **Temperature change RCP2.6 (2081–2100)**
June–August



d) **Temperature change RCP8.5 (2081–2100)**
June–August

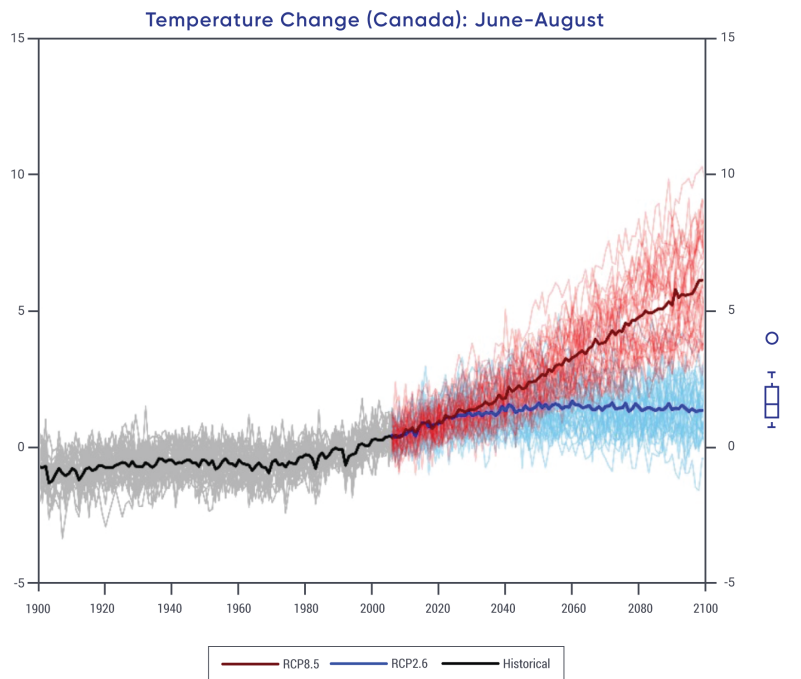
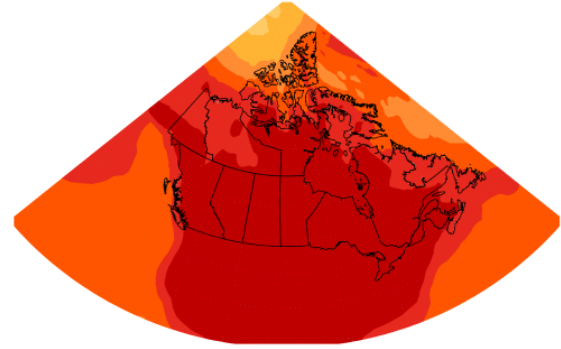


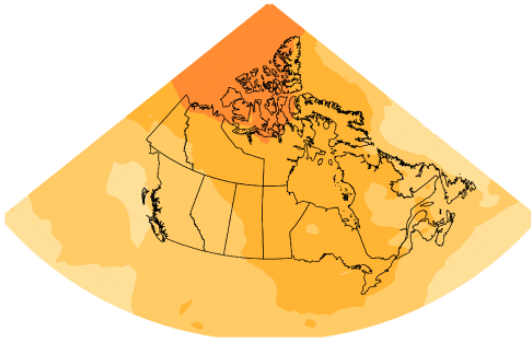
Figure 4.7: Projected temperature changes for summer season



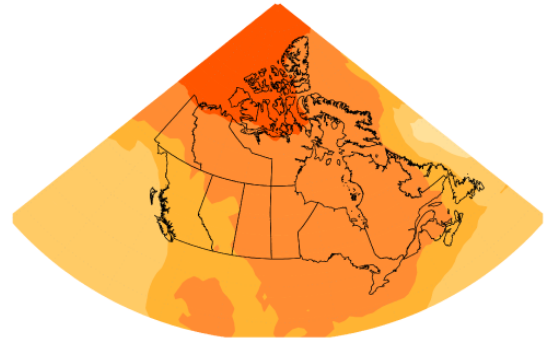
Figure caption: Maps and time series of projected temperature change (°C) for June, July, and August as represented by the median of the CMIP5 multi-model ensemble. Changes are relative to the 1986–2005 period. The upper maps show temperature change for the period 2031–2050 and the lower maps, for the 2081–2100 period. The left-hand maps show changes resulting from the low emission scenario (RCP2.6), whereas the right-hand maps show changes from the high emission scenario (RCP8.5). The time series at the bottom of the figure show the temperature change averaged for the Canadian land area and over the 1900–2100 period. The thin lines show results from the individual CMIP5 models, and the heavy line is the multi-model mean. The spread among models, evident in the thin lines, is quantified by the box and whisker plots to the right of each panel. They show, for the 2081–2100 period, the 5th, 25th, 50th (median), 75th, and 95th percentile values.

FIGURE SOURCE: CLIMATE RESEARCH DIVISION, ENVIRONMENT AND CLIMATE CHANGE CANADA.

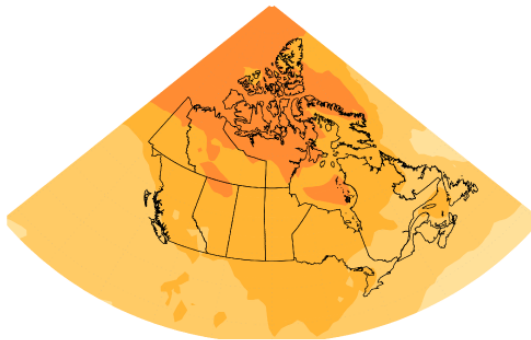
a) **Temperature change RCP2.6 (2031–2050)**
Annual



b) **Temperature change RCP8.5 (2031–2050)**
Annual



c) **Temperature change RCP2.6 (2081–2100)**
Annual



d) **Temperature change RCP8.5 (2081–2100)**
Annual

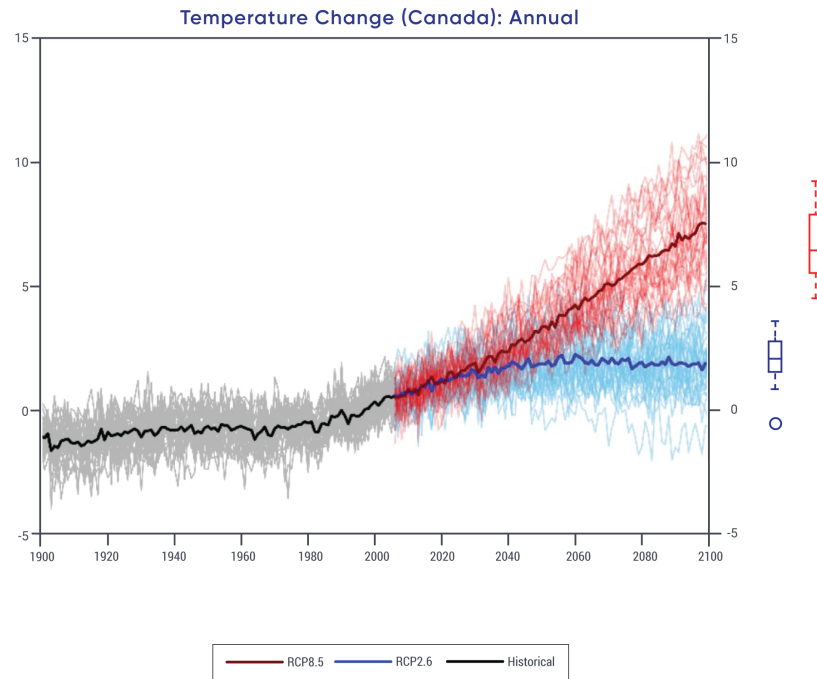
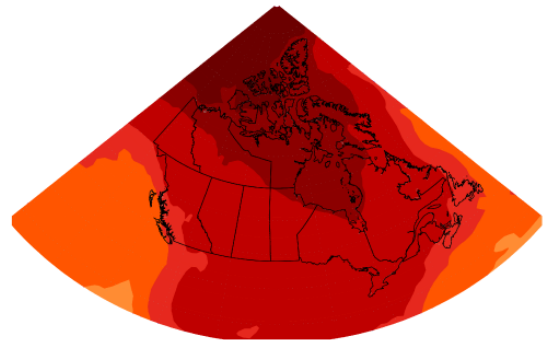


Figure 4.8: Projected annual temperature changes



Figure caption: Maps and time series of projected annual mean temperature change, ($^{\circ}\text{C}$) as represented by the median of the fifth phase of the Coupled Model Intercomparison Project (CMIP5) multi-model ensemble. Changes are relative to the 1986–2005 period. The upper maps show temperature change for the 2031–2050 period and the lower maps, for the 2081–2100 period. The left-hand maps show changes resulting from the low emission scenario (RCP2.6), whereas the right-hand maps show changes from the high emission scenario (RCP8.5). The time series at the bottom of the figure shows the temperature change averaged for the Canadian land area and over the 1900–2100 period. The thin lines show results from the individual fifth phase of the Coupled Model Intercomparison Project (CMIP5) models, and the heavy line is the multi-model mean. The spread among models, evident in the thin lines, is quantified by the box and whisker plots to the right of each panel. They show, for the 2081–2100 period, the 5th, 25th, 50th (median), 75th, and 95th percentile values.

FIGURE SOURCE: CLIMATE RESEARCH DIVISION, ENVIRONMENT AND CLIMATE CHANGE CANADA.

The maps in Figures 4.6, 4.7, and 4.8 illustrate the median projection from the CMIP5 multi-model ensemble – some models project larger changes and some project smaller changes. The spread across models provides an indication of the projection uncertainty discussed in Chapter 3, Section 3.3.2. The spread among the CMIP5 ensemble is only an ad hoc measure of uncertainty. Actual uncertainty could be larger, because CMIP5 models may not represent the full spectrum of plausible representations of all relevant physical processes (Kirtman et al., 2013). The spread across models also includes natural, year-to-year variability, which continues in the future much as it has in the past. Even when averaged for a region as large as Canada, differences in projected temperature among models are on the order of a couple of degrees. Under a low emission scenario (RCP2.6), annual mean warming in Canada stabilizes at about 1.8°C above the 1986–2005 reference period after about 2050, whereas, under a high emission scenario (RCP8.5), annual warming continues throughout the 21st century and beyond, reaching about 6.3°C above the reference period by 2100. Additional values for Canada as a whole and for various regions are presented in Table 4.2.

Temperature change is one of the key indicators of a changing climate, and many other climate variables are directly or indirectly tied to temperature. The changes in mean temperature are the projected response to emissions of GHGs and aerosols from human activities, and natural internal climate variability will continue to be superimposed on these forced changes. Natural internal climate variability is simulated by the climate models used to make projections of future climate change, and this is evident in the year-to-year variability in the Canada-average temperature time series in Figures 4.6, 4.7, and 4.8 (the individual thin lines). Indeed, this year-to-year variability looks much like what has been observed in the past (see Figure 4.2). In contrast, the underlying forced response (approximated by the multi-model average – the thick line in the figures) is a slowly, monotonically changing value that closely tracks the cumulative emissions of GHGs since the pre-industrial era (see Chapter 3, Section 3.4.1). In assessing the impacts of a warming climate, this combination of slow forced change and natural internal variability is important to keep in mind – the future will continue to have extreme warm and cold periods superimposed on a slow warming forced by human activities.

Because the components of the global climate system are closely interconnected, temperature change in a particular region, such as Canada, is closely related to the change in global mean. This is illustrated in the left panel of Figure 4.9, which shows Canadian mean temperature change versus global mean temperature change. As noted previously, Canadian mean temperature is projected to increase at roughly double the global mean rate, regardless of the forcing scenario. That is, the relationship between Canadian and global temperature change remains constant, as shown by the fact that the results from the different scenarios are all aligned. This connection between global mean and Canadian mean temperature change provides a way of estimating the implications of global change for Canada under alternative forcing scenarios. In other words, impacts estimated under one forcing scenario can be scaled to approximate impacts under another forcing scenario, since the ratio of Canadian to global temperature change is roughly constant. Of course, this assumes that impacts scale directly with temperature (which may not always be the case).

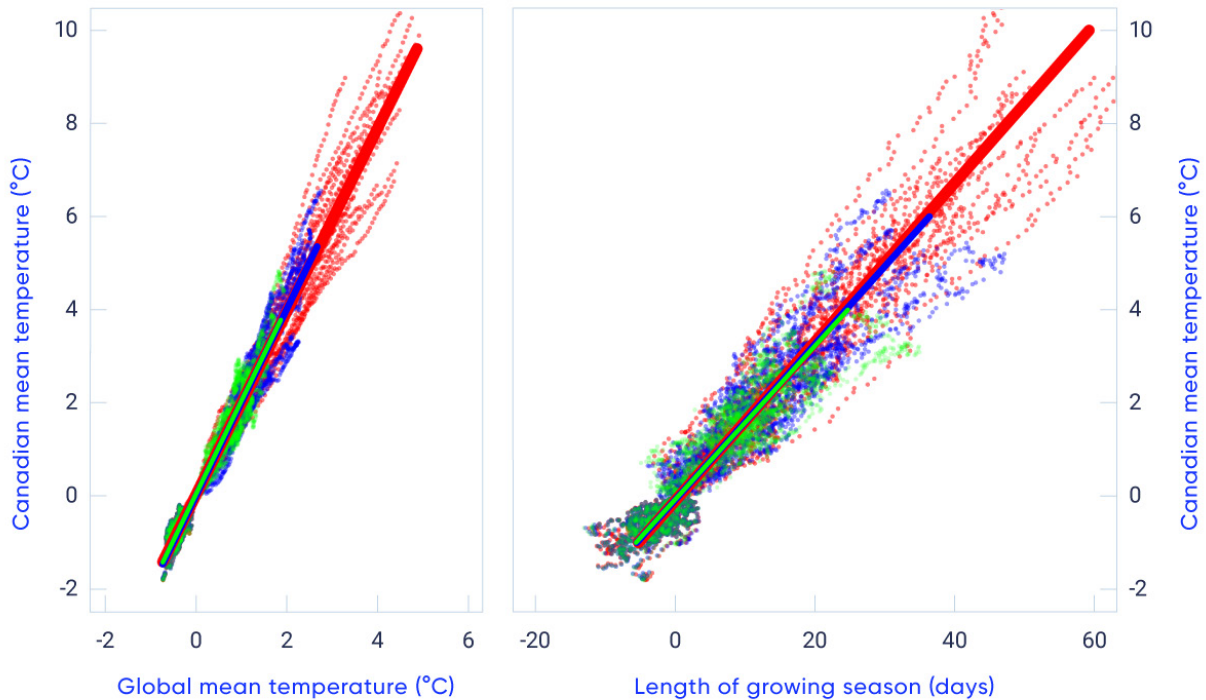


Figure 4.9: Connections between global mean and Canadian mean temperature change, and changes in length of the growing season

Figure caption: The left-hand panel shows Canadian mean temperature change plotted against global mean temperature change (°C for 20-year averages relative to 1986–2005) from fifth phase of the Coupled Model Intercomparison Project (CMIP5) model simulations for three different forcing scenarios (green: RCP2.6; blue: RCP4.5; red: RCP8.5). Heavy lines are least-squares linear fits, whereas thinner dashed lines are individual model results. The right-hand panel shows the changing length of the growing season (in days, see Chapter 1, Section 1.2) for warm-season crops in the Canadian Prairies, as a function of changes in Canadian mean temperature.

FIGURE SOURCE: ADAPTED FROM LI ET AL., 2018.

The IPCC Fifth Assessment concluded that “Global mean temperatures will continue to rise over the 21st century if GHG emissions continue unabated” (Collins et al., 2013, p. 1031). Because of the connection between global mean and Canadian mean temperature changes, it is *virtually certain* that temperature will also continue to increase in Canada as long as GHG emissions continue.

4.2.2: Temperature extremes and other indices

This subsection describes changes in temperature extremes and other indices relevant to impact assessments. All are derived from daily temperature data. Some indices, such as the annual highest and lowest day or night temperatures, represent temperature extremes and have widespread applications, such as in building design. Others are important for specific users. For example, degree days are a commonly used indicator of building cooling or heating demand, and of the amount of heat available for crop growth. Heating degree days (the annual sum of daily mean temperature below 18°C) or cooling degree days (the annual sum of daily mean temperature above 18°C) are used for energy utility planning, while growing degree days (the sum of daily mean temperature above 5°C in a growing season) is an important index for agriculture. Some indices, such as the number of days when daily maximum temperature is above 30°C or when daily minimum temperature is above 22°C, have important health implications (Casati et al., 2013). Observed changes in temperature indices and extremes indicate that warm events are becoming more intense and more frequent, while cold events are becoming less intense and less frequent. These have important implications; for example, extreme winter cold days are important in limiting the occurrence of some forest pests (Goodsman et al., 2018).

4.2.2.1: Observed changes

The annual highest daily maximum temperature, averaged across the country, increased by 0.61°C between 1948 and 2016 (updated from Wan et al., 2018). The largest increases were in northern Canada, while decreases were observed in the southern Prairies (see Figure 4.10a). The highest daily maximum temperature that occurs once in 20 years, on average, also increased (Wang et al., 2014). The annual lowest daily minimum temperature, averaged across the country, increased by 3.3°C between 1948 and 2016, with the strongest warming in the west (see Figure 4.10b) (updated from Wan et al., 2018). The lowest daily minimum temperature that occurs once in 20 years, on average, increased more strongly (Wang et al., 2014). Overall, extreme cold temperatures increased much more rapidly than the extreme warm temperatures, consistent with greater warming in winter than in summer, as well as greater warming in night temperatures than in day temperatures.

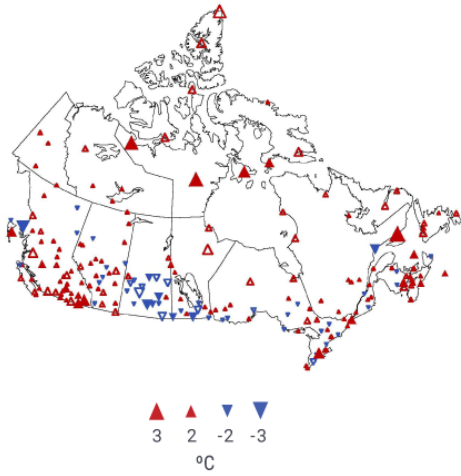
Indices of high temperature, such as hot days and hot nights, are particularly relevant to public health. Hot days, defined as days with maximum temperature above 30°C, are rarely observed in the regions north of 60° north latitude. In southern Canada, the number of hot days annually increased by about 1 to 3 days at a few stations over the 1948–2016 period (see Figure 4.10c; also see Vincent et al., 2018). Most locations in Canada are not warm enough to have hot nights, defined as nights with daily minimum temperature above 22°C, and the number of hot nights has significantly increased only at a few stations in southern Ontario and Quebec.

Warming in winter and spring has resulted in a significant decrease in the number of frost days (days with daily minimum temperature of 0°C or lower) and ice days (days with daily maximum temperature of 0°C or

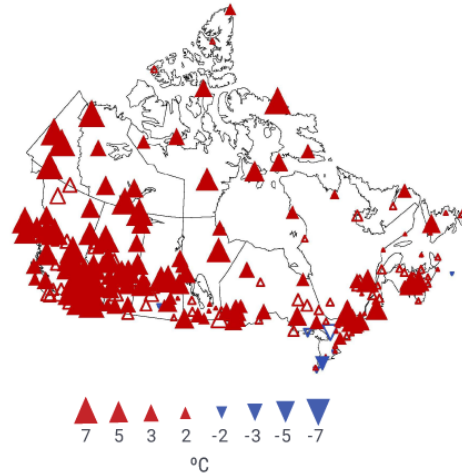


lower), as well as shortened winter seasons (Vincent et al., 2018). Averaged for the country as a whole, frost days have decreased by more than 15 and ice days by more than 10 days from 1948 to 2016. These changes are consistent across the country. As a result, the frost-free season has been extended by 20 days, starting about 10 days earlier and ending about 10 days later. Heating degree days have decreased while cooling degree-days have increased (see Figure 4.10e and f). The length of growing seasons (see Figure 4.10d) and the number of growing degree days have also increased. The growing season, which starts when there are six consecutive days with daily mean temperature above 5°C in spring or summer and ends when this condition fails to be met late in the year, started earlier and ended later, resulting in an increase in growing season length of about 15 days between 1948 and 2016. With the longer growing season, the number of growing degree days increased.

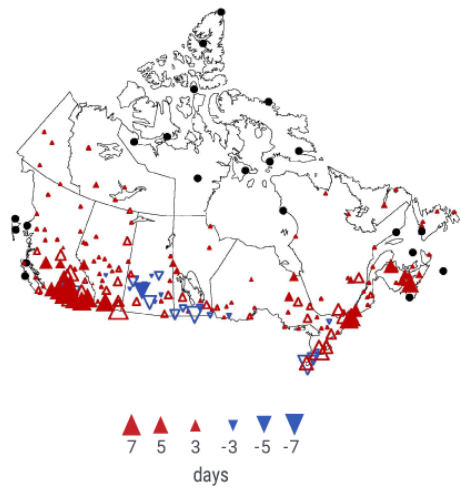
a) Highest daily maximum (°C)



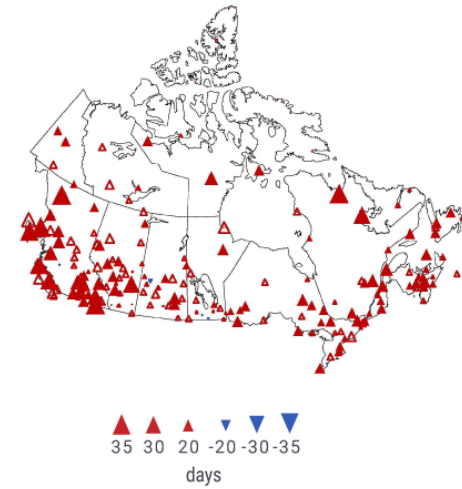
b) Lowest daily minimum (°C)



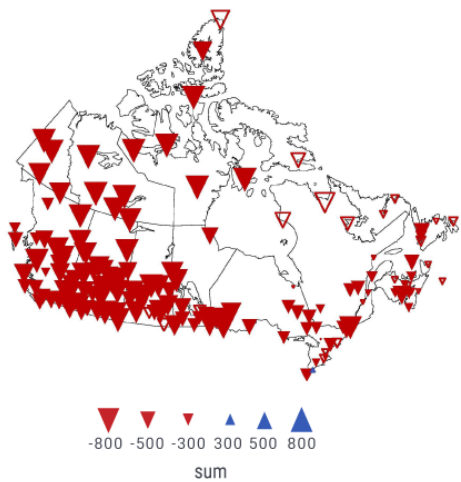
c) Number of hot days (days)



d) Length of growing season (days)



e) Heating degree days (°C-day)



f) Cooling degree days (°C-day)

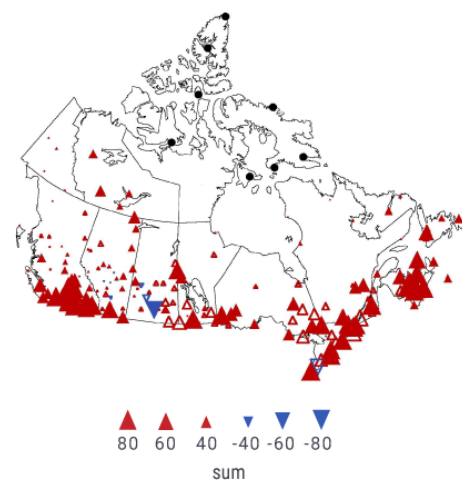


Figure 4.10: Changes in selected temperature indicators, 1948–2016

Figure caption: Observed changes in: (a) annual highest daily maximum temperature, (b) annual lowest daily minimum temperature, (c) annual number of hot days (when daily maximum temperature is above 30°C), (d) length of growing season, and (e) heating and (f) cooling degree days. Changes are computed based on linear trends over the 1948–2016 period. Filled triangles indicate trends significant at the 5% level. The black dots on (c) and (f) mark stations where hot days or daily mean temperature above 18°C do not normally occur. The legend may not include all sizes shown in the figure.

FIGURE SOURCE: ADAPTED FROM VINCENT ET AL., 2018.

4.2.2.2: Causes of observed changes

It is *very likely* that anthropogenic forcing has contributed to the observed changes in the frequency and intensity of daily temperature extremes on the global scale since the mid-20th century (Bindoff et al., 2013; see also Chapter 2, Section 2.3.4). Several detection studies have shown that the annual lowest daily minimum temperature (Zwiers et al., 2011; Min et al., 2013; Kim et al., 2015) and the annual highest daily maximum temperatures (Wang et al., 2017) have been influenced by human activity in three subregions of North America. In Canada, an increase of 3.2°C in the annual lowest daily minimum temperature was observed from 1948 to 2012 (Wan et al., 2018). Only a small fraction (about 0.5°C) of this increase can be related to natural internal climate variability, and anthropogenic influence may have contributed as much as 2.8°C (*likely* range 1.5° to 4.2°C) to the warming (see Figure 4.5). In addition, much of the observed warming seen in the annual highest daily maximum temperature may also be attributable to anthropogenic influence. Overall, most of the observed increase in the coldest (*likely*) and warmest (*high confidence*) daily temperatures of the year in Canada from 1948 to 2012 can be attributed to anthropogenic influence.

While there is a lack of studies directly attributing observed changes in other temperature indices, there is *high confidence* that substantial parts of the observed changes in most of these temperature indices are also due to anthropogenic influence. It is more difficult to detect anthropogenic influence in values such as annual lowest daily minimum temperature, which are sampled once a year, than in other temperature indices that integrate information from many data samples in a year. These indices are less affected by natural internal variability, while nevertheless retaining the climate responses to external forcing.

4.2.2.3: Projected changes and uncertainties

The models used to make projections of future climate are discussed in Chapter 3, Section 3.3. When using climate model projections for impact studies, it is often important to consider that the model simulated



current climate may differ from observed climate — a reflection of model biases (Flato et al. 2013). Many temperature indices are connected to absolute thresholds (like the freezing temperature), and, so, mean biases can substantially alter their usefulness. As a result, where absolute values are important, some form of bias correction is needed. This is a method of correcting the model output to remove, to the extent possible, the influence of model biases. The assessments of projected changes in temperature indices discussed in this subsection are, unless otherwise stated, based on statistically downscaled and bias-corrected data (Li et al., 2018; Murdock et al., 2014; Werner and Cannon, 2016; see Chapter 3, Section 3.5).

Daily extreme temperatures, hot and cold, are projected to increase substantially (see Figure 4.11). Annual highest daily maximum temperature is projected to track the projected changes in summer mean temperature, but at a slightly higher rate (the largest difference between the two is less than 0.5°C, appearing in 2081–2100 under a high emission scenario [RCP8.5]). Annual lowest daily minimum temperature is projected to warm faster than winter mean temperature over most of Canada, increasing the extreme minimum temperature in southern Canada by about 3°C by the end of the century under a high emission scenario (RCP8.5). Table 4.3 summarizes projected changes in Canada. For example, averaged over the country, the annual highest daily maximum temperatures are projected to increase by 1.4°C over the 2031–2050 period under a low emission scenario (RCP2.6), and by 2°C for the same period under a high emission scenario (RCP8.5) compared with the current climate (1986–2005). The corresponding projected increase in 2081–2100 under the low emission scenario (RCP2.6) is 1.5°C, only slightly higher than the increases in 2031–2050. A much larger increase, of about 6°C, is expected in 2081–2100 under the high emission scenario (RCP8.5).

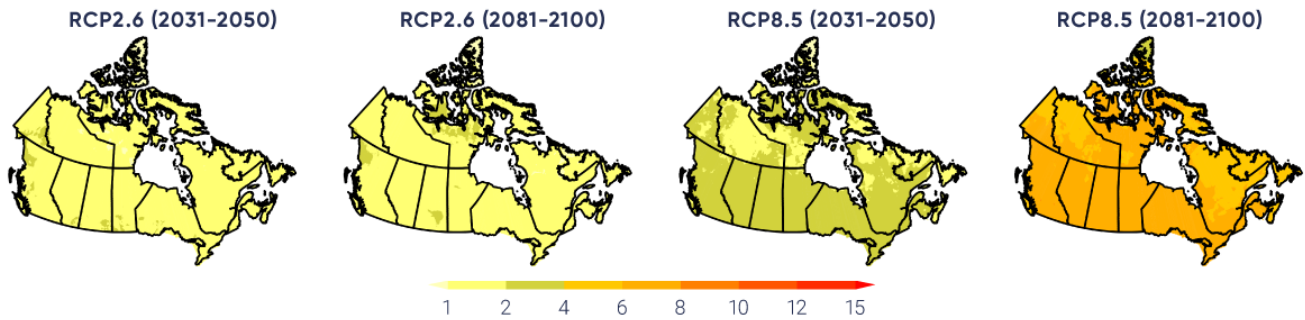
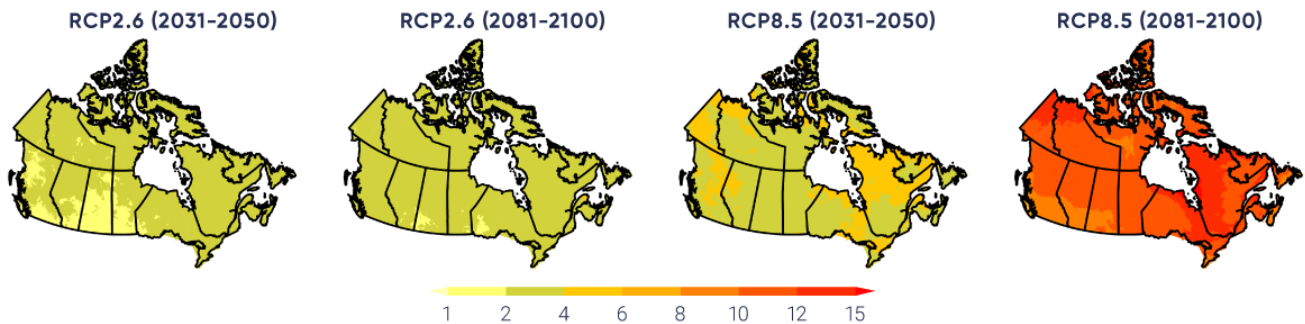
a) Annual highest daily maximum temperature (°C)**b) Annual lowest daily minimum temperature (°C)**

Figure 4.11: Future projections for selected temperature indices (extremes)

Figure caption: Multi-model median projected changes in (a) annual highest daily maximum temperature, (b) annual lowest daily minimum temperature. All maps are based on statistically downscaled and bias-corrected temperature data from simulations by 24 Earth system models. The two left-hand panel show projections for 2031–2050 and 2081–2100 under a low emission scenario (RCP2.6), while the two right-hand panels show projections for 2031–2050 and 2081–2100 under a high emission scenario (RCP8.5).

FIGURE SOURCE: ADAPTED FROM LI ET AL., 2018.

Table 4.3: Multi-model changes in indicators of temperature^a

REGION ^b	SCENARIO; PERIOD; MEDIAN (25%, 75% PERCENTILE)			
	RCP2.6		RCP8.5	
	2031–2050	2081–2100	2031–2050	2081–2100
Annual highest daily maximum temperature, °C				
British Columbia	1.7 (0.9, 2.4)	1.7 (1.2, 2.4)	2.3 (1.6, 3.2)	6.7 (4.9, 7.9)
Prairies	1.6 (0.9, 2.3)	1.6 (1.1, 2.4)	2.5 (1.8, 3.1)	6.9 (5.2, 8.2)
Ontario	1.6 (1.0, 2.4)	1.5 (0.8, 2.2)	2.5 (1.9, 3.0)	6.6 (5.2, 7.7)
Quebec	1.4 (0.8, 2.2)	1.3 (0.7, 2.0)	2.1 (1.5, 2.7)	5.9 (4.7, 7.1)
Atlantic	1.4 (0.9, 1.9)	1.2 (0.6, 1.9)	1.9 (1.4, 2.4)	5.5 (4.6, 6.5)
North	1.3 (0.6, 2.2)	1.5 (0.7, 2.2)	1.8 (0.9, 2.7)	5.7 (3.6, 7.3)
Canada	1.4 (0.7, 2.3)	1.5 (0.8, 2.2)	2.0 (1.2, 2.8)	6.1 (4.2, 7.5)
Annual highest daily minimum temperature, °C				
British Columbia	2.1 (1.1, 3.7)	2.7 (1.4, 4.2)	3.7 (2.4, 5.3)	10.1 (8.5, 11.7)
Prairies	2.1 (1.3, 3.3)	2.5 (1.6, 3.8)	3.5 (2.5, 4.9)	10.5 (9.3, 12.8)
Ontario	2.6 (1.9, 3.5)	2.7 (2.0, 3.8)	3.9 (2.9, 4.7)	11.7 (10, 13.8)
Quebec	2.8 (1.9, 3.9)	3.2 (2.0, 4.4)	4.2 (3.2, 5.3)	12.6 (10.7, 15.7)
Atlantic	2.8 (1.8, 3.8)	3.0 (1.8, 4.5)	3.8 (2.8, 4.9)	11.2 (9.6, 13.6)
North	2.6 (1.8, 3.4)	2.9 (1.9, 4.0)	3.9 (3.0, 4.8)	11.1 (9.4, 14.0)
Canada	2.5 (1.7, 3.5)	2.8 (1.8, 4.1)	3.8 (2.9, 4.9)	11.2 (9.5, 13.8)
Annual number of hot days, days				
British Columbia	1.6 (0.7, 2.5)	1.5 (0.8, 2.5)	2.5 (1.7, 3.6)	16.0 (9.0, 20.0)
Prairies	4.5 (2.5, 6.7)	4.6 (2.6, 6.8)	7.2 (5.2, 9.4)	34.3 (22.8, 40.1)
Ontario	5.4 (3.6, 7.1)	4.7 (2.8, 6.8)	8.8 (6.8, 10.8)	38.0 (28.1, 44.5)
Quebec	1.7 (1.0, 2.3)	1.4 (0.8, 2.1)	2.7 (1.9, 3.4)	14.5 (10.1, 17.3)
Atlantic	1.4 (0.9, 2.0)	1.2 (0.6, 1.8)	2.1 (1.5, 2.8)	12.1 (9.3, 16.7)
North	0.3 (0.1, 0.5)	0.3 (0.1, 0.5)	0.5 (0.3, 0.7)	3.5 (2.0, 5.1)
Canada	1.6 (0.9, 2.3)	1.5 (0.9, 2.3)	2.6 (1.8, 3.3)	13.2 (8.8, 16.2)
Length of growing season for warm-season crops, days				
British Columbia	17.6 (12, 23.5)	22 (14.3, 28.5)	23.3 (17.7, 29.3)	61.1 (48.1, 70.5)
Prairies	11.5 (6.4, 16.0)	13.5 (9.1, 18.3)	15.5 (11.0, 20.5)	43.6 (35.6, 50.8)
Ontario	11.8 (6.9, 17.5)	13.0 (8.0, 19.1)	17.0 (11.8, 22.8)	44.4 (36.9, 53.7)
Quebec	13.6 (8.7, 18.7)	14.0 (7.7, 20.2)	19.3 (13.2, 24.8)	50.1 (40.2, 62.1)
Atlantic	13.7 (8.6, 18.2)	14.3 (8.9, 19.6)	18.6 (13.7, 25.2)	51.1 (42.5, 63.8)
North	8.8 (4.7, 13.4)	10.2 (5.0, 15.3)	12.9 (7.3, 18.4)	37.8 (25.5, 49.9)
Canada	10.8 (6.3, 15.6)	12.4 (7.0, 17.7)	15.3 (9.9, 20.9)	42.8 (31.9, 53.8)

Table 4.3: Multi-model changes in indicators of temperature^a

Cooling degree days, °C-days				
British Columbia	16 (9, 22)	16 (10, 25)	26 (19, 34)	168 (97, 211)
Prairies	52 (32, 74)	55 (32, 79)	85 (66, 108)	386 (260, 461)
Ontario	67 (44, 90)	58 (44, 89)	108 (88, 125)	408 (306, 491)
Quebec	25 (18, 37)	23 (16, 32)	42 (33, 49)	183 (136, 236)
Atlantic	28 (19, 40)	29 (18, 37)	42 (33, 54)	187 (150, 268)
North	6 (4, 10)	7 (4, 10)	10 (7, 13)	58 (34, 83)
Canada	21 (14, 30)	21 (14, 31)	35 (27, 43)	160 (109, 204)
Heating degree days, °C-days				
British Columbia	-497 (-651, -408)	-651 (-829, -502)	-731 (-907, -585)	-1873 (-2115, -1621)
Prairies	-545 (-654, -435)	-648 (-809, -508)	-781 (-957, -635)	-2036 (-2262, -1779)
Ontario	-550 (-681, -448)	-607 (-752, -448)	-770 (-948, -655)	-1990 (-2337, -1749)
Quebec	-596 (-796, -477)	-646 (-913, -480)	-869 (-1061, -690)	-2257 (-2759, -1916)
Atlantic	-524 (-679, -418)	-573 (-839, -428)	-730 (-897, -592)	-1895 (-2372, -1662)
North	-744 (-977, -593)	-884 (-1174, -563)	-1057 (-1352, -877)	-2880 (-3568, -2447)
Canada	-656 (-850, -525)	-772 (-1020, -527)	-936 (-1178, -770)	-2503 (-3033, -2142)

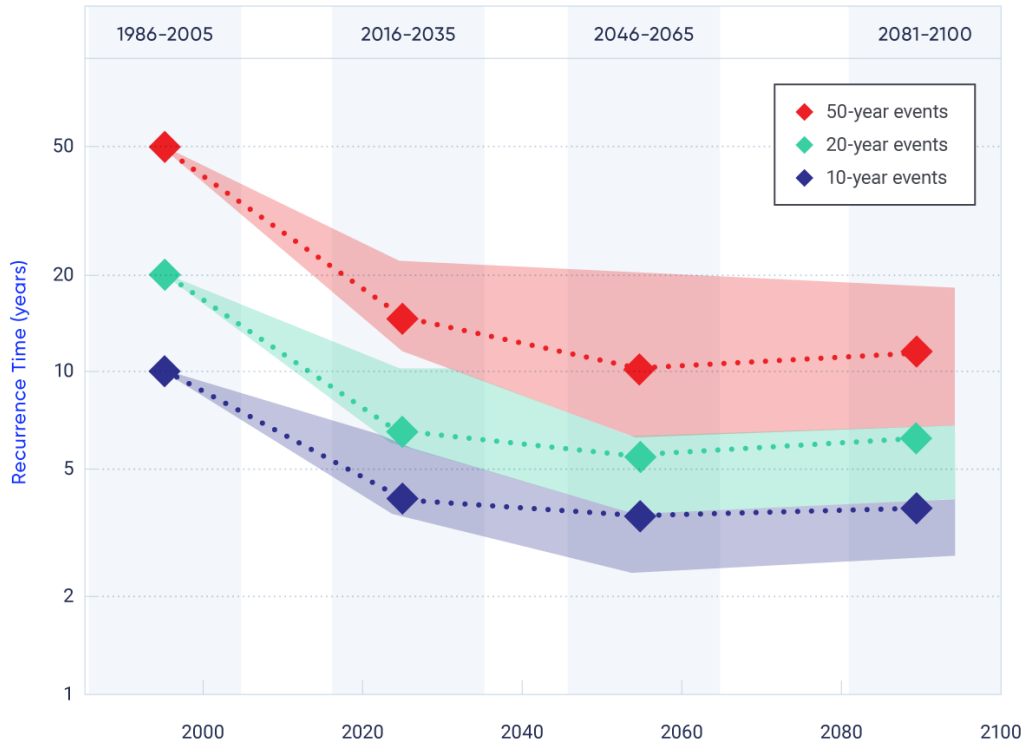
^a Based on statistically downscaled temperature from simulations by 24 Earth system models (adopted from Li et al., 2018).

^b Regions are defined by political boundaries; "North" includes the three territories (see Figure 1.1).

In addition to changes in magnitude, the frequency of certain temperature extremes is also expected to change. Extreme hot temperatures are expected to become more frequent, while extreme cold temperatures less frequent. For example, under a high emission scenario (RCP8.5), the annual highest daily temperature that would currently be attained once every 10 years, on average, will become a once in two-year event by 2050 – a five-fold increase in frequency. The annual highest daily temperature that occurs once every 50 years in the current climate is projected to become a once in five-year event by 2050 – a 10-fold increase in frequency (see Figure 4.12). These projected changes indicate not only more frequent hot temperature extremes, but also relatively larger increases in frequency for more rare events (e.g., 10-year extreme versus 50-year extreme; see also Kharin et al., 2018).



a) Annual maximum temperature RCP2.6



b) Annual maximum temperature RCP8.5

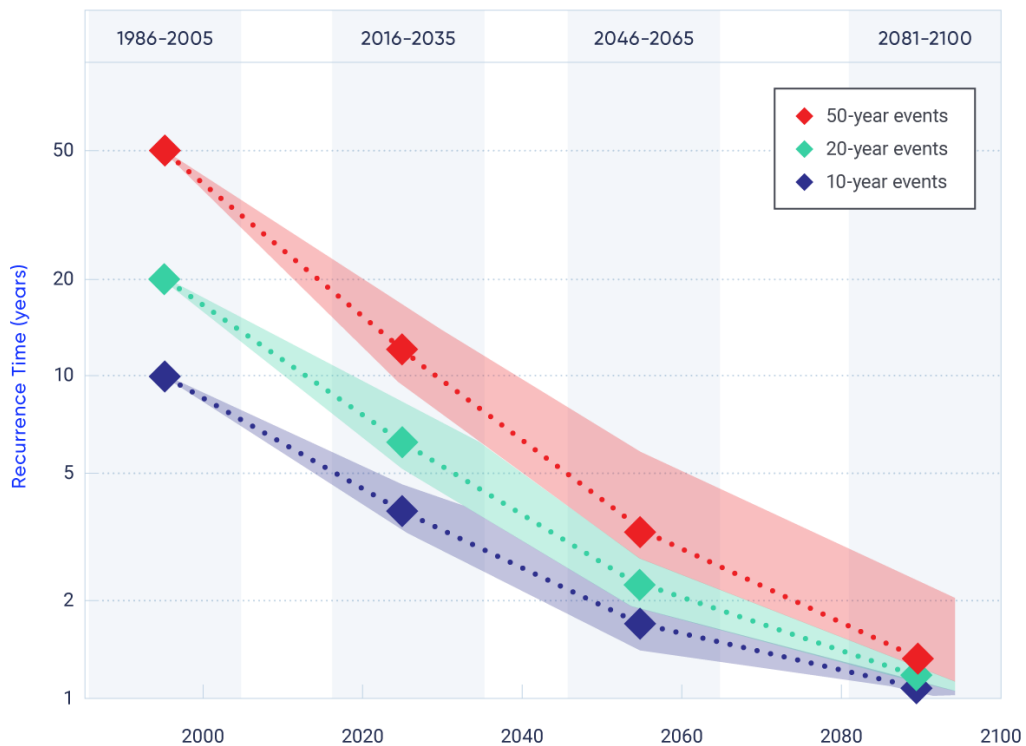


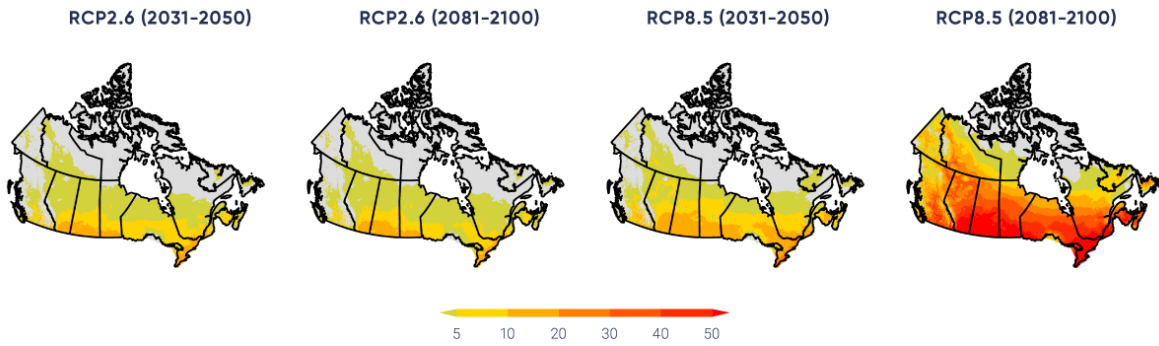
Figure 4.12: Projected changes in recurrence time for extreme temperatures

Figure caption: Projected changes in recurrence time (in years) for annual highest temperatures that occurred, on average, once in 10, 20, and 50 years in the late-20th century across Canada, as simulated by Earth system models contributing to fifth phase of the Coupled Model Intercomparison Project (CMIP5) under a low emission scenario RCP2.6 (upper) and a high emission scenario RCP8.5 (lower). The shading represents the range between the 25th and 75th percentiles

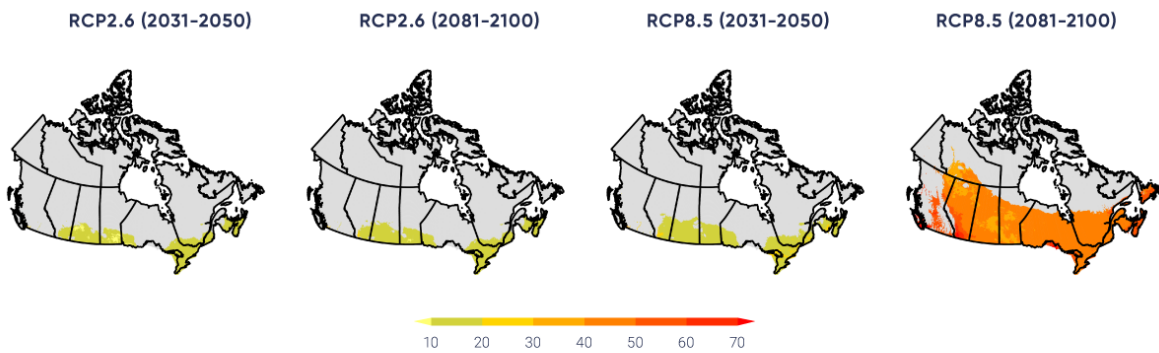
FIGURE SOURCE: VALUES ARE COMPUTED BASED ON KHARIN ET AL., 2013, ADAPTED FROM ECCCL, 2016.

The projected increase in the number of hot days is substantial. In regions that currently experience hot days, the increase may be more than 50 days by the late century under RCP8.5 (see Figure 4.13a). Areas with hot days will progressively expand northward, depending on the level of global warming. The number of frost days and ice days is projected to decrease, with projections ranging from about 10 fewer days in 2031–2050 under the low emission scenario (RCP2.6) to more than 40 fewer days in 2081–2100 under the high emission scenario (RCP8.5) (see Table 4.3) The length of the growing season (see Figure 4.13b) and the number of cooling degree days (see Figure 4.13c) are projected to increase, while heating degree days (see Figure 4.13d) are projected to decrease (see Table 4.3).

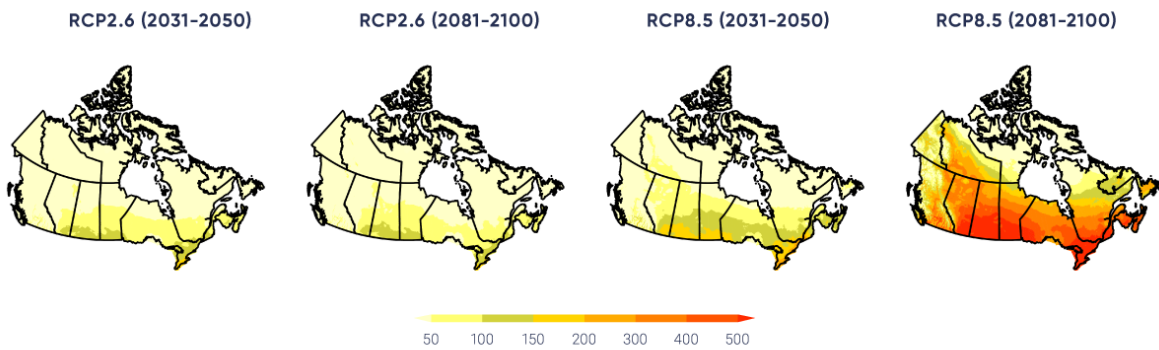
a) Annual number of hot days (days) when daily maximum temperature is above 30°C (TX30)



b) Length of growing season for warm season crops (days) (GSL)



c) Cooling-degree days (°C-days) (CDD)



d) Heating degree days (°C-days) (HDD)

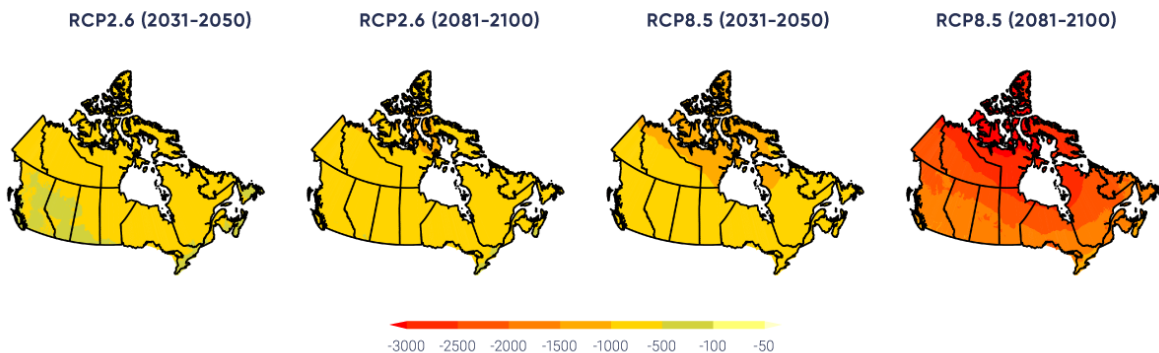


Figure 4.13: Future projections for selected temperature indices (degree days)

Figure caption: Multi-model median projected changes in (a) annual number of hot days (days) when daily maximum temperature is above 30°C (TX30), (b) length of growing season for warm-season crops (days) (GSL), (c) cooling degree days (°C-days) (CDD), (d) heating degree days (°C-days) (HDD). All maps are based on statistically downscaled temperature from simulations by 24 Earth system models. The two left-hand panels show projections for 2031–2050 and 2081–2100 under a low emission scenario (RCP2.6), while two right-hand panels display projections for 2031–2050 and 2081–2100 under a high emissions scenario (RCP8.5), respectively. Areas with less than one hot day per year on average are marked with grey in panel (a), while areas without sufficient cumulative heat during the growing season to support growing warm season crops such as corn or soybean are marked with grey in panel (b)

FIGURE SOURCE: ADAPTED FROM LI ET AL., 2018.

Changes in temperature indices and extremes are closely related to changes in mean temperature. The linear relationship between the change in growing season length and Canadian mean temperature (the right side of Figure 4.9; Li et al., 2018) is one example of how impacts (in this case related to agricultural productivity or forest growth) can be related to temperature change, regardless of the specific pathway of future GHG emissions. Such relationships not only assist impact assessments, but also assist plain-language communication regarding global mitigation efforts and their effect on regional climate impacts. A second example is freezing degree days, a measure of winter severity (e.g., Assel, 1980), which is the annual sum of degrees below freezing for each day, expressed in units of °C-d. A reduction of several hundred °C-d is projected across southern Canada in the late century, with changes of 1000°C-d or more projected for the North (see Figure 4.14). For context, the historical value of freezing degree days at Whitehorse is roughly 1800°C-d, at Edmonton, roughly 1400°C-d, and at Toronto, roughly 375°C-d (based on 1981–2010 data <http://climate.weather.gc.ca/climate_normals/index_e.html>).

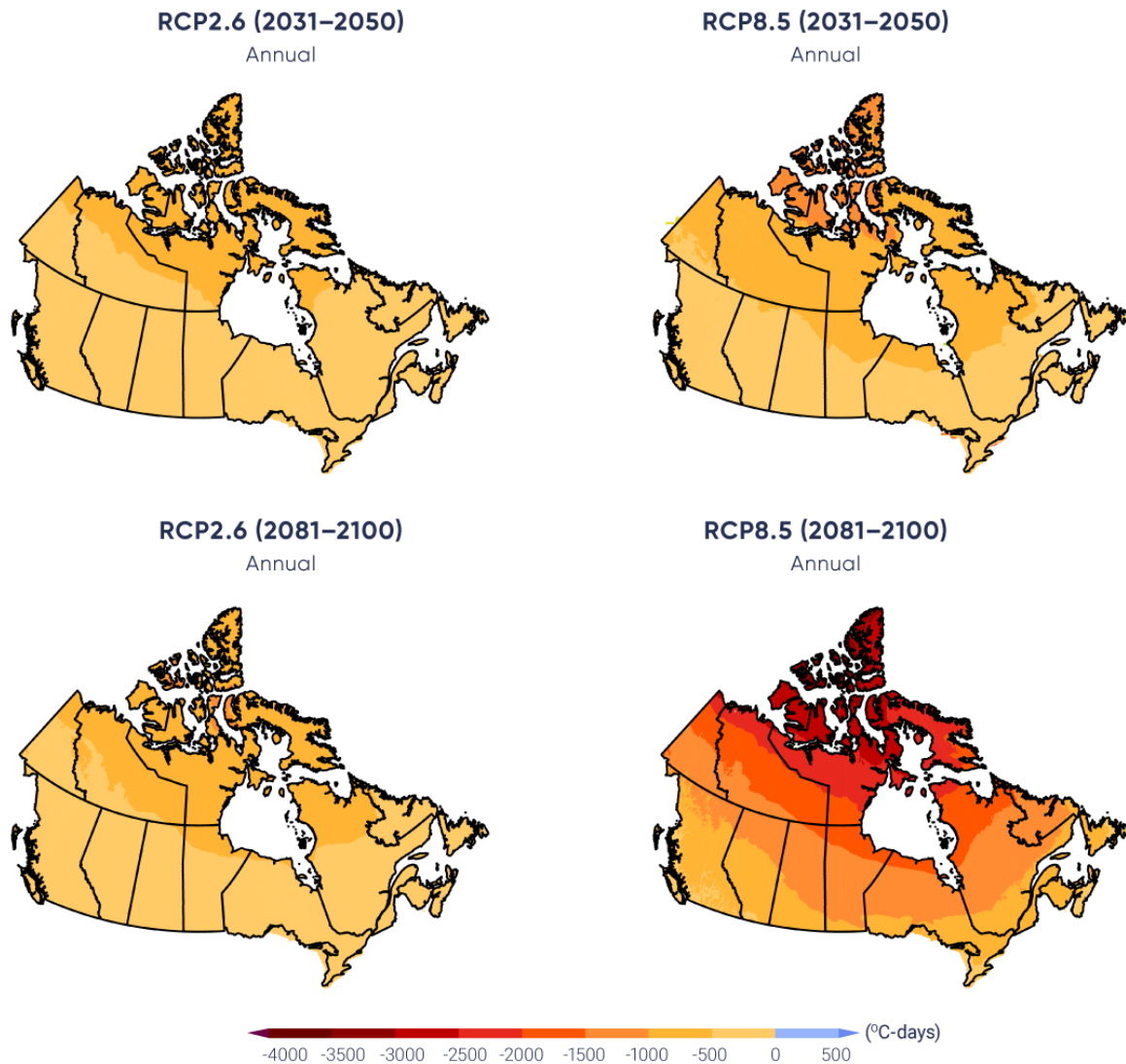


Figure 4.14: Future projections for freezing degree days

Figure caption: Projected change in freezing degree days (°C-d) for the period 2031–2050 (upper panels) and 2081–2100 (lower panels) relative to 1986–2005 average, computed from statistically downscaled daily temperatures based on simulations by 24 models of Fifth phase of the Coupled Model Intercomparison Project (CMIP5) models (Li et al., 2018). The left-hand panels show results for a low emission scenario (RCP2.6) and the right-hand panels show results for a high emission scenario (RCP8.5).

FIGURE SOURCE: LI ET AL., 2018.

For temperature indices and extremes, projections by different models for the near term (2031–2050) under a high emission scenario (RCP8.5) agree on the direction (increasing or decreasing) of changes for almost all

regions. The model projections for the late century (2081–2100) also agree on the direction of changes for all temperature indices and extremes for every region under a high emission scenario (RCP8.5). This indicates the robustness of projected changes in temperature indices for the future.

It is *virtually certain* that, in most places in the world, there will be more hot and fewer cold temperature extremes as global mean temperatures increase (Collins et al. 2013). This will also be the case for Canada.

Section summary

In summary, it is *virtually certain* that the Canadian climate has warmed and that it will warm further in the future, as additional emissions of GHGs are unavoidable. To date, warming has been stronger in winter than in other seasons. Widespread changes in temperature indices and extremes associated with warming have been observed. Both human activities and natural variation of the climate have contributed to this warming, with human factors being dominant. The magnitude of future warming will be determined by the extent of future GHG mitigation. Temperature indices and extremes will continue to change as Canada continues to warm, affecting Canada's natural, social, and economic systems. Substantial changes are projected in temperature extremes. There will be more hot and fewer cold temperature extremes. The increase in Canadian mean temperature is about twice the rate of global mean temperature. This is the case in the historical record and also applies to future change, regardless of the emissions pathway that the Earth will follow. As changes in temperature indices and extremes are closely tied to changes in mean temperature, changes in Canadian climate and their resulting impacts are closely linked to changes in global mean temperature and, ultimately, future emissions of GHGs.

4.3: Precipitation

Key Message

There is *medium confidence* that annual mean precipitation has increased, on average, in Canada, with larger percentage increases in northern Canada. Such increases are consistent with model simulations of anthropogenic climate change.

Key Message

Annual and winter precipitation is projected to increase everywhere in Canada over the 21st century, with larger percentage changes in northern Canada. Summer precipitation is projected to decrease over southern Canada under a high emission scenario towards the end of the 21st century, but only small changes are projected under a low emission scenario.

Key Message

For Canada as a whole, observational evidence of changes in extreme precipitation amounts, accumulated over periods of a day or less, is lacking. However, in the future, daily extreme precipitation is projected to increase (*high confidence*).

Precipitation, as the ultimate source of water for our lands, lakes, and rivers, plays an important role in human society and in shaping and sustaining ecosystems. Human society and natural systems have evolved and adapted to variable precipitation in the past. However, shifts in precipitation beyond its historical range of variability could have profound impacts.

The amount of precipitation varies widely across Canada. The Pacific Coastal and Rocky Mountain ranges of western Canada block much of the moisture brought by westerly winds from the Pacific. As a result, some locations on the west coast receive an average of 3000 mm of precipitation or more in a year. In contrast, the annual mean precipitation can be as low as 300 mm in parts of the Prairies. Because warm air can hold more moisture, the amount of precipitation decreases from south to north, with annual precipitation of only about 200 mm in the far north (Environment Canada, 1995).

Precipitation records for some locations in Canada extend back for more than a century. While the Meteorological Service of Canada has many observational stations at any given time, including more than 2500 stations currently active, only a few hundred stations have continuous long-term records. As with temperature observations, there have been significant changes in observing instruments and/or procedures, including many manned stations having been replaced by automated observing systems. Integrating the data from the manned and automatic observations into one continuous series is challenging, as it requires the accumulation of sufficient data from the new systems to fully understand their characteristics (Milewska and Hogg, 2002). Precipitation measurements have additional challenges when compared with temperature measurements, as they are affected by weather conditions at the time of observation. This is because thermometers are placed in well-protected screens, while precipitation gauges are in the open air. In general, precipitation gauges catch only a portion of precipitation if it is windy, and they become less efficient as wind speed increases (Mekis and Vincent, 2011; Milewska et al., 2018). Additionally, a small amount of precipitation is lost due to evaporation and wetting of the inside of the gauge. Precipitation in the form of snowfall is particularly difficult to observe. A gauge can catch only a small fraction of total snowfall; drifting snow makes it even more complicated to measure snowfall amount. The introduction, over time, of new precipitation gauges has unintentionally introduced data inhomogeneity into the records. The effect of weather conditions and the use of different gauges on observational data need to be carefully adjusted for, to reflect the actual amount of precipitation at a particular site.

Monitoring precipitation over a region is challenging because a gauge measurement is a point observation and thus may not represent precipitation conditions over a large area. As precipitation is sporadic in time and space, point observations of precipitation amount in a day can represent only a very small area surrounding the observational site. However, station observations of precipitation amounts accumulated over longer time

periods (a month or a year) can represent larger areas. For example, total precipitation for a season may be interpolated for a location without observations with reasonable accuracy, if the location is within 20 to 120 km from the observational sites, depending on the season (Milewska and Hogg, 2001). Factors such as topography, season, and dominant weather systems all affect the spatial representativeness of point observations of precipitation.

In general, there is insufficient station density in Canada to compute national average precipitation with desirable accuracy; thus, there is *low confidence* in quantifying regional or national total amounts of precipitation. This is because the distance between observational stations with long-term records (see Figure 4.1) is generally greater than 120 km and because there is a large variation in precipitation over space. In northern Canada, the distance between stations is often more than 1000 km. Locally normalized precipitation (the amount of precipitation divided by its long-term mean) has been used in the past as one alternative. This measure is less variable over space than precipitation amount. As a result, its value at a point location can represent the average over a larger area. Stations with long-term records can provide regional averages for normalized precipitation across southern Canada with reasonable accuracy, although this is not the case for northern Canada (Milewska and Hogg, 2001). As a result, much of the assessment of national or regional changes in precipitation is based on locally normalized precipitation, expressed as a percentage. While this makes it possible to compute some form of national and regional averages, such averages should not be interpreted as normalized spatial averages of precipitation. This is because the local normalization factor is not constant in space.

4.3.1: Mean precipitation

4.3.1.1: Observed changes

Averaged over the country, normalized precipitation has increased by about 20% from 1948 to 2012 (Vincent et al., 2015; Figure 4.15 and Table 4.4). The percentage increase was larger in northern Canada – including Yukon, Northwest Territories, Nunavut, and northern Quebec – than in southern Canada. Nonetheless, significant increases were experienced in parts of southern Canada, including eastern Manitoba, western and southern Ontario, and Atlantic Canada. As mean precipitation is typically higher in southern Canada, the absolute amount of precipitation increase is higher in the south, even though the increase in normalized precipitation is smaller in the region. The regional average of normalized precipitation based on the few available long-term data from stations in northern Canada shows an increase of about 30% from 1948 to 2012 (Vincent et al., 2015); confidence in the regional average is *low*, however. As trends from individual locations in northern Canada are all increasing, there is a *medium confidence* that annual mean precipitation has increased in this region. Taken together, there is *medium confidence* that annual precipitation has increased for Canada as a whole. Additionally, the percentage increase in normalized precipitation is larger than what might be expected from the warming-induced increase in water-holding capacity of the atmosphere, leading to doubt over the magnitude of historical trends. There is *low confidence* in the estimate of the magnitude of the trend.

Precipitation has increased in every season in northern Canada. In southern Canada, precipitation has also increased in most seasons but the increase is generally not statistically significant. However, a statistically significant decrease in winter precipitation has been observed in British Columbia, Alberta, and Saskatchewan (Vincent et al., 2015; Figure 4.16 and Table 4.4).

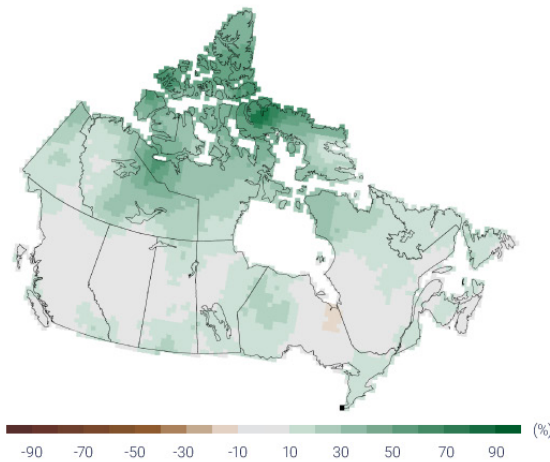
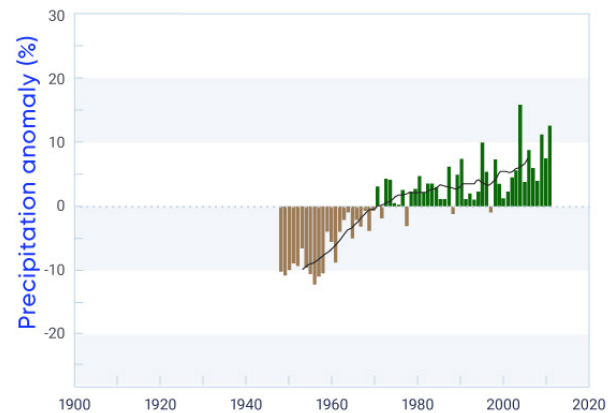
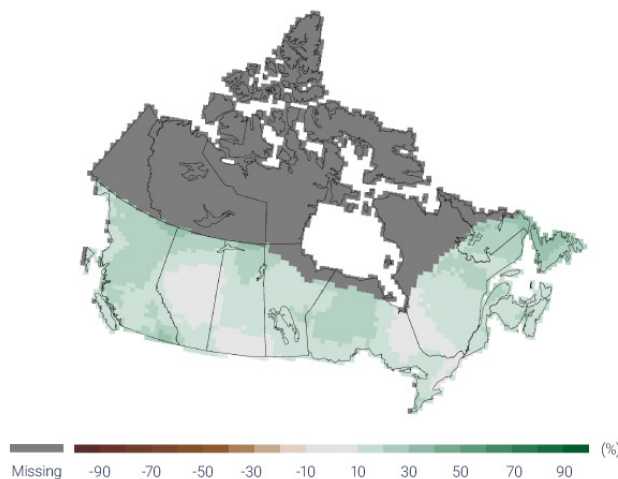
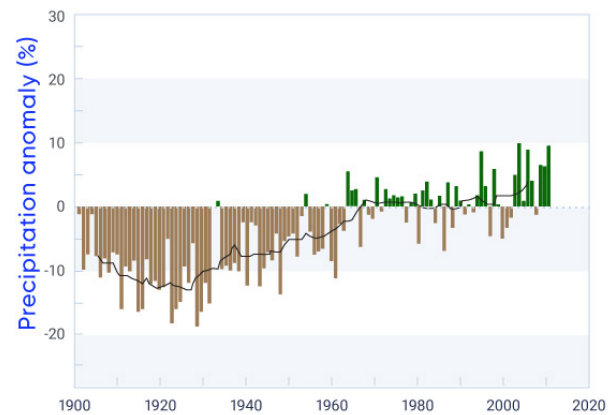
a) 1948–2012**b) 1948–2012****c) 1900–2012****d) 1900–2012**

Figure 4.15: Changes in annual precipitation, 1948–2012 and 1900–2012

Figure caption: Observed changes in locally normalized annual precipitation (%) between (a) 1948 and 2012 and (c) 1900 and 2012; changes are computed based on linear trends over the respective periods. Average of normalized precipitation relative to the 1961–1990 mean (b) across Canada and (d) in southern Canada (south of 60° north latitude); the black lines are 11-year running mean. Estimates are derived from the gridded station data. There is a lack of data in northern Canada (see Figure 4.1).

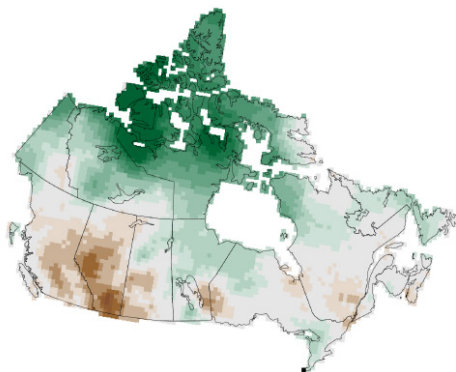
FIGURE SOURCE: UPDATED FROM FIGURE 4 OF VINCENT ET AL., 2015.

Table 4.4: Observed changes in normalized annual and seasonal precipitation between 1948 and 2012 for six regions and for all Canadian land area^a

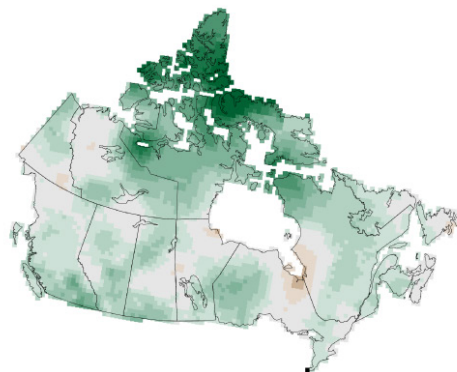
REGION	CHANGE IN PRECIPITATION, %				
	Annual	Winter	Spring	Summer	Autumn
British Columbia	5.0	-9.0	18.2	7.9	11.5
Prairies	7.0	-5.9	13.6	8.4	5.8
Ontario	9.7	5.2	12.5	8.6	17.8
Quebec	10.5	5.3	20.9	6.6	20.0
Atlantic	11.3	5.1	5.7	11.2	18.2
Northern Canada	32.5	54.0	42.2	18.1	32.1
Canada	18.3	20.1	25.3	12.7	19.0

^a Changes are represented by linear trends over the period. Estimates are derived from the gridded station data. There is a lack of data for northern Canada (see Figure 4.1 for the location of stations), which reduces confidence in the estimate.

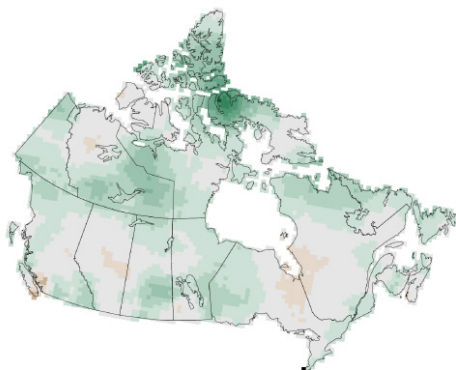
a) Winter



b) Spring



c) Summer



d) Autumn

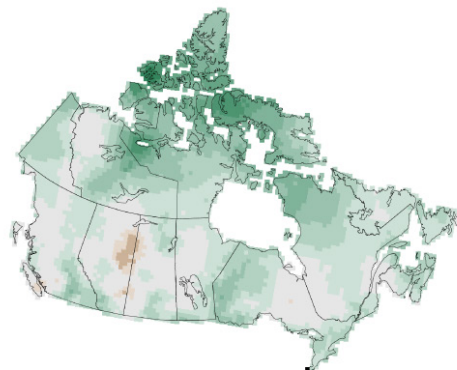


Figure 4.16: Changes in seasonal precipitation, 1948–2012

Figure caption: Observed changes in normalized seasonal precipitation (%) between 1948 and 2012 for the four seasons. Changes are computed based on linear trends over the respective periods. Estimates are derived from the gridded station data. There is a lack of data in northern Canada (see Figure 4.1).

FIGURE SOURCE: FIGURE 5 OF VINCENT ET AL., 2015.

For long-term observed trends, at the century scale, changes in precipitation can be assessed only for southern Canada, due to the lack of data for northern Canada. An increase was observed over all regions of southern Canada since 1900 and is statistically significant at that spatial scale at the 5% level. Warming has resulted in the proportion of the amount of precipitation falling as snow (i.e., the ratio of snowfall to total precipitation) steadily and significantly decreasing over southern Canada, especially during spring and autumn (Vincent et al., 2015). This is also the case for the Arctic region. There is a pronounced decline in summer snowfall over the Arctic Ocean and the Canadian Arctic Archipelago, and this decline is almost entirely caused by snowfall being replaced by rain (Screen and Simmonds, 2012). Such a change in the form of precipitation, from snow to rain, has profound impacts in other components of the physical environment, such as river flow, with the spring freshet becoming significantly earlier (Vincent et al., 2015; see Chapter 6, Section 6.2).

4.3.1.2: Causes of observed changes

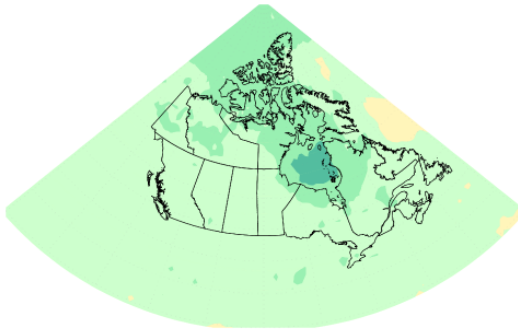
There is *medium confidence* that there is a human-caused contribution to observed global-scale changes in precipitation over land since 1950 (Bindoff et al., 2013). Much of the evidence of human influence on global-scale precipitation results from precipitation increases in the northern mid- to high latitudes (Min et al., 2008; Marvel and Bonfils, 2013; Wan et al., 2014). This pattern of increase is clear in climate model simulations with historical forcing (e.g., Min et al., 2008) and in future projections (Collins et al., 2013). Observed precipitation in northern high latitudes, including Canada, has increased and can be attributed – at least in part – to external forcing (Min et al., 2008; Wan et al., 2014). Atmospheric moisture increases with warming in both observations and model simulations. Natural internal climate variability from decade to decade contributes little to the observed changes (Vincent et al., 2015). This evidence, when combined, leads us to conclude that there is *medium confidence* that the observed increase in Canadian precipitation is at least partly due to human influence.

4.3.1.3: Projected changes and uncertainties

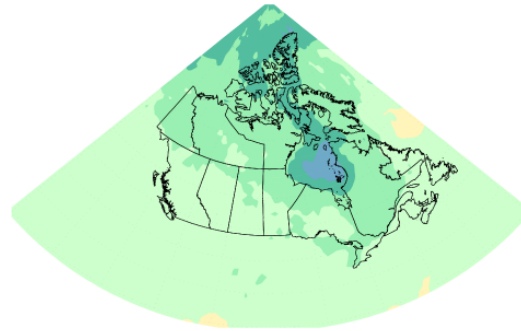
Multi-model projections of percentage changes (relative to 1986–2005) in winter, summer, and annual precipitation in Canada are shown in Figures 4.17, 4.18, and 4.19. The figures include maps of change for the low emission scenario (RCP2.6) and high emission scenario (RCP8.5) for the near term (2031–2050) and late century (2081–2100), and a national average time series of the normalized local changes for Canada as a whole for the period 1900–2100. Unlike for temperature, which is projected to increase everywhere in every season, precipitation has patterns of increase and decrease. In the near term, a small (generally less than 10%) increase in precipitation is projected in all seasons, with slightly larger values in northeastern Canada. In the late century (2081–2100), under the high emission scenario, the changes are much larger, with extensive areas of increased precipitation in northern Canada (more than 30% of the annual mean in the high Arctic). Since annual mean precipitation is low in the Arctic, even modest changes in absolute amount translate into a large percentage change. In contrast, large areas of southern Canada are projected to see a reduction in precipitation in summer under the high emission scenario (RCP8.5); for example, a median reduction of more than 30% is projected for southwestern British Columbia (see Figure 4.18). The projected decrease in summer precipitation (also projected in other parts of the world) is a consequence of overall surface drying and changes in atmospheric circulation (Collins et al., 2013).

As was the case for temperature, the national average time series for precipitation in the lower panels of the three figures show relatively small differences between the low emission scenario (RCP2.6) and high emission scenario (RCP8.5) in the near term (2031–2050). The winter season precipitation changes projected under the two scenarios diverge somewhat by the late century, while the summertime changes are near zero over the entire century, regardless of emission scenario. This small change in national average of locally normalized precipitation hides the fact that summertime precipitation changes are projected to be large (and hence impactful) in many areas of Canada. The large percent increases in northern Canada are generally offset by the large percent decreases in southern Canada, so that the average of percent changes for Canada as a whole in the time series plots shows little overall change in summer precipitation. As mean precipitation is much larger in southern Canada than in northern Canada, the absolute amount of precipitation decrease in the southern Canada is larger than the absolute value of precipitation increase in northern Canada. Regional differences are clearly important for impact studies, and quantitative information at the regional level is provided in Table 4.5. In general, changes in precipitation exhibit more temporal and regional variation than changes in temperature, and, so, projection results for precipitation have less confidence than projection results for temperature.

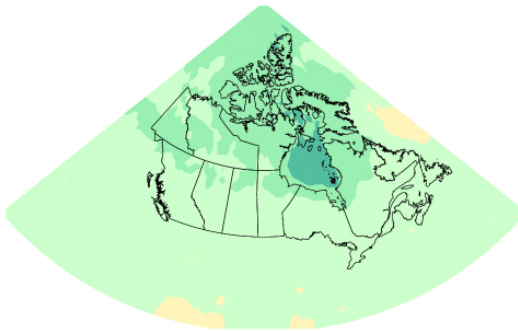
Precipitation change RCP2.6 (2031–2050)
December–February



Precipitation change RCP8.5 (2031–2050)
December–February



Precipitation change RCP2.6 (2081–2100)
December–February



Precipitation change RCP8.5 (2081–2100)
December–February

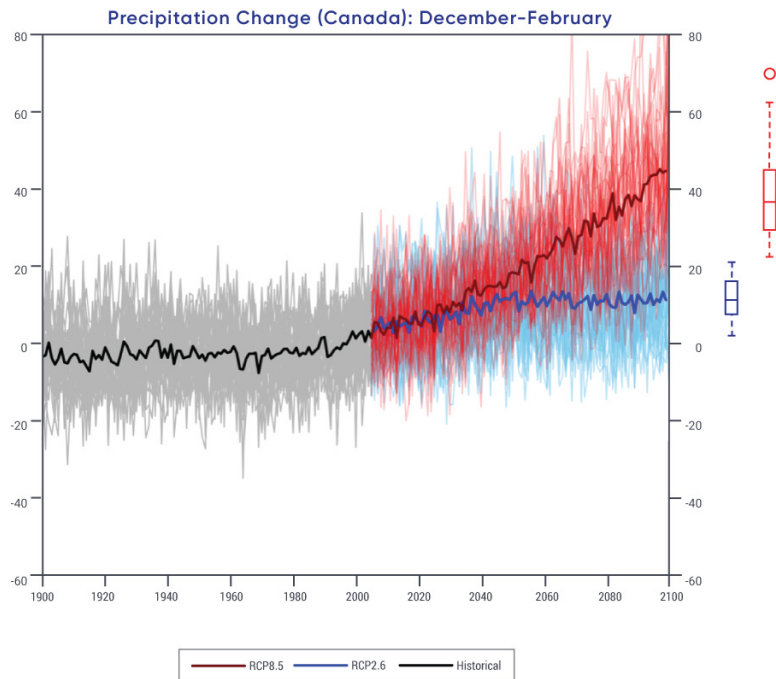
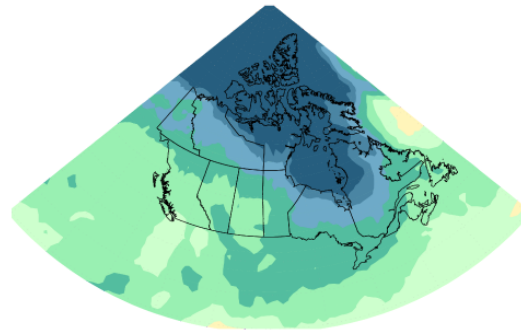


Figure 4.17: Projected precipitation changes for winter season



Figure caption: Maps and time series of projected precipitation change (%) for December, January, and February, as represented by the median of the fifth phase of the Coupled Model Intercomparison Project (CMIP5) multi-model ensemble. Changes are relative to the 1986–2005 period. The upper maps show precipitation change for the 2031–2050 period and the lower maps, for the 2081–2100 period. The left-hand maps show changes resulting from the low emission scenario (RCP2.6), whereas the right-hand maps show changes from the high emission scenario (RCP8.5). The time series at the bottom of the figure shows the change averaged over Canadian land area and spans the 1900–2100 period. The thin lines show results from the individual CMIP5 models, and the heavy line is the multi-model mean. The spread among models, evident in the thin lines, is quantified by the box-and-whisker plots to the right of each panel. They show, for the 2081–2100 period, the 5th, 25th, 50th (median), 75th, and 95th percentile values.

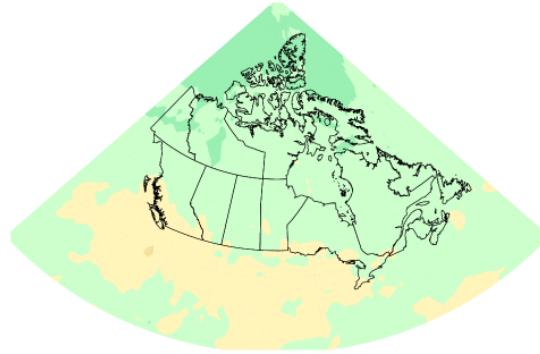
FIGURE SOURCE: CLIMATE RESEARCH DIVISION, ENVIRONMENT AND CLIMATE CHANGE CANADA.

Precipitation change RCP2.6 (2031–2050)

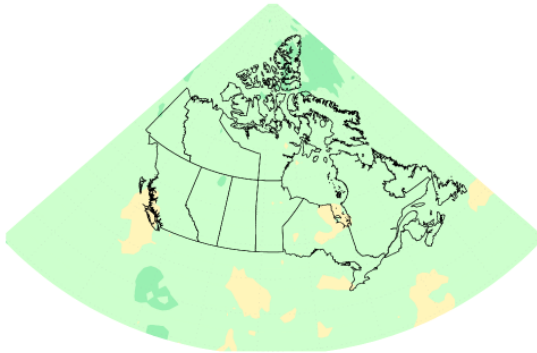
June–August

**Precipitation change RCP8.5 (2031–2050)**

June–August

**Precipitation change RCP2.6 (2081–2100)**

June–August

**Precipitation change RCP8.5 (2081–2100)**

June–August

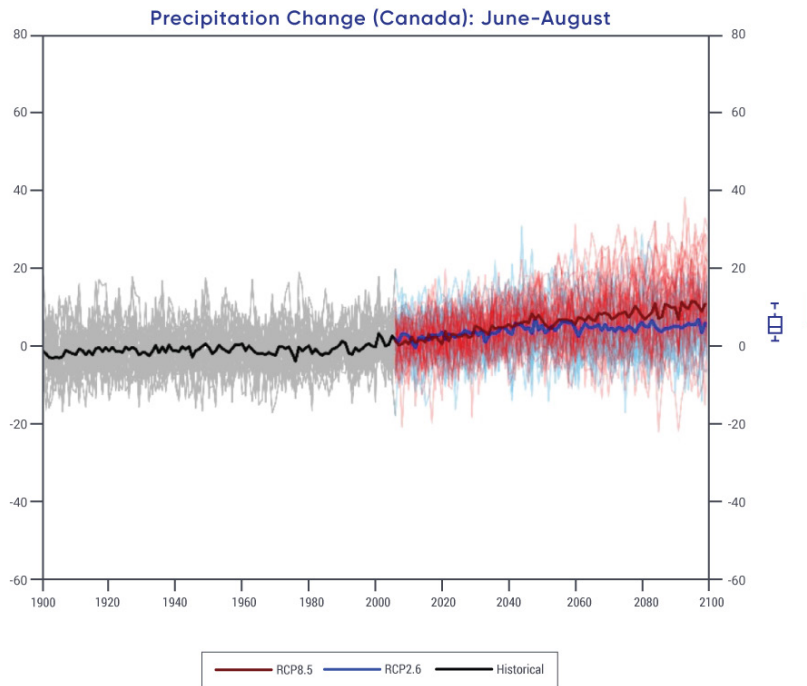
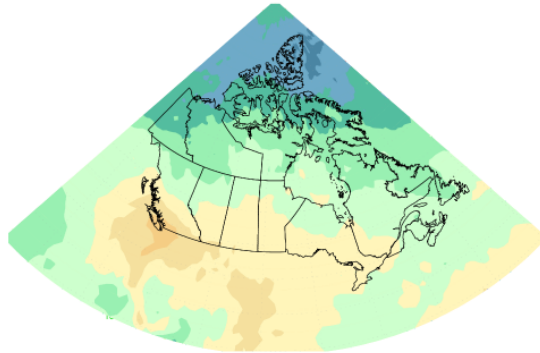


Figure 4.18: Projected precipitation changes for summer season

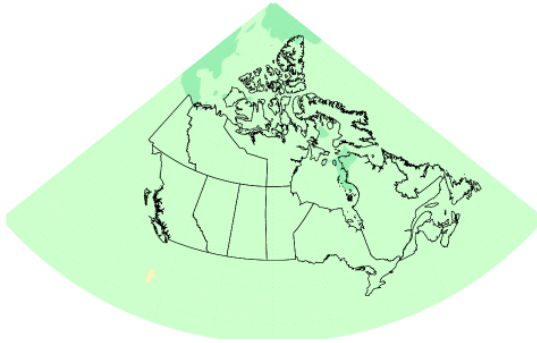


Figure caption: Maps and time series of projected precipitation change (%) for June, July, and August, as represented by the median of the fifth phase of the Coupled Model Intercomparison Project (CMIP5) multi-model ensemble. Changes are relative to the 1986–2005 period. The upper maps show precipitation change for the 2031–2050 period and the lower maps, for the 2081–2100 period. The left-hand maps show changes resulting from the low emission scenario (RCP2.6), whereas the right-hand maps show changes from the high emission scenario (RCP8.5). The time series at the bottom of the figure shows the change averaged over Canadian land area and over the 1900–2100 period. The thin lines show results from the individual CMIP5 models, and the heavy line is the multi-model mean. The spread among models, evident in the thin lines, is quantified by the box-and-whisker plots to the right of each panel. They show, for the 2081–2100 period, the 5th, 25th, 50th (median), 75th, and 95th percentile values.

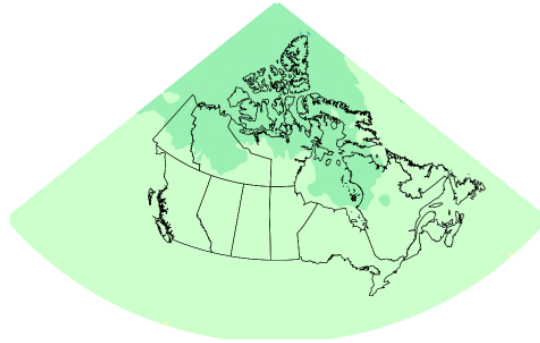
FIGURE SOURCE: CLIMATE RESEARCH DIVISION, ENVIRONMENT AND CLIMATE CHANGE CANADA.

Precipitation change RCP2.6 (2031–2050)

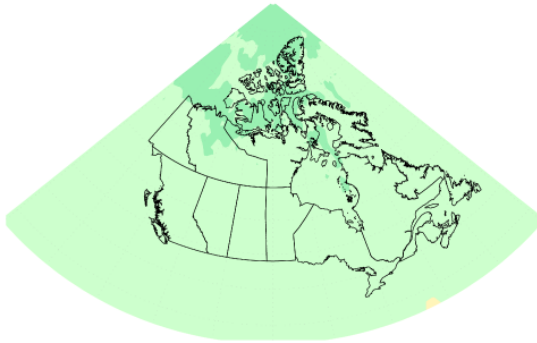
Annual

**Precipitation change RCP8.5 (2031–2050)**

Annual

**Precipitation change RCP2.6 (2081–2100)**

Annual

**Precipitation change RCP8.5 (2081–2100)**

Annual

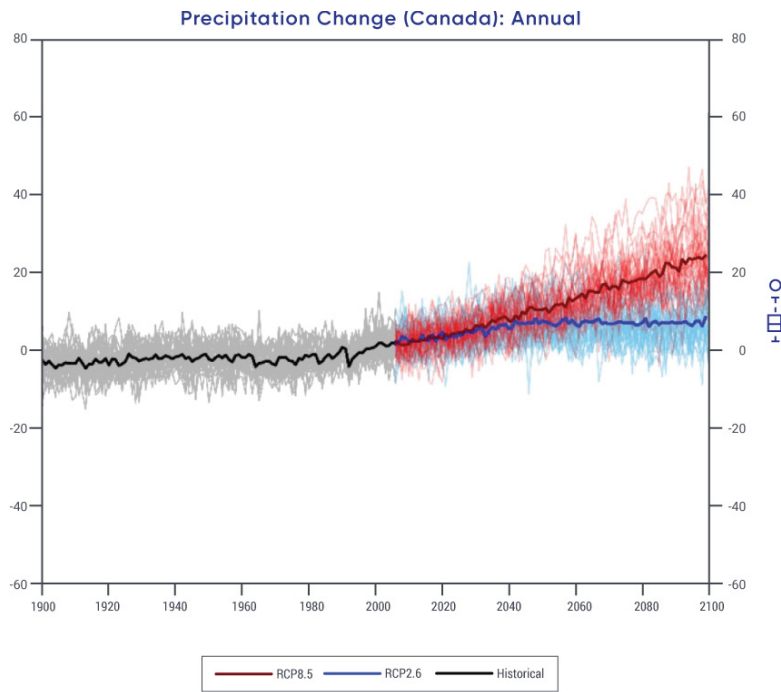
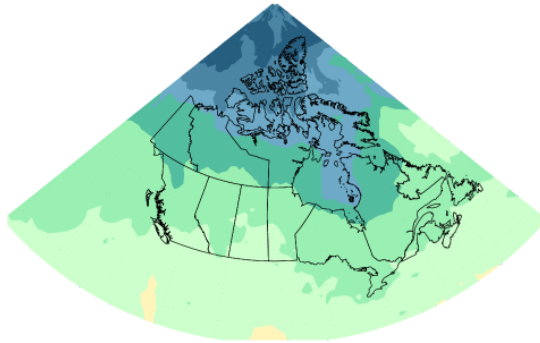


Figure 4.19: Projected annual precipitation changes



Figure caption: Maps and time series of projected annual mean precipitation change (%) as represented by the median of the fifth phase of the Coupled Model Intercomparison Project (CMIP5) multi-model ensemble. Changes are relative to the 1986–2005 period. The upper maps show precipitation change for the 2031–2050 period and the lower maps, for the 2081–2100 period. The left-hand maps show changes resulting from the low emission scenario (RCP2.6), whereas the right-hand maps show changes from the high emission scenario (RCP8.5). The time series at the bottom of the figure shows the change averaged over Canadian land area and over the 1900–2100 period. The thin lines show results from the individual CMIP5 models, and the heavy line is the multi-model mean. The spread among models, evident in the thin lines, is quantified by the box-and-whisker plots to the right of each panel. They show, for the 2081–2100 period, the 5th, 25th, 50th (median), 75th, and 95th percentile values.

FIGURE SOURCE: CLIMATE RESEARCH DIVISION, ENVIRONMENT AND CLIMATE CHANGE CANADA.

Table 4.5: Projected percentage change in annual mean precipitation for six regions and for all Canadian land area relative to 1986–2005^a

REGION ^b	SCENARIO; PERIOD; MEDIAN (25TH, 75TH PERCENTILE), %			
	RCP2.6		RCP8.5	
	2031–2050	2081–2100	2031–2050	2081–2100
British Columbia	4.3 (-0.4, 9.8)	5.8 (0.4, 11.9)	5.7 (0.0, 11.4)	13.8 (5.7, 22.4)
Prairies	5.0 (-0.7, 10.8)	5.9 (-0.2, 12.1)	6.5 (0.4, 13.1)	15.3 (6.3, 24.9)
Ontario	5.5 (0.4, 11.1)	5.3 (-0.1, 10.8)	6.6 (1.8, 12.4)	17.3 (8.5, 26.1)
Quebec	7.1 (2.0, 12.2)	7.2 (2.2, 13.0)	9.4 (4.5, 14.7)	22.5 (14.8, 32.0)
Atlantic	3.8 (-0.8, 9.1)	4.7 (0.3, 9.0)	5.0 (0.6, 9.9)	12.0 (5.7, 19.3)
North	8.2 (2.1, 14.6)	9.4 (2.8, 16.7)	11.3 (5.4, 18.1)	33.3 (22.1, 46.4)
Canada	5.5 (0.2, 11.2)	6.8 (0.4, 14.4)	7.3 (2.0, 13.2)	24.2 (13.7, 36.2)

^a The median or 50th percentile value is based on the CMIP5 multi-model ensemble. The 25th percentile value indicates that 25% of the CMIP5 model projections have a change smaller than this value. The 75th percentile value indicates 25% of CMIP5 model projections have a change larger than this value.

^b Regions are defined by political boundaries; "North" includes the three territories (see Figure 1.1).

As the climate warms, particularly in northern Canada, there will inevitably be an increased likelihood of precipitation falling as rain rather than snow. This is consistent with the observed changes in the snowfall fraction noted earlier. Although there has not been a systematic analysis for Canada, one analysis projected a decrease in the fraction of precipitation falling as snow, especially in the autumn and spring, for southern Alaska and eastern Quebec (Krasting et al., 2013). In addition, regional climate model projections show a general increase in rain-on-snow events over the coming century (Jeong and Sushama, 2017).

These results for changes in mean precipitation are consistent with the IPCC Fifth Assessment, in that the high latitudes are projected to experience a large increase in annual mean precipitation by the late of this century under the high emission (RCP8.5) scenario. The projected increase in annual mean precipitation in the high latitudes is a common feature of generations of climate models. It can be explained by the expected warming-induced large increase in atmospheric water vapour (Collins et al. 2013). Over the historical period, an increase in annual total precipitation in the high latitudes has been detected and can be attributed to human influence (Min et al., 2008; Wan et al., 2014). There is **high confidence** in the projected increase in annual mean precipitation. Confidence in projected changes in seasonal mean precipitation is lower. It should be noted that models generally project less summertime precipitation for southern Canada under a high emission scenario.

4.3.2: Extreme precipitation

Mean precipitation over a day or less can cause localized damage to infrastructure, such as roads and buildings, while heavy multi-day episodes of precipitation can produce flooding over a large region. This section assesses only changes in short-duration (a day or less) extreme precipitation, for which there is relatively more data and research than for longer-duration extremes.

4.3.2.1: Observed changes

There do not appear to be detectable trends in short-duration extreme precipitation in Canada for the country as a whole based on available station data. More stations have experienced an increase than a decrease in the highest amount of one-day rainfall each year, but the direction of trends is rather random over space. Some stations show significant trends, but the number of sites that had significant trends is not more than what one would expect from chance (Shephard et al., 2014; Mekis et al., 2015; Vincent et al., 2018). This seems to be inconsistent with global results (Westra et al., 2013) and the results for the contiguous region of the United States (Barbero et al., 2017). The number of days with heavy rainfall¹⁸ has increased by only 2 to 3 days since 1948 at a few locations in southern British Columbia, Ontario, Quebec, and the Atlantic provinces (Vincent et al., 2018). The number of days with one hour total rainfall greater than 10 mm, with 24-hour total rainfall greater than 25 mm, or with 48-hour total rainfall greater than 50 mm also did not show any consistent change across the country (Mekis et al., 2015). Days with heavy snowfall¹⁹ have decreased by a few days at numerous locations in western Canada (British Columbia to Manitoba), while they have increased at several locations in the North (Yukon, Northwest Territories, and western Nunavut). The highest one-day snowfall amount has decreased by several millimetres (snow water equivalent) at several locations in the southern region of British Columbia and Alberta (Mekis et al., 2015; Vincent et al., 2018).

The lack of a detectable change in extreme precipitation in Canada is not necessarily evidence of a lack of change. On one hand, this is inconsistent with the observed increase in mean precipitation. As the variance of precipitation is proportional to the mean, and as there is a significant increase in mean precipitation, one would expect to see an increase in extreme precipitation. On the other hand, the expected change in response to warming may be small when compared with natural internal variability. Warming has resulted in an increase in atmospheric moisture, which is expected to lead to an increase in extreme precipitation if other conditions, such as atmospheric circulation, do not change. On the global scale, observations indicate an increase in extreme precipitation associated with warming. Moreover, the increase can be attributed to human influence (Min et al., 2011; Zhang et al., 2013). The median increase in extreme precipitation is about 7% per 1°C increase in global mean temperature, consistent with the increase in the water-holding capacity of the atmosphere due to warming (Westra et al., 2013). Compared with the natural internal variability of precipitation,

18 Heavy rainfall is defined as rainfall greater than the annual 90th percentile from all rainfall events greater than 1 mm per day.

19 Heavy snowfall is defined as snowfall greater than the annual 90th percentile from all events greater than 1 mm per day.

this amount of increase would be too small to be detectable at individual locations. Only about 8.5% of all stations over global land areas with more than 30 years of data show an increase in extreme precipitation at the 5% significance level, which is slightly higher than the rate of stations showing an increase (5%) that could be expected from chance (Westra et al., 2013). The detection of the increasing intensity of extreme precipitation over lands on Earth is possible because of the vast amount of data available. On the regional scale, there is much less information, which is the case for Canada, where long-term observations are very limited, and detection becomes more difficult.

4.3.2.2: Projected changes and uncertainties

In the future, extreme precipitation is projected to increase in Canada. Averaged for Canada, extreme precipitation with a return period²⁰ of 20 years in the late century climate is projected to become a once in about 10-year event in 2031–2050 under a high emission scenario (RCP8.5) (see Figure 4.20). Beyond mid-century, these changes are projected to stabilize under the low emission scenario (RCP2.6), but to continue under the high emission scenarios (RCP8.5). An extreme event that currently occurs once in 20 years is projected to become about a once in five-year event by late century under the high emission scenario (RCP8.5). In other words, extreme precipitation of a given magnitude is projected to become more frequent. Moreover, the relative change in event frequency is larger for more extreme and rarer events. For example, an event that currently occurs once in 50 years is projected to occur once in 10 years by late 21st century under a high emission scenario (RCP8.5). The amount of precipitation with a certain recurrence interval is projected to increase. The amount of 24-hour extreme precipitation that occurs once in 20 years on average is projected to increase by about 5% under a low emission scenario (RCP2.6) and by 12% under a high emission scenario (RCP8.5) by 2031–2050, and to increase as much as 25% by 2081–2100 under a high emission scenario (RCP8.5). Differences in the projected percentage changes in annual maximum 24-hour precipitation among regions of Canada for the same emission scenario and time period are notably small. The median value for every region is in general within the range of 25th to 75th percentiles of other regions, except under the high emission scenario toward the late century (see Table 4.6).

20 A return period describes how common an event is. For example, a 20-year return period means the event has a 1 in 20 probability of occurring each year. Thus, a 20-year event would be expected to occur every 20 years, on average.

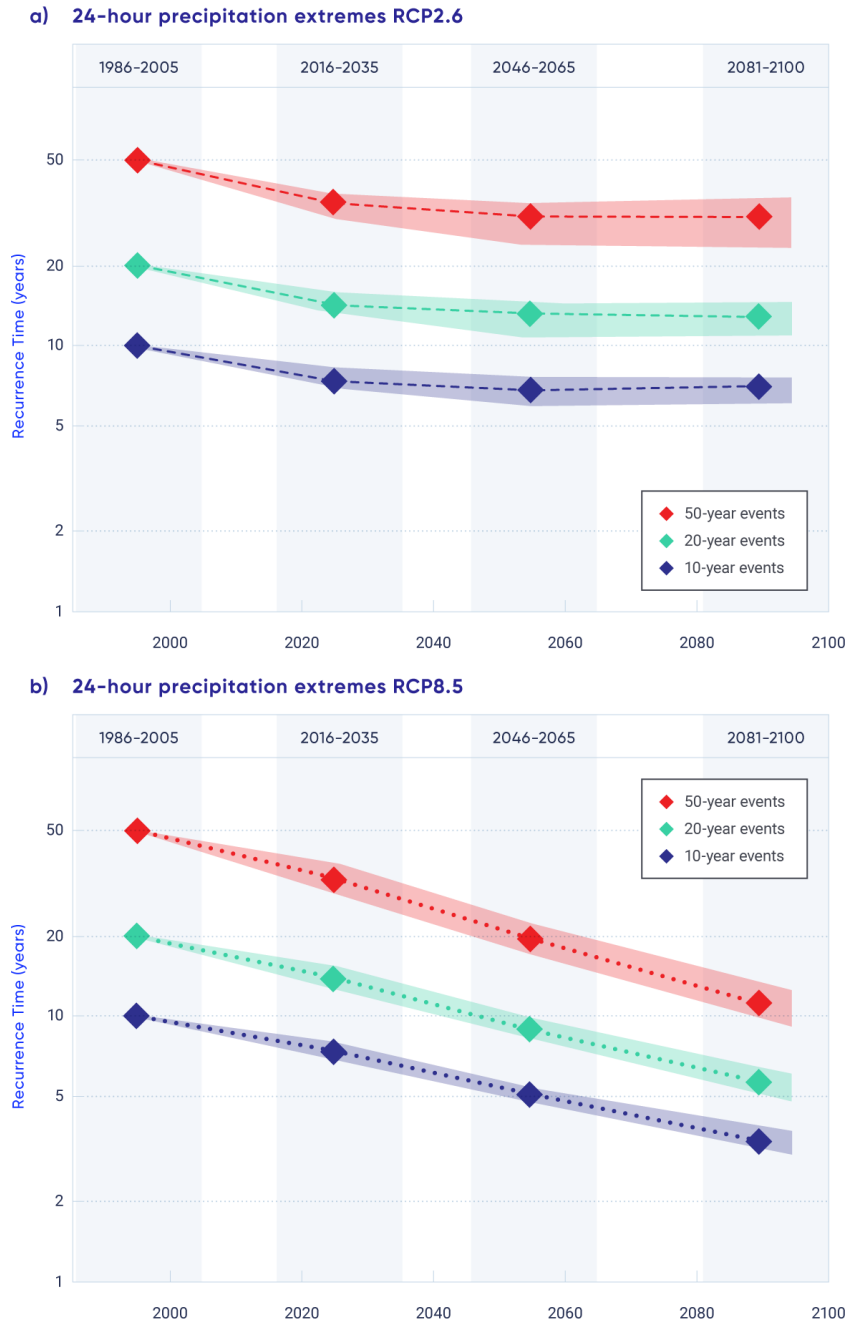


Figure 4.20: Projected changes in recurrence time for extreme precipitation

Figure caption: Projected changes in recurrence time for annual maximum 24-hour precipitation that occurs, on average, once in 10, 20, and 50 years in the late century across Canada, as simulated by Earth system models contributing to the fifth phase of the Coupled Model Intercomparison Project (CMIP5) under a low emission scenario (RCP2.6; upper) and a high emission scenario (RCP8.5; lower). The projections are at global climate model resolution, and the processes that produce 24-hour extreme precipitation at local scale are not well represented. Therefore, projections should be interpreted with caution. The shading represents the range between the 25th and 75th percentiles.

Table 4.6: Projected changes in annual maximum 24-hour precipitation that occur, on average, once in 10, 20, and 50 years, as simulated by Earth system models contributing to the fifth phase of the Coupled Model Intercomparison Project (CMIP5)^a

REGION ^b	SCENARIO; PERIOD; MEDIAN (25TH, 75TH PERCENTILE), %			
	RCP2.6		RCP8.5	
	2031–2050	2081–2100	2031–2050	2081–2100
	10-year return value			
British Columbia	5.9 (3.8, 9.3)	8.0 (4.5, 13.3)	9.8 (7.4, 12.7)	26.1 (20.4, 31.3)
Prairies	5.5 (2.3, 9.2)	5.1 (2.2, 8.9)	7.8 (4.5, 10.1)	17.5 (12.6, 23.8)
Ontario	6.0 (1.4, 8.4)	5.3 (2.1, 10.9)	8.5 (3.6, 11.4)	20.5 (15.4, 26.7)
Quebec	6.8 (2.7, 10.6)	7.2 (4.6, 10.2)	10.0 (6.2, 15.6)	26.0 (17.8, 30.2)
Atlantic	6.8 (3.4, 10.2)	8.5 (6.1, 11.1)	13.5 (7.8, 18.2)	30.2 (22.9, 38.3)
North	7.1 (4.1, 8.7)	7.8 (4.7, 10.8)	10.8 (8.2, 13.5)	29.8 (23.2, 36.2)
Canada	6.1 (4.0, 8.5)	6.7 (4.1, 9.5)	8.4 (6.9, 11.4)	22.9 (18.8, 26.9)
	20-year return value			
British Columbia	6.3 (3.6, 9.9)	6.7 (4.1, 14.1)	9.8 (7.4, 13.6)	25.8 (21.8, 30.8)
Prairies	5.6 (2.6, 10.2)	6.0 (2.6, 10.3)	8.8 (4.7, 10.8)	19.1 (14.1, 25.3)
Ontario	5.7 (0.8, 7.8)	5.1 (2.3, 10.7)	8.2 (2.4, 12.2)	20.1 (16.1, 25.6)
Quebec	6.0 (2.2, 10.8)	8.6 (3.8, 9.9)	10.2 (5.1, 15.8)	25.8 (18.3, 32.0)
Atlantic	7.9 (3.6, 11.9)	9.5 (6.7, 11.8)	13.7 (7.9, 19.2)	30.9 (24.1, 39.1)
North	6.8 (3.6, 9.4)	7.4 (3.1, 11.4)	10.7 (7.9, 13.3)	30.0 (22.9, 35.1)
Canada	6.1 (3.7, 8.7)	6.9 (4.5, 10.0)	8.8 (6.6, 11.6)	24.2 (19.2, 27.8)
	50-year return value			
British Columbia	7.0 (3.0, 10.5)	9.2 (5.1, 16.0)	10.1 (7.5, 15.5)	28.7 (21.9, 33.5)
Prairies	6.1 (2.3, 10.5)	6.5 (2.0, 11.3)	10.0 (6.2, 12.1)	21.3 (14.8, 26.8)
Ontario	4.9 (0.9, 8.4)	7.6 (0.8, 11.0)	8.5 (2.8, 13.0)	20.1 (13.3, 28.0)
Quebec	6.3 (0.9, 9.9)	7.7 (3.3, 11.9)	10.8 (4.7, 17.1)	26.5 (17.9, 33.8)
Atlantic	7.7 (3.5, 12.8)	9.2 (6.6, 14.3)	14.3 (7.9, 21.2)	32.4 (24.9, 42.6)
North	4.9 (2.4, 9.0)	6.4 (1.7, 10.2)	10.8 (7.8, 13.0)	30.1 (24.9, 33.8)
Canada	6.2 (3.8, 9.2)	7.4 (5.0, 10.4)	9.2 (7.0, 11.9)	24.7 (19.6, 29.7)

^a The median or 50th percentile value is based on the CMIP5 multi-model ensemble. The 25th percentile value indicates that 25% of the CMIP5 model projections have a change smaller than this value. The 75th percentile value indicates 25% of CMIP5 model projections have a change larger than this value.

^b Regions are defined by political boundaries; "North" includes the three territories (see Figure 1.1).

While results from global climate model projections (such as those above) are useful for impact assessment and adaptation planning, there is an important caveat, especially for extreme precipitation. It is difficult to interpret these projections at local scales. The spatial resolution of global climate models is coarse (typically 100–250 km). The precipitation extremes in a model therefore represent averages over an area of several thousand square kilometres, and so convey different information than may be required for practical applications. More importantly, climate models may not include all of the physical processes that produce local intense rainstorms. This affects the confidence we can have in statistical downscaling products that transform precipitation from coarse resolution models to smaller areas. While regional climate models may operate at much smaller scales, conventional regional climate models, which are used to conduct most of the dynamical downscaling, do not accurately simulate important processes such as convection. These limitations must be kept in mind when using projections for the purpose of regional and local adaptation; in particular, the projected values given by these global or regional climate models should not be interpreted literally as the measured amount of precipitation at a point location.

Estimating changes in short-duration extreme precipitation at a point location is complex because of the lack of observations in many places and the discontinuous nature of precipitation at small scales. Projection of such extreme precipitation is also difficult because of the shortage of simulations by models with a very high resolution that resolve the physical processes that produce those extreme events (Zhang et al., 2017). Nevertheless, multiple lines of evidence support *high confidence* in projecting an increase in extreme precipitation globally. These lines of evidence include attribution of an observed increase in high-latitude total precipitation to human influence, consistency in projected future increases in extreme precipitation by multiple models, and the physical understanding that warming would result in an increase in atmospheric moisture. It is *likely* that extreme precipitation will increase in Canada in the future, although the magnitude of the increase is much more uncertain.

Box 4.2: The impact of combined changes in temperature and precipitation on observed and projected changes in fire weather

Changes in temperature and in precipitation each have impacts across many sectors. However, combined changes in temperature and precipitation can have additional impacts, and some sectors rely on information regarding concurrent changes in these two variables. An example is fire weather. Changing precipitation and temperature (along with changing wind) alter the risk of extreme wildfires that can result from hot, dry, and windy conditions. Understanding changes in both temperature and precipitation lends insight into changes in wildfire risk and how it might evolve in the future.

The Canadian Forest Fire Weather Index (FWI) System is a collection of indices that use weather variables, including temperature and precipitation, to characterize fire risk. It includes an index, labelled FWI, that synthesizes information from the collection of indices to quantify day-to-day changes in the risk of a spreading fire. A threshold of this index is often used to define days conducive to fire spread (Wang et al., 2015; Jain et

al., 2017). In addition, three of the most commonly used indices are moisture codes, describing the dryness of different categories of fuels (Wotton, 2009). All of the FWI indices represent factors affecting fire potential, with larger values indicating greater fire potential, although the occurrence of a large wildfire also depends on ignition sources, fuel characteristics, and fire management actions.

A few studies have looked at trends in these indices across Canada. Large year-to-year variability in the FWI indices hinders detection of trends (Amiro et al., 2004; Girardin et al. 2004). Trends may sometimes be discerned from a very long record of data, as is the case with increases in the Drought Code²¹ in northern Canada and decreases in the Drought Code in western Canada and parts of eastern Canada during the 20th century (Girardin and Wotton, 2009). Another study found that the mean number of fire spread days across Canada increased over 1979 to 2002, although the trends varied regionally, and only some were significant (Jain et al., 2017). Despite inconsistent trends in the FWI indices, there has been a significant increase in annual area burned across Canada (Podur et al., 2002; Gillett et al., 2004).

Higher temperatures in the future will contribute to increased values of the FWI indices and, therefore, increased fire risk. The increase in precipitation that would be required to offset warming for most of the FWI indices exceeds both projected and reasonable precipitation changes (Flannigan et al. 2016). Increases in extreme values of the Duff Moisture Code²² are projected across most of the forested ecozones of Canada by 2090 (Wotton et al., 2010). Increases in fire spread days and extreme values of the FWI are projected, with the largest changes in the western Prairies (Wang et al., 2015). Several other studies also project increases in the FWI indices and the length of the fire season in Canada in the future (Flannigan et al., 2009; de Groot et al., 2013; Flannigan et al., 2013; Kochtubajda et al., 2006). Although the magnitude of projected changes varied among these studies, most project increases in the FWI indices that correspond to higher fire risk.

Section summary

In summary, there is *medium confidence* that annual mean precipitation has increased, on average, in Canada, with larger percentage increases in northern Canada. There is *low confidence* in the magnitude of the increase because of poor spatial coverage of long-term, observational records. Such increases are consistent with model simulated precipitation response to anthropogenic climate change. Annual and winter precipitation is projected to increase everywhere in Canada over the 21st century, with larger percentage changes in northern Canada. Summer precipitation is projected to decrease over southern Canada under a high emission scenario toward the end of the 21st century, but only small changes are projected under a low emission scenario. For Canada as a whole, there is a lack of observational evidence of changes in daily and short-duration

21 The Drought Code describes dryness in the deepest forest floor layers and in large debris; precipitation influences the amount of moisture in this layer and temperature controls the rate at which the layer dries (Wotton et al., 2009).

22 The Duff Moisture Code describes dryness in the upper layer of forest floor debris; precipitation provides moisture and both temperature and relative humidity control the rate at which the layer dries (Wotton et al., 2009).

extreme precipitation. This is not unexpected, as extreme precipitation response to anthropogenic climate change during the historical period would have been small relative to its natural variability and as such, difficult to detect. However, in the future, daily extreme precipitation is projected to increase (*high confidence*).

4.4: Attribution of extreme events

Key Message

Anthropogenic climate change has increased the likelihood of some types of extreme events, such as the 2016 Fort McMurray wildfire (*medium confidence*) and the extreme precipitation that produced the 2013 southern Alberta flood (*low confidence*).

There has been an increase in costly extreme weather and climate events worldwide (WMO, 2014) and across Canada (Kovacs and Thistlethwaite, 2014; OAGC, 2016; OPBO, 2016). Much of this rise is due to greater exposure to the effects of such extreme events, as Canada's population and the value of its supporting infrastructure have both increased considerably. Changes in the intensity and frequency of damaging extreme weather and climate events due to climate change (IPCC, 2013) may also be playing a role. These extreme weather/climate events attract attention because they are rare and often have notable impacts on our society and economy.

It is generally not feasible to answer the question, Did human-induced climate change cause a particular weather or climate event? Often, that event could have occurred in the absence of human effects. Instead, recent research has focused on whether human activity has influenced the probability of particular weather or climate events or, in some cases, the strength or intensity of the events. As the climate changes, largely due to anthropogenic influences, the likelihood of a particular class of events – all events as extreme as or more extreme than the one defined in the study – also changes (NASEM, 2016). In this sense, an extreme event may be attributable to causes external to the natural climate system. Thus, a new branch of climate science, called event attribution, has emerged that evaluates how the probability or intensity of an extreme event, or more generally, a class of extreme events, has changed as a result of increases in atmospheric GHGs from human activity.

A growing number of extreme events in Canada and worldwide are being examined in this way (e.g., Herring et al., 2017; NASEM 2016). Several of these event attribution analyses are relevant to Canadians (see Table 4.7). Two examples are highlighted in this section, including a description of methods of analysis in Box 4.3.

Table 4.7: Event attribution analyses relevant to Canada

EVENT	REFERENCE	BRIEF OVERVIEW OF CONCLUSIONS
Drought		
2015 drought in western Canada	Szeto et al., 2016 ^a	Anthropogenic climate change increased likelihood of extremely warm spring but no contribution to the observed weather pattern was detected.
Flooding		
2014 flooding in south-east Prairies	Szeto et al., 2015 ^a	Anthropogenic influence may have increased rainfall, but landscape modification played a key role in increased runoff.
2013 Alberta floods	Teufel et al., 2017 ^b	Increased likelihood of extreme rainfall in this region due to the anthropogenic component; no anthropogenic influence detected for runoff.
Cold extremes		
Cold February 2015 in North America	Bellprat et al., 2016	Determined event was mainly due to natural variability, although there might have been some contribution from decreased Arctic sea ice and increased sea surface temperatures.
Extreme cold winter of 2013/2014 in North America	Yu and Zhang, 2015	Suggest warming trend made event less extreme than it might have been.
Extreme cold winter of 2013/2014	Wolter et al., 2015 ^a	Extreme cold events have become much less likely due to the long-term, anthropogenic warming trend.
Warm extremes		
November/December 2016 extreme warm Arctic temperatures	Kam et al., 2017 ^a	Extremely warm Arctic temperatures most likely would not have occurred without the anthropogenic contribution.
2014 extreme warm temperatures in eastern Pacific and western Atlantic	Kam et al., 2015 ^a	Extreme warm temperatures over the eastern Pacific and western Atlantic considerably more likely with the anthropogenic component.

Table 4.7: Event attribution analyses relevant to Canada

Arctic sea ice ^a		
2012 record minimum sea ice extent	Kirchmeier-Young et al., 2017 ^b	Record minimum in summer Arctic sea ice extent would not have occurred without the anthropogenic contribution.
March 2015 record low sea ice extent	Fučkar et al., 2016 ^a	The observed sea ice extent would not have occurred without the underlying climate change influence.
2012 record minimum sea ice extent	Zhang and Knutson, 2013	Record minimum in summer Arctic sea ice extent <i>extremely unlikely</i> to be due to internal variability.
Wildfires		
2016 Fort McMurray wildfire	Kirchmeier-Young et al., 2017 ^{a,b}	Anthropogenic contribution increased likelihood of extreme wildfire risk and the length of fire seasons.
2016 Fort McMurray wildfire	Tett et al., 2017 ^a	Anthropogenic contribution increased likelihood of extreme vapour pressure deficits, which increase fire risk.
2015 Alaska wildfire season	Partain et al., 2016 ^a	Anthropogenic contribution increased likelihood of extreme wildfire risk.

a Included in the annual Bulletin of the American Meteorological Society special reports on event attribution.

b Discussed in more detail in this section.

c Discussed in more detail in Chapter 5.

Box 4.3: Methods for event attribution

Event attribution is used to quantify how human-influenced climate change affects the occurrence of a particular type (or class) of extreme event. Its goals are similar to those of the detection and attribution process described in Chapter 2 (see Section 2.3.4), but it focuses on individual events. Event attribution analyses (NASEM, 2016) compare the likelihood of a particular class of events (e.g., all events as extreme, or more extreme, than the event defined in the study) between a factual world, which includes the human component, and a counter-factual world that comprises only natural factors – that is, the “climate that might have been” in the absence of the human component.

To demonstrate, Figure 4.21 shows distributions of possible values of a climate variable for the world without the human contribution in blue, and for a scenario like the one we have experienced with the human contri-

bution in red. The shaded regions represent the probability that a particular extreme event (an outcome as extreme, or more so, than the one indicated by the vertical bar) will occur in each scenario. The probability of the event increases when the human contribution is included — from 1 in 60 to 1 in 5. The ratio of the probability with the human contribution to the probability without the human contribution is referred to as a “risk ratio.” Although this event could occur in the absence of human influence, it is 12 times as likely (risk ratio of 12) when the human component is included.

The conclusions of an event attribution analysis often depend on how the question is posed. This includes the choices made when defining events and designing the analysis approach. For example, the change in probability between the two scenarios in Figure 4.21 depends on the placement of the vertical bar, or the lower bound on the magnitude that defines the chosen event. Changes in the probabilities of temperature and precipitation extremes depend on the probability of the events in the current climate, with larger risk ratios corresponding to more extreme (rarer) events (Kharin et al., 2018). The uncertainty in the risk ratio (i.e., the event attribution result) becomes larger for rarer events, as it is more difficult to estimate the probabilities of these very rare events. The choice of the variable and/or region to determine the distributions also has an impact on the results.

Two types of questions have been asked in event attribution analyses: How has the probability of the extreme event (frequency) changed, and how has the intensity of the event (magnitude) changed? As an example, event attribution for a flood-producing heavy rainfall event may try to answer, “Has human-induced climate change made this type of heavy rainfall event occur more often?” (frequency) or “Has human-induced climate change increased the amount of rainfall in these types of storms?” (magnitude). The human influence could have a different impact on the frequency than on the magnitude of a particular event. It is thus important to understand the characteristics of the event being assessed and to interpret the results of an event attribution analysis in context.

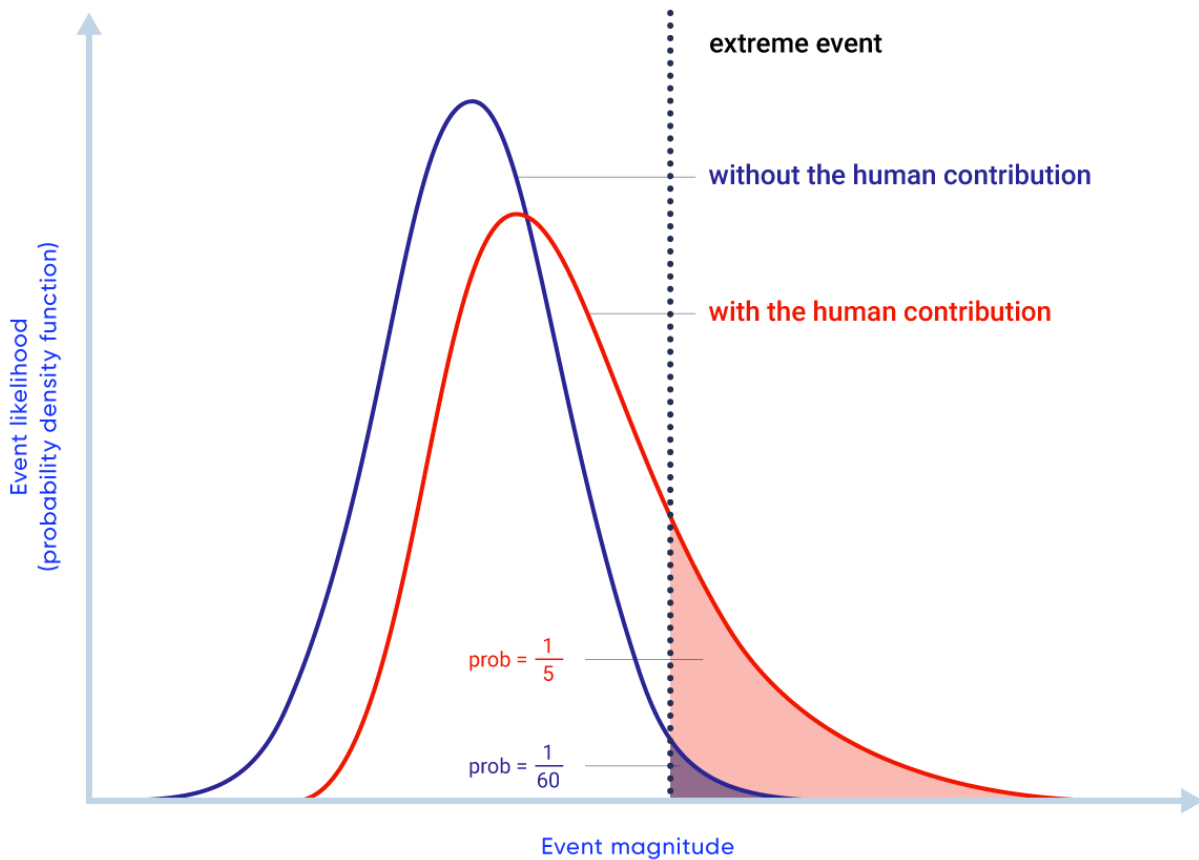


Figure 4.21: Hypothetical illustration of event attribution

Figure caption: The blue distribution represents the possible values of a climate variable in a world without a human influence. The red distribution represents the possible values of the same variable in a world with the human contribution. The shaded areas indicate the probability of experiencing an extreme event (defined by the dashed vertical bar) in each scenario.

FIGURE SOURCE: PRODUCED FOR THIS REPORT BY THE PACIFIC CLIMATE IMPACTS CONSORTIUM (PCIC).

4.4.1: Attribution of two recent events

4.4.1.1: 2013 Southern Alberta flood

In June 2013, an extreme flood event in southern Alberta became Canada's costliest natural disaster to that date, with significant damage to property and infrastructure throughout the region, including in the City of Calgary. The flood displaced almost 100,000 people and resulted in \$6 billion in damage, including \$2 billion in insured losses (ECCC, 2017).

A storm producing heavy rainfall over the region triggered the flooding event in the Bow River basin, but a combination of both meteorological and hydrological factors led to the extreme flooding. A recent study (Teufel et al., 2017) assessed the contributions of several of these factors, including anthropogenic GHG emissions.

The study used the Canadian Regional Climate Model (CRCM5) to run large ensembles of high-resolution simulations for North America. To assess the contribution of human climate change, simulations of the model were run using present-day levels of GHGs and also using pre-industrial levels to represent the time before humans had a discernable impact on the climate.

To estimate the probability of the event, return periods were calculated for three-day rainfall totals during May and June exceeding the observed amount. The return period for the observed event in the present-day climate in the Bow River was estimated to be about 60 years. Using climate projections, the return period is estimated to be reduced to about 20 years by the late 21st century (under both an intermediate emission scenario [RCP4.5] and a high emission scenario [RCP8.5]), implying that the type of extreme rainfall that led to the southern Alberta flooding event will become much more common in the future.

Estimated return periods were compared between the present-day and pre-industrial climates, in order to determine the human contribution (see Figure 4.22). Including human GHG emissions resulted in shorter return periods (the event is more likely) for three-day maximum precipitation over the entire southern Alberta region than for pre-industrial levels (see Figure 4.22a). Weather and climate variability tends to be larger for smaller regions, resulting in a smaller ratio between the anthropogenic influence and natural internal variability. Therefore, the anthropogenic influence on the rainfall events over the smaller Bow River basin region was less pronounced (see Figure 4.22b). There is no discernable difference for maximum three-day surface runoff, and thus no anthropogenic influence is detected for this variable (see Figure 4.22c). The authors acknowledge the uncertainties in modelling complex surface hydrological processes and suggest that any increase in rainfall could be offset by decreases in snowpack or frozen ground conditions.

In summary, human influence was detected for the flood-producing rainfall, particularly over the larger region, but human influence could not be detected for the flood itself. A flood event is the result of many factors in addition to the amount of rainfall, including the ground conditions, characteristics of the snowpack, and size and orientation of the storm. As a result, two events with the same rainfall amounts do not necessarily produce floods of the same magnitude. The complex hydrological processes that occur after the rainfall reaches the ground add additional uncertainty which decreases the ability to detect human influence.

Increased GHG emissions, largely due to human activities, result in increased temperatures. Increased temperatures allow more moisture to be available in the atmosphere for precipitation, leading to increased intensity of extreme rainfall events. The 2013 southern Alberta flood was the result of a combination of many factors, and this study demonstrated that human-induced emission of GHGs had increased the likelihood of an extreme amount of precipitation in southern Alberta, at least as large as the amount observed during this event.

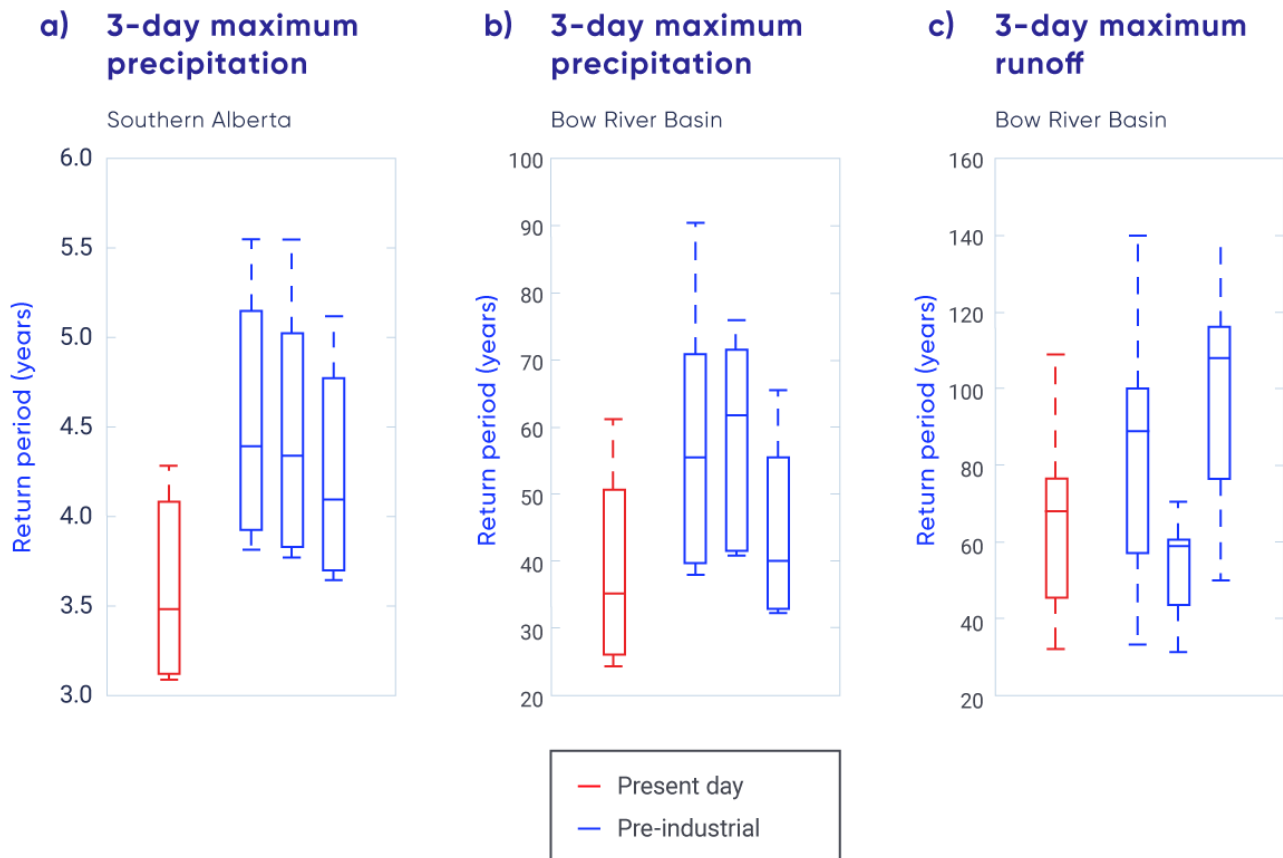


Figure 4.22: Precipitation and runoff that led to the 2013 southern Alberta flood

Figure caption: Return periods for the observed three-day maximum precipitation (a, b) and three-day maximum runoff (c) that led to the 2013 southern Alberta extreme flooding event. Present-day return periods are shown in red, and return periods from three pre-industrial simulations are shown in blue. Analysis is for the larger southern Alberta region (a) and the smaller Bow River basin (b, c). The box plots show the spread in the return periods across different estimates of the observed values from the reference simulations. The box boundaries indicate the range from the 25th to 75th percentiles, the middle line indicates the 50th percentile, and the whiskers extend to 1.5 times the width of the box or the most extreme value.

FIGURE SOURCE: ADAPTED FROM TEUFEL ET AL., 2017.

4.4.1.2: 2016 Fort McMurray wildfire

In early May 2016, a large wildfire burned almost 600,000 ha (a land area covering 6000 square kilometres) in northern Alberta. This fire resulted in the evacuation of all of the residents of Fort McMurray (over 80,000 people) and halted production in the oil sands (Government of Alberta, 2016). Insured losses are estimated at \$3.5 billion (IBC, 2016). The total cost of the event is still being determined, but it is expected to be considerably higher.

The fire ignited near the Horse River amid very dry fuel conditions. High winds a few days later resulted in rapid spread and fire growth. A study has used event attribution to assess the influence of human-induced climate change on several measures of wildfire risk (see Box 4.2), albeit not extreme fire itself, in this region (Kirchmeier-Young et al., 2017a).

Like the previous example, the study used large ensembles of model simulations, in this case employing the Canadian Earth System Model (CanESM2). To assess human influence, the model was run with only natural forcings (solar and volcanic effects) and also with a combination of natural and anthropogenic forcings. The anthropogenic component includes GHG emissions, aerosols, atmospheric ozone changes, and land-use change.

Fire weather (see Box 4.2), fire behaviour, and fire season measures were calculated to characterize fire risk from climate model output. To quantify the anthropogenic contribution, a risk ratio (NASEM, 2016) was calculated as the ratio of two probabilities: one for the event's occurrence when the human component is included, and one for the occurrence of the same event with only natural factors. The risk ratio can be interpreted as how many times as likely the event is as a result of anthropogenic factors. For example, a risk ratio of 1 implies no change in the probability of occurrence, and a risk ratio of 2 implies the event is twice as likely, or that there has been a 100% increase in the probability of the event compared with the unperturbed climate.

Results of the analysis show that three of the fire risk indices – extreme values of the Fire Weather Index (FWI; see Box 4.2), high number of spread days, and long fire seasons – all show risk ratio values greater than 1 (see Figure 4.23), indicating extreme values of each measure of wildfire risk are more likely when anthropogenic warming is included. Risk ratios vary among the different fire risk indices analyzed. However, extreme values of all measures describing wildfire risk are more likely with anthropogenic forcing.

Increasing temperatures, like those observed across Canada (see Section 4.2), will lead to drier fuels, and thus increased fire potential, as well as longer fire seasons. It would require increases in precipitation well beyond what is expected with climate change to offset increasing temperatures in terms of the FWI indices (Flannigan et al., 2016). The study demonstrated that the extreme Alberta wildfire of 2016 occurred in a world where anthropogenic warming has increased fire risk, fire spread potential, and the length of fire seasons across parts of Alberta and Saskatchewan.

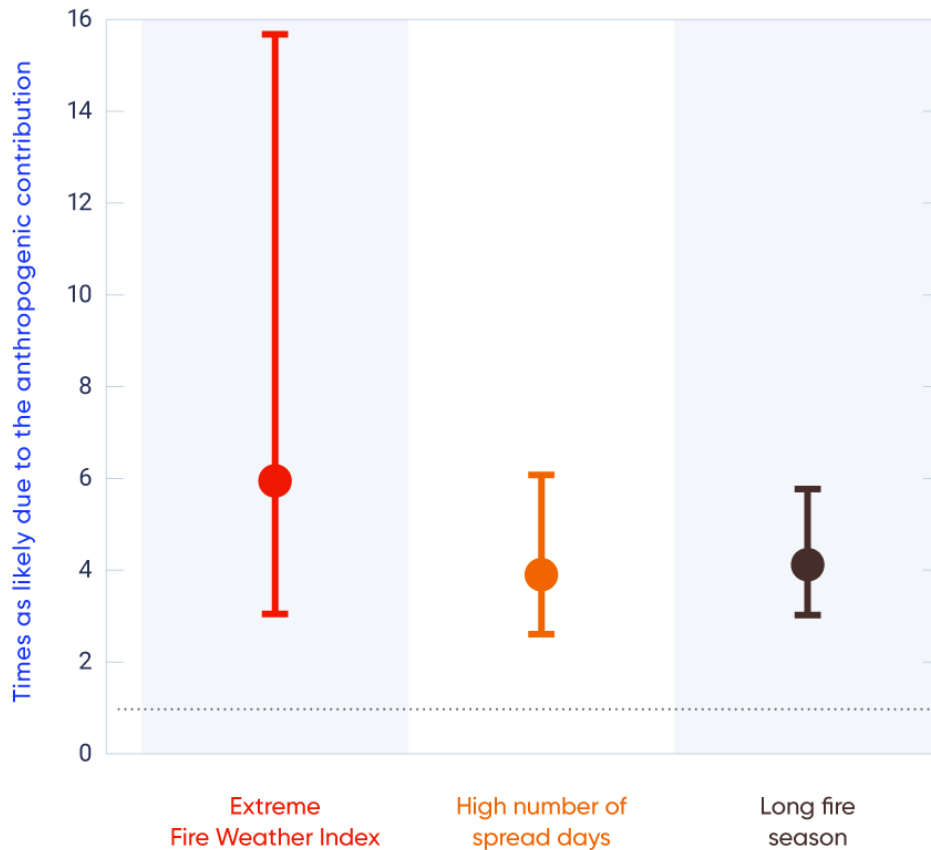


Figure 4.23: Risk ratios for three measures of extreme wildfire risk

Figure caption: Risk ratios for three measures of extreme wildfire risk in the Southern Prairies Homogeneous Fire Regime zone (Boulanger et al., 2014), showing the increase in likelihood due to the anthropogenic contribution. A risk ratio greater than 1 (dashed line) indicates the extreme event is more likely when the human contribution is included. The three measures used to characterize extreme wildfire risk in this region are fire weather (extreme Fire Weather Index), fire behaviour (high number of fire spread days), and fire season (long fire seasons). The error bars represent the 5–95% uncertainty range.

FIGURE SOURCE: ADAPTED FROM KIRCHMEIER-YOUNG ET AL., 2017A.





Section summary

In summary, a new field of event attribution has emerged, which aims to assess the role of human-induced climate change in extreme events. Some recent extreme events across Canada have been analyzed in this way, including the southern Alberta flood in 2013 and the Fort McMurray wildfire of 2016. For the first event, GHG emissions from human activity increased the likelihood of extreme, flood-producing rainfall, but the confidence in this attribution is low because of the difficulties in modelling precipitation extremes, which exhibit large variability at small scales, such as for this event. For the second event, there is *medium confidence* that human-induced climate change increased the likelihood of the extreme wildfire risk associated with the 2016 Fort McMurray wildfire. The assessment of *medium confidence* balances *high confidence* in human influence on the increase in temperature, which affects fire risk strongly, with many other factors contributing to this event that are more difficult to represent in a climate model.

References

Amiro, B.D., Logan, K.A., Wotton, B.M., Flannigan, M.D., Todd, J.B., Stocks, B.J., and Martell, D.L. (2004): Fire weather index system components for large fires in the Canadian boreal forest. *International Journal of Wildland Fire*, v. 13, p. 391–400, doi:10.1071/WF03066.

Assel, R.A. (1980): Maximum freezing degree-days as a winter verity index for the Great Lakes, 1897–1977; *Monthly Weather Review*, v. 108, p. 1440–1445, doi:10.1175/1520-0493(1980)108%3C1440:MFDDAA%3E2.0.CO;2

Barbero, R., Fowler, H.J., Lenerink, G., Blenkinsop, S. (2017): Is the intensification of precipitation extremes with global warming better detected at hourly than daily resolutions? *Geophysical Research Letters*; doi:10.1002/2016GL071917

Bellprat, O., Massonnet, F., García-Serrano, J., Fučkar, N.S., Guemas, V. and Doblas-Reyes, F.J. (2016): The role of Arctic sea ice and sea surface temperatures on the cold 2015 February over North America; in *Explaining Extreme Events of 2015 from a Climate Perspective*; *Bulletin of the American Meteorological Society*, v. 97, p. S36–S41. doi:10.1175/BAMS-D-16-0159.1

Bindoff, N.L., Stott, P.A., AchutaRao, K.M., Allen, M.R., Gillett, N., Gutzler, D., Hansingo, K., Hegerl, G., Hu, Y., Jain, S., Mokhov, I.I., Overland, J., Perlwitz, J., Sebbari R. and Zhang, X. (2013): Detection and attribution of climate change: from global to regional; in *Climate Change 2013: The Physical Science Basis*; Contribution of Working Group I to the Fifth Assessment Report of the Intergovernmental Panel on Climate Change, (ed.) T.F. Stocker, D. Qin, G.-K. Plattner, M. Tignor, S.K. Allen, J. Boschung, A. Nauels, Y. Xia, V. Bex and P.M. Midgley; Cambridge University Press, Cambridge, United Kingdom and New York, NY, p. 867–952, <https://www.ipcc.ch/site/assets/uploads/2018/02/WG1AR5_Chapter10_FINAL.pdf>

Boulanger, Y., Gauthier, S., and Burton, P.J. (2014): A refinement of models projecting future Canadian fire regimes using homogeneous fire regime zones; *Canadian Journal of Forest Research*, v. 44, p. 365–376, doi:10.1139/cjfr-2013-0372.

Casati, B., Yagouti, A. and Chaumont, D. (2013): Regional climate projections of extreme heat events in nine pilot Canadian communities for public health planning; *Journal of Applied Meteorology and Climatology*, v. 52, p. 2669–2698. doi:10.1175/JAMC-D-12-0341.1

Collins, M., Knutti, R., Arblaster, J., Dufresne, J.-L., Fichetef, T., Friedlingstein, P., Gao, X., Gutowski, W.J., Johns, T., Krinner, G., Shongwe, M., Tebaldi, C., Weaver, A.J. and Wehner, M. (2013): Long-term climate change: projections, commitments and irreversibility; in *Climate Change 2013: The Physical Science Basis*; Contribution of Working Group I to the Fifth Assessment Report of the Intergovernmental Panel on Climate Change, (ed.) T.F. Stocker, D. Qin, G.-K. Plattner, M. Tignor, S.K. Allen, J. Boschung, A. Nauels, Y. Xia, V. Bex and P.M. Midgley; Cambridge University Press, Cambridge, United Kingdom and New York, NY, USA; p. 1029–1136, <https://www.ipcc.ch/site/assets/uploads/2018/02/WG1AR5_Chapter12_FINAL.pdf>



de Groot, W.J., Flannigan, M.D. and Cantin, A.S. (2013): Climate change impacts on future boreal fire regimes. *Forest Ecology and Management*, v. 294, p. 35–44. doi:10.1016/j.foreco.2012.09.027.

DeBeer, C.M., Wheeler, H.S., Carey, S.K. and Chun, K.P. (2016): Recent climatic, cryospheric, and hydrological changes over the interior of western Canada: a review and synthesis; *Hydrology and Earth System Sciences*, v. 20, p. 1573–1598. doi: 10.5194/hess-20-1573-2016

ECCC [Environment and Climate Change Canada] (2016): Climate data and scenarios for Canada: Synthesis of recent observation and modelling results. Cat. No.: En84-132/2016E-PDF.

ECCC [Environment and Climate Change Canada] (2017): Canada's top ten weather stories of 2013; <<https://ec.gc.ca/meteo-weather/default.asp?lang=En&n=3318B51C-1>>

Environment Canada (1995): The State of Canada's Climate: Monitoring Variability and Change; A State of the Environment Report; SOE report no. 95-1, Catalogue no. En1-11/95-1E; Environment Canada, Ottawa, ON.

Flannigan, M., Cantin, A.S., de Groot, W.J., Wotton, M., Newbery, A., and Gowman, L.M. (2013): Global wildland fire season severity in the 21st century; *Forest Ecology and Management*, v. 294, p. 54–61. doi:10.1016/j.foreco.2012.10.022.

Flannigan, M.D., Krawchuk, M.A., de Groot, W.J., Wotton, B.M., and Gowman, L.M. (2009): Implications of changing climate for global wildland fire; *International Journal of Wildland Fire*, v. 18, p. 483–507. doi:10.1071/WF08187.

Flannigan, M.D., Wotton, B.M., Marshall, G.A., de Groot, W.J., Johnston, J., Jurko, N. and Cantin, A.S. (2016): Fuel moisture sensitivity to temperature and precipitation: climate change implications. *Climatic Change*, v. 134, p. 59–71. doi:10.1007/s10584-015-1521-0

Flato, G., Marotzke, J., Abiodun, B., Braconnot, P., Chou, S.C., Collins, W., Cox, P., Driouech, F., Emori, S., Eyring, V., Forest, C., Gleckler, P., Guilyardi, E., Jakob, C., Kattsov, V., Reason, C. and Rummukainen, M. (2013): Evaluation of climate models; in *Climate Change 2013: The Physical Science Basis; Contribution of Working Group I to the Fifth Assessment Report of the Intergovernmental Panel on Climate Change*, (ed.) T.F. Stocker, F. Qin, G.-K. Plattner, M. Tignor, S.K. Allen, J. Boschung, A. Nauels, Y. Xia, V. Bex, P.M. Midgley; Cambridge University Press, Cambridge, United Kingdom and New York, NY, USA, p. 741–866, <https://www.ipcc.ch/site/assets/uploads/2018/02/WG1AR5_Chapter09_FINAL.pdf>

Fučkar, N.S., Massonnet, F., Guemas, V., García-Serrano, J., Bellprat, O., Doblas-Reyes, F.J. and Acosta, M. (2016): Record low Northern Hemisphere sea ice extent in March 2015; in *Explaining Extreme Events of 2015 from a Climate Perspective; Bulletin of the American Meteorological Society*, v. 97, p. S136–S140. doi: 10.1175/BAMS-D-16-0153.1

Gillett, N.P., Weaver, A.J., Zwiers, F.W. and Flannigan, M.D. (2004): Detecting the effect of climate change on Canadian forest fires; *Geophysical Research Letters*, v. 31, 4 p. doi:10.1029/2004GL020876

Girardin, M.P., and Wotton, B.M. (2009): Summer moisture and wildfire risks across Canada. *Journal of Applied Meteorology and Climatology*. v. 48, p. 517–533, doi:10.1175/2008JAMC1996.1.



Girardin, M.-P., Tardif, J., Flannigan, M.D., Wotton, B.M., and Bergeron, Y. (2004): Trends and periodicities in the Canadian Drought Code and their relationships with atmospheric circulation for the southern Canadian boreal forest. *Canadian Journal of Forest Research*, v. 34, p. 103–119, doi:10.1139/X03-195.

Goodsman, D.W., Groszklos, G., Aukema, B.H., Whitehouse, C., Bleiker, K.P., McDowell, N.G., Middleton, R.S. and Xu, C. (2018): The effect of warmer winters on the demography of an outbreak insect is hidden by intraspecific competition; *Global Change Biology*, doi:10.1111/gcb.14284

Government of Alberta (2016): Final update 39: 2016 wild-fires; <<https://www.alberta.ca/release.cfm?xID=41701e7EC-BE35-AD48-5793-1642c499FF0DE4CF>>

Gullett, D.W. and Skinner, W.R. (1992): The state of Canada's climate: temperature change in Canada; A State of the Environment Report; SOE report no. 92-2, Cat. no. Enl-11/92-2E; Environment Canada, Ottawa, ON.

Hartmann, D.L., Klein Tank, A.M.G., Rusticucci, M., Alexander, L.V., Brönnimann, S., Charabi, Y., Dentener, F.J., Dlugokencky, E.J., Easterling, D.R., Kaplan, A., Soden, B.J., Thorne, P.W., Wild, M., and Zhai, P.M. (2013): Observations: Atmosphere and Surface; in *Climate Change 2013: The Physical Science Basis. Contribution of Working Group I to the Fifth Assessment Report of the Intergovernmental Panel on Climate Change*, (ed.) T.F. Stocker, D. Qin, G.-K. Plattner, M. Tignor, S.K. Allen, J. Boschung, A. Nauels, Y. Xia, V. Bex and P.M. Midgley; Cambridge University Press, Cambridge, United Kingdom and New York, NY, USA, pp. 159–254. doi:10.1017/CBO9781107415324.008

Herring, S.C., Christidis, N., Hoell, A., Kossin, J.P., Schreck III, C.J. and Stott, P.A. (2017): Explaining extreme events of 2016 from a climate perspective; *Bulletin of the American Meteorological Society*, v. 98, p. S1–S157.

Herring, S.C., Hoell, A., Hoerling, M.P., Kossin, J.P., Schreck III, C.J. and Stott, P.A. (2016): Explaining extreme events of 2015 from a climate perspective; *Bulletin of the American Meteorological Society*, v. 97, p. S1–S145.

IBC [Insurance Bureau of Canada] (2016): Northern Alberta wildfire costliest insured natural disaster in Canadian history – estimate of insured losses: \$3.58 billion; <<http://www.abc.ca/bc/resources/media-centre/media-releases/northern-alberta-wildfire-costliest-insured-natural-disaster-in-canadian-history>>.

IPCC [Intergovernmental Panel on Climate Change] (2013): Summary for policymakers; in *Climate Change 2013: The Physical Science Basis; Contribution of Working Group I to the Fifth Assessment Report of the Intergovernmental Panel on Climate Change*, (ed.) T.F. Stocker, D. Qin, G.-K. Plattner, M. Tignor, S. K. Allen, J. Boschung, A. Nauels, Y. Xia, V. Bex and P.M. Midgley; Cambridge University Press, Cambridge, United Kingdom and New York, NY, USA, p. 3–29. <https://www.ipcc.ch/site/assets/uploads/2018/02/WG1AR5_SPM_FINAL.pdf>.

Jain, P., Wang, X. and Flannigan, M.D. (2017): Trend analysis of fire season length and extreme fire weather in North America between 1979 and 2015; *International Journal of Wildland Fire*, v. 26, p. 1009–1020. doi:10.1071/WF17008

Jeong, D.I. and Sushama, L. (2017): Rain-on-snow events over North America based on two Canadian regional climate models; *Climate Dynamics*. doi:10.1007/s00382-017-3609-x

Kam, J., Knutson, T.R., Zeng, F. and Wittenberg, A.T. (2015): Record annual mean warmth over Europe, the northeast Pacific, and the north-west Atlantic during 2014: assessment of anthropogenic influence; in *Explaining Extreme Events of 2014 from a Climate Perspective*; *Bulletin of the American Meteorological Society*, v. 96, p. S61–S65. doi:10.1175/BAMS-D-15-00101.1

Kam, J., Knutson, T.R., Zeng, F. and Wittenberg, A.T. (2017): CMIP5 model-based assessment of anthropogenic influence on highly anomalous Arctic warmth during November–December 2016; in *Explaining extreme events of 2016 from a climate perspective*; *Bulletin of the American Meteorological Society*, v. 98, p. S34–S38. doi:10.1175/BAMS-D-17-0115.1

Kharin, V.V., Flato, G.M., Zhang, X., Gillett, N.P., Zwiers, F. and Anderson, K. (2018): Risks from climate extremes change differently from 1.5°C to 2.0°C depending on rarity; *Earth's Future*, v. 6, p. 704–715.

Kharin, V.V., Zwiers, F.W., Zhang, X. and Wehner, M. (2013): Changes in temperature and precipitation extremes in the CMIP5 ensemble; *Climatic Change*, v. 119, p. 345–357. doi:10.1007/s10584-013-0705-8

Kim, Y.-H., Min, S.-K., Zhang, X., Zwiers, F., Alexander, L.V., Donat, M.G. and Tung, Y.-S. (2015): Attribution of extreme temperature changes during 1951–2010; *Climate Dynamics*, v. 46, p. 1769–1782. doi: 10.1007/s00382-015-2674-2

Kirchmeier-Young, M.C., Zwiers, F.W., Gillett, N.P. and Cannon, A.J. (2017a): Attributing extreme fire risk in Western Canada to human emissions; *Climatic Change*, v. 144, p. 365–379. doi:10.1007/s10584-017-2030-0

Kirchmeier-Young, M.C., Zwiers, F.W. and Gillett, N.P. (2017b): Attribution of extreme events in Arctic sea ice extent; *Journal of Climate*, v. 30, p. 553–571. doi:10.1175/JCLI-D-16-0412.1

Kirtman, B., Power, S.B., Adedoyin, J.A., Boer, G.J., Bojariu, R., Camilloni, I., Doblas-Reyes, F.J., Fiore, A.M., Kimoto, M., Meehl, G.A., Prather, M., Sarr, A., Schär, C., Sutton, R., van Oldenborgh, G.J., Vecchi, G. and Wang, H.J. (2013): Near-term Climate Change: Projections and Predictability; in *Climate Change 2013: The Physical Science Basis. Contribution of Working Group I to the Fifth Assessment Report of the Intergovernmental Panel on Climate Change*, (ed.) T.F. Stocker, D. Qin, G.-K. Plattner, M. Tignor, S.K. Allen, J. Boschung, A. Nauels, Y. Xia, V. Bex and P.M. Midgley; Cambridge University Press, Cambridge, United Kingdom and New York, NY, USA.

Kochtubajda, B., Flannigan, M.D., Gyakum, J.R., Stewart, R.E., Logan, K.A., and Nguyen, T.-V. (2006): Lightning and fires in the Northwest Territories and responses to future climate change; *Arctic*, v. 59, p. 211–221.

Kovacs, P. and Thistlethwaite, J. (2014): Industry; in *Canada in a Changing Climate: Sector Perspectives on Impacts and Adaptation*, (ed.) F.J. Warren and D.S. Lemmen; Government of Canada, Ottawa, Ontario, p. 135–158.

Krasting, J.P., Broccoli, A.J., Dixon, K.W. and Lanzante, J.R. (2013): Future



changes in Northern Hemisphere snowfall; *Journal of Climate*, v. 26, p. 7813–7828. doi:10.1175/JCLI-D-12-00832.1

Li, G., Zhang, X., Cannon, A.J., Murdock, T., Sobie, S., Zwiers, F.W., Anderson, K. and Qian, B. (2018): Indices of Canada's future climate for general and agricultural adaptation applications; *Climatic Change*, v. 148, p. 249–263.

Marvel, K. and Bonfils, C. (2013): Identifying external influences on global precipitation; *Proceedings of the National Academy of Sciences*, v. 110. doi:10.1073/pnas.1314382110

Mekis, É. and Vincent, L.A. (2011): An overview of the second generation adjusted daily precipitation dataset for trend analysis in Canada; *Atmosphere-Ocean*, v. 49, p. 163–177. doi:10.1080/07055900.2011.583910

Mekis, E., Vincent, L.A., Shephard, M.W. and Zhang, X. (2015): Observed trends in severe weather conditions based on humidex, wind chill, and heavy rainfall events in Canada for 1953–2012; *Atmosphere-Ocean*, v. 53, p. 383–397. doi:10.1080/07055900.2015.1086970

Milewska, E., and Hogg, W.D. (2001): Spatial representativeness of a long-term climate network in Canada. *Atmosphere-Ocean*, v. 39, p. 145–161. doi:10.1080/07055900.2001.9649671

Milewska, E. and Hogg, W.D. (2002): Continuity of climatological observations with automation – temperature and precipitation amounts from AWOS (Automated Weather Observing System). *Atmosphere-Ocean*, v. 40, p. 333–359. doi:10.3137/ao.400304

Milewska, E.J. and Vincent, L.A. (2016): Preserving continuity of long-term daily maximum and minimum temperature observations with automation of reference climate stations using overlapping data and meteorological conditions; *Atmosphere-Ocean*, v. 54, p. 32–47. doi:10.1080/07055900.2015.1135784

Milewska, E.J., Vincent, L.A., Hartwell, M., Charlesworth, K. and Mekis, É. (2019): Adjusting precipitation amounts from Geonor and Pluvio automated weighing gauges to preserve continuity of observations in Canada. *Canadian Water Resources Journal*, doi:10.1080/07011784.2018.1530611.

Min, S.-K., Zhang, X. and Zwiers, F.W. (2008): Human-induced Arctic moistening; *Science*, v. 320, p. 518–520. doi:10.1126/science.1153468

Min, S.-K., Zhang, X., Zwiers, F.W. and Hegerl, G.C. (2011): Human contribution to more intense precipitation extremes; *Nature*, v. 470, p. 378–381. doi:10.1038/nature09763

Min, S.-K., Zhang, X., Zwiers, F., Shiogama, H., Tung, Y.-S. and Wehner, M. (2013): Multi-model detection and attribution of extreme temperature changes; *Journal of Climate*, v. 26, p. 7430–7451. doi: 10.1175/JCLI-D-12-00551.1

Murdock, T.Q., Cannon, A.J. and Sobie, S.R. (2014): Statistical downscaling of future climate projections for North America; Pacific Climate Impacts Consortium; Environment Canada, Victoria, British Columbia, <https://www.pacificclimate.org/sites/default/files/publications/PCIC_EC_downscaling_report_2014.pdf>



- Najafi, M.R., Zwiers, F.W. and Gillett, N.P. (2015): Attribution of Arctic temperature change to greenhouse-gas and aerosol influences; *Nature Climate Change*, v. 5, p. 246–249. doi:10.1038/nclimate2524
- Najafi, M.R., Zwiers, F. and Gillett, N. (2017a): Attribution of the observed spring snowpack decline in British Columbia to anthropogenic climate change; *Journal of Climate*, v. 30, p. 4113–4130.
- Najafi, M.R., Zwiers, F.W. and Gillett, N.P. (2017b): Attribution of observed streamflow changes in key British Columbia drainage basins; *Geophysical Research Letters*, v. 44, p. 11012–11020.
- NASEM [National Academies of Science, Engineering, and Medicine] (2016): Attribution of extreme weather events in the context of climate change; The National Academies Press, Washington, District of Columbia, USA. doi:10.17226/21852
- OAGC [Office of the Auditor General of Canada] (2016): Report 2: Mitigating the impacts of severe weather; Reports of the Commissioner of the Environment and Sustainable Development, <www.oag-bvg.gc.ca/internet/docs/parl_cesd_201605_02_e.pdf>.
- OPBO [Office of the Parliamentary Budget Officer] (2016): Estimate of the average annual cost for disaster financial assistance arrangements due to weather events; Ottawa, Canada. <https://www.pbo-dpb.gc.ca/web/default/files/Documents/Reports/2016/DFAA/DFAA_EN.pdf>.
- Osborn, T.J. and Jones, P.D. (2014): The CRUTEM4 land-surface air temperature data set: construction, previous versions and dissemination via Google Earth; *Earth System Science Data* v. 6, p. 61–68. doi:10.5194/essd-6-61-2014
- Partain, J.L., Alden, S., Bhatt, U.S., Bieniek, P.A., Brettschneider, B.R., Lader, R.T., Olsson, P.Q., Rupp, T.S., Strader, H., Thoman, R.L., Walsh, J., York, A.D. and Ziel, R.H. (2016): An assessment of the role of anthropogenic climate change in the Alaska fire season of 2015; in *Explaining Extreme Events of 2015 from a Climate Perspective*; *Bulletin of the American Meteorological Society*, v. 97, p. S14–S18. doi:10.1175/BAMS-D-16-0149.1
- Podur, J., Martell, D. L., and Knight, K. (2002): Statistical quality control analysis of forest fire activity in Canada; *Canadian Journal of Forest Research*, v. 32, p. 195–205. doi: 10.1139/X01-183
- Screen, J.A. and Simmonds, I. (2012): Declining summer snowfall in the Arctic: causes, impacts and feedbacks; *Climate Dynamics*, v. 38, p. 2243–2256.
- Shephard, M.W., Mekis, E., Morris, R.J., Feng, Y., Zhang, X., Kilcup, K. and Fleetwood, R. (2014): Trends in Canadian short-duration extreme rainfall: including an intensity-duration-frequency perspective; *Atmosphere-Ocean*, v. 52, p. 398–417.
- Szeto, K., Brimelow, J., Gysbers, P. and Stewart, R. (2015): The 2014 extreme flood on the southeastern Canadian Prairies; in *Explaining Extreme Events of 2014 from a Climate Perspective*; *Bulletin of the American Meteorological Society*, v. 96, p. S20–S24. doi:10.1175/BAMS-D-15-00110
- Szeto, K., Zhang, X., White, R.E. and Brimelow, J. (2016): The 2015 extreme drought in western Canada; in *Explaining Extreme Events of 2015*



- from a Climate Perspective; *Bulletin of the American Meteorological Society*, v. 97, p. S42–S46. doi:10.1175/BAMS-D-16-0147.1
- Tett, S.F.B., Falk, A., Rogers, M., Spuler, F., Turner, C., Wainwright, J., Dimdore-Miles, O., Knight, S., Freychet, N., Mineter, M.J. and Lehmann, C.E.R. (2017): Anthropogenic forcings and associated changes in fire risk in western North America and Australia during 2015/16; in *Explaining Extreme Events of 2016 from a Climate Perspective; Bulletin of the American Meteorological Society*, v. 98, p. S60–S64. doi:10.1175/BAMS-D-17-0096.1
- Teufel, B., Diro, G.T., Whan, K., Milrad, S.M., Jeong, D.I., Ganji, A., Huziy, O., Winger, K., Gyakum, J.R., de Elia, R., Zwiers, F.W. and Sushama, L. (2017): Investigation of the 2013 Alberta flood from weather and climate perspectives; *Climate Dynamics*, v. 48, p. 2881–2899. doi:10.1007/s00382-016-3239-8
- Vincent, L.A., Milewska, E.J., Wang, X.L. and Hartwell, M.M. (2017): Uncertainty in homogenized daily temperatures and derived indices of extremes illustrated using parallel observations in Canada; *International Journal of Climatology*, v. 38, p. 692–707. doi:10.1002/joc.5203
- Vincent, L.A., Wang, X.L., Milewska, E.J., Wan, H., Yang, F. and Swail, V. (2012): A second generation of homogenized Canadian monthly surface air temperature for climate trend analysis; *Journal of Geophysical Research*, v. 117. doi:10.1029/2012JD017859
- Vincent, L.A., Zhang, X., Bonsal, B.R. and Hogg, W.D. (2002): Homogenization of daily temperatures over Canada; *Journal of Climate*, v. 15, p. 1322–1334.
- Vincent, L.A., Zhang, X., Brown, R.D., Feng, Y., Mekis, E., Milewska, E.J., Wan, H. and Wang, X.L. (2015): Observed trends in Canada's climate and influence of low-frequency variability modes; *Journal of Climate*, v. 28, p. 4545–4560. doi: <http://dx.doi.org/10.1175/JCLI-D-14-00697.1>
- Vincent, L.A., Zhang, X., Mekis, E., Wan, H. and Bush, E.J. (2018): Monitoring changes in Canada's climate: Trends in temperature and precipitation indices based on daily monitoring data; *Atmosphere-Ocean*, doi: 10.1080/07055900.2018.1514579.
- Wan, H., Zhang, X., Zwiers, F. and Min, S.-K. (2014): Attributing Northern high-latitude precipitation change over the period 1966–2005 to human influence; *Climate Dynamics*, v. 45, p. 1713–1726. doi:10.1007/s00383-014-2423-y
- Wan, H., Zhang, X. and Zwiers, F.W. (2018): Human influence on Canadian temperatures; *Climate Dynamics*, v.52, p. 479-494.
- Wang, X.L., Chen, H., Wu, Y., Feng, Y. and Pu, Q. (2010): New techniques for detection and adjustment of shifts in daily precipitation data series; *Journal of Applied Meteorology and Climatology*, v. 49, p. 2416–2436. doi:10.1175/2010JAMC2376.1
- Wang, X.L., Feng, Y. and Vincent, L.A. (2014): Observed changes in one-in-20 year extremes of Canadian surface air temperatures; *Atmosphere-Ocean*, v. 52, p. 222–231. doi:10.1080/07055900.2013.818526



Wang, X., Thompson, D. K., Marshall, G. A., Tymstra, C., Carr, R., and Flannigan, M.D. (2015): Increasing frequency of extreme fire weather in Canada with climate change. *Climatic Change*, v. 130, p. 573–586. doi:10.1007/s10584-015-1375-5

Wang, X.L., Wen, Q.H. and Wu, Y. (2007): Penalized maximal t test for detecting undocumented mean change in climate data series; *Journal of Applied Meteorology and Climatology*, v. 46, p. 916–931. doi:10.1175/JAM2504.1

Wang, Z., Jiang, Y., Wan, H., Yan, J. and Zhang, X. (2017): Detection and attribution of changes in extreme temperatures at regional scale; *Journal of Climate*, v. 30, p. 7035–7047.

Werner, A.T. and Cannon, A.J. (2016): Hydrologic extremes – an intercomparison of multiple gridded statistical downscaling methods; *Hydrology and Earth System Sciences*, v. 20, p. 1483–1508. doi: 10.5191/hess-20-1483-2016

Westra, S., Alexander, L.V. and Zwiers, F.W. (2013): Global increasing trends in annual maximum daily precipitation; *Journal of Climate*, v. 26, p. 3904–3918. doi:10.1175/JCLI-D-12-00502.1

WMO [World Meteorological Organization] (2014): Atlas of mortality and economic losses from weather, climate and water extremes (1970–2012); WMO No. 1123.

Wolter, K., Hoerling, M., Eischeid, J.K., van Oldenborgh, G.J., Quan, X.-W., Walsh, J.E., Chase, T.N. and Dole, R.M. (2015): How unusual was the cold winter of 2013/14 in the upper Midwest; in *Explaining Extreme Events of 2014 from a Climate Perspective*; *Bulletin of the American Meteorological Society*, v. 96, p. S10–S14. doi:10.1175/BAMS-D-15-0126.1

Wotton, B.M. (2009): Interpreting and using outputs from the Canadian Forest Fire Danger Rating System in research applications; *Environmental and Ecological Statistics*, v. 16, p. 107–131. doi:10.1007/s10651-007-0084-2

Wotton, B.M., Nock, C.A. and Flannigan, M.D. (2010): Forest fire occurrence and climate change in Canada. *International Journal of Wildland Fire*; v. 19, p. 253–271. doi:10.1071/WF09002

Yu, B. and Zhang, X. (2015): A physical analysis of the severe 2013/2014 cold winter in North America; *Journal of Geophysical Research: Atmospheres*; v. 120, p. 10149–10165. doi:10.1002/2015JD02116

Zhang, R., and Knutson, T.R. (2013): The role of global climate change in the extreme low summer Arctic sea ice extent in 2012; in *Explaining Extreme Events of 2012 from a Climate Perspective*; *Bulletin of the American Meteorological Society*, v. 94, p. S23–S26.

Zhang, X., Wan, H., Zwiers, F.W., Hegerl, G.C. and Min, S.-K. (2013): Attributing intensification of precipitation extremes to human influence; *Geophysical Research Letters*, v. 40, p. 5252–5257. doi: 10.1002/grl.51010

Zhang, X., Zwiers, F.W., Li, G., Wan, H. and Cannon, A.J. (2017): Complexity in estimating past and future extreme short-duration rainfall; *Nature Geoscience*, v. 10. doi: 10.1038/ngeo2911



Zhang, X., Zwiers, F.W. and Stott, P. (2006): Multi-model multi-signal climate change detection at regional scale; *Journal of Climate*, v. 19, p. 4294–4307.

Zwiers, F.W., Zhang, X. and Feng, Y. (2011): Anthropogenic influence on long return period daily temperature extremes at regional scales; *Journal of Climate*, v. 24, p. 881–892. doi:10.1175/2010JCLI3908.1





CHAPTER 5

**Changes in
Snow, Ice, and
Permafrost
Across Canada**

CANADA'S CHANGING CLIMATE REPORT



Government
of Canada

Gouvernement
du Canada

Canada



Authors

Chris Derksen, Environment and Climate Change Canada

David Burgess, Natural Resources Canada

Claude Duguay, University of Waterloo

Stephen Howell, Environment and Climate Change Canada

Lawrence Mudryk, Environment and Climate Change Canada

Sharon Smith, Natural Resources Canada

Chad Thackeray, University of California at Los Angeles

Megan Kirchmeier-Young, Environment and Climate Change Canada

Acknowledgements

Recommended citation: Derksen, C., Burgess, D., Duguay, C., Howell, S., Mudryk, L., Smith, S., Thackeray, C. and Kirchmeier-Young, M. (2019): Changes in snow, ice, and permafrost across Canada; Chapter 5 in Canada's Changing Climate Report, (ed.) E. Bush and D.S. Lemmen; Government of Canada, Ottawa, Ontario, p.194–260.



Chapter Table Of Contents

DEFINITIONS

CHAPTER KEY MESSAGES (BY SECTION)

SUMMARY

5.1: Introduction

5.2: Snow cover

5.2.1: Observed changes in snow cover

5.2.2: Projected changes in snow cover

5.3: Sea ice

5.3.1: Observed changes in sea ice

Box 5.1: The influence of human-induced climate change on extreme low Arctic sea ice extent in 2012

5.3.2: Projected changes in sea ice

FAQ 5.1: Where will the last sea ice area be in the Arctic?

5.4: Glaciers and ice caps

5.4.1: Observed changes in glaciers and ice caps

5.4.2: Projected changes in glaciers and ice caps

5.5: Lake and river ice

5.5.1: Observed changes in lake and river ice


5.5.2: Projected changes in lake and river ice

5.6: Permafrost

5.6.1: Observed changes in permafrost

5.6.2: Projected changes in permafrost

5.7: Discussion

A photograph of a glacier landscape, likely in the Canadian Rockies, showing a large glacier flowing over rocky terrain. The sky is overcast and grey. A white rectangular text box is overlaid on the center of the image.

This chapter presents evidence that snow, ice, and permafrost are changing across Canada because of increasing temperatures and changes in precipitation.

Chapter Key Messages

5.2: Snow Cover

The portion of the year with snow cover decreased across most of Canada (*very high confidence*²³) as did the seasonal snow accumulation (*medium confidence*). Snow cover fraction decreased between 5% and 10% per decade since 1981 due to later snow onset and earlier spring melt. Seasonal snow accumulation decreased by 5% to 10% per decade since 1981 with the exception of southern Saskatchewan, and parts of Alberta and British Columbia (increases of 2% to 5% per decade).

It is *very likely* that snow cover duration will decline to mid-century across Canada due to increases in surface air temperature under all emissions scenarios. Scenario-based differences in projected spring snow cover emerge by the end of the century, with stabilized snow loss for a medium emission scenario but continued snow loss under a high emission scenario (*high confidence*). A reduction of 5% to 10% per decade in seasonal snow accumulation is projected through to mid-century for much of southern Canada; only small changes in snow accumulation are projected for northern regions of Canada (*medium confidence*).

5.3: Sea Ice

Perennial sea ice in the Canadian Arctic is being replaced by thinner seasonal sea ice (*very high confidence*). Summer sea ice area (particularly multi-year ice area) declined across the Canadian Arctic at a rate of 5% per decade to 20% per decade since 1968 (depending on region); winter sea ice area decreased in eastern Canada by 8% per decade.

It is *very likely* that increased temperatures under all emissions scenarios will result in continued reduction in sea ice area across the Canadian Arctic in summer and the east coast in winter. Most Canadian Arctic marine regions will be sea ice-free for part of the summer by 2050 (*medium confidence*), although the region to the north of the Canadian Arctic Archipelago and Greenland will be the last area in the Arctic with multi-year ice present during the summer (*very high confidence*). Multi-year ice will, therefore, still drift into the Northwest Passage (and present a navigation hazard for shipping) even when the Arctic Ocean is sea ice-free during the summer.

23 This report uses the same calibrated uncertainty language as in the IPCC's Fifth Assessment Report. The following five terms are used to express assessed levels of confidence in findings based on the availability, quality and level of agreement of the evidence: very low, low, medium, high, very high. The following terms are used to express assessed likelihoods of results: virtually certain (99%–100% probability), extremely likely (95%–100% probability), very likely (90%–100% probability), likely (66%–100% probability), about as likely as not (33%–66% probability), unlikely (0%–33% probability), very unlikely (0%–10% probability), extremely unlikely (0%–5% probability), exceptionally unlikely (0%–1% probability). These terms are typeset in italics in the text. See chapter 1 for additional explanation.

5.4: Glaciers And Ice Caps

Canada's Arctic and alpine glaciers have thinned over the past five decades due to increasing surface temperatures; recent mass loss rates are unprecedented over several millennia (*very high confidence*). Mass loss from glaciers and ice caps in the Canadian Arctic represent the third largest cryosphere contributor to global sea level rise (after the Greenland and Antarctic ice sheets) (*very high confidence*).

Under a medium emission scenario, it is projected that glaciers across the Western Cordillera will lose 74% to 96% of their volume by late century (*high confidence*). An associated decline in glacial meltwater supply to rivers and streams (with impacts on freshwater availability) will emerge by mid-century (*medium confidence*). Most small ice caps and ice shelves in the Canadian Arctic will disappear by 2100 (*very high confidence*).

5.5: Lake And River Ice

The duration of seasonal lake ice cover has declined across Canada over the past five decades due to later ice formation in fall and earlier spring breakup (*high confidence*). Seasonal maximum lake ice cover for the Great Lakes is highly variable since 1971 (*very high confidence*), with no significant trend.

Spring lake ice breakup will be 10 to 25 days earlier by mid-century, and fall freeze-up 5 to 15 days later, depending on the emissions scenario and lake-specific characteristics such as depth (*medium confidence*).

5.6: Permafrost

Permafrost temperature has increased over the past 3–4 decades (*very high confidence*). Regional observations identify warming rates of about 0.1°C per decade in the central Mackenzie Valley and 0.3°C to 0.5°C per decade in the high Arctic. Active layer thickness has increased by approximately 10% since 2000 in the Mackenzie Valley. Widespread formation of thermokarst landforms have been observed across northern Canada.

Increases in mean air temperature over land underlain with permafrost are projected under all emissions scenarios, resulting in continued permafrost warming and thawing over large areas by mid-century (*high confidence*) with impacts on northern infrastructure and the carbon cycle.

Summary

Over the past three decades, the proportion of Canadian land and marine areas covered by snow and ice have decreased, and permafrost temperatures have risen (see Figure 5.1). These changes to the Canadian cryosphere are consistent with those observed in other northern regions (Alaska, northern Europe, and Russia).

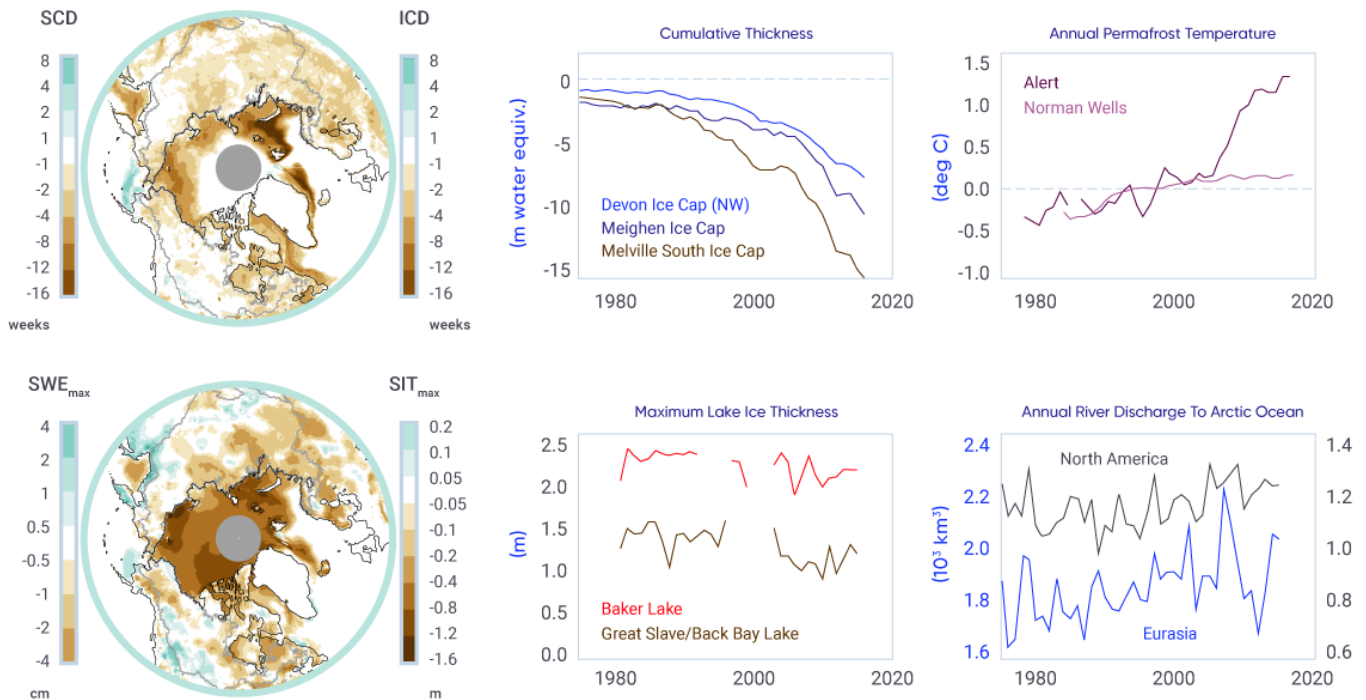


Figure 5.1: Indicators of changes in the cryosphere as a result of warming

Figure caption: Left: Difference in snow cover duration (SCD) and sea ice cover duration (ICD; upper), and in seasonal maximum snow water equivalent (SWE_{max}) and sea ice thickness (SIT_{max}; lower) between the periods 2006–2015 and 1981–1990. Right: Time series of cumulative specific volume change (the running total of ice cap surface mass balance divided by ice cap area) for three ice caps in the Canadian Arctic; annual mean ground temperature departure in the sub-Arctic Mackenzie Valley (Norman Wells) and high Arctic (Alert) relative to the 1988–2007 mean; annual maximum lake ice thickness (Great Slave Lake, Northwest Territories, and Baker Lake, Nunavut); and annual river discharge summed for rivers draining into the Arctic Ocean from North America and Eurasia.

FIGURE SOURCE: SCD AND SWE FROM A BLEND OF FIVE SNOW PRODUCTS; ICD FROM SATELLITE PASSIVE MICROWAVE DATA; AND SIT FROM THE PIOMAS ARCTIC SEA ICE VOLUME REANALYSIS. ICE CAP VOLUME DATA FROM DAVID BURGESS, NATURAL RESOURCES CANADA; GROUND TEMPERATURE DATA FROM SHARON SMITH, NATURAL RESOURCES CANADA; LAKE ICE THICKNESS DATA FROM CLAUDE DUGUAY, UNIVERSITY OF WATERLOO; ARCTIC RIVER DISCHARGE DATA FROM STEPHEN DERY, UNIVERSITY OF NORTHERN BRITISH COLUMBIA.

Snow cover fraction (SCF) decreased across most of Canada during the 1981–2015 period due to delayed snow cover onset in fall and earlier snow melt in spring. Regional and seasonal variability in the SCF trends reflects internal climate variability in surface temperature trends. Over the same time period, seasonal maximum snow water equivalent (SWE_{max}), which is indicative of seasonally accumulated snow available for spring melt, decreased across the Maritimes, southern Ontario, and nearly all of Canadian land areas north of 55° north latitude, while it increased across southern Saskatchewan and parts of Alberta and British Columbia.

Significant reductions in sea ice area over the period 1968–2016 were evident in the summer and fall across the Canadian Arctic (5% to 20% per decade, depending on region), and in winter and spring in eastern Canadian waters (5% to 10% per decade). Perennial sea ice in the Canadian Arctic is being replaced by thinner seasonal sea ice: multi-year ice losses are greatest in the Beaufort Sea and the Canadian Arctic Archipelago (CAA), approaching 10% per decade. Sixty-year records of landfast sea ice thickness show evidence of thinning ice in the CAA.

Glaciers in Canada have receded over the past century, with a rapid acceleration in area and mass losses over the past decade, due primarily to increasing air temperature. Recent mass loss rates are unprecedented over several millennia. Lake ice cover is changing across Canada, driven primarily by earlier spring breakup. Seasonal ice cover duration declined for approximately 80% of Arctic lakes between 2002 and 2015. Permafrost in the central and southern Mackenzie Valley has warmed at a rate of approximately 0.2°C per decade since the mid-1980s. While modest, these increases are important because permafrost temperatures in these regions are currently close to zero, so the ground is vulnerable to thawing. Permafrost temperatures in the high Arctic have increased at higher rates than in the sub-Arctic, ranging between 0.7°C and 1°C per decade.

These changes to the cryosphere during recent decades are in large part a response to increasing surface temperatures. Regional and seasonal variability are due to natural climate variability in surface temperature trends, changes in the amount and the phase (rain or snow) of precipitation, and to remote influences within the global climate system (such as variations in ocean circulation and sea surface temperatures). Changes to individual components of the cryosphere are interconnected. For example, snow is an effective insulator, so changes in the timing of snow cover onset and the seasonal accumulation of snow strongly influence underlying ground temperature and the thickness of lake and sea ice.

Further changes to the cryosphere over the coming decades are *virtually certain*, as temperatures are projected to increase under all future emission scenarios. There is robust evidence that snow cover extent and accumulation, sea ice extent and overall thickness, and the mass of land ice will continue to decrease across Canada throughout the 21st century. Most Canadian Arctic marine regions could be sea ice-free for at least one month in the summer by 2050, but sea ice will continue to be found along the northern coast of the CAA. Reductions in glacier mass in western Canada will impact the magnitude and seasonality of streamflow, affecting the availability of freshwater for human use. Warming will lead to a loss of permafrost and alteration of the landscape as thawing occurs. These changes to the cryosphere will not be spatially uniform due to regional effects of natural climate variability at decadal to multi-decadal time scales.

5.1: Introduction

The term “cryosphere” refers to places on the Earth where water is frozen, and includes snow, sea ice, land ice (glaciers and ice caps), freshwater ice (lake and river ice), permafrost, and seasonally frozen ground. Although the term may not be broadly familiar to Canadians, the cryosphere is a defining component of Canada’s landscape for at least part of each year, and for the entire year at higher latitudes and elevations.

The cryosphere plays a key role in the climate system by influencing surface reflectivity (albedo – snow and ice are highly reflective of incoming solar energy; see Chapter 2, Box 2.3), heat transfer (snow is a highly effective insulator of the underlying soil or ice), and hydrological processes (water storage and runoff). It also has important ecosystem linkages, as many organisms have adapted to living in or on snow and ice. These range from distinctive microbial communities, to seals and polar bears, which rely on sea ice for breeding, feeding, and mobility. Ice cover influences the algae growing season, water temperature, and oxygen levels, as well as allowing wildlife to reach shorelines and cross water bodies. The state of the cryosphere also influences the Canadian economy by supplying freshwater from snow and glaciers for human use during melt periods, impacting shipping and offshore operations, facilitating northern transportation and resource extraction through ice roads, and supporting winter recreation. It also contributes to a wide range of hazards such as spring flooding, avalanches, as well as landscape instability as permafrost thaws. The cryosphere is also critically important in the traditional ways of life of many Indigenous communities, particularly in the North. As well as influencing the abundance and location of land, freshwater, and marine resources on which these communities depend, snow, ice, and permafrost also affect access to these resources.

This chapter provides an assessment of observed and projected changes in the Canadian cryosphere. This updates a review conducted as part of the 2007/2008 International Polar Year (Derksen et al., 2012) and a previous overview of Canada’s changing climate (Bush et al., 2014), as well as complementing recent assessments of the global (Vaughan et al., 2013) and Arctic (AMAP, 2017a) cryosphere. When appropriate, the longest available datasets of continuous surface measurements from observation sites are provided (for example, glacier mass balance, permafrost temperature). Otherwise, validated datasets from remote sensing and land surface models are utilized to provide information for large areas (for example, sea ice concentration, snow cover fraction, lake ice cover). The historical periods vary between components of the cryosphere, depending on the available data, but extend from at least 1981 to present. Projected changes to the cryosphere are based on state-of-the-art climate model simulations from the fifth phase of the Coupled Model Intercomparison Project (CMIP5) (<https://esgf-node.llnl.gov/projects/cmip5/>) (see Chapter 3, Box 3.1). In some cases, these models simulate variables that can be directly compared with observations – for example, snow cover fraction. In other cases, analysis of model projections is more complicated, either because the models do not directly simulate the variable of interest (e.g., permafrost area needs to be inferred from soil temperature) or the spatial resolution of global models is too coarse to provide information on individual features of interest (i.e., specific lakes or glaciers) (see Chapter 3, Figure 3.2 for an explanation of models).

Changes in temperature and precipitation are the primary drivers of variability and change in the cryosphere – these variables are discussed for all of Canada in Chapter 4. Temperature influences the timing, duration, and intensity of melt periods, as well as whether precipitation falls as rain or snow. Snowfall events determine the accumulation of seasonal snow, an important reflective and insulating layer, while changes in snow depth influence ice thickness (both lake and sea ice) and ground temperature.

5.2: Snow cover

Key Message

The portion of the year with snow cover decreased across most of Canada (*very high confidence*) as did the seasonal snow accumulation (*medium confidence*). Snow cover fraction decreased between 5% and 10% per decade since 1981 due to later snow onset and earlier spring melt. Seasonal snow accumulation decreased by 5% to 10% per decade since 1981 with the exception of southern Saskatchewan, and parts of Alberta and British Columbia (increases of 2% to 5% per decade).

Key Message

It is *very likely* that snow cover duration will decline to mid-century across Canada due to increases in surface air temperature under all emissions scenarios. Scenario-based differences in projected spring snow cover emerge by the end of the century, with stabilized snow loss for a medium emission scenario but continued snow loss under a high emission scenario (*high confidence*). A reduction of 5% to 10% per decade in seasonal snow accumulation is projected through to mid-century for much of southern Canada; only small changes in snow accumulation are projected for northern regions of Canada (*medium confidence*).

Snow cover is a defining characteristic of the Canadian landscape for a few months each winter along the southern margins of the country and for up to nine or 10 months each year in the high Arctic. Snow is responsible for a cascade of interactions and feedbacks that affect the climate system, freshwater availability, vegetation, biogeochemical activity including exchanges of carbon dioxide and trace gases, and ecosystem services (Brown et al., 2017). To understand changes in snow, it is necessary to consider multiple variables, including snow cover fraction (SCF), which is affected by the timing of snow onset and snow melt, and the maximum seasonal snow water equivalent (SWE_{max}), the amount of water stored by snow and available for melt in spring. These variables affect the exchange of energy between the surface and the atmosphere (with important feedbacks to the global climate system) and freshwater availability, as nearly all Canadian watersheds are snow-dominated in the winter. Snow is critical to winter travel and tourism in many regions of the country and is a key requirement for the construction of winter roads that connect remote communities and mines, particularly in the Northwest Territories, northern Manitoba, and northern Ontario.

Surface observations of snow depth from climate monitoring stations (such observations are referred to as "in situ data") are not well suited for detecting trends and variability in snow cover because they measure snow only at individual points (Brown and Braaten, 1998). Snow depth can vary significantly at the local scale because of interactions with vegetation and topography (typically driven by winds), which means single point measurements may not capture the mean snow depth on the landscape (Neumann et al., 2003). In addition, climate stations are exceptionally sparse above 55° north latitude in Canada and are biased to lower elevations in mountainous areas and in coastal areas in the sub-Arctic and Arctic. It is, therefore, challenging to use the conventional Canadian climate observing network for a national-scale assessment of snow. Satellite

observations and land surface models are available that provide daily, spatially continuous data across all of Canada, extending back for decades. These products have a coarse spatial resolution (25–50 km), which presents problems for alpine areas and regions with mixed land cover. Researchers have made significant efforts to determine the agreement among datasets to ensure robust analysis of trends (Mudryk et al., 2018).

5.2.1: Observed changes in snow cover

Based on an analysis of multiple datasets covering 1981–2015, SCF (characterized as the proportion of days within each month that snow was present on the ground) decreased by 5% to 10% across most of Canada during most seasons (Mudryk et al., 2018; see Figure 5.2), notably, for eastern Canada in spring (April/May/June) and most of the Canadian land area in the fall (October/November/December). This loss of snow cover is consistent with previous studies using in situ datasets covering a longer time period (Brown and Braaten, 1998; Vincent et al., 2015), but the 1981–2015 period is characterized by stronger reductions in snow cover during the snow onset period for eastern Canada in response to enhanced fall warming (consistent with Brown et al., 2018). Decreasing SCF trends over high latitudes of Canada are consistent with documented reductions in annual snow cover duration (SCD; the number of days with snow cover) across circumpolar Arctic land areas of two to four days per decade (approximately 1% to 2% per decade, assuming 250 days mean snow cover) (Brown et al., 2017). Some studies (Derksen and Brown, 2012; Derksen et al., 2016; Brutel-Vuilmet et al., 2013; Hernández-Henríquez et al., 2015; Mudryk et al., 2017) identified spring snow cover losses slightly stronger than those in Figure 5.2, because different datasets and time periods were considered. Despite these differences, all studies consistently show reductions in spring SCF.

Analysis of surface temperature from a blend of six atmospheric reanalysis datasets showed that warming trends over the 1981–2015 period are found in all Canadian land areas with SCF reductions (Mudryk et al., 2018). Cooling trends in winter and spring are associated with the regions of increasing SCF (see Figure 5.2). Observations from climate stations in the regions where SCF trends increased over 1981–2015 also show decreased maximum snow depth and SCD over the longer 1950–2012 period (Vincent et al., 2015), so the positive trends over 1981–2015 reflect nature variability in regional surface temperatures and precipitation.

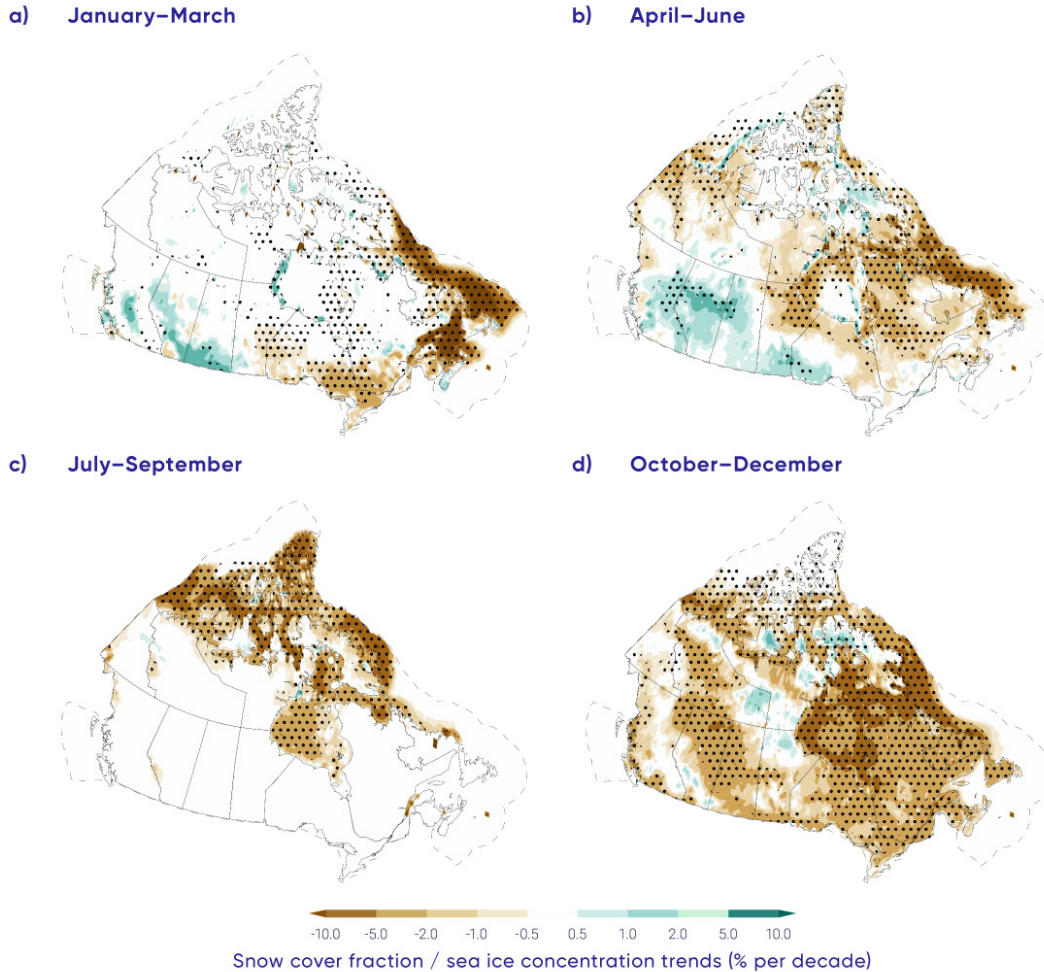


Figure 5.2: Snow cover fraction and sea ice concentration trends, 1981–2015

Figure caption: Terrestrial snow cover fraction and sea ice concentration seasonal trends for 1981–2015. Stippling indicates statistical significance (there is only a 10% possibility that such changes are due to chance). Dashed line denotes limit of Canadian marine territory. Changes in sea ice are discussed in Section 5.3.

FIGURE SOURCE: MUDRYK ET AL. (2018)

While SCF information is important for identifying changes in where snow covers the ground, from a water-resources perspective, it is important to understand how much water is stored in the form of snow. This is determined from the pre-melt SWE_{max} . SWE_{max} declined by 5% to 10% across much of Canada during the period 1981–2015, according to the multi-dataset analysis shown in Figure 5.3 (Mudryk et al., 2018). This is consistent with snow depth trends from surface measurements (Brown and Braaten, 1998; Vincent et al., 2015) and other observational studies (for example, Mudryk et al., 2015). Increases in SWE_{max} are evident across parts of British Columbia, Alberta, and southern Saskatchewan. The influences of temperature and precipitation changes need to be separated to understand the driving mechanisms behind trends in SWE_{max} (Raisanen, 2008; Brown and Mote, 2009; Mankin and Diffenbaugh, 2014; Sospedra-Alfonso and Merryfield, 2017).

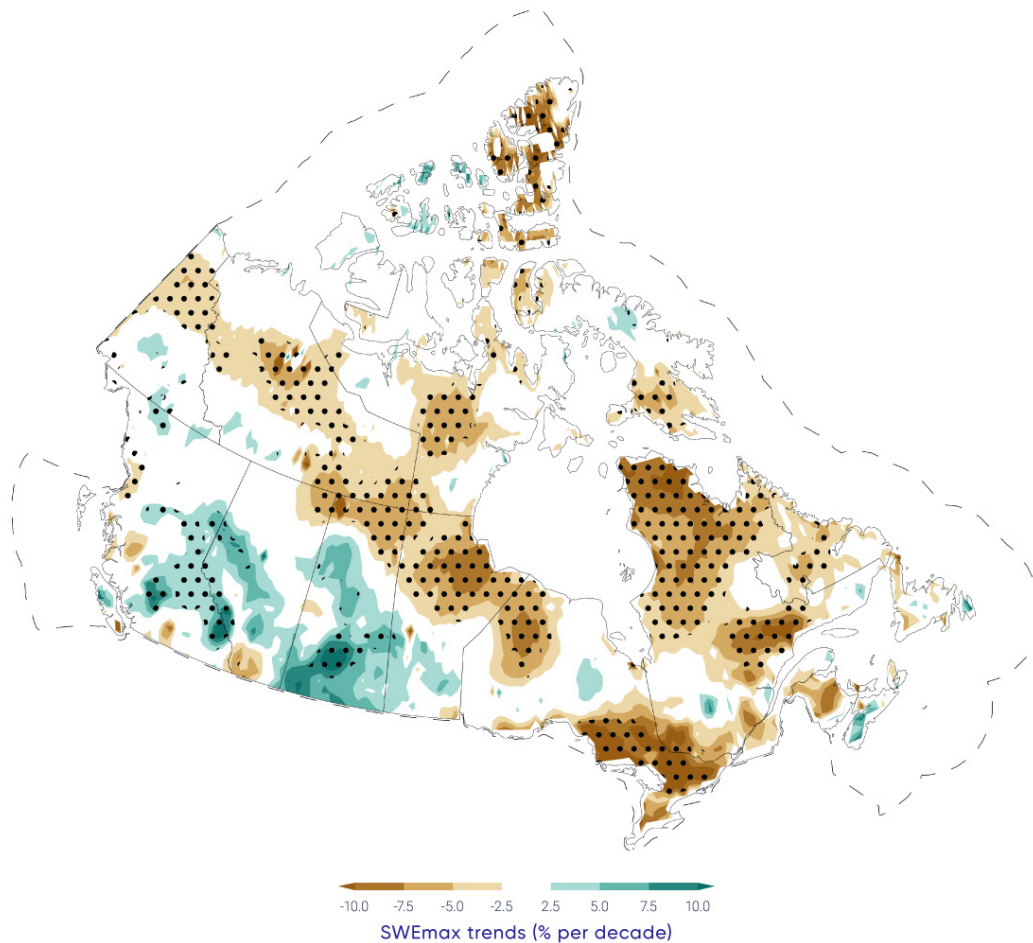


Figure 5.3: Trends in maximum snow water equivalent, 1981–2015

Figure caption: Trends in maximum snow water equivalent (SWE_{max}) (% per decade) for 1981–2015. Stippling indicates statistical significance (there is only a 10% possibility that such changes are due to chance).

FIGURE SOURCE: MUDRYK ET AL. (2018).

5.2.2: Projected changes in snow cover

Projections of surface temperatures across Canada for the near-term under a high emission scenario (RCP8.5) show warming in all seasons in the multi-model average (see Chapter 4, Section 4.2.1.3), with concurrent decreases in projected SCF across all of Canada during all seasons (Figure 5.4; Mudryk et al., 2018). During winter, projected snow cover reductions will be greatest across southern Canada, where temperature increases result in less snowfall as a proportion of the total precipitation. Temperatures will remain

sufficiently cold at higher latitudes that winter (January/February/March) SCF in this region is not projected to change in response to warming. During spring, the region of snow sensitivity to temperature forcing is projected to shift north, as snow cover retreats across the boreal forest, sub-Arctic, and high Arctic. This leads to projected negative SCF trends (loss of snow) across these regions during the April through June period. Important differences in spring snow cover projections between emissions scenarios emerge by the end of the century, with stabilized snow loss under a medium emission scenario (RCP4.5) but continued loss under a high emission scenario (RCP8.5) (Brown et al., 2017).

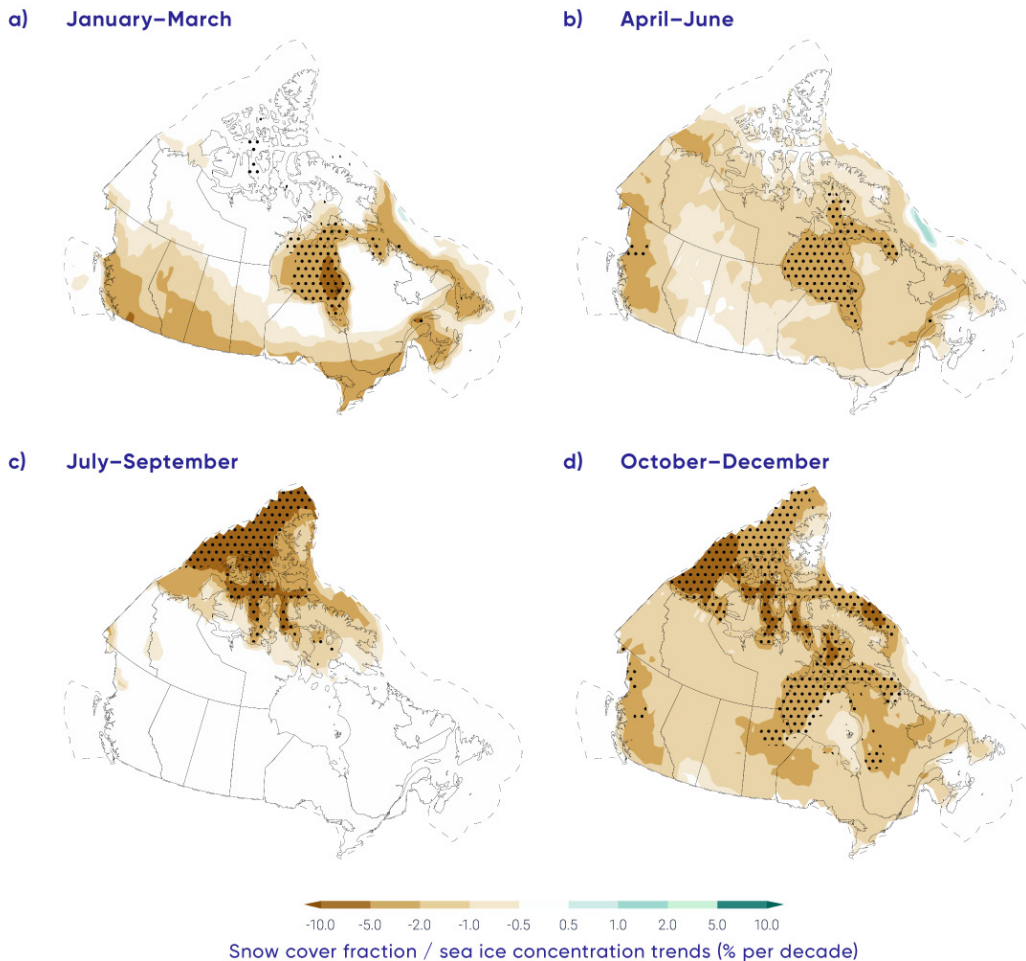


Figure 5.4: Projected snow cover fraction and sea ice concentration trends, 2020–2050

Figure caption: Projected terrestrial snow cover fraction and sea ice concentration seasonal trends (% per decade) for the 2020–2050 period for Canadian land and marine areas. Trends are calculated from the multi-model mean of an ensemble of climate models (Coupled Model Intercomparison Project - CMIP5), using a high emission scenario (RCP8.5). Stippling indicates statistical significance (there is only a 10% possibility that such changes are due to chance).

FIGURE SOURCE: MUDRYK ET AL. (2018)

Projected changes in SWE_{max} indicate that reductions will be extensive (5% to 10% per decade through 2050, or a cumulative loss of 15% to 30% over the entire 2020–2050 period) over much of southern Canada, with the greatest changes in the Maritimes and British Columbia (see Figure 5.5). The decreases across the prairies, Ontario, Quebec, and the Maritimes are attributable to increasing temperatures that will shift the proportion of total precipitation that currently falls as snow toward rain (Sospedra-Alfonso and Merryfield, 2017). (Note that the greatest near-term reductions in SWE_{max} , according to the climate model projections, will be just south of the Canadian border.) Projected changes in British Columbia are consistent with projected SWE_{max} reductions in the Western Cordillera (Fyfe et al., 2017). While SWE_{max} is projected to increase by mid-century in the Eurasian Arctic (Brown et al., 2017), minimal change is projected across high-latitude land areas of Canada because increased snowfall is expected to be offset by increasing temperatures that shorten the snow accumulation season.

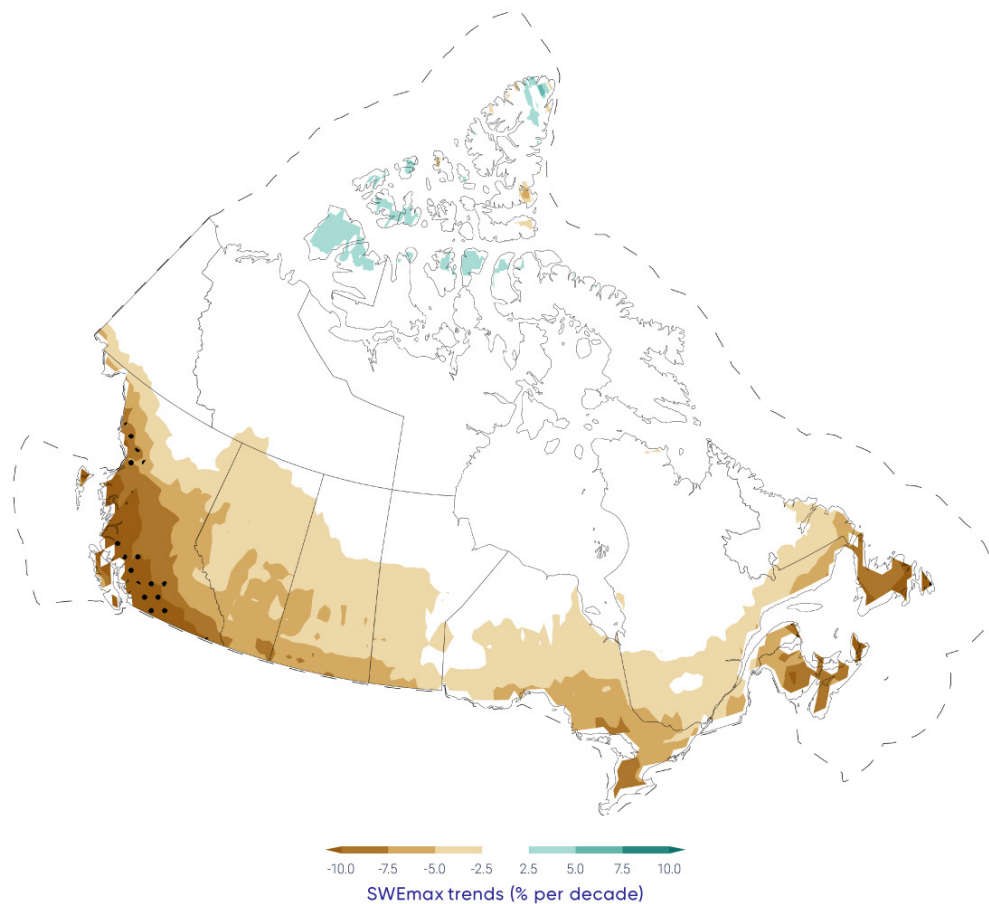


Figure 5.5: Projected trends in maximum snow water equivalent, 2020–2050

Figure caption: Projected trends in maximum snow water equivalent (SWE_{max} % per decade) for 2020–2050 for Canadian land areas. Trends are calculated from the multi-model mean of an ensemble climate models (Coupled Model Intercomparison Project - CMIP5), using a high emission scenario (RCP8.5). Stippling indicates statistical significance (there is only a 10% possibility that such changes are due to chance).

The greatest snow loss across Canada during the 2020–2050 period is projected to occur in the shoulder seasons (October–November and May–June; Thackeray et al., 2016) (see Figure 5.6). During mid-winter, there is minimal percentage change in projected snow cover extent because winter temperatures across northern regions of Canada will remain cold enough to sustain snow cover and there is greater climatological snow extent in winter, which results in smaller percentage changes (see Figure 5.5). The projected trends are similar to the rate of change already observed during the historical period (see Section 5.2.1). Trends from a large ensemble of simulations from the Canadian Earth System Model (CanESM2) are slightly stronger than the CMIP5 multi-model mean because projected warming is greater in CanESM2 than in the CMIP5 multi-model mean (Thackeray et al., 2016).

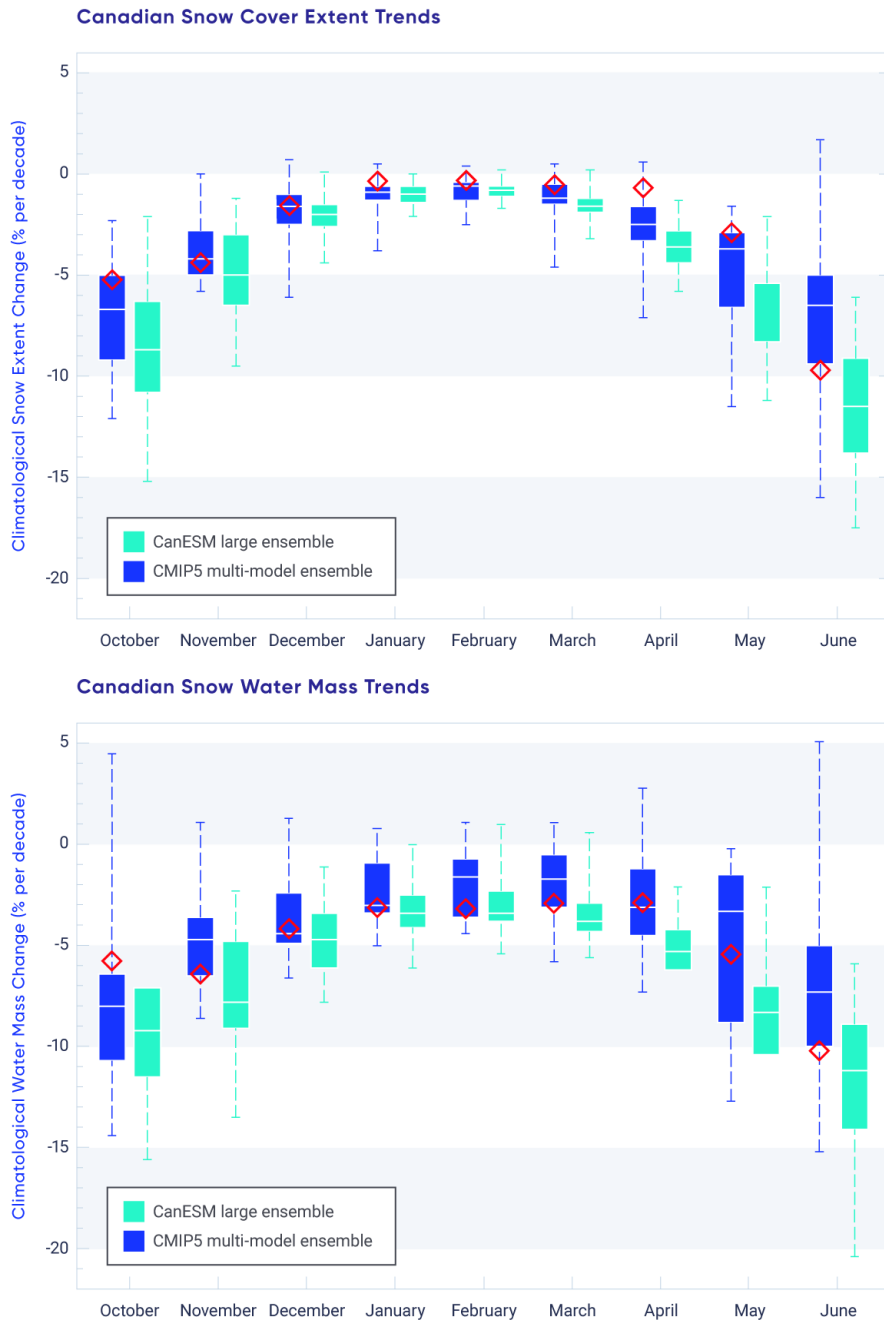


Figure 5.6: Observed (1981–2015) and projected trends in Canadian snow cover extent and snow water mass, 2020–2050

Figure caption: Monthly projected trends in Canadian snow cover extent (upper) and snow water mass (lower) from the Coupled Model Intercomparison Project (CMIP5) multi-model ensemble (blue) and from the Canadian Earth System Model (CanESM) large ensemble (aqua), under a high emission scenario (RCP8.5). Monthly mean observational trends (1981–2015) from the snow dataset used in Section 5.1.1 are shown in red. Boxes show the 25th–75th percentile range, the horizontal line shows the median, and the dashed whiskers illustrate the minimum and maximum.

FIGURE SOURCE: MUDRYK ET AL. (2018)

Section summary

In summary, analysis of multiple sources of SCF data from satellite remote sensing and land surface models over the 1981–2015 period show the portion of the year with snow cover decreased across Canada at a rate of 5% to 10% per decade. There is *very high confidence* in these trends based on consistency among multiple datasets and quantitative relationships with surface temperature trends in which there is also *high confidence* (see Chapter 4). Seasonal snow accumulation decreased by a rate of 5% to 10% per decade across most of Canada (1981–2015), with the exception of southern Saskatchewan, Alberta, and British Columbia (increases of 2% to 5% per decade), driven by both temperature and precipitation changes. Because of greater uncertainty in sources of data on snow accumulation (compared to those on SCF), we have *medium confidence* in these trends. It is *very likely* that snow cover duration will decline to mid-century across Canada as a result of increases in surface air temperature under all emission scenarios. This likelihood assessment is based on the strongly established sensitivity of snow cover to surface temperature in both observations and climate models. Scenario-based differences in projected spring snow cover emerge by the end of the century, with stabilized snow loss for low and medium emission scenarios (RCP2.6 and 4.5) but continued snow loss under a high emission scenario (RCP8.5). A reduction of 5% to 10% per decade in seasonal snow accumulation (through 2050) is projected across much of southern Canada; only small changes in snow accumulation are projected across northern regions of Canada because increases in winter precipitation are expected to offset a shorter snow accumulation period. There is greater uncertainty in SWE projections (compared to SCD) because of greater spread in climate model responses due to the competing effects of temperature and precipitation, so there is *medium confidence* in these results.

5.3: Sea ice

Key Message

Perennial sea ice in the Canadian Arctic is being replaced by thinner seasonal sea ice (*very high confidence*). Summer sea ice area (particularly multi-year ice area) declined across the Canadian Arctic at a rate of 5% per decade to 20% per decade since 1968 (depending on region); winter sea ice area decreased in eastern Canada by 8% per decade.

Key Message

It is *very likely* that increased temperatures under all emissions scenarios will result in continued reduction in sea ice area across the Canadian Arctic in summer and the east coast in winter. Most Canadian Arctic marine regions will be sea ice-free for part of the summer by 2050 (*medium confidence*), although the region to the north of the Canadian Arctic Archipelago and Greenland will be the last area in the Arctic with multi-year ice present during the summer (*very high confidence*). Multi-year ice will, therefore, still drift into the Northwest Passage (and present a navigation hazard for shipping) even when the Arctic Ocean is sea ice-free during the summer.

Climate-driven changes to sea ice affect local ecosystems throughout Arctic Canada and influence northern residents through impacts on travelling, hunting, and fishing, with implications for people's lives, livelihoods, cultural practices, and economic activities. Satellite data show dramatic changes in Arctic sea ice cover during the past 40 years, which are unprecedented over the past 150 years (Walsh et al., 2017). The once-dominant ice that lasts over at least one complete summer melt season (multi-year ice, MYI) in the Arctic Ocean has been largely replaced by ice that melts completely during the summer (seasonal first-year ice, FYI) (Maslanik et al., 2011; Comiso, 2012). This change is important because FYI drifts and melts more readily (Tandon et al., 2018; Stroeve et al., 2012). Average ice thickness over the Arctic Ocean has decreased considerably (Kwok and Rothrock, 2009; Haas et al., 2010; Laxon et al., 2013; Richter-Menge and Farrell, 2013; Kwok and Cunningham, 2015; Tilling et al., 2015). Since 2007, a series of new record-low Arctic sea ice extents have been recorded in the month of September (when sea ice extent reaches the annual minimum), with a loss rate of approximately 13% per decade relative to the 1981–2010 mean (<<http://nsidc.org/arcticseaice-news/>>; Stroeve et al. 2012). Concurrent with these changes in ice cover, shipping activity in Canadian Arctic waters has increased over the past decade (Pizzolato et al., 2016; Dawson et al., 2018). Decreases in sea ice extent are no longer confined to the months of low ice cover (August/September/October), but are now also observed during the once-stable winter season (Serreze et al. 2007; Parkinson, 2014).

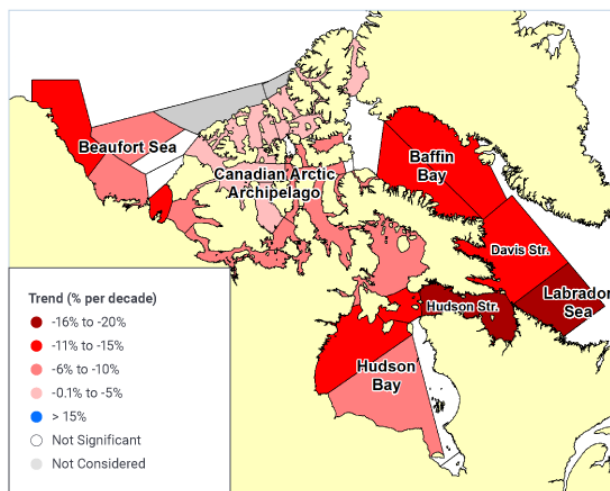
While the changes in sea ice extent and character across the Arctic are dramatic, there is considerable regional variability. Canadian sea ice areas are composed of portions of the open Arctic Ocean where ice can circulate freely (the western Arctic/Beaufort Sea region), contrasted with the narrow waterways of the Canadian Arctic Archipelago (CAA), where ice is landfast for most of the year. Along the more temperate east coast and in Hudson Bay, the ice melts completely each spring. (Sea ice does not occur on the Pacific coast.)

5.3.1: Observed changes in sea ice

Estimates of total ice and MYI area within Canadian Arctic waters are available from the Canadian Ice Service Digital Archive (CISDA), which is an integration of a variety of datasets, including satellite measurements, surface observations, airborne and ship reports, and operational model results (see Canadian Ice Service, 2007 and Tivy et al., 2011a for complete details). This record has been shown to provide more accurate estimates of sea ice concentration (SIC) in Canadian waters compared to satellite passive microwave estimates (Agnew and Howell, 2003). Analysis of seasonally averaged trends in SIC over the 1981–2015 period (selected to match the period of snow datasets described in Section 5.2.1) found reductions over Canadian waters in all seasons (see Figure 5.2). Regions with the strongest SIC declines were eastern Canadian waters in winter and spring, and the CAA and Hudson Bay in summer and fall. SIC trend patterns are closely associated with warming patterns during the seasons of ice onset and growth (from October through March). However, dynamic effects (such as wind, which redistributes sea ice) also influence the observed ice reductions in spring and summer (Mudryk et al., 2018).

The CISDA archive also extends the record of total and MYI back to 1968, almost 10 years earlier than coverage by satellite passive microwave observations. Between 1968 and 2016, sea ice area, averaged over the summer period, has decreased significantly in almost every region of the Canadian Arctic, by up to 20% per decade in some regions (e.g., the Hudson Strait and Labrador Sea; see Figure 5.7). Compared with trends computed over the periods 1968–2008 (Tivy et al., 2011a) and 1968–2010 (Derksen et al., 2012), more regions are now experiencing significant decreases, and the rate of decline is stronger in all regions except Hudson Bay. The largest declines in MYI have occurred in the CAA (approximately 9% per decade) and Beaufort Sea (approximately 7% per decade).

All Ice



Multi-year Ice

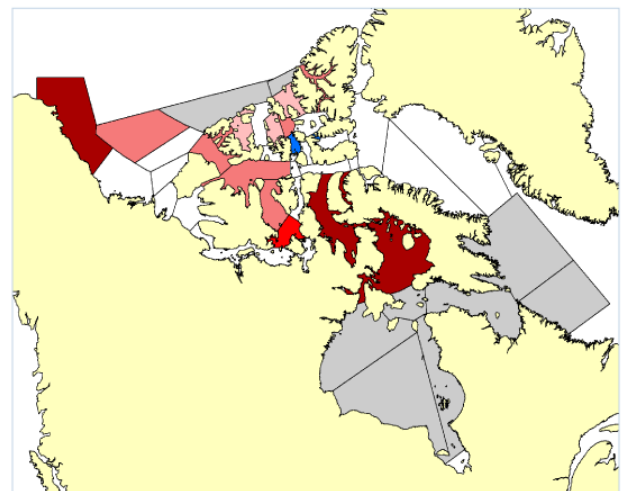


Figure 5.7: Trends in Arctic summer total ice and multi-year ice, 1968–2016

Figure caption: Trends in summer total ice (left) and multi-year ice (MYI, right) area from 1968 to 2016. Summer is defined as June 25 to October 15 for the Beaufort Sea, CAA, and Baffin Bay regions, and from June 18 to November 19 for Hudson Bay, Hudson Strait, Davis Strait, and Labrador Sea, consistent with Tivy et al. (2011a) and Derksen et al. (2012). Only trends significant at the 5% level (there is only a 5% possibility that the trend is due to chance) are shown.

FIGURE SOURCE: CANADIAN ICE SERVICE DIGITAL ARCHIVE; MUDRYK ET AL. (2018)

While there are high year-to-year differences due to natural variability, time series of sea ice area (see Figure 5.8) clearly show negative trends. The Beaufort Sea experienced record-low sea ice area in 2012, becoming virtually ice free near the end of the melt season (Figure 5.8a; Babb et al., 2016). This was nearly repeated in 2016. The CAA had record-low ice years in 2011 and 2012, eclipsing the previous record set in 1998 (Figure 5.8b; Howell et al., 2013). Baffin Bay has experienced consistently low sea ice area since 1999 (Figure 5.8c), while Hudson Bay sea ice area has declined since the mid-1990s (see Figure 5.8d; Tivy et al., 2011b; Hochheim and Barber, 2014). Modelling has demonstrated that the recent extreme lows in Arctic SIC would not have occurred without anthropogenic climate change (see Box 5.1).

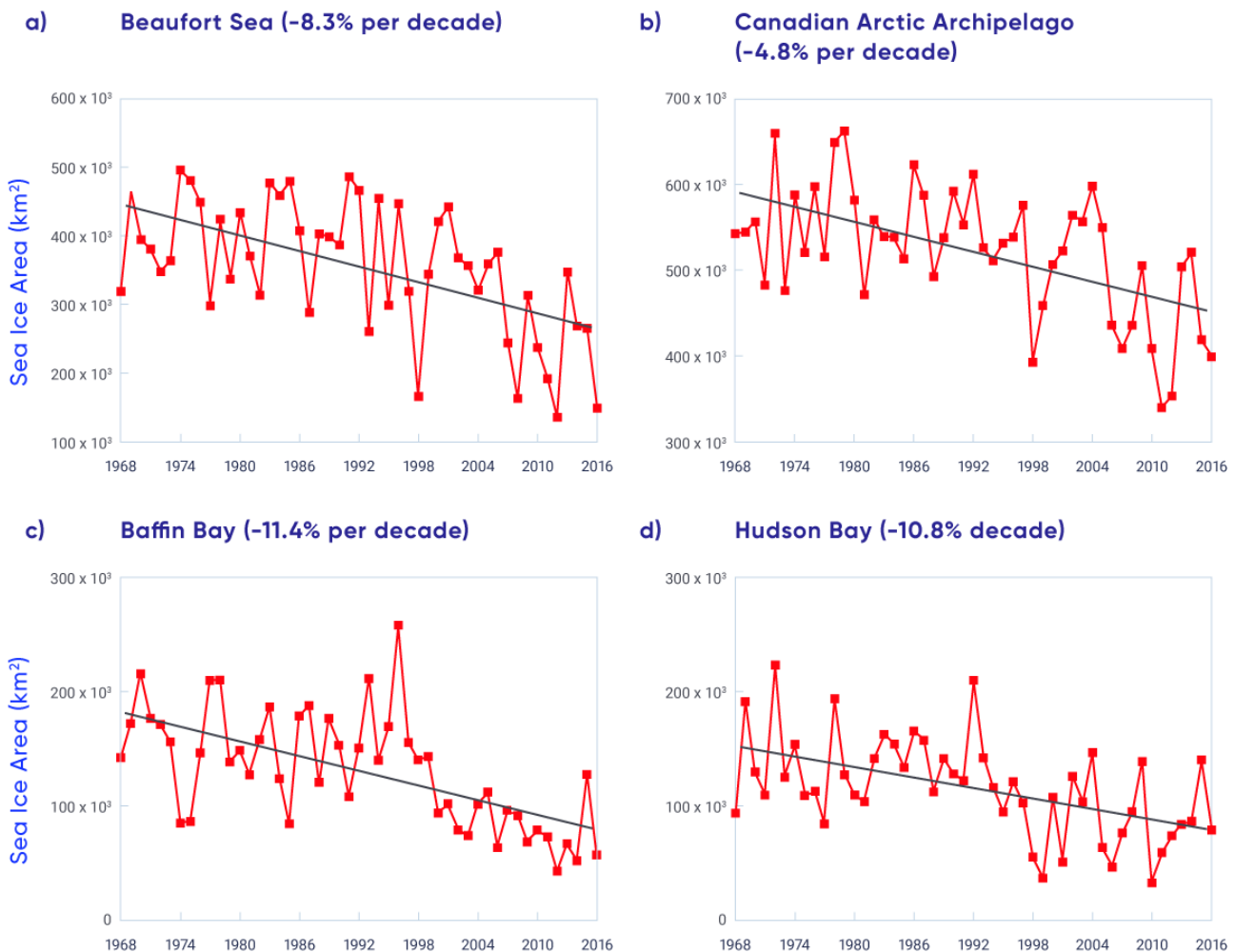


Figure 5.8: Arctic summer total sea ice area, 1968–2016

Figure caption: Time series of summer total sea ice area for the (a) Beaufort Sea, (b) Canadian Arctic Archipelago (CAA), (c) Baffin Bay, and (d) Hudson Bay regions from 1968 to 2016.

FIGURE SOURCE: CANADIAN ICE SERVICE DIGITAL ARCHIVE; MUDRYK ET AL. (2018)

Box 5.1: The influence of human-induced climate change on extreme low Arctic sea ice extent in 2012

The Arctic experienced a record-low sea ice extent (SIE) in September 2012. Extreme low SIEs can have impacts on Arctic communities, ecosystems, and economic activities. Determining the role of human-induced climate change in extreme low Arctic SIEs is important, because understanding the role of anthropogenic greenhouse gases compared to natural variability provides a basis for understanding future projections and potential adaptation measures.

Event attribution methods are used to determine the influence of human-induced climate change on the occurrence (or intensity) of extreme events (NASEM, 2016). The probability of a particular extreme event is compared between two different sets of climate model simulations: those that include the contribution from human activities and those that include only natural factors. The difference in these probabilities indicates the effect of human-induced climate change on the event. Attribution studies are described in more detail in Chapter 4, Section 4.4.

Increasing temperatures in the Arctic have been attributed to human-induced factors in many studies (Gillett et al., 2008; Najafi et al., 2015; Min et al., 2008). Furthermore, attribution studies show that the record-low SIE in 2012 was **extremely unlikely** to be due to natural variability in the climate system alone (Zhang and Knutson, 2013) and that it would not have occurred without human influence on climate (Kirchmeier-Young et al., 2017). Figure 5.9a shows September Arctic SIE over time from climate model simulations using only natural factors (blue line) and simulations that also include the human-induced component (red line). Simulations that include the human-induced component show a strong decreasing trend, similar to the observed decline in SIE (black line). On the other hand, the simulations with only natural forcings show similar year-to-year variability but no trend.

To compare the probability of the 2012 event from each set of simulations, probability distributions are shown in Figure 5.9b. The distributions describe possible values that might be expected in each scenario and how likely they are. The observed 2012 record-low SIE event (vertical dashed line) is within the distribution from the simulations that include the human-induced component and is much lower than any values in the distribution with only natural forcings. With the human-induced component included, there is a 10.3% possibility of a September SIE more extreme than the observed 2012 event. For the natural-only simulations, this probability is extremely small. Therefore, the record-low September SIE in 2012 was **extremely unlikely** to be due to only natural variability of the climate and would not have occurred without the human influence on climate (Kirchmeier-Young et al., 2017).

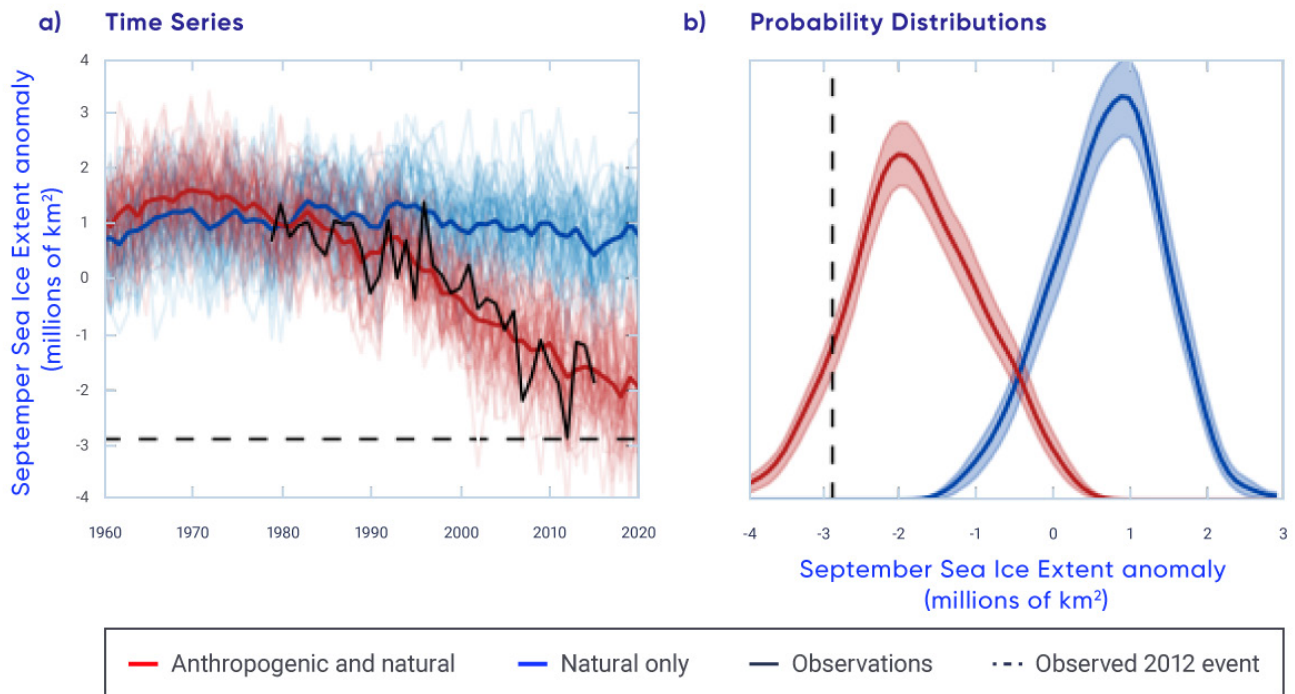


Figure 5.9: Comparison of Arctic sea ice extent between simulations with and without the contribution of human activities

Figure caption: (a) Time series of September Arctic sea ice extent (SIE) simulations that include the human-induced component (red) and simulations that include only natural factors (blue), shown as anomalies. Time series from 50 realizations of the Canadian Earth System Model (CanESM2) are shown, with the mean shown in bold. The time series of observations from the National Snow and Ice Data Center is shown in black. The horizontal dashed line indicates the record-low 2012 SIE. (b) Probability distributions for values from each set of simulations with (red) and without (blue) the human-induced component. Shading represents the uncertainty in the estimated distributions and the vertical dashed line indicates the record-low 2012 SIE.

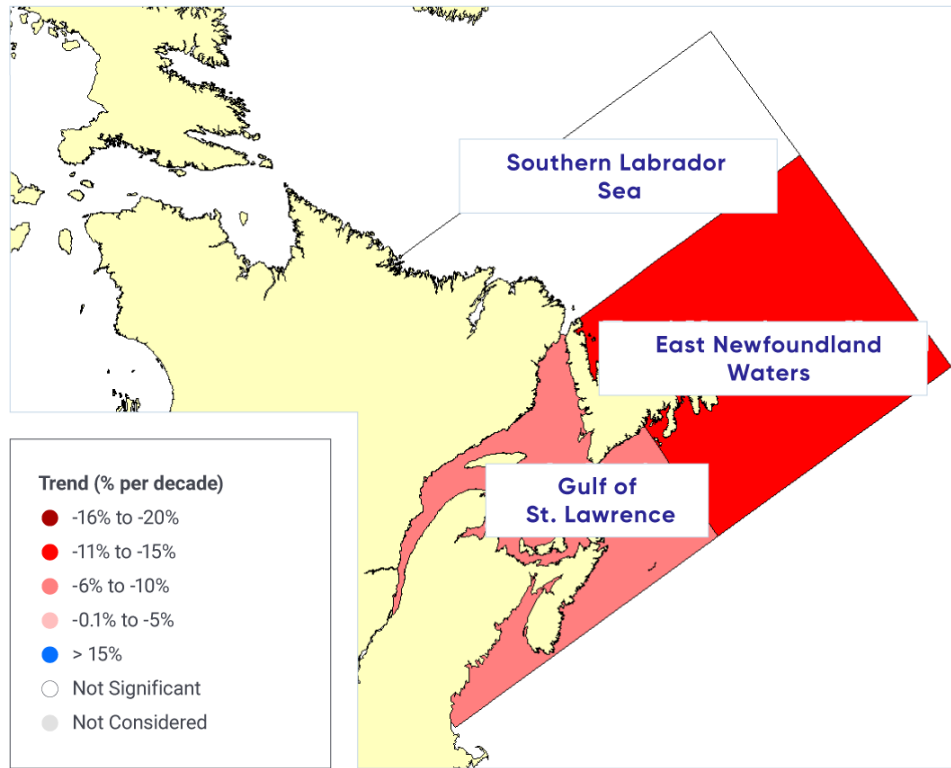
FIGURE SOURCE: ADAPTED FROM KIRCHMEIER-YOUNG ET AL. (2017).

The decline of sea ice across the Canadian Arctic is driven by increasing spring air temperature and resulting increases in the length of the melt season. This results in more open water, increased absorption of solar radiation (which further contributes to ice melt), increased water temperature, and delayed fall freeze-up (Howell et al., 2009a; Tivy et al., 2011a; Stroeve et al., 2014; Parkinson, 2014). Changes in sea ice cover are also driven by atmospheric circulation. The Beaufort Sea was once a region where ice would thicken and age before being transported to the Chukchi Sea and recirculated in the Arctic (Tucker et al., 2001; Rigor et al., 2002), but now the region has become a considerable contributor to the Arctic's MYI loss (Kwok and Cunningham, 2010; Maslanik et al., 2011; Krishfield et al., 2014; Galley et al., 2016). Ice is still being sequestered from the Canada Basin (one of the two ocean basins in the Arctic Ocean) and transported through the Beaufort Sea during the summer months, but this ice is now younger and thinner and melts en route to the Chukchi Sea (Howell et al., 2016a). The CAA was also a region with historically heavy MYI throughout the melt season, but MYI conditions have become lighter in recent years (see Figure 5.7; Howell et al., 2015).

Arctic sea ice thickness has declined in recent years, largely associated with a reduction and thinning of the MYI fraction (e.g., Kwok and Rothrock, 2009; Haas et al., 2010; Laxon et al., 2013; Richter-Menge and Farrell, 2013; Kwok and Cunningham, 2015; Tilling et al., 2015). These studies indicate thickness declines are greater in the Beaufort Sea compared with the north-facing coast of the CAA, which still contains some of the thickest sea ice in the world (Haas and Howell, 2015). Unfortunately, the spaceborne sensors used to obtain sea ice thickness information over the Arctic Ocean are not of sufficient spatial resolution to provide thickness estimates within the narrow channels of the CAA. Although there are only four locations with consistent records and point measurements may not capture regionally representative conditions, the Canadian Ice Service record of in situ landfast ice thickness represents one of the longest datasets in the Arctic, spanning over five decades. Maximum ice thickness has declined significantly at three sites in the CAA (Cambridge Bay, Eureka, and Alert), with decreases ranging from 3.6 to 5.1 cm (± 1.7 cm) per decade from the late 1950s to 2016 (Howell et al., 2016b). No significant trend was found at Resolute, a result that differs from an earlier study by Brown and Cote (1992), which reported a significant increase in maximum ice thickness at Resolute over the 1950–1989 period.

Sea ice along the east coast of Canada is seasonal, with ice melting completely each spring. A robust indicator of change is winter season sea ice area, defined as the average from January through March of each year. The rate of decline between 1969 and 2016, determined from the CISDA for the entire east coast region, is 7.5% per decade (statistically significant at the 1% level; there is only a 1% possibility that the decline is due to chance; see Figure 5.10). This is consistent with the passive microwave time series, which indicates a decline of 9.5% per decade over the 1979–2015 period (Peng and Meier, 2017). There is regional variability within the east coast region, as the rate of decline for the Gulf of St. Lawrence (8.3% per decade) is less than that for eastern Newfoundland waters (10.6% per decade), while the decline for the southern Labrador Sea is not statistically significant at the 5% level (there is a possibility of more than 5% that the decline is due to chance; see Figure 5.10). Years with extensive ice cover are more prominent before 1995, but the region has experienced recent heavy ice years as well (in 2014 and 2015). Sea ice variability in this region is driven largely by temperature and atmospheric circulation (i.e., winds) associated with the Arctic Oscillation (also called the Northern Annular Mode [see Chapter 2, Box 2.5]; Deser and Tang, 2008; Peterson et al., 2015).

a)



b) East Coast (-7.6% per decade)

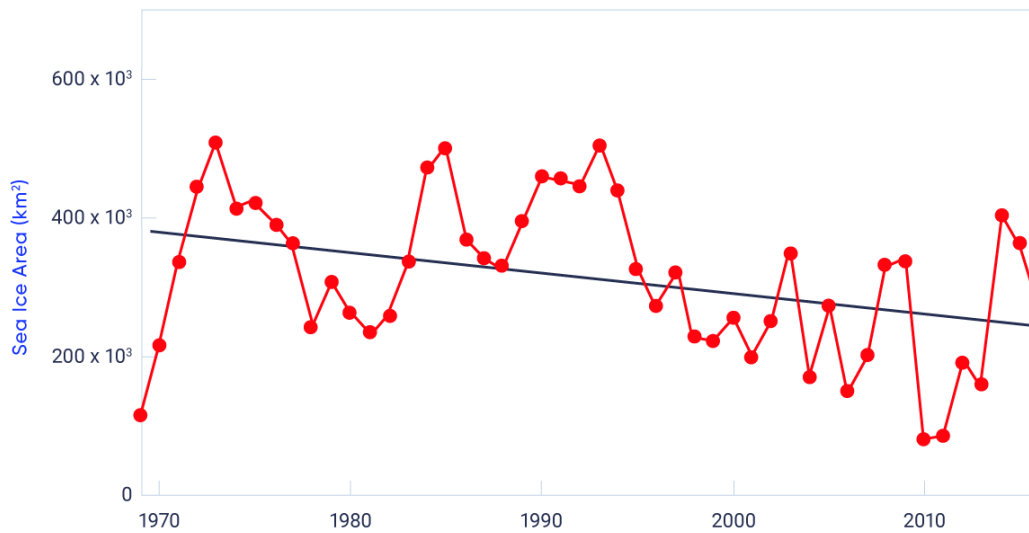


FIGURE 5.10: East coast sea ice area trends, 1969–2016

Figure caption: (a) Map of average January–March sea ice area trends for subregions of the east coast and (b) time series of average January–March sea ice area trends for the entire region, 1969–2016.

5.3.2: Projected changes in sea ice

The narrow channels in Canadian Arctic waters are poorly represented by the coarse spatial resolution of climate models. While uncertainty in model projections is therefore higher for the CAA than for the pan-Arctic, evaluation of historical simulations shows the CMIP5 multi-model ensemble (see Chapter 3, Box 3.1) still provides a quantitative basis for projecting future sea ice conditions (Laliberté et al., 2016). Under a high emission scenario (RCP8.5), the CMIP5 multi-model projections indicate widespread reductions in SIC for the ice melt (summer) and ice formation (fall) seasons (Mudryk et al., 2018; see Figure 5.4). For the east coast, virtually ice-free conditions during the winter months are projected by mid-century under a high emission scenario (RCP8.5) with uncertainty in these projections due to potential changes in the transport of sea ice from the Arctic to the east coast (Loder et al., 2015).

The probability and timing of future sea ice-free conditions are sensitive to the definition of 'ice-free' (Laliberté et al., 2016). When using a threshold of 5% ice area, there is a 50% probability that all Canadian regions will be sea ice-free in September by 2050 under a high emission scenario (RCP8.5; see Figure 5.11). The probability that all regions will be ice free is similar for August, but lower for October and November. Hudson Bay, which is already largely ice free in August and September, has a high probability of being ice free for four consecutive months (August through November) by 2050. Using a definition of 30% ice area, more persistent ice-free conditions are projected. Baffin Bay is projected to be ice free for August through October, and the Beaufort Sea and the CAA may be ice free in August and September by 2050.

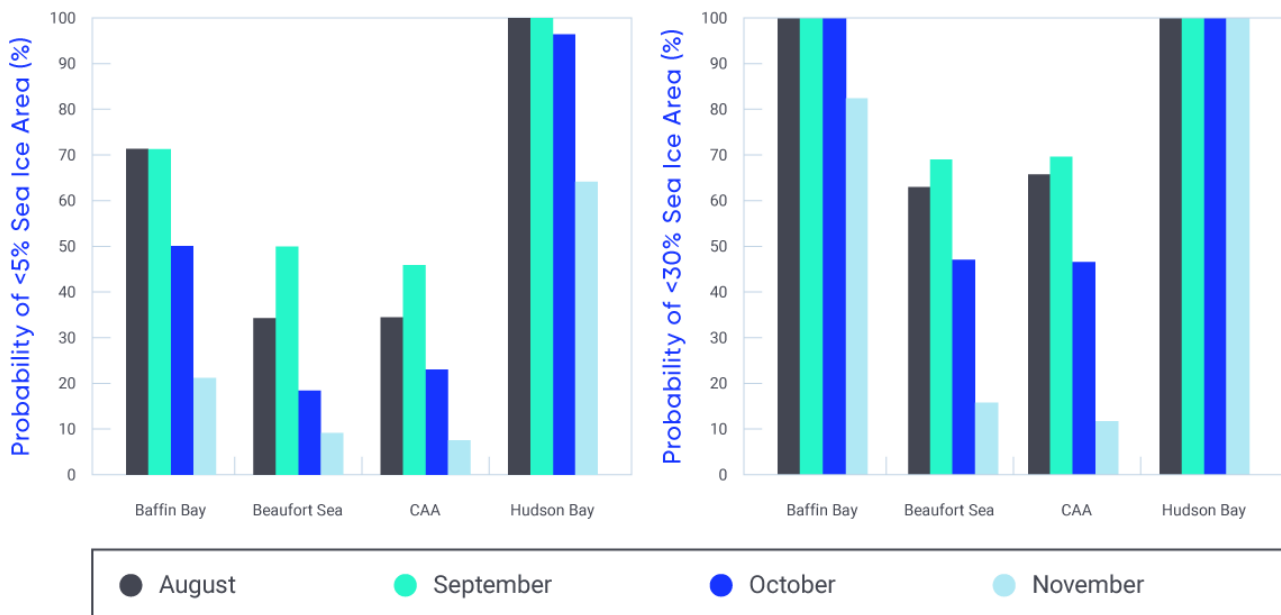


Figure 5.11: Probability of sea ice-free conditions by 2050

Figure caption: Probability of sea ice-free conditions by 2050 under a high emission scenario (RCP8.5) from the Coupled Model Intercomparison Project (CMIP5) multi-model mean using a definition of ice-free conditions of 5% (left) and 30% (right) sea ice area.

FIGURE SOURCE: MUDRYK ET AL. (2018)

The likelihood of summer ice-free conditions in the central Arctic is connected to the magnitude of projected global temperature increases, with a much greater probability of ice-free conditions for 2°C global warming compared to 1.5°C (Jahn, 2018; Sigmond et al., 2018). The area to the north of the CAA and Greenland will be the last refuge for summer sea ice (including MYI) in the Arctic during the summer (Wang and Overland, 2012; Laliberté et al., 2016), so ice will still drift into the Northwest Passage, where it will present a navigation hazard for shipping, even when the Arctic Ocean is sea ice-free during the summer (see FAQ 5.1: Where will the last ice area be in the Arctic?).

FAQ 5.1: Where will the last sea ice area be in the Arctic?

Short answer:

The last sea ice area in the Arctic during the summer months will be along the northern coasts of Greenland and the Canadian Arctic Archipelago (CAA), as well as areas between the northern islands of the CAA (Figure 5.12), providing an important refuge for sea ice-dependent species. As long as there is sea ice within this region during the summer months, it will continue to be transported southward into the major shipping channels of the CAA, presenting an ongoing potential hazard for shipping in this region, even while the majority of the Arctic is free of sea ice.

Full answer:

The decline of summer Arctic sea ice extent associated with observed warmer temperatures is perhaps the most visible feature of climate change over the past 30 years or more (Comiso, 2012; Fyfe et al., 2013). Arctic sea ice is also thinner because older and thicker MYI has been gradually replaced by younger seasonal ice (Kwok and Cunningham, 2015). Continued declines in both sea ice extent and thickness as a result of further warming from greenhouse gas emissions are projected by the latest state-of-the-art climate models, and this has led to questions about when the Arctic will become free of sea ice during the summer months. The consensus from climate models is that a summertime sea ice-free Arctic could be a reality under a high emissions scenario by mid-century; however, there is considerable regional variability in the timing of projected sea ice-free conditions during the summer months (Laliberté et al., 2016).

The “last ice area” (LIA) refers to regions of the Arctic immediately north of Greenland and the CAA, as well as areas between the northern islands of the CAA (Figure 5.12). The concept of the LIA was borne from climate model simulations that project sea ice within the LIA, even when the rest of the Arctic is virtually sea ice-free during September (Laliberté et al., 2016). Sea ice will persist in the LIA because of the influence of large-scale atmospheric circulation (prevailing winds) on sea ice motion, with the atmospheric Beaufort High driving the counter-clockwise (anti-cyclonic) movement of sea ice in the Beaufort Gyre. As a result, Arctic Ocean sea ice converges against the northern coasts of Greenland and the CAA, creating some of the thickest sea ice in the world, with some floes over 5 m thick (Kwok and Cunningham, 2015). This thick sea ice is more resistant to melt under a warming Arctic. So, assuming no major changes in future atmospheric circulation patterns, sea ice will persist in the LIA during the summer, even when the rest of the Arctic is sea ice-free.



Figure 5.12: Location of the last ice area

Figure caption: Approximate area (shaded in white) of the last sea ice area in the Arctic during the summer months.

FIGURE SOURCE: BASEMAP – [HTTPS://NOAA.MAPS.ARCGIS.COM/HOME/ITEM.HTML?ID=94F14EB0995E4BFC9D2439FC868345DA](https://noaa.maps.arcgis.com/home/item.html?id=94f14eb0995e4bf9c9d2439fc868345da);
LAST ICE AREA ESTIMATE – [HTTP://WWW.WWF.CA/CONSERVATION/ARCTIC/LIA/](http://www.wwf.ca/conservation/arctic/lia/)

Recent scientific attention, in the context of the Paris Agreement under the United Nations Framework Convention on Climate Change, has focused on the probability that the Arctic will become sea ice-free in the summer. The Paris Agreement aims to strengthen the global response to climate change by limiting the increase in global mean temperature to within 2°C above pre-industrial levels, while pursuing efforts to limit warming even more, to 1.5°C. Climate model simulations show that a sea ice-free Arctic becomes increasingly more likely as global mean temperatures increase beyond 1.5°C and reach 2°C (e.g., Jahn, 2018; Sigmond et al., 2018). These studies define sea ice-free conditions for the Arctic as a threshold of 1 million km² sea ice extent; this remnant ice cover will be located in the LIA.

The LIA will be an important refuge for marine species who rely on sea ice for habitat and hunting, as well as for communities that depend on these species. The persistence of sea ice within the LIA has implications for shipping in the Arctic. For instance, even when the majority of the Arctic is sea ice-free during the summer, thick multi-year ice from the LIA will continue to be transported southward into the channels of the Northwest Passage, presenting a hazard to transiting ships (Haas and Howell, 2015).

Section summary

In summary, the Arctic sea ice environment has changed profoundly over recent decades (Barber et al., 2017). Perennial sea ice that survives the summer melt is being replaced by thinner seasonal sea ice that melts in the summer. Summer sea ice area (particularly MYI) declined across the Canadian Arctic by 5% to 20% per decade (1968–2016, depending on region); winter sea ice area decreased in eastern Canada (by 7.6% per decade, 1969–2016). There is **very high confidence** in these trends, which are derived by trained analysts from Canadian Ice Service ice charts that provide region-specific sea ice information. It is **very likely** that continued reductions in summer and fall sea ice across the Canadian Arctic, and winter sea ice in eastern Canadian waters, will result from increased temperatures under all emission scenarios. Most Canadian Arctic marine regions could be sea ice-free for at least one month in the summer by 2050 (**high confidence**) based on simulations from CMIP5 models. There is **very high confidence** that the region to the north of the CAA and Greenland will be the last area where thick MYI will be present in the Arctic during the summer. Current understanding of sea ice dynamics, based on satellite observations, indicates this MYI will continue to drift into Canadian waters.

5.4: Glaciers and ice caps

Key Message

Canada's Arctic and alpine glaciers have thinned over the past five decades due to increasing surface temperatures; recent mass loss rates are unprecedented over several millennia (*very high confidence*). Mass loss from glaciers and ice caps in the Canadian Arctic represent the third largest cryosphere contributor to global sea level rise (after the Greenland and Antarctic ice sheets) (*very high confidence*).

Key Message

Under a medium emission scenario, it is projected that glaciers across the Western Cordillera will lose 74 to 96% of their volume by late century (*high confidence*). An associated decline in glacial meltwater supply to rivers and streams (with impacts on freshwater availability) will emerge by mid-century (*medium confidence*). Most small ice caps and ice shelves in the Canadian Arctic will disappear by 2100 (*very high confidence*).

Canada's landmass supports approximately 200,000 km² of ice, which includes glaciers and ice caps in western Canada, the Canadian Arctic Archipelago (CAA), and northern Labrador (Radic et al., 2014; Clarke et al., 2015). These glaciers are responding to long-term climate changes since the Little Ice Age, as well as the anthropogenic rapid warming of recent decades. The largest ice caps are located in Queen Elizabeth Islands and Baffin Island of the Canadian Arctic. Because they drain to the Arctic Ocean, these ice caps represent the greatest potential contribution from Canadian territory to sea level increases (Radic et al., 2014). Mountain glaciers of western Canada cover a much smaller area and have less potential to affect global sea levels. However, they are an important source of meltwater runoff, as melt from these glaciers is a significant contributor to summer streamflow in river systems (Jost et al., 2012; Naz et al., 2014; Bash and Marshall, 2014). The loss of mountain glaciers can therefore influence how much water is available, and when, in downstream areas that can extend far from the source regions.

A key measure of health for glaciers and ice caps is surface mass balance, the difference between annual mass gained through snow accumulation and mass lost due to melt runoff. In the relatively dry Canadian Arctic, surface mass balance is determined primarily by the duration and intensity of the summer melt season (Koerner, 2005), while glaciers in more temperate regions of Canada are also influenced significantly by year-to-year variations in snowfall. Remote sensing measurements generally cannot be used to directly estimate mass balance, with the exception of very coarse resolution gravimetric measurements from the NASA GRACE mission (approximately 450 km × 450 km), but remote sensing does contribute valuable information on the melt/freeze state (Wang et al., 2005), changes in ice thickness (Gray et al., 2016; Krabill et al., 2002; Berthier et al., 2014), and glacier motion and iceberg calving (Strozzi et al., 2008, van Wychen et al., 2016, Gray et al., 2001). For larger regions, models can be used to estimate mass balance (Lenaerts et al., 2013; Gardner et al., 2011). Long-term records of surface mass balance measurements from a small number of Canadian glaciers are available through the World Glacier Monitoring Service (<<http://wgms.ch/latest-glacier-mass-balance-data/>>). Acquiring surface measurements for the determination of glacier mass balance is logistically difficult, so only selected glaciers in the CAA and western Cordillera are monitored (see Figure 5.13).

5.4.1: Observed changes in glaciers and ice caps

Climate warming, combined with periods of reduced precipitation in Western Canada, has contributed to total thinning of glaciers in the southern Cordillera by 30 to 50 m since the early 1980s (see Figure 5.13) (Zemp et al., 2015). By the mid-1980s, glaciers in Garibaldi Provincial Park, southern British Columbia, had contracted in area by 208 km² since the Little Ice Age maximum extent of 505 km², with accelerated shrinkage by another 52 km² (or 7% of the Little Ice Age maximum) by 2005 (Koch et al., 2009). Glacier extent at several sites in the central and southern Canadian Rocky Mountains decreased by approximately 40% from 1919 to 2006 (Tennant et al., 2012). Glaciers of the Columbia Icefield, in the Canadian Rocky Mountains, also experienced dramatic changes from 1919 to 2009, losing 22.5% of total area while retreating more than 1.1 km on average (Tennant and Menounos, 2013). Aerial photography shows that all glaciers in British Columbia's Cariboo Mountains receded over the 1952–2005 period, with a loss of approximately 11% in surface area (Beedle et al., 2015). In eastern Canada, small alpine glaciers in the Torngat Mountains, Labrador (see Figure 5.13 for location) shrunk by 27% between 1950 and 2005, with current thinning rates as high as 6 m per year across the 22 km² of glaciers that remain in this area (Barrand, et al., 2017).

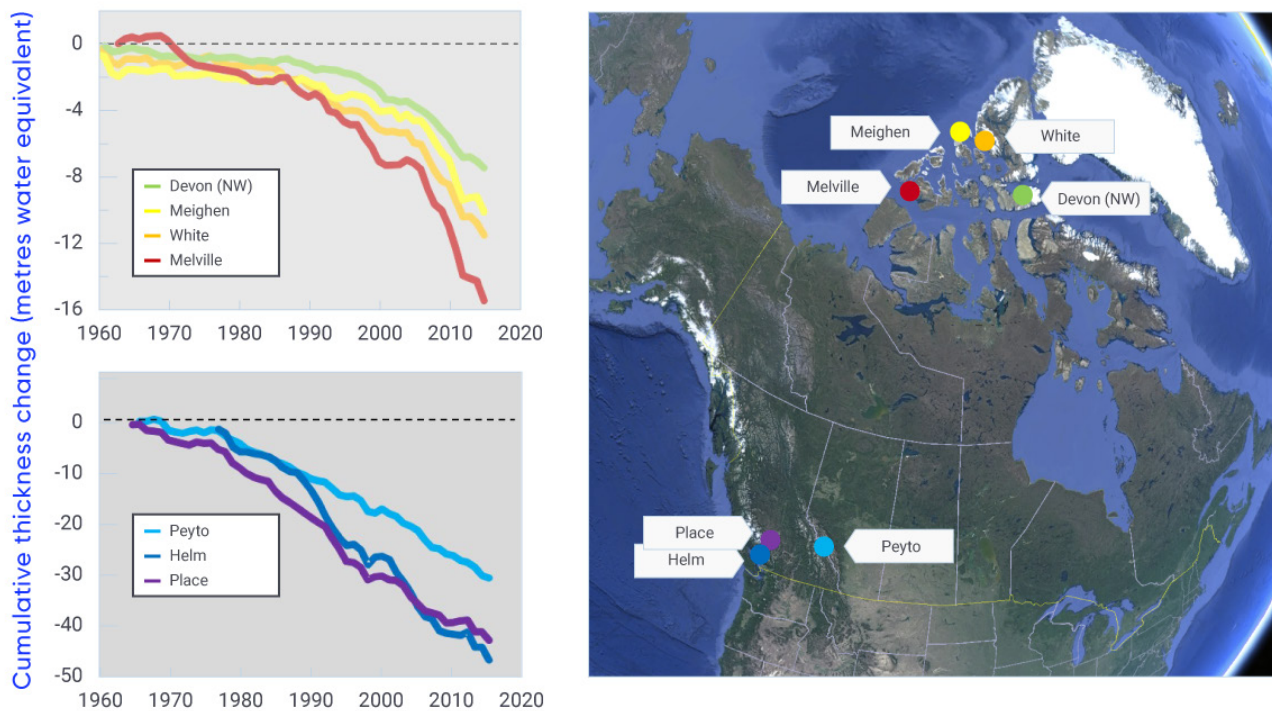


FIGURE 5.13: Cumulative thickness change at long-term glacier monitoring sites in Canada

Figure caption: Map shows location of monitoring sites in the Canadian Arctic Archipelago and the Western Cordillera (image courtesy of Google Earth). Graphs show change in cumulative thickness of reference glaciers in the Canadian high Arctic (top left) and Western Cordillera (bottom left) since the early 1960s. Note the difference in y-axis scale between graphs.

FIGURE SOURCE: MASS BALANCE DATA FOR DEVON (NORTHWEST), MEIGHEN, MELVILLE, AND ALL SITES IN THE WESTERN CORDILLERA ARE FROM THE GEOLOGICAL SURVEY OF CANADA ARCHIVES, AND DATA FOR THE WHITE GLACIER WERE OBTAINED FROM TRENT UNIVERSITY (1960–2012; G. COGLEY) AND UNIVERSITY OF OTTAWA (2013–2015; L. COPLAND).

Glaciers and ice fields covering approximately 10,000 km² of the Yukon have decreased in area by approximately 22% between 1957 and 2007, and thinned by 0.78 m water equivalent (90% uncertainty range 0.44 to 1.12 m per year) contributing 1.12 mm (90% uncertainty range 0.63 to 1.61 mm) to global sea level over this period (Barrand and Sharp, 2010). Mass balance of glaciers, measured at three monitoring sites in Alaska (all within 300 km of the Kluane ice field, Yukon) indicate a rapid change from positive to negative glacier mass balance in this region beginning in the late 1980s (Wolken et al., 2017).

Long-term in situ glacier monitoring indicates a trend of significant loss of mass for glaciers and ice caps in the CAA beginning in the early 1990s (see Figure 5.13). Acceleration of glacier thinning in this region in the mid-2000s coincided with increases in summer warming driven by the advection of warm air masses to the Arctic from more southerly latitudes (Sharp et al., 2011; Mortimer et al., 2016). Based on satellite measurements and surface mass-budget models, total mass loss from glaciers and ice caps in the CAA has increased more than two-fold, from 22 gigatonnes (Gt) per year between 1995 and 2000 (Abdalati et al., 2004), to 60 Gt per year (90% uncertainty range 52 to 66 Gt per year) over the 2004–2009 period (Gardner et al., 2013), and 67 Gt per year (90% uncertainty range 61 to 73 Gt per year) over the 2003–2010 period (Jacob et al., 2012), with mass losses continuing to accelerate to 2015 (Harig and Simons, 2016). According to the most recent assessments of regional glacier change, glacier melting in the CAA has contributed 0.16 mm per year to global sea-level rise since 1995, 23% of the contribution of the Greenland ice sheet and 75% of the Antarctic Ice Sheet (Gardner et al., 2103; Shepard et al., 2012; Sharp et al., 2016).

The Barnes Ice Cap on Baffin Island, the last remnant of the Laurentide Ice Sheet that covered most of Canada during the last glaciation, lost 17% of its mass from 1900 to 2010 (Gilbert et al., 2016). Approximately 10% of the total area of ice in the CAA is composed of small, stagnant ice caps (the oldest are less than 3000 years old), located almost entirely under the regional equilibrium line altitude, meaning they do not have an accumulation zone and experience net thinning across their entire area in most years. These ice caps are shrinking rapidly (Serreze et al., 2017) and fragmenting (Burgess, 2017), with many expected to completely disappear within the next few decades. Of similar age to the small ice caps are the ice shelves of northern Ellesmere Island, which are composed of floating glacier ice and/or very thick old sea ice. These ice shelves have decreased in area by about 90% since 1900 (with more than 50% of that loss since 2003) and are expected to survive for only the next decade or two (Mueller et al., 2017).

Like many glaciers in the world, Canada's glaciers are out of equilibrium with current climatic conditions and will continue to lose mass for the foreseeable future. Summer warming in the Arctic has driven extreme melting of ice caps and glaciers over the past two decades, resulting in this region becoming the most significant cryosphere contributor to global sea-level rise after the Greenland and Antarctic ice sheets.

5.4.2: Projected changes in glaciers and ice caps

Climate model projections indicate that western Canada and the western United States together (grouped together in many studies because of their similar mountainous domain) could lose approximately 85% (90% uncertainty range 74% to 96%) of the 2006 volume of glaciers by the end of the century under a medium emission scenario (RCP4.5). Under a high emission scenario (RCP8.5), this loss could exceed 95% (Radic et al., 2014). Glaciers in the coastal ranges of western Canada are predicted to lose 75% (90% uncertainty range 65% to 85%) of their 2005 ice area and 70% (90% uncertainty range 60% to 80%) of their volume by 2100 based on the mean of four emission scenarios (RCP2.6, 4.5, 6.0, 8.5) (Clarke et al., 2015). Glaciers in the western Canadian interior are projected to lose more than 90% of the 2005 volume under all scenarios except a low emission scenario (RCP2.6) (Clarke et al., 2015). These changes, in combination with the projected loss of alpine snow cover, will impact regional water resources (Fyfe et al., 2017; see Chapter 6, Section 6.2). Glacier-fed rivers may experience periods of increased discharge due to greater meltwater contributions in a warmer climate, but this response is finite, and glacier mass loss associated with warming is projected to result in reduced summer streamflow by mid-century (Clarke et al., 2015). The rate and timing of this transition will have important consequences for stream and river water quality and temperature, and for the availability of water for human uses such as hydro-electricity generation and agriculture.

Regional land ice models project that glaciers and ice caps in the Canadian Arctic will lose 18% of their total mass by 2100 (Radic et al., 2014; relative to a baseline mass reference estimated by Radic and Hock, 2011) under a medium emission scenario (RCP4.5), equivalent to 35 mm of global sea-level rise (Lenaerts et al., 2013; Marzeion et al., 2012). This loss of land ice volume in Arctic Canada by 2100 will contribute 41 mm of sea-level equivalent (90% uncertainty range 26 to 56 mm) under RCP4.5, and 57 mm of sea-level equivalent (90% uncertainty range 39 to 75 mm) under a high emission scenario (RCP8.5) (Radic et al., 2014). Densification of high-elevation firn (partially compacted granular snow that is the intermediate stage between snow and glacial ice) has reduced or eliminated the internal storage capacity of the larger (more than 2000 km²) ice caps in this region, thus increasing their sensitivity to future warming (Noël et al., 2018). Based on the trajectories of observed loss over recent decades, many of the remaining small ice caps (less than 2000 km²) and ice shelves in the Canadian Arctic are expected to disappear by 2100.

Section summary

In summary, Canada's Arctic and alpine glaciers have thinned over the past three to five decades, due to increasing surface temperatures (*very high confidence*). While spatial sampling is sparse, these long-term trends in glacier thickness change have been measured annually following standardized protocols and agree with independent remote sensing and model-based approaches. Multiple assessments using satellite data and models show that mass loss from glaciers and ice caps in the Canadian Arctic represents the largest cryosphere contributor to global sea-level rise after the Greenland and Antarctic ice sheets (*very high confidence*). Based on a regional mass balance model forced by future climate scenarios, glaciers across the Western Cordillera are projected to lose up to 85% of their volume by the end of the century (*high confidence*).

This will lead to a decline in glacial meltwater supply to rivers and streams, although there is only *medium confidence* in the absolute impacts on freshwater availability because of multiple other contributors to projected streamflow changes (see Chapter 6, Section 6.2). Based on output from various independent models, glaciers and ice caps in the Canadian Arctic will lose 18% of their total mass by the end of the century, and so will remain important contributors to global sea-level rise beyond 2100 (*high confidence*). Small ice caps and ice shelves in the Canadian Arctic are shrinking rapidly. Based on observed changes in recent decades, and ice cap and ice shelf sensitivity to projected temperature increases, most are expected to disappear well before 2100 (*very high confidence*).

5.5: Lake and river ice

Key Message

The duration of seasonal lake ice cover has declined across Canada over the past five decades due to later ice formation in fall and earlier spring breakup (*high confidence*). Seasonal maximum lake ice cover for the Great Lakes is highly variable since 1971 (*very high confidence*), with no significant trend.

Key Message

Spring lake ice breakup will be 10 to 25 days earlier by mid-century, and fall freeze-up 5 to 15 days later, depending on the emissions scenario and lake-specific characteristics such as depth (*medium confidence*).

Canada is a lake-rich country, particularly across the north, with approximately 20% to 25% of the Arctic coastal lowlands covered by lakes (Duguay et al., 2003). Therefore, the timing of lake and river ice freeze-up and breakup (known as ice phenology) and ice thickness are important indicators of climate variability and change. Ice phenology is sensitive to changes in air temperature, whereas changes in ice thickness are linked to changes in both air temperature and snowfall. Due to the insulating properties of snow, the timing of snow accumulation on new ice and the seasonal accumulation of snow influence ice thickness. In situ records of ice cover across much of Canada are limited, because surface-based ice monitoring is not practical in many regions, so satellite remote sensing is commonly used to monitor lake and river ice (Howell et al., 2009).

Changes to ice phenology and thickness influence the role that lakes play in regional energy and water cycles (Rouse et al., 2005). Ice cover also has strong effects on lake biogeochemical processes in cold regions: changes in the ecological productivity of high Arctic lakes on Ellesmere Island are predominantly determined by variations in ice cover duration (Griffiths et al., 2017). Reductions in ice cover may also allow greater emissions of methane (a greenhouse gas) from Arctic lakes (Greene et al., 2014; Tan and Zhuang, 2015). The importance of ice cover to ecosystems is not limited to the Arctic. For instance, earlier ice melt across the Great Lakes is linked to turbidity and phytoplankton activity through enhanced wind-induced mixing (Bai et al., 2015). Seasonal roads across frozen lakes serve as a critical supply lines to remote communities and mines during winter months, while stable lake and river ice is a necessity for safe winter season recreation and travel for residents of northern communities.

5.5.1: Observed changes in lake and river ice

Surface observations show that ice breakup is occurring earlier, and freeze onset later, across small lakes in southern Quebec, Ontario, Manitoba, and Saskatchewan (Brown and Duguay, 2010). A significant declining trend in annual maximum ice cover was observed for the Laurentian Great Lakes over the 1973–2010 period (71% decline for all of the Laurentian Great Lakes), with the largest declines occurring in Lake Ontario (88%), Lake Superior (79%), and Lake Michigan (77%) (Wang et al., 2012). Heavy ice years in 2014, 2015, and 2018, however, result in no trend over the full 1973–2018 period (Figure 5.14). The large year-to-year variation is associated with the Arctic Oscillation/North Atlantic Oscillation (AO/NAO) and El Niño–Southern Oscillation (ENSO) (see Chapter 2, Box 2.5). For example, the record-breaking low in maximum ice cover in the winter of 2011/2012 occurred during a strong positive-phase AO/NAO and the cold phase of ENSO (La Niña event) (Bai et al., 2015). Whether variable ice cover contributes to observed increases in water temperature in the Laurentian Great Lakes is a topic under debate. Recent findings suggest that changes in winter lake ice cover play only a minor role in the observed warming trend (Zhong et al., 2016), whereas ice cover duration was linked to summer surface water temperature (particularly in nearshore areas) when the lakes were examined at a finer spatial scale (Mason et al., 2016).

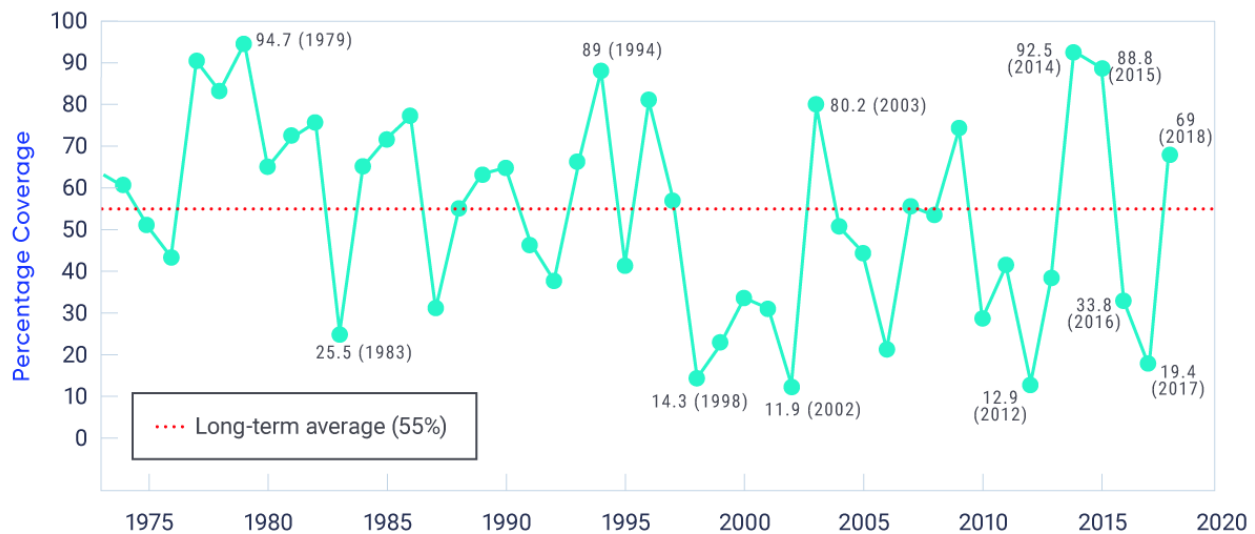


FIGURE 5.14: Laurentian Great Lakes annual maximum ice cover, 1973–2018.

Figure caption: Laurentian Great Lakes annual maximum ice cover (%) (1973–2018). Red dashed line indicates the long-term average.

FIGURE SOURCE: NOAA GREAT LAKES ENVIRONMENTAL RESEARCH LABORATORY, [HTTPS://WWW.GLERL.NOAA.GOV/DATA/ICE/](https://www.glerl.noaa.gov/data/ice/)



Satellite measurements show that lakes in Arctic Canada have also been experiencing an earlier ice minimum (the last date of floating ice cover on the lake surface) and an earlier date when the water is clear of ice (see Figure 5.15; see also Duguay et al., 2006; Prowse, 2012; Cooley and Pavelsky, 2016). These changes are consistent with a recent circumpolar assessment, which showed that approximately 80% of Arctic lakes experienced declines in ice cover duration from 2002 to 2015, due to both a later freeze-up and an earlier breakup (Du et al., 2017). Results from northern Alaska (which are likely similar to those in northwestern Canada) show that lake ice has begun to thin in recent decades (Alexeev et al., 2016). From 1992 to 2011, approximately one-third of shallow lakes in which the entire water volume historically froze to the bed by the end of winter had changed to floating ice (Arp et al., 2012; Surdu et al., 2014). Canada's northernmost lake, Ward Hunt Lake (located on Ward Hunt Island), had maintained stable, continuous year-round ice cover for many decades until very warm summers of 2011 and 2012, when the ice cover fully melted (Paquette et al., 2015). This loss of inland perennial freshwater ice cover occurred nearly simultaneously with the collapse of the nearby Ward Hunt ice shelf (Mueller et al., 2009; Veillette et al., 2010). Analysis of a 15-year time series (1997–2011) of radar and optical satellite imagery provides further evidence that some lakes in the central and eastern Canadian high Arctic are transitioning from continuous (year-round) to seasonal ice cover (Surdu et al., 2016).

It is difficult to provide an assessment of river ice changes across Canada because of sparse observations and a lack of recent assessments of the available data. There is evidence of earlier river ice breakup, consistent with increases in surface temperature (Prowse, 2012). However, the impact that climate-driven changes in ice phenology and thickness, combined with changing seasonal flow regimes (see Chapter 6, Section 6.2) and the influence of hydraulic processes (i.e., changing ice strength), will have on ice jams and flood events is not fully understood (Beltaos and Prowse, 2009).

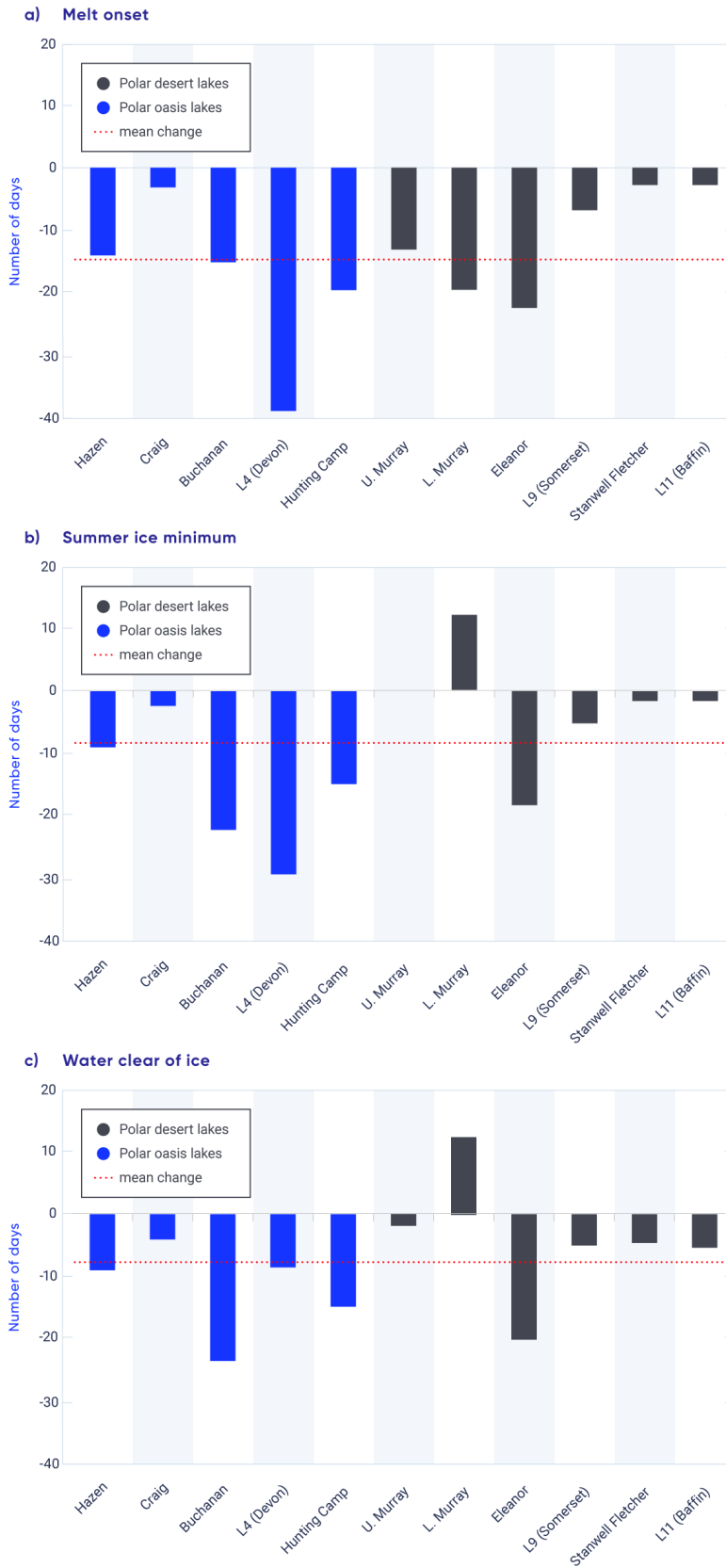


Figure 5.15: Changes in ice cover for selected lakes in the Canadian high Arctic, 1997–2011

Figure caption: Number of days earlier (negative numbers) or later (positive numbers) of (a) melt onset, (b) summer ice minimum, and (c) date that water is clear of ice for selected lakes in the central and eastern Canadian high Arctic from 1997 to 2011. Number of days' change is reported relative to the 1997–2011 mean date (from remote sensing observations). Lakes in polar-oasis (relatively high annual precipitation) environments are shown as blue bars and lakes in polar-desert environments (relatively low annual precipitation) are shown as black bars. The red dashed line indicates the 1997–2011 mean change.

FIGURE SOURCE: SURDU ET AL., 2016

5.5.2: Projected changes in lake and river ice

Changes in lake ice can be projected only indirectly, because lake models are not embedded within global climate models and individual lakes are not spatially resolved. When forced by a future climate under a medium emission scenario (RCP4.5), lake ice models project that spring breakup will occur between 10 and 25 days earlier by mid-century (compared with 1961–1990), and freeze-up will be five to 15 days later across Canada (Brown and Duguay, 2011; Dibike et al., 2012) (Figure 5.16). This results in a reduction of ice cover duration of 15 to 40 days for much of the country. More extreme reductions of up to 60 days are projected in coastal regions. The range in projected changes is due to regional variability in temperature and snowfall changes, and to lake-specific variables such as size and depth. The Laurentian Great Lakes can be resolved by lake models if the projected climate forcing data are downscaled. This approach has identified consistent results, with reduced ice cover duration of between 25 to 50 days across the Laurentian Great Lakes by mid-century, due to both later freeze-up and earlier melt (Gula and Peltier, 2012). Mean seasonal maximum ice thickness is projected to decrease by 10 to 50 cm by mid-century, with a more pronounced decrease in the eastern Canadian high Arctic (Brown and Duguay, 2011).

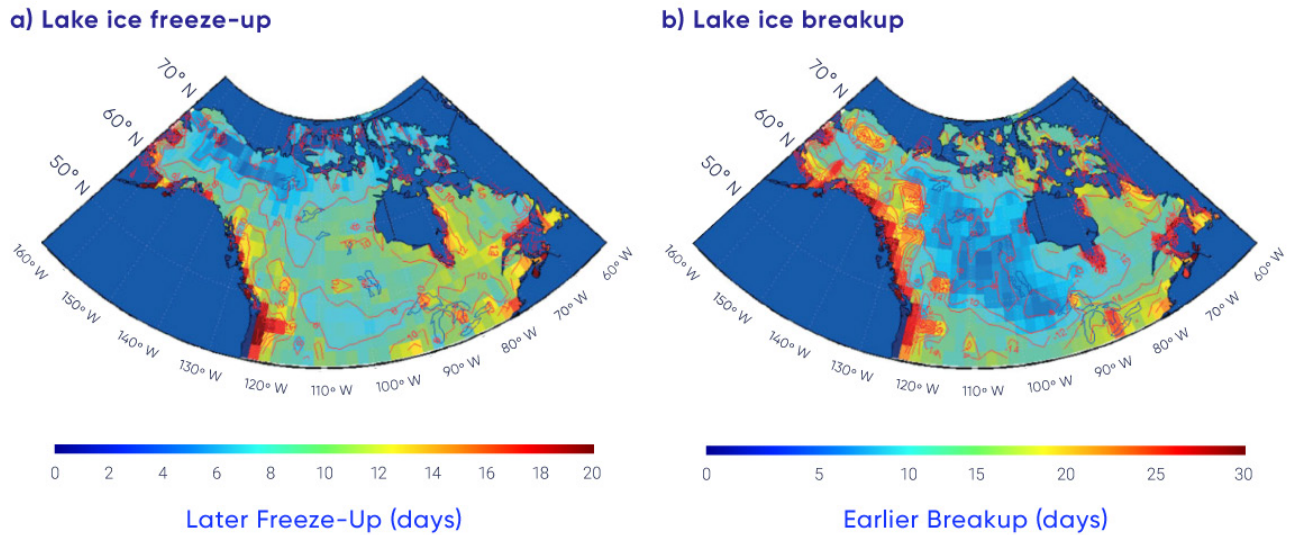


Figure 5.16: Projected change in ice freeze-up and ice breakup dates for Canadian lakes

Figure caption: Change in mean date (number of days) of (a) freeze-up and (b) breakup between the current (1961–1990) and future (2041–2070) climatic periods for a hypothetical lake of 20 m depth. Note that all changes are in the positive direction (later ice freeze-up and earlier ice breakup). Simulations performed with the Canadian Regional Climate Model (CRCM4.2) using the SRES A2 emission scenario.

FIGURE SOURCE: DIBIKE ET AL., 2012

Warming is projected to drive an earlier river ice breakup in spring, which is due to decreased mechanical ice strength and earlier onset of peak discharge (Cooley and Pavelsky, 2016). More frequent mid-winter breakup and associated ice jam events are anticipated (Beltaos and Prowse, 2009), although projected changes in river ice properties may reduce ice obstructions during the passage of the spring freshet (the increased flow resulting from snow and ice melt in the spring) (Prowse et al., 2010). A shorter ice cover season and reduced ice thickness may affect food security for northern communities by reducing the reliability of traditional ice-based hunting routes and the safety of ice-based travel. The reliability and predictability of ice roads as supply lines to northern communities and development sites is not fully dependent on climate, because these ice roads are partially engineered each season (i.e., snow is removed to accelerate ice growth). However, there have been instances of severely curtailed ice-road shipping seasons due to unusually warm conditions in the early winter (Sturm et al., 2016). The seasonal operational duration for such ice roads is expected to decrease as a result of winter warming (Perrin et al., 2015; Mullan et al., 2017).

Section summary

In summary, the duration of seasonal lake ice cover is declining across Canada due to later ice formation in fall and earlier spring breakup, with implications for freshwater ecosystem services, tourism and recreation, and transportation. Although the surface monitoring network is sparse, there is *high confidence* in this trend because of consistency between satellite observations and historical lake ice model simulations. There is a weak negative trend in seasonal maximum lake ice cover for the Laurentian Great Lakes (1971–2017); large year-to-year variation is the primary feature of the time series (*very high confidence*). Changes in lake ice are difficult to project because lake models are not embedded within global climate models and individual lakes are not spatially resolved. Instead, estimates of changing lake ice phenology are derived from lake ice models forced by projected future climates. These simulations indicate spring lake ice breakup will be 10 to 25 days earlier by mid-century, with a 5 to 15 day delay in fall freeze-up, depending on the emission scenario. While the impact of warming temperatures on ice phenology is clear, there is only *medium confidence* in these projections because of numerous sources of uncertainty, including the quality of snowfall projections, the limitations of lake ice models, and the role of lake-specific characteristics such as depth and morphology.

5.6: Permafrost

Key Message

Permafrost temperature has increased over the past 3-4 decades (*very high confidence*). Regional observations identify warming rates of about 0.1°C per decade in the central Mackenzie Valley and 0.3°C to 0.5°C per decade in the high Arctic. Active layer thickness has increased by approximately 10% since 2000 in the Mackenzie Valley. Widespread formation of thermokarst landforms have been observed across northern Canada.

Key Message

Increases in mean air temperature over land underlain with permafrost are projected under all emissions scenarios, resulting in continued permafrost warming and thawing over large areas by mid-century (*high confidence*) with impacts on northern infrastructure and the carbon cycle.

Permafrost is an important component of the Canadian landscape, underlying about 40% of the landmass and extending under the ocean in parts of the Canadian Arctic. Soil properties (including both the deep mineral soil and any overlying layers of organic matter), ground cover, and the thickness of overlying snow cover (because of snow's insulating properties) have important influences on ground temperatures and, therefore, permafrost characteristics. The soil layer above the permafrost that thaws and freezes annually is referred to as the "active layer."

Understanding current permafrost conditions and how they may evolve in response to a changing climate is essential for the assessment of climate change impacts and the development of adaptation strategies in northern Canada. Permafrost conditions are linked to hydrological (e.g., drainage) and land surface processes (e.g., erosion and slope movements); ground warming and thawing can therefore affect ecosystems. Thawing of ice-rich permafrost results in ground instability; if not considered in the design phase, this can affect the integrity of infrastructure such as buildings and airstrips. Coastal communities face unique challenges because of processes related to thawing of the shore face (Ford et al., 2016). The northern circumpolar permafrost region holds reserves of carbon (approximately 1000 petagrams [Pg] in the upper 3 m) as large as the total amount of carbon in the atmosphere (Hugelius et al., 2014; Olefeldt et al., 2016). If permafrost thaws, it could therefore release massive amounts of greenhouse gases (carbon dioxide and methane) into the atmosphere (Romanovsky et al., 2017a). Northern soils efficiently store mercury, which is vulnerable to release as a consequence of permafrost thaw (Schuster et al., 2018). Permafrost thawing can also release other compounds and dissolved material (e.g., Kokelj and Jorgenson, 2013; Kokelj et al., 2013), including contaminants associated with waste facilities that may depend on permafrost for containment (e.g., Prowse et al., 2009; Thienpont et al., 2013).

5.6.1: Observed changes in permafrost

Permafrost conditions are challenging to monitor because they cannot be directly determined using satellite measurements. They are therefore determined largely from in situ monitoring, which results in gaps in the spatial distribution of measurement sites because of the relative inaccessibility of large portions of northern Canada and historical emphasis in monitoring regions with infrastructure development potential (such as the Mackenzie Valley; Smith et al., 2010). Changes in permafrost conditions over the last few decades can be assessed by tracking changes in two key indicators: permafrost temperature and thickness of the active layer. Ground temperature, measured below the depth where it varies from one season to the next, is a good indicator of decadal to century changes in climate, while the active layer responds to shorter-term climate fluctuations (Romanovsky et al., 2010).

Ground temperature is measured in boreholes, generally up to 20 m deep, across northern Canada. Some of these monitoring sites have been operating for more than two decades, while many others were installed during the International Polar Year (IPY, 2007–2009) to establish baseline measurements of the temperature of permafrost (Smith et al., 2010; Derksen et al., 2012). A comparison of data collected for about five years after the establishment of the IPY baseline indicates that permafrost has warmed at many sites from the boreal forest to the tundra (Smith et al., 2015a), with greater changes in the colder permafrost of the eastern and high Arctic, where temperatures increased by more than 0.5°C at some sites over this short time period. Continued data collection has extended the time series beyond 30 years for some sites, allowing researchers to place the changes since IPY in the context of a longer record.

The temperature of warm permafrost (above -2°C) in the central and southern Mackenzie Valley (i.e., Norman Wells, Wrigley) has increased since the mid-1980s, but the rate of temperature increase has generally been lower since 2000 – less than about 0.2°C per decade (see Figure 5.17 and Table 5.1). The low rate of increase is observed because permafrost temperatures are already close to 0°C in this region, so energy is directed toward the latent heat required to melt ground ice rather than raising the temperature further. In the Yukon, comparison of recent ground temperature measurements with those made in the late 1970s and early 1980s suggests similar warming of approximately 0.2°C per decade (Duguay, 2013; Smith et al., 2015b). In contrast, in the northern Mackenzie Valley (sites designated Norris Ck and KC-07 in Figure 5.17 and Table 5.1), recent increases in permafrost temperature have been up to 0.9°C per decade, likely associated with the greater increases in surface air temperature in this region over the last decade when compared with the southern Mackenzie Valley (Wrigley, Norman Wells in Figure 5.17; Smith et al., 2017).

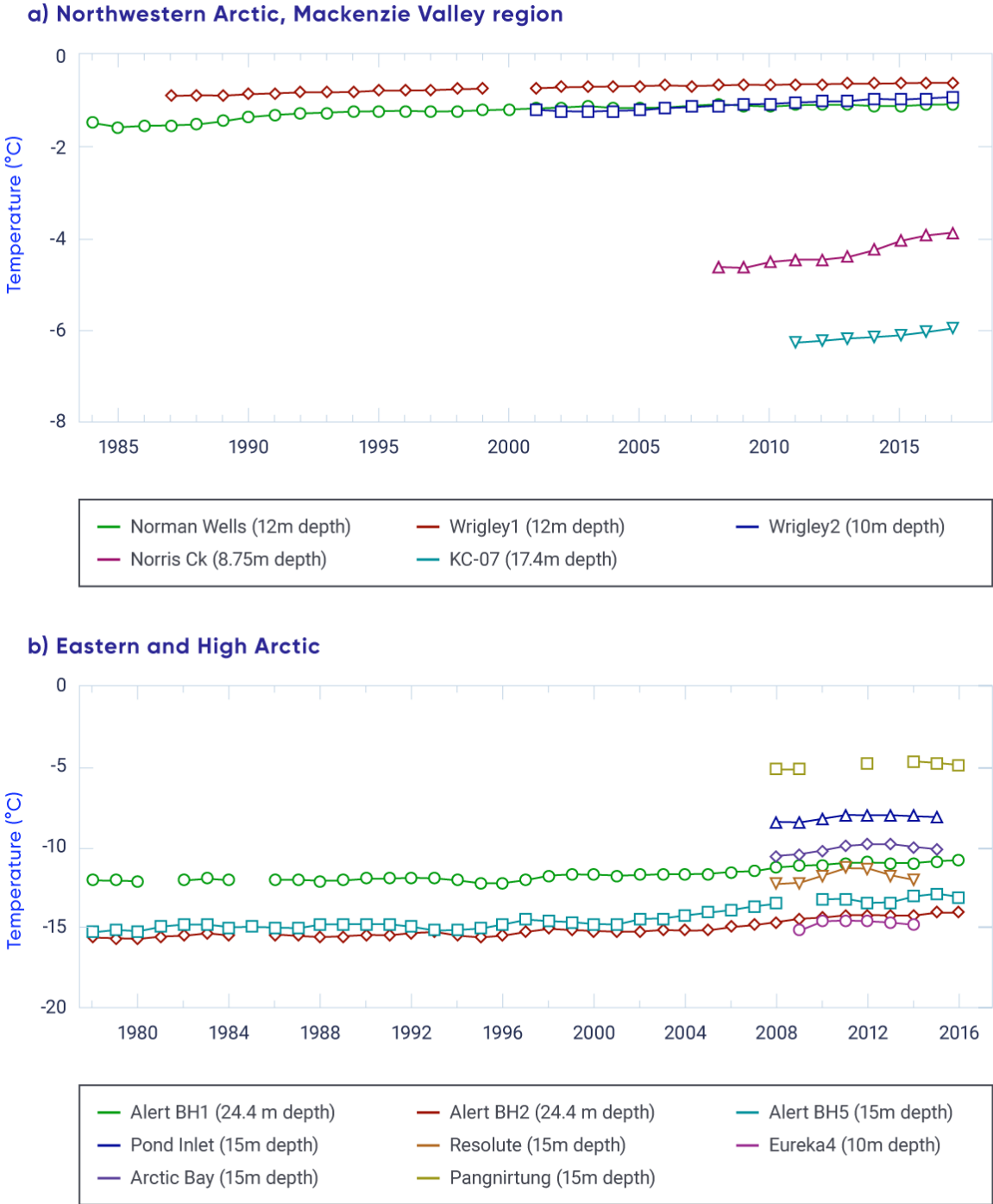


Figure 5.17: Trends in permafrost temperatures

Figure caption: Observed trends in permafrost temperatures for locations in the northwestern Arctic, Mackenzie Valley region (top) and eastern and high Arctic (bottom). Note that the range of the y-axis differs between graphs.

FIGURE SOURCE: BASED ON UPDATES FROM ROMANOVSKY ET AL., 2017B; EDNIE AND SMITH, 2015; SMITH ET AL., 2017.

Table 5.1: Changes in permafrost temperature for selected sites across northern Canada

Region	Sites	Increase per decade, °C	
		Entire record	Since 2000
Central Mackenzie Valley	Norman Wells, Wrigley	Up to 0.1	< 0.1 to 0.2
Northern Mackenzie	Norris Ck, KC-07	NA	0.5 to 0.9
Baffin Island	Pond, Arctic Bay, Pangnirtung	NA	0.5 to 0.7
High Arctic	Resolute, Eureka	NA	0.4 to 0.7
High Arctic	Alert	0.5 (15 m), 0.3 to 0.4 (24 m)	1.2 (15 m), 0.7 to 0.9 (24 m)
Northern Quebec (Nunavik)	Akulivik, Salluit, Quaqtaq, Puvirnituq, Tasiujaq, Umiujaq (11–20 m)	0.7 to 1.0	0.5 to 0.9

SOURCE: NORTHWEST TERRITORIES AND NUNAVUT UPDATED FROM ROMANOVSKY ET AL. (2017B); NORTHERN QUEBEC FROM ALLARD ET AL. (2016).

Since 2000, high Arctic permafrost temperatures have increased at higher rates than those observed in the sub-Arctic, ranging between 0.7°C and 0.9°C at 24 m depth and more than 1.0°C per decade at 15 m depth (see Table 5.1), consistent with greater increases in air temperature since 2000 (Smith et al., 2015a). Short records from sites in the Baffin region indicate warming at 10–15 m depth since 2000 (see Figure 5.17 and Table 5.1), but there has been a decline in permafrost temperatures since 2012 (Ednie and Smith, 2015) that likely reflects lower air temperatures in this region since 2010. In northern Quebec, where measurements at some sites began in the early 1990s, permafrost continues to warm at rates between 0.5°C to 1.0°C per decade (Smith et al., 2010; Allard et al., 2016). Permafrost can exist at high elevations in more southerly locations. Canada's most southerly occurrence of permafrost, at Mont Jacques-Cartier on the Gaspé Peninsula, shows an overall warming trend at 14 m depth of 0.2°C per decade since 1977 (Gray et al., 2017).



A network of thaw tubes throughout the Mackenzie Valley has provided information on trends in the active layer thickness (ALT) between 1991 and 2016 (see Figure 5.18; Smith et al., 2009). ALT exhibits greater variability among years than does deeper ground temperature, with higher values of ALT in extremely warm years such as 1998 (Duchesne et al., 2015). ALT generally increased between 1991 and 1998 but decreased over the following decade in response to lower annual air temperatures in the region. Since 2008, there has been a general increase in ALT in Mackenzie Valley, with peak values in 2012 (Duchesne et al., 2015; Smith et al., 2017). At sites where the permafrost is ice-rich, increases in summer thawing have been accompanied by significant settlement (subsidence) of the ground surface (Duchesne et al., 2015).

A number of recent studies provide other evidence of changing permafrost conditions. Observations of landscape change over time, often based on air photo or satellite imagery interpretation, have identified areas undergoing thermokarst processes, such as lake formation and collapse of peat plateaus and palsas (e.g., Olefeldt et al., 2016; Kokelj and Jorgenson, 2013). Over the last 50 years in northern Quebec, there has been a loss of permafrost mounds, collapse of lithalsas, and increases in the size of thermokarst ponds (Bouchard et al., 2014; Beck et al., 2015; Jolivel and Allard, 2017), while palsa decay has been observed in the Mackenzie mountains of the Northwest Territories (Mamet et al., 2017). A recent repeat of a 1964 survey of permafrost conditions along the Alaska Highway corridor between Whitehorse and Fort St. John indicated that permafrost continues to persist in organic-rich soils, but is no longer found at other sites (James et al., 2013). Changes in lake area in Old Crow Flats since 1951 have also been linked to thermokarst processes (Lantz and Turner, 2015). A recent intensification of thaw slumping may also be tied to changes in climate, including increases in precipitation (Kokelj et al., 2015, 2017a; Segal et al., 2016; Rudy et al., 2017). In the southern Northwest Territories, forest die-off has been attributed to permafrost thawing and ground subsidence (Sniderhan and Baltzer, 2016). Erosion of Arctic coasts in the form of retrogressive thaw slumps can result from a combination of mechanical (wave action) and thermal (warming permafrost) processes, potentially exacerbated by sea-level rise (see Chapter 7, Section 7.5; Ford et al., 2016; Lamoureux et al., 2015; Lantuit and Pollard, 2008).

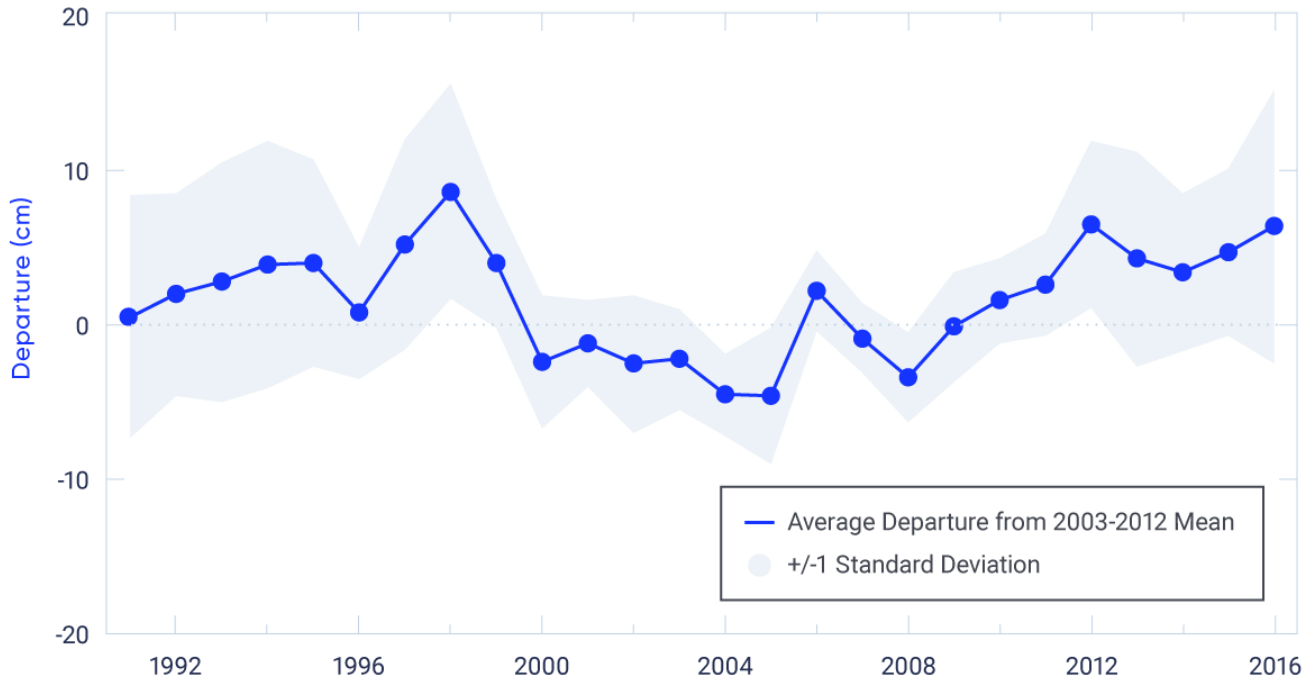


Figure 5.18: Active layer thickness departures, Mackenzie Valley, Northwest Territories, 1991–2016

Figure caption: Departures from the 2003–2012 mean (solid line) in measured active layer thickness (and standard deviation, shaded area) for 25 thaw tube sites in the Mackenzie Valley, Northwest Territories.

FIGURE SOURCE: UPDATED FROM DUCHESNE ET AL., 2015; SMITH ET AL., 2017

5.6.2: Projected changes in permafrost

Climate models project large increases in mean surface temperature (approximately 8°C) across present-day permafrost areas by the end of the 21st century under a high emission scenario (RCP8.5) (Koven et al., 2013) (see Chapter 3, Section 3.3.3). While this dramatic warming will no doubt affect permafrost temperatures and conditions (e.g., Slater and Lawrence, 2013; Guo and Wang, 2016; Chadburn et al., 2017), it is challenging to project associated reductions in permafrost extent from climate model simulations because of inadequate representation of soil properties (including ice content) and uncertainties in understanding the response of deep permafrost (which can exceed hundreds of metres below the surface). Simulations from a model considering deeper permafrost and driven by low and medium emission scenarios project that the area underlain by permafrost in Canada will decline by approximately 16%–20% by 2090, relative to a 1990 baseline (Zhang et al., 2008a). These declines are smaller than projections from other modelling studies that only examined near-surface ground temperature (Koven et al., 2013; Slater and Lawrence, 2013). These simulations also show that permafrost thaw would continue through the late 21st century, even if air temperatures stabilize by mid-century (Zhang et al., 2008b).

Other climate-related effects also influence the future response of permafrost to warming and complicate modelling of future conditions (e.g., Kokelj et al., 2017b; Romanovsky et al., 2017a). For example, intensification of rainfall appears to be strongly linked to thaw slumping (Kokelj et al., 2015). New shrub growth in the tundra can promote snow accumulation and lead to warmer winter ground conditions (Lantz et al., 2013). Thaw and collapse of peat plateaus and palsas into adjacent ponds increase overall permafrost degradation, and gullies that form because of degrading ice wedges can result in thermal erosion and further permafrost degradation (Mamet et al., 2017; Beck et al., 2015; Quinton and Baltzer, 2013; Godin et al., 2016; Perreault et al., 2017). Damage to vegetation and the organic layer due to wildfires (which are projected to occur more frequently under a warming climate) can lead to warming of the ground, increases in ALT, and degradation of permafrost (Smith et al., 2015c; Zhang et al., 2015; Fisher et al., 2016). Similarly, vegetation clearing and surface disturbance due to human activity and infrastructure construction can also lead to ground warming and thawing and enhance the effects of changing air temperatures on permafrost environments (Smith and Riseborough, 2010; Wolfe et al., 2015).

Section summary

In summary, a large proportion of the northern Canadian landscape has undergone, or will soon undergo, changes brought about by permafrost thaw. The temperature of permafrost is increasing across sub-Arctic and Arctic Canada, and the ALT has increased over the past decade in the Mackenzie Valley (*high confidence*). The rate of increase differs within and among regions due to variability in surface temperature changes, soil properties, and preceding temperature conditions. There is *high confidence* in these trends: they are derived from high-quality borehole measurements (permafrost temperature) and thaw tube networks (ALT), although the measurements are spatially sparse. The observed permafrost temperature and ALT changes are consistent with regional surface air temperature trends, but additional factors such as snow cover, vegetation changes, and disturbance can also modulate the response of permafrost to a changing climate. Ongoing landscape change across northern Canada associated with the expansion of thermokarst landforms was identified from surface observations and remote sensing. There is *medium confidence* in the assessment of thermokarst changes: they are associated with well-understood processes associated with the thaw of ice-rich permafrost, but region-specific rates of change are difficult to determine. Projected increases in mean air temperature over land underlain with permafrost under all emission scenarios will result in permafrost warming and thawing across large areas of Canada by the middle of the 21st century (*high confidence*), with impacts on northern infrastructure and the carbon cycle. This is the expected permafrost response to the high probability of increased surface temperature across Arctic land areas, with additional factors such as changes to snow cover, surface wetness, vegetation, and disturbance also influencing permafrost conditions. Confidence in projected permafrost changes from climate model simulations is affected by inadequate representation of soil properties (including ice content) and uncertainties in understanding the response of deep permafrost.

5.7: Discussion

This assessment of observed and projected changes to the Canadian cryosphere shows that the proportion of Canadian land and marine areas covered by seasonal snow, lake and river ice, and sea ice are decreasing over time; glaciers and ice caps are losing area and mass; and permafrost is warming and thawing. Further changes to the cryosphere are inevitable over the coming decades, driven by increasing air temperature. These changes will have major impacts on terrestrial, aquatic, and marine ecosystems, and on many sectors of the Canadian economy. Impacts will include risks to freshwater supply, from changes in peak pre-melt snow mass and the timing of snow melt across the country (Sturm et al., 2017; Fyfe et al., 2017) and from loss of glaciers in the Coastal Mountains and western Rockies. More precipitation falling as rain rather than snow, combined with earlier spring thaw, will result in earlier peak streamflows, with subsequent reduced summer and autumn flows. Determining the likely timing of summer sea ice-free conditions for Canadian regions (Laliberté et al., 2016) has important implications for marine shipping in the Arctic (Pizzolato et al., 2016). Lake and river ice conditions are important for overland transportation in the sub-Arctic and Arctic, both for goods transported via ice roads (Sturm et al., 2016; Furgal and Prowse, 2008) and for local access to the land (Tremblay et al., 2008). Thawing permafrost can release greenhouse gases (Olefeldt et al., 2016) and contaminants (Schuster et al., 2018), while permafrost degradation has effects on northern infrastructure, further adding to the high cost of northern development (AMAP, 2017b; Pendakur, 2017; Prowse et al., 2009).

There is a strong reliance on satellite remote sensing to provide spatially continuous and long time series of cryosphere data for climate analysis. While these data are subject to limitations, there would be essentially no monitoring capability for Canadian snow and ice (especially in the Arctic) without satellite data. Models are another important source of information, albeit limited by uncertainties in both model performance and the data used to drive the models. Glacier mass balance and permafrost changes are determined from observed measurements from a limited number of locations. While the individual measurements are high-quality, spatial coverage and representativeness is poor. Some variables are difficult to monitor at all. For example, alpine snow poses a unique challenge because the coarse resolution of snow mass data from satellites and global models and the sparse networks of surface observations do not capture land cover variability and steep topographic gradients in areas of complex terrain. Addressing these methodological challenges and information gaps, potentially through the use of regional climate model simulations (Wrzesien et al., 2018) is important because alpine regions are extremely sensitive to climate change and have a large impact on water resources (Fyfe et al., 2017; Berg and Hall, 2017; Sospedra-Alfonso et al., 2015). A second example is sea ice thickness in the Canadian Arctic, where surface observations are few and current satellite data are unable to provide estimates within the narrow channels and waterways of the CAA. Snow depth on sea ice influences how thick ice can grow, but measurements are currently limited to airborne surveys, with limited sampling over time periods and geographic areas.

Detection and attribution studies show that climate change induced by human activity has driven observed changes to the cryosphere. This includes the decline in Northern Hemisphere spring snow cover (Najafi et al., 2016), summer Arctic sea ice loss (Min et al., 2008; Kirchmeier-Young et al., 2017), and declines in land ice mass balance (Marzeion et al., 2014).



Projected changes to the cryosphere are closely tied to the amount of future warming (Thackeray et al., 2016; Mudryk et al., 2017; Notz and Stroeve, 2016). While continued temperature increases are *very likely*, there will be natural variability at the decadal scale. This suggests that the influence of natural climate variability on air temperature trends will modulate the response of components of the cryosphere across different regions of Canada over the coming decades. Regardless of this decadal-scale natural variability, the two key messages from this integrated assessment of historical observations and future climate model projections of the Canadian cryosphere are clear. The proportion of Canadian land and marine areas covered by snow and ice have decreased, and permafrost temperatures are rising. These observed changes to the cryosphere are *virtually certain* to continue over the coming century in response to long-term increases in surface air temperatures under all emission scenarios.

References

- Abdalati, W., Krabill, W., Frederick, E., Manizade, S., Martin, C., Sonntag, J., Swift, R., Thomas, R., Yungel, J. and Koerner, R. (2004): Elevation changes of ice caps in the Canadian Arctic Archipelago; *Journal of Geophysical Research*, v. 109. doi:10.1029/2003JF000045
- Agnew, T. and Howell, S. (2003): The use of operational ice charts for evaluating passive microwave ice concentration data; *Atmosphere-Ocean*, v. 41, p. 317–331. doi:10.3137/ao.410405
- Alexeev, V., Arp, C., Jones, B. and Cai, L. (2016): Arctic sea ice decline contributes to thinning lake ice trend in northern Alaska; *Environmental Research Letters*, v. 11. doi:10.1088/1748-9326/11/7/074022
- Allard, M., Sarrazin, D. and L'Hérault, E. (2016): Températures du sol dans des forages et près de la surface dans le nord-est du Canada, v. 1.4 (1988-2016); *Nordicana D8*. doi:10.5885/45291SL-34F28A9491014AFD
- AMAP [Arctic Monitoring and Assessment Programme] (2017a): Snow, Water, Ice and Permafrost in the Arctic (SWIPA) 2017; Arctic Monitoring and Assessment Programme (AMAP), Oslo, Norway; xiv + 269 p.
- AMAP [Arctic Monitoring and Assessment Programme] (2017b): Adaptation Actions for a Changing Arctic: Perspectives from the Bering-Chukchi-Beaufort Region; Arctic Monitoring and Assessment Programme (AMAP), Oslo, Norway; xiv + 255 p.
- Arp, C., Jones, B., Lu, Z. and Whitman, M. (2012): Shifting balance of thermokarst lake ice regimes across the Arctic Coastal Plain of northern Alaska; *Geophysical Research Letters*, v. 39, p. 1–5. doi:10.1029/2012GL052518
- Babb, D., Galley, R., Barber, D. and Rysgaard, S. (2016): Physical processes contributing to an ice free Beaufort Sea during September 2012; *Journal of Geophysical Research*, v. 121, p. 267–283. doi:10.1002/2015JC010756
- Bai, X., Wang, J., Austin, J., Schwab, D., Assel, R., Clites, A., Bratton, J., Colton, M., Lenters, J., Lofgren, B., Wohlleben, T., Helfrich, S., Vanderploeg, H., Luo, I. and Leshkevich, G. (2015): A record-breaking low ice cover over the Great Lakes during winter 2011/2012: Combined effects of a strong positive NAO and La Nina; *Climate Dynamics*, v. 44, p. 1187-1213. doi:10.1007/s00382-014-2225-2
- Barber, D.G., Meier, W.N., Gerland, S., Mundy, C.J., Holland, M., Kern, S., Li, Z., Michel, C., Perovich, D.K., Tamura, T., Berge, J., Bowman, J., Christiansen, J.S., Ehn, J.K., Ferguson, S., Granskog, M.A., Kikuchi, T., Kuosa, H., Light, B., Lundholm, N., Melnikov, I.A., Polashenski, C., Smedsrud, L.H., Spreen, G., Tschudi, M., Vihma, T., Webster, M. and Zhang, L. (2017): Arctic Sea Ice; in *Snow Water Ice and Permafrost in the Arctic (SWIPA) 2017 Assessment*, Arctic Monitoring and Assessment Programme, Oslo, Norway, p. 103–136.
- Barrand, N. and Sharp, M. (2010): Sustained rapid shrinkage of Yukon glaciers since the 1957/58 International Geophysical Year; *Geophysical Research Letters*, v. 37. doi:10.1029/2009GL042030



Barrand, N., Way, R., Bell, T. and Sharp, M. (2017): Recent changes in area and thickness of Torngat Mountain glaciers (northern Labrador, Canada); *The Cryosphere*, v. 11, p. 157–168. doi:10.5194/tc-11-157-2017

Bash, E. and Marshall, S. (2014): Estimation of glacial melt contributions to the Bow River, Alberta, Canada, using a radiation-temperature melt model; *Annals of Glaciology*, v. 55, issue 66, p. 138–152. doi:10.3189/2014AoG66A226

Beck, I., Ludwig, R., Bernier, M., Levesque, E. and Boike, J. (2015): Assessing permafrost degradation and land cover changes (1986–2009) using remote sensing data over Umiujaq, sub-Arctic Québec; *Permafrost and Periglacial Processes*, v. 26, p. 129–141. doi:10.1002/ppp.1839

Beedle, M., Menounos, B. and Wheate, R. (2015): Glacier change in the Cariboo Mountains, British Columbia, Canada (1952–2005); *The Cryosphere*, v. 9, p. 65–80. doi:10.5194/tc-9-65-2015

Beltaos, S. and Prowse, T. (2009): River-ice hydrology in a shrinking cryosphere; *Hydrological Processes*, v. 23, p. 122–144. doi:10.1002/hyp.7165

Berg, N. and Hall, A. (2017): Anthropogenic warming impacts on California snowpack during drought; *Geophysical Research Letters*, v. 44, p. 2511–2518. doi:10.1002/2016GL072104

Berthier, E., Vincent, C., Magnússon, E., Gunnlaugsson, Á., Pitte, P., Le Meur, E., Masiokas, M., Ruiz, L., Pálsson, F., Belart, J. and Wagnon, P. (2014): Glacier topography and elevation changes derived from Pléiades sub-meter stereo images; *The Cryosphere*, v. 8, p. 2275–2291. doi:10.5194/tc-8-2275-2014

Bouchard, F., Francus, P., Pientz, R., Laurion, I. and Feyte, S. (2014): Subarctic thermokarst ponds: Investigating recent landscape evolution and sediment dynamics in thawed permafrost of northern Québec (Canada); *Arctic, Antarctic, and Alpine Research*, v. 46, p. 251–271. doi:10.1657/1938-4246-46.1.251

Brown, R. and Braaten, R. (1998): Spatial and temporal variability of Canadian monthly snow depths, 1946–1995; *Atmosphere-Ocean*, v. 36, p. 37–45. doi:10.1080/07055900.1998.9649605

Brown, R. and Cote, P. (1992): Interannual variability of landfast ice thickness in the Canadian high Arctic, 1950–89; *Arctic*, v. 45, p. 273–284.

Brown, L. and Duguay, C. (2010): The response and role of ice cover in lake-climate interactions; *Progress in Physical Geography*, v. 34. doi:10.1177/0309133310375653

Brown, L. and Duguay, C. (2011): The fate of lake ice in the North American Arctic; *The Cryosphere*, v. 5, p. 869–892. doi:10.5194/tc-5-869-2011

Brown, R. and Mote, P. (2009): The response of Northern Hemisphere snow cover to a changing climate; *Journal of Climate*, v. 22, p. 2124–2145. doi:10.1175/2008JCLI2665.1

Brown, R., Barrette, C., Brown, L., Chaumont, D., Grenier, P., Howell, S. and Sharp, M. (2018): Climate variability, trends and projected change; in *From Science to Policy in the Eastern Canadian Arctic: An Integrated Regional Impact Study (IRIS) of Climate Change and Modernization*, (ed.)



- Bell, T., and Brown, T.M.; ArcticNet, Quebec City, Quebec, p. 57–93.
- Brown, R., Schuler, D., Bulygina, O., Derksen, C., Luoju, K., Mudryk, L., Wang, L. and Yang, D. (2017): Arctic terrestrial snow; in Snow Water Ice and Permafrost in the Arctic (SWIPA) 2017 Assessment, Arctic Monitoring and Assessment Programme, Oslo, Norway, p. 40.
- Brutel-Vuilmet, C., Ménégoz, M. and Krinner, G. (2013): An analysis of present and future seasonal Northern Hemisphere land snow cover simulated by CMIP5 coupled climate models; *The Cryosphere*, v. 7, p. 67–80. doi:10.5194/tc-7-67-2013
- Burgess, D. (2017): Mass balance of ice caps in the Queen Elizabeth Islands: 2014–2015; Geological Survey of Canada, Open File 8223, p. 36. doi:10.4095/300231
- Bush, E., Loder, J., James, T., Mortsch, L. and Cohen, S. (2014): An Overview of Canada's Changing Climate; in *Canada in a Changing Climate: Sector Perspectives on Impacts and Adaptation*, (ed.) F.J. Warren and D.S. Lemmen; Government of Canada, Ottawa, Ontario, p. 23–64.
- Canadian Ice Service (2007): Regional Charts: History, Accuracy, and Caveats, CIS Archive Documentation Series No. 1, Ottawa, Ontario, <http://ice.ec.gc.ca/IA_DOC/cisads_no_001_e.pdf> [July 2018].
- Chadburn, S., Burke, E., Cox, P., Friedlingstein, P., Hugelius, G. and Westermann, S. (2017): An observation-based constraint on permafrost loss as a function of global warming; *Nature Climate Change*, v. 7, p. 40–44. doi:10.1038/NCLIMATE3262
- Clarke, G., Jarosch, A., Anslow, F., Radić, V., & Menounos, B. (2015): Projected deglaciation of western Canada in the in the 21st century; *Nature Geoscience*, v. 8, p. 372–377. doi:10.1038/NGEO2407
- Comiso, J. (2012): Large decadal decline of the Arctic multiyear ice cover; *Journal of Climate*, v. 25, p. 1176–1193. doi:10.1175/JCLI-D-1100113.1
- Cooley, S. and Pavelsky, T. (2016): Spatial and temporal patterns in Arctic river ice breakup revealed by automated ice detection from MODIS imagery; *Remote Sensing of Environment*, v. 175, p. 310–322. doi:10.1016/j.rse.2016.01.004
- Dawson, J., Pizzolato, L., Howell, S., Copland L. and Johnston, M. (2018): Temporal and spatial patterns of ship traffic in the Canadian Arctic from 1990 to 2015; *Arctic*, v. 71, issue 7, p. 15–26. doi:10.14430/arctic4698
- Derksen, C., and Brown, R. (2012): Spring snow cover extent reductions in the 2008–2012 period exceeding climate model projections; *Geophysical Research Letters*, v. 39. doi:10.1029/2012GL053387
- Derksen, C., Brown, R., Mudryk, L. and Luoju, K. (2016): Terrestrial Snow (Arctic). In *State of the Climate in 2015*; *Bulletin of the American Meteorological Society*, v. 97, S145–S147.
- Derksen, C., Smith, S., Sharp, M., Brown, L., Howell, S., Copland, L., Mueller, D., Gauthier, Y., Fletcher, C., Tivy, A., Bernier, M., Bourgeois J., Brown, R., Burn, C., Duguay, C., Kushner, P., Langlois, A., Lewkowicz, A., Royer, A. and Walker, A. (2012): Variability and change in the Canadian Cryosphere; *Climatic Change*, v. 115, p. 59–88. doi:10.1007/s10584-012-0470-0



Deser, C., and Teng, H. (2008): Evolution of Arctic sea ice concentration trends and the role of atmospheric circulation forcing, 1979–2007; *Geophysical Research Letters*, v. 35. doi:10.1029/2007GL032023

Dibike, Y., Prowse, T., Bonsal, B., de Rham, L. and Saloranta, T. (2012): Simulation of North American lake-ice cover characteristics under contemporary and future climate conditions; *International Journal of Climatology*, v. 32, p. 695–709. doi:10.1002/joc.2300

Du, J., Kimball, J., Duguay, C., Kim, Y. and Watts, J. (2017): Satellite microwave assessment of Northern Hemisphere lake ice phenology from 2002 to 2015; *The Cryosphere*, v. 11, p. 47–63. doi:10.5194/tc-11-47-2017

Duchesne, C., Smith, S., Ednie, M. and Bonnaventure, P. (2015): Active layer variability and change in the Mackenzie Valley, Northwest Territories; in *GEOQuébec 2015, Proceedings, 68th Canadian Geotechnical Conference and 7th Canadian Conference on Permafrost*, Québec, Quebec.

Duguay, M. (2013): Permafrost changes along the Alaska Highway Corridor, Southern Yukon, from ground temperature measurements and DC electrical resistivity tomography; MSc Thesis, University of Ottawa, Ottawa, Ontario. doi:10.20381/ruor-3084

Duguay, C., Flato, G., Jeffries, M., Menard, P., Morris, K. and Rouse, W. (2003): Ice-cover variability on shallow lakes at high latitudes: Model simulations and observations; *Hydrological Processes*, v. 17, p. 3465–3483. doi:10.1002/hyp.1394

Duguay, C., Prowse, T., Bonsal, B., Brown, R. Lacroix, M. and Ménard, P. (2006): Recent trends in Canadian lake ice cover; *Hydrological Processes*, v. 20, p. 781-801. doi:10.1002/hyp.6131

Ednie, M. and Smith, S. (2015): Permafrost temperature data 2008–2014 from community-based monitoring sites in Nunavut; *Geological Survey of Canada, Open File 7784*. doi:10.4095/296705

Fisher, J., Estop-Aragones, C., Thierry, A., Charman, D., Wolfe S., Hartley I., Murton, J., Williams, M. and Phoenix, G. (2016): The influence of vegetation and soil characteristics on active-layer thickness of permafrost soils in boreal forest; *Global Change Biology*, v. 22, p. 3127–3140. doi:10.1111/gcb.13248

Ford, J., Bell, T. and Couture, N. (2016): Perspectives on Canada's North Coast region; in *Canada's Marine Coasts in a Changing Climate*, (ed.) Lemmen, D.S, Warren, F.J., James, T.S. and Mercer Clarke, C.S.L.; Government of Canada, Ottawa, Ontario, p. 153–206.

Furgal, C. and Prowse, T. (2008): Northern Canada; in *From impacts to adaptation: Canada in a changing climate 2007*, (ed.) Lemmen, D.S., Warren, F.J., Lacroix, J., Bush, E.; Government of Canada, Ottawa, Ontario, p. 57–118.

Fyfe, J., Derksen, C., Mudryk, L., Flato, G., Santer, B., Swart, N., Molotch, N., Zhang, X., Wan, H., Arora, V., Scinocca, J. and Jiao, Y. (2017): Large near-term projected snowpack loss over the western United States; *Nature Communications*, v. 8. doi:10.1038/NCOMMS14996

Fyfe, J.C., von Salzen, K., Gillett, N.P., Aurora, V.K., Flato, G.F and McConnell, J.R. (2013): One hundred years of Arctic surface temperature



variation due to anthropogenic influence. *Scientific Reports*, v. 3, article no. 2645. doi:10.1038/srep02645.

Galley, R., Babb, D., Ogi, M., Else, B., Geilfus, N.-X., Crabeck, O., Barber, D. and Rysgaard, S. (2016): Replacement of multiyear sea ice and changes in the open water season duration in the Beaufort Sea since 2004; *Journal of Geophysical Research*, v. 121, p. 1806–1823. doi:10.1002/2015JC011583

Gardner, A., Moholdt, G., Cogley, J., Wouters, B., Arendt, A., Wahr, J., Berthier, E., Hock, R., Pfeffer, W., Kaser, G., Ligtenberg, S., Bolch, T., Sharp, M., Hagen, J., Van Den Broeke, M. and Paul, F. (2013): A reconciled estimate of glacier contributions to sea level rise: 2003 to 2009; *Science*, v. 340, p. 852–857. doi:10.1126/science.1234532

Gardner, A., Moholdt, G., Wouters, B., Wolken, G., Burgess, D., Sharp, M., Cogley, G., Braun, C. and Labine, C. (2011): Sharply increased mass loss from glaciers and ice caps in the Canadian Arctic Archipelago. *Nature*, v. 473, p. 357–360. doi:10.1038/nature10089

Gilbert, A., Flowers, G., Miller, G., Rabus, B., van Wychen, W., Gardner, A. and Copland, L. (2016): Sensitivity of Barnes Ice Cap, Baffin Island, Canada, to climate state and internal dynamics; *Journal of Geophysical Research*, v. 121, p. 1516–1539. doi:10.1002/2016JF003839

Gillett, N., Stone, D., Stott, P., Nozawa, T., Karpechko, A., Hegerl, G., Wehner, M. and Jones, P. (2008): Attribution of polar warming to human influence; *Nature Geoscience*, v. 1, p. 750–754. doi:10.1038/ngeo338

Godin, E., Fortier, D. and Levesque, E. (2016): Nonlinear thermal and moisture response of ice-wedge polygons to permafrost disturbance increases heterogeneity of high Arctic wetland; *Biogeosciences*, v. 13, p. 1439–1452. doi:10.5194/bg-13-1439-2016

Gray, J., Davense, G., Fortier D. and Godin, E. (2017): The thermal regime of mountain permafrost at the summit of Mont Jacques-Cartier in the Gaspé Peninsula, Québec, Canada: A 37 year record of fluctuations showing an overall warming trend; *Permafrost and Periglacial Processes*, v. 28, p. 266–274. doi:10.1002/ppp.1903

Gray, L., Burgess, D., Copland, L., Dunse, T., Langley, K. and Schuler, T. (2015): Cryosat delivers monthly and inter-annual surface elevation change for Arctic ice caps; *The Cryosphere*, v. 9, p. 1895–1913. doi:10.5194/tc-9-1895-2015

Gray, L., Short, N., Mattar, K. and Jezek, K. (2001): Velocities and flux of the Filchner Ice Shelf and its tributaries determined from speckle tracking interferometry; *Canadian Journal of Remote Sensing*, v. 27, p. 193–206. doi:10.1080/07038992.2001.10854936

Greene, S., Walter Anthony, K., Archer, D., Sepulveda-Jauregui, A. and Martinez-Cruz, K. (2014): Modeling the impediment of methane ebullition bubbles by seasonal lake ice; *Biogeosciences*, v. 11, p. 6791–6811. doi:10.5194/bg-11-6791-2014

Griffiths, K., Michelutti, N., Sugar, M., Douglas, M. and Smol, J. (2017): Ice-cover is the principal driver of ecological change in High Arctic lakes and ponds; *PLoS ONE*, v. 12. doi:10.1371/journal.pone.0172989



- Gula, J. and Peltier, W. (2012): Dynamical downscaling over the Great Lakes basin of North America using the WRF regional climate model: the impact of the Great Lakes system on regional greenhouse warming; *Journal of Climate*, v. 25, p. 7723–7742. doi:10.1175/JCLI-D-00388.1
- Guo, D. and Wang, H. (2016): CMIP5 permafrost degradation projection: A comparison among different regions; *Journal of Geophysical Research*, v. 121, p. 4499–4517. doi:10.1002/2015JD024108
- Haas, C. and Howell, S. (2015): Ice thickness in the Northwest Passage; *Geophysical Research Letters*, v. 42, p. 7673–7680. doi:10.1002/2015GL065704
- Haas, C., Hendricks, S., Eicken, H. and Herber, A. (2010): Synoptic airborne thickness surveys reveal state of Arctic sea ice cover; *Geophysical Research Letters*, v. 37, issue 9. doi:10.1029/2010GL042652
- Harig, C. and Simons, F. (2016): Ice mass loss in Greenland, the Gulf of Alaska, and the Canadian Archipelago: Seasonal cycles and decadal trends; *Geophysical Research Letters*, v. 43. doi:10.1002/2016GL067759
- Hernández-Henríquez, M., Déry, S. and Derksen, C. (2015): Polar amplification and elevation-dependence in trends of Northern Hemisphere snow cover extent, 1971–2014; *Environmental Research Letters*, v. 10. doi:10.1088/1748-9326/10/4/044010
- Hochheim, K. and Barber, D. (2014): An update on the ice climatology of the Hudson Bay system; *Arctic Antarctic and Alpine Research*, v. 46, p. 66–83. doi:10.1657/1938-4246-46.1.66
- Howell, S., Brady, M., Derksen, C. and Kelly, R. (2016a): Recent changes in sea ice area flux through the Beaufort Sea during the summer; *Journal of Geophysical Research*, v. 121, p. 2659–2672. doi:10.1002/2015JC011464
- Howell, S., Brown, L., Kang, K. and Duguay, C. (2009): Variability in ice phenology on Great Bear Lake and Great Slave Lake, Northwest Territories Canada, from SeaWinds/QuikSCAT: 2000–2006; *Remote Sensing of Environment*, v. 113, p. 813–834. doi:10.1016/j.rse.2008.12.007
- Howell, S., Derksen, C., Pizzolato, L. and Brady, M. (2015): Multiyear ice replenishment in the Canadian Arctic Archipelago: 1997–2013; *Journal of Geophysical Research*, v. 120, p. 1623–1637. doi:10.1002/2015JC010696
- Howell, S., Duguay, C. and Markus, T. (2009a): Sea ice conditions and melt season duration variability within the Canadian Arctic Archipelago: 1979–2008; *Geophysical Research Letters*, v. 36. doi:10.1029/2009GL037681
- Howell, S., Laliberté, F., Kwok, R., Derksen, C. and King, J. (2016b): Landfast ice thickness in the Canadian Arctic Archipelago from Observations and Models; *The Cryosphere*, v. 10. doi:10.5194/tc-10-1463-2016
- Howell, S., Wohlleben, T., Komarov, A., Pizzolato, L. and Derksen, C. (2013): Recent extreme light years in the Canadian Arctic Archipelago: 2011 and 2012 eclipse 1998 and 2007; *The Cryosphere*, v. 7, p. 1753–1768. doi:10.5194/tc-7-1753-2013
- Hugelius, G., Strauss, J., Zubrzycki, S., Harden, J., Schuur, E., Ping, C-L., Schirmermeister, L., Grosse, G., Michaelson, G., Koven, C., O'Donnell, J., Elberling, B., Mishra, U., Camill, P., Yu, Z., Palmtag, J. and Kuhry, P. (2014):



Estimated stocks of circumpolar permafrost carbon with quantified uncertainty ranges and identified data gaps; *Biogeosciences*, v. 11, p. 6573–6593. doi:10.5194/bg-11-6573-2014

Jacob, T., Wahr, J., Pfeffer, W. and Swenson, W. (2012): Recent contributions of glaciers and ice caps to sea level rise; *Nature*, v. 482, p. 514–518. doi:10.1038/nature10847

Jahn, A. (2018): Reduced probability of ice-free summers for 1.5 °C compared to 2 °C warming; *Nature Climate Change*, v. 8, p. 409–413. doi:10.1038/s41558-018-0127-8

James, M., Lewkowicz, A., Smith, S. and Miceli, C. (2013): Multi-decadal degradation and persistence of permafrost in the Alaska Highway corridor, northwest Canada; *Environmental Research Letters*, v. 8. doi:10.1088/1748-9326/8/4/045013

Jolivel, M. and Allard, M. (2017): Impact of permafrost thaw on the turbidity regime of a subarctic river: the Sheldrake River, Nunavik, Quebec; *Arctic Science*, v. 3. p. 451–474. doi:10.1139/as-2016-0006

Jost, G., Moore, R., Menounos, B. and Wheate, R. (2012): Quantifying the contribution of glacier runoff to streamflow in the upper Columbia River Basin, Canada; *Hydrology and Earth System Sciences*, v. 16, p. 849–860. doi:10.5194/hess-16-849-2012

Kirchmeier-Young, M., Zwiers, F. and Gillett, N. (2017): Attribution of extreme events in Arctic sea ice extent; *Journal of Climate*, v. 30, p. 553–571. doi:10.1175/JCLI-D-16-0412.1

Koch, J., Clague, J. and Osborn, G. (2014): Alpine glaciers and permanent ice and snow patches in western Canada approach their smallest sizes since the mid-Holocene, consistent with global trends; *The Holocene*, v. 24, p. 1639–1648. doi:10.1177/0959683614551214

Koch, J., Menounos, B. and Clague, J. (2009): Glacier change in Garibaldi Provincial Park, southern Coast Mountains, British Columbia, since the Little Ice Age; *Global and Planetary Change*, v. 66, p. 161–178. doi:10.1016/j.gloplacha.2008.11.006

Koerner, R.M. (2005): Mass balance of glaciers in the Queen Elizabeth Islands, Nunavut, Canada; *Annals of Glaciology*, v. 42, p. 417–423. doi:10.3189/172756405781813122

Kokelj, S. and Jorgenson, M. (2013): Advances in thermokarst research; *Permafrost and Periglacial Processes*, v. 24, p. 108–119. doi:10.1002/ppp.1779

Kokelj, S., Lacelle, D., Lantz, T., Tunnicliffe, J., Malone, L., Clark, I. and Chin, K. (2013): Thawing of massive ground ice in mega slumps drives increases in stream sediment and solute flux across a range of watershed scales; *Journal of Geophysical Research*, v. 118, p. 681–692. doi:10.1002/jgrf.20063

Kokelj, S., Lantz, T., Tunnicliffe, J., Segal, R. and Lacelle, D. (2017a): Climate-driven thaw of permafrost preserved glacial landscapes, northwestern Canada; *Geology*, v. 45, p. 371–374. doi:10.1130/G38626.1

Kokelj, S., Palmer, M., Lantz, T. and Burn, C. (2017b): Ground temperatures



and permafrost warming from forest to tundra, Tuktoyaktuk Coastlands and Anderson Plain, NWT, Canada; *Permafrost and Periglacial Processes*, v. 28, p. 543–551. doi:10.1002/ppp.1934

Kokelj, S., Tunnicliffe, J., Lacelle, D., Lantz, T., Chin, K. and Fraser, R. (2015): Increased precipitation drives mega slump development and destabilization of ice-rich permafrost terrain, northwestern Canada; *Global and Planetary Change*, v. 129, p. 56–68. doi:10.1016/j.gloplacha.2015.02.008

Koven, C., Riley, W. and Stern, A. (2013): Analysis of permafrost thermal dynamics and response to climate change in the CMIP5 Earth system models; *Journal of Climate*, v. 26, p. 1877–1900. doi:10.1175/JCLI-D-12-00228.1

Krabill, W., Frederick, E., Manizade, S., Martin, C., Sonntag, J., Swift, R., Thomas, R., Wright, W., Yungel, J. and Abdalati, W. (2002): Aircraft laser altimetry measurements of changes of the Greenland ice sheet: Technique and accuracy assessment; *Journal of Geodynamics*, v. 34, p. 357–376. doi:10.1016/S0264-3707(02)00040-6

Krishfield, R., Proshutinsky, A., Tateyama, K., Williams, W., Carmack, E., McLaughlin, F. and Timmermans, M.-L. (2014): Deterioration of perennial sea ice in the Beaufort Gyre from 2003 to 2012 and its impact on the oceanic freshwater cycle; *Journal of Geophysical Research*, v. 119, p. 1271–1305. doi:10.1002/2013JC008999

Kwok, R. and Cunningham, G. (2010): Contribution of melt in the Beaufort Sea to the decline in Arctic multiyear sea ice coverage: 1993–2009; *Geophysical Research Letters*, v. 37. doi:10.1029/2010GL044678

Kwok, R. and Cunningham, G. (2015): Variability of Arctic sea ice thickness and volume from CryoSat-2; *Philosophical Transactions of the Royal Society A*, v. 373. doi:10.1098/rsta.2014.0157

Kwok, R. and Rothrock, D. (2009): Decline in Arctic sea ice thickness from submarine and ICESat records: 1958–2008; *Geophysical Research Letters*, v. 36. doi:10.1029/2009GL039035

Laliberté, F., Howell, S., and Kushner, P. (2016): Regional variability of a projected sea ice-free Arctic during the summer months; *Geophysical Research Letters*, v. 43. doi:10.1002/2015GL066855

Lamoureux, S., Forbes, D., Bell, T. and Manson, G. (2015): The impact of climate change on infrastructure in the western and central Canadian Arctic; in *From Science to Policy in the Western and Central Canadian Arctic: An Integrated Regional Impact Study (IRIS) of climate change and modernization*, (ed.) Stern, G.A., and Gaden, A.; ArcticNet, Quebec, p. 301–341.

Lantuit, H. and Pollard, W. (2008): Fifty years of coastal erosion and retrogressive thaw slump activity on Herschel Island, southern Beaufort Sea, Yukon Territory, Canada; *Geomorphology*, v. 95, p. 84–102. doi:10.1016/j.geomorph.2006.07.040

Lantz, T. and Turner, K. (2015): Changes in lake area in response to thermokarst processes and climate in Old Crow Flats, Yukon; *Journal of Geophysical Research*, v. 120, p. 513–524. doi:10.1002/2014JG002744



Lantz, T., Marsh, P. and Kokelj, S. (2013): Recent shrub proliferation in the Mackenzie Delta uplands and microclimatic implications; *Ecosystems*, v. 16, p. 47–59. doi:10.1007/s10021-012-9595-2

Laxon, S., Giles, K., Ridout, A., Wingham, D., Willatt, R., Cullen, R., Kwok, R., Schweiger, A., Zhang, J., Haas, C., Hendricks, S., Krishfield, R., Kurtz, N., Farrell, S. and Davidson, M. (2013): CryoSat-2 estimates of Arctic sea ice thickness and volume; *Geophysical Research Letters*, v. 40, p. 732–737. doi:10.1002/grl.50193

Lenaerts, J., van Angelen, J., van den Broeke, M., Gardner, A., Wouters, B. and van Meijgaard, E. (2013): Irreversible mass loss of Canadian Arctic Archipelago glaciers; *Geophysical Research Letters*, v. 40, p. 870–874. doi:10.1002/grl.50214

Loder, J., van der Baaren, A. and Yashayaev, I. (2015): Climate comparisons and change projections for the Northwest Atlantic from six CMIP5 models; *Atmosphere-Ocean*, v. 53, p. 529–555. doi:10.1080/07055900.2015.1087836

Mamet, S., Chun, K., Kershaw, G., Loranty, M. and Kershaw, G. (2017): Recent increases in permafrost thaw rates and areal loss of palsas in the western Northwest Territories, Canada; *Permafrost and Periglacial Processes*, v. 28, p. 619–633. doi:10.1002/ppp.1951

Mankin, J. and Diffenbaugh, N. (2014): Influence of temperature and precipitation variability on near-term snow trends; *Climate Dynamics*, v. 45, p. 1099–1116. doi:10.1007/s00382-014-2357-4

Marzeion, B., Cogley, J. G., Richter, K. and Parkes, D. (2014): Attribution of global glacier mass loss to anthropogenic and natural causes; *Science*, v. 345, p. 919–921. doi:10.1126/science.1254702

Marzeion, B., Jarosch, A., and Hofer, M. (2012): Past and future sea-level change from the surface mass balance of glaciers; *The Cryosphere*, v. 6, p. 1295–1322. doi:10.5194/tc-6-1295-2012

Maslanik, J., Stroeve, J., Fowler, C. and Emery, W. (2011): Distribution and trends in Arctic sea ice age through spring 2011; *Geophysical Research Letters*, v. 38. doi:10.1029/2011GL047735

Mason, L., Riseng, C., Gronewold, A., Rutherford, E., Wang, J., Clites, A., Smith, S. and McIntyre, P. (2016): Fine-scale spatial variation in ice cover and surface temperature trends across the surface of the Laurentian Great Lakes; *Climatic Change*, v. 138, p. 71–83. doi:10.1007/s10584-016-1721-2

Min, S.-K., Zhang, X., Zwiers, F. and Agnew, T. (2008): Human influence on Arctic sea ice detectable from early 1990s onwards; *Geophysical Research Letters*, v. 35. doi:10.1029/2008GL035725

Mortimer, C., Sharp, M. and Wouters, B. (2016): Glacier surface temperatures in the Canadian High Arctic, 2000–15; *Journal of Glaciology*, v. 62, p. 963–975. doi:10.1017/jog.2016.80

Mudryk, L., Derksen, C., Howell, S., Laliberté, F., Thackeray, C., Sospedra-Alfonso, R., Vionnet, V., Kushner, P. and Brown, R. (2018): Canadian snow and sea ice: historical trends and projections; *The Cryosphere*, v. 12, p. 1157–1176. doi:10.5194/tc-12-1157-2018



Mudryk, L., Derksen, C., Kushner, P. and Brown, R. (2015): Characterization of Northern Hemisphere snow water equivalent datasets, 1981–2010; *Journal of Climate*, v. 28, p. 8037–8051. doi:10.1175/JCLI-D-15-0229.1

Mudryk, L., Kushner, P., Derksen, C. and Thackeray, C. (2017): Snow cover response to temperature in observational and climate model ensembles; *Geophysical Research Letters*, v. 44. doi:10.1002/2016GL071789

Mueller, D., Copland, L. and Jeffries, M. (2017): Changes in Canadian Arctic ice shelf extent since 1906; in *Arctic Ice Shelves and Ice Islands*, (ed.) L. Copland and D. Mueller, Springer-Verlag.

Mueller, D., van Hove, P., Antoniadis, D., Jeffries, M. and Vincent, W. (2009): High Arctic lakes as sentinel ecosystems: Cascading regime shifts in climate, ice cover, and mixing; *Limnology and Oceanography*, v. 54, p. 2371–2385. doi:10.4319/lo.2009.54.6_part_2.2371

Mullan, D., Swindles, G., Patterson, T., Galloway, J., Macumber, A., Falck, H., Crossley, L., Chen, J. and Pisaric, M. (2017): Climate change and the long-term viability of the World's busiest heavy haul ice road; *Theoretical and Applied Climatology*, v. 129, p. 1089–1108. doi:10.1007/s00704-016-1830-x

Najafi, M., Zwiers, F. and Gillett, N. (2015): Attribution of Arctic temperature change to greenhouse-gas and aerosol influences; *Nature Climate Change*, v. 5, p. 246–249. doi:10.1038/nclimate2524

Najafi, M., Zwiers, F. and Gillett, N. (2016): Attribution of the spring snow cover extent decline in the Northern Hemisphere, Eurasia and North America to anthropogenic influence; *Climatic Change*, v. 136, p. 571–586. doi:10.1007/s10584-016-1632-2

NASEM [National Academies of Science, Engineering, and Medicine] (2016): Attribution of extreme weather events in the context of climate change; The National Academies Press, p. 186. doi:10.17226/21852

Naz, B., Frans, C., Clarke, G., Burns, P. and Lettenmaier, D. (2014): Modeling the effect of glacier recession on streamflow response using a coupled glacio-hydrological model; *Hydrology and Earth System Sciences*, v. 18, p. 787–802. doi:10.5194/hess-18-787-2014

Neumann, N., Smith, C., Derksen, C. and Goodison, B. (2006): Characterizing local scale snow cover using point measurements; *Atmosphere-Ocean*, v. 44 p. 257–269. doi:10.3137/ao.440304

Noël, B., van de Berg, W., Lhermitte, S., Wouters, B., Schaffer, N. and van den Broeke, M. (2018): Six decades of glacial mass loss in the Canadian Arctic Archipelago; *Journal of Geophysical Research*, v. 123. doi:10.1029/2017JF004304

Notz, D. and Stroeve, J. (2016): Observed Arctic sea-ice loss directly follows anthropogenic CO₂ emission; *Science*, v. 354. doi:10.1126/science.aag2345

Olefeldt, D., Goswami, S., Grosse, G., Hayes, D., Hugelius, G., Kuhry, P., McGuire, A., Romanovsky, V., Sannel, A., Schuur, E. and Turetsky, M. (2016): Circumpolar distribution and carbon storage of thermokarst landscapes; *Nature Communications*, v. 7, p. 1–11. doi:10.1038/ncomms13043



- Paquette, M., Fortier, D., Mueller, D., Sarrazin, D. and Vincent, W. (2015): Rapid disappearance of perennial ice on Canada's most northern lake; *Geophysical Research Letters*, v. 42, p. 1433–1440. doi:10.1002/2014GL062960
- Parkinson, C. (2014): Spatially mapped reductions in the length of the Arctic sea ice season; *Geophysical Research Letters*, v. 41, p. 4316–4322. doi:10.1002/2014GL060434
- Pendakur, K. (2017): Northern Territories; in *Climate risks and adaptation practices for the Canadian transportation sector 2016*; (ed.) Palko, K. and Lemmen, D.S.; Government of Canada, Ottawa, Ontario, p. 27–64.
- Peng, G. and Meier, W. (2017): Temporal and regional variability of Arctic sea-ice coverage from satellite data; *Annals of Glaciology*, v. 59, p. 191–200. doi:10.1017/aog.2017.32
- Perrault, N., Levesque, E., Fortier, D., Gratton, D. and Lamarque, L. (2017): Remote sensing evaluation of High Arctic wetland depletion following permafrost disturbance by thermo-erosion gully processes; *Arctic Science*, v. 3, p. 237–253. doi:10.1139/as-2016-0047
- Perrin, A., Dion, J., Eng, S., Sawyer, D., Nodleman, J., Comer, N., Auld, H., Sparling, E., Harris, M., Nodelman, J. and Kinnear, L. (2015): Economic implications of climate change adaptations for mine access roads in northern Canada. *Northern Climate ExChange*, Yukon Research Centre, Yukon College, p. 93.
- Peterson, I., Pettipas, R. and Rosing-Asvid, A. (2015): Trends and variability in sea ice and icebergs off the Canadian East Coast; *Atmosphere-Ocean*, v. 53, p. 582–594. doi:10.1080/07055900.2015.1057684
- Pizzolato, L., Howell, S., Dawson, J., Laliberté, F. and Copland, L. (2016): The influence of declining sea ice on shipping activity in the Canadian Arctic; *Geophysical Research Letters*, v. 43. doi:10.1002/2016GL071489
- Prowse, T. (2012): Lake and River ice in Canada; in *Changing Cold Environments: A Canadian Perspective*, 1st edition, (eds.) H. French, and O. Slaymaker, John Wiley & Sons, p. 163–181.
- Prowse, T., Furgal, C., Chouinard, R., Melling, H., Milburn, D. and Smith, S. (2009): Implications of climate change for economic development in Northern Canada: energy, resource, and transportation sectors; *Ambio*, v. 38, p. 272–281. doi:10.1479/0044-7447-38.5.272
- Prowse, T., Shrestha, R., Bonsal, B. and Dibike, Y. (2010): Changing spring air-temperature gradients along large northern rivers: Implications for severity of river-ice floods; *Geophysical Research Letters*, v. 37. doi:10.1029/2010GL044878
- Quinton, W., and Baltzer, J. (2013): The active-layer hydrology of a peat plateau with thawing permafrost (Scotty Creek, Canada); *Hydrogeology Journal*, v. 21, p. 201–220. doi: 10.1007/s10040-012-0935-2
- Radić, V., and Hock, R. (2011): Regionally differentiated contribution of mountain glaciers and ice caps to future sea-level rise; *Nature Geoscience*, v. 4, p. 91–94. doi:10.1038/ngeo1052
- Radić, V., Bliss, A., Beedlow, A., Hock, R., Miles, E. and Cogley, J.G. (2014):



Regional and global projections of twenty-first century glacier mass changes in response to climate scenarios from global climate models; *Climate Dynamics*, v. 42, p. 37–58. doi:10.1007/s00382-013-1719-7

Raisanen, J. (2008): Warmer climate: less or more snow?; *Climate Dynamics*, v. 30, p. 307–319. doi: 10.1007/s00382-007-0289-y

Richter-Menge, J. and Farrell, S. (2013): Arctic sea ice conditions in spring 2009–2013 prior to melt; *Geophysical Research Letters*, v. 40, p. 5888–5893. doi:10.1002/2013GL058011

Rigor, I., Wallace, J. and Colony, R. (2002): Response of sea ice to the Arctic oscillation; *Journal of Climate*, v. 15, p. 2648–2663. doi: 10.1175/1520-0442(2002)015%3C2648:ROSITT%3E2.0.CO;2

Romanovsky, V., Isaksen, K., Drozdov, D., Anisimov, O., Instanes, A., Leibman, M., McGuire, A., Shiklomanov, N., Smith, S., and Walker, D. (2017a): Changing permafrost and its impacts; in *Snow Water Ice and Permafrost in the Arctic (SWIPA) 2017; Assessment, Arctic Monitoring and Assessment Programme*, Oslo, Norway, p. 65–102.

Romanovsky, V., Smith, S. and Christiansen, H. (2010): Permafrost thermal state in the polar Northern Hemisphere during the International Polar Year 2007-2009: a synthesis; *Permafrost and Periglacial Processes*, v. 21, p. 106–116. doi:10.1002/ppp.689

Romanovsky, V., Smith, S., Isaksen, K., Shiklomanov, N., Streletskiy, D., Kholodov, A., Christiansen, H., Drozdov, D., Malkova, G. and Marchenko, S. (2017b): Terrestrial Permafrost; in *Arctic Report Card 2017*, (ed.) J. Richter-Menge, J.E. Overland, J.T. Mathis, and E. Osborne <<http://www.arctic.noaa.gov/Report-Card>> [July 2018].

Rouse, W., Oswald, C., Binyamin, J., Spence, C., Schertzer, W., Blanken, P., Bussieres, N. and Duguay, C. (2005): The role of northern lakes in a regional energy balance; *Journal of Hydrometeorology*, v. 6, p. 291–305.

Rudy, A., Lamoureux, S., Kokelj, S., Smith, I. and England, J. (2017): Accelerating thermokarst transforms ice-cored terrain triggering a downstream cascade to the ocean; *Geophysical Research Letters*, v. 47. doi:10.1002/2017GL074912

Schuster, P., Schaefer, K., Aiken, G., Antweiler, R., Dewild J., Gryziec, J., Gusmeroli, A., Hugelius, G., Jafarov, E., Krabbenhoft, D., Liu, L., Herman-Mercer, N., Mu, C., Roth, D., Schaefer, T., Striegl, R., Wickland, K. and Zhang, T. (2018): Permafrost stores a globally significant amount of mercury; *Geophysical Research Letters*, v. 45, p. 1463–1471. doi:10.1002/2017GL075571

Segal, R., Lantz, T. and Kokelj, S. (2016): Acceleration of thaw slump activity in glaciated landscapes of the Western Canadian Arctic; *Environmental Research Letters*, v. 11. doi:10.1088/1748-9326/11/3/034025

Serreze, M., Holland, M. and Stroeve, J. (2007): Perspectives on the Arctic's shrinking sea ice cover; *Science*, v. 315, p. 1533–1536.

Serreze, M., Raup, B., Braun, C., Hardy, D. and Bradley, R. (2017): Rapid wastage of the Hazen Plateau ice caps, northeastern Ellesmere Island, Nunavut, Canada; *The Cryosphere*, v. 11, p. 169–177. doi:10.5194/tc-11-169-2017



Sharp, M., Burgess, D., Cawkwell, F., Copland, L., Davis, J., Dowdeswell, E., Dowdeswell, J., Gardner, A., Mair, D., Wang, L., Williamson, S., Wolken, G. and Wyatt, F. (2016): Remote sensing of recent glacier changes in the Canadian Arctic; in *Global Land Ice Measurements from Space*, (ed.) J. Kargel, G. Leonard, M. Bishop, A. Kääb, and B. Raup; Springer, p. 205–227. doi: 10.1007/978-3-540-79818-7doi

Sharp, M., Burgess, D., Cogley, J. G., Ecclestone, M., Labine, C. and Wolken, G. (2011): Extreme melt on Canada's Arctic ice caps in the 21st century; *Geophysical Research Letters*, v. 38, p. 3–7. doi:10.1029/2011GL047381

Shepard, A., Ivins, E., Geruo, A., Barletta, V., Bentley, M., Bettadpur, S., Briggs, K., Bromwich, D., Forsberg, R., Galin, N., Horwath, M., Jacobs, S., Joughin, I., King, M., Lenaerts, J., Li, J., Ligtenberg, S., Luckman, A., Luthcke, S., McMillan, M., Meister, R., Milne, G., Mouginot, J., Muir, A., Nicolas, J., Paden, J., Payne, A., Pritchard, H., Rignot, E., Rott, H., Sørensen, L., Scambos, T., Scheuchl, B., Schrama, E., Smith, B., Sundal, A., Van Angelen, J., Van De Berg, W., Van Den Broeke, M., Vaughan, D., Velicogna, I., Wahr, J., Whitehouse, P., Wingham, D., Yi, D., Young, D. and Zwally, H. (2012): A reconciled estimate of ice-sheet mass balance; *Science*, v. 338, p. 1183–1189.

Sigmond, M., Fyfe, J. and Swart, N. (2018): Ice-free Arctic projections under the Paris Agreement; *Nature Climate Change*, v. 8, p. 404–408. doi:10.1038/s41558-018-0124-y

Slater, A. and Lawrence, D. (2013): Diagnosing present and future permafrost from climate models; *Journal of Climate*, v. 26, p. 5608–5623. doi:10.1175/JCLI-D-12-00341.1

Smith, S. and Riseborough, D. (2010): Modelling the thermal response of permafrost terrain to right-of-way disturbance and climate warming; *Cold Regions Science and Technology*, v. 60, p. 92–103.

Smith, S., Chartrand, J., Duchesne, C. and Ednie, M. (2017): Report on 2016 field activities and collection of ground thermal and active layer data in the Mackenzie Corridor, Northwest Territories; Geological Survey of Canada, Open File 8303. doi:10.4095/306212

Smith, S., Lewkowicz, A., Duchesne, C. and Ednie, M. (2015a): Variability and change in permafrost thermal state in northern Canada; Paper 237 in *GEOQuébec 2015, Proceedings, 68th Canadian Geotechnical Conference and 7th Canadian Conference on Permafrost*, Québec, Quebec.

Smith, S., Lewkowicz, A., Ednie, M., Duguay, M. and Bevington, A. (2015b): A characterization of permafrost thermal state in the southern Yukon; Paper 331, in *GEOQuébec 2015, Proceedings, 68th Canadian Geotechnical Conference and 7th Canadian Conference on Permafrost*, Québec, Quebec.

Smith, S., Riseborough, D. and Bonnaventure, P. (2015c): Eighteen year record of forest fire effects on ground thermal regimes and permafrost in the central Mackenzie Valley, NWT, Canada; *Permafrost and Periglacial Processes*, v. 26, p. 289–303. doi:10.1002/ppp.1849

Smith, S., Romanovsky, V., Lewkowicz, A., Burn, C., Allard, M., Clow, G., Yoshikawa, K., and Throop, J. (2010): Thermal state of permafrost in North



America - A contribution to the International Polar Year; Permafrost and Periglacial Processes, v. 21, p. 117–135. doi:10.1002/ppp.690

Smith, S., Wolfe, ST., Riseborough, D. and Nixon, F. (2009): Active-layer characteristics and summer climatic indices, Mackenzie Valley, Northwest Territories, Canada; Permafrost and Periglacial Processes, v. 20, p. 201–220.

Sniderhan, A. and Baltzer, J. (2016): Growth dynamics of black spruce (*Picea mariana*) in a rapidly thawing discontinuous permafrost peatland; Journal of Geophysical Research, v. 121, p. 2988–3000. doi:10.1002/2016JG003528

Sospedra-Alfonso, R. and Merryfield, W. (2017): Influences of temperature and precipitation on historical and future snowpack variability over the Northern Hemisphere in the Second Generation Canadian Earth System Model; Journal of Climate, v. 30, p. 4633–4656. doi:10.1175/JCLI-D-16-0612.1

Sospedra-Alfonso, R., Melton, J. and Merryfield, W. (2015): Effects of temperature and precipitation on snowpack variability in the Central Rocky Mountains as a function of elevation; Geophysical Research Letters, v. 42, p. 4429–4438. doi:10.1002/2015GL063898

Stroeve, J., Markus, T., Boisvert, L., Miller, J. and Barrett, A. (2014): Changes in Arctic melt season and implications for sea ice loss; Geophysical Research Letters, v. 41, p. 1216–1225. doi:10.1002/2013GL058951

Stroeve, J., Serreze, M., Kay, J., Holland, M., Meier, W. and Barrett, A. (2012): The Arctic's rapidly shrinking sea ice cover: A research synthesis; Climatic Change, v. 110, p. 1005–1027. doi:10.1007/s10584-011-0101-1

Strozzi, T., Kouraev, A., Wiesmann, A., Wegmüller, U., Sharov, A. and Werner, C. (2008): Estimation of Arctic glacier motion with satellite L-band SAR data; Remote Sensing of Environment, v. 112, p. 636–645. doi:10.1016/j.rse.2007.06.007

Sturm, M., Goldstein, M., Huntington, H. and Douglas, T. (2016): Using an option pricing approach to evaluate strategic decisions in a rapidly changing climate: Black–Scholes and climate change; Climatic Change, v. 140, p. 437–449. doi:10.1007/s10584-016-1860-5

Sturm, M., Goldstein, M. and Parr, C. (2017): Water and life from snow: A trillion-dollar science question; Water Resources Research, v. 53, p. 3534–3544. doi:10.1002/2017WR020840

Surdu, C., Duguay, C., Brown, L. and Fernández Prieto, D. (2014): Response of ice cover on shallow lakes of the North Slope of Alaska to contemporary climate conditions (1950–2011): Radar remote-sensing and numerical modeling data analysis; The Cryosphere, v. 8, p. 167–180. doi:10.5194/tc-8-167-2014

Surdu, C., Duguay, C. and Fernández Prieto, D. (2016): Evidence of recent changes in the ice regime of high arctic lakes from spaceborne satellite observations; The Cryosphere, v. 10, p. 941–960. doi:10.5194/tc-10-941-2016

Tan, Z. and Zhuang, Q. (2015): Arctic lakes are continuous methane sources to the atmosphere under warming conditions; Environmental



Research Letters, v. 10, p. 1–9. doi:10.1088/1748-9326/10/5/054016

Tandon, N., Kushner, P., Docquier, D., Wettstein, J. and Li, C. (2018): Reassessing sea ice drift and its relationship to long term Arctic sea ice loss in coupled climate models; *Journal of Geophysical Research*. doi:10.1029/2017JC013697

Tennant, C. and Menounos, B. (2013): Glacier change of the Columbia Icefield, Canadian Rocky Mountains, 1919–2009; *Journal of Glaciology*, v. 59, p. 671–686. doi:10.3189/2013JoG12J135

Tennant, C., Menounos, B., Wheate, R. and Clague, J. (2012): Area change of glaciers in the Canadian Rocky Mountains, 1919 to 2006; *The Cryosphere*, v. 6, p. 1541–1552. doi:10.5194/tc-6-1541-2012

Thackeray, C., Fletcher, C., Mudryk, L. and Derksen, C. (2016): Quantifying the uncertainty in historical and future simulations of Northern Hemisphere spring snow cover; *Journal of Climate*, v. 29, p. 8647–8663. doi:10.1175/JCLI-D-16-0341.1

Thienpont, J., Kokelj, S., Korosi, J., Cheng, E., Desjardins, C., Kimpe, L., Blais, J., Pisaric, M. and Smol, J. (2013): Exploratory hydrocarbon drilling impacts to Arctic lake ecosystems; *PLoS ONE*, v. 8. doi:10.1371/journal.pone.0078875

Tilling, R., Ridout, A., Shepherd, A. and Wingham, D. (2015): Increased Arctic sea ice volume after anomalously low melting in 2013; *Nature Geoscience*, v. 8, p. 643–646. doi:10.1038/ngeo2489

Tivy, A., Howell, S., Alt, B., McCourt, S., Chagnon, R., Crocker, G., Carrieres, T. and Yackel, J. (2011a): Trends and variability in summer sea ice cover in the Canadian Arctic based on the Canadian Ice Service Digital Archive, 1960–2008 and 1968–2008; *Journal of Geophysical Research*, v. 116. doi:10.1029/2009JC005855

Tivy A, Howell, S., Alt, B., Yackel, J. and Carrieres, T. (2011b): Origins and levels of seasonal forecast skill for sea ice in Hudson Bay using canonical correlation analysis; *Journal of Climate*, v. 24. doi:10.1175/2010JCLI3527.1

Tremblay, M., Furgal, C., Larrivee, C., Annanack, T., Tookalook, P., Qiisik, M., Angiyou, E., Swappie, N., Savard, J. and Barrett, M. (2008): Climate change in Northern Quebec: Adaptation strategies from community-based research; *Arctic*, v. 61, p. 27–34.

Tucker III, W. Weatherly, J., Eppler, D., Farmer, L. and Bentley, D. (2001): Evidence for rapid thinning of sea ice in the western Arctic Ocean at the end of the 1980s; *Geophysical Research Letters*, v. 28, p. 2851–2854. doi:10.1029/2001GL012967

Van Wychen, W., J. Davis, D. O. Burgess, L. Copland, L. Gray, M. Sharp, and C. Mortimer (2016), Characterizing interannual variability of glacier dynamics and dynamic discharge (1999–2015) for the ice masses of Ellesmere and Axel Heiberg Islands, Nunavut, Canada, *J. Geophys. Res. Earth Surf.*, 121, 39–63, doi:10.1002/2015JF003708.



Vaughan, D., Comiso, J., Allison, I., Carrasco, J., Kaser, G., Kwok, R., Mote, P., Murray, T., Paul, F., Ren, J., Rignot, E., Solomina, O., Steffen, K. and Zhang, T. (2013): Observations: Cryosphere; in *Climate Change 2013: The Physical Science Basis (Contribution of Working Group I to the Fifth Assessment Report of the Intergovernmental Panel on Climate Change)*; (ed.) T. Stocker, D. Qin, G.-K. Plattner, M. Tignor, S. Allen, J. Boschung, A. Nauels, Y. Xia, V. Bex and P. Midgley, Cambridge University Press, Cambridge, United Kingdom and New York, NY, USA, p. 317–382. doi:10.1017/CBO9781107415324.012

Veillette, J., Martineau, M., Antoniades, D., Sarrazin, D. and Vincent, W. (2010): Effects of loss of perennial lake ice on mixing and phytoplankton dynamics: Insights from High Arctic Canada; *Annals of Glaciology*, v. 51, p. 56–70. doi: 10.3189/172756411795931921

Vincent, L., Zhang, X., Brown, R., Feng, Y., Mekis, E., Milewska, E., Wan, H. and Wang, X. (2015): Observed trends in Canada's climate and influence of low-frequency variability modes; *Journal of Climate*, v. 28, p. 4545–4560. doi: 10.1175/JCLI-D-14-00697.1

Walsh, J., Fetterer, F., Stewart, J. and Chapman, W. (2017): A database for depicting Arctic sea ice variations back to 1850; *Geographical Review*, v. 107, p. 89–107. doi: 10.1111/j.1931-0846.2016.12195.x

Wang, J., Bai, X., Hu, H., Clites, A., Colton, M., and Lofgren, B. (2012): Temporal and spatial variability of Great Lakes ice cover, 1973–2010; *Journal of Climate*, v. 25, p. 1318–1329. Doi: 10.1175/2011JCLI4066.1

Wang, L., Sharp, M., Rivard, B., Marshall, S. and Burgess, D. (2005): Melt season duration on Canadian Arctic ice caps, 2000–2004; *Geophysical Research Letters*, v. 32. doi:10.1029/2005GL023962

Wang, M. and Overland, J. (2012): A sea ice free summer Arctic within 30 years: An update from CMIP5 models; *Geophysical Research Letters*, v. 39. doi:10.1029/2012GL052868

Wolfe, S., Morse, P., Hoeve, T., Sladen, W., Kokelj, S., and Arenson, L. (2015): Disequilibrium permafrost conditions on NWT Highway 3; Paper 115 in *GEOQuébec 2015, Proceedings, 68th Canadian Geotechnical Conference and 7th Canadian Conference on Permafrost*, Québec, Québec.

Wolken, G., Sharp, M., Andreassen, L.-M., Burgess, D., Copland, L., Kohler, J., O'Neel, S., Pelto, M., Thomson, L. and Wouters, B. (2017): Glaciers and Ice Caps Outside Greenland; Section F of Chapter 5: The Arctic, in *State of the Climate in 2016*, (ed.) Blunden, J. and Arndt, D.S.; *Bulletin of the American Meteorological Society* v. 98, p. 140–145.

Wrzesien, M., Durand, M., Pavelsky, T., Kapnick, S., Zhang, Y., Guo, J. and Shum, C. K. (2018): A new estimate of North American mountain snow accumulation from regional climate model simulations; *Geophysical Research Letters*, v. 45, p. 1423–1432. doi: 10.1002/2017GL076664

Zemp, M., Frey, H., Gärtner-Roer, I., Nussbaumer, S., Hoelzle, M., Paul, F., Haerberli, W., Denzinger, F., Ahlström, A., Anderson, B., Bajracharya, S., Baroni, C., Braun, L., Càceres, B., Casassa, G., Cobos, G., Dàvila, L., Delgado Granados, H., Demuth, M., Espizua, L., Fischer, A., Fujita, K., Gadek, B., Ghazanfar, A., Hagen, J., Holmlund, P., Karimi, N., Li, Z., Pelto, M., Pitte, P., Popovnin, V., Portocarrero, C., Prinz, R., Sangewar, C., Severskiy, I.,



Sigurdsson, O., Soruco, A., Usubaliev, R., Vincent, C. (2015): Historically unprecedented global glacier changes in the early 21st century; *Journal of Glaciology*, v. 61, p. 745–762. doi:10.3189/2015JoG15J017

Zhang, R. and Knutson, T. (2013): The role of global climate change in the extreme low summer Arctic sea ice extent in 2012; in *Explaining Extreme Events of 2012 from a Climate Perspective*, (ed.) T.C. Peterson, M.P. Hoerling, P.A. Stott, and S.C. Herring; *Bulletin of the American Meteorological Society*, v. 94, p. S23–S26.

Zhang, Y., Chen, W. and Riseborough, D. (2008a): Transient projections of permafrost distribution in Canada during the 21st century under scenarios of climate change; *Global and Planetary Change*, v. 60, p. 443–456.

Zhang, Y., Chen, W. and Riseborough, D. (2008b): Disequilibrium response of permafrost thaw to climate warming in Canada over 1850–2100; *Geophysical Research Letters*, v. 35. doi:10.1029/2007GL032117

Zhang, Y., Wolfe, S., Morse, P., Olthof, I. and Fraser, R. (2015): Spatiotemporal impacts of wildfire and climate warming on permafrost across a subarctic region, Canada; *Journal of Geophysical Research*, v. 120, p. 2338–2356. doi: 10.1002/2015JF003679

Zhong, Y., Notaro, M., Vavrus, S. and Foster, M. (2016): Recent accelerated warming of the Laurentian Great Lakes: Physical drivers; *Limnology and Oceanography*, v. 61, p. 1762–1786. doi:10.1002/lno.10331





CHAPTER 6

**Changes in
Freshwater
Availability
Across Canada**

CANADA'S CHANGING CLIMATE REPORT



Government
of Canada

Gouvernement
du Canada

Canada



Authors

Barrie R. Bonsal, Environment and Climate Change Canada

Daniel L. Peters, Environment and Climate Change Canada

Frank Seglenieks, Environment and Climate Change Canada

Alfonso Rivera, Natural Resources Canada

Aaron Berg, University of Guelph

Acknowledgement

Hayley O'Neil, University of Victoria

Recommended citation: Bonsal, B.R., Peters, D.L., Seglenieks, F., Rivera, A., and Berg, A. (2019): Changes in freshwater availability across Canada; Chapter 6 in Canada's Changing Climate Report, (ed.) E. Bush and D.S. Lemmen; Government of Canada, Ottawa, Ontario, p. 261–342.



Chapter Table Of Contents

SUMMARY

6.1: Introduction

6.2: Surface runoff: streamflow

Box 6.1: Canada's hydrometric network

6.2.1: Streamflow magnitude

6.2.2: Streamflow timing

6.2.3: Streamflow regime

Box 6.2: Streamflow regimes

6.2.4: Streamflow-related floods

FAQ 6.1: Will there be more droughts and floods in Canada in a warmer climate?

6.3: Surface water levels: lakes and wetlands

6.3.1: Laurentian Great Lakes

6.3.2: Other lakes

6.3.3: Wetlands and deltas

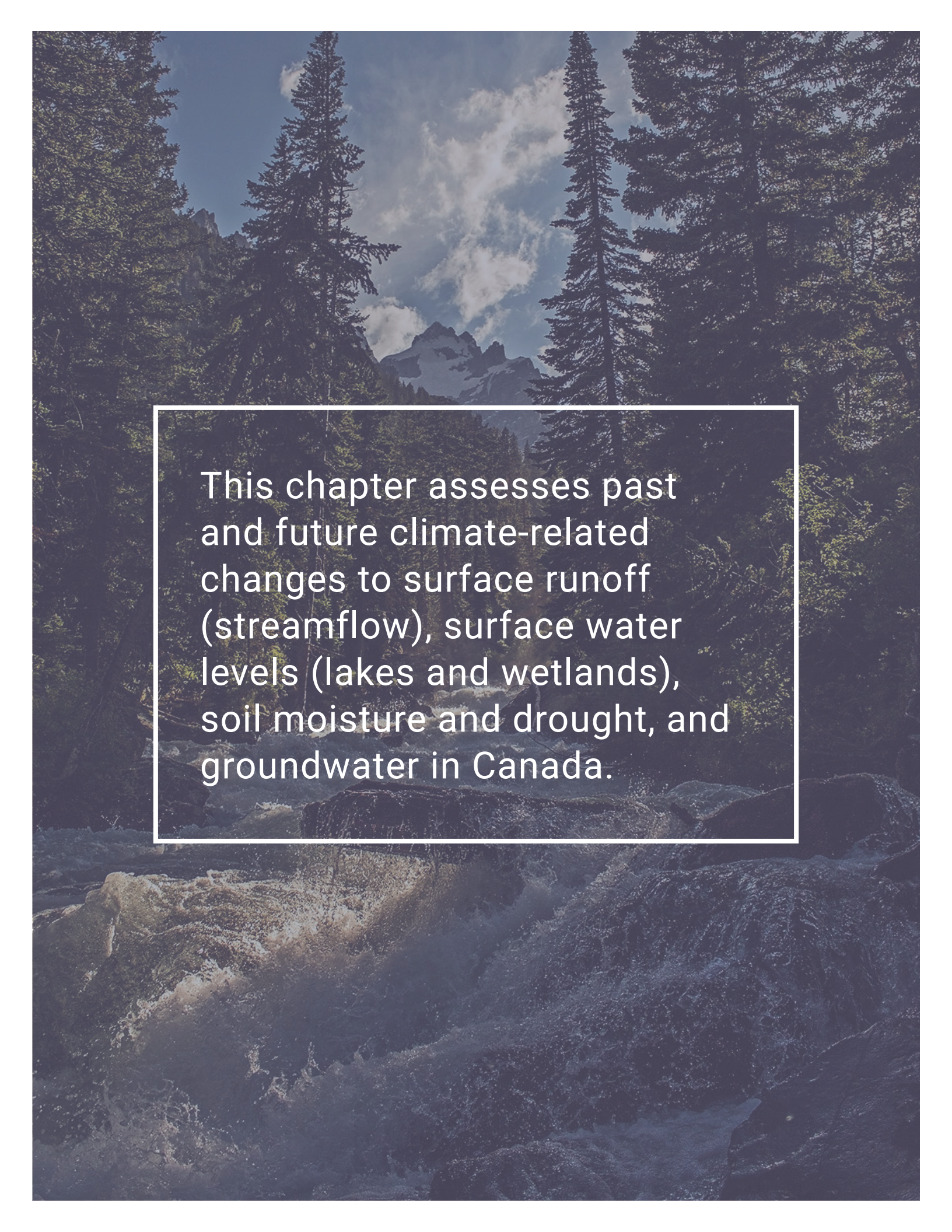
6.4: Soil moisture and drought

6.4.1: Soil moisture

6.4.2: Drought

6.5: Groundwater

Box 6.3: Monitoring groundwater from space



This chapter assesses past and future climate-related changes to surface runoff (streamflow), surface water levels (lakes and wetlands), soil moisture and drought, and groundwater in Canada.

Chapter Key Messages

6.2: Surface Runoff: Streamflow

The seasonal timing of peak streamflow has shifted, driven by warming temperatures. Over the last several decades in Canada, spring peak streamflow following snowmelt has occurred earlier, with higher winter and early spring flows (*high confidence*²⁴). In some areas, reduced summer flows have been observed (*medium confidence*). These seasonal changes are projected to continue, with corresponding shifts from more snowmelt-dominated regimes toward rainfall-dominated regimes (*high confidence*).

There have been no consistent trends in annual streamflow amounts across Canada as a whole. In the future, annual flows are projected to increase in most northern basins but decrease in southern interior continental regions (*medium confidence*).

Streamflow-related floods result from many factors, and in Canada these mainly include excess precipitation, snowmelt, ice jams, rain-on-snow, or a combination of these factors. There have been no spatially consistent trends in these flood-causing factors or in flooding events across the country as a whole. Projected increases in extreme precipitation are expected to increase the potential for future urban flooding (*high confidence*). Projected higher temperatures will result in a shift toward earlier floods associated with spring snowmelt, ice jams, and rain-on-snow events (*medium confidence*). It is uncertain how projected higher temperatures and reductions in snow cover will combine to affect the frequency and magnitude of future snowmelt-related flooding.

6.3: Surface Water Levels: Lakes And Wetlands

In regions of Canada where there are sufficient data, there is no indication of long-term changes to lake and wetland levels. Future levels may decline in southern Canada, where increased evaporation may exceed increased precipitation (*low confidence*). Projected warming and thawing permafrost has the potential to cause future changes, including rapid drainage, in many northern Canadian lakes (*medium confidence*).

24 This report uses the same calibrated uncertainty language as in the IPCC's Fifth Assessment Report. The following five terms are used to express assessed levels of confidence in findings based on the availability, quality and level of agreement of the evidence: very low, low, medium, high, very high. The following terms are used to express assessed likelihoods of results: virtually certain (99%–100% probability), extremely likely (95%–100% probability), very likely (90%–100% probability), likely (66%–100% probability), about as likely as not (33%–66% probability), unlikely (0%–33% probability), very unlikely (0%–10% probability), extremely unlikely (0%–5% probability), exceptionally unlikely (0%–1% probability). These terms are typeset in italics in the text. See chapter 1 for additional explanation.



6.4: Soil Moisture And Drought

Periodic droughts have occurred across much of Canada, but no long-term changes are evident. Future droughts and soil moisture deficits are projected to be more frequent and intense across the southern Canadian Prairies and interior British Columbia during summer, and to be more prominent at the end of the century under a high emission scenario (*medium confidence*).

6.5: Groundwater

The complexity of groundwater systems and a lack of information make it difficult to assess whether groundwater levels have changed since records began. It is expected that projected changes to temperature and precipitation will influence future groundwater levels; however, the magnitude and even direction of change is not clear. Spring recharge of groundwater aquifers over most of the country is anticipated to occur earlier in the future, as a result of earlier snowmelt (*medium confidence*).

Summary

Freshwater availability in Canada is influenced by a multitude of factors: some natural, some as a result of human activity. Changes in precipitation and temperature have a strong influence, both directly and indirectly, through changes to snow, ice, and permafrost. Disturbances of the water cycle by humans (dams, diversions, and withdrawals) make it difficult to discern climate-related changes. Direct measurements of freshwater availability indicators are inconsistent across the country and, in some cases, too sparse to evaluate past changes. In addition, future changes are determined from a multitude of hydrological models, using output from numerous climate models with different emission scenarios. These factors make it challenging to conduct a pan-Canadian assessment of freshwater availability, and even more difficult to determine whether past changes can be attributed to anthropogenic climate change. In this chapter, national and regional studies are considered, along with information on changes in temperature and precipitation from Chapter 4 and changes to the cryosphere from Chapter 5, to assess changes to freshwater availability in Canada.

Past changes in the seasonality of streamflow have been characterized by earlier spring freshets (the increased flow resulting from snow and ice melt in the spring) due to earlier peaks in spring snowmelt, higher winter and early spring flows, and, for many regions, reduced summer flows. These changes are consistent with observed warming and related changes to snow and ice. During the last 30 to 100 years, annual streamflow magnitudes, surface water levels, soil moisture content and droughts, and shallow groundwater aquifers have, for the most part, been variable, with no clear increasing or decreasing trends. This variability corresponds to observed year-to-year and multi-year variations in precipitation, which are partly influenced by naturally occurring large-scale climate variability (see Chapter 2, Box 2.5). However, for many indicators, there is a lack of evidence (particularly in northern regions of the country) to assess Canada-wide past changes in freshwater availability.

Continued warming and associated reductions in snow cover, shrinking mountain glaciers, and accelerated permafrost thaw are expected to continue to drive changes in the seasonality of streamflow. This includes increased winter flows, even earlier spring freshets, and reduced summer flows, as well as corresponding shifts from more snowmelt-dominated regimes toward rainfall-dominated regimes. Annual streamflow is projected to increase in some areas (mainly northern regions), but decline in others (southern interior regions). Thawing permafrost could cause future changes in many northern Canadian lakes, including rapid drainage. The frequency and intensity of future streamflow-driven flooding are uncertain, because of the complexity of factors involved. Projected increases in extreme precipitation are expected to increase the potential for future urban flooding. However, it is uncertain how projected higher temperatures and reductions in snow cover will combine to affect the frequency and magnitude of future snowmelt-related flooding. Lower surface water levels of lakes and wetlands are expected, especially toward the end of this century, under higher emission scenarios (see Chapter 3, Section 3.2), due to higher temperatures and increased evaporation. However, the magnitude of these decreases will depend on how much future precipitation increases offset increased evaporation.

Future increases in drought and decreases in surface soil moisture are anticipated during summer in the southern Canadian prairies and interior British Columbia, where moisture deficits from increased evapotranspiration are projected to be greater than precipitation increases. These changes are expected to be more



prominent toward the end of this century under higher emission scenarios; however, there is considerable uncertainty in their magnitude. Groundwater systems are complex, and, although it is expected that changes to temperature and precipitation will influence future levels, the magnitude and even direction of change is not clear. However, in the future, spring recharge of groundwater aquifers over most of the country is anticipated to occur earlier, as a result of earlier snowmelt.

These anticipated changes from anthropogenic climate warming will directly affect the timing and amount of future freshwater supplies, and they may be exacerbated by human management alterations to freshwater systems. The impacts are expected to be more prominent toward the end of this century under higher emission scenarios, given the larger associated climate changes. Of particular concern are impacts in regions that currently rely on snow and ice melt as freshwater sources, as well as continental interior areas, where increased evapotranspiration from warmer temperatures could reduce future water supplies. However, freshwater supplies in all regions of Canada are expected to be affected in one way or another. It is also anticipated that water-related extremes, such as droughts and floods, will intensify these impacts.

6.1: Introduction

Canada has vast amounts of freshwater, in the form of lakes, rivers, and wetlands, aquifers with groundwater reserves, as well as water stored in snowpacks, glaciers, and the soil. There are over 8500 rivers and more than 2 million lakes covering almost 9% of Canada (Monk and Baird, 2011), while wetlands occupy an estimated 16% of the country's landmass (National Wetlands Working Group, 1988, 1997). This freshwater is fundamental to the environment (e.g., aquatic ecosystems) and to many social and economic activities, including agriculture, industry, hydroelectricity generation, provision of drinking water, and recreation.

Freshwater availability is primarily governed by processes and interactions within the water cycle (see Figure 6.1). Rain or snowmelt water can run off over the land surface into lakes and streams, but direct surface runoff is rare in many natural areas, such as forests. Rather, much of the precipitation infiltrates into the ground, accumulates on the surface as snow, or fills surface water bodies, where it eventually infiltrates into the soil or evaporates. Some of the infiltrated water remains in shallow soil, where it is taken up by vegetation and transpired back to the atmosphere. Soil water may flow rapidly to streams and lakes through highly permeable subsoils or percolate down to recharge deeper groundwater aquifers. This deeper water flows to streams much more slowly, over periods ranging from days to thousands of years, depending on the permeability of the geologic formations. Human water management — including dams, reservoirs, and water withdrawals — has also become an important component of the water cycle.

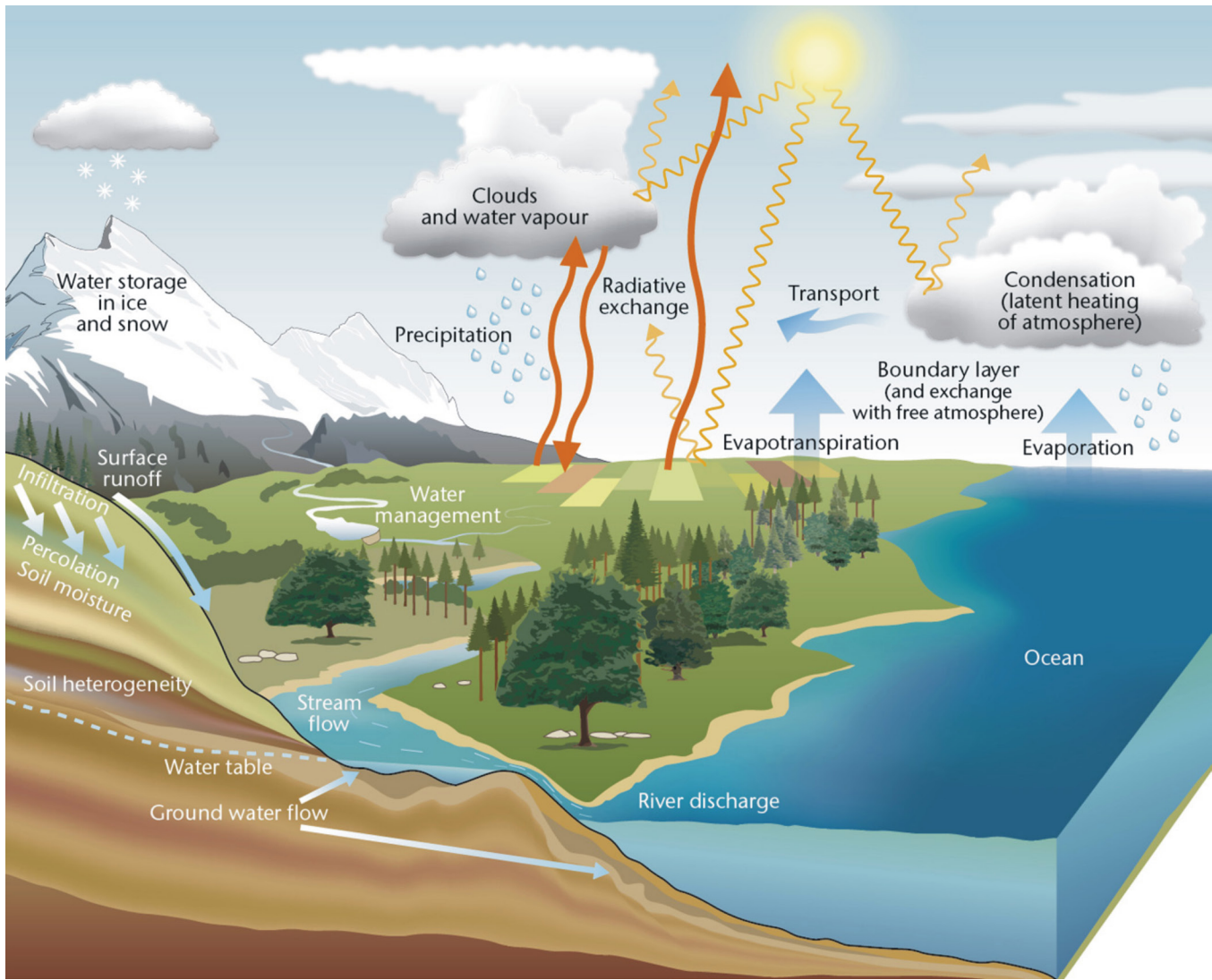


Figure 6.1: The water cycle, its components, relevant processes, and interactions

Figure caption: In the water cycle, water that evaporates from oceans is transported over land, where it falls as precipitation. It then either moves back to the atmosphere through evapotranspiration, is stored as ice or snow, or makes its way to rivers/streams (via various pathways), where it eventually flows back to the ocean.

FIGURE SOURCE: UK MET OFFICE (2018).

Within the water cycle, the amount and timing of freshwater is influenced by several natural factors, including size of the watershed; type of landforms; storage characteristics (on the surface and in subsurface soil); type, rate, and amount of precipitation; presence of ice; amount of vegetation; soil properties (including permafrost); and evaporation. Each of these acts on a variety of scales in time and space. This complexity is particularly prominent in Canada, with its large land mass, diverse climate and eco-regions, and varied geology. Furthermore, much of the surface water is currently managed by humans (especially in the more heavily populated southern regions), making it difficult to separate the effects of climate from those of management.

Freshwater monitoring varies across Canada, with spatially dense monitoring at many points in some areas, but a lack of monitoring in others, especially in much of northern Canada. Most research on past and future freshwater availability is on individual large watersheds or specified geographic regions, and changes are evaluated over different periods, depending on data availability, with few Canada-wide assessments. Studies on future changes use many different hydrological models driven by output from global climate models (GCMs) and regional climate models (RCMs) (see Chapter 3, Section 3.3). As a result, assessing past and future changes of freshwater availability in a pan-Canadian context is difficult. However, freshwater is greatly influenced by surface temperature and precipitation (see Chapter 4) as well as the cryosphere (snow, glaciers, freshwater ice, and permafrost) (see Chapter 5), and there is considerable information on past and future changes in these variables across most of Canada. In much of the country, the proportion of total precipitation falling as snow is declining, the extent and duration of snow cover are decreasing, glaciers are receding, permafrost is thawing, air temperature and resulting evapotranspiration are increasing, and precipitation is increasing. These trends are projected to continue, and all affect the amount and timing of freshwater availability.

In this chapter, freshwater availability is defined as water available at the surface (streams, lakes, and wetlands), in the soil, and in aquifers (groundwater). The assessment focuses primarily on water bodies unaffected by human management, using information from federal and provincial/territorial monitoring networks. Since floods and droughts are directly related to freshwater availability, past and future changes in these events are also assessed (Chapter 6, Sections 6.2.4 and 6.4.2). Climate change impacts on water quality are not addressed in this assessment.

6.2: Surface runoff: streamflow

Key Message

The seasonal timing of peak streamflow has shifted, driven by warming temperatures. Over the last several decades in Canada, spring peak streamflow following snowmelt has occurred earlier, with higher winter and early spring flows (*high confidence*). In some areas, reduced summer flows have been observed (*medium confidence*). These seasonal changes are projected to continue, with corresponding shifts from more snowmelt-dominated regimes toward rainfall-dominated regimes (*high confidence*).

Key Message

There have been no consistent trends in annual streamflow amounts across Canada as a whole. In the future, annual flows are projected to increase in most northern basins but decrease in southern interior continental regions (*medium confidence*).

Key Message

Streamflow-related floods result from many factors, and in Canada these mainly include excess precipitation, snowmelt, ice jams, rain-on-snow, or a combination of these factors. There have been no spatially consistent trends in these flood-causing factors or in flooding events across the country as a whole. Projected increases in extreme precipitation are expected to increase the potential for future urban flooding (*high confidence*). Projected higher temperatures will result in a shift toward earlier floods associated with spring snowmelt, ice jams, and rain-on-snow events (*medium confidence*). It is uncertain how projected higher temperatures and reductions in snow cover will combine to affect the frequency and magnitude of future snowmelt-related flooding.

Canada has more than 8500 rivers and streams of various lengths (Monk and Baird, 2011). Many are affected by human alterations, such as flow regulation (dams, weirs, and locks), water withdrawals, and diversions, often associated with hydroelectric facilities (CDA, 2016). Studies on climate-related past changes in streamflow rely heavily on data from streams that are not subject to these forms of human regulation (i.e., unregulated) or those with limited regulation (see Box 6.1). In a few cases, studies have attempted to account for regulation by determining naturalized flow using various hydrological models (Peters and Buttle, 2010). Future streamflow changes are assessed using climate output (e.g., precipitation and temperature) from various GCMs and/or RCMs that provide input to a hydrological model. The multitude of climate and hydrological models used in these studies adds uncertainty to future streamflow changes (e.g., Seneviratne et al., 2012).

Box 6.1: Canada's hydrometric network

Hydrometric stations are located on lakes, rivers, and streams of many sizes, ranging from drainage basins as small as a few hectares to large watersheds such as the Mackenzie Basin (1,680,000 km²). Over 2600 active water-level and streamflow stations are currently operated under federal-provincial and federal-territorial cost-sharing agreements. Streamflow is the volume of water flowing past a point on a river in a unit of time (e.g., cubic metres per second). Most stations are located in the southern part of the country; as a result, the network is often inadequate to describe water characteristics and trends in northern Canada. The Reference Hydrometric Basin Network (RHBN) is a subset of stations from the national network that are used primarily for the detection, monitoring, and assessment of climate change (ECCC, 2017). These stations are characterized by near-pristine or stable hydrological conditions and have been active for at least 20 years (Harvey et al., 1999) (see Figure 6.2). However, the RHBN is also unevenly distributed across Canada (with almost no

representation of the high Arctic Islands), and the length of data records varies (Whitfield et al., 2012).

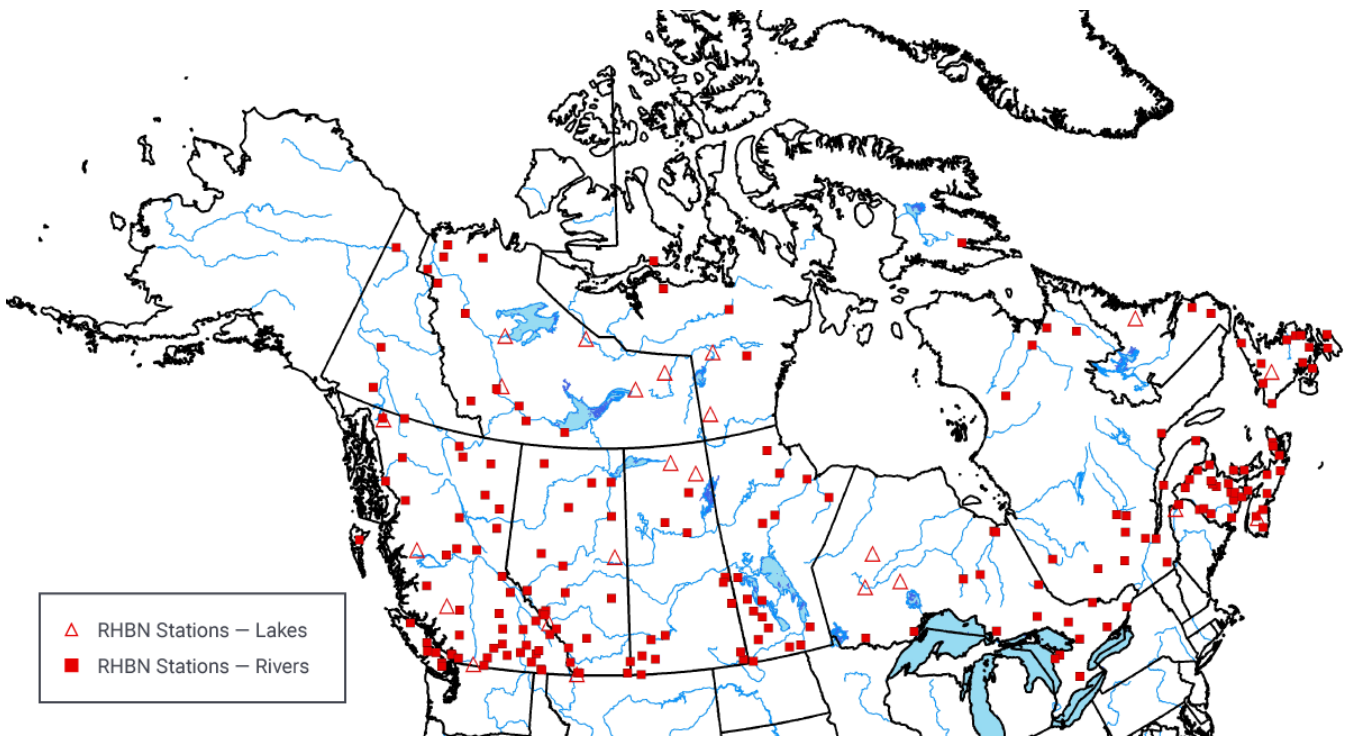


Figure 6.2: Current Reference Hydrometric Basin Network river and lake stations across Canada

Figure caption: Canada's Reference Hydrometric Basin Network (RHBN), a subset of stations that have experienced little or no flow alteration and have thus widely been used for streamflow-related studies. This assessment relies on literature that incorporated primarily stations from the RHBN.

FIGURE SOURCE: DERIVED USING DATA FROM THE WATER SURVEY OF CANADA (ECCC, 2017) <[HTTPS://WATEROFFICE.EC.GC.CA/](https://wateroffice.ec.gc.ca/)>.

6.2.1: Streamflow magnitude

Streamflow magnitude (runoff) is a key indicator for evaluating changes in surface water. It is assessed at monthly, seasonal, and annual timescales to determine changes in overall flow volumes, and on daily to weekly scales to assess high and low streamflow extremes. In all cases, pan-Canadian analyses are infrequent and, in most cases, older than regional studies. For Canada as a whole, annual streamflow trends were mixed. Significant declines occurred at 11% of stations and significant increases at 4% of stations for the 1967–1996 period. Most decreases were in southern Canada (Zhang et al., 2001; similar results in Burn and Hag Elnur, 2002). Seasonal runoff over the 1970–2005 period, in most of the 172 stations evaluated, was dominated by natural variability. Twelve per cent of stations showed significant increases in winter runoff (December to February), while only 5% had significant winter decreases. Spring and summer trends were mixed, with no spatial pattern (Monk et al., 2011). From 1960 to 1997, significant increases in April flow occurred at almost 20% of stations, and significant decreases in summer flow (May to September) were observed at 14% of the sites (Burn and Hag Elnur, 2002). The increases in April flow were also found (25% of stations) for the longer 1950–2012 period (Vincent et al., 2015).

Regional studies of trends in annual and seasonal streamflow magnitudes are summarized in Table 6.1. Although these individual studies use different time periods, hydrometric stations, and analysis techniques, the findings are mostly consistent with the Canada-wide analyses. Annual flows over western Canada have varied from one region to another, with both increasing and decreasing trends since approximately the 1960s and 1970s (e.g., DeBeer et al., 2016). Most declines were observed in rivers draining the eastern slopes of the central/southern Rocky Mountains, including the Athabasca, Peace, Red Deer, Elbow, and Oldman rivers (Burn et al., 2004a; Rood et al., 2005; Schindler and Donahue, 2006; St. Jacques et al., 2010; Yip et al., 2012; Peters et al., 2013; Bawden et al., 2014). Long-term streamflow records (over more than 30 years) from the Northwest Territories, including the Mackenzie River, indicated increasing annual flows (St. Jacques and Sauchyn, 2009; Rood et al., 2017). However, annual runoff from rivers draining into northern Canada as a whole (western Arctic Ocean, western Hudson and James Bay, and Labrador Sea) showed no significant trends for the period 1964–2013 (Déry et al., 2016). Rivers in Yukon, British Columbia, Ontario, and Quebec reported mixed annual trends (Fleming and Clarke, 2003; Brabets and Walvoord, 2009; Fleming, 2010; Fleming and Weber, 2012; Déry et al., 2012; Nalley et al., 2012; Hernández-Henríquez et al., 2017).

Table 6.1: Observed trends in annual, winter, and summer streamflow magnitudes from basin-wide case studies in Canada

Watershed (west to east)	Annual runoff or streamflow trend	Winter runoff or streamflow trend	Summer runoff or streamflow trend	Source
Pan-Arctic	→ (no significant trend) 1964–2013 into Bering Sea, western Arctic Ocean, western Hudson and James Bay, and Labrador Sea ↑ and ↓ to the eastern Hudson and James Bay (eastern Arctic Ocean)			Déry et al. (2016)
Yukon River (YT)	→ 1944–2005; ↑ during warm Pacific Decadal Oscillation (PDO) 1976–2005	↑ 1944–2005, due to warm PDO, 1976–2005	↓ During warm PDO, 1976–2005	Brabets and Walvoord (2009)
White River, Alsek River; glacier in basins (YT)	↑ 1975–1999			Fleming and Clarke (2003)
Dezadeash River, no glacier in basin (YT)	↓ 1953–1999			Fleming and Clarke (2003)
Big Creek, no glacier in basin (YT)	↓ 1975–1999			Fleming and Clarke (2003)
BC region	Mixture of trends 1966–2015		Most positive detectable trends occur in spring in glacierized westward rivers located > 1200 m	Hernández-Henríquez et al. (2017)
Campbell, Stave, Cheakamus, and other rivers in south coastal BC	↑ 1984–2007	↑ December–January, ↓ February, 1984–2007		Fleming and Weber (2012)
Cowichan River (BC)			↓ August, 1961–2006	Fleming (2010)
Fraser River (BC)	Variability increasing			Déry et al. (2012)
Fraser River (BC)			↓ June–August 1958–2012	BCMOE (2016)
Castle River near Beaver Mines (BC)	↓ 1946–1948, 1951–2002			Rood et al. (2005)
Bridge River (BC)	Possible small ↑ 1984–2007	Small ↑ 1984–2007	Possible small ↑ June–July, ↓ August, 1984–2007	Fleming and Weber (2012)

Table 6.1: Observed trends in annual, winter, and summer streamflow magnitudes from basin-wide case studies in Canada

Columbia River (BC)	Possible small ↑ 1984–2007	↑ 1984–2007	Possible small ↓ August, 1984–2007	Fleming and Weber (2012)
Columbia River at Fairmont Hot Springs (BC)	↓ 1946–1995			Rood et al. (2005)
Peace River (BC)	→ 1984–2007	→ 1984–2007	→ 1984–2007	Fleming and Weber (2012)
Peace River at town of Peace River (AB)			↓ -57%, 1912–2003	Schindler and Donahue (2006)
	↑ 1916–2013			Rood et al. (2017)
Mackenzie River (BC, AB, YT, SK, NT)	1961–2002			Yip et al. (2012)
	↑ 1965–2007			St. Jacques and Sauchyn (2009)
	↑ 1940–2013			Rood et al. (2017)
Liard River (YT, BC, AB, NT)	↓ annual mean, 1960–1999	↑ 1975–1999, and 1960–1999	↓ June and August, 1975–1999	Burn et al. (2004a)
	↑ annual minimum, 1960–1999			
	↓ annual maximum, 1975–1999			
	↑ 1944–2013	↑ 1944–2013	↑ 1944–2013	Rood et al. (2017)
Peel River above Fort McPherson (NT)	→ 1975–2013			Rood et al. (2017)
Athabasca River below Fort McMurray (AB)	Significant ↓ 1958–2009		↓ -19% from 1958–2003	Schindler and Donahue (2006)
			↓ -33.3% 1970–2003	Peters et al. (2013)
			↓ -30% to -20%, 1958–2009	
Athabasca River at Athabasca (AB)	→ 1913–2013			Rood et al. (2017)
				Peters et al. (2013)
Athabasca and Peace River sub-basins (BC, AB, SK)	↓ 1966–2010	Mostly ↓ 1966–2010, with increases in several sub-basins	Majority ↓ 1966–2010	Bawden et al. (2014)

Table 6.1: Observed trends in annual, winter, and summer streamflow magnitudes from basin-wide case studies in Canada

Red Deer River (AB)	↓ 1913–2002			Rood et al. (2005)
Bow River (AB)	Small ↓ 1911–2002 and 1912–2007			St. Jacques et al. (2010)
Elbow River below Glenmore Dam (AB)	↓ 1912–2001			St. Jacques et al. (2010)
Oldman River near Lethbridge (AB)	↓ 1912–2001			St. Jacques et al. (2010)
			↓ -42% 1915–2003	Schindler and Donahue (2006)
South Saskatchewan River at Medicine Hat (AB)	↓ 1913–1930, 1936–2002; ↑ 1912–2001 (naturalized, climate only)			Rood et al. (2005); St. Jacques et al. (2010)
South Saskatchewan River at Saskatoon (AB, SK)			↓ -84% 1912–2003	Schindler and Donahue (2006)
North Saskatchewan River at Edmonton (AB)	↓ 1911–2007			St. Jacques et al. (2010)
Prairie unregulated streams	↓ 1966–2005		↓ 1966–2005	Burn et al. (2008)
Winnipeg River (MB)	↑ +58% since 1924	↑ since 1924	→ since 1924	St. George (2007)
Hudson Bay (MB)	↓ 1964–1980s; ↑ 1980s–2008	↑ 1964–2008	↓ 1964–2008	Déry et al. (2011)
Churchill (MB)	↓ 1964–2008			Déry et al. (2011)
Nagagami River (ON)	↑ 1954–2008			Nalley et al. (2012)
Missinaibi River (ON)	↑ 1954–2008			Nalley et al. (2012)
Black River (ON)	↑ 1954–2008			Nalley et al. (2012)
Richelieu River (QC)	↑ 1954–2008			Nalley et al. (2012)
Eaton River (QC)	Small ↓ 1954–2007			Nalley et al. (2012)

Table 6.1: Observed trends in annual, winter, and summer streamflow magnitudes from basin-wide case studies in Canada

St. Lawrence River, south shore tributaries (QC)	↓ 1950–2000	Assani et al. (2012)
St. Lawrence River, tributaries north and west of Montreal (QC)	↑ 1950–2000	Assani et al. (2012)
Thirteen rivers in New Brunswick	↑ 11/13 (5 significant at 70%), ↓ 2/13, 1969–2006	↓ 9/13 (5 significant at 70%) 1969–2006 Arisz et al. (2011)

TABLE SOURCE: UPDATED FROM MORTSCH ET AL. (2015).

Seasonally, there has been a consistent pattern of increasing winter flows in many regions (see Table 6.1), particularly for more northern basins, such as the Mackenzie and Yukon rivers and those draining into Hudson Bay. Summer flows have been generally declining over most regions of Canada, although the declines are not as widespread as for winter. Note that these studies are mostly consistent on the direction of change, but there are large differences in the rate of these changes. Many of these regional trends in flow were linked to precipitation trends or variability affecting the entire basin, although winter warming and associated snow-melt explained several of the increases in winter/early spring flow (e.g., DeBeer et al., 2016). In addition, several flows were associated with naturally occurring internal climate variability (mainly El Niño–Southern Oscillation, Pacific Decadal Oscillation [PDO], and Arctic Oscillation [AO]; see Chapter 2, Box 2.5), particularly for western Canada during winter (e.g., Bonsal and Shabbar, 2008; Whitfield et al., 2010), the Mackenzie Basin (St. Jacques and Sauchyn, 2009), and rivers draining into Hudson Bay (Déry and Wood, 2004).

Changes in extreme short-term streamflow are important indicators of flood risk. One-day maximum flow magnitudes (the highest one-day flow recorded during the year) from 1970 to 2005 revealed that 11% of hydrometric sites across Canada have significantly decreasing trends (lower maximum flow levels), while only less than 4% have increasing trends (higher maximum flow levels) (Monk et al., 2011). A more recent study using an expanded set of RHBN stations (280) for the 1961–2010 period yielded very similar results, with 10% of the sites showing significant decreases and less than 4% significant increases (Burn and Whitfield, 2016) (see Figure 6.3).

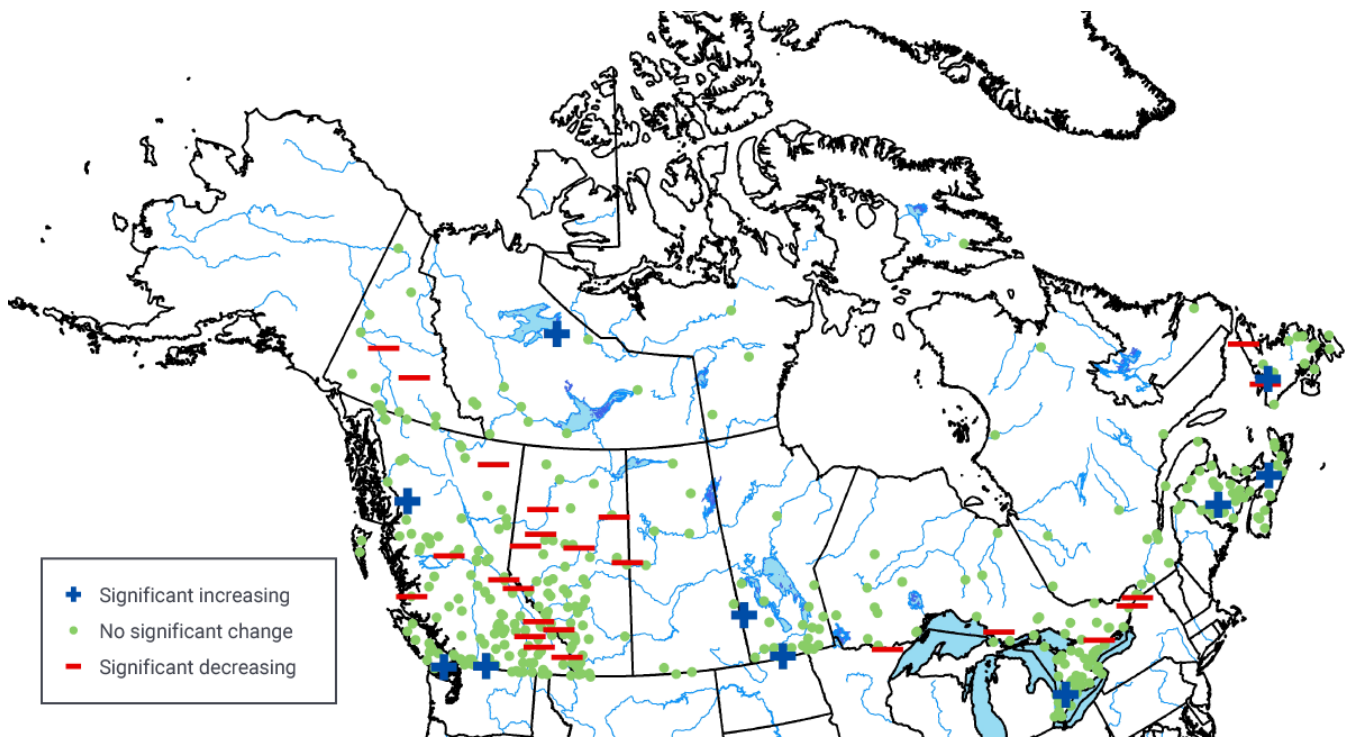


Figure 6.3: Streamflow changes in Canada, trends in maximum flow, 1961–2010

Figure caption: Summary of trends in one-day maximum flow in Canada using stations on unregulated streams from the Reference Hydrometric Basin Network (see Box 6.1). Significant trends denote that there is only a 5% possibility that such changes are due to chance.

FIGURE SOURCE: MODIFIED FROM BURN AND WHITFIELD (2016).

Equally important to aquatic ecosystems and society are low flows, since they represent periods of decreased water availability. More stations show significantly lower one-day minimum flow trends (18%) than show significantly higher ones (8%) (see Figure 6.4) (Monk et al., 2011). Results from a smaller subset of RHBN stations (Ehsanzadeh and Adamowski, 2007, for 1961–2000 and Burn et al., 2010, for 1967–2006) revealed similar tendencies in seven-day low flows, with more sites having significantly lower values (36% and 18% for each study, respectively) than higher values (7% and 5%, respectively).

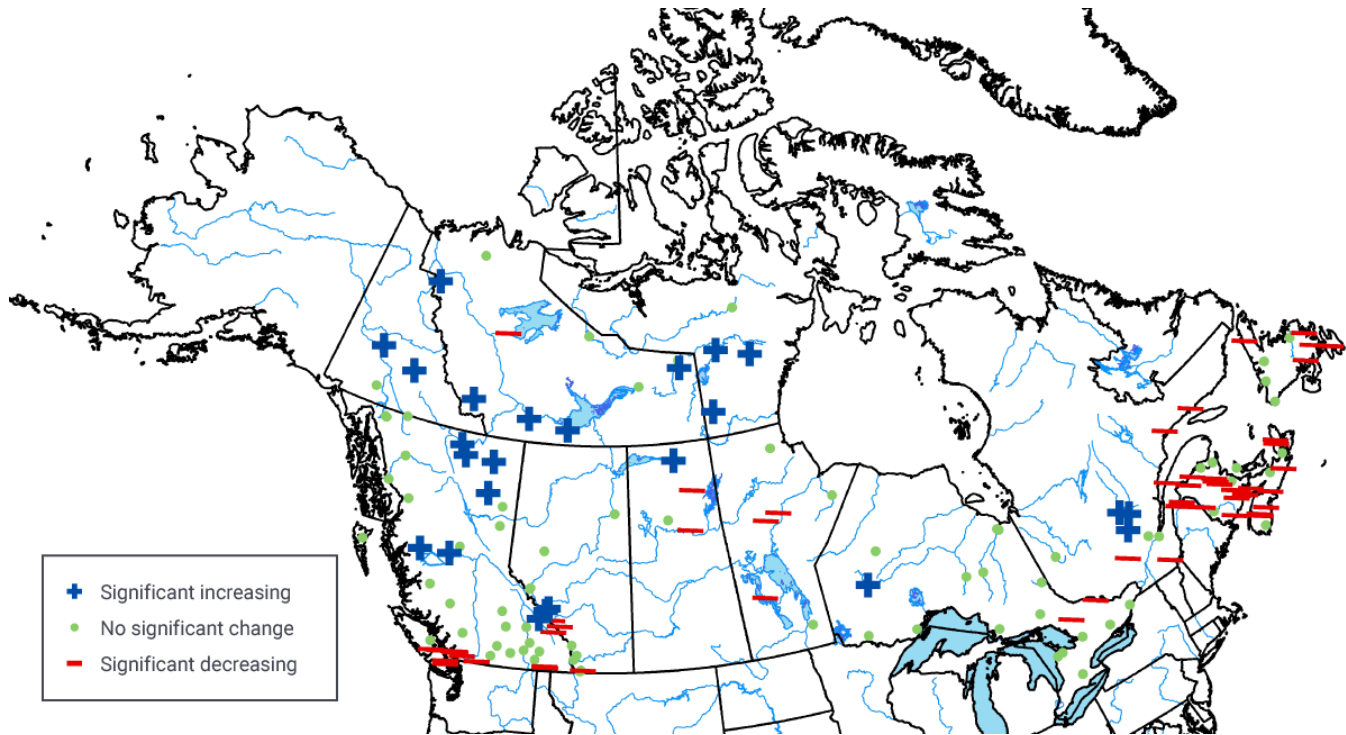


Figure 6.4: Streamflow changes in Canada, trends in minimum flow, 1970–2005

Figure caption: Summary of trends in one-day minimum flow in Canada using stations on unregulated streams from the Reference Hydrometric Basin Network (see Box 6.1). Significant trends denote that there is only a 10% possibility that such changes are due to chance.

FIGURE SOURCE: MODIFIED FROM MONK ET AL. (2011).

Another indicator of freshwater availability is baseflow, the portion of streamflow resulting from seepage of water from the ground (related to groundwater; see Section 6.5). Baseflow often sustains river water supply during low-flow periods. For the vast majority of sites in Canada, annual baseflow trends did not significantly change from 1966 to 2005 (Rivard et al., 2009). However, an analysis of a baseflow index across Canada found some locations with significantly decreasing trends (11% of stations) and others with increasing trends (9%) (Monk et al., 2011). Additionally, in northwestern Canada, winter baseflow has increased significantly in 39% of the 23 rivers analyzed. The likely explanation is enhanced water infiltration from permafrost thawing due to climate warming (St. Jacques and Sauchyn, 2009).

Only one published study directly attributed changes in streamflow magnitude within Canada to anthropogenic climate change. This included recent observed declines in summer (June–August) streamflow in four British Columbia rivers (Najafi et al., 2017b). The decreases were due to smaller late-spring snowpacks (and consequently, lower summer runoff), which were attributed to the human influence on warming of cold-season temperatures (Najafi et al., 2017a) (see Chapter 4, Section 4.3.1.2).

Projected future changes in Canadian streamflow magnitudes have not been extensively examined on a national scale, although several regional assessments have been conducted (see Table 6.2 and Figure 6.5). The majority of these studies are based on the third phase of the Coupled Model Intercomparison Project (CMIP3) climate models and SRES emission scenarios (see Chapter 3, Section 3.3) unless otherwise specified. The findings are mostly consistent on the direction of change, although there are large uncertainties in magnitude. In general, for the mid-21st century, watersheds in British Columbia and northern Alberta are projected to have increases in annual and winter runoff, whereas some watersheds in Alberta, southwest British Columbia, and southern Ontario are projected to have declines in summer flow (Kerkhoven and Gan, 2011; Poitras et al., 2011; Bennett et al., 2012; Bohrn, 2012; Harma et al., 2012; Schnorbus et al., 2011; 2014; Shrestha et al., 2012a; Eum et al., 2017; Islam et al., 2017). In the Prairie region, most rivers in southern Alberta and Saskatchewan are projected to have decreases in both annual and summer runoff (Lapp et al., 2009; Shepherd et al., 2010; Forbes et al., 2011; Kerkhoven and Gan, 2011; Kienzle et al., 2012; Tanzeeba and Gan, 2012; St. Jacques et al., 2013, 2017). However, rivers in southern and northern Manitoba are projected to have increasing flow (Poitras et al., 2011; Shrestha et al., 2012b; Stantec, 2012). Projected changes in future annual runoff are mixed in Ontario (EBNFLO Environmental and AquaResource Inc., 2010; Grillakis et al., 2011), while in Quebec the majority of studies project increasing annual flows (Quilbe et al., 2008; Minville et al., 2008, 2010; Boyer et al., 2010; Chen et al., 2011; Guay et al., 2015). A Quebec study using several models from the fifth phase of the Coupled Model Intercomparison Project (CMIP5) found that mid-century (2041–2070) flows for southern rivers under both medium and high emission scenarios (RCP4.5 and RCP8.5) will be characterized by earlier and smaller spring peak flow and lower summer runoff. Annual mean flow is anticipated to increase in northern regions and decrease in the south (CEHQ, 2015). Annual streamflow is projected to increase for New Brunswick (El-Jabi et al., 2013) and Labrador (Roberts et al., 2012). In northwestern Canada, there is evidence that watersheds such as the Mackenzie and Yukon river basins will see an increase in annual flow, mainly due to the higher precipitation amounts projected at higher latitudes (e.g., Poitras et al., 2011; Thorne, 2011; Vetter et al., 2017).

Table 6.2: Projected changes in annual and seasonal streamflow from basin-wide case studies across Canada

Watershed (west to east)	Projections	Key references
Baker River (BC)	Most scenarios for the 2050s project increased winter runoff and decreased summer runoff, including decreased snow water equivalent	Bennett et al. (2012)
Campbell River (BC)	Increase in 2050s winter runoff, and decrease in summer runoff; no consensus on changes in mean annual runoff	Schnorbus et al. (2011); Bennett et al. (2012)

Table 6.2: Projected changes in annual and seasonal streamflow from basin-wide case studies across Canada

Trepanier Creek, Okanagan Basin (BC)	Decrease in 2050s mean annual and summer streamflow, with spring freshet occurring two weeks earlier, compared with 1983–1993 period	Harma et al. (2012)
Ingenika River (BC)	Increase in 2050s winter runoff; no consensus on changes in summer runoff	Bennett et al. (2012)
Fraser River (BC)	No consensus for 2050s mean annual flow projection for the Fraser River; flow during summer would decline in all scenarios	Shrestha et al. (2012a)
	Earlier spring snowmelt in the 2050s (approximately 25 days), yielding more runoff in the winter and spring, and earlier recession to low-flow volumes in summer at mouth	Islam et al. (2017)
Columbia River (BC); Peace River (BC, AB)	Streamflow projections for the 2050s indicate these rivers will retain the characteristics of a nival regime by mid-century, although streamflow-timing shifts result in the form of generally higher winter, earlier freshet onset, higher spring runoff, and reduced summer runoff. An overall increase in annual runoff is projected	Schnorbus et al. (2014)
Liard River (NT)	General increase in annual flow under warming climate scenarios	Thorne (2011)
Mackenzie River (NT)	Increasing tendency for mean annual runoff over the 21 st century	Vetter et al. (2017)
Athabasca River (AB)	Projected increases in spring and winter flows, increases in minimum and maximum flows, with summer flows projected to decrease in the 2050s and 2080s; overall increase in annual runoff reaching the river mouth	Eum et al. (2017)

Table 6.2: Projected changes in annual and seasonal streamflow from basin-wide case studies across Canada

Southern Prairies (tributaries of Saskatchewan River) (AB, SK)	Decreases in 2050s annual runoff, except for increase in Cline River, AB, due to large increase in winter runoff; increases in Red River and decreases in Old Man River, AB; a shift to an earlier spring peak in runoff and drier late summer expected	Lapp et al. (2009); Shepherd et al. (2010); Forbes et al. (2011); Kienzle et al. (2012); St. Jacques et al. (2013, 2017)
Churchill (MB)	In a hydrological model intercomparison, two of three hydrological model projections for a range of climate scenarios projected increases in annual runoff, while a third model projected decreases	Bohrn (2012)
Lake Winnipeg – Upper Assiniboine and Morris Basins (MB)	Increased annual runoff projected for the Upper Assiniboine and for most scenarios in the Morris Basin	Shrestha et al. (2012b); Stantec (2012)
Western Canada basins: Columbia, Fraser, Yukon, Mackenzie, Churchill, Nelson, Saskatchewan rivers	Increased annual mean flow projected for 2050s; increase in magnitude of winter streamflow and earlier spring peak flow for northern basins; significant increase in 10-year return frequency of 15-day winter and fall low flows and one-day high flows for high-latitude western Canadian basins; decrease in high-flow events for the more southern basins (Churchill, Saskatchewan, and Athabasca)	Poitras et al. (2011)
Spencer Creek (ON)	Increase in mean annual and fall–winter streamflow and decrease in March–April spring peak flow	Grillakis et al. (2011)
Credit River (ON)	Mixed projections of annual streamflow	EBNFLO Environmental and AquaResource Inc. (2010)
305 Tributaries in QC	Increase in mean annual streamflow for majority of Quebec watersheds; decreased June–August contribution to annual streamflow	Guay et al. (2015)

Table 6.2: Projected changes in annual and seasonal streamflow from basin-wide case studies across Canada

Quebec Rivers south of approximately 50 degrees north	Mean annual flows are projected in 2050s to decrease in southern regions and increase in more northern areas; spring floods projected to be earlier, with the volume and peak decreasing in the south; summer–fall peak flood flows projected to be higher over a large portion of southern Quebec; summer flows lower	CEHQ (2015)
Tributaries of the St. Lawrence (QC) (including Richelieu, St. François, Yamachiche, St. Maurice and Bati-scan rivers)	Increases in 2050s mean winter runoff, with most scenarios projecting decreased summer runoff and increased annual runoff	Boyer et al. (2010)
Chaudière (QC)	Slight decrease in annual runoff for the 2020s	Quilbe et al. (2008)
Chute-du-Diable (QC)	Most scenarios suggest increases in the winter, spring, and fall runoff, whereas summer is expected to see a decrease, with increases in annual runoff for 2050s and 2080s	Minville et al. (2008)
Peribonka River (QC)	Generally earlier spring freshet timing, slightly higher spring peak, and slightly higher annual runoff projected for 2050s and 2080s	Minville et al. (2010)
Saint John, Nashwaak, Canaan, Kennebecasis, Restigouche, and Miramichi Rivers (NB)	Increase in 2050s mean annual streamflow; depending on the scenario and the time slice used, increase in flood and drought frequencies	El-Jabi et al. (2013)
Pinus River Basin (Labrador, NL)	Increase in 2050s mean annual streamflow, with spring peak occurring two weeks earlier compared with the 1971–2000 period	Roberts et al. (2012)

TABLE SOURCE: MODIFIED AND UPDATED FROM COHEN ET AL. (2015).

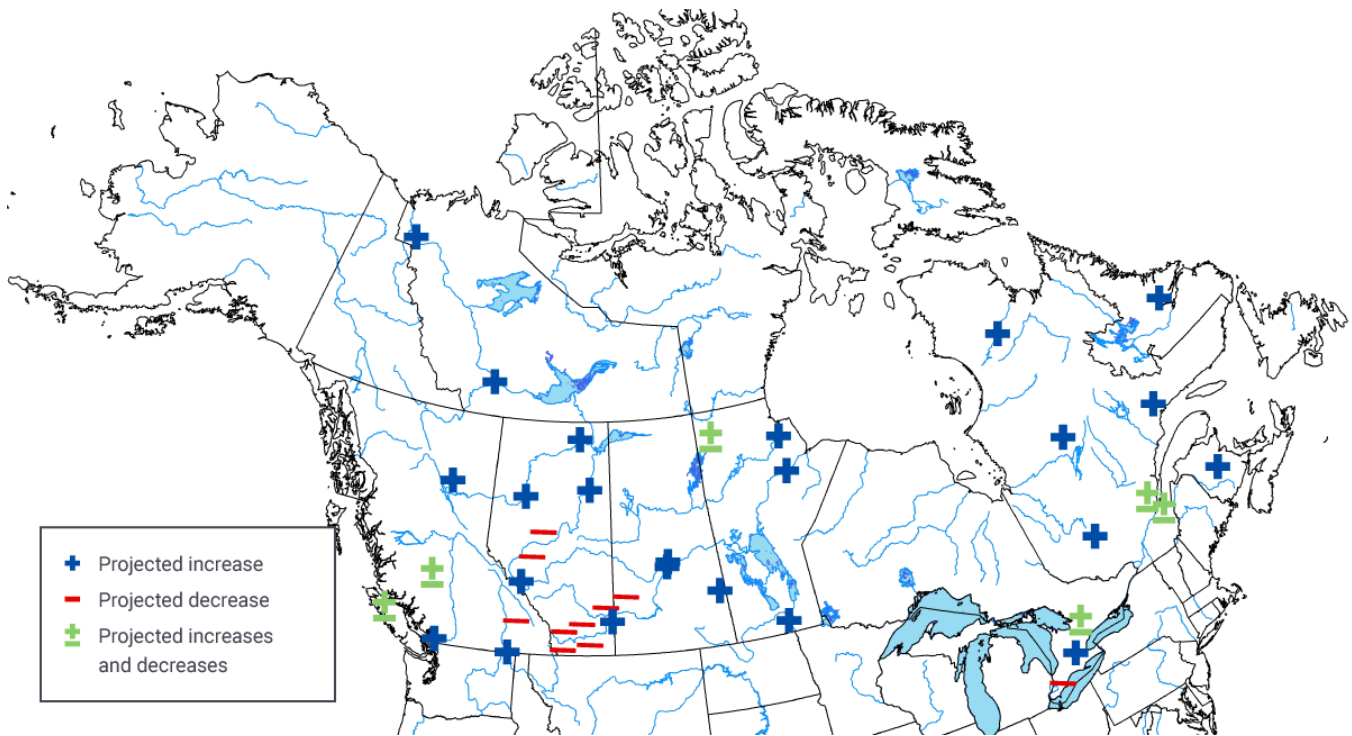


Figure 6.5: Projected future changes to annual streamflow in Canada

Figure caption: Summary of projected future changes to annual streamflow across Canada for the mid- to late 21st century based on various emission scenarios.

FIGURE SOURCE: UPDATED FROM BUSH ET AL. (2014) AND COHEN ET AL. (2015).

6.2.2: Streamflow timing

Reliable streamflow is important for water users and aquatic ecosystems, which have become accustomed to having adequate water supplies at certain times of the year. As a result, streamflow timing and related streamflow regimes (see Section 6.2.3) are important indicators of freshwater availability. The timing of streamflow events is significantly influenced by climate. Such events include the spring freshet, when flow dramatically increases due to snowmelt, and shorter-duration (usually one- to seven-day) maximum and minimum flows during the year. Pan-Canadian studies have generally reported that the spring high-flow season is coming earlier (Zhang et al., 2001; Déry et al., 2009; Vincent et al., 2015). This finding is supported by a study using 49 RHBN hydrometric stations with more than 30 years of data up to 2010 (Jones et al., 2015; see Figure 6.6). The average rate of change for stations with earlier trends was approximately two days per decade, consistent with other studies showing earlier freshets (e.g., Prowse et al., 2002).

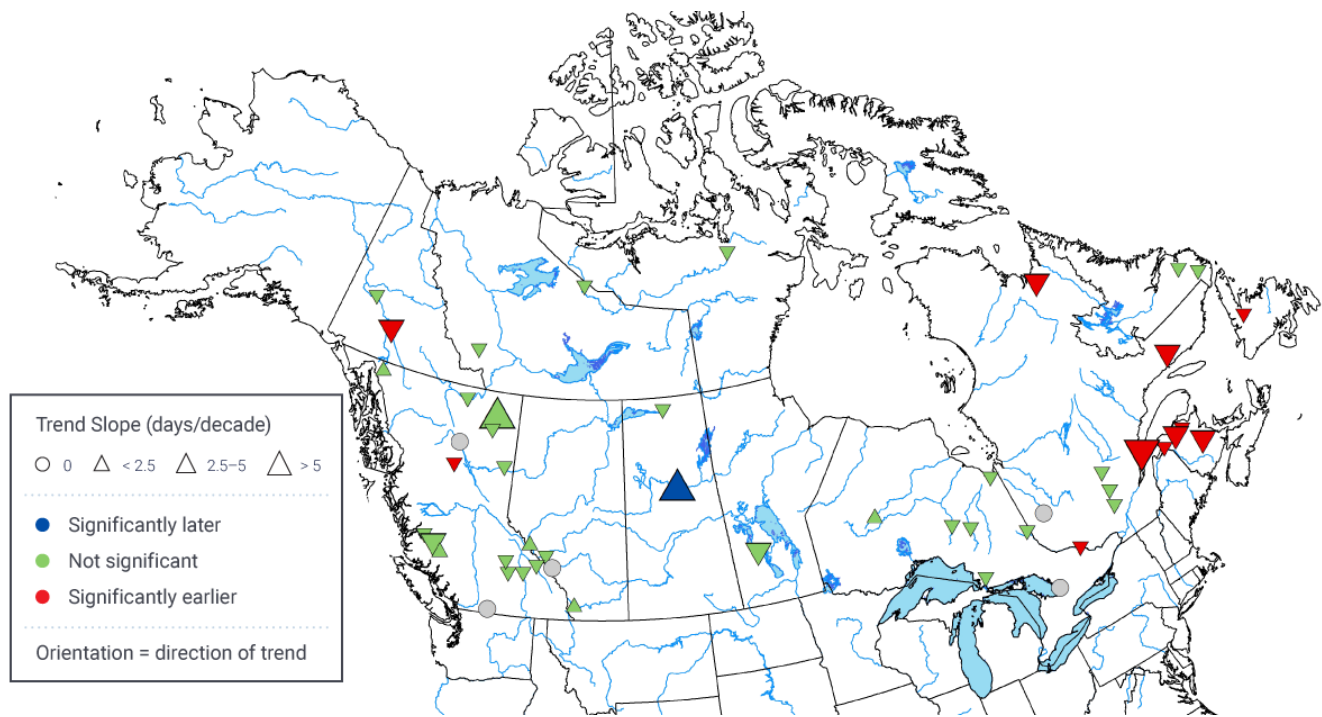


Figure 6.6: Past changes in timing of spring freshet

Figure caption: Trends in spring freshet timing (in days per decade with magnitude proportional to the size of the triangle) for 49 stations in unregulated streams from the Reference Hydrometric Basin Network (RHBN; see Box 6.1). Downward-pointing triangles represent earlier freshets and upward-pointing triangles represent later freshets. Green triangles indicate the trend is not significant. Significant trends denote that there is only a 5% possibility that such changes are due to chance. Data lengths range from 30 to 100 years.

FIGURE SOURCE: MODIFIED FROM JONES ET AL. (2015).

Several regional studies in western Canada, including the Northwest Territories, have also found an earlier onset of spring freshet over the past several decades (Burn et al., 2004a, 2004b; Abdul Aziz and Burn, 2006; Burn, 2008; Rood et al., 2008; Cunderlik and Ouarda, 2009). For example, the Fraser River in British Columbia displayed a trend toward smaller mountain snowpacks and earlier melt onsets that resulted in a 10-day advance of the spring freshet (with subsequent reductions in summer flows) for the 1949–2006 period (Kang et al., 2016). In the Mackenzie Basin (British Columbia, Alberta, and Northwest Territories), spring freshet advanced by approximately 2.7 days per decade over the last 25 years (Woo and Thorne, 2003). These trends are consistent with increasing spring temperatures (see Chapter 4, Section 4.2.1.1) and the resulting earlier spring snowmelt (e.g., DeBeer et al., 2016).

The timing of annual low flows of various durations (one, seven, 15, and 30 days) was significantly earlier in the year over the 1954–2003 period in southern British Columbia, central and southwestern Alberta, central Saskatchewan, much of Ontario, as well as Quebec and the Atlantic provinces. Northern British Columbia, Yukon, Northwest Territories, Nunavut, and the Laurentian Great Lakes region had significant trends toward later dates. Similar spatial results were also observed for winter and summer low flows (Khaliq et al., 2008). For the timing of high flows, summer rainfall-driven peak events in some regions of the Prairies were found to occur earlier (Burn et al., 2008); however, western Canada as a whole showed no consistent trends in the timing of rainfall-dominated high flows (e.g., Cunderlik and Ouarda, 2009).

No Canadian studies have directly attributed change in streamflow timing to anthropogenic climate change. However, since earlier spring freshets are the result of strong winter and spring warming, and most the observed warming in Canada is due to human influence (see Chapter 4, Section 4.2.1.2), there is strong reasoning that observed changes in streamflow seasonality are at least partly attributable to anthropogenic warming. Furthermore, trends toward earlier snowmelt-driven streamflow in the western United States since 1950 (including the Columbia River basin that extends into southern British Columbia) have been attributed to anthropogenic climate warming (Hidalgo et al., 2009).

There are few studies of future streamflow timing in Canada. An earlier snowmelt peak and resulting spring freshet is projected for mid-century (2041–2070) over western Canada, particularly for northern basins, using the Canadian Regional Climate Model and a high emission scenario (A2). For the majority of western Canada basins, this earlier shift was also projected for the end-of-winter low-flow events (Poitras et al., 2011). Earlier spring freshet flows for the mid-century period (2041–2070) are also projected using several CMIP5 models under a medium (RCP4.5) and a high (RCP8.5) emission scenario. Spring freshets are projected to advance by an average of 25 days (RCP4.5 and RCP8.5) in the Fraser River, British Columbia (Islam et al., 2017), and by 15 days (RCP4.5) and 20 days (RCP8.5) for rivers in southern Quebec (CEHQ, 2015). Given the continued spring warming projected for Canada (see Chapter 4, Section 4.2.1.3), earlier spring freshet flows in the future are also probable in other regions of Canada.

6.2.3: Streamflow regime

In a warming climate, the following changes to current streamflow regimes (see Box 6.2) are expected: (1) earlier onset of spring freshet; (2) smaller magnitude of snowmelt events; (3) more rainfall-generated flows; (4) a transition from nival catchments to mixed regimes and from mixed regimes to pluvial regimes (Burn et al., 2016). Regional studies have yielded similar results. For example, trends in southern areas of western Canada (Fraser and Columbia river watersheds) are associated with changes in runoff timing, including a shorter snow- and glacier-melt season, earlier onset of spring melt, and decreased summer flows during approximately the last 50 years (e.g., Rood et al., 2008; Déry et al., 2009). Shifts from nival to mixed or even pluvial regimes were observed for small prairie streams (Burn et al., 2008; Shook and Pomeroy, 2012; Duman-ski et al., 2015).

Box 6.2: Streamflow regimes

Streamflow regime refers to the seasonal distribution of flow, influenced predominantly by the prevailing climate in the region (e.g., Moore et al., 2017). Temperature affects the type of precipitation (rain versus snow), the accumulation of a snowpack, and the timing and amount of ice and snowmelt runoff. Precipitation determines the potential magnitude of flow generated during different periods of the year. In Canada, streamflow regimes are classified as nival (snowmelt-dominated), glacial (glacier-dominated), pluvial (rainfall-dominated), or mixed (see Figure 6.7). Across much of the country, most of the winter precipitation falls as snow and melts during spring and early summer. As a result, the vast majority of rivers are nival (see Figure 6.8). These regimes exhibit high flows in spring and early summer (due to snowmelt), and the timing depends on geographic location (since snowmelt is later farther north or at higher elevations) and on the size of the catchment (see Figure 6.7a). Glacial regimes are confined to mountainous regions of western Canada and the high Arctic islands, where glaciers and ice caps are present. These regimes are associated with an initial snowmelt runoff, followed by continued flow into late summer sustained from ice melt (see Figure 6.7b). Pluvial regimes are driven by the seasonal distribution of rainfall. At lower elevations on the west coast of Canada, this consists of high flows during winter and low flows during summer and autumn (see Figure 6.7c). On the east coast, higher flows are most common in spring and autumn. Combinations of these regimes (known as mixed regimes) are also found in Canada (see Figure 6.7d). For instance, nivo-pluvial regimes are influenced by both snow and rainfall, the exact proportion depending on the location of the stream. In British Columbia, for example, the seasonal flow patterns transition from pluvial (rain-dominated) in coastal/low-elevations to nival (snow-dominated) toward the continental interior of the province and higher elevations (Moore et al., 2017).

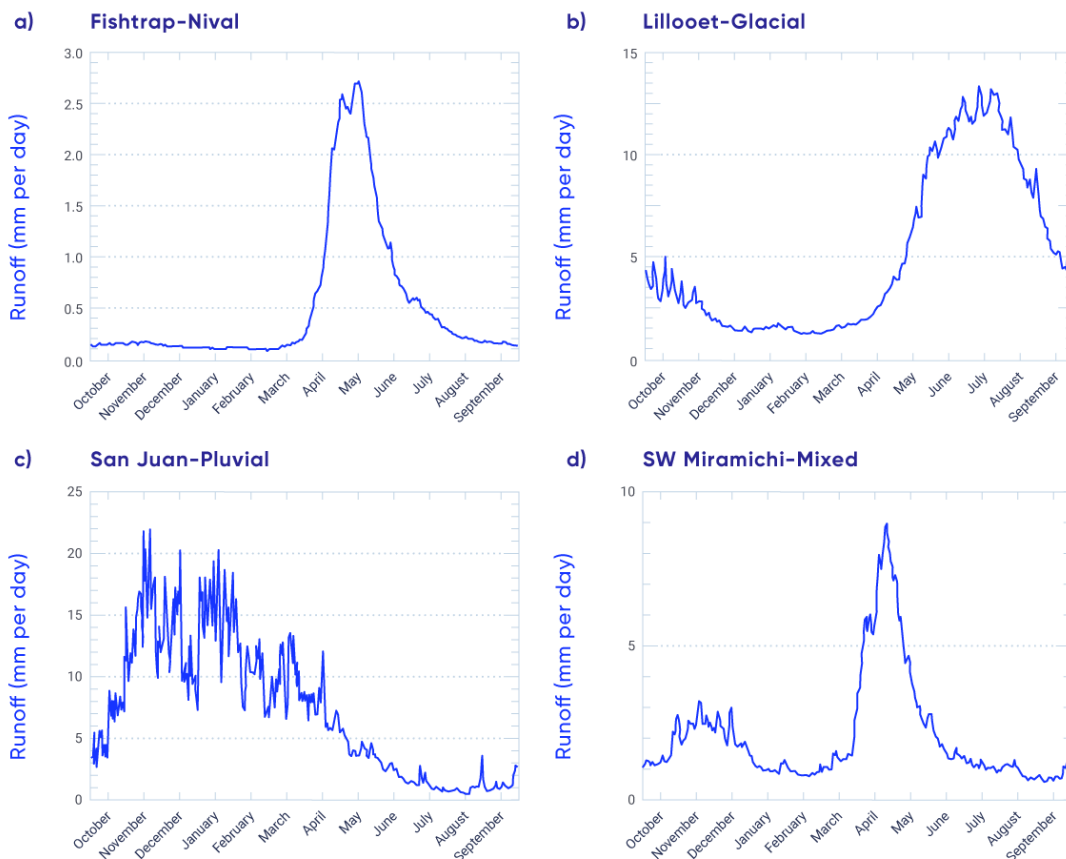


Figure 6.7: Typical streamflow regimes across Canada

Figure caption: Long-term mean amounts of daily runoff for (a) Fishtrap Creek near McLure, British Columbia (nival), (b) Lillooet River near Pemberton, British Columbia (glacial), (c) San Juan River near Port Renfrew, British Columbia (pluvial), and (d) southwest Miramichi River at Blackville, New Brunswick (mixed). All data are for the 1981–2000 period.

FIGURE SOURCE: MODIFIED FROM DÉRY ET AL. (2009) WITH DATA OBTAINED FROM WATER SURVEY OF CANADA (ECCC, 2017; <[HTTPS://WATEROFFICE.EC.GC.CA/](https://wateroffice.ec.gc.ca/)>).

Nival catchments are predominantly found in northern and western Canada, while pluvial basins are located on the east and west coasts, and mixed catchments are mainly in southern Ontario and Quebec and Atlantic Canada (see Figure 6.8). Glacial regimes were not identified in this analysis (Burn et al., 2016). The characterization of regimes is based on longer-term hydroclimatic averages, but, in most of Canada, there is considerable year-to-year variability in these patterns.

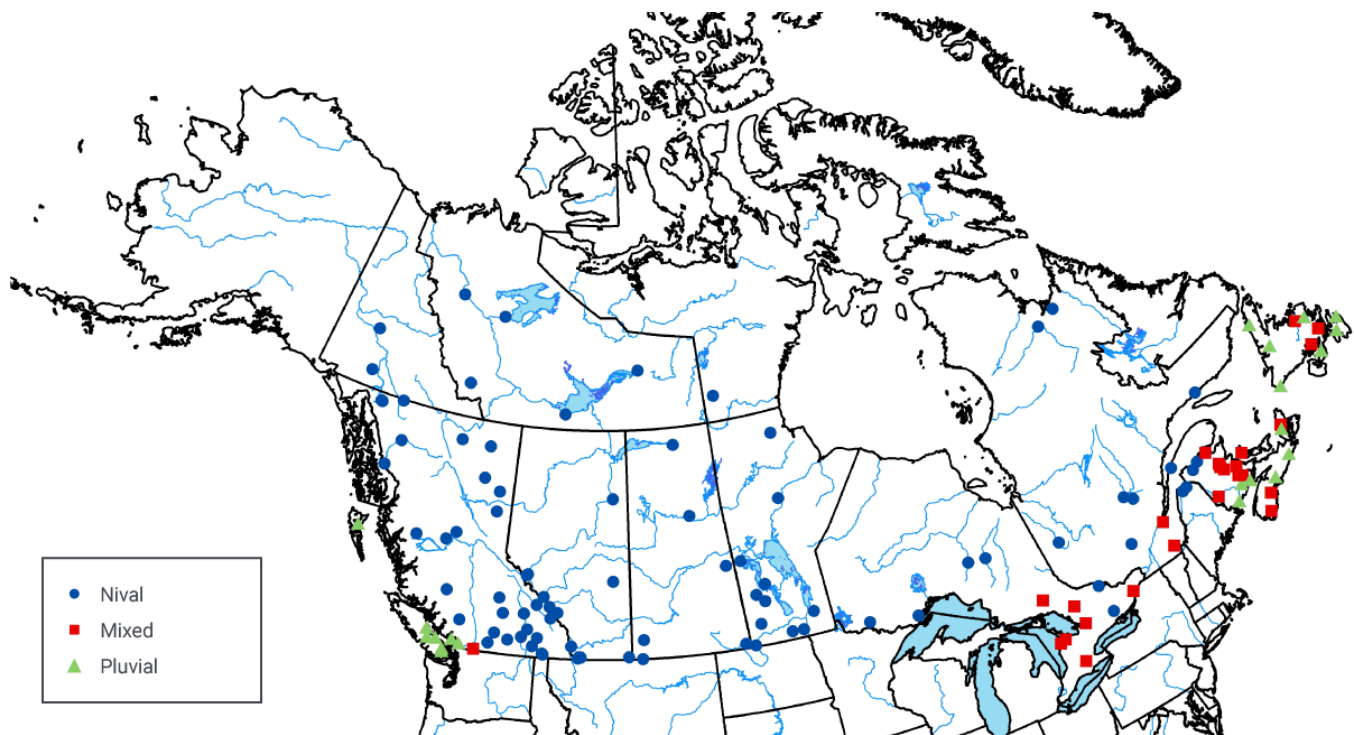


Figure 6.8: Spatial distribution of streamflow regimes across Canada

Figure caption: Locations of nival (snowmelt-dominated), pluvial (rainfall-dominated), and mixed streamflow regimes across Canada based on a subset of Reference Hydrometric Basin Network stations for the 1963–2012 period. Glacial regimes were not identified in this analysis.

FIGURE SOURCE: MODIFIED FROM BURN ET AL. (2016).

6.2.4: Streamflow-related floods

A flood is the overflowing of the normal confines of a stream or other body of water, or the accumulation of water over areas that are not normally submerged. Flooding typically occurs at local to watershed scales. There are several types, including streamflow (fluvial), urban, flash, and coastal flooding (see FAQ 6.1 and, for coastal flooding, Chapter 7, Section 7.5.3; Seneviratne et al., 2012). This section assesses only streamflow-related floods, although implications for urban floods are discussed. The main causes of streamflow floods are intense and/or long-lasting precipitation, snow/ice melt, rain-on-snow, river ice jams, or a combination of these causes. Flood risk is also affected by drainage basin conditions, such as pre-flood water levels in the rivers; the presence of snow and ice; soil character (e.g., whether it is frozen, its moisture content); urbanization; and the existence of dikes, dams, and reservoirs (e.g., Bates et al., 2008).

Streamflow flooding is a common and natural occurrence, but large events are often a costly disaster for Canadians (Buttle et al., 2016; Peters et al., 2016). Given the range of potential drivers, flooding can occur any time of the year somewhere in Canada. Flooding from snowmelt and ice jams typically occurs during the spring but can also result from mid-winter melts. Floods generated by intense and/or excessive rainfall typically occur in late spring and summer, when atmospheric convective precipitation (generally brief but intense rain showers resulting from heat convection forming cumulonimbus clouds) is more common. An example of a costly event was the June 2013 southern Alberta flood, which was driven mainly by extreme rainfall (including rain-on-snow at higher elevations) associated with an intense weather system (Liu et al., 2016; Teufel et al., 2017) (see Chapter 4, Section 4.4.1.1). By contrast, ice jams on the lower Peace and Athabasca Rivers in northern Alberta in 2014 led to widespread inundation of delta wetland areas, which was beneficial to maintaining the aquatic ecosystem in the region (Peters et al., 2016). In 2014 as well, a delayed spring onset of snowmelt and an extremely wet May and June resulted in major flooding in the southeastern Canadian prairies (Szeto et al., 2015).

Different areas of Canada are classified according to the type of floods they generally experience. Across the country, 32% of 136 stream gauge sites (1913–2006) are classified as spring freshet/ice breakup flood-dominated, 42% as open-water flood-dominated (i.e., during the warm season), and 23% as a mix of these two classes. The timing of ice-influenced peak water levels and ice breakup (which can lead to flooding) has shifted earlier since the late 1960s (von de Wall et al., 2009; 2010) (see also Chapter 5, Section 5.5). There are also areas of Canada, such as the Saint John River, New Brunswick, where floodplains have been subject to more frequent mid-winter ice jams and higher April flows, both of which increase the risk of major flooding (Beltaos, 2002). However, more recent analyses of both spring freshet- and open-water flood-dominated rivers across Canada revealed that changes in magnitude, timing, number, and duration of high-flow events showed varying trends across Canada, increasing in some cases and decreasing in others. For nival catchments, this included trends toward smaller and earlier flood events; both consistent with a reduction in winter snowpack (Burn and Whitfield, 2016). In addition, examination of the seasonality of past flood regimes in 132 RHBN stations over four periods ranging from 50 to 80 years revealed the decreased importance of snowmelt flood events and the increased importance of both rain-on-snow and rainfall-driven flood events (Burn et al., 2016). To the authors' knowledge, no studies have assessed past trends in urban flooding across Canada.

Complex interactions among the many factors that lead to streamflow floods complicate the attribution of these events to anthropogenic climate change. An event-attribution study of the 2013 southern Alberta flood determined that human-induced warming increased the likelihood of extreme precipitation, at least as large as the amount observed during this event (Teufel et al., 2017). However, since the flood resulted from a combination of many meteorological and hydrological factors, human influence could not be detected for the flood itself (see Chapter 4, Section 4.4.1.1). Similarly, an event-attribution study of the 2014 flood in the south-eastern prairies was unable to detect human influence on that flood, owing to multiple contributing factors (Szeto et al., 2015).

It is expected that a changing climate will impact several of the factors affecting future streamflow flood occurrence (see FAQ 6.1). These include precipitation amount, type, and intensity; the amount and duration of snow cover; the timing and frequency of ice jams; and the potential for rain-on-snow events. However, interactions between flood-generating factors at the watershed scale lead to large uncertainties regarding the frequency and intensity of future floods (Whitfield, 2012). Some studies have suggested that the contribution of snowmelt to spring floods is expected to generally decline due to depleted snowpacks (e.g., Whitfield and Cannon, 2000; Zhang et al., 2001; Peters et al., 2006). However, there are only a few watershed-scale studies on future streamflow flooding (and/or their related factors) in Canada, which use climate model projections as input into a hydrological model. For example, depletion of the snowpack by mid-winter melt events are projected to lead to a major reduction in the frequency of spring ice jam flooding, but could increase the potential for mid-winter ice jam flooding in the Peace–Athabasca delta in northern Alberta (Beltaos et al., 2006). Two British Columbia watersheds, one on the coast and one in the interior, are both projected to experience increased flooding potential, due to more rainfall and winter rain-on-snow events in the coastal watershed and to more spring rain and more rapid snowmelt events in the interior watershed (Loukas et al., 2000; 2002). For the Red River Basin in Manitoba, snow accumulation during winter is expected to decrease, while rainfall is expected to increase during the snowmelt period. However, due to the variability among climate models, it is difficult to project whether flood magnitude will increase or decrease (Rasmussen, 2015). In the Châteauguay watershed in Quebec, spring, summer, and autumn peak flood events are projected to be reduced in magnitude under a medium emission scenario (B2), but there are large differences among the three models used (Mareuil et al., 2007). The only study of projected changes in rain-on-snow events suggested general increases in these events from November to March for most of Canada by mid-century (2041–2070) for both medium (RCP4.5) and high (RCP8.5) emission scenarios (Jeong and Sushama, 2018). To the authors' knowledge, no studies have assessed projected changes to urban floods across Canada; however, increases in extreme precipitation are considered a factor that will affect their future occurrence (e.g., Buttle et al., 2016; Sandink, 2016).

FAQ 6.1: Will there be more droughts and floods in Canada in a warmer climate?

Short Answer:

When droughts and floods occur, there are usually multiple contributing factors. This makes projecting future changes in these events very challenging. Some contributing factors will be affected by human-induced climate warming, and some will change due to other human influences (such as changes to the landscape). As well, natural climate variability will continue to play a role. As temperatures rise, the threat of drought will increase across many regions of Canada. Projected increases in extreme rainfall in a warmer climate are expected to increase the likelihood of rain-generated flooding in some regions. Snowmelt-related floods are expected to occur earlier in the year, but it is uncertain how projected warming and reductions in snow cover will combine to affect their frequency and magnitude.

Long Answer:

As temperatures rise, the threat of drought is projected to increase across many regions of Canada. This includes the southern Canadian prairies and the interior of British Columbia, as well as regions that depend on snowmelt and/or glacial meltwater for their main dry-season water supply. However, there is considerable uncertainty in future drought projections. Similarly, while future warming is expected to affect future factors causing floods, such as extreme precipitation, and the amount and timing of snow/ice melt, it is not straightforward how these changes will interact to affect the frequency and magnitude of future floods across Canada.

Warmer air can hold more moisture. Therefore, in a warmer world, the hydrological cycle is expected to become more intense, with more rainfall concentrated in extreme events and longer dry spells in between (e.g., Houghton, 2004). Water availability in Canada is naturally variable, with periodic droughts and floods. Whether both dry and wet extremes will increase in the future in Canada as a result of anthropogenic climate change is a question that challenges climate change adaptation.

Droughts

In a warmer world, most climate models project more frequent, longer-lasting warm spells; overall increased summer dryness in the middle-interior regions of North America; and earlier, less-abundant snowmelt (e.g., Trenberth, 2011). Since Canada is projected to warm in all seasons under a range of emission scenarios, drought risk is expected to increase in many regions of the country. In summer, higher temperatures cause increased evaporation, including more loss of moisture through plant leaves (transpiration). This leads to more rapid drying of soils if the effects of higher temperatures are not offset by other changes (such as reduced wind speed or increased humidity) (Sheffield et al., 2012). How much summer droughts will increase in frequency and intensity depends on whether future summer precipitation will offset increased evaporation and transpiration. Current climate models suggest that the southern Canadian prairies and the interior of British Columbia will be at a higher risk for drought in the future, but there is considerable uncertainty in future drought projections. Smaller snowpacks and earlier snow and ice melt associated with warming temperatures could increase drought risk in the many snowmelt-fed basins across Canada that rely on this water source, as well as in regions that depend on glacial meltwater for their main dry-season water supply (e.g., Barnett et al., 2005). Therefore, as temperatures rise, the threat of drought will increase across many regions of Canada.

Floods

Flooding typically occurs at local to watershed scales. There are several types of floods that affect Canadians, but the most damaging are those related to rivers and those in urban areas (sometimes associated with river flooding). In Canada, the main causes of river floods are intense and/or long-lasting precipitation, snow/ice melt (including rain on snow), river ice jams, or a combination of these causes. Changes to the landscape, such as deforestation (including that caused by fires and tree diseases) and wetland drainage, exacerbate river floods. Urban flooding is usually caused by short-duration intense rainfall events (e.g., those associated with thunderstorms). Urbanization creates large areas of impervious surfaces (roads, parking lots, buildings) that increase immediate runoff, and heavy downpours can exceed the capacity of storm drains (Melillo et al., 2014).

While future warming is expected to affect flood-causing factors, it is not straightforward how these changes will interact to affect the frequency and magnitude of future floods across Canada. Projected increases in extreme precipitation (see Chapter 4) are expected to increase the likelihood of rain-generated urban flooding in some regions. Furthermore, when extreme rainfall occurs in drought-stricken areas, the drier and more compact soils are less able to absorb water, thus increasing the likelihood of overland flow and the potential to cause flooding (e.g., Houghton, 2004). Projected higher winter and spring temperatures will result in changes to the timing of snow and ice melt and imply a higher potential for rain-on-snow events. The potential for river-ice jams may also increase as a result of winter thaws. However, given that warmer temperatures will be associated with smaller snowpacks, it is unclear how warming will affect the frequency and magnitude of future snowmelt-related floods (e.g., Whitfield, 2012). Nonetheless, snowmelt-related floods are expected to occur earlier in the year, on average, in association with higher temperatures. Some evidence for this shift to earlier flood events following snowmelt has already been observed in some Canadian streams over the last few decades (Burn and Whitfield, 2016).



Questions for future research

Climate change may also affect weather patterns and storms. For example, climate models predict changes in phenomena that can cause extreme precipitation events, such as atmospheric rivers (narrow bands of concentrated moisture in the atmosphere that enter western Canada from the Pacific Ocean; e.g., Radic et al., 2015), and rapidly intensifying storm systems (sometimes referred to as “weather bombs”; e.g., Seiler et al., 2018). These changes could influence the future occurrence and location of floods in Canada. In addition, naturally occurring modes of climate variability, including El Niño–Southern Oscillation, the Pacific Decadal Oscillation, and the North Atlantic Oscillation, have been shown to influence Canadian droughts and floods (e.g., Bonsal and Shabbar, 2008). Anthropogenic climate change may result in changes to these modes of climate variability over the 21st century, thus affecting future droughts and floods in Canada. All of these topics are active areas of research.

Section summary

In summary, numerous regional and a few national studies have examined past changes to surface runoff over the last several decades. Most have incorporated RHBN stations (see Box 6.1), thus minimizing the effects of water regulation. There is high agreement among these analyses – and thus *high confidence* – that the spring freshet has shifted earlier, with higher winter and early-spring flows (see Table 6.1 and Figure 6.6). There is less evidence – and thus *medium confidence* – that summer flows have decreased, which has been mainly documented in western Canada (see Table 6.1). All of these changes are consistent with the observed winter and spring warming (see Chapter 4, Section 4.2.1.1) and resulting changes to snow cover, including less snow at higher elevations, which often sustains summer runoff (see Chapter 5, Section 5.2.1). They also may be partly attributed to anthropogenic climate change. National and regional studies on past annual flow revealed little consistency across Canada (see Table 6.1) and generally reflect regional variations in precipitation and natural climate variability (see Chapter 2, Section 2.3.3).

Given the projected warming (see Chapter 4, Section 4.2.1.3) and resulting reductions in snow cover and mountain glaciers and increased permafrost thaw (see Chapter 5), there is *high confidence* that the observed seasonal changes in streamflow will continue. Consistent evidence for these projected changes, characterized by even earlier spring freshets, higher winter flows, and reduced summer flows, is provided in numerous regional studies (see Table 6.2). These changes in physical climate are expected to cause streams to shift from nival (snowmelt-dominated) toward pluvial (rainfall-dominated) regimes. There are, however, large uncertainties in the magnitude of projected changes. Regional studies project both increases and decreases in annual streamflow, with increases mainly in more northern basins, and decreases mainly in western interior basins (see Table 6.2 and Figure 6.5). Due to modelling uncertainties, and the complexity of factors associated with annual flow, there is *medium confidence* in these projected annual changes.

Streamflow-related floods result from many factors, including intense and/or long-lasting precipitation, snowmelt, ice jams, rain-on-snow, or a combination of these factors. Studies reveal no spatially consistent trends in these factors, including extreme one-day high streamflow events (see Figure 6.3), across the country. There is also no indication of spatially consistent trends in streamflow-related or urban flooding events for Canada as a whole. It is expected that a changing climate will affect these flood-causing factors in various ways. For example, although no studies assessing future changes to urban floods were identified, it follows directly – and thus there is *high confidence*, – that projected increases in extreme precipitation (see Chapter 4, Section 4.3.2.2) will result in a higher incidence of rain-generated urban flooding in some regions. Projected higher temperatures (see Chapter 4, Section 4.2.1.3) suggest a shift toward earlier snowmelt-related floods, including those associated with spring snowmelt, ice jams, and rain-on-snow events. This shift is consistent with observed earlier spring freshet trends (see Section 6.2.2) and with a few studies that have found trends toward earlier snowmelt-related flood events and earlier ice-affected peak streamflow levels during the last few decades. However, given the complexity of factors associated with snowmelt-related flooding, and the limited studies, there is only *medium confidence* in this shift. There is considerable uncertainty as to how these higher temperatures and reductions in snow cover (see Chapter 5, Section 5.2.2) will affect the frequency and magnitude of future snowmelt-related floods. Smaller snowpacks imply that the contribution of snowmelt

to flooding will decline, including floods induced by river ice jams or rain-on-snow events. Individual studies have identified smaller snowmelt-related flood events in some nival catchments across the country during the last few decades and a projected decrease in future ice-jam flooding in the Peace-Athabasca Delta due to smaller snow packs. Warmer temperatures also imply a higher potential for rain-on-snow, and one study has shown projected increases in these events across Canada. However, given that snowpacks are expected to be smaller in the future, it is uncertain whether an increase in rain-on-snow will lead to greater flood potential. As a result, there is a lack of consistent evidence regarding the effects of climate change on future snowmelt-related flooding across the country.

6.3: Surface water levels: lakes and wetlands

Key Message

In regions of Canada where there are sufficient data, there is no indication of long-term changes to lake and wetland levels. Future levels may decline in southern Canada, where increased evaporation may exceed increased precipitation (*low confidence*). Projected warming and thawing permafrost has the potential to cause future changes in many northern Canadian lakes, including rapid drainage (*medium confidence*).

Canada has more than 2 million lakes covering 7.6% of the country's area, with 578 having an area greater than 100 km² (Canadian National Committee, 1975; Monk and Baird, 2011). There is a wide range of lake types, including the Laurentian Great Lakes (Superior, Michigan, Huron, Erie, and Ontario) and Mackenzie Great Lakes (Great Slave and Great Bear), Arctic and sub-Arctic lakes, glacial, boreal, prairie, and shallow enclosed saline lakes (Schertzer et al., 2004). Some lake levels are monitored by Canada's Hydrometric Network (see Box 6.1). Other than in a select few cases, there is limited information on past trends and projected future changes in lake levels. Furthermore, many of the larger lakes are regulated by humans, and there is no comprehensive national dataset for unregulated lakes. Thus, a Canada-wide assessment of past trends and future changes is challenging. This section focuses on major lakes and water bodies, reflecting the available literature and monitoring data.

The levels of freshwater lakes and wetlands are governed by a simple equation:

$$\text{Inputs} - \text{Outputs} = \text{Change in storage (i.e., water level, or net basin supplies [NBS])}$$

The main inputs include river inflow (runoff), direct precipitation onto the water body, snowmelt, and groundwater inflow. Outputs involve river outflow, evaporation, and exchange with groundwater. The contribution from these variables varies greatly with the size of the water body. Larger lakes within very large drainage basins are affected by events far upstream, in addition to local/regional climate. Smaller lakes and wetlands are more responsive to local climatic conditions. Surface water bodies in Canada are becoming increasingly vulnerable to a variety of stresses, both climate-related and from human management (flow regulation and land-use change) (e.g., Schertzer et al., 2004).

6.3.1: Laurentian Great Lakes

Given their importance to Canada and the United States, the Laurentian Great Lakes are among the most studied water bodies in North America. Levels of these lakes have been monitored for more than 100 years by Canadian and US federal agencies. The levels show a large degree of variability due to natural climate variations, as well as to direct human management (e.g., dredging, diversions). These fluctuations have significant impacts on shoreline erosion, flooding of property, navigation, recreation, economy, aquatic ecosystems, and human health. Seasonally, water levels typically progress from a summer maximum to a minimum in the winter/spring (Argyilan and Forman, 2003). The lakes also exhibit year-to-year and multi-year fluctuations of less than 2.0 m, varying by lake (Wilcox et al., 2007; DFO, 2013).

All of the Laurentian Great Lakes have experienced considerable variability in overall NBS and its primary individual components (basin-wide precipitation, lake evaporation, and river runoff) during the last several decades (see Figure 6.9). This year-to-year and multi-year variability is significantly influenced by naturally occurring large-scale modes of climate variability including PDO, AO, and the Atlantic Multi-decadal Oscillation (see Chapter 2, Box 2.5) (e.g., Ghanbari and Bravo, 2008; Hanrahan et al., 2010). Given the large geographic expanse of the Laurentian Great Lakes basin, trends in NBS and individual components vary from one lake to another. In Lake Superior, evaporation is increasing and runoff is decreasing, resulting in a significant decrease in NBS. These trends are also seen for Lake Erie (although not at statistically significant levels). In Lake Ontario, NBS has increased significantly, mainly due to increases in precipitation and runoff, although changes in these individual components are not significant. For the other lakes, trends are insignificant and mixed. For example, runoff is declining for Lake Erie, but rising for Lakes Michigan, Huron, and Ontario. Evaporation has increased over the last 70 years in Lakes Superior and Erie but shows relatively little change in the other lakes (although values have been higher since around 1998). Precipitation has increased in Lake Ontario but decreased in Lake Superior, while no trend is evident in the other lakes.

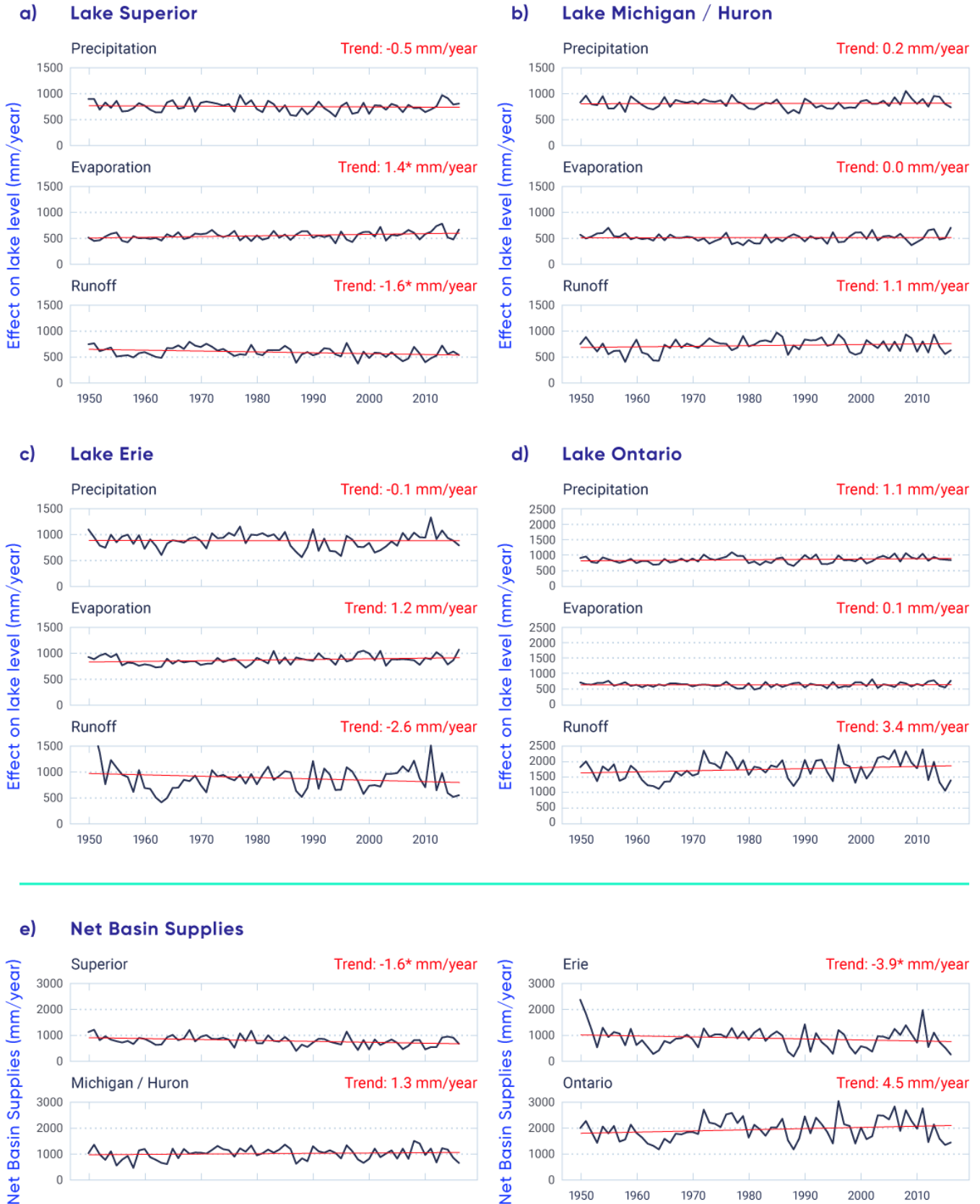


Figure 6.9: Historical time series for water variables, Laurentian Great Lakes, 1950–2016

Figure caption: Time series of mean over-lake precipitation, evaporation, and river runoff (measured as the effect on lake level) for the 1950–2016 period for (a) Lake Superior, (b) Lakes Michigan/Huron, (c) Lake Erie, and (d) Lake Ontario. (e) Time series of net basin supplies (NBS) for the 1950–2016 period for Lakes Superior, Michigan/Huron, Erie, and Ontario. Red lines and text represent linear trends. *Significant trends (there is only a 5% possibility that such changes are due to chance). Lakes Michigan and Huron are connected by the Straits of Mackinac and thus have the same water level. They are therefore considered as one lake.

From 1998 to 2013, all the Laurentian Great Lakes experienced a long period of low levels, including record lows in Lakes Michigan and Huron in December 2012 and January 2013. This period ended with a quick rise in all lake levels starting in 2013. September 2014 was the first month since 1998 that all lakes were above long-term (1918–2013) average levels. The 2013 rise was attributed to increased precipitation, while the 2014 rise resulted from a combination of below-average evaporation and above-average precipitation and runoff (Gronewold et al., 2016). During spring 2017, a series of above-average precipitation events caused the level of Lake Ontario to reach its highest level since reliable measurements began in 1918 (IJC, 2017). These two opposite extremes, occurring within a few years of each other, reveal the variability in the Laurentian Great Lakes' levels and illustrate the difficulty in projecting future lake levels in response to climate change.

Most studies of future levels have been based on CMIP3 GCM projections (see Chapter 3, Box 3.1) that have been run through RCMs (Angel and Kunkel, 2010; Hayhoe et al., 2010; IUGLS, 2012; MacKay and Seglenieks, 2013). RCMs are essential for modelling the Laurentian Great Lakes, since their finer spatial resolution (typically around 50 km versus GCM grids of around 200 to 250 km; see Chapter 3, Section 3.5) allows explicit modelling of the individual lakes. As a result, models include phenomena that can have significant effects on water balance, such as lake-effect snow, which transfers large amounts of water from the lake to the land surface. Projected NBS shows considerable changes to the seasonal cycle of Lakes Michigan and Huron for 2041–2070 compared with 1961–2000 (see Figure 6.10). These changes include an increase in NBS during the winter and early spring and a decrease in summer and early fall, largely due to projected changes in seasonal precipitation. Other lakes have similar results. Overall, these projected seasonal changes are expected to result in a decrease in NBS of 1.7% to 3.9% in Lakes Superior, Michigan, Huron, and Erie, and of 0.7% in Lake Ontario (IUGLS, 2012). On average, under a range of emission scenarios, most RCM studies project a lowering of future lake levels by 0.2 m for the 30-year time period centred on the 2050s, as compared to the 1971–2000 mean. However, there is a considerable range (from a 0.1 m increase to a 0.5 m decrease) (Angel and Kunkel, 2010; Hayhoe et al., 2010; IUGLS, 2012). These changes are less than those projected using statistically downscaled GCM output that does not incorporate the individual lakes (MacKay and Seglenieks, 2013). All studies agree that there will continue to be large year-to-year and multi-year variability in lake levels, possibly even above and below the historically observed extremes (IUGLS, 2012; Music et al., 2015).

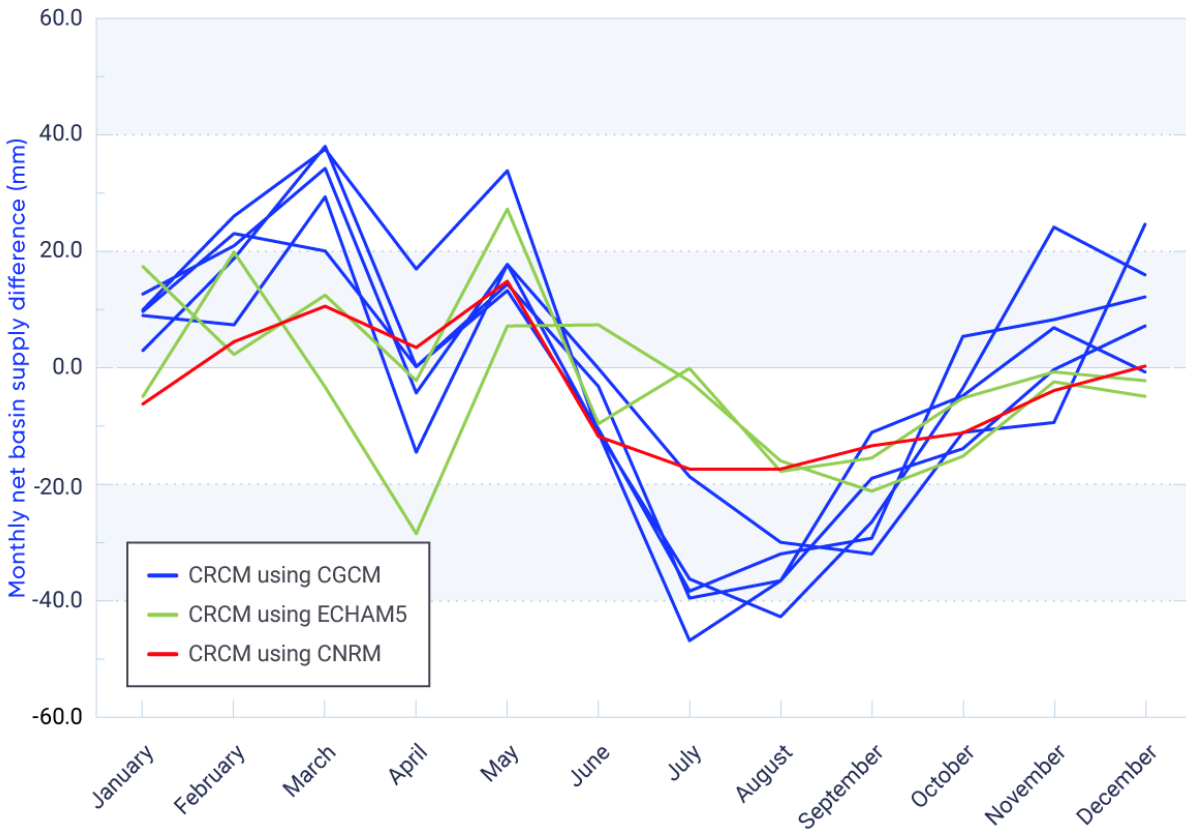


Figure 6.10: Differences in future monthly Lake Michigan/Huron net basin supply

Figure caption: Difference in monthly Lake Michigan/Huron net basin supply (NBS) between 2041–2070 and 1961–2000 using the Canadian Regional Climate Model (CRCM) driven by three global climate models used in the third phase of the Coupled Model Intercomparison Project (CMIP3): Canadian Global Climate Model version 3 (CGCM) (five separate simulations), ECHAM Climate Model version 5 (ECHAM5) (two separate simulations), and Centre National de Recherches Meteorologiques version 5.1 (CNRM) (one simulation).

FIGURE SOURCE: ADAPTED FROM IUGLS, 2012.

6.3.2: Other lakes

Although levels of most other large lakes in Canada (e.g., Lakes Winnipeg, Athabasca, and Great Slave Lake) are monitored, these lakes are influenced by human regulation, making it difficult to assess past climate-related trends. An exception is Great Bear Lake in the Northwest Territories, which is unregulated. Figure 6.11 illus-

trates recurring high and low levels of this lake, with no discernible long-term trend. The levels have varied, in part, due to regional climatic conditions. In particular, the driest years were in the late 1940s and early 1950s, when water levels reached an all-time low, with another low recorded in the mid-1990s. The wettest years and highest levels were in the early to mid-1960s, with another peak in the early 1970s (MacDonald et al., 2004).

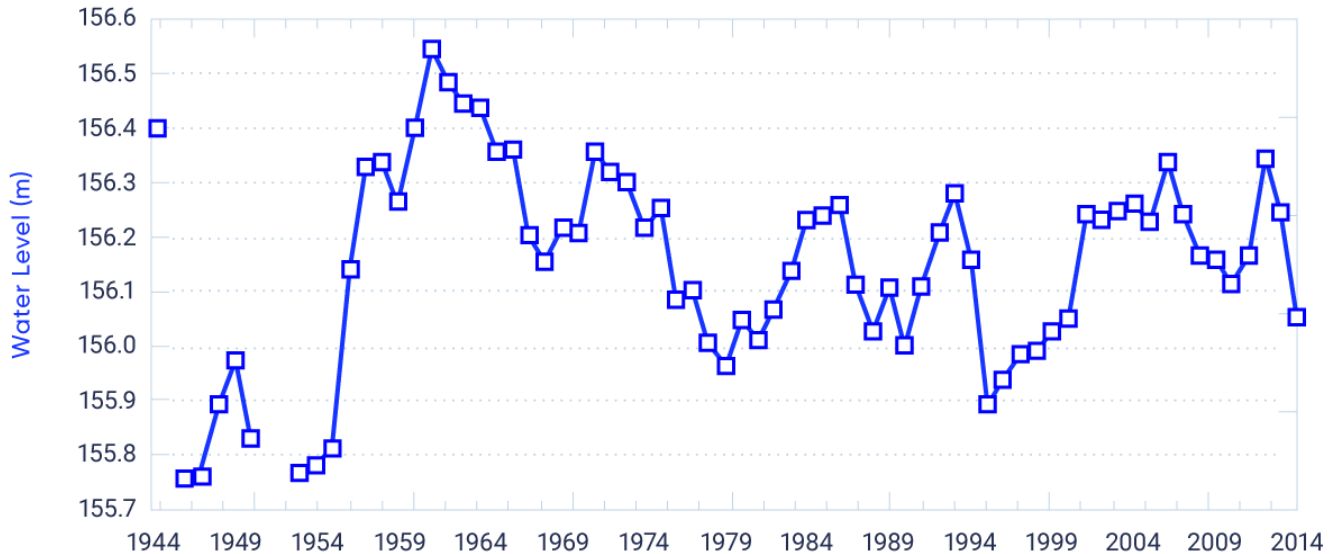


Figure 6.11: Water levels for Great Bear Lake, 1944–2014

Figure caption: Annual (September to August) surface water levels for Great Bear Lake from 1944 to 2014.

FIGURE SOURCE: ORIGINAL FIGURE FROM MACDONALD ET AL. (2004) <[HTTP://WWW.DFO-MPO.GC.CA/LIBRARY/278592.PDF](http://www.dfo-mpo.gc.ca/library/278592.pdf)>. THE FIGURE HAS BEEN MODIFIED AND UPDATED THROUGH 2014 USING DAILY FLOW LEVEL DATA OBTAINED FROM WATER SURVEY OF CANADA (ECCC, 2017) <[HTTPS://WATEROFFICE.EC.GC.CA/](https://wateroffice.ec.gc.ca/)>.

In the Prairie region, glaciation and dry climate have resulted in numerous closed-basin saline lakes, which drain internally and rarely spill runoff. Water storage in these lakes is sensitive to climate, driven by precipitation, local runoff, and evaporation. From 1910 to 2006, levels in several closed-basin lakes across the Prairie region showed an overall decline of 4 to 10 m (see Figure 6.12), due, in part, to higher warm-season temperatures (and resulting increased evaporation) and declining snowmelt runoff to the lakes. However, climate variables alone did not explain the declines, and other contributing factors, such as land-use changes (dams, ditches, wetland drainage, and dugouts) and changes in agricultural practices, were also involved (van der Kamp et al., 2008). From the late 2000s through 2016 (see Figure 6.12), there has been an abrupt reversal in



levels of many of these lakes (a rise of as much as 6 to 8 m), reflecting the exceptionally wet conditions on the Prairies over these years (e.g., Bonsal et al., 2017). The reversal has resulted in several cases of overland flooding, exemplifying the natural hydroclimatic variability in this region and the susceptibility of surface water bodies to precipitation extremes, both dry and wet. Although no studies have investigated future climate impacts on these lake levels, they will continue to be affected by dry and wet extremes. However, given the projected higher temperatures (see Chapter 4, Section 4.2.1.3) and resulting increased evaporation, future levels are expected to decline, although the magnitude will depend on how much future precipitation increases will offset evaporation.

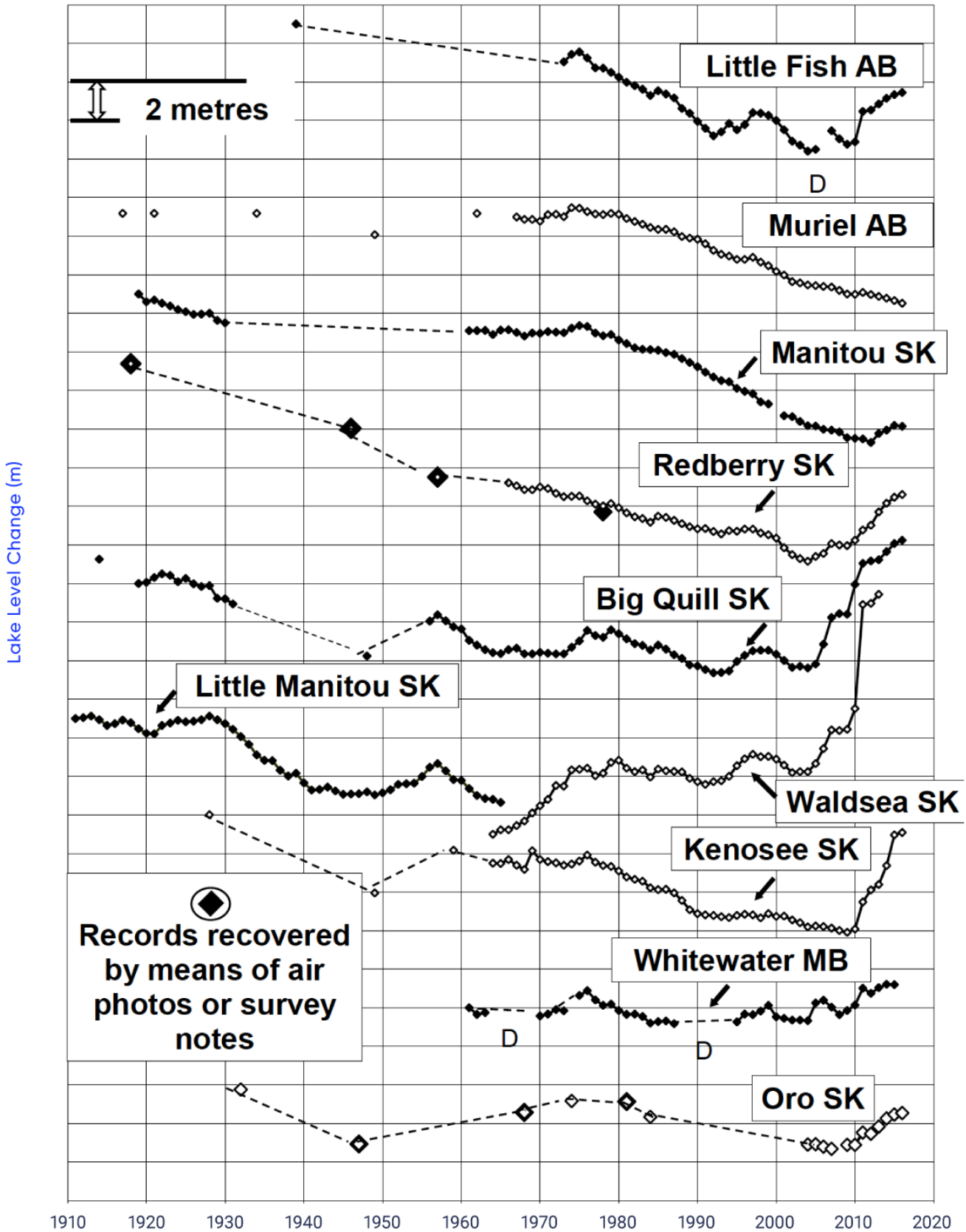


Figure 6.12: Water-level changes for 10 representative lakes across the southern Canadian prairies, 1910–2016

Figure caption: Relative water-level changes for 10 representative closed-basin lakes across the southern Canadian Prairies for their period of record. Dashed lines connecting separated data points are not representative of measured water levels between the points. "D" indicates that the lake was dry at the time of measurement.

FIGURE SOURCE: VAN DER KAMP ET AL. (2008); DATA UPDATED THROUGH 2016.

Smaller lakes and ponds are a characteristic feature of the Canadian Arctic, with large numbers of permafrost thaw lakes found in northern Yukon and the Northwest Territories (see Chapter 5, Section 5.6). These water bodies are variable in size, with diameters of 10 to 10,000 m and depths of 1 to 20 m (Plug et al., 2008; Vincent et al., 2012). Warming due to Arctic amplification at high latitudes can affect the size of permafrost lakes. In particular, those in continuous permafrost may expand due to acceleration of the permafrost thaw processes that formed them, whereas those in discontinuous permafrost (i.e., patches of permafrost) may shrink and even disappear due to rapid drainage as the underlying permafrost completely thaws (e.g., Hinzman et al., 2005; Smith et al., 2005). Some evidence for these processes has been observed in certain high-latitude regions, including Canada. For example, total lake area in the Old Crow Flats (Yukon) declined by approximately 6000 hectares between 1951 and 2007, with close to half of this loss being caused by rapid and persistent drainage of 38 large lakes. This drainage also resulted in the formation of numerous smaller residual ponds. Catastrophic lake drainages in this region have become more than five times more frequent in recent decades, and it has been suggested that these changes are associated with increases in regional temperature and precipitation (Lantz and Turner, 2015). This observation is consistent with local perceptions that lakes in the Old Crow Flats are showing declining water levels (e.g., Wolfe et al., 2011). However, other Canadian Arctic studies have revealed mixed results. For example, aerial photographs and topographic maps showed that, in a 10,000 km² region east of the Mackenzie delta in the Northwest Territories, 41 lakes drained between 1950 and 2000, but the rate of drainage has decreased over time (Marsh et al., 2009). Similarly, total lake area on the Tuktoyaktuk Peninsula on the Arctic Ocean coast of the Northwest Territories from 1978 to 2001 ranged from a 14% increase to an 11% decrease. The increases occurred primarily between 1978 and 1992 and decreases between 1992 and 2001, depending strongly on annual precipitation (Plug et al., 2008).

Future warming and further permafrost thaw (see Chapter 5, Section 5.6.2) are anticipated to have a substantial impact on surface water in the Arctic. Permafrost thaw lakes currently have natural cycles of expansion, erosion, drainage, and reformation (e.g., van Huissteden et al., 2011), which may accelerate under warmer climate conditions. GCMs project increased precipitation over the Canadian Arctic (see Chapter 4, Section 4.3.1.3); however, these increases will be partially offset by greater evaporation due to both warmer temperatures in summer and decreased duration of ice cover. In addition, many high Arctic lakes depend on year-round snow and glaciers and are thus vulnerable to the rapid warming of the cryosphere. As a result, the extent of northern lakes is highly vulnerable to change as a result of increased water loss from evaporation and/or drainage (e.g., Vincent et al., 2012).

6.3.3: Wetlands and deltas

Wetlands are land saturated with water all or most of the time, with poorly drained soils and vegetation adapted to wet environments. They are often associated with standing surface water, and depths are generally less than 2 m. Canada has approximately 1.5 million km² of wetlands – commonly referred to as swamps, marshes, bogs, muskegs, ponds, and sloughs – representing about 16% of the country's landmass (National Wetlands Working Group, 1988, 1997). The majority of wetlands are peatlands in the Arctic, sub-Arctic, boreal, prairie, and temperate regions (van der Kamp and Marsh, 2004). Canada also has several deltas that form from sediments deposited by rivers entering a large lake or ocean. The most prominent examples include the Mackenzie (with more than 25,000 shallow lakes and wetlands), Fraser, Peace–Athabasca, Slave, Saskatchewan, and St. Clair river deltas. Critical to the resilience of delta ecosystems are occasional low- and high-water events. High-water events can result in overland flow (ice jam and open-water flooding) and are a crucial source of water replenishment to disconnected water bodies perched above the main flow system (see below; Peters et al., 2013).

By storing water and releasing it slowly, wetlands and deltas are important to Canada's freshwater availability. Under certain conditions, wetlands can alleviate floods, maintain groundwater levels and streamflow, filter sediments and pollutants, cycle nutrients, and sequester carbon (Federal, Provincial and Territorial Governments of Canada, 2010). They are closely linked with climate, as they gain water from direct precipitation, runoff from surrounding uplands, and groundwater inflow. They lose water via evapotranspiration and surface/groundwater outflow. Some wetlands also owe their existence in part to cold Canadian winters and resulting permafrost, snowmelt, and river ice jams. Thus, both shorter winters and increased evaporation due to longer summers will increase stress on wetland environments, unless increases in precipitation offset the loss of water through evaporation (van der Kamp and Marsh, 2004).

Despite the importance of wetlands, a comprehensive inventory or monitoring program for the entire country does not exist (Fournier et al., 2007). However, since 1979, Ducks Unlimited Canada has used aerial photography and satellite imagery to inventory millions of hectares of wetlands across Canada. In addition, the US Fish and Wildlife Service produces an annual report that summarizes the status of North American waterfowl populations and their habitats, with input from Canada (US Fish and Wildlife Service, 2017). Figure 6.13 shows Canadian prairie pond counts during May from 1961 to 2017. The series shows substantial multi-year variability and no long-term trends. The levels closely correspond to long-term precipitation variability in the region. In many regions of Canada, wetlands are being lost due to land conversion, water-level control, and climate change (e.g., Watmough and Schmoll, 2007; Ducks Unlimited Canada, 2010).

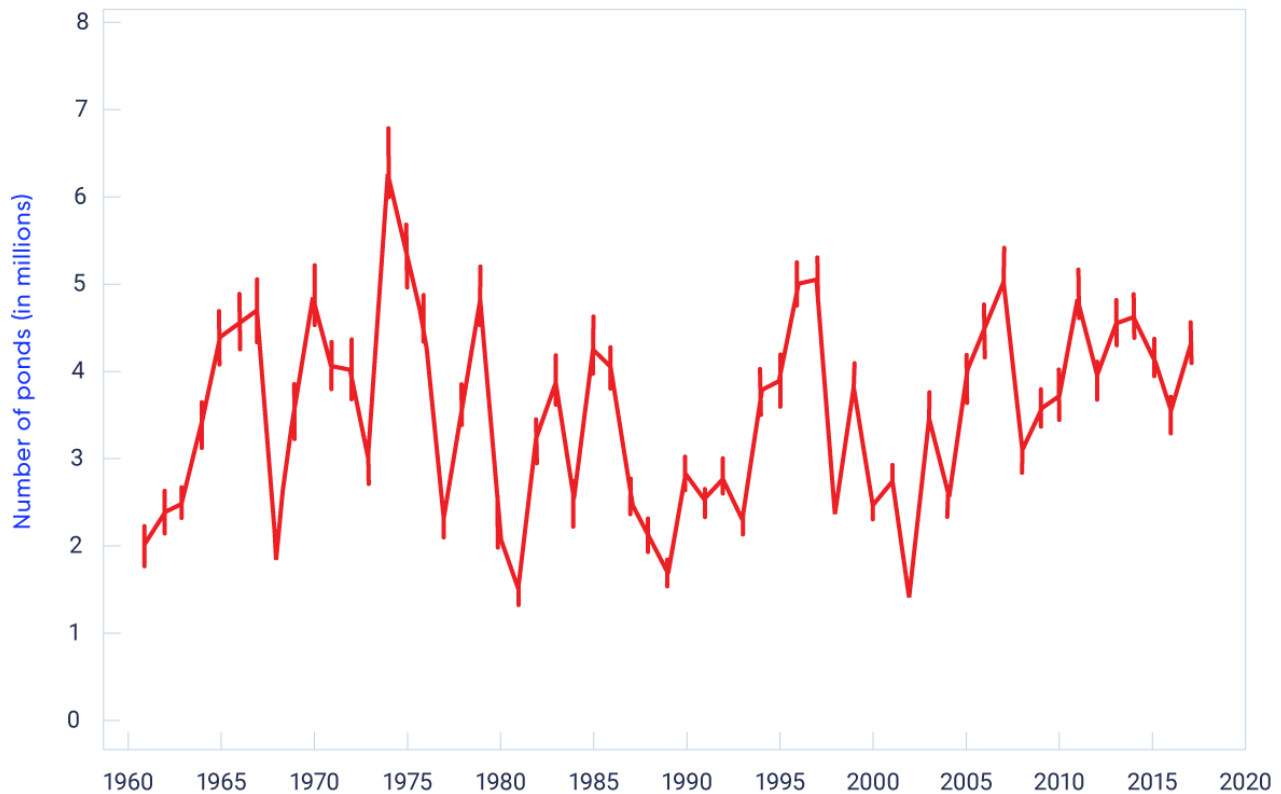


Figure 6.13: Ponds in the Canadian Prairies, 1961–2016

Figure caption: Number of ponds during May in the Canadian Prairies. Vertical bars show 90% confidence intervals.

FIGURE SOURCE: ADAPTED FROM US FISH AND WILDLIFE SERVICE (2017).

Many small lakes in freshwater delta systems are “perched basins,” located at a higher elevation than the nearby rivers. These basins typically experience declines in water levels during drier periods and replenishment during flood events in a continuous cycle (e.g., Marsh and Lesack, 1996; Peters et al., 2006; Lesack and Marsh, 2010). For example, in the Peace–Athabasca delta, evaporation exceeded precipitation from 1900 to 1940; opposite conditions prevailed from 1940 to the mid-1970s; and this was followed by a return to drier conditions that has continued through 2009 (Peters et al., 2006; Peters, 2013). The Mackenzie, Slave, and Saskatchewan river deltas had similar variability (e.g., Lesack and Marsh, 2010; Peters, 2013). Under a warmer and wetter future climate (2070–2099; ensemble of CMIP3 GCMs; high emission (A2) and medium emission (B2) scenarios), a shorter ice season (by two to four weeks), thinner ice cover, and depletion of the snowpack by mid-winter melt events are projected to lead to a major reduction in the frequency of spring ice jam flooding in the Peace–Athabasca delta (Beltaos et al., 2006). This reduction would have serious ecological implications, including accelerated loss of aquatic habitat, unless summer flood levels can reach the perched basins (Peters et al., 2006).

Section Summary

In summary, changes in surface water levels are affected by many factors, including the seasonal distribution of precipitation, inputs from snowmelt and rivers, evaporation (influenced by duration of ice cover and surface temperature), outflows, exchanges with groundwater, and the presence of permafrost. Many of the larger lakes are regulated by humans, while most other surface water bodies in Canada are monitored infrequently or not at all. For the few regions where analyses have been carried out (primarily the prairies and the Laurentian Great Lakes), evidence reveals that water levels have varied on year-to-year and multi-year timescales, with no long-term trends (see Figures 6.9, 6.11, 6.12, 6.13). Precipitation appeared to be the main driver of these fluctuations, with some of this variation being influenced by naturally occurring internal climate variability (see Chapter 2, Box 2.5). There is some evidence that high-latitude warming (see Chapter 4, Section 4.2.1.1) and associated permafrost thaw (see Chapter 5, Section 5.6.1) have affected the levels of lakes in northwestern Canada, including a higher incidence of rapid lake drainage; however, results are inconsistent.

The Laurentian Great Lakes are the only region of Canada where projected changes to future surface water levels have been examined, and these lakes are projected to show small average declines (0.2 m) in levels by the mid-21st century. However, water levels are expected to change seasonally, with an increase in water levels during the winter and early spring and a decrease in summer and early fall (see Figure 6.10). Given the close association between past water levels and surface climate, projected changes to precipitation and temperature are expected to affect future levels. However, the direction and magnitude of change will depend on the balance between future precipitation increases and increases in evaporation due to higher temperatures and longer ice-free periods. Regions of southern Canada may see declines in future water levels due to projected decreases in summer precipitation under a high emission (RCP8.5) scenario (see Chapter 4, Section 4.3.2.2) and higher evaporation associated with projected higher temperatures. There is, however *low confidence* in this assessment, due to the lack of future water-level studies and the complexity of factors that affect surface water levels. Since high-latitude warming (see Chapter 4, Section 4.2.1.1) and associated permafrost thaw Chapter 5, Section 5.6.1 have affected the levels of permafrost thaw lakes in northwestern Canada, projected warming in northern Canada (see Chapter 4, Section 4.2.1.3) and continued permafrost thaw (Chapter 5, Section 5.6.2) are expected to alter many Arctic lakes, including causing rapid drainage. Since no studies have directly assessed future water-level changes across northern Canada, there is only *medium confidence* in this assessment.

6.4: Soil moisture and drought

Key Message

Periodic droughts have occurred across much of Canada, but no long-term changes are evident. Future droughts and soil moisture deficits are projected to be more frequent and intense across the southern Canadian Prairies and interior British Columbia during summer, and to be more prominent at the end of the century under a high emission scenario (*medium confidence*).

Soil moisture directly influences runoff and flooding, since it strongly affects the amount of precipitation/snowmelt that makes its way into surface water bodies. It also determines the exchange of water and heat energy between the land surface and the atmosphere through evaporation and plant transpiration, and influences occurrence of precipitation through the recycling of moisture (see Seneviratne et al., 2010 for a detailed explanation of soil moisture–climate interactions). There are few direct measurements of soil moisture in Canada, and amounts are therefore estimated through remote sensing (e.g., with satellites) and/or modelling. The lack of an extensive monitoring network makes it difficult to make large-scale assessments of past trends (e.g., Mortsch et al., 2015). Future changes in soil moisture are primarily assessed using direct soil moisture output from GCMs. These changes are influenced by future precipitation and evaporation (the latter of which may be affected by changes in vegetation). However, modelled soil moisture is associated with large uncertainties, due to complexities in the representation of actual evapotranspiration, vegetation growth, and water use efficiency under enhanced atmospheric carbon dioxide concentrations (e.g., Seneviratne et al., 2010; Wehner et al., 2017). Longer-term climate variability, including droughts and excessive wet periods, are often directly related to soil moisture (and other aspects of freshwater availability). As a result, this section also assesses past and future changes to relevant indicators of drought.

6.4.1: Soil moisture

Quantifying soil moisture over large domains is challenging, as a result of the variability of soil moisture over time and among regions (Famiglietti et al., 2008). Several national-scale soil moisture networks exist globally (Doringo et al., 2011), including two in the United States (Schaefer et al., 2007; Bell et al., 2013). While there is no national network across Canada, there are some regional/provincial sites. For example, Alberta has monitored drought for the past 15 years, including soil moisture conditions, over a large network within the province, while Saskatchewan, Manitoba, and Ontario have established soil moisture and weather monitoring stations for selected regions. These networks have been used for validation of remote sensing data (described below) (e.g., Adams et al., 2015; Pacheco et al., 2015; Champagne et al., 2016) and for calibration and validation of hydrological models (Hayashi et al., 2010). Due to the difficulties (including high costs) of direct soil moisture monitoring, numerous remote sensing approaches have been used (Chan et al., 2016; Colliander et al., 2017). At present, continuous estimates of soil moisture for Canada as a whole are available from the Soil Moisture and Ocean Salinity (SMOS) satellite mission (2010–present) and more recently as part of the Soil Moisture Active Passive (SMAP) Mission (2015–present) (e.g., Champagne et al., 2011, 2012). SMOS data are distributed by Agriculture and Agri-Food Canada (<<http://open.canada.ca/data/en/dataset/723bb-b4c-d209-4599-b39b-0ede5a0a0371>>).

A limitation to estimates of soil moisture from remote sensing is the relatively shallow observation depth, which is generally limited to the top few centimetres from the surface. Deeper values within the root zone (i.e., the top metre) are often determined using data assimilation systems, in which soil moisture data from satellite sensors are merged with estimates from a hydrological model (e.g., Reichle et al., 2017). In Canada, this is done operationally and nationally as part of the Canadian Land Data Assimilation System (Carrera et al., 2015). Due to the relatively short record, no studies have examined trends in these data. Daily soil moisture values in the Canadian prairie provinces for three soil layer depths (0–20 cm, 20–100 cm and 0–100 cm) were, however, reconstructed from 1950 to 2009 using the Variable Infiltration Capacity (VIC) land-surface hydrology model. The reconstructed soil moisture matched past observations across the prairies, but no trends were reported (Wen et al., 2011).

There have been a few global studies of future soil moisture using GCM output. An ensemble of 15 CMIP3 GCMs projected a decrease in June–August soil moisture for most of Canada for the late century under a medium-high emission scenario (SRES 1Ab) (Wang, 2005). Projected late-century changes in surface, total, and layer-by-layer soil moisture from 25 GCMs included in CMIP5 under a high emission scenario (RCP8.5) indicated that, in most mid-latitudes of the Northern Hemisphere, including southern Canada, the top 10 cm of soil will become drier during the summer, but the remainder of the soil, down to 3 m, will stay wet (Berg et al., 2016; Wehner et al., 2017).

6.4.2: Drought

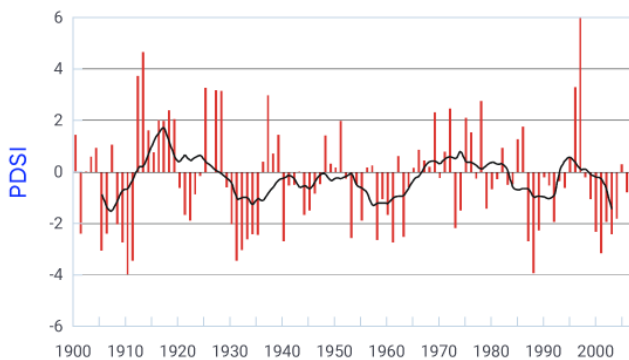
Drought is often defined as a period of abnormally dry weather long enough to cause a serious hydrological imbalance (e.g., Seneviratne et al., 2012) and therefore impacts on several components of the water cycle. These impacts can also be exacerbated by increases in evapotranspiration associated with high temperatures. Drought impacts differ, however, depending on their timing. In general, warm-season droughts affect not only agricultural production (usually due to soil moisture deficits) but also surface and subsurface water levels. Precipitation deficits associated with the runoff season (including winter snow accumulation) primarily affect the replenishment of freshwater systems.

Numerous indices of drought (which also identify moisture surplus) have been used to characterize their occurrence and intensity. The indices incorporate various hydroclimatic inputs (e.g., precipitation, temperature, streamflow, groundwater, and snowpack), and each index has its own strengths and weaknesses (see WMO, 2016 for a comprehensive list). Some indices are based on precipitation alone (e.g., the Standardized Precipitation Index [SPI] (McKee et al., 1993)) and do not take into account that higher temperatures are often associated with below-normal precipitation. As a result, enhanced evapotranspiration is not considered. A few indices incorporate precipitation and estimates of potential evapotranspiration (based on air temperature) – for example, the Palmer Drought Severity Index (PDSI) (Palmer, 1965) and the Standardized Precipitation Evapotranspiration Index (SPEI) (Vicente-Serrano et al., 2010). A shortcoming of these indices is that they use potential evapotranspiration as a proxy for actual evapotranspiration and, thus, do not consider how soil moisture and vegetation may limit evapotranspiration and subsequent drought development. This can lead to overestimation of drought intensity, particularly for climate change projections (e.g., Donohue et al., 2010;

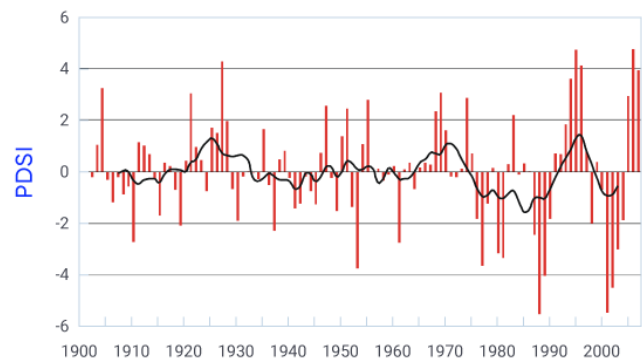
Milly and Dunne, 2011, 2016; Shaw and Riha, 2011). The vast majority of global-scale and Canadian analyses of historical trends and projected future changes to drought have used indices based on precipitation alone or on the combined effects of temperature and precipitation (e.g., Bonsal et al., 2011), and these are the focus of this assessment.

A few global studies have highlighted past trends in specific regions, including, for example, drying over mid-latitude regions of Canada from 1950 to 2008 (Dai, 2011 using PDSI). However, since the beginning of the 20th century, the frequency of global drought remains generally unchanged; it appears that, over this longer period, increases in global temperature and potential evapotranspiration have been offset by increases in annual precipitation (e.g., Sheffield et al., 2012; McCabe and Wolock, 2015). Trend analyses in Canadian drought are fragmented, with no comprehensive country-wide analyses to date. The majority have focused on the Prairie region, because of the greater frequency of drought in this region (e.g., Mortsch et al., 2015). A Canadian drought review (Bonsal et al., 2011) provided examples of 20th-century changes in PDSI for individual stations in various regions of the country (1900 to 2007) (see Figure 6.14). Considerable multi-year variability is evident, with no discernible long-term trends. This variability was also apparent in regional studies of SPEI (1900–2011) in summer (June–August) and over the “water year” (October–September) in southeastern Alberta and southwestern Saskatchewan (Bonsal et al., 2017) and the Athabasca River Basin (Bonsal and Cuell, 2017). Other Canadian Prairie region drought studies have highlighted periodic droughts during the 1890s, 1910s, 1930s, 1980s, and early 2000s (e.g., Chipanshi et al., 2006; Bonsal and Regier, 2007; Bonsal et al., 2013). From the mid-to-late 2000s to approximately 2014, the Prairie region has experienced exceptionally wet conditions, highlighting the high variability in this region (e.g., Bonsal et al., 2017).

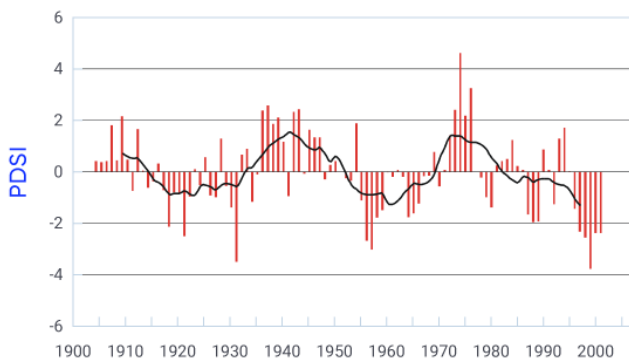
a) Kamloops, BC



b) Saskatoon, SK



c) Sherbrooke, QC



d) Yarmouth, NS

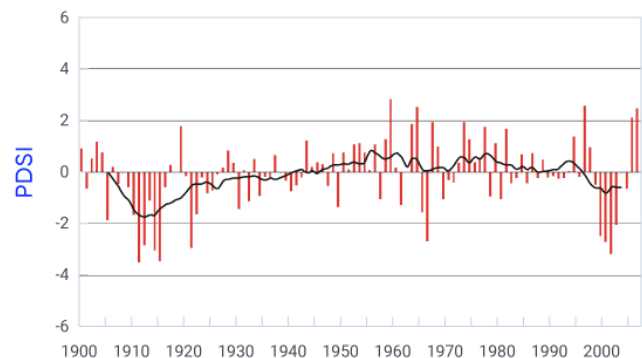


Figure 6.14: Annual Palmer Drought Severity Index for four selected Canadian locations, 1900–2007

Figure caption: Annual Palmer Drought Severity Index (PDSI) values from 1900 to 2007 for (a) Kamloops, British Columbia, (b) Saskatoon, Saskatchewan, (c) Sherbrooke, Quebec, and (d) Yarmouth, Nova Scotia. Solid lines represent 10-year running means. Positive values indicate wetter conditions, negative values indicate drier conditions.

FIGURE SOURCE: BONSAI ET AL. (2011).

In other areas of the country, the Canadian Drought Code (based on maximum temperature and precipitation) showed that drought severity over the southern boreal forest regions of Canada was variable, with no long-term trend from 1913 to 1998 (Girardin et al., 2004). A more recent analysis using PDSI and the Climate Moisture Index (difference between annual precipitation and annual potential evapotranspiration) indicated that, for the Canadian boreal zone as a whole, several regions experienced significant drying between 1951 and 2010, but there were also some areas with significant wetting (Wang et al., 2014). An analysis of 20th century (1920–1999) drought events in southern Ontario revealed occurrences in 1930, 1933, 1934, 1936, 1963, 1998, and 1999, with no long-term trend (Klaassen, 2002). Canada-wide trends in actual evapotranspiration from 1960 to 2000 showed significant increasing values at 35% of the station locations, mainly on the Pacific and Atlantic coasts and in the Laurentian Great Lakes/St. Lawrence zones (Fernandes et al., 2007). Other studies found that annual actual evapotranspiration trends in the Prairie region were mixed (e.g., Gan, 1998). Observed pan evaporation and estimated potential evapotranspiration for 11 Prairie region sites from the 1960s to early 2000s showed significant decreasing and increasing trends at different sites. Overall, more locations had decreases in potential evapotranspiration, and these were concentrated during June and July (Burn and Hesch, 2006).

No Canadian studies have attempted to directly attribute past trends in drought to anthropogenic climate change, although there has been some research on the 2015 extreme drought event in western Canada. Anthropogenic climate change increased the likelihood of the extremely warm spring, but no human influence was detected on the persistent drought-producing weather pattern (Szeto et al., 2016).

To date, no Canada-wide studies of future drought projections have been carried out. There are, however, several regional-scale analyses, with the majority focusing on the Prairie region and incorporating one or more drought indices. For example, output from three CMIP3 GCMs incorporating high (A2), medium-high (A1B), and medium (B2) emission scenarios were used to project future (2011–2100) summer PDSI over the southern Canadian prairies. More persistent droughts are projected, particularly after 2040, and multi-year droughts of 10 or more years are projected to become more probable (Bonsal et al., 2013). Similarly, the Canadian Regional Climate Model, under a high emission (A2) scenario, projected that long droughts of six to 10 months will increase and become more severe by mid-century across southern Manitoba and Saskatchewan and the eastern slopes of the Rocky Mountains. However, in the northern Prairie region, long drought events will be less severe and less frequent (PaiMazumder et al., 2012). A number of other studies of the Prairie region have

examined drought changes for the mid-century period using several climate models that are part of the North American Regional Climate Change Assessment Program (Mearns et al., 2009). For the southern Prairie region, results under a high emission scenario (A2) indicated an overall increased drought risk for both summer and winter. There were considerable differences among models, with projections ranging from a substantial increase in drought with a higher degree of year-to-year variability, to relatively no change from current conditions (Jeong et al., 2014; Masud et al., 2017; Bonsal et al., 2017). Further north, in the Athabasca River Basin, projections revealed an average change toward more summer drought, but, again, there was a substantial range among the climate models (Bonsal and Cuell, 2017). Future annual and summer SPEI changes over all western Canadian river basins were assessed with six CMIP5 GCMs for the periods 2041–2070 and 2071–2100 (relative to 1971–2000) using medium emission (RCP4.5) and high emission (RCP8.5) scenarios. Southern watersheds showed a gradual increase in annual water deficit throughout the 21st century, while the opposite was true for northern basins. For summer, however, all river basins except those in the extreme north are expected to experience decreasing water availability (see Figure 6.15) (Dibike et al., 2017). Twelve CMIP3 GCMs incorporating medium (B1), medium-high (A1B), and high (A2) emission scenarios showed that, by the end of the 21st century, the combined changes in precipitation and temperature will lead to generally drier conditions in much of the boreal forest region of western Canada and to a higher likelihood of drought. However, some regions in the east may become slightly wetter (Wang et al., 2014).

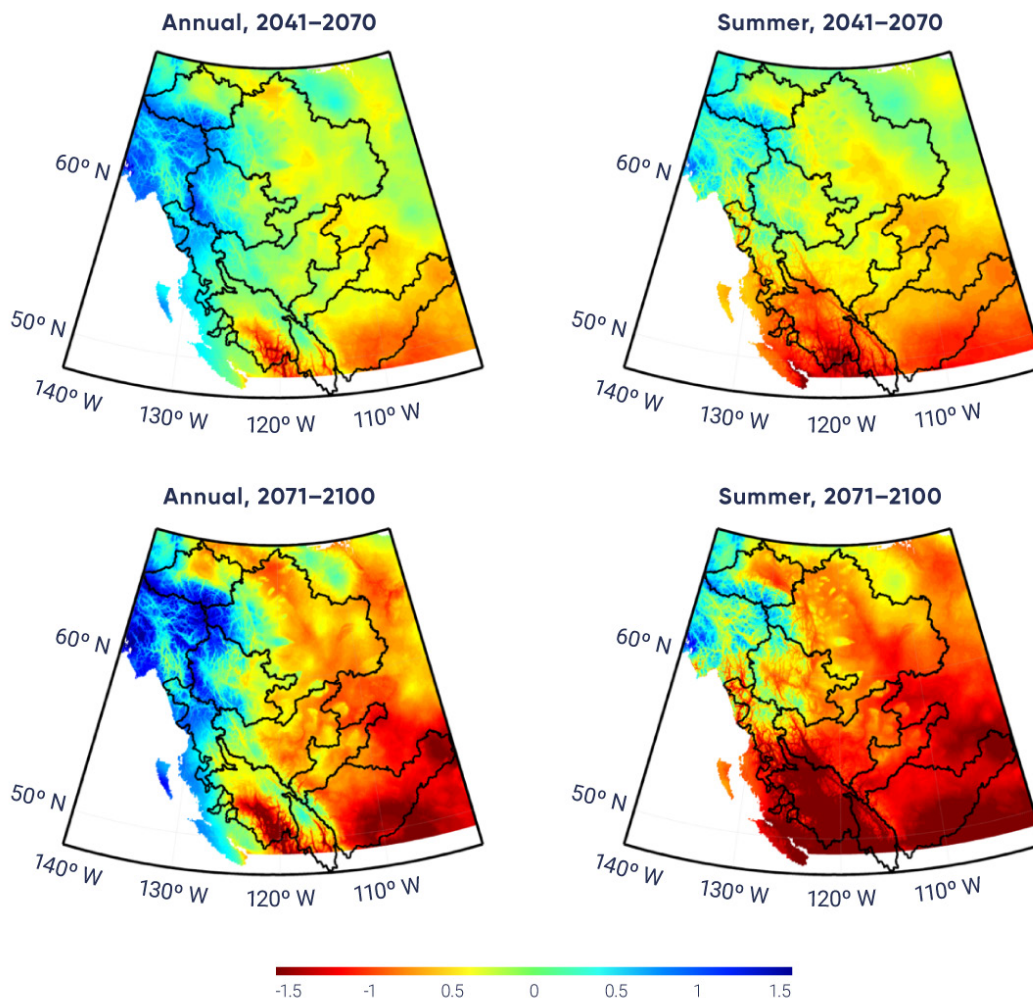


Figure 6.15: Changes in mean annual Standardized Precipitation Evapotranspiration Index for western Canadian watersheds

Figure caption: Changes in mean annual Standardized Precipitation Evapotranspiration Index (SPEI) (left) and summer (June–August) SPEI (right) between the baseline (1971–2000) and 2041–2070 (top) and between baseline and 2071–2100 (bottom) for western Canadian watersheds. SPEI is determined from temperature and precipitation output from an ensemble of six CMIP5 GCMs under a high emission (RCP8.5) scenario. Positive values indicate wetter conditions, negative values indicate drier conditions.

FIGURE SOURCE: DIBIKE ET AL. (2017).

These future projections are consistent with other North American and global-scale studies using similar drought indices. For instance, drought projections using numerous CMIP5 GCMs (medium emission (RCP4.5) scenario) showed that the frequency of severe-to-extreme drought conditions is expected to increase by the late 21st century for much of southern Canada, including southeast British Columbia, the prairies and Ontario (as measured by PDSI and soil moisture) (Dai, 2012; Zhao and Dai, 2015, 2016). Similar results have been projected using PDSI and SPEI under a high emission (RCP 8.5) scenario (Cook et al., 2014; Touma et al., 2015). This included increases in drought magnitude and frequency over western, central, and eastern North America, with the greatest change over western and central regions. Year-to-year variability in SPI was projected to increase by the end of century (2080–2099) in various regions of North America, suggesting more extremes; however, there was considerable uncertainty in these results, due to large differences among regions and among the 21 CMIP5 GCMs (Swain and Hayhoe, 2015). Although there is overall consistency regarding the increased likelihood of future drought over southern interior continental regions of Canada, there is uncertainty concerning the magnitude of these changes. This is primarily due to shortcomings of the indices that estimate potential evapotranspiration, which may lead to an overestimation of drought intensity (e.g., Sheffield et al., 2012; Trenberth et al., 2014; Milly and Dunne, 2016).

Section summary

In summary, records of directly measured and/or remotely sensed soil moisture are not long enough to assess past changes. Climate change impacts on soil moisture specifically for Canada have not been studied, although there have been a few global-scale studies. Results revealed a general consensus that summer soil moisture will decrease at the end of this century under medium to high emission scenarios in several interior continental regions of the globe, including southern Canada (interior British Columbia and the southern prairies). These are also the areas of Canada where droughts are projected to become more frequent, due to increased evapotranspiration from higher temperatures. However, there is considerable uncertainty in future soil moisture projections, due to the complexity of interactions among precipitation, evapotranspiration, and vegetation, which are inherently difficult to model and simulated in varying ways among individual models. Therefore, there is *medium confidence* that summer soil moisture will decrease in future in southern interior regions of Canada.

There have been several regional-scale assessments of past drought occurrence, with the majority focusing on the Prairie region. Results revealed that, for the most part, droughts have been characterized by year-to-year and multi-year variations (see Figure 6.14). This finding is consistent with the assessment of surface water levels (see Section 6.3). No Canada-wide studies of projected future droughts are currently available, but several have been carried out in western Canada (primarily the Prairie region). There is agreement among these studies concerning increased frequency and intensity of droughts, particularly at the end of century under higher emission scenarios. This is consistent with several global-scale drought studies that primarily showed increased drought potential in summer over continental interior regions (including interior British Columbia and the southern Prairie region). However, all of these studies incorporated drought indices in which large increases in potential evapotranspiration (based solely on future temperature changes) were considered the major reason for widespread drying. Approaches using potential evapotranspiration as a proxy for actual evapotranspiration do not consider how soil moisture and vegetation may limit evapotranspiration and subsequent drought development. Therefore, these studies tend to overestimate future drought intensity, thus increasing the uncertainty of future drought projections. As a result, there is only *medium confidence* in the projected increased frequency and intensity of droughts over southern interior regions of Canada (see FAQ 6.1).



6.5: Groundwater

Key Message

The complexity of groundwater systems and a lack of information make it difficult to assess whether groundwater levels have changed since records began. It is expected that projected changes to temperature and precipitation will influence future groundwater levels; however, the magnitude and even direction of change is not clear. Spring recharge of groundwater aquifers over most of the country is anticipated to occur earlier in the future, as a result of earlier snowmelt (*medium confidence*).

Groundwater is water found underground in the cracks and spaces in soil, sand, and rock. It is formed from precipitation and surface water that seeps into the ground to form aquifers (a body of saturated rock through which water can easily move). Ground and surface water are inextricably interconnected, as groundwater discharges into rivers, lakes, wetlands, and reservoirs. Thus, the amount and availability of groundwater influence surface water. In addition, groundwater plays an important role in sustaining baseflow for many Canadian rivers (see Section 6.2.1). Groundwater is generally measured at local (individual wells) or aquifer scales (hundreds of square kilometres). In Canada, the principal source of data is provincial government agencies, which hold observations of groundwater levels, water well records, hydrogeological maps, and information on groundwater extraction (CCME, 2010). Although provincial wells represent direct data for the estimation of aquifer recharge, the data are localized and typically short-term (around 30 years, with none longer than 50 years) (Rivard et al., 2009). Wells may not be located near climate and/or streamflow stations, making comparisons with surface conditions difficult, and can also be affected by groundwater withdrawal (Rivera et al., 2004). Recently, however, large-scale aquifers have been mapped using remote sensing, a method that shows great future potential (see Box 6.3). Future groundwater changes are assessed using climate output (e.g., precipitation and surface air temperature) from numerous GCMs that are incorporated into various groundwater and hydrological models. These numerous models and the complexity of groundwater systems make for a large degree of uncertainty in assessing future groundwater changes (e.g., Smerdon, 2017).

Box 6.3: Monitoring groundwater from space

Remote sensing from satellites is a powerful means of mapping aquifers and assessing groundwater resources. Current research involves mapping groundwater from the Gravity Recovery and Climate Experiment (GRACE) satellites. GRACE operated from March 2002 to October 2017, and one of its key objectives was to monitor changes in water storage. This monitoring is continuing with the launch of another GRACE satellite in May 2018. During the past decade, several studies have aimed to analyze changes in water storage from GRACE data at the best possible resolution in time and space. Natural Resources Canada has various experimental projects to map the variability of groundwater over time in major water basins across the country using GRACE data and other measurements of snow, ice, surface water, and soil moisture, as well as point-source groundwater measurements. These maps provide a new, comprehensive, national view of ground-

water and have been used to quantify recent changes in groundwater storage in four Canadian regions: the Laurentian Great Lakes Basin, Alberta, the eastern Rocky Mountains, and Canada as a whole. Two of these are discussed below.

Groundwater storage changes within the Laurentian Great Lakes Basin

Groundwater storage (GWS) changes within the Laurentian Great Lakes Basin using GRACE and auxiliary data have been estimated for the 2002–2010 period (see Figure 6.16). Average GWS changes reveal distinct annual cycles, with a peak-to-peak magnitude of about 50 mm in water thickness equivalent (i.e., a 50 mm layer of water over all land areas of the basin). Average GWS losses were 5.0 km³/year during this period (equivalent to 6.5 mm groundwater loss per year over all land areas of the basin) (Huang et al., 2012). This trend should be interpreted with caution, given the short period of analysis and uncertainty in the models used for soil moisture changes. Further GRACE observations are required to assess the longer-term GWS change in the Laurentian Great Lakes Basin.

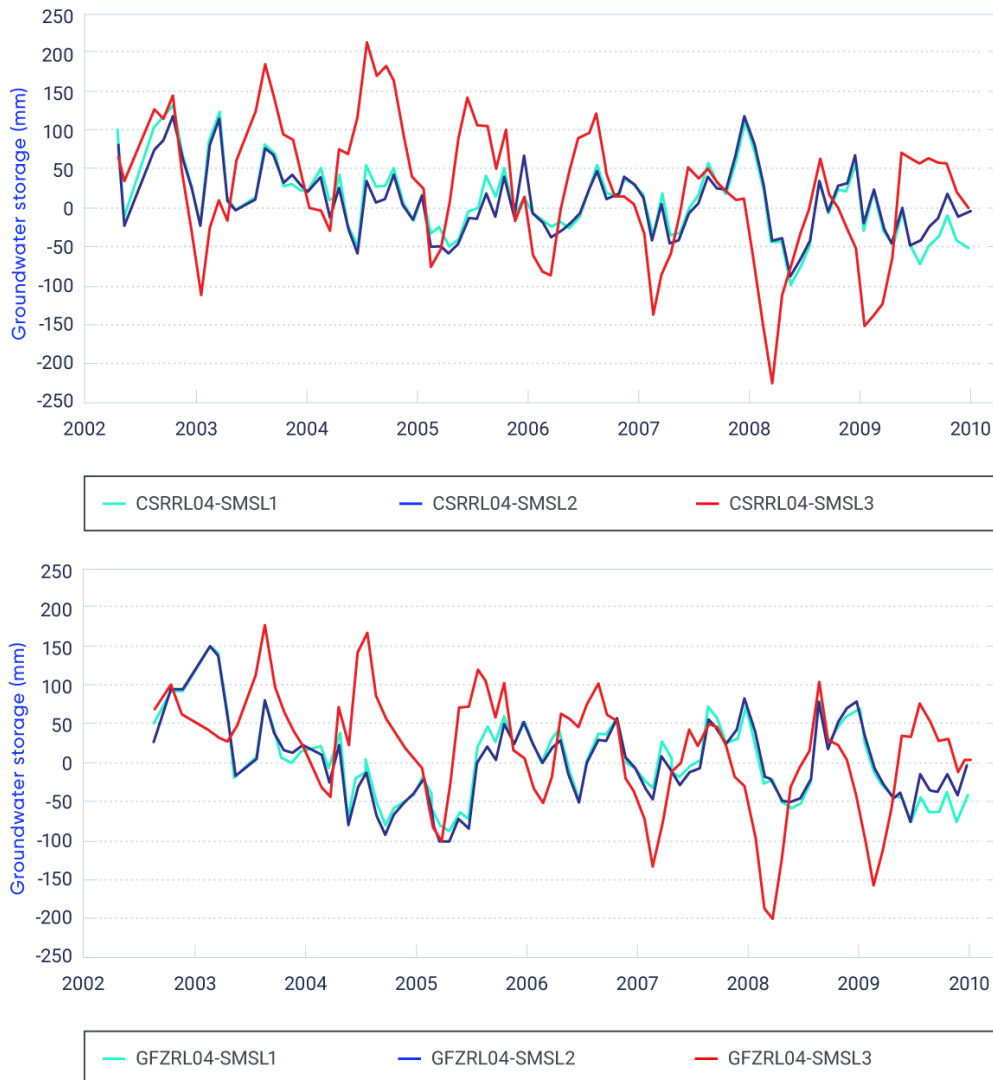


Figure 6.16: Variation in groundwater storage in the Laurentian Great Lakes Basin, 2002–2010

Figure caption: Derived groundwater storage (GWS) measured in water thickness equivalent over the land areas of the Great Lakes Basin using the Center for Space Research (CSR) release 04 (RL04) (top) and GeoForschungsZentrum (GFZ) release 04 (RL04) (bottom) Gravity Recovery and Climate Experiment (GRACE) models. Each model incorporates three soil moisture, snow, and lake (SMSL) water storage fields that have different land-surface models.

FIGURE SOURCE: HUANG ET AL. (2012)

Mapping groundwater storage variations in Alberta

GRACE data were used to represent broad-scale patterns of variations in GWS in Alberta for the 2002–2014 period (see Figure 6.17) (Huang et al., 2016). GWS showed a positive trend that increased from west to east. The average trend for the entire province was 11 mm per year. The GWS variations were validated using provincial groundwater-monitoring wells and showed strong associations. This short-term trend should be interpreted with caution, but these results are promising for future monitoring of groundwater in prairie landscapes using GRACE.

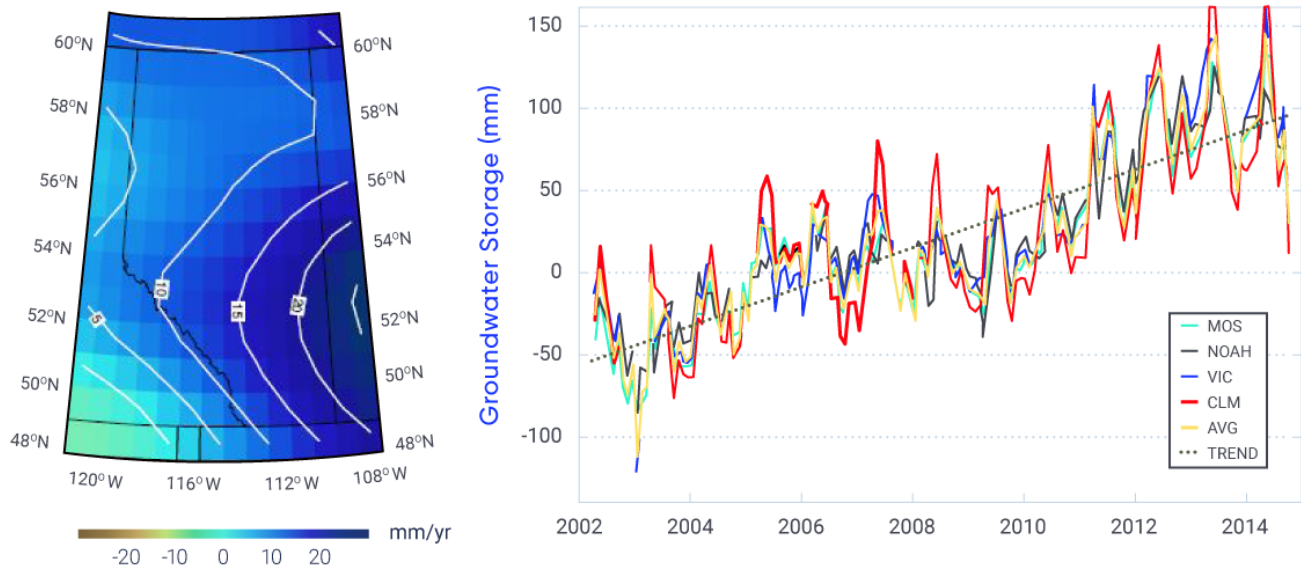


Figure 6.17: Groundwater storage trends in Alberta, 2002–2014

Figure caption: Average groundwater storage (GWS) trends in Alberta using the release 05 monthly GRACE gravity model for the period April 2002 to October 2014 (left). The average is determined using four land-surface models from the Global Land Data Assimilation System: Mosaic (MOS), Noah, Variable Infiltration Capacity (VIC), and Community Land Model (CLM). Time series averaged over the entire province for each model (as well as the average of all four models [AVG]), and the linear trend are provided on the right. Twelve mean monthly GWS variation maps were generated from the 139 monthly GWS variation grids to characterize the annual GWS variations.

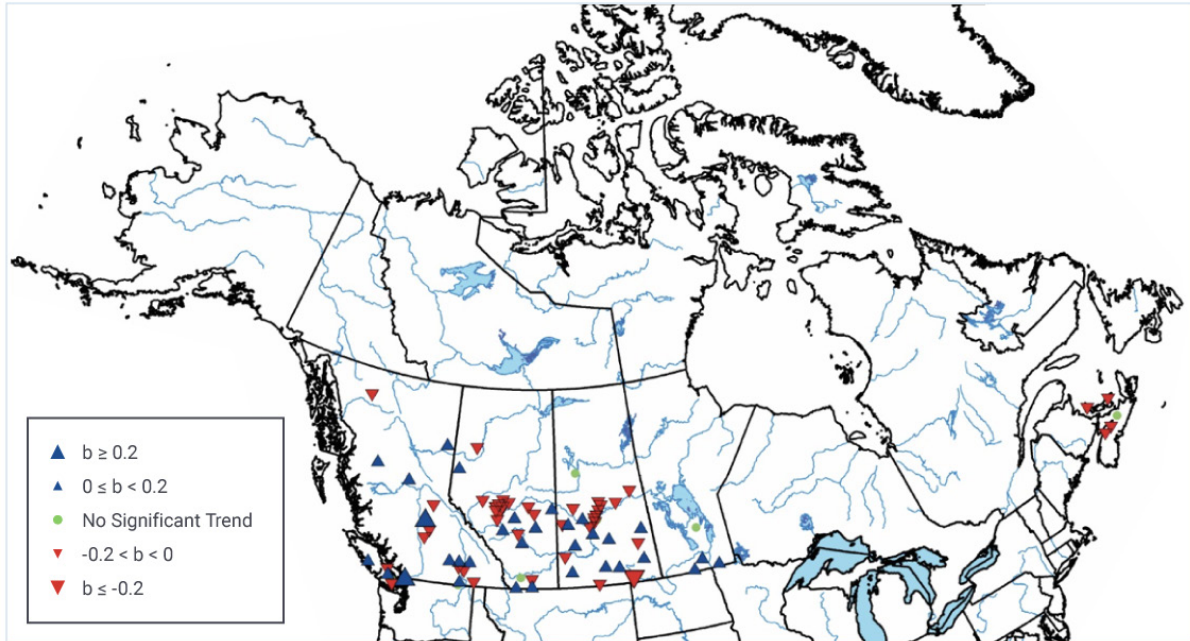
FIGURE SOURCE: HUANG ET AL. (2016).

Groundwater recharge (replenishment) occurs several ways: through infiltration of rain and/or snowmelt water, via exchange from rivers or reservoirs, and from depressions in the landscape fed by surface runoff (Allen et al., 2014). Most studies consider recharge as a percentage of precipitation, but the percentage varies greatly, depending on the region's climate and the geological and hydraulic characteristics of the aquifer. In Canada, recharge rates are typically 65% or less of annual precipitation (Rivera, 2014) but are difficult to quantify, particularly over large regions. Determining these rates normally requires measuring precipitation and then performing a water balance by approximating all the other surface water fluxes (runoff, evaporation, and transpiration). There are marked regional differences in groundwater recharge estimates across the Canadian landmass. In eastern Canada, these vary between 1000 and 1500 mm per year; in the Prairie region, between 50 and 400 mm per year; and in British Columbia, 500 to 2000 mm per year (although considerable uncertainty exists) (Allen et al., 2014). There is not enough information to estimate recharge rates for northern Canada.

Groundwater discharge (i.e., loss of water) occurs through discharge to a surface water body, flow through formations, or pumping from a well. In semi-arid regions, such as the Canadian prairies, direct evaporation and/or evapotranspiration from the shallow water table is the primary mechanism for groundwater loss. Groundwater discharge is also difficult to quantify, especially in areas dominated by well pumping or evaporation.

Only one study of trends in groundwater levels in Canada has been carried out. Analyses of available data from provincial wells (138 with 30 years' data and 53 with 40 years' data, distributed over six provinces) showed that approximately 80% of the wells had significant trends (see Figure 6.18). Mixed trends were generally observed across most of western Canada, while, for the Maritime provinces, decreasing trends dominated in the 30-year record. Overall, the number of upward and downward trends was similar, and, in some cases, nearby wells had opposite trends. This is not surprising, since some wells are more affected by pumping than others. The authors stated that these trends could be attributed to climate variations (e.g., more rain that has not been counterbalanced by increased evapotranspiration) but also to human activities (changes in land use, pumping, artificial recharge) or to the statistical methods used for trend estimation (Rivard et al., 2009).

30 years



40 years

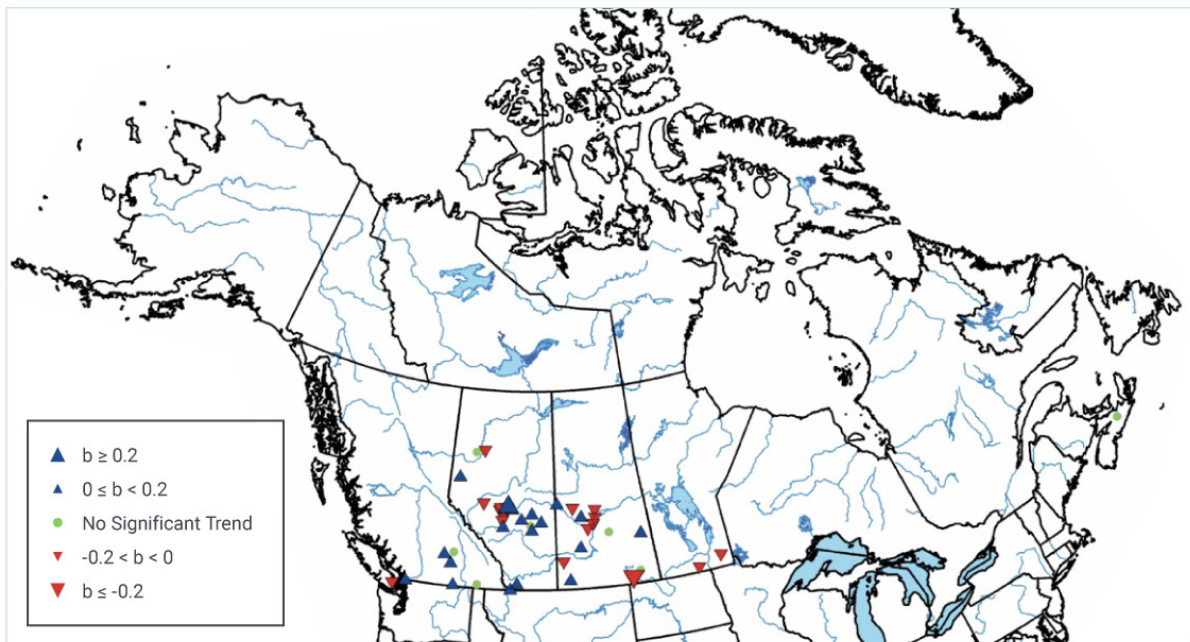


Figure 6.18: Annual mean groundwater level trends for selected areas of Canada

Figure caption: Trends for annual mean groundwater levels for 30-year (1976–2005, top) and 40-year (1966–2005, bottom) series. b represents the magnitude of the trend in metres per year. Significant trends denote that there is only a 10% possibility that such changes are due to chance.

FIGURE SOURCE: MODIFIED FROM RIVARD ET AL. (2009).

Some case studies have compared groundwater levels with precipitation (i.e., wet and dry periods) and determined that the two variables tend to mirror each other, with groundwater levels responding to precipitation after a delay, which varies depending on the region (e.g., Chen et al., 2002, 2004). For example, Figure 6.19 shows annual precipitation at the Winnipeg James Armstrong Richardson International Airport and average water levels from 24 groundwater wells in the Winnipeg area. The groundwater response has a delay of approximately 2.2 years (upper graph). If annual precipitation is shifted forward by 2.2 years, the two variables are significantly correlated (there is only a 5% possibility that such changes are due to chance) ($r = 0.85$, lower graph). Annual mean temperature had a significant negative correlation ($r = -0.72$) with groundwater levels (Chen et al., 2004). Over the last few decades, the annual recharge in a small prairie watershed in Alberta was significantly correlated with a combination of growing season (May–September) precipitation and snowmelt runoff (Hayashi and Farrow, 2014). For eastern Canada, aquifer recharge in Quebec, New Brunswick, and Prince Edward Island varied in a similar fashion to precipitation (over the 1960–2000 period), particularly at the New Brunswick site (Allen et al., 2014). The relationship was most prevalent on long-term timescales (decades), but was not consistent over time. Therefore, there is some evidence that precipitation variability can affect groundwater recharge, with shallower systems responding more quickly than deeper aquifers (Allen et al., 2014).

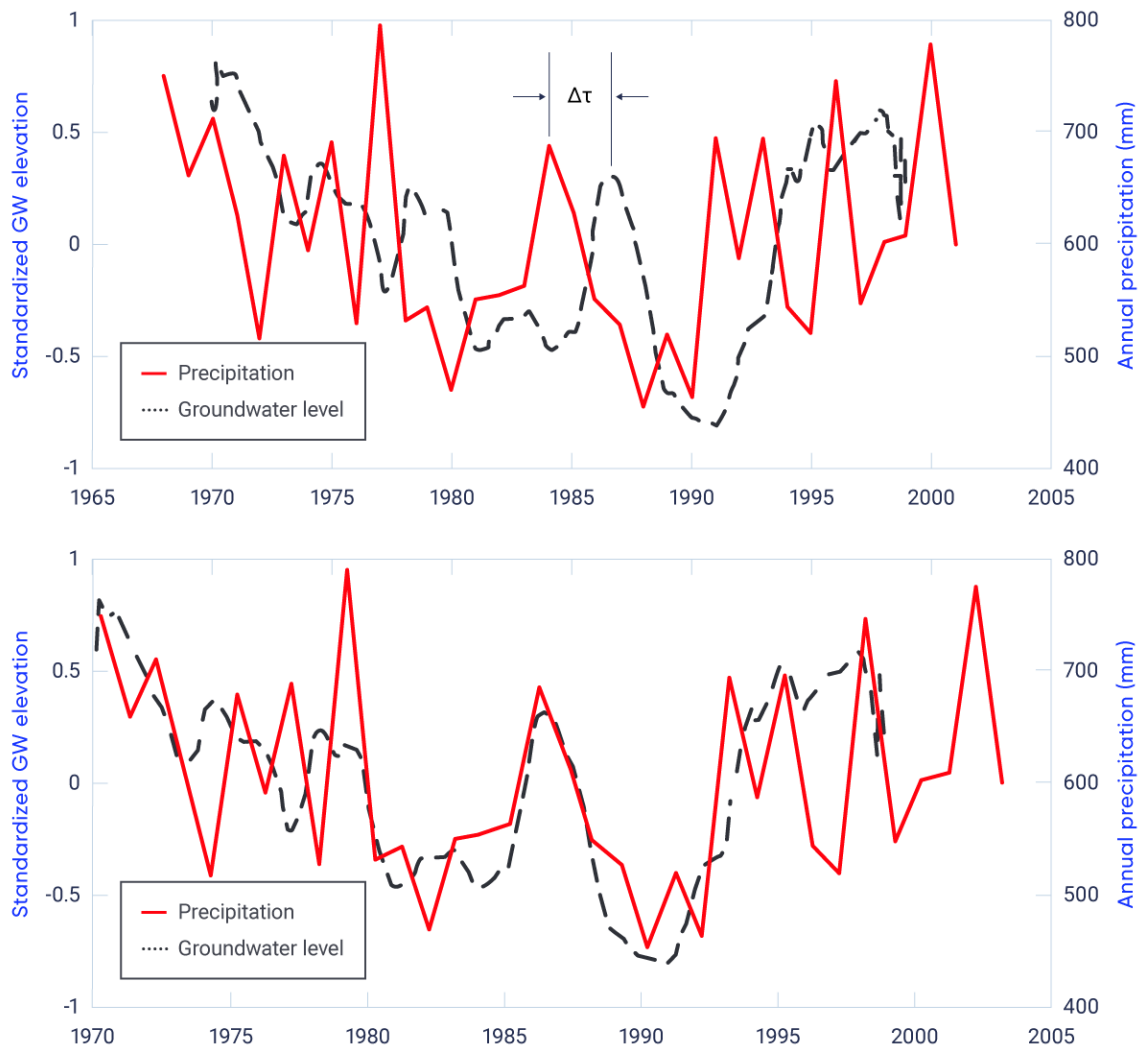


Figure 6.19: Precipitation and groundwater levels in the Winnipeg area, 1968–2003

Figure caption: Annual precipitation and average standardized groundwater levels in 24 monitoring wells in the Winnipeg, Manitoba, area. The upper graph shows actual values, while the lower graph provides values with precipitation shifted later by 2.2 years (as denoted by the Δt in the upper graph).

FIGURE SOURCE: ALLEN ET AL. (2014).

Future changes in temperature and precipitation are expected to alter groundwater recharge (through changes to runoff, evapotranspiration, and snow accumulation). Several studies have reviewed various aspects of climate change and groundwater recharge over different regions of the world and emphasized the large degree of uncertainty in modelling future recharge. At present, it is not possible to clearly project the magnitude of future groundwater recharge or whether recharge will increase or decrease (e.g., Rivard et al., 2009; Smerdon, 2017). There have been a few regional-scale studies of the potential effect of climate change on future (various time periods) recharge across Canada, and these also show a wide range of results. For example, in south-central British Columbia, higher recharge is projected from spring to summer (Scibek and Allen, 2006), whereas, in southern Manitoba's shallow aquifers, recharge may decrease, mainly due to increasing temperature (Chen et al., 2004). For Ontario as a whole, projected recharge rates for several watersheds averaged between increases of 32% and decreases of 3% (Southarm et al., 1999; Jyrkama and Sykes, 2007; Sultana and Coulibaly, 2011; Oni et al., 2014; Nikolik and Simonovic, 2015; Motiee and McBean, 2017). Quebec tended to show lower recharge changes, ranging from decreases of 10% to increases of 20% (Sulis et al., 2011, 2012; Bourgault et al., 2014; Levison et al., 2014a, 2014b; CEHQ, 2015; Lemieux et al., 2015; Levison et al., 2016), while, in the Atlantic provinces, average changes were between decreases of 8% and increases of 30% (Kurylyk and MacQuarrie, 2013; Green and MacQuarrie, 2014; Kurylyk et al., 2014; Rivard et al., 2014). In most of these eastern Canadian analyses, a shift to earlier recharge due to earlier snowmelt was consistently projected.

Section summary

In summary, groundwater levels are difficult to assess, due their complexity within the Canadian landscape and due to human pressures (e.g., withdrawals). The only national-scale analysis (for provinces where data were available) identified both increasing and decreasing trends in groundwater levels over the past 30 to 40 years; in some cases, nearby wells had opposite trends (see Figure 6.18). In some regional studies, observed changes in levels were reflected in longer-term variations in precipitation and snowmelt, particularly for shallow aquifers (see Figure 6.19). However, relationships in many regions of the country have not been analyzed, and, as a result, it is difficult to establish a direct climate-groundwater link for the period of observations.

A few studies have assessed impacts of climate change on groundwater recharge over different regions of the world and emphasized the large degree of uncertainty in modelling future recharge. Site-specific climate change studies in Canada revealed both increases and decreases. These studies incorporate different surface and groundwater models, as well as a variety of climate models, emission scenarios, and future time horizons. In addition, they do not include all regions of the country, with notable gaps in northern Canada. Since there is evidence for an association between precipitation, snowmelt, and – to a lesser extent – temperature, on the one hand, and groundwater recharge, on the other, it is anticipated that projected future changes in these variables will impact future groundwater levels. However, due to the complexities and lack of consistent evidence, there is a high degree of uncertainty in the magnitude and even the direction of change. Furthermore, the extent of future groundwater withdrawals is unknown, thus adding to the uncertainty. Nonetheless, many studies show a seasonal shift toward earlier recharge in association with projected earlier snowmelt and, thus, there is *medium confidence* that spring recharge of groundwater aquifers over most of the country will occur earlier in the future.



References

- Abdul Aziz, O.I. and Burn, D.H. (2006): Trends and variability in the hydrological regime of the Mackenzie River Basin; *Journal of Hydrology*, v. 319, p. 282–294.
- Adams, J.R., McNairn, H., Berg, A.A. and Champagne, C. (2015): Evaluation of near-surface soil moisture data from an AAFC monitoring network in Manitoba, Canada: Implications for L-band satellite validation; *Journal of Hydrology*, v. 521, p. 582–592.
- Allen, D., Hayashi, M., Nastev, M., Chen, Z. and Turner, B. (2014): Recharge and Climate; Chapter 4 in *Canada's Groundwater Resources*, (ed.) A. Rivera; Fitzhenry & Whiteside Limited, Markham, Ontario, p. 101–148.
- Angel, J.R. and Kunkel, K.E. (2010): The response of Great Lakes water levels to future climate scenarios with an emphasis on Lake Michigan-Huron; *Journal of Great Lakes Research*, v. 36, p. 51–58.
- Argyilan, E.P. and Forman, S.L. (2003): Lake level response to seasonal climatic variability in the Lake Michigan-Huron system from 1920 to 1995; *Journal of Great Lakes Research*, v. 29, p. 488–500.
- Arisz, H., Dalton, S., Scott, D. and Burrell, B.C. (2011): Trends in New Brunswick hydrometric data; in *Proceedings of the Annual Conference of the Canadian Society for Civil Engineering*, 14–17 June 2011, Ottawa, Ontario, p. 2995–3005.
- Assani, A.A., Landry, R. and Laurencelle, M. (2012): Comparison of interannual variability modes and trends of seasonal precipitation and streamflow in Southern Quebec (Canada); *River Research and Applications*, v. 28, p. 1740–1752.
- Barnett, T.P., Adam, J.C. and Lettenmaier, D.P. (2005): Potential Impacts of a warming climate on water availability in snow-dominated regions; *Nature*, v. 438, p. 303–309.
- Bates, B.C., Kundzewics, Z.W., Wu, S. and Palutikof, J.P. (2008): *Climate Change and Water*; Technical Paper of the Intergovernmental Panel on Climate Change, IPCC Secretariat, Geneva, Switzerland, 210 p.
- Bawden, A.J., Linton, H.C., Burn, D.H. and Prowse, T.D. (2014): A spatio-temporal analysis of hydrological trends and variability in the Athabasca River region, Canada; *Journal of Hydrology*, v. 509, p. 333–342.
- BCMOE [British Columbia Ministry of the Environment] (2016): *Indicators of Climate Change for British Columbia 2016 Update*; British Columbia Ministry of the Environment, <http://www2.gov.bc.ca/assets/gov/environment/research-monitoring-and-reporting/reporting/envreportbc/archived-reports/climate-change/climatechangeindicators-13sept2016_final.pdf>.
- Bell, J.E., Palecki, M.A., Baker, C.B., Collins, W.G., Lawrimore, J.H., Leeper, R.D., Hall, M.E., Kochendorfer, J., Meyers, T.P., Wilson, T. and Diamond, H.J. (2013): U.S. Climate Reference Network soil moisture and temperature observations; *Journal of Hydrometeorology*, v. 14, p. 977–988.



Beltaos S. (2002): Effects of climate on mid-winter ice jams; *Hydrological Processes*, v. 16, p. 789–804.

Beltaos, S., Prowse, T., Bonsal, B., Carter, T., MacKay, R., Romolo, L., Pietroniro, A. and Toth, B. (2006): Climatic effects on ice-jam flooding of the Peace-Athabasca Delta; *Hydrological Processes*, v. 20, p. 4031–4050.

Bennett, K.E., Werner, A.T. and Schnorbus, M. (2012): Uncertainties in hydrologic and climate change impact analyses in headwater basins of British Columbia; *Journal of Climate*, v. 25, p. 5711–5730.

Berg, A., Sheffield, J. and Milly, P.C.D (2016): Divergent surface and total soil moisture projections under global warming; *Geophysical Research Letters*, v. 44, p. 236–244.

Born, S.K. (2012): Climate change impacts assessment and uncertainty analysis at the hydrology of a northern, data-sparse catchment using multiple hydrological models; Master's thesis, Civil Engineering, University of Manitoba, Winnipeg, 207 p., <<http://mspace.lib.umanitoba.ca/handle/1993/13692>>

Bonsal, B.R. and Cuell, C. (2017): Hydro-climatic variability and extremes over the Athabasca river basin: Historical trends and projected future occurrence; *Canadian Water Resources Journal*, v. 42, p. 315–335. doi:10.1080/07011784.2017.1328288

Bonsal, B.R. and Regier, M. (2007): Historical comparison of the 2001/2002 drought in the Canadian Prairies; *Climate Research*, v. 33, p. 229–242.

Bonsal, B.R. and Shabbar, A. (2008): Impacts of large-scale circulation variability on low streamflows over Canada: A review; *Canadian Water Resources Journal*, v. 33, p. 137–154.

Bonsal, B.R., Aider, R. Gachon, P. and Lapp, S. (2013): An Assessment of Canadian Prairie drought: Past, present, and future; *Climate Dynamics*, v. 41, p. 501–516.

Bonsal, B.R., Cuell, C., Wheaton, E., Sauchyn, D.J. and Barrow E. (2017): An assessment of historical and projected future hydro-climatic variability and extremes over southern watersheds in the Canadian Prairies; *International Journal of Climatology*, v. 37, p. 3934–3948. doi:10.1002/joc.4967

Bonsal, B.R., Wheaton, E.E., Chipanshi, A., Lin, C., Sauchyn, D.J. and Wen, L. (2011): Drought research in Canada: A review; *Atmosphere-Ocean*, v. 49, p. 303–319.

Bourgault, M.A., Larocque, M. and Roy, M. (2014): Simulation of aquifer-peatland-river interactions under climate change; *Hydrology Research*, v. 45, p. 425–440.

Boyer, C., Chaumont, D., Chartier, I. and Roy, A.G. (2010): Impact of climate change on the hydrology of St. Lawrence tributaries; *Journal of Hydrology*, v. 384, p. 65–83.

Brabets, T.P. and Walvoord, M.A. (2009): Trends in streamflow in the Yukon River Basin from 1944 to 2005 and the influence of the Pacific Decadal Oscillation; *Journal of Hydrology*, v. 371, p. 108–119.



Burn, D.H. (2008): Climatic influences on streamflow timing in the headwaters of the Mackenzie River Basin; *Journal of Hydrology*, v. 352, p. 225–238.

Burn, D.H. and Hag Elnur, M.H. (2002): Detection of hydrologic trends and variability; *Journal of Hydrology*, v. 255, p. 107–122.

Burn, D.H. and Hesch, N.M. (2006): A comparison of trends in potential and pan evaporation for the Canadian Prairies; *Canadian Water Resources Journal*, v. 31, p. 173–184.

Burn D.H. and Whitfield, P.H. (2016): Changes in floods and flood regimes in Canada; *Canadian Water Resources Journal*, v. 41, p. 139–150. doi: 10.1080/07011784.2015.1026844

Burn, D.H., Abdul Aziz, O.I. and Pietroniro, A. (2004a): A comparison of trends in hydrological variables for two watersheds in the Mackenzie River Basin; *Canadian Water Resources Journal*, v. 29, p. 283–298.

Burn, D.H., Cunderlik, J.M. and Pietroniro, A. (2004b): Hydrological trends and variability in the Liard River basin; *Hydrological Sciences Journal*, v. 49, p. 53–67.

Burn, D.H., Fan, L. and Bell, G. (2008): Identification and quantification of streamflow trends on the Canadian Prairies; *Hydrological Sciences Journal*, v. 53, p. 538–549.

Burn, D.H., Sharif, M. and Zhang, K. (2010): Detection of trends in hydrological extremes for Canadian watersheds; *Hydrological Processes*, v. 24, p. 1781–1790. doi: 10.1002/hyp.7625

Burn, D.H., Whitfield, P.H. and Sharif, M. (2016): Identification of changes in floods and flood regimes in Canada using a peaks over threshold approach; *Hydrological Processes*, v. 30, p. 3303–3314. doi: 10.1002/hyp.10861

Bush, E.J., Loder, J.W., James, T.S., Mortsch, L.D. and Cohen, S.J. (2014): An Overview of Canada's Changing Climate; Chapter 2 in *Canada in a Changing Climate: Sector Perspectives on Impacts and Adaptation*, (ed.) F.J. Warren and D.S. Lemmen; Government of Canada, Ottawa, Ontario, p. 23–64, <https://www.nrcan.gc.ca/sites/www.nrcan.gc.ca/files/earth-sciences/pdf/assess/2014/pdf/Chapter2-Overview_Eng.pdf>

Buttle, J.M., Allen, D.M., Cassie, D., Davison, B., Hayashi, M., Peters, D.L., Pomeroy, J.W., Simonovic, S., St-Hilaire, A. and Whitfield, P.H. (2016): Flood processes in Canada, regional and special aspects; Special Issue on Floods in Canada; *Canadian Water Resources Journal*, v. 41, p. 7–30. doi: 10.1080/07011784.2015.1131629

Canadian National Committee (1975): Canadian survey on the water balance of lakes; in *International Hydrological Decade Report*; Environment Canada, Ottawa, Ontario.

Carrera, M.L., Bélair, S. and Bilodeau, B. (2015): The Canadian land data assimilation system (CaLDAS): Description and synthetic evaluation study; *Journal of Hydrometeorology*, v. 16, p. 1293–1314. doi: 10.1175/JHM-D-14-0089.1

CCME [Canadian Council of Ministers of the Environment] (2010): Review and assessment of Canadian groundwater resources, management, current research mechanisms and priorities; Canadian Council of Ministers of the Environment, <http://www.ccme.ca/files/Resources/water/groundwater/gw_phase1_smry_en_1.1.pdf>.

CDA [Canadian Dam Association] (2016): Dams in Canada; Canadian Dam Association, Toronto, Ontario <https://www.cda.ca/EN/Dams_in_Canada/EN/Dams_In_Canada.aspx?hkey=11c76c52-7794-4ddf-b541-584f9ea2d-be9>.

CEHQ [Centre d'Expertise Hydrique Québec] (2015): Hydroclimatic atlas of southern Québec: The impact of climate change on high, low and mean flow regimes for the 2050 horizon; Centre d'expertise hydrique du Québec, Québec, Quebec, 81 p. <https://www.cehq.gouv.qc.ca/hydrometrie/atlas/Atlas_hydroclimatique_2015EN.pdf>

Champagne, C., Berg, A.A., McNairn, H., Drewitt, G. and Huffman, T. (2012): Evaluation of soil moisture extremes for agricultural productivity in the Canadian prairies; *Agricultural and Forest Meteorology*, v. 165, p. 1–11.

Champagne, C., McNairn, H. and Berg, A.A. (2011): Monitoring agricultural soil moisture extremes in Canada using passive microwave remote sensing; *Remote Sensing of Environment*, v. 115, p. 2434–2444.

Champagne, C., Rowlandson, T., Berg, A., Burns, T., L'Heureux, J., Tetlock, E., Adams, J.R., McNairn, H., Toth, B. and Itenfisu, D. (2016) Satellite surface soil moisture from SMOS and Aquarius: Assessment for applications in agricultural landscapes; *International Journal of Applied Earth Observation and Geoinformation*, v. 45, p. 143–154.

Chan, S.K., Bindlish, R., O'Neill, P.E., Njoku, E., Jackson, T., Colliander, A., Chen, F., Burgin, M., Dunbar, S., Piepmeier, J., Yuch, S., Entekhabi, D., Cosh, M.H., Caldwell, T., Walker, J., Wu, X., Berg, A., Rowlandson, T., Pacheco, A., McNairn, H., Thibeault, M., Martinez-Fernandez, J., Gonzalez-Zamora, A., Seyfried, M., Bosch, D., Starks, P., Goodrich, D., Prueger, J., Palecki, M., Small, E.E., Zreda, M., Calvet, J.C., Crow, W. and Kerr, Y. (2016): Assessment of the SMAP passive soil moisture product; *IEEE Transactions on Geoscience and Remote Sensing*, v. 54, p. 4994–5007.

Chen, J., Brissette, F.P., Poulin, A. and Leconte, R. (2011): Overall uncertainty study of the hydrological impacts of climate change for a Canadian watershed; *Water Resources Research*, v. 47. doi: 10.1029/2011WR010602

Chen, Z., Grasby, S. and Osadetz, K. (2002): Predicting groundwater variation from climatic variables: an empirical model; *Journal of Hydrology*, v. 260, p. 102–117.

Chen, Z., Grasby, S. and Osadetz, K. (2004): Relation between climate variability and groundwater levels in the upper carbonate aquifer, southern Manitoba, Canada; *Journal of Hydrology*, v. 290, p. 43–62.

Chipanshi, A.C., Findlater, K.M., Hadwen, T. and O'Brien, E.G. (2006): Analysis of consecutive droughts on the Canadian Prairies; *Climate Research*, v. 30, p. 175–187.

Cohen, S., Koshida, G. and Mortsch, L. (2015): Climate and water availability indicators in Canada: Challenges and a way forward. Part III – Future scenarios; *Canadian Water Resources Journal*, v. 40, p. 160–173.



Colliander, A., Jackson, T.J., Bindlish, R. Chan, S., Das, N., Kim, S.B., Cosh, M.H., Dunbar, R.S., Dang, L., Pashaian, L., Asanuma, J., Aida, K., Berg, A., Rowlandson, T., Bosch, D., Caldwell, T., Caylor, K., Goodrich, D., al Jassar, H., Lopez-Baeza, E., Martínez-Fernandez, J., Gonzalez-Zamora, A., Livingston, S., McNairn, H., Pacheco, A., Moghaddam, M., Montzka, C., Notarnicola, C., Niedrist, G., Pellarin, T., Prueger, J., Pulliainen, J., Rautiainen, K., Ramos, J., Seyfried, M., Starks, P., Su, Z., Zeng, Y., van der Velde, R., Thibeault, M., Dorigo, W., Vreugdenhil, M., Walker, J.P., Wu, X., Monerris, A., O'Neill, P.E., Entekhabi, D., Njoku, E.G. and Yueh, S. (2017): Validation of SMAP surface soil moisture products with core validation sites; *Remote Sensing of Environment*, v. 191, p. 215–231.

Cook, B.I., Smerdon, J.E., Seager, R. and Coats, S. (2014): Global Warming and 21st Century Drying; *Climate Dynamics*, v. 43, p. 2607–2627.

Cunderlik, J.M. and Ouarda, T.M.B.J. (2009): Trends in the timing and magnitude of floods in Canada; *Journal of Hydrology*, v. 375, p. 471–480.

Dai, A. (2011): Characteristics and trends in various forms of the Palmer Drought Severity Index during 1900–2008; *Journal of Geophysical Research*, v. 116, D12115. doi: 10.1029/2010JD015541

Dai, A. (2012): Increasing Drought under Global Warming in Observations and Models; *Nature Climate Change*, v. 3, p. 52–58.

DeBeer, C.M., Wheeler, H.S., Carey, S.K. and Chun, K.P. (2016): Recent, climatic, cryospheric, and hydrological changes over the interior of western Canada: A review and synthesis; *Hydrology and Earth System Sciences*, v. 20, p. 1573–1598.

Déry, S.J. and Wood, E.F. (2004): Teleconnection between the Arctic Oscillation and Hudson Bay river discharge; *Geophysical Research Letters*, v. 31, L18205. doi: 10.1029/2004GL020729

Déry, S.J., Hernández-Henríquez, M.A., Owens, P.N., Parkes, M.W. and Petticrew, E.L. (2012): A century of hydrological variability and trends in the Fraser River Basin; *Environmental Research Letters*, v. 7, 024019. doi:10.1088/1748-9326/7/2/024019

Déry, S.J., Mlynowski, T.J., Hernández-Henriquez, M.A. and Straneo, F. (2011): Interannual variability and interdecadal trends in Hudson Bay streamflow; *Journal of Marine Systems*, v. 88, p. 341–351.

Déry, S.J., Stadnyk, T.A., MacDonald, M.K. and Gauli-Sharma, B. (2016): Recent trends and variability in river discharge across northern Canada; *Hydrology and Earth System Sciences*, v. 20, p. 4801–4818.

Déry, S.J., Stahl, K., Moore, R.D., Whitfield, P.H., Menounos, B. and Burford, J.E. (2009): Detection of runoff timing changes in pluvial, nival, and glacial rivers of western Canada; *Water Resources Research*, v. 45, W04426. doi:10.1029/2008WR006975

DFO [Fisheries and Oceans Canada] Canadian Hydrographic Service (2013): Water levels, Great Lakes and Montreal harbour; *Monthly Water Level Bulletin*, <<http://publications.gc.ca/site/eng/9.500663/publication.html>>.

Dibike, Y.D., Prowse, T.D., Bonsal, B.R. and O'Neil, H.C.L. (2017): Implications of future climate on water availability in the western Canadian river basins; *International Journal of Climatology*, v. 37, p. 3247–3263.



Donohue, R.J., McVicar, T.R. and Roderick, M.L. (2010): Assessing the ability of potential evaporation formulations to capture the dynamics in evaporative demand within a changing climate; *Journal of Hydrology*, v. 386, p. 186–197.

Doringo, W.A., Wagner, W., Hohensinn, R., Hahn, S., Paulik, C., Xaver, A., Gruber, A., Drusch, M., Mecklenburg, S., van Oevelen, P., Robock, A. and Jackson, T. (2011): The international soil moisture network: a data hosting facility for global in situ soil moisture measurements; *Hydrology and Earth System Sciences*, v. 15, p. 1675–1698.

Ducks Unlimited Canada (2010): Southern Ontario wetland conversion analysis: final report; Ducks Unlimited; Barrie, Ontario, 23 p. <http://www.ducks.ca/assets/2010/10/duc_ontariowca_optimized.pdf>.

Duguay, C., Ernou, Y. and Hawkings, J. (1999): SAR and optical satellite observations of ice covered thermokarst lakes, Old Crow Flats, Yukon Territory; paper presented at 56th Eastern Snow Conference, Fredericton, New Brunswick, Canada.

Dumanski, S., Pomeroy, J.W. and Westbrook, C.J. (2015): Hydrological regime changes in a Canadian Prairie basin; *Hydrological Processes*, v. 29, p. 3893–3904.

EBNFLO Environmental and AquaResource Inc. (2010): Guide for assessment of hydrologic effects of climate change in Ontario; prepared for the Ontario Ministry of Natural Resources and Ministry of the Environment in partnership with Credit Valley Conservation, <https://www.researchgate.net/profile/Linda_Mortsch/publication/309565142_Guide_for_assessment_of_hydrologic_effects_of_climate_change_in_Ontario/links/58adeba892851cf7ae85b0db/Guide-for-assessment-of-hydrologic-effects-of-climate-change-in-Ontario.pdf>.

ECCC [Environment and Climate Change Canada] (2017): Water level and flow; Environment and Climate Change Canada, <<https://wateroffice.ec.gc.ca/>>.

Ehsanzadeh, E. and Adamowski, K. (2007): Detection of trends in low flows across Canada; *Canadian Water Resources Journal*, v. 32, p. 251–264.

El-Jabi, N., Turkkan, N. and Caissie, D. (2013): Regional climate index for floods and droughts using Canadian Climate Model (CGCM3.1); *American Journal of Climate Change*, v. 2, p. 106–115.

Eum, H., Dibike, Y. and Prowse, T. (2017): Climate-induced alteration of hydrologic indicators in the Athabasca River Basin, Alberta, Canada; *Journal of Hydrology*, v. 544, p. 327–342.

Famiglietti, J.S., Ryu, D., Berg, A., Rodell, M. and Jackson, T.J. (2008): Field observations of soil moisture availability across scales; *Water Resources Research*, v. 44, W01423. doi:10.1029/2006WR005804

Federal, Provincial and Territorial Governments of Canada (2010): Canadian Biodiversity: Ecosystem Status and Trends 2010; Canadian Councils of Resource Ministers, Ottawa, Ontario, 142 p.

Fernandes, R., Korolevych, V. and Wang, S. (2007): Trends in land evapotranspiration over Canada for the period 1960–2000 based on in situ



climate observations and a land surface model; *Journal of Hydrometeorology*, v. 8, p. 1016–1030.

Fleming, S.W. (2010): Signal-to-noise ratios of geophysical and environmental time series; *Environmental and Engineering Geoscience*, v. 16, p. 389–399.

Fleming, S.W. and Clarke, G.K.C. (2003): Glacial control of water resource and related environmental responses to climatic warming: Empirical analysis using historical streamflow data from Northwestern Canada; *Canadian Water Resources Journal*, v. 28, p. 69–86.

Fleming, S.W. and Weber, F.A. (2012): Detection of long-term change in hydroelectric reservoir inflows: Bridging theory and practice; *Journal of Hydrology*, v. 470, p. 36–54.

Forbes, K.A., Kienzle, S.W., Coburn, C.A., Byrne, J.M. and Rasmussen, J. (2011): Simulating the hydrological response to predicted climate change on a watershed in southern Alberta, Canada; *Climatic Change*, v. 105, p. 555–576.

Fournier, R.A., Grenier, M., Lavoie, A. and Hélie, R. (2007): Towards a strategy to implement the Canadian Wetland Inventory using satellite remote sensing; *Canadian Journal of Remote Sensing*, v. 33, p. S1–S16.

Gan, T.Y. (1998): Hydroclimatic trends and possible climatic warming in the Canadian Prairies; *Water Resources Research*, v. 34, p. 3009–3015.

Ghanbari, R.N. and Bravo, H.R. (2008): Coherence between atmospheric teleconnections, Great Lakes water levels, and regional climate; *Advances in Water Resources*, v. 31, p. 1284–1298.

Girardin, M.P., Tardif, J., Flannigan, M.D., Wotton, B.M. and Bergeron, Y. (2004): Trends and periodicities in the Canadian drought code and their relationships with atmospheric circulation for the southern boreal forest; *Canadian Journal of Forest Research*, v. 34, p. 103–119.

GLERL [Great Lakes Environmental Research Laboratory] (2017): GLERL Great Lakes monthly hydrologic data (1860–Recent), <www.glerl.noaa.gov/ahps/mnth-hydro.html>.

Green, N.R. and MacQuarrie, K.T.B. (2014): An evaluation of the relative importance of the effects of climate change and groundwater extraction on seawater intrusion in coastal aquifers in Atlantic Canada; *Hydrogeology Journal*, v. 22, p. 609–623.

Grillakis, M.G., Koutroulis, A.G. and Tsanis, I.K. (2011): Climate change impact on the hydrology of Spencer Creek watershed in Southern Ontario, Canada; *Journal of Hydrology*, v. 409, p. 1–19.

Gronewold, A.D., Bruxer, J., Durnford, D., Smith, J.P., Clites, A.H., Seglenieks, F., Qian, S.S., Hunter, T.S. and Fortin, V. (2016): Hydrological drivers of record-setting water level rise on Earth's largest lake system; *Water Resources Research*, v. 52, p. 4026–4042. doi:10.1002/2015WR018209

Guay C., Minville M. and Braun M. (2015): A global portrait of hydrological changes at the 2050 horizon for the province of Quebec; *Canadian Water Resources Journal*, v. 40, p. 285–302.

- Hanrahan, J.L., Kravtsov, S.V. and Roebber, P.J. (2010): Connecting past and present climate variability to the water levels of Lakes Michigan and Huron; *Geophysical Research Letters*, v. 37, L01701. doi:10.1029/2009GL041707
- Harma, K. J., Johnson, M.S. and Cohen, S.J. (2012): Future water supply and demand in the Okanagan basin, British Columbia: A scenario-based analysis of multiple, interacting stressors; *Water Resources Management*, v. 26, p. 667–689.
- Harvey, K.D., Pilon, P.J. and Yuzyk, T.R. (1999): Canada's Reference Hydrometric Basin Network (RHBN); in *Proceedings of the Canadian Water Resources Association 51st Annual Conference, Partnerships in Water Resources Management*, Nova Scotia, Canada.
- Hayashi, M. and Farrow, C.R. (2014): Watershed-scale response of groundwater recharge to inter-annual and inter-decadal variability in precipitation (Alberta, Canada); *Hydrogeology Journal*, v. 22, p. 1825–1839.
- Hayashi, M., Jackson, J.F. and Xu, L. (2010): Application of the versatile soil moisture budget model to estimate evaporation from prairie grassland; *Canadian Water Resources Journal*, v. 35, p. 187–208.
- Hayhoe, K., VanDorn, J., Croley, T., Schlegal, N. and Wuebbles, D. (2010): Regional climate change projections for Chicago and the US Great Lakes; *Journal of Great Lakes Research*, v. 36, p. 7–21.
- Hernández-Henríquez, M.A., Sharma, A.R. and Déry, S.J. (2017): Variability and trends in runoff in the rivers of British Columbia's Coast and Insular Mountains; *Hydrological Processes*, v. 31, p. 3269–3282.
- Hidalgo, H.G., Das, T., Dettinger, M.D., Cayan, D.R., Pierce, D.W., Barnett, T.P., Bala, G., Mirin, A., Wood, A.W., Bonfils, C., Santer, B.D. and Nozawa, T. (2009): Detection and attribution of streamflow timing changes to climate change in the western United States; *Journal of Climate*, v. 22, p. 3838–3855.
- Hinzman, L.D., Bettez, N.D., Bolton, W.R., Chapin, F.S., Dyurgerov, M.B., Fastie, C.L., Griffith, B., Hollister, R.D., Hope, A., Huntington, H.P., Jensen, A.M., Jia, G.L., Jorgenson, T., Kane, D.L., Klein, D.R., Kofinas, G., Lynch, A.H., Lloyd, A.H., McGuire, A.D., Nelson, F.E., Thomas, W.C., Osterkamp, E., Racine, C.H., Romanovsky, V.E., Stone, R.S., Stow, D.A., Sturm, M., Tweedie, C.E., Vourlitis, G.L., Walker, M.D., Walker, D.A., Webber, P.J., Welker, J.M., Winker, K.S., Yoshikawa, K. (2005): Evidence and implications of recent climate change in northern Alaska and other Arctic regions; *Climatic Change*, v. 72, p. 251–298.
- Houghton, J. (2004): *Global Warming: The Complete Briefing* (3rd edition); Cambridge University Press, Cambridge, United Kingdom, 351 p.
- Huang, J., Halpenny, J., van der Wal, W., Klatt, C., James, T.S. and Rivera, A. (2012): Detectability of groundwater storage change within the Great Lakes Water Basin using GRACE; *Journal of Geophysical Research*, v. 117. doi:10.1029/2011JB008876
- Huang, J., Pavlic, G., Rivera, A., Palombi, D. and Smerdon, B. (2016): Mapping groundwater storage variations with GRACE: a case study in Alberta, Canada; *Hydrogeology Journal*, v. 24, p. 1663–1680.



IJC [International Joint Commission] (2017): Extreme conditions and challenges during high water levels on Lake Ontario and the St. Lawrence River, <<https://ijc.org/en/extreme-conditions-and-challenges-during-high-water-levels-lake-ontario-and-st-lawrence-river/>>.

Islam, S.U., Déry, S.J. and Werner, A.T. (2017): Future climate change impacts on snow and water resources of the Fraser River Basin, British Columbia; *Journal of Hydrometeorology*, v. 18, p. 473–496.

IUGLS [International Upper Great Lakes Study] (2012): Lake Superior regulation: Addressing uncertainty in upper Great Lakes water levels; Final Report to the International Joint Commission, March 2012, 215 p.

Jeong, D.I. and Sushama, L. (2018): Rain-on-snow events over North America based on two Canadian regional climate models; *Climate Dynamics*, v. 50, p. 303–316.

Jeong, D.I., Sushama, L. and Khaliq, M.N. (2014): The role of temperature in drought projections over North America; *Climatic Change*, v. 127, p. 289–303.

Jones, N.E., Petreman, I.C. and Schmidt, B.J. (2015): High flows and freshet timing in Canada: Observed trends; *Climate Change Research Report CCRR-42*, Ontario Ministry of Natural Resources and Forestry, Science and Research Branch, Peterborough, Ontario, <http://www.climateontario.ca/MNR_Publications/CCRR42.pdf>.

Jyrkama, M.I. and Sykes, J.F. (2007): The impact of climate change on spatially varying groundwater recharge in the Grand River watershed (Ontario); *Journal of Hydrology*, v. 338, p. 237–250.

Kang, D.H., Gao, H., Shi, H., Islam, S. and Dery, S.J. (2016): Impacts of a rapidly declining mountain snowpack on streamflow timing in Canada's Fraser River basin; *Scientific Reports*, v. 6. doi: 10.1038/srep19299

Kerkhoven, E. and Gan, T.Y. (2011): Differences and sensitivities in potential hydrologic impact of climate change to regional-scale Athabasca and Fraser River basins of the leeward and windward sides of the Canadian Rocky Mountains respectively; *Climatic Change*, v. 106, p. 583–607.

Khaliq, M.N., Ouara, T.B.M.J., Gachon, P. and Sushama, L. (2008): Temporal evolution of low-flow regimes in Canadian rivers; *Water Resources Research*, v. 44. doi:10.1029/2007WR006132

Kienzle, S.W., Nemeth, M.W., Byrne, J.M. and MacDonald, R.J. (2012): Simulating the hydrological impacts of climate change in the upper North Saskatchewan River basin, Alberta, Canada; *Journal of Hydrology*, v. 412–413, p. 76–89.

Klaassen, J. (2002): A climatological assessment of major 20th century drought in southern Ontario, Canada; *Proceedings of the 13th Conference on Applied Climatology*, 13–16 May 2002; American Meteorological Society, Portland, Oregon.

Kurylyk, B.L. and MacQuarrie, K.T.B. (2013): The uncertainty associated with estimating future groundwater recharge: A summary of recent research and an example from a small unconfined aquifer in a northern humid-continental climate; *Journal of Hydrology*, v. 492, p. 244–253.



Kurylyk, B.L., MacQuarrie, K.T.B. and Voss, C.I. (2014): Climate change impacts on the temperature and magnitude of groundwater discharge from shallow, unconfined aquifers; *Water Resources Research*, v. 50, p. 3253–3274.

Lantz, T.C. and Turner, K.W. (2015): Changes in lake area in response to thermokarst processes and climate in Old Crow Flats, Yukon; *Journal of Geophysical Research: Biogeosciences*, v. 120, p. 513–524.

Lapp, S., Sauchyn, D.J. and Toth, B. (2009): Constructing scenarios of future climate and water supply for the SSRB: Use and limitations for vulnerability assessment; *Prairie Forum*, v. 34, p. 153–180.

Lemieux, J.M., Hassaoui, J., Molson, J., Therrien, R., Therrien, P., Chouteau, M. and Ouellet, M. (2015): Simulating the impact of climate change on the groundwater resources of the Magdalen Islands, Québec, Canada; *Journal of Hydrology: Regional Studies*, v. 3, p. 400–423.

Lesack, L.F.W. and Marsh, P., (2010): River-to-lake connectivities, water renewal, and aquatic habitat diversity in the Mackenzie River Delta; *Water Resources Research*, v. 46. doi:10.1029/2010WR009607

Levison, J., Larocque, M., Fournier, V., Gagné, S., Pellerin, S. and Ouellet, M.A. (2014a): Dynamics of a headwater system and peatland under current conditions and with climate change; *Hydrological Processes*, v. 28, p. 4808–4822.

Levison, J., Larocque, M. and Ouellet, M.A. (2014b): Modeling low-flow bedrock springs providing ecological habitats with climate change scenarios; *Journal of Hydrology*, v. 515, p. 16–28.

Levison, J., Larocque, M., Ouellet, M.A., Ferland, O. and Poirier, C. (2016): Long-term trends in groundwater recharge and discharge in a fractured bedrock aquifer – past and future conditions; *Canadian Water Resources Journal*, v. 41, p. 500–514.

Liu, A.Q., Mooney, C., Szeto, K., Thériault, J.M., Kochtubajda, B., Stewart, R.E., Boodoo, S., Goodson, R., Li, Y. and Pomeroy, J. (2016): The June 2013 Alberta Catastrophic Flooding Event: Part 1—Climatological aspects and hydrometeorological features; *Hydrological Processes*, v. 30, p. 4899–4916.

Loukas, A., Vasiliades, L. and Dalezios, N.R. (2000): Flood producing mechanisms identification in southern British Columbia, Canada; *Journal of Hydrology*, v. 227, p. 218–235.

Loukas, A., Vasiliades, L. and Dalezios, N.R. (2002): Climatic impacts on the runoff generation processes in British Columbia, Canada; *Hydrology and Earth System Sciences*, v. 6, p. 211–227.

MacDonald, D.D., Levy, D.A., Czarnecki, A., Low, G. and Richea, N. (2004): State of the Aquatic Knowledge of Great Bear Watershed; Prepared for: Water Resources Division Indian and Northern Affairs Canada, Yellowknife, Northern Territory <<http://www.dfo-mpo.gc.ca/Library/278592.pdf>>.

MacKay, M. and Seglenieks, F. (2013): On the simulation of Laurentian Great Lakes water levels under projections of global climate change; *Climatic Change*, v. 117, p.55–67.



Mareuil, A., Leconte, R., Rissette, F. and Minville, M. (2007): Impacts of climate change on the frequency and severity of floods in the Châteauguay River basin, Canada; *Canadian Journal of Civil Engineering*, v. 34, p. 1048–1060.

Marsh P. and Lesack L. (1996): The hydrologic regime of perched lakes in the Mackenzie Delta: Potential responses to climate change; *Limnology and Oceanography*, v. 41, p. 849–856.

Marsh, P., Russell, M., Pohl, S., Haywood, H. and Onclin, C. (2009): Changes in thaw lake drainage in the Western Canadian Arctic from 1950 to 2000; *Hydrological Processes*, v. 23, p. 145–158.

Masud, M.B., Khaliq, M.N. and Wheeler, H.S. (2017): Future changes to drought characteristics over the Canadian Prairie Provinces based on NARCCAP multi-RCM ensemble; *Climate Dynamics*, v. 48, p. 2685–2705.

McCabe, G.J. and Wolock, D.M. (2015): Variability and trends in global drought; *Earth and Space Science*, v. 2, p. 223–228.

McKee, T.B., Doeskin, N.J. and Kleist, J. (1993): The relationship of drought frequency and duration to time scales; *Proceedings of the 8th Conference on Applied Climatology*, 17–22 January 1993, American Meteorological Society, Boston, Massachusetts, p. 179–184.

Mearns, L.O., Gutowski, W.J., Jones, R., Leung, L.Y., McGinnis, S., Nunes, A.M.B. and Qian, Y. (2009): A regional climate change assessment program for North America; *EOS*, v. 90, p. 311–312.

Melillo, J.M., Richmond, T.C. and Yohe, G.W. (ed.) (2014): *Highlights of Climate Change Impacts in the United States: The Third National Climate Assessment*; U.S. Global Change Research Program, 148 p.

Milly, P.C.D. and Dunne, K.A. (2011): Hydrologic adjustment of climate-model projections: The potential pitfall of potential evapotranspiration; *Earth Interactions*, v. 15, p. 1–14.

Milly, P.C.D. and Dunne, K.A. (2016): Potential evapotranspiration and continental drying; *Nature Climate Change Letters*, v. 6, p. 946–949.

Minville, M., Brissette, F. and Leconte, R. (2008): Uncertainty of the impact of climate change on the hydrology of a Nordic watershed; *Journal of Hydrology*, v. 358, p. 70–83.

Minville, M., Krau, S., Brissette, F. and Leconte, R. (2010): Behaviour and performance of a water resource system in Québec (Canada) under adapted operating policies in a climate change context; *Water Resources Management*, v. 24, p. 1333–1352.

Monk, W.A. and Baird, D.J. (2011): Ecosystem status and trends report: biodiversity in Canadian lakes and rivers; *Canadian Biodiversity: Ecosystem Status and Trends 2010*; Technical Thematic Report No. 20, Canadian Councils of Resource Ministers, Ottawa, Ontario, 79 p.

Monk, W.A., Peters, D.L., Curry, R.A. and Baird, D.J. (2011): Quantifying trends in indicator hydroecological variables for regime-based groups of Canadian rivers; *Hydrological Processes*, v. 25, p. 3086–3100.



Moore, R.D., Sidle, R.C., Eaton, B., Takahashi, G. and Wilford, D. (2017): Water and watersheds; Chapter 7 in Innes, (ed.) J.L. and Tikina, A.V.; Sustainable Forest Management: From Concept to Practice, Routledge, Taylor and Francis Group, New York, NY, USA 396 p.

Mortsch, L., Cohen, S. and Koshida, G. (2015): Climate and water availability indicators in Canada: Challenges and a way forward. Part II – Historic trends; Canadian Water Resources Journal, v. 40, p. 146–159.

Motiee, H. and McBean, E. (2017): Assessment of climate change impacts on groundwater recharge for different soil types-Guelph region in Grand River basin, Canada; ECOPERSIA, v. 5, p. 1731–1744.

Music B., Frigon A., Longfren B., Turcotte R. and Cyr J.F. (2015): Present and future Laurentian Great Lakes hydroclimatic conditions as simulated by regional climate models with an emphasis on Lake Michigan-Huron; Climate Change, v. 130, p. 603–618.

Najafi, M.R., Zwiers, F. and Gillett, N. (2017a): Attribution of the observed spring snowpack decline in British Columbia to anthropogenic climate change; Journal of Climate, v. 30, p. 4113–4130.

Najafi, M.R., Zwiers, F. and Gillett, N. (2017b): Attribution of observed streamflow changes in key British Columbia drainage basins; Geophysical Research Letters, v. 44, p. 11012–11020.

Nalley, D., Adamowski, J. and Khalil, B. (2012): Using discrete wavelet transforms to analyze trends in streamflow and precipitation in Quebec and Ontario (1954–2008); Journal of Hydrology, v. 475, p. 204–228.

National Wetlands Working Group (1988): Wetlands of Canada; Ecological Land Classification Series No. 24; Sustainable Development Branch, Environment Canada, Ottawa, ON, and Polyscience Publications Inc., Montréal, Quebec, 452 p.

National Wetlands Working Group (1997): The Canadian wetland classification system (2nd edition), (Ed.) B.G. Warner and C.D.A. Rubec; The Wetlands Research Centre, University of Waterloo, Waterloo, Ontario, 68 p.

Nikolik, V.V. and Simonovic, S.P. (2015): Multi-method modeling framework for support of integrated water resources management; Environmental Processes, v. 2, p. 461–483.

Oni, S.K., Futter, M.N., Molot, L.A., Dillon, P.J. and Crossman, J. (2014): Uncertainty assessments and hydrological implications of climate change in two adjacent agricultural catchments of a rapidly urbanizing watershed; Science of the Total Environment, v. 473–474, p. 326–337.

Pacheco, A., McNairn, H., Mahmoodi, A., Champagne, C. and Kerr, Y.H. (2015): The impact of national land cover and soils data on SMOS soil moisture retrieval over Canadian agricultural landscapes; IEEE Journal of Selected Topics in Applied Earth Observations and Remote Sensing, v. 8, p. 5281–5293.

PaiMazumder, D., Sushama, L., Laprise, R., Khaliq, M.N. and Suachyn, D. (2012): Canadian RCM projected changes to short and long-term drought characteristics over the Canadian Prairies; International Journal of Climatology, v. 33, p. 1409–1423.



Palmer, W.C. (1965): Meteorological Drought; Research Paper No. 45, Weather Bureau, Washington, District of Columbia, 58 pp.

Peters, D.L. (2013): Multi-Scale Hydroclimatic Controls on the Duration of Pondered Water in Wetland-Lake Environments of a Cold Regions Delta. WSTD Contribution No. 11-083; National Hydrology Research Centre, Saskatoon, Saskatchewan, 43 p.

Peters, D.L. and Buttle, J.M. (2010): The effects of flow regulation and climatic variability on obstructed drainage and reverse flow contribution in a Northern river–lake–delta complex, Mackenzie basin headwaters; *River Research and Application*, v. 26, p. 1065–1089.

Peters, D.L., Atkinson, D., Monk, W.A., Tenenbaum, D.E. and Baird, D.J. (2013): A multi-scale hydroclimatic analysis of runoff generation in the Athabasca, River, western Canada; *Hydrological Processes*, v. 27, p. 1915–1934.

Peters D.L., Cassie, D., Monk, W.A., Rood, S. and St-Hilaire, A. (2016): Ecological Aspects of Floods in Canada: Special Issue on Floods in Canada; *Canadian Water Resources Journal*, v. 41, p. 288–306.

Peters, D.L., Prowse, T.D., Pietroniro, A. and Leconte, R. (2006): Flood hydrology of the Peace-Athabasca Delta, northern Canada; *Hydrological Processes*, v. 20, p. 4073–4096.

Plug, L.J., Walls, C. and Scott, B.M. (2008): Tundra lake changes from 1978 to 2001 on the Tuktoyaktuk Peninsula, western Canadian Arctic; *Geophysical Research Letters*, v. 35. doi:10.1029/2007GL032303

Poitras, V., Sushama, L., Seglenieks, F., Khaliq, M.N. and Soulis, E. (2011): Projected changes to streamflow characteristics over western Canada as simulated by the Canadian RCM; *Journal of Hydrometeorology*, v. 12, p. 1395–1413.

Prowse, T.D., Bonsal, B.R., Lacroix, M.P. and Beltaos, S. (2002): Trends in river-ice breakup and related temperature controls; in *Ice in the Environment*, (ed.) V.A. Squire and P. Lannghome; Proceedings of the 16th IAHR Conference on Sea Ice Processes, International Association of Hydraulic Engineering and Research, Dunedin, New Zealand, p. 64–71.

Quilbe, R., Rousseau, A.N., Moquet, J.S., Trinh, N.B., Dibike, Y., Gachon, P. and Chaumont, D. (2008): Assessing the effect of climate change on river flow using general circulation models and hydrological modelling: Application to the Chaudière River, Quebec, Canada; *Canadian Water Resources Journal*, v. 33, p. 73–94.

Radic, V., Cannon, A.J., Menounos, B. and Gi, N. (2015): Future changes in autumn atmospheric river events in British Columbia, Canada, as projected by CMIP5 global climate models; *Journal of Geophysical Research: Atmospheres*, v. 120, p. 9279–9302.

Rasmussen, P.F. (2015): Assessing the impact of climate change on the frequency of floods in the Red River basin; *Canadian Water Resources Journal*, v. 41, p. 331–342.

Reichle, R.H., Draper, C.S., Liu, Q., Giroto, M., Mahanama, S.P.P., Koster, R.D. and De Lannoy, G.J.M. (2017): Assessment of MERRA-2 land surface hydrology estimates; *Journal of Climate*, v. 30, p. 2937–2960.



- Rivard, C., Paniconi, C., Vigneault, H. and Chaumont, D. (2014): A watershed-scale study of climate change impacts on groundwater recharge (Annapolis Valley, Nova Scotia, Canada); *Hydrological Sciences Journal*, v. 59, p. 1437–1456.
- Rivard, C., Vigneault, H., Piggott, A.R., Larocque, M. and Anctil, F. (2009): Groundwater recharge trends in Canada; *Canadian Journal of Earth Sciences*, v. 46, p. 841–854.
- Rivera, A. (2014): Groundwater Basics; Chapter 2 in *Canada's Groundwater Resources* (ed.) A. Rivera; Fitzhenry & Whiteside Limited, Markham, Ontario, p. 22–61.
- Rivera, A., Allen, D.M. and Maathuis, M. (2004). Climate Variability and Change: Groundwater Resources; Chapter 10 in *Threats to Water Availability in Canada*, NWRI Scientific Assessment Report Series No. 3 and ACSD Science Assessment Series No. 1.; National Water Research Institute, Burlington, Ontario, p. 77–83.
- Roberts, J., Pryse-Phillips, A. and Snelgrove, K. (2012): Modeling the potential impacts of climate change on a small watershed in Labrador, Canada; *Canadian Water Resources Journal*, v. 37, p. 231–251.
- Rood, S.B., Kaluthota, S., Philipsen, L.J., Rood, N.J. and Zanewich, K.P. (2017): Increasing discharge from the Mackenzie River system to the Arctic Ocean; *Hydrological Processes*, v. 31, p. 150–160.
- Rood, S.B., Pan, J., Gill, K.M., Franks, C.G., Samuelson, G.M. and Shepherd, A. (2008): Declining summer flows of Rocky Mountain rivers: Changing seasonal hydrology and probable impacts on floodplain forests; *Journal of Hydrology*, v. 349, p. 397–410.
- Rood, S.B., Samuelson, G.M., Weber, J.K. and Wywrot, K.A. (2005): Twentieth-century decline in streamflows from the hydrographic apex of North America; *Journal of Hydrology*, v. 306, p. 215–233.
- Sandink, D. (2016): Urban flooding and ground-related homes in Canada: an overview; *Journal of Flood Risk Management*, v. 9, p. 208–223.
- Schaefer, G.L., Cosh, M.H. and Jackson, T.J. (2007): The USDA natural resources conservation service soil climate analysis network (SCAN); *Journal of Atmospheric and Oceanic Technology*, v. 24, p. 2073–2077.
- Schertzer, W.M., Rouse, W.R., Lam, D.C.L., Bonin, D. and Mortsch, L.D. (2004): Chapter 12. Climate Variability and Change: Lakes and Reservoirs; Chapter 12 in *Threats to Water Availability in Canada*, NWRI Scientific Assessment Report Series No. 3 and ACSD Science Assessment Series No. 1.; National Water Research Institute, Burlington, Ontario, p. 91–99.
- Schindler, D.W. and Donahue, W.F. (2006): Inaugural article: An impending water crisis in Canada's western prairie provinces; *Proceedings of the National Academy of Sciences*, v. 103, p. 7210–7216.
- Schnorbus, M.A., Bennett, K.E., Werner, A.T. and Berland, A.J. (2011): Hydrologic impacts of climate change in the Peace, Campbell and Columbia Watersheds, British Columbia, Canada; *Hydrologic Modelling Project Final Report (Part II)*, Victoria British Columbia; University of Victoria, Pacific Climate Impacts Consortium, <<https://pacificclimate.org/sites/default/files/publications/Schnorbus.HydroModelling.FinalReport2.Apr2011.pdf>>.



Schnorbus, M., Werner, A. and Bennett, K. (2014): Impacts of climate change in three hydrologic regimes in British Columbia, Canada; *Hydrological Processes*, v. 28, p. 1170–1189.

Scibek, J. and Allen, D.M. (2006): Modeled impacts of predicted climate change on recharge and groundwater levels; *Water Resources Research*, v. 41. doi: 10.1029/2005WR004742

Seiler, C., Zwiers, F.W., Hodges, K.I. and Scinocca, A.F. (2018): How does dynamical downscaling affect model biases and future projections of explosive extratropical cyclones along North America's Atlantic coast?; *Climate Dynamics*, v. 50, p. 677–692.

Seneviratne, S.I., Corti, T., Davin, E.L., Hirschi, M., Jaeger, E.B., Lehner, I., Orlowsky, B. and Teuling, A.J. (2010): Investigating soil moisture-climate interactions in a changing climate: a review; *Earth-Science Reviews*, v. 99, p. 125–161.

Seneviratne, S.I., Nicholls, N., Easterling, D., Goodess, C.M., Kanae, S., Kossin, J., Luo, Y., Marengo, J., McInnes, K., Rahimi, M., Reichstein, M., Sorteberg, A., Vera, C. and Zhang, X. (2012): Changes in climate extremes and their impacts on the natural physical environment; in *Managing the Risks of Extreme Events and Disasters to Advance Climate Change Adaptation*, (ed.) C.B. Field, V. Barros, T.F. Stocker, D. Qin, D.J. Dokken, K.L. Ebi, M.D. Mastrandrea, K.J. Mach, G.K. Plattner, S.K. Allen, M. Tignor and P.M. Midgley; A Special Report of Working Groups I and II of the Intergovernmental Panel on Climate Change; Cambridge University Press, Cambridge, United Kingdom and New York, NY, USA, p. 109–230.

Shaw, S.B. and Riha, S.J. (2011): Assessing temperature-based PET equations under a changing climate in temperate, deciduous forests; *Hydrological Processes*, v. 25, p. 1466–1478.

Sheffield, J., Wood, E.F. and Roderick, M.L. (2012): Little change in global drought over the past 60 years; *Nature*, v. 491, p. 435–438.

Shepherd, A., Gill, K.M. and Rood, S.B. (2010): Climate change and future flows of Rocky Mountain rivers: Converging forecasts from empirical trend projection and down-scaled global circulation modelling; *Hydrological Processes*, v. 24, p. 3864–3877.

Shook, K. and Pomeroy, J. (2012): Changes in the hydrological character of rainfall on the Canadian Prairies; *Hydrological Processes*, v. 26, p. 1752–1766.

Shrestha, R.R., Berland, A.J., Schnorbus, M.A. and Prowse, T.D. (2012b): Modelling of climate-induced hydrologic changes in the Lake Winnipeg watershed; *Journal of Great Lakes Research*, v. 38, p. 83–94.

Shrestha, R.R., Schnorbus, M.A., Werner, A.T. and Berland, A.J. (2012a): Modelling spatial and temporal variability of hydrologic impacts of climate change in the Fraser River basin, British Columbia, Canada; *Hydrological Processes*, v. 26, p. 1840–1860.

Smerdon, B.D. (2017): Synopsis of climate change effects on groundwater recharge; *Journal of Hydrology*, v. 555, p. 125–128.

Smith, L.C., Sheng, Y., MacDonald, G.M. and Hinzman, L.D. (2005): Disappearing Arctic lakes; *Science*, v. 308, p. 1429.



Southam, C.F., Mills, B.N., Moulton, R.J. and Brown, D.W. (1999): The potential impact of climate change in Ontario's Grand River basin: Water supply and demand issues; *Canadian Water Resources Journal*, v. 24, p. 307–328.

St. George, S. (2007): Streamflow in the Winnipeg River basin, Canada: Trends, extremes and climate linkages; *Journal of Hydrology*, v. 332, p. 396–411.

St. Jacques, J.M. and Sauchyn, D.J. (2009): Increasing winter baseflow and mean annual streamflow from possible permafrost thawing in the Northwest Territories, Canada; *Geophysical Research Letters*, v. 36. doi:10.1029/2008GL035822

St. Jacques, J.M., Andreichuk, Y., Sauchyn, D.J. and Barrow, E. (2017): Projecting Canadian Prairie Runoff for 2041–2070 with North American Regional Climate Change Assessment Program (NARCCAP) Data; *Journal of the American Water Resources Association*. doi:10.1111/1752-1688.12642

St. Jacques, J.M., Lapp, S.L., Zhao, Y., Barrow, E.M. and Sauchyn, D.J. (2013): Twenty-first century central Rocky Mountain river discharge scenarios under greenhouse forcing; *Quaternary International*, v. 310, p. 34–46.

St. Jacques, J.M., Sauchyn, D.J. and Zhao, Y. (2010): Northern Rocky Mountain streamflow records: Global warming trends, human impacts or natural variability? *Geophysical Research Letters*, v. 37.

Stantec (2012): Assiniboine River Basin Hydrologic Model - Climate Change Assessment; prepared for Manitoba Conservation, Climate Change Branch, 102 p., <http://www.parc.ca/rac/fileManagement/upload/2/FINAL_AssiniboineRBasin_Hydrologic_Model_20120323.pdf>.

Sulis, M., Paniconi, C., Marrocu, M., Huard, D. and Chaumont, D. (2012): Hydrologic response to multimodel climate output using a physically based model of groundwater/surface water interactions; *Water Resources Research*, v. 48.

Sulis, M., Paniconi, C., Rivard, C., Harvey, R. and Chaumont, D. (2011): Assessment of climate change impacts at the catchment scale with a detailed hydrological model of surface-subsurface interactions and comparison with a land surface model; *Water Resources Research*, v. 47.

Sultana, Z. and Coulibaly, P. (2011): Distributed modelling of future changes in hydrological processes of Spencer Creek watershed; *Hydrological Processes*, v. 25, p. 1254–1270.

Swain, S. and Hayhoe, K. (2015): CMIP5 projected changes in spring and summer drought and wet conditions over North America; *Climate Dynamics*, v. 44, p. 2737–2750.

Szeto, K., Brimelow, J., Gysbers, P. and Stewart, R. (2015): The 2014 extreme flood on the southeastern Canadian Prairies; in *Explaining Extremes of 2014 from a Climatic Perspective*, *Bulletin of the American Meteorological Society*, v. 96, S20–S24.

Szeto, K., Zhang, X., White, R.E. and Brimelow, J. (2016): The 2015 extreme drought in western Canada; in *Explaining Extremes of 2015 from a Climatic Perspective*; *Bulletin of the American Meteorological Society*, v. 97, S42–S46.



Tanzeeba, S. and Gan, T.Y. (2012): Potential impact of climate change on the water availability of South Saskatchewan River Basin; *Climatic Change*, v. 112, p. 355–386.

Teufel, B., Diro, G.T., Whan, K., Milrad, S.M., Jeong, D.I., Ganji, A., Huziy, O., Winger, K., Gyakum, J.R., de Elia, R., Zwiers, F.W. and Sushama, L. (2017): Investigation of the 2013 Alberta flood from weather and climate perspectives; *Climate Dynamics*, v. 48, p. 2881–2899.

Thorne, R. (2011): Uncertainty in the impacts of projected climate change on the hydrology of a subarctic environment: Liard River Basin; *Hydrology Earth System Sciences*, v. 15, p. 1483–1492.

Touma, D., Ashfaq, M., Nayak, M.A., Kao, S.C. and Diffenbaugh, N.S. (2015): A multi-model and multi-index evaluation of drought characteristics in the 21st century; *Journal of Hydrology*, v. 526, p. 196–207.

Trenberth, K.E. (2011): Changes in precipitation with climate change; *Climate Research*, v. 47, p. 123–138.

Trenberth, K.E., Dai, A., van der Schrier, G., Jones, P.D., Barichivich, J., Briffa, K.R. and Sheffield, J. (2014): Global warming and changes in drought; *Nature Climate Change*, v. 4, p. 17–22.

UK Met Office [United Kingdom Meteorological Office] (2018): Water cycle for kids, <<http://www.metoffice.gov.uk/learning/weather-for-kids/water-cycle/>>.

US Fish and Wildlife Service (2017): Waterfowl population status, 2017; U.S. Department of the Interior, Washington, District of Columbia, United States, <<https://www.fws.gov/migratorybirds/pdf/surveys-and-data/Population-status/Waterfowl/WaterfowlPopulationStatusReport17.pdf>>.

van der Kamp, G. and Marsh, P. (2004). Climate Variability and Change: Wetlands; Chapter 13 in *Threats to Water Availability in Canada*, NWRI Scientific Assessment Report Series No. 3 and ACSD Science Assessment Series No. 1.; National Water Research Institute, Burlington, Ontario, p. 101–106.

van der Kamp, G., Keir, D. and Evans, M.S. (2008): Long-term water-level changes in closed-basin lakes of the Canadian prairies; *Canadian Water Resources Journal*, v. 33, p. 23–38.

van Huissteden, J., Berrittella, C., Parmentier, F.J.W., Mi, Y., Maximov, T.C. and Dolman, A.J. (2011): Methane emissions from permafrost thaw lakes limited by lake drainage; *Nature Climate Change*, v. 1, p. 119–123.

Vetter, T., Reinhart, J., Florke, M., van Griensven, A., Hattermann, F., Huang, S., Koch, H., Pechlivanidis, I.G., Plotner, S., Seidou, O., Su, B., Vervoort, R.W. and Krysanova, V. (2017): Evaluation of sources of uncertainty in projected hydrological change under climate change in 12 large-scale river basins; *Climatic Change*, v. 141, p. 419–433.

Vicente-Serrano, S.M., Begueria, S. and Lopez-Moreno, J.I. (2010): A multiscale drought index sensitive to global warming: The Standardized Precipitation Evapotranspiration Index; *Journal of Climate*, v. 23, p. 1696–1718.



Vincent, L.A., Zhang, X., Brown, R.D., Feng, Y., Mekis, E., Milewska, E.J., Wan, H. and Wang, X.L. (2015): Observed trends in Canada's climate and influence of low frequency variability modes; *Journal of Climate*, v. 28, p. 4545–4560.

Vincent, W.F., Laurion, I., Pienitz, R. and Walter-Anthony, K.M. (2012): Climate impacts on Arctic lake ecosystems; in *Climatic Change and Global Warming of Inland Waters: Impacts and Mitigation for Ecosystems and Societies*; (ed.) C.R. Goldman, M. Kumagai, and R.D. Robarts; John Wiley & Sons, 496 p.

von de Wall, S., de Rham L.P. and Prowse, T.D. (2009): Open water and ice-induced extreme water levels on Canadian rivers; in *Proceedings of the 17th International Northern Research Basins Symposium and Workshop, 12–18 August 2009*; (ed.) K.L. Young and W. Quinton; Iqaluit-Pangnirtung-Kuuujjaq, Nunavut, p. 337–347.

von de Wall, S., de Rham, L.P. and Prowse, T.D. (2010): The river ice break-up season in Canada: Variations in water levels and timing; in *Proceedings of the 67th Eastern Snow Conference, 8–10 June, 2010*, Hancock, Massachusetts, p. 5–15.

Wang, G. (2005): Agricultural drought in a future climate: Results from 15 Global Climate Models participating in the IPCC 4th assessment; *Climate Dynamics*, v. 25, p. 739–753.

Wang, Y., Hogg, E.H., Price, D.T., Edwards, J. and Williamson, T. (2014): Past and projected future changes in moisture conditions in the Canadian boreal forest; *The Forestry Chronicle*, v. 90, p. 678–691.

Watmough, M.D. and Schmoll, M.J. (2007): Environment Canada's Prairie and Northern Region habitat monitoring program phase II: recent habitat trends in the Prairie Habitat Joint Venture; *Technical Report Series No. 493*; Environment Canada, Canadian Wildlife Service, Edmonton, Alberta, 135 p.

Wehner, M.F., Arnold, J.R., Knutson, T. Kunkel, K.E. and LeGrande, A.N. (2017): Droughts, floods, and wildfires; in *Climate Science Special Report: Fourth National Climate Assessment*, v. 1, (ed.) D.J. Wuebbles, D.W. Fahey, K.A. Hibbard, D.J. Dokken, B.C. Stewart and T.K. Maycock, U.S. Global Change Research Program, Washington, District of Columbia, United States, p. 231–256.

Wen, L., Lin, C.A., Wu, Z., Lu, G., Pomeroy, J. and Zhu, Y. (2011): Reconstructing sixty year (1950–2009) daily soil moisture over the Canadian Prairies using the Variable Infiltration Capacity model; *Canadian Water Resources Journal*, v. 36, p. 83–102.

Whitfield, P.H. (2012): Floods in future climates: a review; *Journal of Flood Risk Management*, v. 5, p. 336–365.

Whitfield, P.H. and Cannon, A.J. (2000): Recent variations in climate and hydrology in Canada; *Canadian Water Resources Journal*, v. 25, p. 19–65.

Whitfield, P.H., Burn, D.H., Hannaford, J., Higgins, H., Hodgkins, G.A., Marsh, T. and Looser, U. (2012): Reference hydrologic networks: The status and potential future directions of national reference hydrologic networks for detecting trends; *Hydrological Sciences Journal*, v. 57, p. 1562–1579.



Whitfield, P.H., Moore, R.D., Fleming, S.W. and Zawadzki, A. (2010): Pacific Decadal Oscillation and the hydroclimatology of western Canada — Review and prospects; *Canadian Water Resources Journal*, v. 35, p. 1–28.

Wilcox, D.A., Thompson, T.A., Booth, R.K. and Nicholas, J.R. (2007): Lake-level variability and water availability in the Great Lakes; Circular 1311, US Geological Survey, National Water Availability and Use Program, Virginia, United States.

Wolfe, B.B., Humphries, M.M., Pisaric, M.F.J., Balasubramaniam, A.M., Burn, C.R., Chan, L., Cooley, D., Froese, D.G., Graupe, S., Hall, R.I., Lantz, T., Porter, T.J., Roy-Leveillee, P., Turner, K.W., Wesche, S.D. and Williams, M. (2011): Environmental change and traditional use of the Old Crow Flats in Northern Canada: An IPY opportunity to meet the challenges of the New Northern Research Paradigm; *Arctic*, v. 64, p. 127–135.

Woo, M.K and Thorne, R. (2003): Streamflow in the Mackenzie Basin, Canada; *Arctic*, v. 56, p. 328–340.

World Meteorological Organization (WMO) and Global Water Partnership (GWP) (2016): *Handbook of Drought Indicators and Indices*; (ed.) M. Svoboda and B.A. Fuchs; Integrated Drought Management Programme (IDMP), Integrated Drought Management Tools and Guidelines Series 2, Geneva, Switzerland.

Yip, Q.K.Y., Burn, D.H., Seglenieks, F., Pietroniro, A. and Soulis, E.D. (2012): Climate impacts on hydrological variables in the Mackenzie River Basin; *Canadian Water Resources Journal*, v. 37, p.209–230.

Zhang, X., Harvey, K.D., Hogg, W.D. and Yuzyk, T.R. (2001): Trends in Canadian streamflow; *Water Resources Research*, v. 37, p. 987–998.

Zhao, T. and Dai, A. (2015): The magnitude and causes of global drought changes in the twenty-first century under a low-moderate emissions scenario; *Journal of Climate*, v. 28, p. 4490–4512.

Zhao, T. and Dai, A. (2016): Uncertainties in historical changes and future projections of drought: Part II: Model simulated historical and future drought changes; *Climatic Change*, v. 144, p. 535–548. doi:10.1007/s10584-016-1742-x





CHAPTER 7

Changes in Oceans Surrounding Canada

CANADA'S CHANGING CLIMATE REPORT



Government
of Canada

Gouvernement
du Canada

Canada



Authors

Blair J. W. Greenan, Fisheries and Oceans Canada

Thomas S. James, Natural Resources Canada

John W. Loder, Fisheries and Oceans Canada

Pierre Pepin, Fisheries and Oceans Canada

Kumiko Azetsu-Scott, Fisheries and Oceans Canada

Debby Ianson, Fisheries and Oceans Canada

Roberta C. Hamme, University of Victoria

Denis Gilbert, Fisheries and Oceans Canada

Jean-Éric Tremblay, Université Laval

Xiaolan L. Wang, Environment and Climate Change Canada

Will Perrie, Fisheries and Oceans Canada

Acknowledgments

Jim Christian, Fisheries and Oceans Canada

Eugene Colbourne, Fisheries and Oceans Canada

Peter Galbraith, Fisheries and Oceans Canada

Phil Greyson, Fisheries and Oceans Canada

Guoqi Han, Fisheries and Oceans Canada

Dave Hebert, Fisheries and Oceans Canada

Roger Pettipas, Fisheries and Oceans Canada

Marie Robert, Fisheries and Oceans Canada

Tetjana Ross, Fisheries and Oceans Canada

Nadja Steiner, Fisheries and Oceans Canada

Igor Yashayaev, Fisheries and Oceans Canada

Li Zhai, Fisheries and Oceans Canada

Recommended citation: Greenan, B.J.W., James, T.S., Loder, J.W., Pepin, P., Azetsu-Scott, K., Ianson, D., Hamme, R.C., Gilbert, D., Tremblay, J-E., Wang, X.L. and Perrie, W. (2019): Changes in oceans surrounding Canada; Chapter 7 in (eds.) Bush and Lemmen, Canada's Changing Climate Report; Government of Canada, Ottawa, Ontario, p. 343–423.



Chapter Table Of Contents

CHAPTER KEY MESSAGES (BY SECTION)

SUMMARY

7.1: Introduction

Box 7.1: Canada's marine coasts

Box 7.2: Oceans currents and gyres

7.2: Ocean temperature

7.2.1: Observations

7.2.1.1: Northeast Pacific Ocean

7.2.1.2: Northwest Atlantic Ocean

7.2.1.3: Arctic Ocean

7.2.2: Future projections

7.3: Ocean salinity and density stratification

Box 7.3: Brine rejection

Box 7.4: Ocean density stratification

7.3.1: Observations

7.3.1.1: Northeast Pacific Ocean

7.3.1.2: Northwest Atlantic Ocean

7.3.1.3: Arctic Ocean

7.3.2: Future projections

7.4: Marine winds, storms, and waves

7.4.1: Marine winds and storms

7.4.2: Waves

7.5: Sea level

7.5.1: Historical sea level

7.5.2: Future projections



- 7.5.2.1: Global sea-level rise
- 7.5.2.2: Vertical land motion
- 7.5.2.3: Other effects
- 7.5.2.4: Projections of relative sea-level rise

7.5.3: Extreme water levels

Box 7.5: Storm surge flooding

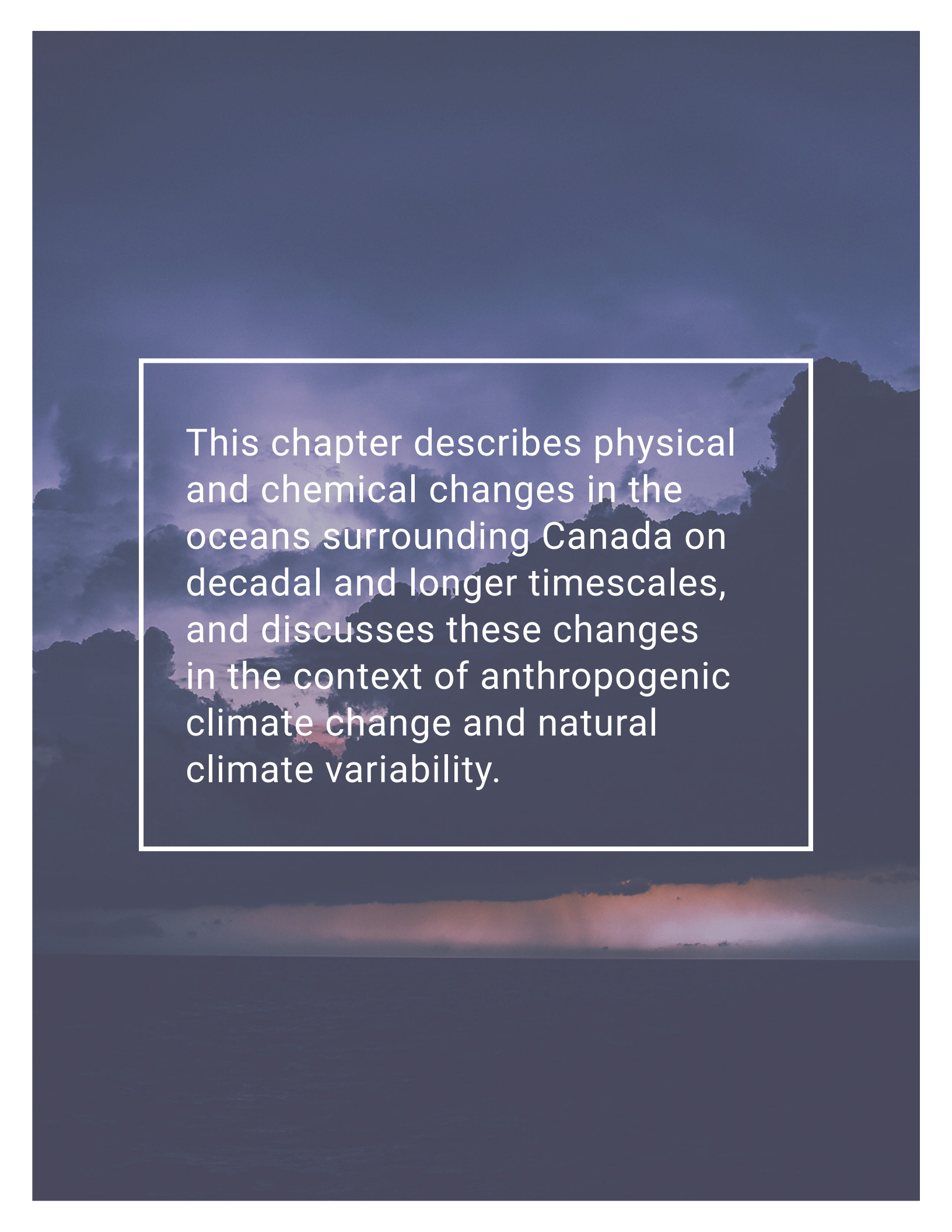
7.6: Ocean chemistry

7.6.1: Ocean acidification

Box 7.6: Ocean carbon cycle

7.6.2: Dissolved oxygen and hypoxia

7.6.3: Ocean nutrients



This chapter describes physical and chemical changes in the oceans surrounding Canada on decadal and longer timescales, and discusses these changes in the context of anthropogenic climate change and natural climate variability.

Chapter Key Messages

7.2: Ocean Temperature

Upper-ocean temperature has increased in the Northeast Pacific and most areas of the Northwest Atlantic over the last century, consistent with anthropogenic climate change (*high confidence*²⁵). The upper ocean has warmed in the Canadian Arctic in summer and fall as a result of increases in air temperature and declines in sea ice (*medium confidence*).

Oceans surrounding Canada are projected to continue to warm over the 21st century in response to past and future emissions of greenhouse gases. The warming in summer will be greatest in the ice-free areas of the Arctic and off southern Atlantic Canada where subtropical water is projected to shift further north (*medium confidence*). During winter in the next few decades, the upper ocean surrounding Atlantic Canada will warm the most, the Northeast Pacific will experience intermediate warming rates and the Arctic and eastern sub-Arctic ocean areas (including Hudson Bay and Labrador Sea) will warm the least (*medium confidence*).

7.3: Ocean Salinity and Density Stratification

There has been a slight long-term freshening of upper-ocean waters in most areas off Canada as a result of various factors related to anthropogenic climate change, in addition to natural decadal-scale variability (*medium confidence*). Salinity has increased below the surface in some mid-latitude areas, indicating a northward shift of saltier subtropical water (*medium confidence*).

Freshening of the ocean surface is projected to continue in most areas off Canada over the rest of this century under a range of emission scenarios, due to increases in precipitation and melting of land and sea ice (*medium confidence*). However, increases in salinity are expected in off-shelf waters south of Atlantic Canada due to the northward shift of subtropical water (*medium confidence*). The upper-ocean freshening and warming is expected to increase the vertical stratification of water density, which will affect ocean sequestration of greenhouse gases, dissolved oxygen levels, and marine ecosystems.

7.4: Marine Winds, Storms, and Waves

Surface wave heights and the duration of the wave season in the Canadian Arctic have increased since 1970 and are projected to continue to increase over this century as sea ice declines (*high confidence*). Off Canada's east coast, areas that currently have seasonal sea ice are also anticipated to experience increased wave activity in the future, as seasonal ice duration decreases (*medium confidence*).

25 This report uses the same calibrated uncertainty language as in the IPCC's Fifth Assessment Report. The following five terms are used to express assessed levels of confidence in findings based on the availability, quality and level of agreement of the evidence: very low, low, medium, high, very high. The following terms are used to express assessed likelihoods of results: virtually certain (99%–100% probability), extremely likely (95%–100% probability), very likely (90%–100% probability), likely (66%–100% probability), about as likely as not (33%–66% probability), unlikely (0%–33% probability), very unlikely (0%–10% probability), extremely unlikely (0%–5% probability), exceptionally unlikely (0%–1% probability). These terms are typeset in italics in the text. See chapter 1 for additional explanation.

A slight northward shift of storm tracks, with decreased wind speed and lower wave heights off Atlantic Canada, has been observed and is projected to continue in future (*low confidence*). Off the Pacific coast of Canada, wave heights have been observed to increase in winter and decrease in summer, and these trends are projected to continue in future (*low confidence*).

7.5: Sea Level

Globally, sea level has risen, and is projected to continue to rise. The projected amount of global sea-level rise in the 21st century is many tens of centimetres and it may exceed one metre. However, relative sea level in different parts of Canada is projected to rise or fall, depending on local vertical land motion. Due to land subsidence, parts of Atlantic Canada are projected to experience relative sea-level change higher than the global average during the coming century (*high confidence*).

Where relative sea level is projected to rise (most of the Atlantic and Pacific coasts and the Beaufort coast in the Arctic), the frequency and magnitude of extreme high water-level events will increase (*high confidence*). This will result in increased flooding, which is expected to lead to infrastructure and ecosystem damage as well as coastline erosion, putting communities at risk. Adaptation actions need to be tailored to local projections of relative sea-level change.

Extreme high water-level events are expected to become larger and occur more often in areas where, and in seasons when, there is increased open water along Canada's Arctic and Atlantic coasts, as a result of declining sea ice cover, leading to increased wave action and larger storm surges (*high confidence*).

7.6: Ocean Chemistry

Increasing acidity (decreasing pH) of the upper-ocean waters surrounding Canada has been observed, consistent with increased carbon dioxide uptake from the atmosphere (*high confidence*). This trend is expected to continue, with acidification occurring most rapidly in the Arctic Ocean (*high confidence*).

Subsurface oxygen concentrations have decreased in the Northeast Pacific and Northwest Atlantic oceans off Canada (*high confidence*). Increased upper-ocean temperature and density stratification associated with anthropogenic climate change have contributed to this decrease (*medium confidence*). Low subsurface oxygen conditions will become more widespread and detrimental to marine life in future, as a result of continuing climate change (*medium confidence*).

Nutrient supply to the ocean-surface layer has generally decreased in the North Pacific Ocean, consistent with increasing upper-ocean stratification (*medium confidence*). No consistent pattern of nutrient change has been observed for the Northwest Atlantic Ocean off Canada. There are no long-term nutrient data available for the Canadian Arctic.

Summary

The global ocean covers approximately 71% of the Earth's surface and is a vast reservoir of water, energy, carbon, and many other substances. It is a key component of the climate system and interacts directly with the atmosphere and cryosphere. Freshwater resources are also linked to the ocean via runoff in coastal areas. The ocean plays an important role in mitigating anthropogenic climate change through its ability to absorb substantial amounts of heat and carbon.

Canada is surrounded by oceans on three sides – the Pacific, Arctic, and Atlantic oceans. There is strong evidence of human-induced changes during the past century in key ocean-climate properties – such as temperature, sea ice, sea level, acidity, and dissolved oxygen – off Canada. Warmer ocean temperature has contributed to declining sea ice and increasing sea level. However, there is an area south of Greenland where there has been little ocean warming, so regional trends do differ. Warming and a slight freshening of the upper ocean have reduced its density resulting in increased vertical differences in density (referred to as “density stratification”) in oceans off Canada; this could affect the vertical transport of heat, carbon, and nutrients and, thereby, ecosystem health and services.

Global sea levels are rising due to ocean thermal expansion, and diminishing glaciers and ice sheets which deliver water to the oceans. Changes in sea level relative to Canada's coastline are also affected by vertical land motion (upward, called “uplift” or downward, called “subsidence”) in response to the retreat of the last glacial ice sheet. Relative sea level has increased in most regions of Canada over the last century and even exceeded the global rate of change in southern Atlantic Canada, where land is subsiding. However, there are regions of Canada (e.g., Hudson Bay) where relative sea level has fallen as a result of the rate of uplift being higher than the rate of global sea-level rise. Increasing relative sea level is also increasing risks for coastal infrastructure and communities. This is compounded by increases in ocean wave heights in areas that have experienced seasonal reductions in sea ice.

Ocean chemistry has undergone changes, such as increasing acidity and decreasing subsurface oxygen concentrations, as a result of anthropogenic climate change. The physical and chemical trends observed in the oceans surrounding Canada are consistent with changes observed in the atmosphere, cryosphere, freshwater systems, and adjoining oceans.

The fundamental principles that govern how the physical and chemical environment of the ocean will respond to increased atmospheric carbon dioxide have allowed model-based projections of future conditions in the oceans surrounding Canada under a range of emission scenarios. In general, warming and freshening at the ocean surface is projected during this century, which will continue to increase stratification and reduce sea ice. Sea-level rise along some Canadian coastlines will be higher than the global average during this century, leading to increased flooding and erosion. Ocean acidification and decreasing subsurface oxygen levels will continue, with increasingly adverse implications for marine ecosystems.

7.1: Introduction

The global ocean — composed of an interconnected system of oceans — is an integral component of the climate system and is experiencing change in its physical, chemical, and biological properties. The ocean has absorbed more than 90% of the increase in heat energy in the climate system between 1971 and 2010 (Rhein et al., 2013; Jewett and Romanou, 2017). This has led to an increase in ocean heat content, which is a robust indicator of global warming (Cheng et al., 2017). The ocean also stores and distributes water from melting land glaciers and ice sheets, making it a very important reservoir in the global water cycle. Increased heat content, which causes water to expand and occupy more volume, and added meltwater from glaciers are the predominant sources of global sea-level rise, accounting for about three-quarters of the change between 1971 and 2010 (Church et al., 2013). The ocean has also absorbed more than one-quarter of all carbon dioxide (CO₂) emissions to the atmosphere from human activity over the period of 1750 to 2011 (Rhein et al., 2013), and this has increased the acidity of seawater (ocean acidification).

Canada's coastline is vast, approximately 230,000 km in length, with over half bordering the Arctic Ocean (see Box 7.1). The oceans off Canada generally have a relatively narrow coastal zone, with embayments and shallow water; a plateau-like continental shelf with typical water depths of 100–300 m; and a continental slope with depths increasing to 3000–5000 m in the major ocean basins. There are large regional differences in ocean temperatures surrounding Canada (see Figure 7.1). The west coast is influenced by the eastward-flowing North Pacific Current, which supplies source water for both the North Pacific subpolar and subtropical gyres (see Box 7.2). The resulting northward-flowing Alaska Current and the southward-flowing California Current regions are both important upwelling zones, which bring nutrient-rich water to the surface and support diverse marine ecosystems. Pacific water is transported to the western Arctic through the Bering Strait between Alaska and Russia. Circulation in the Arctic Ocean is complex, but the primary feature of the western Arctic off Canada is the counterclockwise-flowing Beaufort Gyre, with eastward coastal flow. Some of the Pacific water that enters the Arctic flows out through the Canadian Arctic Archipelago to Baffin Bay and south to the Labrador Sea and beyond. The North Atlantic Ocean off Canada is influenced by the intense western boundary currents of its two basin-scale gyres — the subpolar gyre's Labrador Current and the subtropical gyre's Gulf Stream. As shown in Figure 7.1, the Labrador and Newfoundland Shelf and Slope regions and the Gulf of St. Lawrence are linked to outflow from the Arctic via the Labrador Current, but the Gulf of St. Lawrence is a nearly enclosed coastal sea that is also strongly influenced by freshwater runoff from the St. Lawrence River system. The Scotian Shelf, Gulf of Maine, southern Newfoundland Shelf, and their adjoining continental slope regions have strong spatial gradients (or differences) in temperature and salinity associated with the cold and fresh Labrador Current flowing southward along the shelf edge and the warm and saline Gulf Stream flowing northeastward further offshore.

Box 7.1: Assessment of Canada's marine coasts

A recent scientific assessment, *Canada's Marine Coasts in a Changing Climate*, focused on Canada's coastlines (Lemmen et al., 2016). It included an overview of the physical setting of Canada's coastlines, expected impacts of climate change, a discussion of the challenges for coastal adaptation, and numerous adaptation case studies. Regional chapters discussed Canada's east, north, and west coasts separately. It also provided sea-level projections for Canadian coastal areas, based on global sea-level rise projections from the Intergovernmental Panel on Climate Change's Fifth Assessment Report (Church et al., 2013). In this chapter, there is an updated discussion of sea-level projections and extreme water levels, but *Canada's Marine Coasts in a Changing Climate* is recommended for more detailed information on Canada's coastlines.



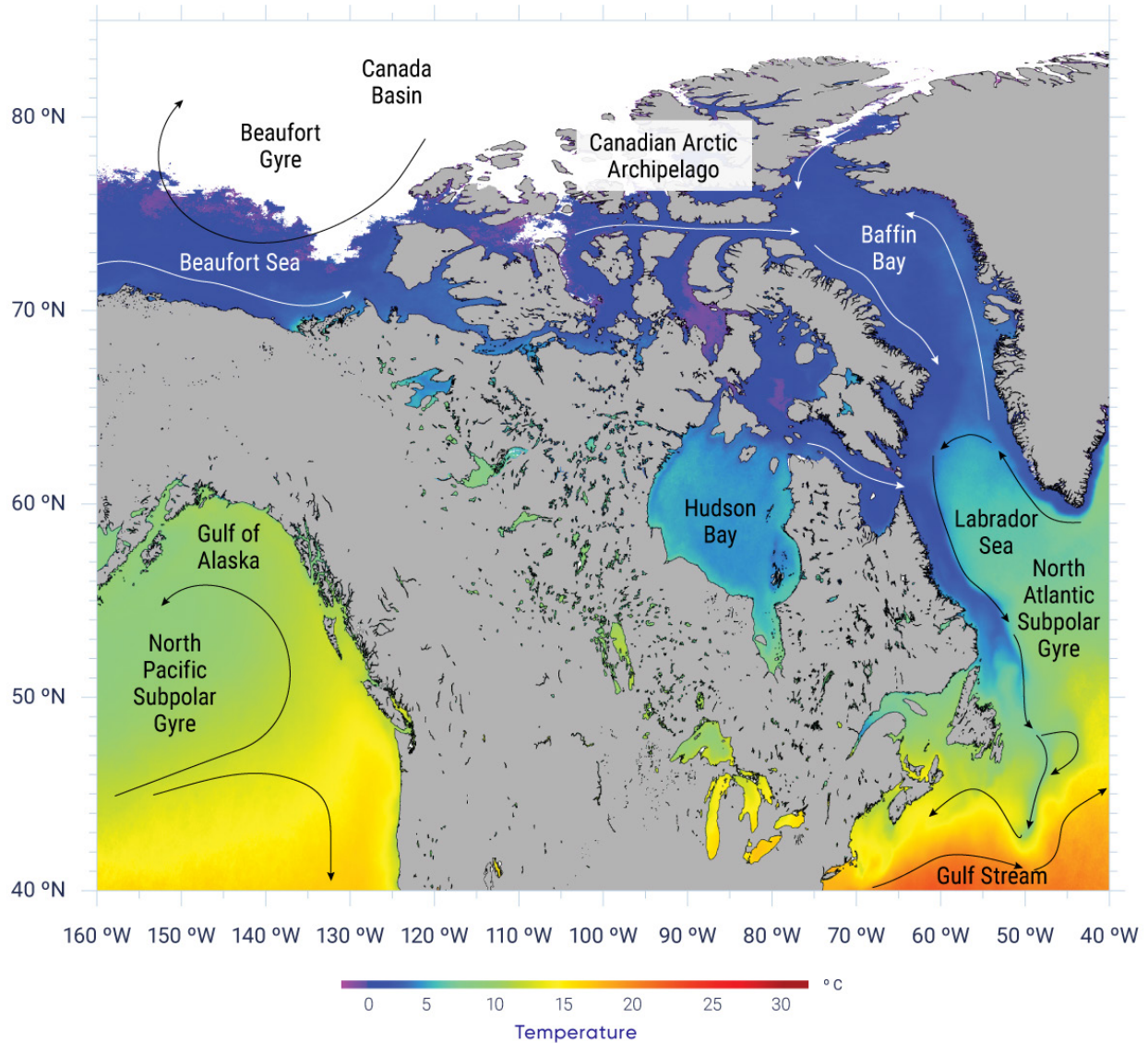


Figure 7.1: Sea surface temperatures, currents, and gyres in the oceans surrounding Canada

Figure caption: Fall (September–November) average sea surface temperature (1985–2013) in the oceans surrounding Canada, based on advanced very-high-resolution radiometer satellite infrared imagery. The lines (both black and white) with arrowheads represent the general direction of upper-ocean currents. Ice-covered marine areas are coloured white.

FIGURE SOURCE: ADAPTED FROM LAROCHE AND GALBRAITH (2016).

Box 7.2: Ocean currents and gyres

Large-scale ocean circulation is commonly described in terms of major ocean currents and gyres. In this context, ocean currents are coherent streams of water (like rivers) in the ocean, analogous to the jet streams in the atmosphere. They can extend over long distances, as is evident in features such as the Gulf Stream in the North Atlantic or its counterpart, the Kuroshio Current (and its extension, the North Pacific Current) in the Pacific, as well as over smaller scales in both coastal waters and the open ocean. Ocean currents are naturally variable in flow patterns and intensity over time. The large-scale ocean currents are formed primarily by wind blowing across the surface of the ocean and by spatial differences in the temperature, salinity, and pressure of seawater. Their patterns are influenced by the Earth's rotation as well as the location of the continents and topography of the ocean bottom. They are important because they can transport water, sea ice, heat, salt, dissolved gases such as carbon dioxide and oxygen, and other materials over long distances, resulting in the ocean being a critical component of the Earth's climate system. Other ocean currents with variability on short timescales (such as tidal and storm currents) also contribute to ocean climate by generating turbulence, which is important to vertical mixing of various ocean properties (e.g., temperature, salt, nutrients) among its upper, intermediate, and deep layers.

An important aspect of persistent ocean currents is that they sometimes carry water back to its original position through quasi-closed circuits, referred to as ocean gyres. These can range in scale from the basin-wide subtropical and subpolar gyres (of which major currents like the Gulf Stream and Labrador Current are key components), to regional ones like the Beaufort Gyre, to smaller-scale gyres over submarine banks on continental shelves. Gyres are essentially rotating water masses, often with significantly different properties (e.g., temperature and salinity) than the surrounding waters. Many aspects of ocean-climate variability can be described in terms of the changes in position, strength, properties, and interactions of these gyres.

The largest-scale system of currents is the meridional overturning circulation, a three-dimensional circulation pattern that moves water (and properties such as heat and carbon) between the upper and deep ocean and among the world's ocean basins. It plays a major role in regulating the Earth's climate by transporting heat from equatorial to polar regions. The subpolar and subtropical gyres contribute to this larger-scale circulation. Paleoceanography studies indicate that the meridional overturning circulation changed substantially during historical glacial–interglacial cycles, and it is expected to play a regulating role in anthropogenic climate change.

The Labrador Sea between Atlantic Canada and Greenland plays a key role in the global climate system because it is one of the few regions in the global ocean where surface waters become dense enough, as a result of winter cooling, to sink to intermediate ocean depths of up to 2400 m, through a process called “deep convection.” This supplies a branch of the global ocean's meridional overturning circulation (sometimes referred to as the “global conveyor belt”), a system of surface and deep currents that transports large amounts of water, heat, salt, carbon, nutrients, and other substances around the globe. Under anthropogenic climate

change, surface warming and freshening, and the associated increase in upper-ocean stratification (see Box 7.4) are expected to reduce convection depths in the Labrador Sea; in turn, this would reduce the sequestration of anthropogenic carbon into the deep ocean (see Box 7.6). Such deep-ocean sequestration prevents carbon from coming in contact with the atmosphere for centuries. These changes are also expected to affect the strength of the Atlantic branch of the meridional overturning circulation and ocean conditions off Atlantic Canada, as well as global climate.

Global measures of ocean heat content and sea-level rise have provided indicators that anthropogenic climate change is changing the ocean on a global scale (Cheng et al., 2017). However, it is more difficult to determine the causes of observed changes at regional scales. Natural internal climate variability plays a larger role on regional spatial scales and on timescales of years to decades (see Chapter 2, Section 2.3.3). The large expanse of ocean surrounding Canada poses significant logistical challenges for climate monitoring, especially in the remote Arctic, and systematic monitoring programs beyond satellite remote sensing are somewhat limited. Inferences about the role of anthropogenic climate change from records of less than 50 years duration need to be made with caution, considering known contributions from natural variability (see Sections 7.2 and 7.3). Given the rapid changes occurring in the Arctic (e.g., air temperature increase, sea ice decline), signs of anthropogenic climate change have emerged there earlier than in ocean regions off southern Canada. Past and future changes in the atmosphere, cryosphere, and freshwater systems that are drivers of changes in the ocean are covered in the preceding chapters of this report. Key among these are rising air and sea surface temperatures (SST) (see Chapter 2, Section 2.2.1 and Chapter 4, Section 4.2), precipitation changes (Chapter 2, Section 2.2.2 and Chapter 4, Section 4.3), reductions in sea and land ice (Chapter 5, Sections 5.3 and 5.4) and changes in the seasonality and magnitude of streamflow from freshwater systems (Chapter 6, Section 6.2).

Climate variability detection and projection are more difficult for the coastal zones (involving small embayments and nearshore waters) surrounding Canada because of: the highly irregular coastline and seabed topography; influences from atmosphere, land, and offshore ocean; and the sensitivity of coastal ocean circulation to the orientation of the coastline relative to the varying winds. Consequently, it is more difficult to make inferences from limited observations and coarse-scale climate models. However, some long-term coastal observation sites are representative of offshore waters (and also neighbouring coastal waters), as will be discussed in this chapter.

7.2: Ocean temperature

Key Message

Upper-ocean temperature has increased in the Northeast Pacific and most areas of the Northwest Atlantic over the last century, consistent with anthropogenic climate change (*high confidence*). The upper ocean has warmed in the Canadian Arctic in summer and fall as a result of increases in air temperature and declines in sea ice (*medium confidence*).

Key Message

Oceans surrounding Canada are projected to continue to warm over the 21st century in response to past and future emissions of greenhouse gases. The warming in summer will be greatest in the ice-free areas of the Arctic and off southern Atlantic Canada, where subtropical water is projected to shift further north (*medium confidence*). During winter in the next few decades, the upper ocean surrounding Atlantic Canada will warm the most, the Northeast Pacific will experience intermediate warming rates and the Arctic and eastern sub-Arctic ocean areas (including Hudson Bay and Labrador Sea) will warm the least (*medium confidence*).

The ocean absorbs incoming radiation from the sun and greenhouse gases in the atmosphere, and stores it as heat in its upper layers, some of which eventually spreads to deeper waters. Water has a much higher heat capacity than air, meaning the ocean can absorb larger amounts of heat energy with smaller increases in temperature. Because it takes centuries for upper-ocean heat changes to spread to abyssal depths everywhere, the vertical extent of warming in the ocean is much less than in the lower atmosphere, even though it has absorbed more than 90% of the Earth's extra accumulated heat since 1955. During 1971–2010, the upper 75 m of the global ocean warmed at a rate of 0.11°C per decade, but the warming rate was only 0.015°C per decade at 700 m (Rhein et al., 2013).

Global average SST had a warming trend of 0.07°C per decade during 1900–2016 (Jewett and Romanou, 2017) and 0.1°C per decade during 1950–2016 (Huang et al., 2017). Similar to global mean combined air and sea surface temperature (see Chapter 2, Section 2.2.1), SST also shows a multi-decadal variation related to changes in greenhouse gas and aerosol emissions and to natural internal climate variability, and shorter-term variations mainly due to volcanic eruptions and El Niño and La Niña events. Regionally, SST is also influenced by other dominant modes of natural climate variability, such as the Atlantic Multi-decadal Oscillation, the North Atlantic Oscillation, and the Pacific Decadal Oscillation. These variability modes generally involve large-scale patterns in atmospheric and/or oceanic circulation, which result in changes in surface winds over the ocean and transfers of heat across the air-sea interface (see Chapter 2, Box 2.5).

7.2.1: Observations

Sustained temperature observations in the oceans surrounding Canada began in the early 20th century, but these time series are limited to a few locations. In the Arctic Ocean, there have been very few continuous observations, and those that do exist are limited to the last several decades. Ocean temperature observations have evolved from the 19th century sampling of the ocean from ships to a more systematic and near-global coverage from satellites for surface waters (e.g., Larouche and Galbraith, 2016) and Argo floats (autonomous profilers that measure the temperature and salinity of the upper 2000 m of the ocean) for the deep ocean (Riser et al., 2016). Observations of subsurface ocean temperature on the continental shelves surrounding Canada continue to be acquired primarily through vertical profiles taken by research vessels, supplemented by continuous time series (typically with hourly sampling) from scattered moored instruments. This section will focus on long-term ocean temperature observations collected by Fisheries and Oceans Canada (DFO) monitoring programs, which draw on data from various sources of regular sampling initiated at some sites in the early 20th century. The site-specific time series presented in this section are representative of temperature over broader shelf and open-ocean regions (Ouellet et al., 2011, Petrie and Dean-Moore, 1996).

7.2.1.1: Northeast Pacific Ocean

Sea surface and upper-ocean temperatures in the Northeast Pacific are strongly influenced by natural variability associated with the El Niño–Southern Oscillation (ENSO) and Pacific Decadal Oscillation (Christian and Foreman, 2013; Huang et al., 2017). On the west coast of Canada, DFO has two long-term monitoring programs that provide continuing ocean temperature data: the British Columbia Shore Station Oceanographic Program, which has coastal time series (representative of near-surface shelf waters) dating back to 1914 (Chandler et al., 2017), and the Line P program, which has been monitoring the deep ocean since 1956, out to the former Ocean Weather Station Papa (Crawford et al., 2007) (see Figure 7.2). Long-term warming trends of 0.08°C per decade have been observed at Amphitrite Point and Kains Island on the west coast of Vancouver Island and of 0.15°C per decade, at Entrance Island on the Strait of Georgia (see Figure 7.3). In the offshore upper ocean (10–50 m) at Station P, the long-term warming trend is 0.14°C per decade, while the subsurface (100–150 m) waters show a weaker warming (0.07°C per decade) and a decadal-scale variation similar in magnitude to that in the upper-ocean waters. These upper-ocean rates of increase are similar to SST trends (1950–2016) observed for the US Northwest (0.07°C per decade) and Alaska (0.12°C per decade) coastal regions (Jewett and Romanou, 2017).

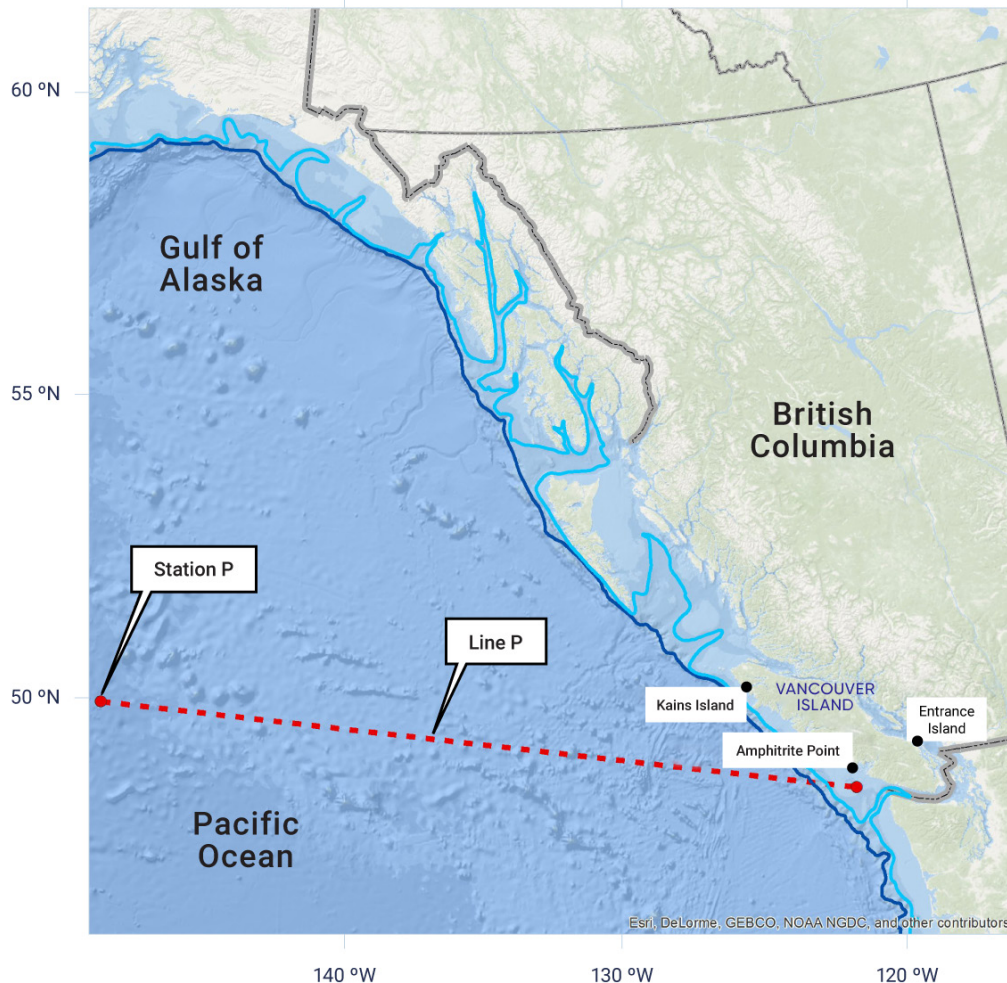


Figure 7.2: Locations of monitoring sites in the North Pacific off British Columbia

Figure caption: Map showing locations of British Columbia Shore Station Oceanographic Program sites on the east (Entrance Island) and west (Amphitrite Point and Kains Island) coasts of Vancouver Island. Offshore ocean temperature, salinity and other observations are collected by the DFO Line P monitoring program extending out to Station P, which is the former location of the Ocean Weather Station Papa. The 200 m and 1000 m depth contours are indicated by the light and dark blue lines.

FIGURE SOURCE: FISHERIES AND OCEANS CANADA

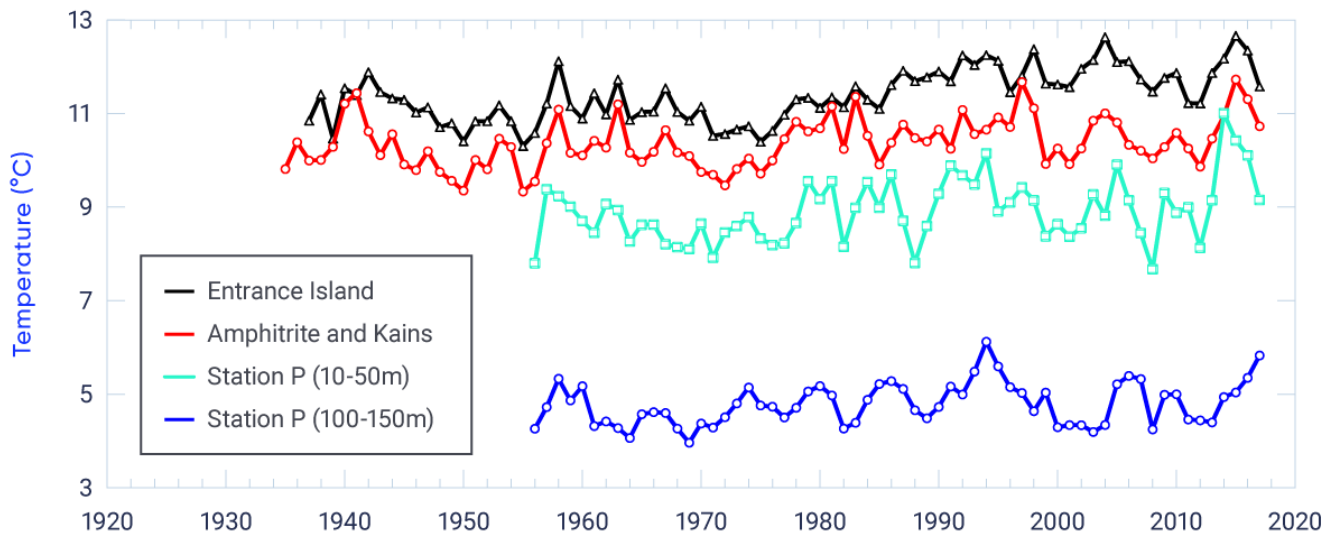


Figure 7.3: Annual mean temperatures in the Northeast Pacific Ocean off British Columbia

Figure caption: Coastal temperature time series collected at DFO monitoring sites on the east (Entrance Island, positive trend 0.15°C per decade, significant at 1% level [there is only a 1% possibility that such changes are due to chance]) and west (Amphitrite Point and Kains Island, positive trend 0.08°C per decade, significant at 1% level) coasts of Vancouver Island. Offshore ocean temperature at Station P is presented for the upper ocean (10–50 m, positive trend 0.14°C per decade, significant at 1% level) and the depth range of the permanent thermocline (layer in which temperature decreases strongly with depth; 100–150 m, positive trend 0.07°C per decade, significant at 5% level).

FIGURE SOURCE: DATA FROM DFO MONITORING PROGRAMS. BRITISH COLUMBIA SHORE STATION OCEANOGRAPHIC PROGRAM <[HTTP://WWW.PAC.DFO-MPO.GC.CA/SCIENCE/OCEANS/DATA-DONNEES/LIGHTSTATIONS-PHARES/INDEX-ENG.HTML](http://www.pac.dfo-mpo.gc.ca/science/oceans/data-donnees/lightstations-phares/index-eng.html)>. LINE P MONITORING PROGRAM <[HTTP://WWW.DFO-MPO.GC.CA/SCIENCE/DATA-DONNEES/LINE-P/INDEX-ENG.HTML](http://www.dfo-mpo.gc.ca/science/data-donnees/line-p/index-eng.html)>.

7.2.1.2: Northwest Atlantic Ocean

In the Northwest Atlantic Ocean off the Atlantic provinces (Figure 7.4), long-term warming trends are apparent from in situ data (Galbraith et al., 2017; Hebert et al., 2016) collected in the Gulf of St. Lawrence, Scotian Shelf, and Gulf of Maine (Figure 7.5 and Figure 7.6). Variability in annual mean surface temperature since 1985 in the Gulf of St. Lawrence has been highly correlated with that in regional air temperature, including a warming trend (Galbraith et al., 2012). The higher near-bottom warming rate (0.23°C per decade) is related to an increasing influence of subtropical waters from the Gulf Stream transported at depth into the Laurentian Channel (Gilbert et al., 2005), a submarine valley running from the mouth of the St. Lawrence River, through the Gulf of St. Lawrence, to the edge of the continental shelf.

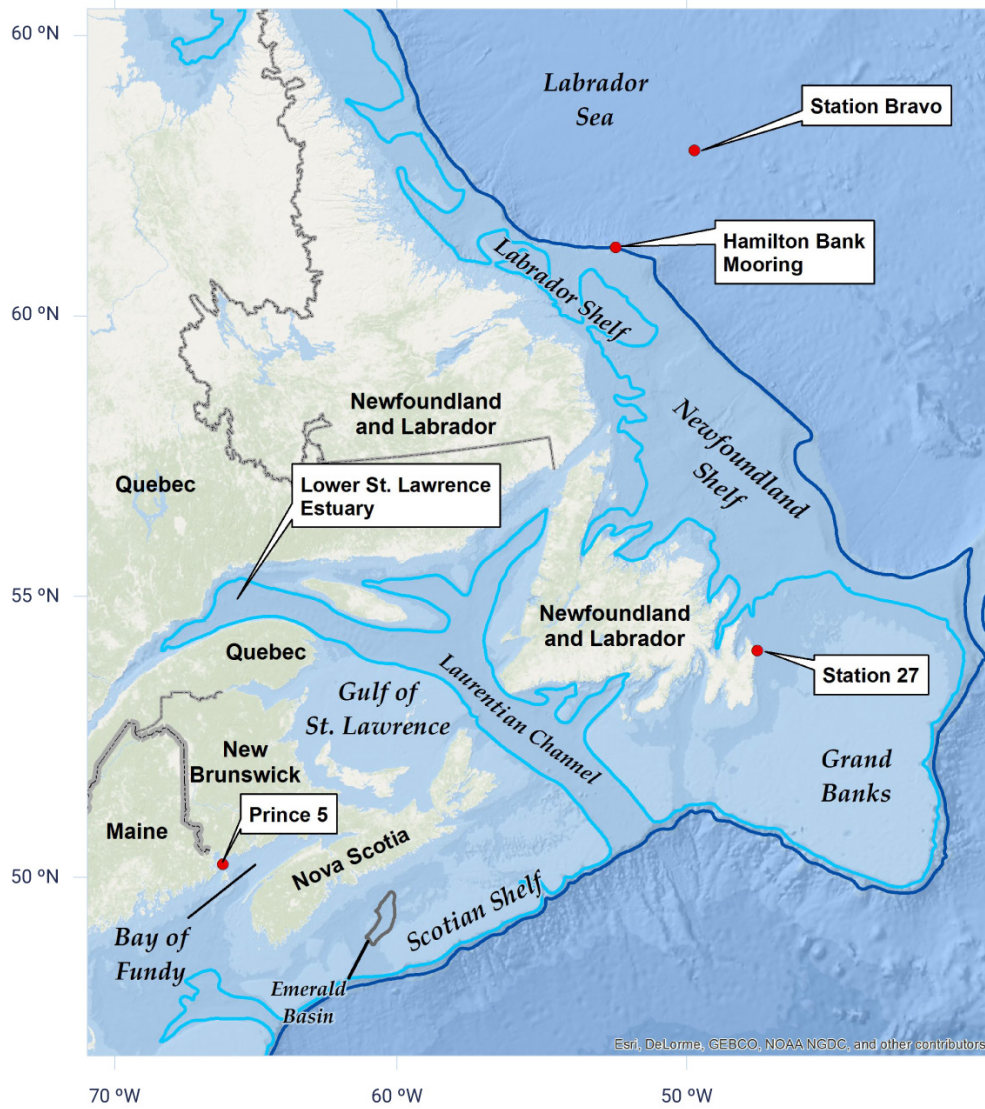


Figure 7.4: Sampling locations in the Northwest Atlantic Ocean off the Atlantic provinces

Figure caption: Map identifying areas of the Northwest Atlantic Ocean in which temperature and salinity time series are presented in this report. These areas include the Labrador Sea, Newfoundland Shelf, Scotian Shelf, Gulf of St. Lawrence, and Bay of Fundy. Ocean observations are collected by DFO Atlantic zone monitoring programs. The 200 m and 1000 m depth contours are indicated by the light and dark blue lines.

FIGURE SOURCE: FISHERIES AND OCEANS CANADA

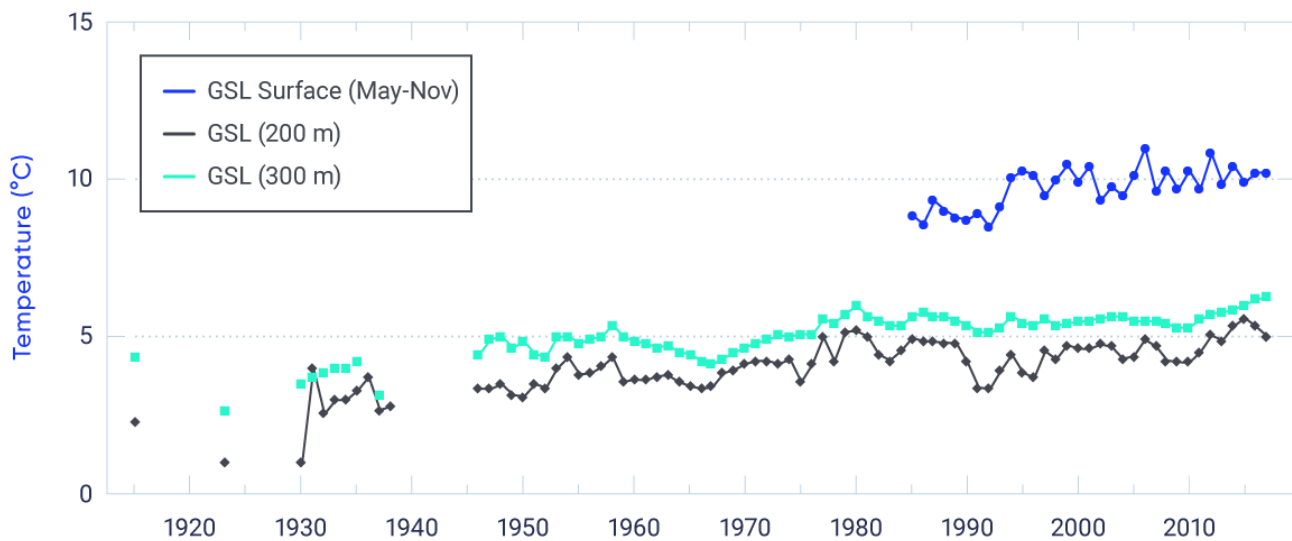


Figure 7.5: Ocean temperature in the Gulf of St. Lawrence

Figure caption: Ocean temperature time series for the surface and at depths of 200 and 300 m in the Gulf of St. Lawrence collected by DFO monitoring programs. Sea surface temperature (May to November average, ice-free period) from advanced very-high-resolution radiometer satellite observations (1985–2017, positive trend of 0.46°C per decade, significant at 1% level). Temperature from in situ observations at depths of 200 m (1915–2017, positive trend of 0.25°C per decade, significant at 1% level) and 300 m (1915–2017, positive trend of 0.23°C per decade, significant at 1% level) indicate warming in the deep Gulf of St. Lawrence over the past half-century.

FIGURE SOURCE: DATA FROM DFO MONITORING PROGRAMS (GALBRAITH ET AL., 2012; GALBRAITH ET AL., 2017). ATLANTIC ZONE MONITORING PROGRAM <[HTTP://WWW.MEDS-SDMM.DFO-MPO.GC.CA/ISDM-GDSI/AZMP-PMZA/INDEX-ENG.HTML](http://www.meds-sdmm.dfo-mpo.gc.ca/isdm-gdsi/azmp-pmza/index-eng.html)>

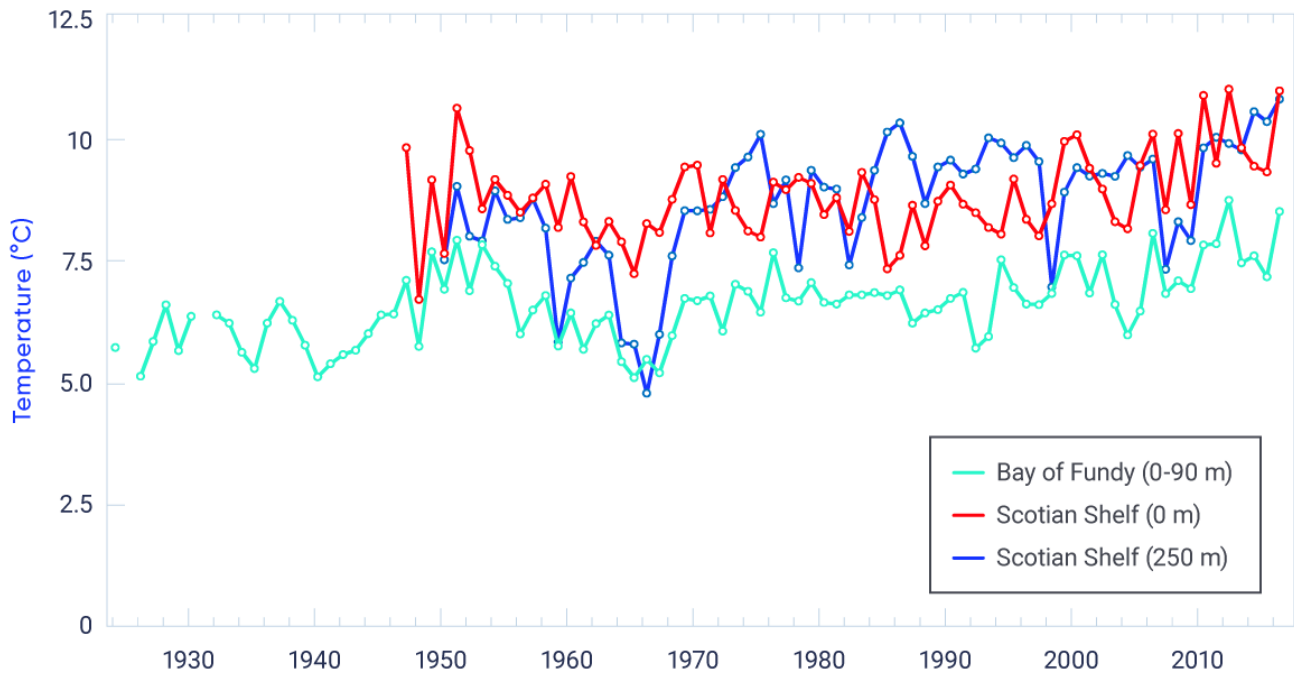


Figure 7.6: Annual mean temperatures in the Scotian Shelf and the Bay of Fundy

Figure caption: Ocean temperature time series in the Scotian Shelf and one for the Bay of Fundy collected by DFO monitoring programs. Long-term increases are observed from in situ sea surface temperature (0 m, 1947–2016, positive trend of 0.15°C per decade, significant at 1% level) and for the deeper layer (250 m, 1947–2016, positive trend of 0.36°C per decade, significant at 1% level) of the Emerald Basin region of the Scotian Shelf. Depth-averaged ocean temperature (0–90 m) from the Prince 5 station in the Bay of Fundy (1924–2016, positive trend of 0.16°C per decade, significant at 1% level) indicates a similar long-term warming trend.

FIGURE SOURCE: DATA FROM DFO MONITORING PROGRAMS (HEBERT ET AL., 2016). ATLANTIC ZONE MONITORING PROGRAM
<[HTTP://WWW.MEDS-SDMM.DFO-MPO.GC.CA/ISDM-GDSI/AZMP-PMZA/INDEX-ENG.HTML](http://www.meds-sdmm.dfo-mpo.gc.ca/isdm-gdsi/azmp-pmza/index-eng.html)>

In contrast to the areas discussed above (which are west of the Grand Banks and the island of Newfoundland), no significant warming trend in the past century has been shown in temperature averaged over all depths at the Newfoundland Shelf monitoring site (Station 27, see Figure 7.4) nor in the upper ocean (averaged over 20–150 m) in the central Labrador Sea near the former Ocean Weather Station Bravo site (Colbourne et al., 2017; Yashayaev and Loder, 2017). However, surface warming is evident over the past several decades on the Labrador and Newfoundland Shelves, as illustrated by the warming trend of 0.13°C per decade at Station 27 since 1950 (see Figure 7.7).

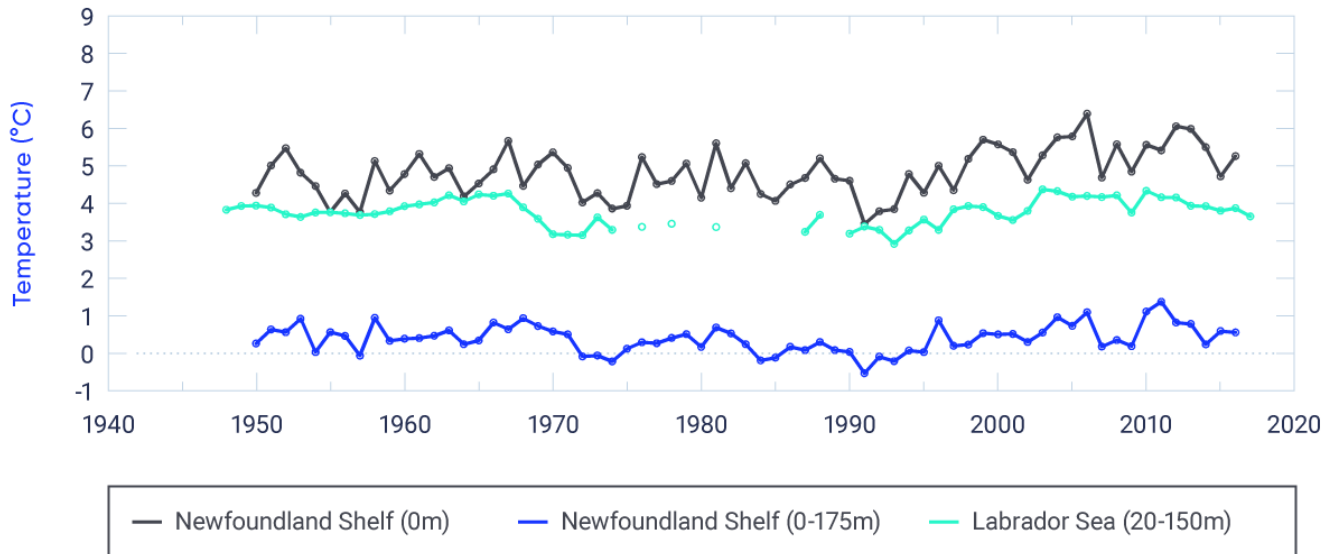


Figure 7.7: Annual mean temperatures in the Newfoundland Shelf and Labrador Sea

Figure caption: Ocean temperature time series in the Newfoundland Shelf and Labrador Sea collected by DFO monitoring programs. Sea surface temperature (0 m) on the Newfoundland Shelf at AZMP Station 27 near St. John's (1950–2016, positive trend of 0.13°C per decade, significant at 1% level [there is only a 1% possibility that the trend is due to chance]) and depth-averaged ocean temperature (0–175 m) from that site (1950–2016, non-significant positive trend of 0.02°C per decade). Upper-ocean temperature (20–150 m) of the central Labrador Sea basin (OWS Bravo) does not demonstrate long-term warming (1948–2016, non-significant positive trend of 0.03°C per decade).

FIGURE SOURCE: DATA FROM DFO MONITORING PROGRAMS (COLBOURNE ET AL., 2017; YASHAYAEV AND LODER, 2017). ATLANTIC ZONE MONITORING PROGRAM <[HTTP://WWW.MEDS-SDMM.DFO-MPO.GC.CA/ISDM-GDSI/AZMP-PMZA/INDEX-ENG.HTML](http://www.meds-sdmm.dfo-mpo.gc.ca/isdm-gdsi/azmp-pmza/index-eng.html)>. ATLANTIC ZONE OFF-SHELF MONITORING PROGRAM <[HTTP://WWW.BIO.GC.CA/SCIENCE/MONITORING-MONITORAGE/AZOMP-PMZAO/AZOMP-PMZAO-EN.PHP](http://www.bio.gc.ca/science/monitoring-monitorage/azomp-pmzao/azomp-pmzao-en.php)>.

Confidence in the Northwest Atlantic temperature changes over the last century is strengthened by comparisons of in situ measurements from DFO monitoring sites (Colbourne et al., 2017; Galbraith et al., 2017; Hebert et al., 2016; Yashayaev and Loder, 2017) with three global monthly interpolated SST datasets that extend back to the late 19th century (Loder and Wang, 2015). Trends in annual mean SST off Atlantic Canada since 1900 and 1950 are generally similar to global ones (Jewett and Romanou, 2017), except in the offshore Labrador Sea, where trends are weak (and not statistically significant). Trends since 1981 are generally two to three times larger than the longer-term ones, due to a combination of anthropogenic global warming and a warming phase of the Atlantic Multi-decadal Oscillation since the 1970s (Loder and Wang, 2015).

The absence of a long-term warming trend in the subpolar Labrador Sea region is consistent with the large area south of Greenland, where there has been no net warming observed in surface air and water temperatures over the past century (Lozier et al., 2008; IPCC, 2013; Loder and Wang, 2015). This is usually attributed to the predominance of natural climate variability in this area (e.g., Delworth and Zeng, 2016) and a possible reduction in the strength of Atlantic Meridional Overturning Circulation (e.g., Rahmstorf et al., 2015). An example of the importance of (and the pitfalls associated with) decadal-scale variability in the Northwest Atlantic is provided by the longest available temperature record from moored instruments off Atlantic Canada, specifically from a depth of 1000 m on the Labrador Slope. This record showed little (less than 0.2°C) net warming between 1987 and 2015 but warming by over 0.5°C between 1995 and 2011 as a result of record deep convection and subsurface cooling in the Labrador Sea during the early 1990s (Yashayaev and Loder, 2016). Longer time series of temperatures from the central Labrador Sea (see Figure 7.7) indicate no net warming of this water mass (which is of importance to the Atlantic Meridional Overturning Circulation) since 1950. Clearly, caution is warranted in inferring anthropogenic climate change from observational records of only a few decades' duration in the Atlantic and Pacific Ocean waters off Canada. To date, natural decadal-scale variability in these waters is of comparable magnitude to that of global anthropogenic climate change.

Changes in seasonality of SST in Atlantic Canada in recent decades have been studied by determining when threshold spring- and fall-like temperatures were reached each year, estimated from satellite data (Galbraith and Larouche, 2013). All regions of Atlantic Canada experienced earlier spring warming between 1985 and 2011, with trends varying between 0.6 weeks per decade earlier on the Scotian Shelf to 1.6 weeks per decade earlier on the Labrador Shelf. However, only a few limited regions experienced trends statistically different from zero for changes in the timing of fall cooling, with rates of 0.5 to 0.7 weeks per decade later in the year. If these changes were associated entirely with atmospheric warming, some regions of Atlantic Canada could see summertime SST conditions extended by as much as two weeks for each overall 1°C increase in regional air temperature. Over the period 1982–2014, it has been similarly estimated that summer duration increased by as much as three weeks per decade in the Scotian Shelf–Gulf of Maine region (Thomas et al., 2017), but this change likely includes a significant contribution from decadal-scale variability.

7.2.1.3: Arctic Ocean

Detecting and understanding climate change in the Canadian sector of the Arctic Ocean over the last century present challenges owing to the lack of adequate long-term observational records. However, there is strong evidence that surface air temperatures have increased in the Canadian Arctic and that sea ice extent and volume have declined (see Chapter 4, Section 4.2.1 and Chapter 5, Section 5.3.1). These changes point to associated upper-ocean warming in the region (especially considering the heat involved in changing sea ice to ocean water).

Satellite observations indicate that the August SST in most seasonal open-water areas in the Beaufort Sea, Hudson Bay, and Baffin Bay increased by more than 0.5°C per decade during 1982–2017 (Timmermans et al., 2018; also see Larouche and Galbraith, 2016) but also indicate limited or no warming in other areas (which may just reflect sparse data in marginal ice zones). In the Beaufort Sea at 50 m depth on the mid-continental shelf, no significant trend has been observed over the past 25 years (Steiner et al., 2015). This lack of a tem-

perature trend is consistent with observations of the upper-ocean mixed layer in the southern Beaufort Sea and the Canada Basin (one of two basins in the Arctic Ocean; Peralta-Ferriz and Woodgate, 2015). In the off-shelf basins of the Arctic Ocean, subsurface temperatures (at 150–900 m depth) have increased by 0.48°C per decade since 1970 (Polyakov et al., 2012).

In the Canadian Arctic Archipelago, temperatures near the seabed at 145 m depth in the western Lancaster Sound have increased by about 0.2°C (2002–2011), indicating a warming of the deeper layer of Arctic water passing through this passage into the Northwest Atlantic (Hamilton and Wu, 2013; Steiner et al., 2015). For the Baffin Island Shelf, no trend in temperature can be identified in the upper 50 m layer (1950–2005), but in the 50–200 m layer there is a slight cooling trend of 0.05°C per decade (Hamilton and Wu, 2013; Zweng and Münchow, 2006). In central Baffin Bay, a cooling trend of about 0.16°C per decade has been observed in the surface (0–50 m) and no trend observed in the 50–200 m layer since 1950, and a warming trend of about 0.13°C per decade has been seen in the deep basin (600–800 m) since 1960 (Hamilton and Wu, 2013; Zweng and Münchow, 2006).

7.2.2: Future projections

Because the heat capacity of water is much higher than that of air, anthropogenic ocean warming is expected to be somewhat less than that in the lower atmosphere over land, except possibly in some places where there are changes in ocean circulation (e.g., the warm Gulf Stream shifting northward). Projections from models in the fifth phase of the Coupled Model Intercomparison Project (CMIP5; see Chapter 3, Box 3.1) used in the Intergovernmental Panel on Climate Change's (IPCC's) Fifth Assessment Report (AR5) generally indicate widespread warming of the upper oceans around Canada during the 21st century, with greater warming for higher emission scenarios. Substantial variability is evident between seasons and from one region to another (Loder et al., 2015; Christian and Holmes, 2016; Steiner et al., 2015; Christian and Foreman, 2013). Projected changes in SST to mid-century (average for 2046–2065 relative to that for 1986–2005) for a high emission scenario (RCP8.5) have been computed as the ensemble mean of six of the CMIP5 models (Loder et al., 2015). Global emissions since 2005 (e.g., Peters et al., 2013; 2017), and climate-policy decisions (e.g., Sanford et al., 2014) have been closer to this scenario than to the low emission scenario (RCP2.6). The projected mid-century SST increases for the medium emission scenario (RCP4.5) are about 70% of those for RCP8.5 with similar spatial patterns, consistent with the scalability of projected air temperature changes discussed in Chapter 4 (also see Markovic et al., 2013). As a good approximation, these projected increases can be taken to apply until mid-century, assuming only limited further reductions in emissions.

In the Northeast Pacific off British Columbia, the projected SST increases to mid-century are roughly 2°C in winter and 3°C in summer, with a small and smooth increase with latitude (see Figure 7.8). In contrast, the projected increases in Canadian Arctic waters (including Hudson Bay) and the Northwest Atlantic have larger seasonal and spatial variations. The projected SST changes in the Arctic in winter are very small (because of the projected continued presence of winter sea ice), but those in summer are up to 4°C in areas such as the Beaufort Sea and Hudson Bay, where reduced sea ice cover is projected. The CMIP5 models do not have adequate spatial resolution and representations of sea ice and ocean physics in the complex Canadian Arctic Archipelago to reliably project the details of ocean temperature changes in summer and fall there, but sub-

stantial spatial structure in the ocean changes associated with changes in sea ice can be expected (e.g., Sou and Flato, 2009; Hu and Myers, 2014; Steiner et al., 2015). Reliable projections of ocean conditions in this region will probably require a combination of higher spatial resolution in global climate models and inclusion of both sea ice and ocean components in the regional climate models used in dynamical downscaling (see Chapter 3.5).

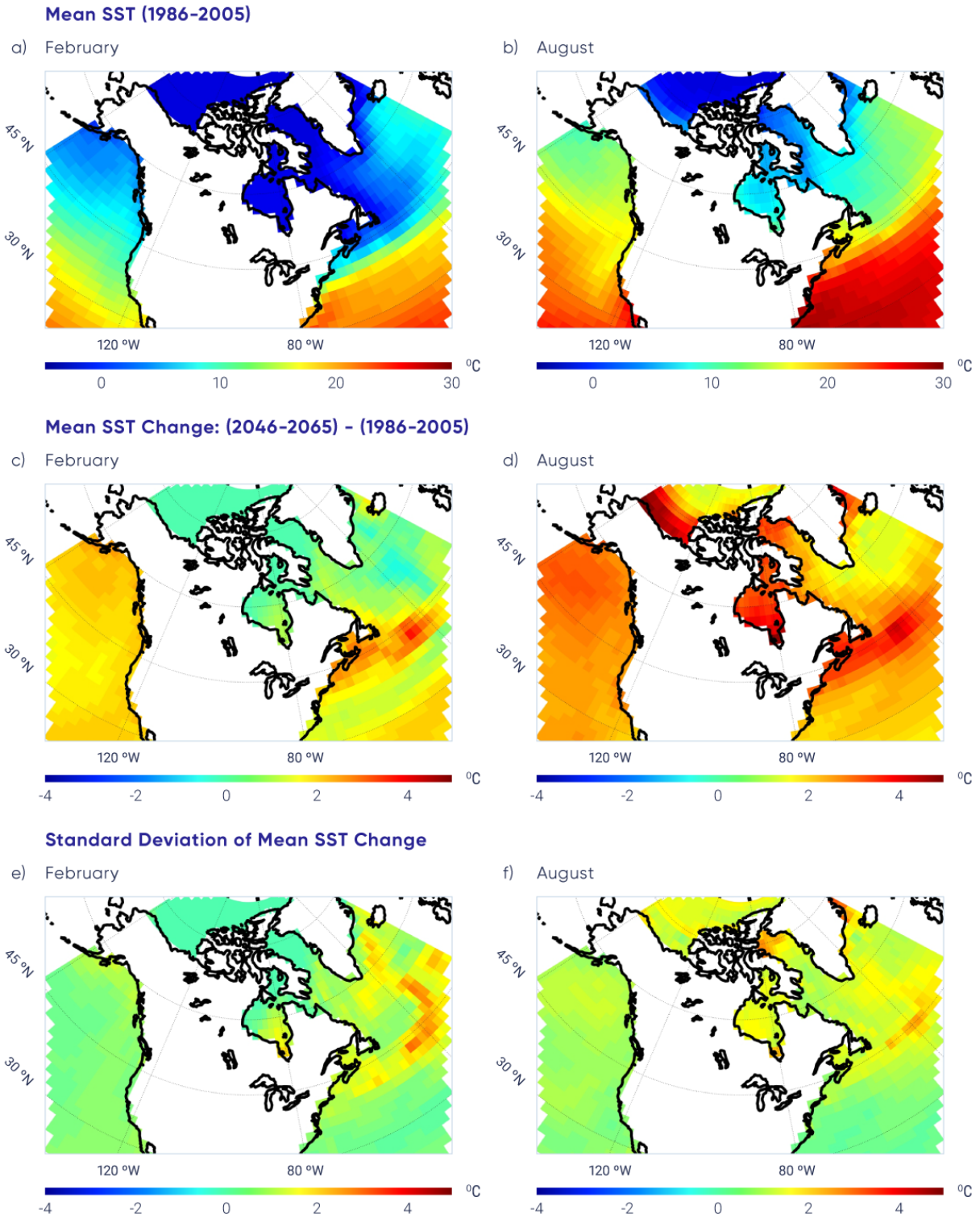


Figure 7.8: Projected future sea surface temperatures in oceans surrounding Canada

Figure caption: Fifth phase of the Coupled Model Intercomparison Project (CMIP5) ensemble mean sea surface temperature (SST) for the period of 1986–2005 (top row) for February (a) and August (b). Change in the mean SST for mid-century (2046–2065) relative to 1986–2005 for February (c) and August (d) for the high emission scenario (RCP8.5). Standard deviation in the SST change for mid-century relative to 1986–2005 for February (e) and August (f). In general, the standard deviation is small, indicating agreement among models, except for northern Baffin Bay and the regions south of Nova Scotia, Newfoundland, and Greenland; this can be attributed to the difficulty in modelling the ocean dynamics of these regions.

FIGURE SOURCE: ADAPTED FROM LODER AND VAN DER BAAREN (2013).

Air temperature increases are projected to be larger than the SST increases in most parts of the Northwest Atlantic (Loder et al., 2015), consistent with atmospheric warming being the primary driver of ocean warming (e.g., Collins et al., 2013; Hegerl et al., 2007). The latitudinal variation of future SST change in offshore waters will be different from the increase with latitude of air temperature over the land associated with Arctic amplification. In contrast to air temperature for Canada as a whole, the SST increase in the Northwest Atlantic is projected to be largest at mid-latitudes and smaller proceeding north into subpolar waters. Winter SST increases by mid-century of up to 3°C off the Maritime provinces, but only 1°C off Labrador, are projected for the high emission scenario (RCP8.5). Similarly, mid-century summer SST increases of up to 4°C are projected off the Maritime provinces, but increases are limited to 2°C off Labrador. The mid-latitude maximum in the SST increase is related to projected changes in large-scale ocean circulation and to a slight northward expansion of the subtropical gyre (and shift of the Gulf Stream), in particular.

In the North Atlantic south of Greenland, most models indicate that future warming will be more limited, with the Atlantic Meridional Overturning Circulation transporting less heat northward (Drijfhout et al., 2012). However, substantial uncertainty remains about the potential for significant reduction of this circulation in the future, due to the complexity of the atmosphere–ice–ocean system in the Northwest Atlantic and the limited capability of current climate models to simulate important processes in this complex system (Sgubin et al., 2017).

As is the case for the Canadian Arctic Archipelago, the coarse horizontal resolution of the ocean in the CMIP5 Earth system models (of approximately 100 km) poses a challenge for modelling the ocean off Atlantic Canada, where the coastline and seafloor topography are complex. This results in a warm bias in SST due to a misrepresentation of the boundary between the subpolar and subtropical gyres; thus, existing climate change projections are based on a modelled regional ocean circulation that differs from current reality (Loder et al., 2015; Saba et al., 2016). This is important for Atlantic Canada, in particular, which is in a region of large spatial differences in ocean temperature (Figure 7.1). Regional climate downscaling has provided detailed information on the spatial structure of potential changes for Atlantic Canada (Long et al., 2016), but the overall magnitude of the changes is uncertain.

Section Summary

In summary, upper-ocean temperature has increased in the Northeast Pacific and most areas of the Northwest Atlantic over the last century, consistent with anthropogenic climate change (*high confidence*). This statement of confidence is based on high-quality in situ observations of sea surface and subsurface temperature, which are generally consistent with the regional variations in global interpolated SST datasets. The number of locations with long subsurface time series is limited and, although these data are expected to be representative of large areas, there is lower confidence in them. Natural decadal variability is comparable in magnitude to the long-term changes in ocean temperature; there is a region south of Greenland where there has been little or no warming over the last century. There are no long-term ocean temperature measurements for the Arctic Ocean, but warming is expected to have occurred in the summer and fall periods, based on observed increases in air temperature (see Chapter 4, Section 4.2.1) and declines in sea ice (see Chapter 5, Section 5.3.1) (*medium confidence*). This statement of confidence is based on a few short temperature time series and on expert judgment of the coupling of the atmosphere, cryosphere, and upper ocean.

Oceans surrounding Canada are projected to continue to warm over the 21st century in response to past and future emissions of greenhouse gases. The warming in summer will be greatest in the ice-free areas of the Arctic and off southern Atlantic Canada where subtropical water is projected to shift further north (*medium confidence*). During winter in the next few decades, the upper ocean surrounding Atlantic Canada will warm the most, the Northeast Pacific will experience intermediate warming rates and the Arctic and eastern sub-Arctic ocean areas (including Hudson Bay and Labrador Sea) will warm the least (*medium confidence*). These statements of confidence are based on an analysis of six CMIP5 model projections of SST for the oceans surrounding Canada, which show an increase in SST in all seasons in the Northeast Pacific and Northwest Atlantic oceans. The statements are also based on physical understanding of the processes related to increasing surface air temperature, resulting in a positive heat transfer to the ocean surface waters. The level of confidence is medium rather than high owing to differences in the regional projections from the Earth system models.



7.3: Ocean salinity and density stratification

Key Message

There has been a slight long-term freshening of upper-ocean waters in most areas off Canada as a result of various factors related to anthropogenic climate change, in addition to natural decadal-scale variability (*medium confidence*). Salinity has increased below the surface in some mid-latitude areas, indicating a northward shift of saltier subtropical water (*medium confidence*).

Key Message

Freshening of the ocean surface is projected to continue in most areas off Canada over the rest of this century under a range of emission scenarios, due to increases in precipitation and melting of land and sea ice (*medium confidence*). However, increases in salinity are expected in off-shelf waters south of Atlantic Canada due to the northward shift of subtropical water (*medium confidence*). The upper-ocean freshening and warming is expected to increase the vertical stratification of water density, which will affect ocean sequestration of greenhouse gases, dissolved oxygen levels, and marine ecosystems.

The ocean is a key component of the Earth's water cycle (see Chapter 6, Figure 6.1), and changes in the rates of evaporation and precipitation are reflected in the relative freshness or salinity of the ocean surface water (Helm et al., 2010). Salinity can also change in response to freshwater runoff from the continent, melting and freezing of sea ice (see Box 7.3), and ocean circulation and mixing. Changes near the sea surface affect the ocean interior (intermediate and deep layers) through processes such as vertical mixing and deep convection (e.g., Yashayaev and Loder, 2016). Ocean salinity, together with temperature and pressure (depth), determines the density of seawater, which, in turn, affects ocean circulation, vertical density stratification (see Box 7.4), and vertical mixing. The differences in sea surface salinity between different areas of the global ocean have become stronger since the 1950s. Relatively saline surface waters in the evaporation-dominated lower mid-latitudes have become more saline, while relatively fresh surface waters in rainfall-dominated tropical and ice-influenced polar regions have become fresher (Rhein et al., 2013).

Box 7.3: Brine rejection

Brine rejection is a process that occurs during sea ice formation, in which salt is pushed from the ice, as it forms, into the surrounding seawater. This results in sea ice being fresher than the seawater from which it formed. When sea ice melts, a freshwater layer develops at the ocean surface where the melt occurs.

Box 7.4: Ocean density stratification

The density of seawater is a function of its temperature, salinity, and pressure (which increases with depth below the sea surface). Ocean density stratification refers to the vertical difference in water density. Light, relatively warm and fresh near-surface water generally overlies cold, denser, subsurface water. In the upper ocean, this stratification is seasonal. It develops in spring and summer as a result of the warming of near-surface water by sunlight and atmospheric heating and the freshening of near-surface water due to continental runoff, sea ice melting, or precipitation. It then disappears with fall cooling and wind-driven mixing. Weaker stratification persists year-round below the winter mixed layer. Stratification limits vertical mixing in the ocean, particularly in the upper ocean in spring and summer. The variability of this stratification from region to region and over time has significant implications for mixing heat and carbon dioxide down into the ocean and for mixing nutrients (needed for plankton growth) up into the surface layers. With increased warming and runoff of fresh water into the Arctic and subpolar oceans under anthropogenic climate change, stratification in these waters is expected to increase. This effect may reduce the ocean's ability to absorb carbon dioxide from human activities, thereby amplifying global warming. It could also reduce the upwelling of nutrients to the waters surrounding Canada, affecting food sources for the entire marine food web.

7.3.1: Observations

Ocean salinity observations have been made since the late 19th century by research cruises. The coverage of these observations is, however, more sparse than observations of temperature, as salinity is more difficult to measure than temperature. Observations of ocean salinity on the continental shelves surrounding Canada are primarily acquired through vertical profiles taken by research vessels, supplemented by continuous time series from sparse moored instruments.

7.3.1.1: Northeast Pacific Ocean

As with ocean temperatures in the North Pacific (see Section 7.2.1.1), sea surface salinity is strongly influenced by natural variability associated with the seasons, freshwater runoff from land, and longer-term processes such as ENSO and the Pacific Decadal Oscillation. Observations at offshore Station P show a slight long-term freshening (a decline in salinity of 0.015 per decade²⁶) near the surface and a slight long-term salinity increase (but not statistically different from zero) at depth (see Figure 7.9). Coastal waters along the west coast of Vancouver Island show slight freshening (a decline of 0.043 per decade), which is consistent with Station P, while those along the east coast (in the Strait of Georgia) show slight salinity increases of the same magnitude. The complexity of freshwater runoff contributes to the variability observed at these coastal stations.

26 Salinity is a dimensionless (i.e., without units) quantity which corresponds to parts per thousand (of salt in seawater), or grams of salt per kilogram of seawater.

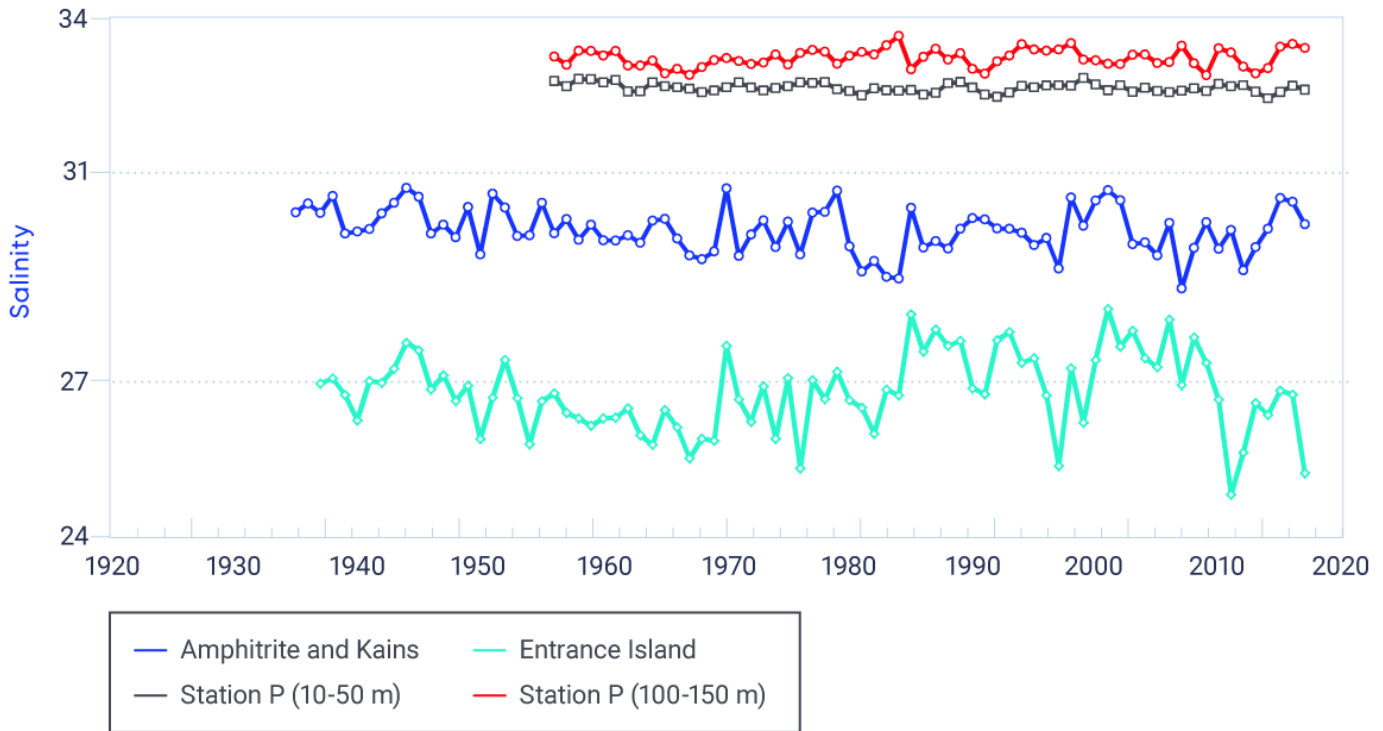


Figure 7.9: Ocean salinity changes in the Pacific Ocean off Canada's west coast

Figure caption: Annual mean salinity in the Pacific Ocean off British Columbia at same sites as the mean temperature in Figure 7.2. Long-term trends in these time series are small but statistically different from zero for the Station P (10–50 m) near-surface layer (1956–2017, declining trend of 0.015 per decade, significant at 5% level, (there is only a 5% possibility that the trend is due to chance)) and Amphitrite and Kains Islands (1935–2017, declining trend of 0.043 per decade, significant at 5% level). Interannual and decadal variability is large at Entrance Island (east Vancouver Island) relative to the sites on the west coast of Vancouver Island and at Station P. Long-term trends are not statistically different from zero at Entrance Island (1937–2017, increasing trend of 0.038 per decade) nor at Station P (100–150 m) deep layer (1956–2017, increasing trend of 0.013 per decade).

FIGURE SOURCE: DATA ARE FROM DFO MONITORING PROGRAMS. BRITISH COLUMBIA SHORE STATION OCEANOGRAPHIC PROGRAM <[HTTP://WWW.PAC.DFO-MPO.GC.CA/SCIENCE/OCEANS/DATA-DONNEES/LIGHTSTATIONS-PHARES/INDEX-ENG.HTML](http://www.pac.dfo-mpo.gc.ca/science/oceans/data-donnees/lightstations-phares/index-eng.html)>. LINE P MONITORING PROGRAM <[HTTP://WWW.DFO-MPO.GC.CA/SCIENCE/DATA-DONNEES/LINE-P/INDEX-ENG.HTML](http://www.dfo-mpo.gc.ca/science/data-donnees/line-p/index-eng.html)>.

Stratification of the upper ocean along Line P increased over the period 1956 to 2011 (Freeland, 2013). This is primarily driven by the freshening of the near-surface waters (Durack and Wijffels, 2010; Durack et al., 2012), supplemented by the tendency toward increasing salinity below 100 m.

7.3.1.2: Northwest Atlantic Ocean

Off the Atlantic coast, long-term salinity changes have generally shown a slight freshening (decreasing) trend of the upper ocean and an increasing trend in the deep water of the Gulf of St. Lawrence (see Figure 7.10). The multiple factors that contribute to the long-term trends in salinity are partly offsetting at mid-latitudes, such that decade-to-decade natural variability is important. On the Newfoundland Shelf, there was a freshening, with salinity declining by about 0.013 per decade (Colbourne et al., 2017). In the central Labrador Sea and Bay of Fundy, the upper ocean has a similar weak trend to that observed on the Newfoundland Shelf but it is not statistically different from zero (Hebert et al., 2016; Yashayaev et al., 2014; Yashayaev and Loder, 2016). The largest and most robust salinity trend in Atlantic Canadian waters has been found in the deep (200–300 m below the surface) waters of the Gulf of St. Lawrence, where there has been a statistically significant increase in salinity of 0.019 per decade over the past 90 years. This trend is consistent with a northward shift of higher-salinity subtropical waters, which is also indicated by temperature (see Section 7.2.1.2) and oxygen (see Section 7.6.2) observations (Gilbert et al., 2005; Galbraith et al., 2017).

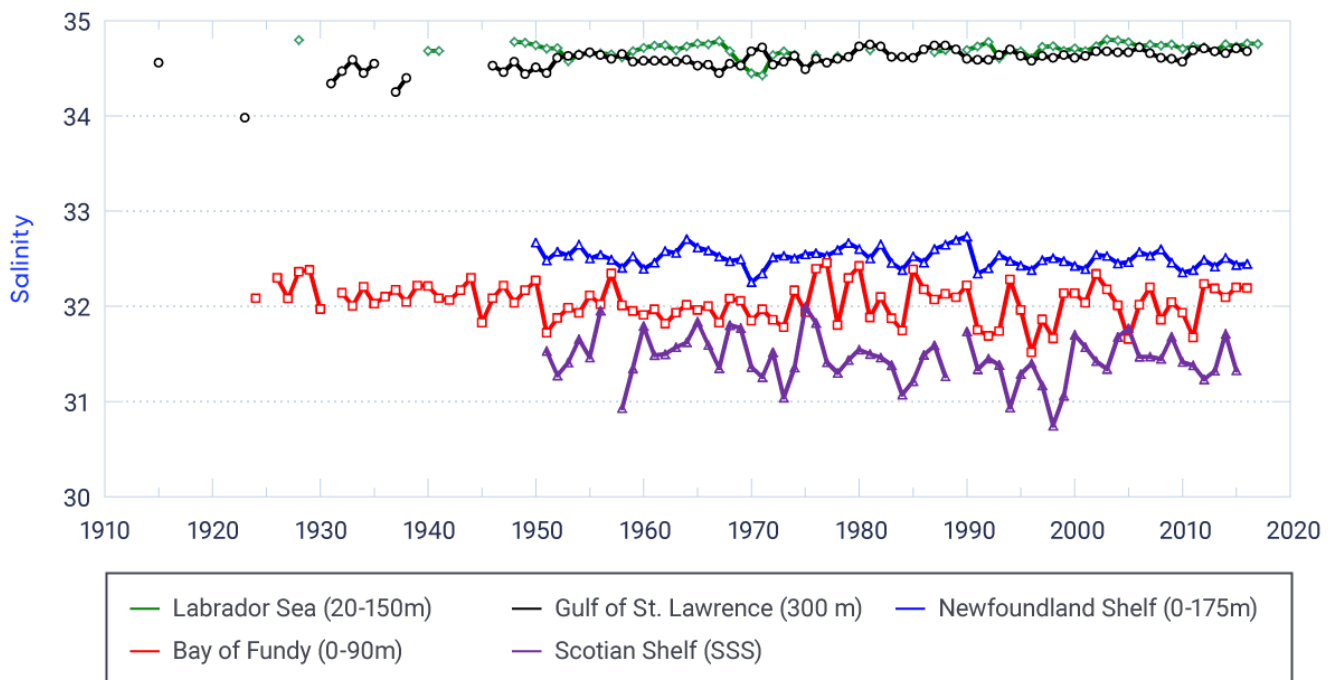


Figure 7.10: Ocean salinity changes in the Atlantic Ocean off Canada's east coast

Figure caption: Annual mean salinity at representative sites from five different areas off Atlantic Canada, from Fisheries and Oceans Canada (DFO) monitoring programs. The Gulf of St. Lawrence (300 m depth) long-term trend is significantly positive (1915–2016, trend 0.019 per decade, significant at 1% level), in contrast to the other

sites, which all have negative trends. The decreasing trend on the Newfoundland Shelf (Station 27, 0–175 m, 1950–2016, declining trend of 0.013 per decade, significant at 5% level) is statistically different from zero. The remaining sites do not have trends that are statistically different from zero (Labrador Sea, 20–150 m, 1928–2012, declining trend of 0.005 per decade; Scotian Shelf (Emerald Basin), 1951–2016, declining trend of 0.022 per decade; Bay of Fundy, 0–90 m, 1924–2016, declining trend of 0.009 per decade).

FIGURE SOURCE: DATA ARE FROM DFO MONITORING PROGRAMS (HEBERT ET AL., 2016; COLBOURNE ET AL., 2017; GALBRAITH ET AL., 2017; YASHAYAEV AND LODER, 2017).

There is evidence of a long-term increase in upper-ocean stratification for the period 1948–2017, with the rate on the Scotian Shelf being about twice that observed on the Newfoundland Shelf (see Figure 7.11). This trend is a result of long-term changes in both surface temperature and salinity. In general, these trends are consistent with positive trends in stratification observed for many areas over the continental shelves in Atlantic Canada, which were assessed over the 1951–2009 period (Hebert, 2013). However, it is also evident that multi-decadal natural variability is an important influence on stratification in this area (see Figure 7.11). There are some regions where there has been decreasing stratification in the last few decades, such as the western Gulf of St. Lawrence and St. Lawrence Estuary, which are strongly influenced by changes in freshwater discharges (Galbraith et al., 2017).

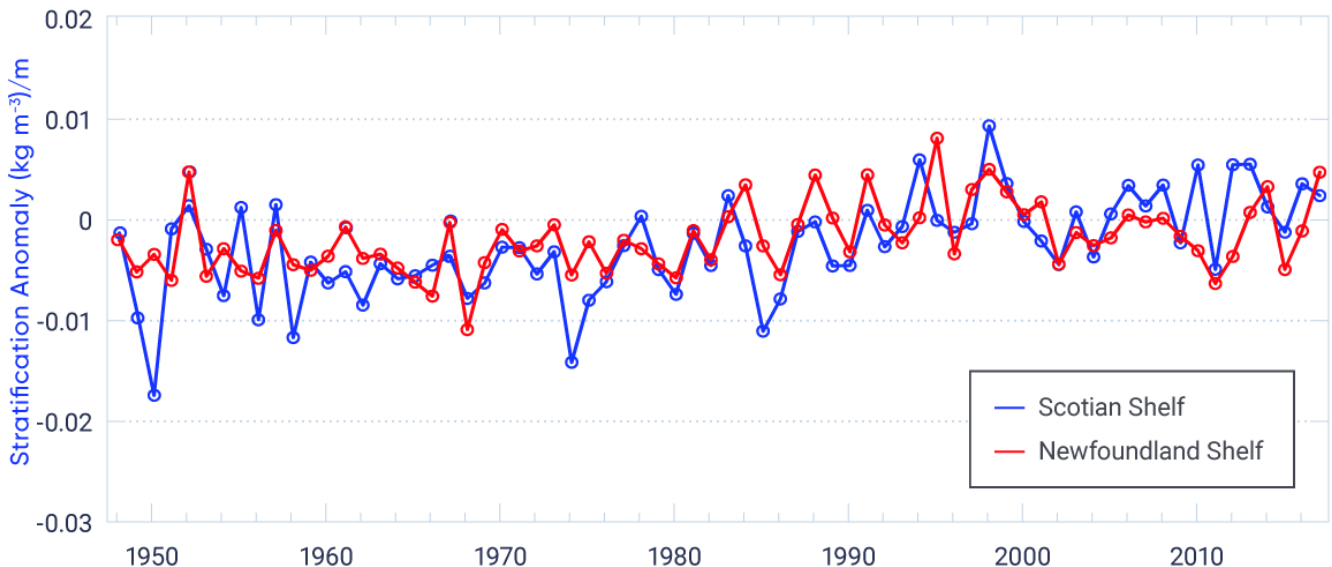


Figure 7.11: Ocean stratification changes on the Scotian Shelf and Newfoundland Shelf

Figure caption: Stratification index (density difference from the ocean surface [0 m] to the depth of 50 m) is expressed as a mean annual anomaly (departure from normal) for the period 1948–2017. The time series for the Scotian Shelf is derived from data collected from several areas across the shelf, which are combined to provide one annual anomaly estimate. The time series for the Newfoundland Shelf is based on data collected at the AZMP Station 27. The long-term trend is significantly positive for both the Scotian Shelf (1948–2017, positive trend 0.0015 (kg/m³) per decade, significant at 1% level) and the Newfoundland Shelf (1948–2017, positive trend 0.00074 (kg/m³) per decade, significant at 1% level).

FIGURE SOURCE: DATA FROM DFO MONITORING PROGRAMS (HEBERT ET AL., 2016; COLBOURNE ET AL., 2017).

7.3.1.3: Arctic Ocean

Freshwater is accumulating in the Arctic, Canadian Arctic Archipelago, and Baffin Bay, with more freshwater present in the decade of the 2000s compared to the 1980–2000 average (Haine et al., 2015); this accumulation is particularly strong in the Beaufort Gyre. In contrast to the widespread freshening of the Arctic Ocean mixed layer, the summer southern Beaufort Sea has shown salinity increasing at a rate of approximately 2 per decade for the 1982–2012 period (Peralta-Ferriz and Woodgate, 2015). The southern Beaufort Sea is strongly influenced by the freshwater runoff from the Mackenzie River as well as changes in the Beaufort Gyre circulation and its effects on coastal waters, and it is difficult to assess the robustness and origin of this salinity increase. Salinity has been measured at a mid-shelf site in the Beaufort Sea since 1999, but there is no discernable trend in the data collected (Steiner et al., 2015).

In the Canadian Arctic Archipelago, salinity near the seabed at 145 m depth in the western Lancaster Sound increased over the 2002–2011 period, concurrent with warming at this location (Steiner et al., 2015; Hamilton and Wu, 2013). For the Baffin Island Shelf, no trend in salinity can be identified in the upper 50 m layer (1950–2005), but in the 50–200 m layer there was a freshening trend (decline of 0.15 per decade) over the period 1976–2002 (Hamilton and Wu, 2013). In central Baffin Bay, there is no significant long-term trend in salinity in either the 0–50 m or the 600–800 m depth layer (Zweng and Münchow, 2006).

7.3.2: Future projections

In the global context, the CMIP5 climate model projections suggest that subtropical regions with high sea surface salinity, dominated by net evaporation, will become more saline as the century progresses. High-latitude regions with lower sea surface salinity are projected to freshen over the coming century (Collins et al., 2013).

For the northeastern Pacific off Canada, future projections show significant freshening by mid-century (see Figure 7.12), with little change in the spatial structure under either a medium (RCP4.5) or high (RCP8.5) emission scenario (Christian and Foreman, 2013).

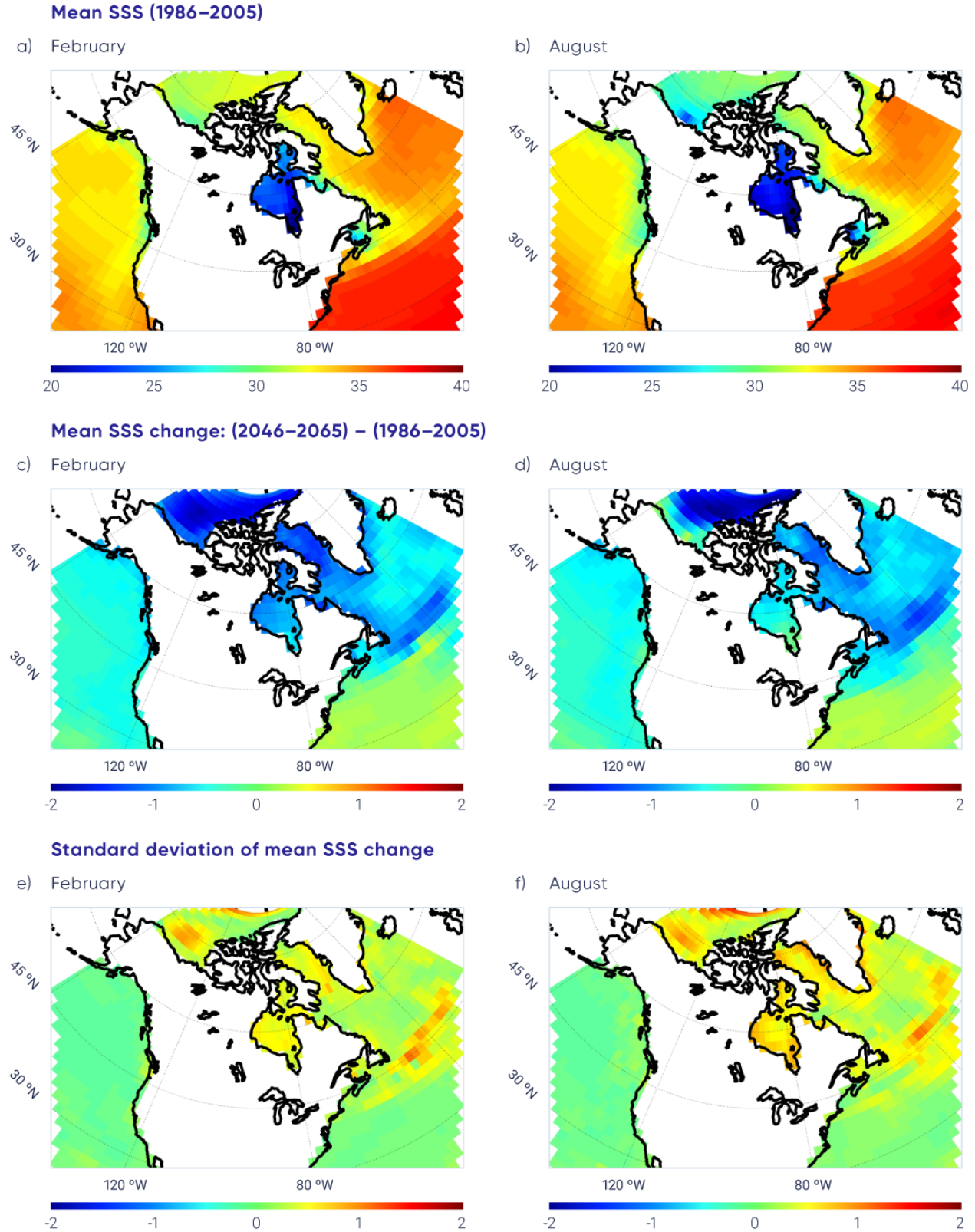


Figure 7.12: Future changes in salinity in the oceans surrounding Canada

Figure caption: Fifth phase of the Coupled Model Intercomparison Project (CMIP5) ensemble mean sea surface salinity (SSS) for the period 1986–2005 (top row) for February (a) and August (b). Change in the mean SSS for mid-century (2046–2065) relative to 1986–2005 for February (c) and August (d) for a high emission scenario (RCP8.5). Standard deviation in the SSS change for mid-century relative to 1986–2005 for February (e) and August (f). Panels (c) and (d) show a general freshening of the sea surface in the Northeast Pacific and in the Northwest Atlantic north of 40° north latitude (decrease generally less than 1). In the North Atlantic subtropical gyre, the projection indicates an increase in salinity (increase generally less than 1). In the Northeast Pacific, the standard deviation is small, indicating agreement among models. In many areas of the Arctic and Northwest Atlantic Oceans, the large standard deviation indicates larger discrepancies between model projections in these areas, where sea ice and complex ocean dynamics are important processes that are difficult to simulate.

FIGURE SOURCE: ADAPTED FROM LODER AND VAN DER BAAREN (2013).

Significant freshening by mid-century for the subpolar Northwest Atlantic Ocean is also projected under medium (RCP4.5) and high (RCP8.5) emission scenarios (see Figure 7.12; also Loder et al., 2015). On the other hand, increased salinity is projected in the subtropical gyre, thereby increasing the difference in salinity between the two gyres of the North Atlantic Ocean. The increased difference is important, because small changes in the boundary between the gyres will result in shifts in local salinity (and, potentially, stratification and circulation). The boundary for the shift from increasing to decreasing salinity trends generally lies around 40° north latitude (Loder et al., 2015) but there are significant differences among projections for this region from different CMIP5 models; therefore, confidence in the pattern of future projections of sea surface salinity is low. A high-resolution climate model projects significantly larger changes in salinity on the ocean bottom on the continental shelf in southern Atlantic Canada, (i.e., Scotian Shelf), suggesting that the CMIP5 climate change projections for the Northwest Atlantic shelf between Cape Hatteras and the Grand Banks may underestimate expected changes in salinity (Saba et al., 2016). The CMIP5 global models do not resolve the topography of the continental shelf or the spatial structure of the ocean overlying the shelf. CMIP5 global models also do not properly resolve the Gulf Stream separation off Cape Hatteras, North Carolina; therefore, the position of the Gulf Stream is too far north in the models' simulations of past and present-day regional ocean climate.

Projected continued losses of sea ice will add fresh meltwater to the ocean (see Box 7.3) which, combined with projected increased precipitation (see Chapter 4, Section 4.3.1.3), will affect the freshwater input into the Arctic Ocean. The CMIP5 global model simulations project a fresher (decrease of approximately 2 by mid-century) near-surface ocean in the Beaufort Sea and area north of the Canadian Arctic Archipelago under the high emission scenario (RCP8.5) (see Figure 7.12). The spatial pattern of surface salinity shows increased freshening with distance north from the coast in the Beaufort Sea (Steiner et al., 2015). A high-resolution model simulation for the Canadian Arctic Archipelago projects strong decadal variability in surface salinity but no clear trend by mid-century (Hu and Myers, 2014). The southward transport of freshwater that is currently tied up in sea ice in the Arctic will be a contributor to the southward extent of low-salinity water off Atlantic Canada. With less seasonal sea ice, this transport mechanism is expected to weaken and, once there is no seasonal ice cover, eventually disappear.

Section Summary

In summary, there has been a slight long-term freshening of upper-ocean waters in most areas off Canada as a result of various factors related to anthropogenic climate change, in addition to natural decadal-scale variability (*medium confidence*). Salinity has increased below the surface in some mid-latitude areas, indicating a northward shift of saltier subtropical water (*medium confidence*). These statements of confidence are based on agreement among high-quality in situ observations of surface and subsurface salinity, available from DFO databases. The number of locations with long time series is more limited than those of ocean temperature, and this reduces confidence in the broader-scale representativeness of trends. Natural decadal variability is comparable in magnitude to the long-term changes in ocean salinity in most areas, which also reduces confidence in trends. Observations from the Arctic Ocean as a whole indicate freshening in most areas, but increased salinity in some others. Given the lack of data, no confidence statement has been made about climate change trends for ocean salinity in the Arctic.

Freshening of the ocean surface is projected to continue in most areas off Canada over the rest of this century under a range of emission scenarios, due to increases in precipitation and melting of land and sea ice (*medium confidence*). However, increases in salinity are expected in off-shelf waters south of Atlantic Canada due to the northward shift of subtropical water (*medium confidence*). The upper-ocean freshening and warming is expected to increase the vertical stratification of water density, which will affect ocean sequestration of greenhouse gases, dissolved oxygen levels, and marine ecosystems. These statements of confidence are based on the analysis of six CMIP5 model projections of sea surface salinity for the oceans surrounding Canada, and regional model studies. There are differences in the magnitude of salinity change among the CMIP5 model projections in the Northwest Atlantic, which means there is more uncertainty in projections for this region.



7.4: Marine winds, storms, and waves

Key Message

Surface wave heights and the duration of the wave season in the Canadian Arctic have increased since 1970 and are projected to continue to increase over this century as sea ice declines (*high confidence*). Off Canada's east coast, areas that currently have seasonal sea ice are also anticipated to experience increased wave activity in the future, as seasonal ice duration decreases (*medium confidence*).

Key Message

A slight northward shift of storm tracks, with decreased wind speed and lower wave heights off Atlantic Canada, has been observed and is projected to continue in future (*low confidence*). Off the Pacific coast of Canada, wave heights have been observed to increase in winter and decrease in summer, and these trends are projected to continue in future (*low confidence*).

Marine storms have impacts on both the offshore economy and coastal communities. Winds are an important feature of marine storms, and waves result directly from the wind blowing over the surface of the ocean. While changes in storminess (frequency and intensity of storms) have potential negative consequences (e.g., disruption of fisheries), uncertainty in past and future global storminess remains high, as a result of poor historical observational data, inconsistencies among research studies, and differences in the projections from global and regional climate models (Hartmann et al., 2013). Because storms are dynamic, short-lived events, it is challenging to determine whether observed regional changes are a result of natural internal climate variability or attributable to anthropogenic climate change. Hence, there is lower confidence in atmospheric circulation-related projections (e.g., storminess) than in changes in thermodynamic properties such as temperature (Hartmann et al., 2013; Shepherd, 2014).

7.4.1: Marine winds and storms

As is the case globally, the assessment of historical changes in winds and storms for the oceans surrounding Canada is hampered by limited evidence, in part related to sparse observations and challenges in integrating early marine observations, instrumental records, and satellite data. However, there is evidence of a slight northward shift of storm tracks of about 180 km over the North Atlantic Ocean (60° west to 10° east) and about 260 km for Canada as a whole (120° west to 70° west) for the 1982–2001 period relative to 1958–1977 (Wang et al., 2006). This trend is consistent with global assessments, which have observed a poleward shift of storm tracks and the jet stream since the 1970s (Wu et al., 2012; Hartmann et al., 2013), and is projected to continue through this century (Collins et al., 2013). The poleward shift results in a modest projected decrease in wind speed and wave heights over marine areas in Atlantic Canada (Casas-Prat et al., 2018).

An increasing trend in the frequency of autumn (October–December) extreme storms (low-pressure systems of core pressure less than 980 hPa) over the 1958–2010 period has been observed over marine areas of Atlantic Canada, but there are no statistically significant trends for extreme storms in other seasons for the Atlantic and Pacific coasts of Canada (Wang et al., 2016). This is consistent with research that has demonstrated that human activities have contributed to an observed upward trend in North Atlantic hurricane activity since the 1970s (Kossin et al., 2017). Model projections of late-summer and autumn storms off Atlantic Canada suggest a slight northward shift of storm tracks and a modest reduction in intensities of storms, although extreme storms may have increased intensities (Jiang and Perrie, 2007, 2008; Perrie et al., 2010; Guo et al., 2015).

For the Arctic above 75° north latitude, an increasing trend in storm frequency and intensity has been seen in all long-term datasets that cover 1958–2010 or 1900–2010 periods (see Wang et al., 2016). This trend is independent of different storm identification and analysis methods and is consistent with the increasing trend in ocean surface wave heights in this region, as seen in satellite data (Francis et al., 2011; Liu et al., 2016) and wave reanalysis data (Wang et al., 2015; see also Section 7.4.2). However, observations are sparse in the Arctic region, which lowers our confidence in storminess trends in this region. Increases in surface wind speed over Canadian sectors of the Arctic Ocean are projected, largely related to the projected declines in sea ice (Casas-Prat et al., 2018).

7.4.2: Waves

Waves are an important physical feature of the ocean surface that affects fluxes of energy, heat, and gases between the atmosphere and ocean, as well as marine safety and transportation. Surface waves are generated by wind forcing, and “significant wave height” is a measure that is approximately equal to the average of the highest one-third of wave heights. Global and regional time series of wave characteristics are available from buoy data, voluntary observing ship reports, satellite measurements, and model wave reanalysis/hindcasts (i.e., simulations of past conditions using observations of other climate variables).

In the Arctic, over the 1970–2013 period, significant wave heights have increased over the Canadian Beaufort Sea westward to the northern Chukchi Sea in September, with the Beaufort–Chukchi–Siberian Seas regional mean significant wave height increasing at a rate of 3% to 8% per decade in July–September (Wang et al., 2015). These trends suggest that increasing wave energy could constitute a mechanism to break up sea ice and accelerate ice retreat (Thomson and Rogers, 2014; Wang et al., 2015); however, the rate of sea ice reduction could also be enhanced by wave mixing in the upper ocean, causing an added release of heat (Smith et al., 2018). For areas experiencing loss of sea ice (see Chapter 5, Section 5.3), significant seasonal increases in waves are projected for the future (Casas-Prat et al., 2018). Reduced sea ice cover will result in greater distances of open water for waves to travel across and, with a southward mean wave direction for the Arctic Ocean, this will result in increased wave impacts on coastal infrastructure and communities in the Canadian Arctic.

For the waters off the Pacific coast, an analysis of buoy wave records revealed that wave heights in the region off British Columbia have decreased significantly over the past three to four decades in summer and increased slightly in winter, showing small decreasing annual trends (Gemrich et al., 2011). The same trends and trend seasonality are evident in other studies (Wang and Swail, 2001) and are also projected to continue into the future (Wang et al., 2014; Casas-Prat et al., 2018; Erikson et al., 2015). The wintertime increase in wave height in this region is also seen in observations from voluntary observing ships (VOS) for 1958–2002, but these results show much larger increases (Gulev and Griforieva, 2006). The reason for the difference between the VOS and other results is uncertain.

Over the past half-century, the large-scale pattern of North Atlantic wave heights is characterized by increases in the Northeast Atlantic, with decreases in the mid-latitude North Atlantic in winter (Wang and Swail, 2001,



2002; Wang et al., 2012; Bromirski and Cayan, 2015). For the waters off Atlantic Canada, small increases (around 2 cm per decade) in summertime wave heights and insignificant wintertime decreases were observed for the 1948–2008 period (Bromirski and Cayan, 2015). Similar trends are also seen in other observational wave studies (Wang and Swail, 2001, 2002). These results differ from VOS observations for 1958–2002, which show wintertime increases of around 0.1 m per decade for the waters off Atlantic Canada (Gulev and Griforieva, 2006), and the reason for this discrepancy is unclear. Modest decreases in wave height in the region off Atlantic Canada are projected over the coming century (Wang et al., 2014; Casas-Prat et al., 2018). In the Gulf of St. Lawrence, downscaled projections suggest decreased mean significant wave heights in summer and increased wave heights in winter, with reduced seasonal sea ice playing an important role (Long et al., 2015; Perrie et al., 2015; Wang et al., 2018)

Section Summary

In summary, consistent significant trends in winds, storminess, and waves have not been found for most of the waters off Canada, in part due to limited data and strong effects of natural variability. Long-term data are very limited, tend to have very coarse spatial resolution, and do not cover nearshore areas. A slight northward shift of storm tracks, with decreased wind speed and lower wave heights off Atlantic Canada, has been observed and is projected to continue (*low confidence*). Off the Pacific coast, wave heights have been observed to increase in winter and decrease in summer, and these trends are projected to continue in future (*low confidence*). These confidence statements reflect the limited amount of published literature specific to winds and waves in the marine regions off Canada, the lack of high-quality historical data, and discrepancies in trends derived from different datasets.

Surface wave heights and the duration of the wave season in the Canadian Arctic have increased since 1970 and are projected to continue to increase over this century as sea ice declines (*high confidence*). Off Canada's east coast, areas that currently have seasonal sea ice are also anticipated to experience increased wave activity in the future, as seasonal ice duration decreases (*medium confidence*). This key message is based on limited wave time series in regions with seasonal ice coverage and a few published regional studies; however, there is strong evidence of past trends and future projections of declines in sea ice in both the Arctic and Atlantic Canada (see Chapter 5, Section 5.3). Increased wave activity resulting from sea ice decline is based on modelling results and expert judgment regarding the understanding of air–sea interaction processes.

7.5: Sea level

Key Message

Globally, sea level has risen, and is projected to continue to rise. The projected amount of global sea-level rise in the 21st century is many tens of centimetres and it may exceed one metre. However, relative sea level in different parts of Canada is projected to rise or fall, depending on local vertical land motion. Due to land subsidence, parts of Atlantic Canada are projected to experience relative sea-level change higher than the global average during the coming century (*high confidence*).

Key Message

Where relative sea level is projected to rise (most of the Atlantic and Pacific coasts and the Beaufort coast in the Arctic), the frequency and magnitude of extreme high water-level events will increase (*high confidence*). This will result in increased flooding, which is expected to lead to infrastructure and ecosystem damage as well as coastline erosion, putting communities at risk. Adaptation actions need to be tailored to local projections of relative sea-level change.

Key Message

Extreme high water-level events are expected to become larger and occur more often in areas where, and in seasons when, there is increased open water along Canada's Arctic and Atlantic coasts, as a result of declining sea ice cover, leading to increased wave action and larger storm surges (*high confidence*).

Global mean sea level is projected to rise by 28–98 cm during this century, and possibly more, due primarily to thermal expansion of the oceans and decreasing land ice (glaciers, ice caps, and ice sheets) (e.g., IPCC, 2013; Church et al., 2013). Recent publications raise the possibility of larger amounts of global sea-level rise by 2100, primarily due to enhanced delivery of Antarctic ice to the oceans (e.g., Ritz et al., 2015; Deconto and Pollard, 2016). Sea-level rise leads to increased coastal flooding and erosion, depending on the physical nature of the coastline. Thus, projections of sea-level change are important for forecasting risk to populations, for infrastructure planning and maintenance, and for habitat management (e.g., Nicholls et al., 2011).

Global mean sea-level change is commonly discussed in terms of “absolute” sea level, meaning that it is referenced to the centre of the Earth. At coastal locations, the sea-level change that is experienced relative to land is known as “relative” sea-level change; this can differ from absolute sea-level change because of geophysical processes that cause land to move upward (“uplift”) or downward (“subsidence”). Relative (local) sea-level projections for Canada's coasts (James et al., 2014, 2015; Lemmen et al., 2016) based on CMIP5 and other results (Church et al., 2013) are reviewed and updated in this section.

Projections of relative sea-level change are provided for a number of Representative Concentration Pathway (RCP) scenarios as well as an enhanced scenario. The low emission scenario (RCP2.6) represents a strong mitigation pathway requiring concerted global action (Moss et al., 2010). At present, atmospheric carbon dioxide concentrations are tracking above the low scenario (UNEP 2017), and it is advisable to consider the risks associated with higher emission scenarios in adaptation planning.

7.5.1: Historical sea level

Globally, for most of the 20th century (up to 1990), sea level rose at a mean rate slightly larger than 1 mm/year (average [90% uncertainty range]: 1.2 [1.0 to 1.4] mm per year [Hay et al., 2015]; 1.1 [0.5 to 1.7] mm per year [Dangendorf et al., 2017]). Recently, the rate of mean sea-level rise has increased, and the rate of global mean sea-level rise after 1993 is nearly three times as large (average [90% uncertainty range]: 3.0 [2.3 to 3.7] mm per year, 1993–2010 [Hay et al., 2015]; 3.1 [0.3 to 5.9] mm per year, 1993–2012 [Dangendorf et al., 2017]).

The long-term trends in relative sea level observed at tide gauges in Canada vary substantially from one location to another. Some of the variability is due to oceanographic factors affecting the absolute elevation of the sea surface, but a major determinant of relative sea-level change in Canada is vertical land motion. Land subsidence (sinking) increases relative sea-level, while land uplift does the opposite. Across much of Canada, land uplift or subsidence is mainly due to the delayed effects of the last continental glaciation (ice age), called glacial isostatic adjustment (GIA). GIA is still causing uplift of the North American continental crust in areas close to the centre of former ice sheets, such as Hudson Bay, and subsidence in regions that were on the edge of former ice sheets, such as the southern part of Atlantic Canada, as shown in Global Positioning System (GPS) data (see Figure 7.13). On the west coast, active tectonics, and, on the Fraser delta, sediment consolidation (Mazzotti et al., 2009), contribute to vertical land motion.

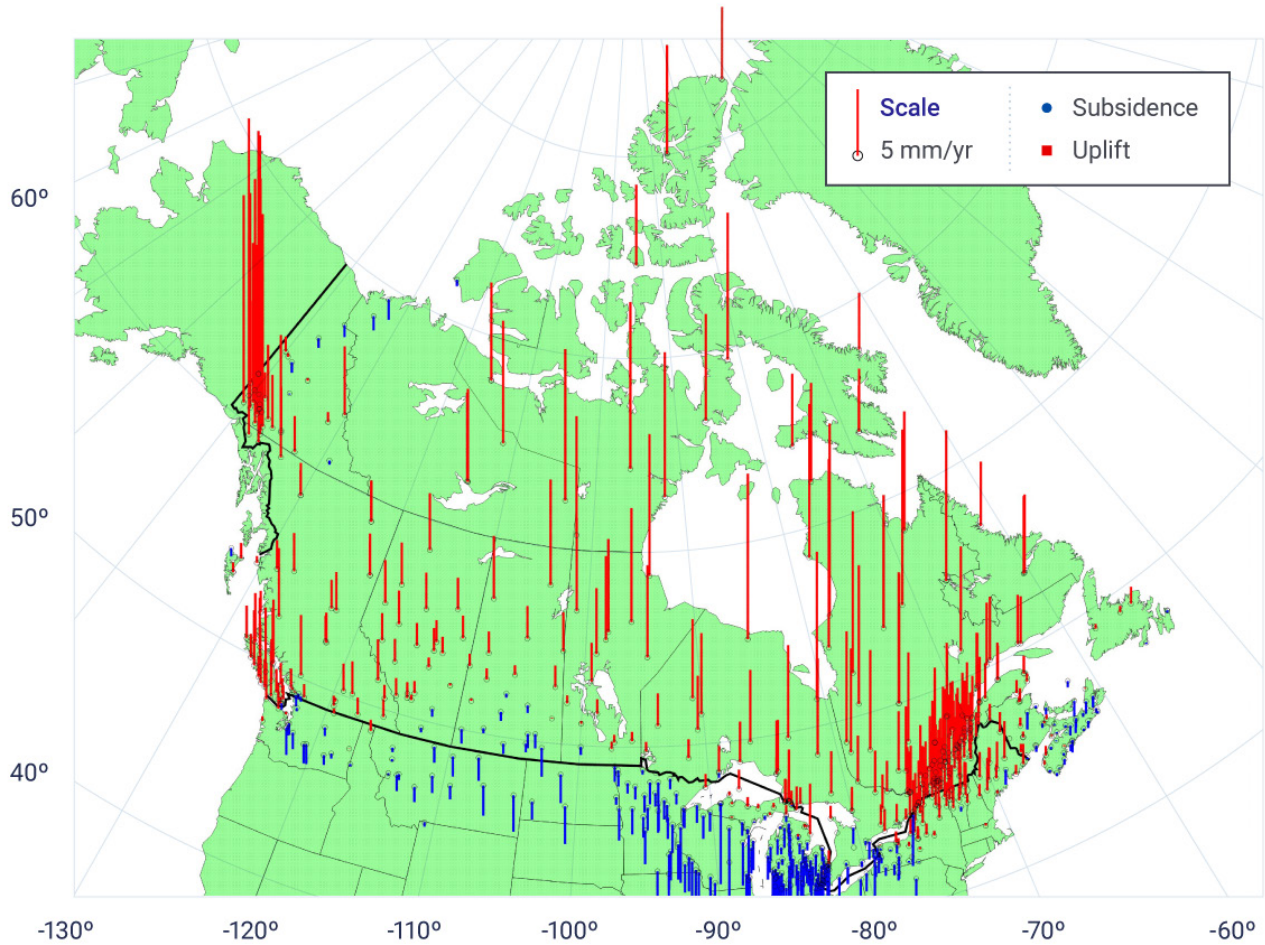


Figure 7.13: Crustal uplift and subsidence rates for the Canadian landmass

Figure caption: Rates of land uplift and subsidence determined from Global Positioning System (GPS)-derived data (in millimetres per year).

FIGURE SOURCE: CRAYMER AND ROBIN, 2016.

In the Atlantic region, vertical measured land motion ranges from uplift rates of about 1–4.5 mm per year for Quebec sites to subsidence of up to about 2 mm per year at some locations in Nova Scotia (see Figure 7.13). On the west coast of Canada, vertical motion rates vary from negligible values near Vancouver to uplift of almost 4 mm per year in the middle part of Vancouver Island, and smaller rates of uplift further north. The largest variation in vertical land motion is observed in the Arctic. Hudson Bay coastlines are rising at a rate of 10 mm per year or more. Significant portions of the Canadian Arctic Archipelago coastline are uplifting at a rate of a few millimetres per year from a combination of GIA and the response of Earth's crust to present-day changes in ice mass, whereas the Beaufort Sea coastline in the western Arctic is subsiding due to GIA at a rate of 1–2 mm per year.

The effects of vertical land motion are evident in tide gauge records (see Figure 7.14). Where the land is uplifting rapidly due to GIA, such as at Churchill, Manitoba (on Hudson Bay), sea level has been falling rapidly, at a rate of 9.3 mm per year. Where the land is sinking due to GIA, such as much of the Maritimes, southern Newfoundland, and along the Beaufort Sea coast of the Northwest Territories and Yukon, sea level is rising faster than the global average. At Halifax, sea level rose at a rate of about 3.3 mm per year during the 20th century.

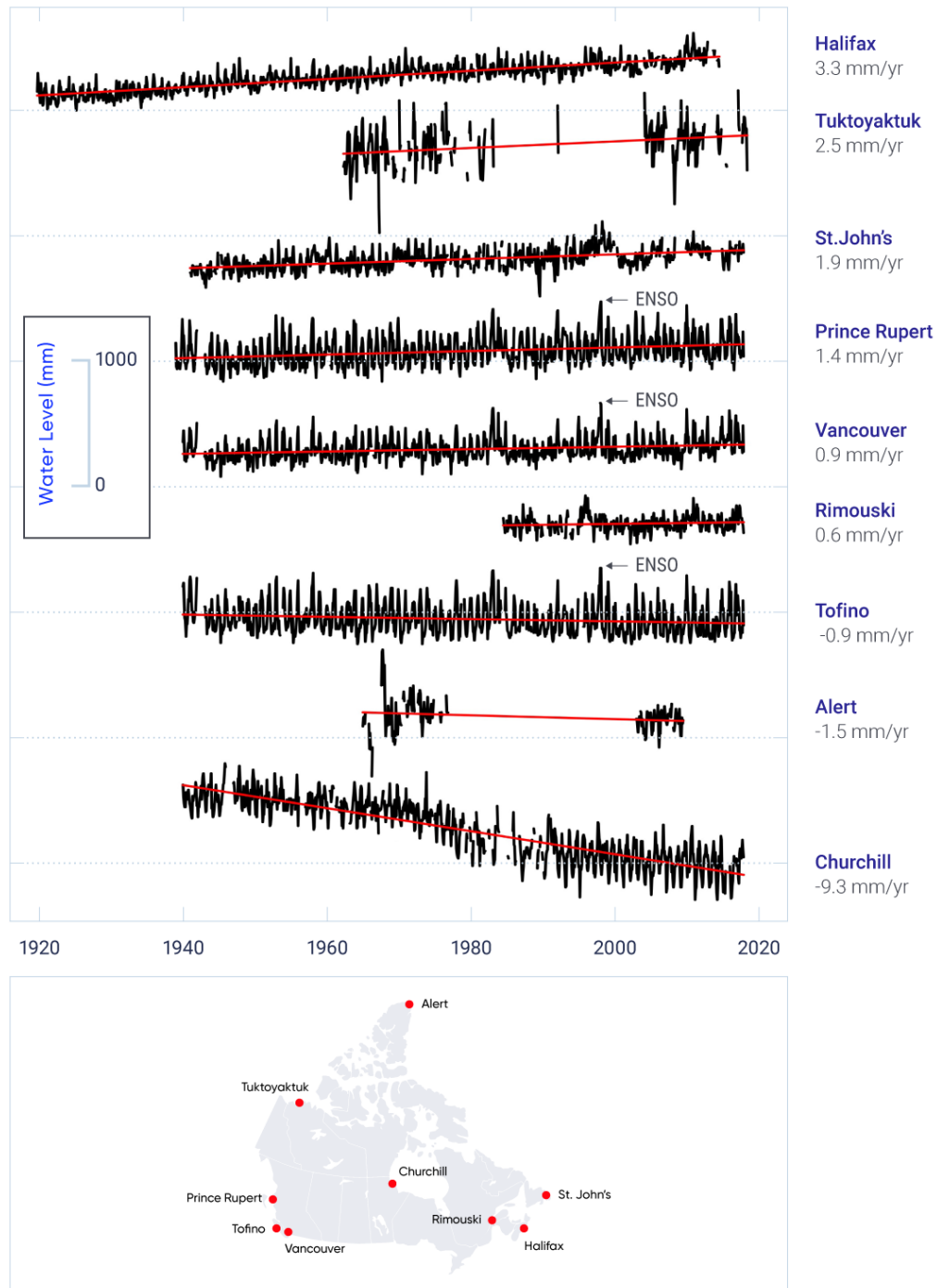


Figure 7.14: Long-term trends of relative sea-level change at representative sites across Canada

Figure caption: The water-level records (monthly values, with tides removed) of nine tide gauges distributed around Canada. The records show differing linear trends from one location to another, primarily indicating different amounts of vertical land motion arising from glacial isostatic adjustment and other factors. Superposed on this long-term change is substantial variability from year to year, indicating the changing nature of the oceans and the influence of climate cycles and other processes. For the west coast, the 1997/98 El Niño–Southern Oscillation event (ENSO, indicated by arrows) was a time of high water levels during the winter months. Individual tide gauge records are vertically offset for display purposes.

FIGURE SOURCE: TIDE GAUGE DATA OBTAINED FROM THE PERMANENT SERVICE FOR MEAN SEA LEVEL AT <[HTTP://WWW.PSMSL.ORG/DATA/OBTAINING](http://www.psmsl.org/data/obtaining)> AND ACCESSED 19 SEPTEMBER 2017.

7.5.2: Future projections

Projections of relative sea-level changes for coastal Canada, based on the CMIP5 model projections used in IPCC AR5 (Church et al., 2013), take into account projections of global sea-level change, vertical land motion, dynamic oceanographic changes, and redistribution of meltwater from glaciers, ice caps, and ice sheets in the oceans (James et al., 2014, 2015; Han et al., 2015b, 2015c; Zhai et al., 2015; Lemmen et al., 2016). The following gives a brief description of the factors contributing to sea-level change.

7.5.2.1: Global sea-level rise

Global (absolute) sea-level change results from a variety of sources: thermal expansion of warming ocean waters; addition of water from mountain glaciers, ice caps, and the Greenland and Antarctic ice sheets; and human activities that directly contribute to sea-level rise (i.e., groundwater depletion) and to sea-level fall (from water impoundment behind newly built dams).

Global (absolute) mean sea level is projected, in IPCC AR5, to rise by 28 to 98 cm by 2100, relative to 1986–2005 (Church et al., 2013; see Figure 7.15), depending on the emission scenario. But global mean sea-level rise could exceed 1 m by 2100 if additional contributions of water come from the marine-based sectors of the Antarctic Ice Sheet (Church et al., 2013). There is a potential for collapse of parts of the ice sheet that are in direct contact with warming ocean waters, through ice shelves extending out into the ocean. There is *medium confidence* that this additional contribution would not exceed several tenths of a metre of sea-level rise during the 21st century (Church et al., 2013). Most recent modelling findings are consistent with the IPCC AR5 assessment (Cornford et al., 2015; Golledge et al., 2015; Joughin et al., 2014; Levermann et al., 2014; Ritz et al., 2015). An exception is a modelling study (DeConto and Pollard, 2016) that projects up to a metre or more of sea-level rise from Antarctica alone for a high emission scenario (RCP8.5) by 2100. These larger amounts of global sea-level rise would have significant impacts on coastal populations.

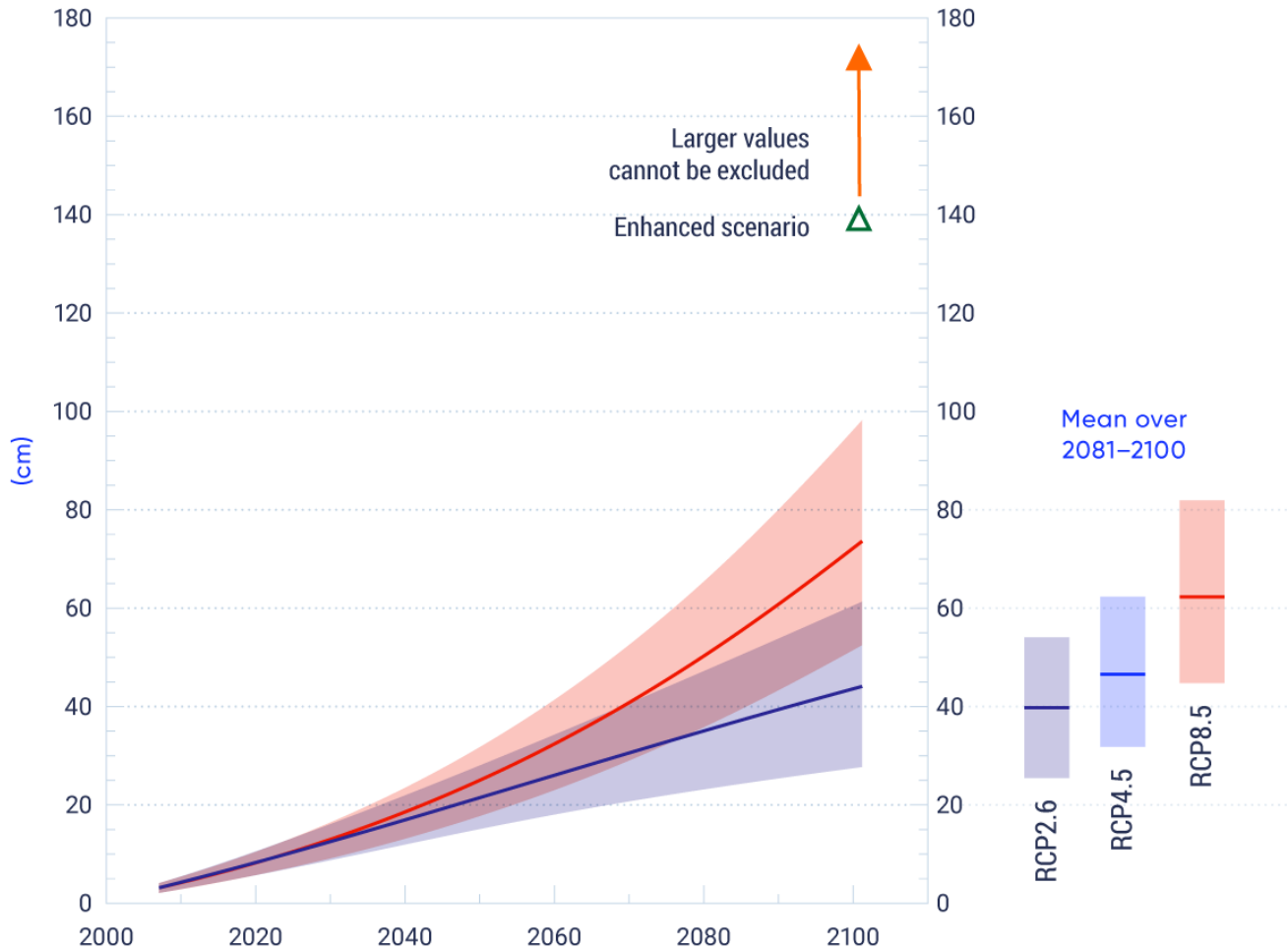


Figure 7.15: Projected global sea-level rise during the 21st century

Figure caption: Projections of global average (mean) sea-level rise relative to 1986–2005 for low (RCP2.6) and high (RCP8.5) emission scenarios from IPCC AR5 (Church et al., 2013). Also shown is an enhanced scenario reflecting greater amounts of ice discharged from Antarctica and contributing to global sea-level rise (see Table 7.1). The lines indicate the median projection, and the shading indicates the assessed range (5th–95th percentile, or 90% uncertainty range). The projected global mean sea-level rise over 2081–2100 (relative to 1986–2005) is given on the right for these scenarios and for a medium emission scenario (RCP4.5). Lines and shading are the same as in the main graph.

FIGURE SOURCE: FIGURE SPM.9, IPCC, 2013.

Global sea-level change scenarios used to generate relative sea-level projections across Canada are reported in Table 7.1 for low [RCP2.6], medium [RCP4.5], and high [RCP8.5] emission scenarios and an enhanced high scenario. The enhanced high scenario specifically evaluates the effect of more rapid drawdown of portions of the West Antarctic Ice Sheet on relative sea-level change in Canada. The enhanced scenario was created by augmenting the high emission scenario (RCP8.5), the scenario most likely to be associated with rapid ice-sheet discharge, by an additional 65 cm of sea-level rise²⁷ originating from West Antarctica. This scenario, with a total global sea-level rise of 139 cm by 2100, lies above most recent Antarctic modelling results and within the range of the results of the recent study of DeConto and Pollard (2016). It is a plausible extreme scenario, but even larger amounts of global sea-level rise cannot be ruled out.

Table 7.1: Projected global sea-level rise by 2100

Emission scenario	<i>Likely</i> global sea-level rise by 2100 (cm), median [90% uncertainty range] ¹
Low (RCP2.6)	44 [28 to 61]
Medium (RCP4.5)	53 [36 to 71]
High (RCP8.5)	74 [52 to 98]
Enhanced; RCP8.5 plus Antarctic Ice Sheet reduction ²	74 + 65 = 139

¹Relative to 1986–2005.

²Scenario is indicative, so percentile values (uncertainty range) are not provided.

TABLE SOURCE: TABLE 2, P. 50, ATKINSON ET AL., 2016

The potential impacts of extreme sea-level rise on human settlement, economic activity, and coastal ecosystems are substantial and would pose great challenges to adaptation (e.g., Parris et al., 2012; Mercer Clarke et al., 2016). It may be appropriate to consider even larger global sea-level rise scenarios, given the large uncertainties regarding the stability of the marine sectors of the Antarctic Ice Sheet. The US National Climate Assessment considers an “extreme” scenario of 2.5 m of global sea-level rise by 2100 that is intended to “test plans and policies against extreme cases with a low probability of occurrence but severe consequences if realized” (Sweet et al., 2017).

27 The value of 65 cm is derived from the average of four papers available to the IPCC AR5 (Church et al., 2013) indicating the additional amount of global sea-level rise that could be delivered by the Antarctic Ice Sheet by 2100 due to marine ice sheet instability (see James et al. [2014] for more information on the derivation of the scenario).

7.5.2.2: Vertical land motion

As discussed in Section 7.5.1, vertical land motion strongly influences changes in relative sea level (Figure 7.13). Vertical land motion due to GIA will continue at rates close to rates currently observed.

7.5.2.3: Other effects

Meltwater from glaciers, ice caps, and ice sheets is not distributed uniformly throughout the world's oceans (Farrell and Clark, 1976; Mitrovica et al., 2001, 2011), because the Earth's crust responds elastically to ice-mass changes and ocean water is subjected to reduced gravitational attraction of any nearby shrinking ice mass. These effects are incorporated into calculations of meltwater redistribution to determine relative sea-level change.

Global ocean currents are associated with spatial variations in "dynamic" sea surface topography of up to 1 m in amplitude (i.e., about 2 m from peak to trough). Changes to ocean currents can lead to changes in both absolute and relative sea level. Enhanced sea-level rise due to reductions in the Atlantic Meridional Overturning Circulation (see Section 7.1) projected in CMIP5 models is expected for northeastern coastal North America, including Atlantic Canada, in the coming century (Yin et al., 2010; Yin, 2012; Church et al., 2013).

7.5.2.4: Projections of relative sea-level change

Relative sea-level projections for coastal communities and other locations in Canada, incorporating the factors described above (see also Han et al., 2015b), show the effect of global sea-level rise as well as differences from one area to another due to vertical land motion (James et al., 2014; see Figure 7.16).²⁸ The projected sea-level changes generally differ from one area to another in a similar way to historical relative sea-level change measured at tide gauges (see Figure 7.14).

28 Regional sea level data from IPCC AR5 distributed in netCDF format by the Integrated Climate Data Center (ICDC), University of Hamburg, Hamburg, Germany, is available from <<http://icdc.cen.uni-hamburg.de/1/daten/ocean/ar5-slr.html>>. The modelled vertical crustal motion was removed from the data files and replaced with measured vertical land motion at GPS sites to generate the sea-level projections described here. See James et al. (2014) for more information on how the relative sea-level projections, including projections for the enhanced scenario, were generated.

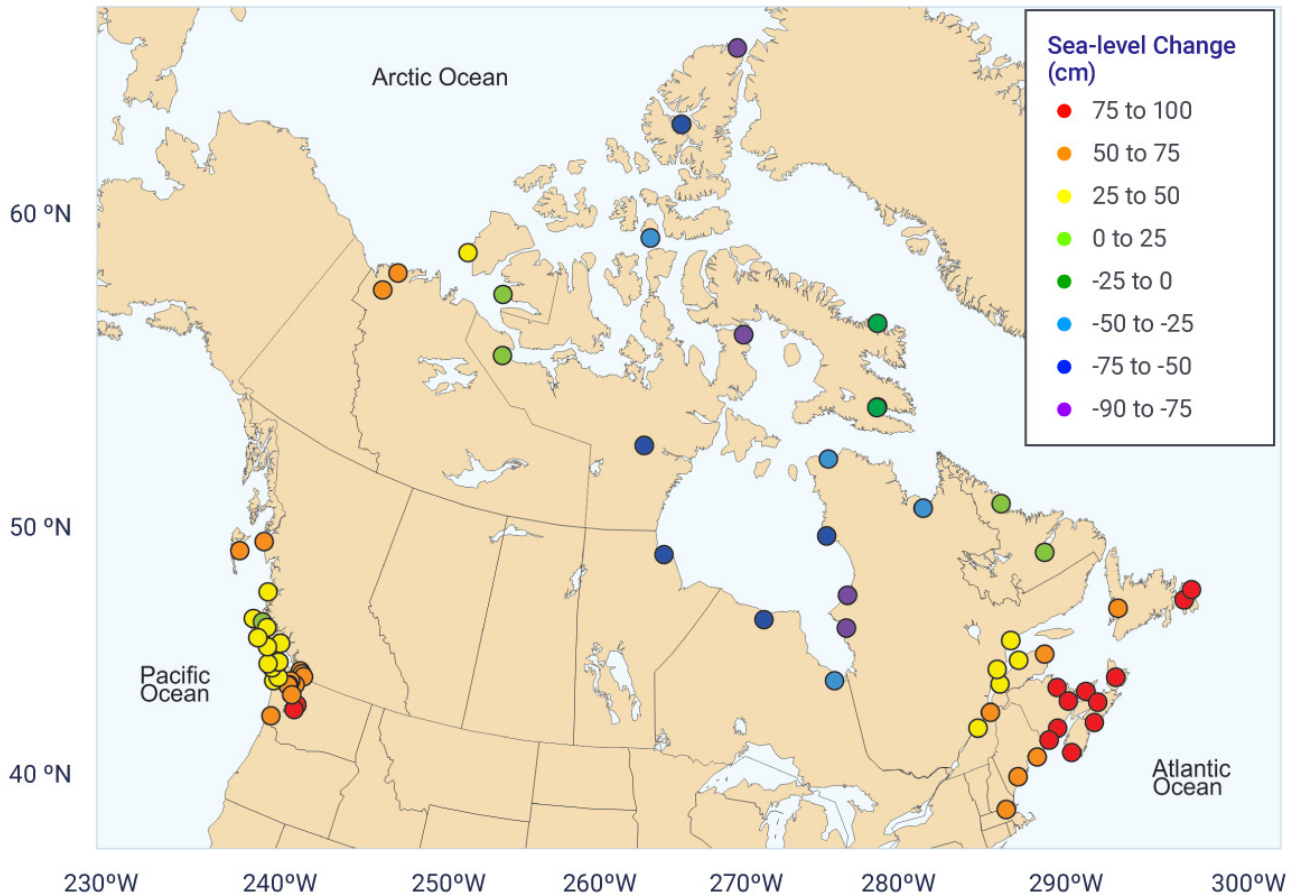


Figure 7.16: Projected relative sea-level change along Canadian coastlines at the end of the century

Figure caption: Projected relative sea-level changes shown at 2100 for the median of a high emission scenario (RCP8.5) at 69 coastal locations in Canada and the northern United States. Values range from a sea-level fall of 84 cm to a sea-level rise of 93 cm and are relative to the average conditions in the 1986–2005 period. For comparison, the projected median global sea-level change at 2100 for the high emission scenario is 74 cm.

FIGURE SOURCE: JAMES ET AL. (2014, 2015); LEMMEN ET AL (2016).

The largest projected sea-level rise, exceeding 75 cm for the median projection of the high emission scenario by 2100 (red dots on Figure 7.16), is projected where the land is currently sinking due to GIA in Atlantic Canada (see Figure 7.13). Other areas where the land is also sinking or uplifting at low rates due to GIA, with projected sea-level rise larger than 50 cm (orange dots on Figure 7.16), include the Beaufort Sea coastline,

parts of southern Newfoundland and Quebec, and the Fraser River lowland and northern British Columbia. Where the land is currently uplifting fastest, in Hudson Bay and the central Canadian Arctic Archipelago, sea level is projected to continue to fall by more than 50 cm by 2100 (dark blue and purple dots on Figure 7.16). In the high Arctic and eastern Arctic, the effects of present-day ice-mass changes (due to loss of Arctic glaciers and ice caps, and the Greenland Ice Sheet) contribute to reduced projected sea-level rise or small sea-level fall (see Section 7.5.2.3).

Figure 7.17 summarizes the sea-level projections for all scenarios for Halifax, Nova Scotia; Vancouver, British Columbia; Nain, Newfoundland and Labrador; and La Grande 1, Quebec. These locations span a range of vertical crustal motion, from sinking at about 1 mm per year (Halifax) to uplifting rapidly at 15 mm per year (La Grande 1). The enhanced high scenario (green triangle) is notable in providing projections of relative sea-level change exceeding 150 cm at Halifax by 2100 and only negligible sea-level fall at the fastest land-uplifting location of La Grande 1. In contrast, the low emission scenario (RCP2.6) anticipates about 50 cm of sea-level rise at Halifax and more than 100 cm of sea-level fall at La Grande 1. Further details on the regional variability of projected sea-level changes are presented in Lemmen et al. (2016; see Chapter 2 of that report for an overview, and regional Chapters 4, 5, and 6 of that report).

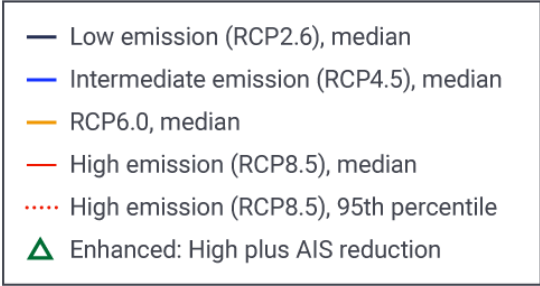


Figure 7.17: Projected relative sea-level change for representative coastal locations across Canada

Figure caption: Projected relative sea-level change based on global sea-level projections from Church et al. (2013), and vertical (V) crustal motion (uplift rate, given to nearest 0.5 mm per year) derived from Global Positioning System (GPS) observations indicated in each panel for (a) Halifax, (b) Vancouver, (c) Nain, and (d) La Grande 1 (James et al., 2014, 2015; Lemmen et al., 2016). Projections are given through the current century for low emission (RCP2.6), medium emission (RCP4.5), and high emission (RCP8.5) scenarios. The projected value by 2100 is also given for the enhanced scenario (RCP8.5 plus 65 cm reflecting Antarctic Ice Sheet (AIS) reduction; green triangle). Rectangles show the 90% uncertainty range (5th–95th percentile) of the average projection over the 2081–2100 period and also include the medium (RCP6.0) emission scenario; the dashed red line shows the 95th percentile value for the high emission scenario.

FIGURE SOURCE: JAMES ET AL. (2014, 2015), LEMMEN ET AL. (2016).

Global sea level will continue to rise for centuries beyond 2100, with rates dependent on future greenhouse gas emissions and the potential melting of the Greenland and West Antarctic ice sheets (Church et al., 2013; Atkinson et al., 2016). The general spatial patterns of projected relative sea-level change in Canada beyond 2100 are expected to be similar to those for the current century. Relative sea-level rise at rates above the global average is expected in areas where land is sinking, sea-level fall is expected to continue (but at reduced rates) in areas where land is uplifting relatively quickly, and there could be a change from falling to rising sea level in some areas.

7.5.3: Extreme water levels

Ocean-surface heights vary on timescales from seconds to hours to years, due to waves, tides, and atmospheric and ocean circulation. These fluctuations may arise from the large-scale modes of internal climate variability (ENSO, Pacific Decadal Oscillation, and North Atlantic Oscillation events; see Chapter 2, Box 2.5), seasonal warming and runoff, storms, and changes to ocean circulation. Extreme ENSO events can result in coastal sea-level changes of a few tens of centimetres (see Figure 7.14; see the high-water levels at the British Columbia sites at the end of 1997 and beginning of 1998). The ENSO cycle may intensify with global warming (Cai et al., 2014), and this could generate larger peak water levels during El Niño events on Canada's west coast. Together, these factors, superimposed on the tidal cycle, produce variability that causes peak water levels to vary substantially throughout the year, and from year to year.

One of the most serious consequences of sea-level rise is its effect on extreme high coastal water-level and flooding events. These events are typically associated with storm surges that coincide with high tides (see Box 7.5). Storm surges can have heights of 1 m or more above high tide levels (Bernier and Thompson, 2006; Han et al., 2012; Ma et al., 2015; Manson and Solomon, 2007; Thomson et al., 2008), with wave run-up further adding to the extent of flooding. Where relative sea level is projected to rise, extreme high water levels (combined tide and surge) are expected to be even higher and more frequent in the future.

Box 7.5: Storm surge flooding

Storm surges have produced extreme high water-level events on all three of Canada's coasts, causing flooding of infrastructure and habitat as well as erosion of coastlines (see photos). Storm surge flooding usually occurs during high tides, when large storms approach landfall (see Figure 7.18).



LEFT – Storm surge on the Sunshine Coast Highway (Highway 101) at Davis Bay, British Columbia, located on the mainland coast north of Vancouver, British Columbia, on February 6, 2006. Photo courtesy of B. Oakford.

RIGHT – Example of coastal erosion and roadway damage at Conrads Road on Queensland Beach, Nova Scotia, following the January 4, 2018, blizzard. (see <https://en.wikipedia.org/wiki/January_2018_North_American_blizzard>). Photo credit: Colleen Jones, CBC, January 5, 2018.

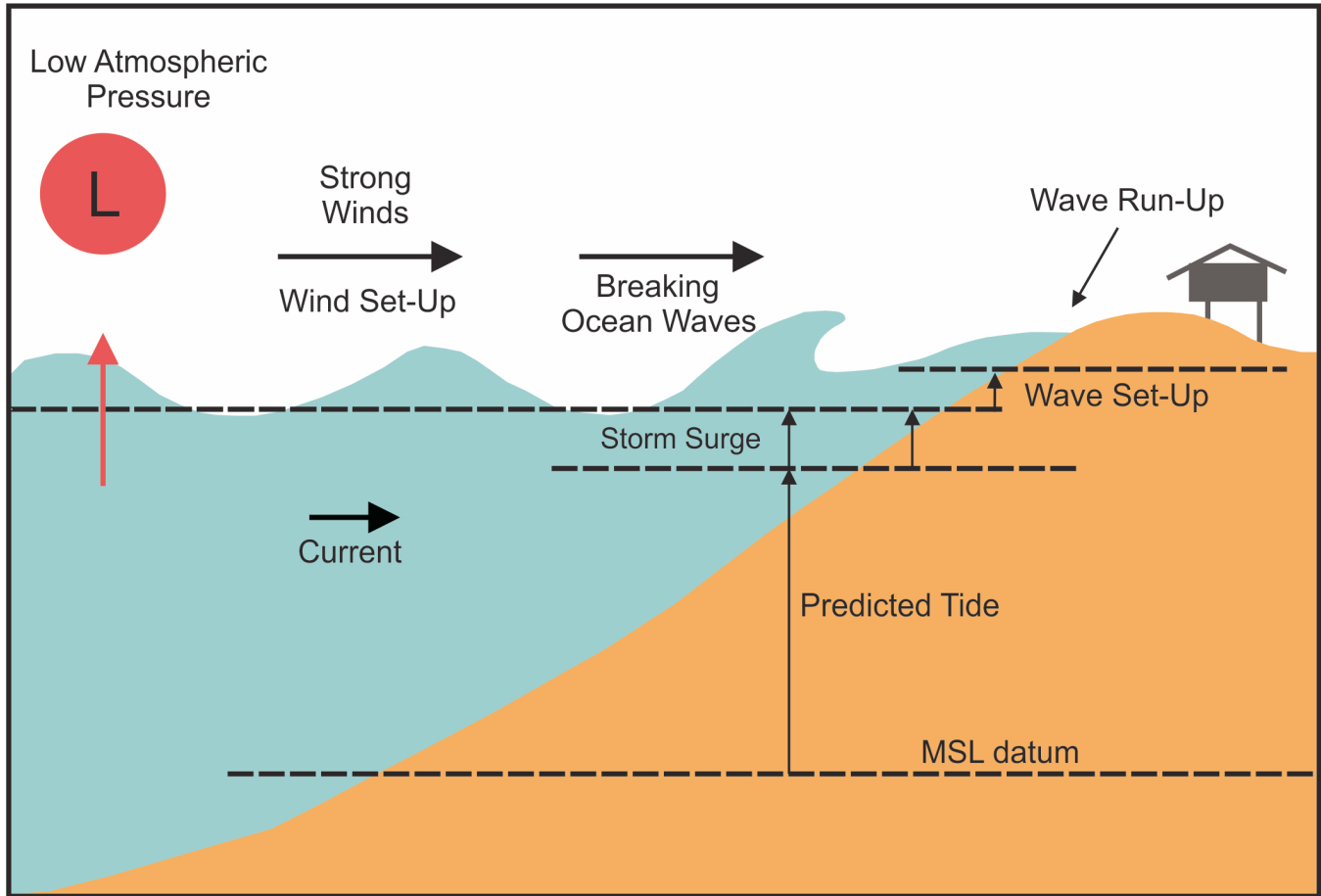


Figure 7.18: Factors contributing to storm surges

Figure caption: A storm surge results from an atmospheric low-pressure system and strong winds blowing onshore during large storms. Strong low-pressure systems raise the surface of the ocean due to their reduced atmospheric pressure. Winds that blow onshore cause water to flow toward the coastline, resulting in wind set-up (rise in water level from wind stresses on the surface of the water). As waves enter shallow coastal water and break, wave set-up (rise in water level due to breaking waves) further raises the water level. Waves rushing up a beach or structure generate additional wave run-up. All of these factors contribute to high water levels that are superimposed on the predicted tide. MSL datum = mean sea-level datum.

FIGURE SOURCE: ADAPTED FROM MULLAN ET AL., 2005.

Extreme high water-level events pose risks to communities, transportation networks, and ecosystems (Lemmen et al., 2016). Adaptation measures must be designed in light of regional projections of changes in relative sea level, sea ice, storminess, and other climate factors affecting coastal regions. Adaptation tools for coastal infrastructure planning for projected extreme water levels are being developed for application in Canada (e.g., Zhai et al., 2014, 2015).

The effect of sea-level rise on extreme water levels is illustrated for Halifax (see Figure 7.19). Sea-level has been rising at Halifax, and the number of water levels exceeding the 2.3 m flood level (red line in Figure 7.19) has increased through the 20th and early 21st century. The record shows that, for this particular flood level, 131 flooding events have occurred in the historical record (1901–2018), while for a 2.1 m flood level (aqua line) there have been 596 flooding events, which is more than four times as many. A 20 cm rise in mean sea level, which is projected to occur within two to three decades at Halifax for all emission scenarios (Figure 7.17), can therefore be anticipated to increase 2.3 m flooding events at this location by about the same factor of four. Generally, a projected rise in mean sea level is expected to increase the number of extreme water-level events at a given flood level as well as increase the largest flood height (Church et al., 2013). For example, large, impactful events, such as the water level reached once every 50 years at Halifax in the past, may occur as frequently as every two years by mid-century under the relative sea-level rise caused by a high emission scenario (Atkinson et al., 2016).

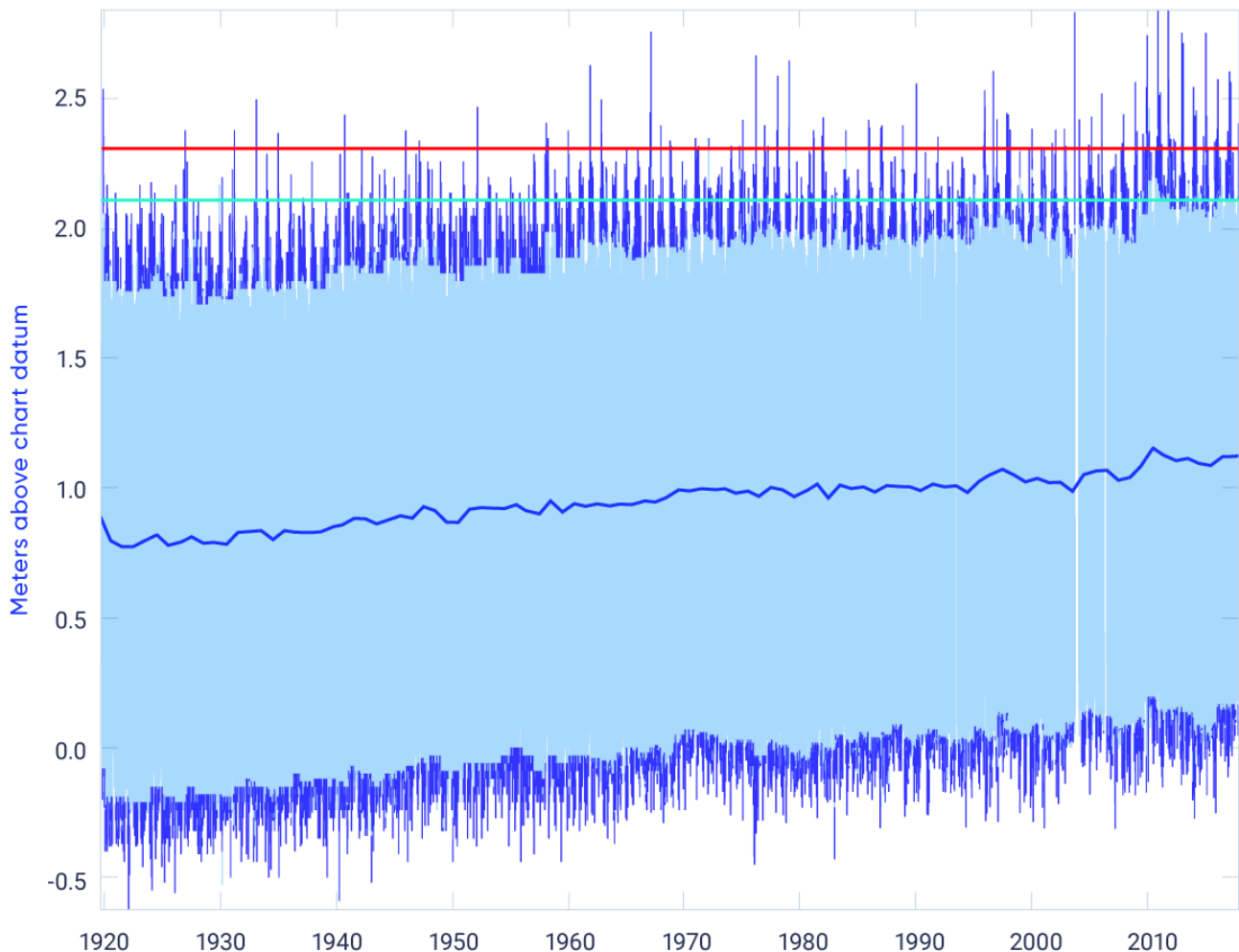


Figure 7.19: Halifax Harbour tide gauge record and extreme water levels

Figure caption: Hourly water levels recorded at Halifax Harbour for 1920 to 2018, with 5% extremes shown in dark blue and the 90% mid-range in light blue. Mean sea level (thick blue line) exhibits short-term variability su-

perposed on a long-term increase throughout the record duration. Flood levels at 2.3 m (red line) and 2.1 m (aqua line) show increasing numbers of extreme water-level events throughout the record duration, a consequence of the rise in mean sea level. The number of events at the lower 2.1 m flood level (596) is much higher than at the higher 2.3 m level (131).

FIGURE SOURCE: CANADIAN HYDROGRAPHIC SERVICE, FISHERIES AND OCEANS CANADA.

Increases in storm frequency or intensity would contribute to further increases in the occurrence of extreme high water-level events; however, projecting such increases is difficult because region-specific projections of storminess are not robust (Hartmann et al., 2013; see Section 7.4.1). While more thermal energy in a warmer atmosphere is projected to lead to increased storminess on a global scale, storminess may or may not increase in any given region, depending on storm-source regions and storm tracks. Projections of changes to wave height in the oceans surrounding Canada are also uncertain (see Section 7.4.2), but where winds and wind-driven waves increase, wave set-up and run-up (the maximum level waves reach) will also increase (see Box 7.5). Larger waves generally have greater erosive power and damage potential.

Reductions in sea ice cover (see Chapter 5, Section 5.3) also have important implications for wind-driven waves (see Section 7.4.2), storm surges, and extreme high water levels. Sea ice in the nearshore prevents waves from breaking directly onshore and reduces wave run-up (Forbes and Taylor, 1994; Allard et al., 1998). Ice further offshore reflects waves and reduces their height before they reach the shoreline (Wadhams et al., 1988; Squire, 2007). A greater amount of open water leads to larger waves, even if the winds are unchanged (e.g., Lintern et al., 2011). Increased winds over open water and higher waves, arising from reduced sea ice that would otherwise diminish storm surges, lead to higher extreme water levels. Thus, in areas where sea ice is projected to continue to diminish, such as Atlantic Canada in winter and spring (Han et al., 2015a) and the Arctic in summer and fall, there is the potential for increased extreme high water levels due to stronger storm surges and wave run-up.

Section Summary

In summary, global mean sea level has risen globally and is projected to continue to rise by many tens of centimetres, possibly exceeding a metre, by 2100. This is primarily attributable to ocean thermal expansion and water delivered to the oceans from diminishing glaciers and ice sheets. Across Canada, however, relative sea level is projected to rise or fall, depending on the amount of global sea-level rise and local vertical land motion. Due to post-glacial land subsidence, parts of Atlantic Canada are projected to experience relative sea-level change higher than the global average during the upcoming century (*high confidence*). This statement of confidence is based on a strong mechanistic understanding of processes controlling global and relative sea levels. Uncertainty remains about the magnitude of some sources of global sea-level, especially the projected amount of water delivered by the Antarctic Ice Sheet. All emission scenarios are projected to result in global mean sea-level rise, with the magnitude of change diverging among scenarios in the latter half of the 21st century. Vertical land motion measurements are consistent over broad spatial scales, which contribute to the confidence in the relative sea-level projections. Adaptation actions need to be tailored to local projections of relative sea-level change.

Where relative sea level is projected to rise (most of the Atlantic and Pacific coasts and the Beaufort coast in the Arctic), the frequency and magnitude of extreme high water-level events will increase (*high confidence*). This will result in increased flooding, which is expected to lead to infrastructure and ecosystem damage as well as coastline erosion, putting communities at risk. The statement of confidence is based on long-term measurements of coastal sea level and mechanistic understanding of the processes controlling extreme water-level events. Where relative sea level is projected to rise, extreme high water levels (combined tide and surge) will be even higher and more frequent in the future. As yet, projections of regional storm intensity and frequency are not robust, so their potential contribution to changes in extreme water-level events is uncertain.

Extreme high water-level events are expected to become larger and occur more often in areas where, and in seasons when, there is increased open water along Canada's Arctic and Atlantic coasts, as a result of declining sea ice cover, leading to increased wave action and larger storm surges (*high confidence*). The statement of confidence is based on a mechanistic understanding of the processes controlling extreme water-level events and expert judgment. This finding is supported by Chapter 5, which demonstrates significant declines in summer sea ice area observed across the Canadian Arctic, while winter sea ice area is decreasing in eastern Canada (e.g., Gulf of St. Lawrence). Sea ice is projected to continue to decline in the Canadian Arctic, and further reductions of seasonal sea ice are projected for eastern Canada (Chapter 5, Section 5.3.2).

7.6: Ocean chemistry

Key Message

Increasing acidity (decreasing pH) of the upper-ocean waters surrounding Canada has been observed, consistent with increased carbon dioxide uptake from the atmosphere (*high confidence*). This trend is expected to continue, with acidification occurring most rapidly in the Arctic Ocean (*high confidence*).

Key Message

Subsurface oxygen concentrations have decreased in the Northeast Pacific and Northwest Atlantic oceans off Canada (*high confidence*). Increased upper-ocean temperature and density stratification associated with anthropogenic climate change have contributed to this decrease (*medium confidence*). Low subsurface oxygen conditions will become more widespread and detrimental to marine life in future, as a result of continuing climate change (*medium confidence*).

Key Message

Nutrient supply to the ocean-surface layer has generally decreased in the North Pacific Ocean, consistent with increasing upper-ocean stratification (*medium confidence*). No consistent pattern of nutrient change has been observed for the Northwest Atlantic Ocean off Canada. There are no long-term nutrient data available for the Canadian Arctic.

While there are a broad range of ocean chemistry topics related to climate variability and change, this section focuses on ocean acidification, dissolved oxygen levels, and nutrients. Ocean acidification is strongly linked to uptake of CO₂ from the atmosphere and its sequestration in the ocean. Uptake and sequestration are strongly influenced by the physical processes within the ocean, including vertical mixing (upward and downward movement of water) and deep convection, which result in ocean ventilation (the injection of surface waters into the ocean interior and export away from their sources). Changes in oxygen concentrations in the ocean are linked to climate change through increasing upper-ocean temperature and density stratification, which also affect nutrient availability. Modification of ocean chemistry as a result of climate change has significant impacts on the marine ecosystem, and some changes could cause positive feedbacks, amplifying atmospheric CO₂ concentrations.

7.6.1: Ocean acidification

An increasing concentration of CO₂ in the atmosphere is not only contributing to greenhouse warming of the global climate system, it is also affecting the ocean carbon cycle (see Box 7.6) and changing the fundamental chemistry of the ocean. The ocean has taken up more than a quarter of the CO₂ produced by human activities, mainly from fossil fuel burning, since the start of the Industrial Era (Sabine et al., 2004; Rhein et al., 2013; Jewett and Romanou, 2017). While this uptake has helped to slow the rate of anthropogenic climate change, it has also resulted in increased acidity of the ocean (referred to as ocean acidification).

Box 7.6: Ocean carbon cycle

The ocean carbon cycle (see Figure 7.20) is composed of processes that exchange carbon within the ocean as well as among the atmosphere, coasts and seafloor. Part of the ocean carbon cycle transforms carbon between non-living and living matter, represented by the marine biota. The ocean contains about 50 times as much inorganic carbon (carbon not associated with living things, such as CO₂) as is found in the atmosphere (Raven and Falkowski, 1999). As the concentration of anthropogenic CO₂ increases in the atmosphere, the oceans absorb more of it, and one of the results of this is increasing acidity of seawater.

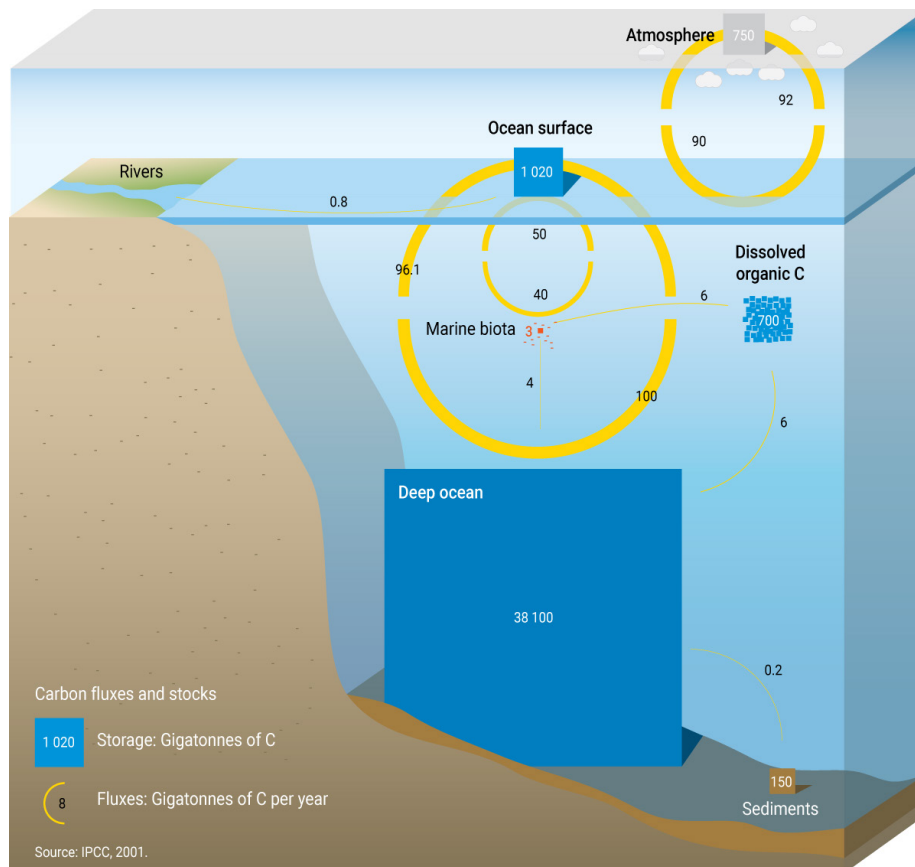


Figure 7.20: Ocean carbon cycle

Figure caption: The ocean carbon cycle is represented by fluxes (yellow arrows), which include the annual net transfer of carbon dioxide (CO₂) between the atmosphere and ocean surface. The carbon inventory (rectangles) indicates that the deep ocean is a large storage reservoir and important to the Earth's climate system.

FIGURE SOURCE: RICCARDO PRAVETTONI, UNEP/GRID-ARENDA, <[HTTP://WWW.GRIDA.NO/RESOURCES/7555](http://www.grida.no/resources/7555)>

Acidification takes place after CO₂ gas from the atmosphere is transferred into the surface of the ocean, where it dissolves and forms carbonic acid. This process causes a decrease in pH and in the concentration of carbonate ions (CO₃²⁻), a building block of organisms with calcium carbonate () shells and skeletons. This process also results in a decrease in the ocean's saturation state (a measure of the thermodynamic potential for a particular mineral to form in a solid state or to be dissolved) with respect to CaCO₃. These changes can result in seawater having a corrosive effect on shells and skeletons, dissolving them, inhibiting their growth, or causing them to require more energy to grow. Ocean acidification may have many other harmful effects for marine organisms, including increased mortality of young, changes in behaviour, food web changes, reduction in suitable habitat for some species, and increases in harmful algal blooms (Haigh et al., 2015).

Observations confirm that pH, a measure of acidity, has a present-day range of 7.95–8.35 (mean 8.11) in the surface waters of the open ocean (Feely et al., 2009). Globally, the pH²⁹ of ocean surface waters has decreased by 0.1 since the beginning of the Industrial Era (Rhein et al., 2013). The largest reduction has occurred in the northern North Atlantic, and the smallest reduction, in the subtropical South Pacific (Sabine et al., 2004). Oceans have not experienced pH changes this rapid for at least the last 66 million years and possibly the last 300 million years (Hönisch et al., 2012). Some acidification events in Earth's history have led to some species becoming extinct and others recovering slowly (Hönisch et al., 2012). This raises serious concerns about the resilience of marine ecosystems to increasing atmospheric CO₂.

Nearshore and coastal waters are affected by the same processes as open-ocean waters and are additionally affected by freshwater inputs from rivers, glacial meltwater, and sea ice melt that decrease the capacity of coastal waters to buffer CO₂, making them more vulnerable to acidification (Ianson et al., 2016; Moore-Maley et al., 2016; Azetsu-Scott et al., 2014). Another factor in some coastal areas is nutrient inputs from human and industrial activities via rivers, and other runoff, which increase primary production in coastal waters. In turn, various forms of planktonic organisms and their decay products are consumed by bacteria that contribute to local ocean acidification and reduced oxygen concentrations (see Section 7.6.2) through bacterial respiration, which produces CO₂.

29 Because the pH scale is logarithmic, a change of one pH unit corresponds to a 10-fold change in hydrogen ion concentration.

Each of Canada's marine regions (Pacific, Arctic, and Atlantic) has distinct factors that affect the degree of ocean acidification, and these regions are interconnected through ocean circulation patterns (see Section 7.1). Levels of dissolved carbon in the Northeast Pacific are naturally high due to the global ocean's meridional overturning circulation patterns (Feely et al. 2008). In this region, water below the winter mixed layer has been travelling through the ocean interior for years to decades (out of contact with the atmosphere), accumulating additional organic matter from sinking biological production that decomposes to nutrients and CO₂ (Feely et al., 2004). Summer upwelling there brings this nutrient- and CO₂-rich water to the surface and causes intermittent periods of exceptionally low pH (7.6) at ocean depths above 100 m (Ianson et al., 2003, 2009; Haigh et al., 2015). These processes make for a system with considerable variability over time and space. The key issue for ocean acidification in this region is that the upwelled waters will have increasingly more CO₂ and lower pH in the future (Feely et al., 2008).

The Canadian Arctic Archipelago (Chierici and Fransson, 2009) and Canada Basin of the Arctic Ocean (Yamamoto-Kawai et al., 2009) are the first ocean regions off Canada to show low saturation state; that is, corrosive surface waters. The observed increase in acidity resulting from global CO₂ emissions has been augmented in the Arctic Ocean by rapid increases in freshwater input from accelerated ice melt and increased river input, which has reduced the CaCO₃ saturation state. In addition, in cold Arctic waters, CaCO₃ shells are even more soluble, making shelled organisms especially vulnerable to the effects of acidification. Rapid changes are projected to continue for the Arctic Ocean surrounding Canada, and this region is expected to be the first to experience undersaturation of surface waters (Feely et al., 2009).

In the central Labrador Sea, deep convection during wintertime transports anthropogenic CO₂ as deep as 2300 m (Azetsu-Scott et al., 2010). Annual sampling of the Labrador Sea since 1996 has shown a steady decline of pH (of 0.029 per decade) in a layer 150–500 m below the ocean surface, which is ventilated every year by vertical mixing during winter (see Figure 7.21). Further south, the pH of the bottom waters in the Lower St. Lawrence Estuary (in the Gulf of St. Lawrence; see Figure 7.4), have decreased by 0.2 to 0.3 since the 1930s (rate of 0.021 per decade; see Figure 7.21), which is greater than can be attributed solely to the uptake of anthropogenic CO₂ (Mucci et al., 2011). The pH decrease has been accompanied by a decline in the CaCO₃ saturation state.

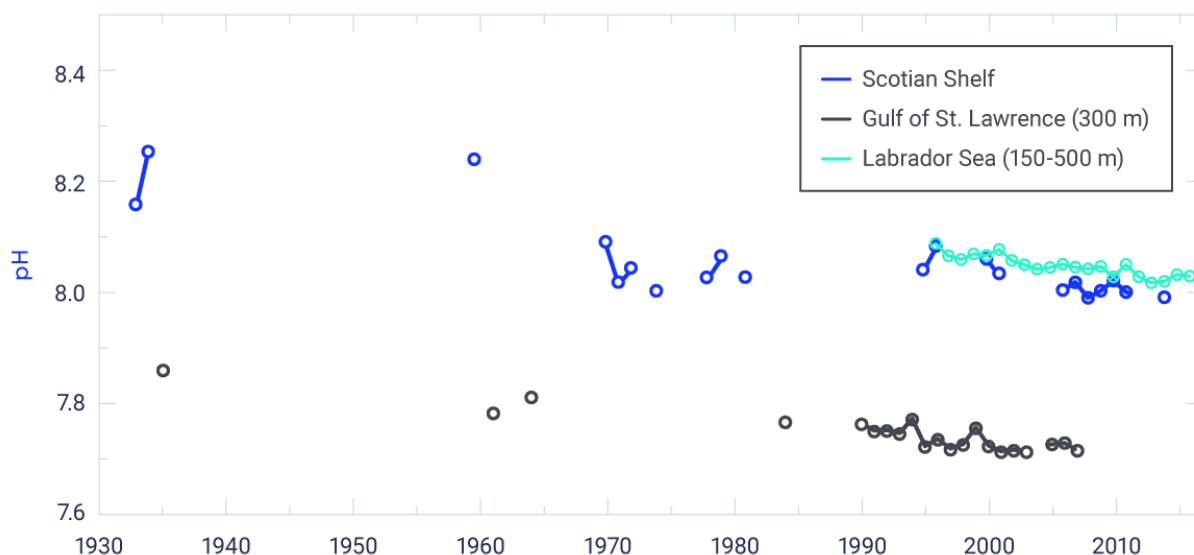


Figure 7.21: pH time series for the waters off Atlantic Canada

Figure caption: pH (depth-averaged) time series over the Scotian Shelf (1933–2014, declining trend of 0.026 per decade; 1995–2014, declining trend of 0.044 per decade); near-bottom estimate (approximately 300 m) of pH in the Gulf of St. Lawrence (1935–2007, declining trend of 0.021 per decade; 1990–2007, declining trend of 0.026 per decade); and pH from the central Labrador Sea in the annually ventilated layer (150–300 m) (1996–2016, declining trend of 0.029 per decade). Estimates of pH before the 1990s have a high level of uncertainty because of the quality of the measurements and should be interpreted with caution. Therefore, no assessment of statistical confidence is provided for the observed trends.

FIGURE SOURCE: DATA FOR THE SCOTIAN SHELF AND LABRADOR SEA FROM THE DFO MONITORING DATABASE. DATA FOR THE GULF OF ST. LAWRENCE DERIVED FROM MUCCI ET AL. (2011).

Waters of the Scotian Shelf have the lowest saturation states of the entire New England/Nova Scotia region (except for episodic nearshore events), due to cold water temperatures in the winter (Gledhill et al., 2015). As in other regions, the saturation state is modified by seasonal biological processes (Shadwick et al., 2011). A summary of the long-term trend from upper-ocean samples collected over the Scotian Shelf and Slope indicates that pH is declining at a rate of 0.026 per decade; however, there is a high level of uncertainty in data collected before the 1990s (before the establishment of international protocols and standards) (Dickson et al., 2007). For the 1995–2014 period, the trend on the Scotian Shelf is pH declining at a rate of 0.044 per decade (see Figure 7.21).

The circulation patterns connecting Canada's ocean regions are also important for understanding differences in acidity (see Section 7.1). The naturally high levels of dissolved carbon in waters of the Northeast Pacific result in water entering the western Arctic Ocean (through Bering Strait) with low saturation states. The saturation state of the Pacific Ocean water is further decreased through the addition of sea ice meltwater and river input, as well as respiration of organic matter, in the Arctic Ocean. Outflow through the Canadian Arctic Archipelago in the eastern Arctic can be traced along western Baffin Bay and Davis Strait to the northwestern Atlantic Ocean. While local mixing in the northern Labrador Sea modifies this Arctic outflow, low saturation states can still be identified over the Labrador/Newfoundland Shelf (Azestu-Scott et al., 2010; Yamamoto-Kawai, 2009). Within the Atlantic region, seasonally varying outflows from the Gulf of St. Lawrence and the Labrador/Newfoundland Shelf regions bring fresher and cooler water onto the Scotian Shelf and the Gulf of Maine, which seasonally increases ocean acidification.

Under all future emission scenarios for the 21st century, global ocean acidification is expected to continue to increase in the upper ocean, with pH expected to stabilize and remain above saturation under the low emission scenario (RCP2.6) (Bopp et al., 2013). The high emission scenario (RCP8.5) would result in the Arctic surface waters becoming undersaturated by mid-century.

7.6.2: Dissolved oxygen and hypoxia

The oxygen content of the ocean is important because it constrains biological productivity, biodiversity, and biogeochemical cycles (Breitburg et al., 2018). Waters with low levels of oxygen are described as “hypoxic” (dissolved oxygen concentration of less than $61 \mu\text{mol/kg}$) while those that are devoid of oxygen are described as “anoxic” (zero dissolved oxygen concentration). As the global ocean warms under anthropogenic climate change, a loss of dissolved oxygen is expected (Gruber, 2011). The reason for this in the open ocean is twofold. First, as ocean temperature increases, the solubility of oxygen decreases, and therefore the ocean’s capacity to hold oxygen decreases. Second, increased upper-ocean stratification caused by warming and freshening of surface water (see Box 7.4) tends to reduce vertical mixing and ventilation of the main thermocline (an ocean layer where water temperature changes rapidly with depth), resulting in a decreased supply of oxygen from its surface to subsurface waters. The global ocean has lost about 2% of its oxygen since 1960, with large variations among ocean basins and at various depths (Schmidtko et al., 2017). For the upper ocean, over the 1958–2015 period, trends in oxygen concentration and ocean heat content are highly correlated (Ito et al., 2017).

There is only qualitative agreement between computer models and observations with regard to the amount of oxygen loss in the surface of the ocean. CMIP5 models consistently simulate a decline in the global dissolved oxygen inventory equal to only about half of the observation-based estimates and also predict different spatial patterns of oxygen change (Schmidtko et al., 2017, Bopp et al., 2013; Oschlies et al., 2008). This suggests that mechanisms of oxygen decline are not well represented in current ocean models.

Human activities can play a major role in changes in dissolved oxygen in coastal waters, which can be exacerbated by the impacts of anthropogenic climate change. Coastal and inland waters are particularly vulnerable to decreasing oxygen trends (Gilbert et al., 2010), because eutrophication (an increase in the rate of supply of organic matter to an ecosystem) is generally higher in these areas and because physical flushing may not be adequate to disperse oxygen-depleted waters. It can be difficult to separate the effects of nutrient enrichment and climate change in assessing changes in oxygen concentration in these waters. A general overview of oxygen status and trends in Canadian marine waters is provided in Figure 7.22.

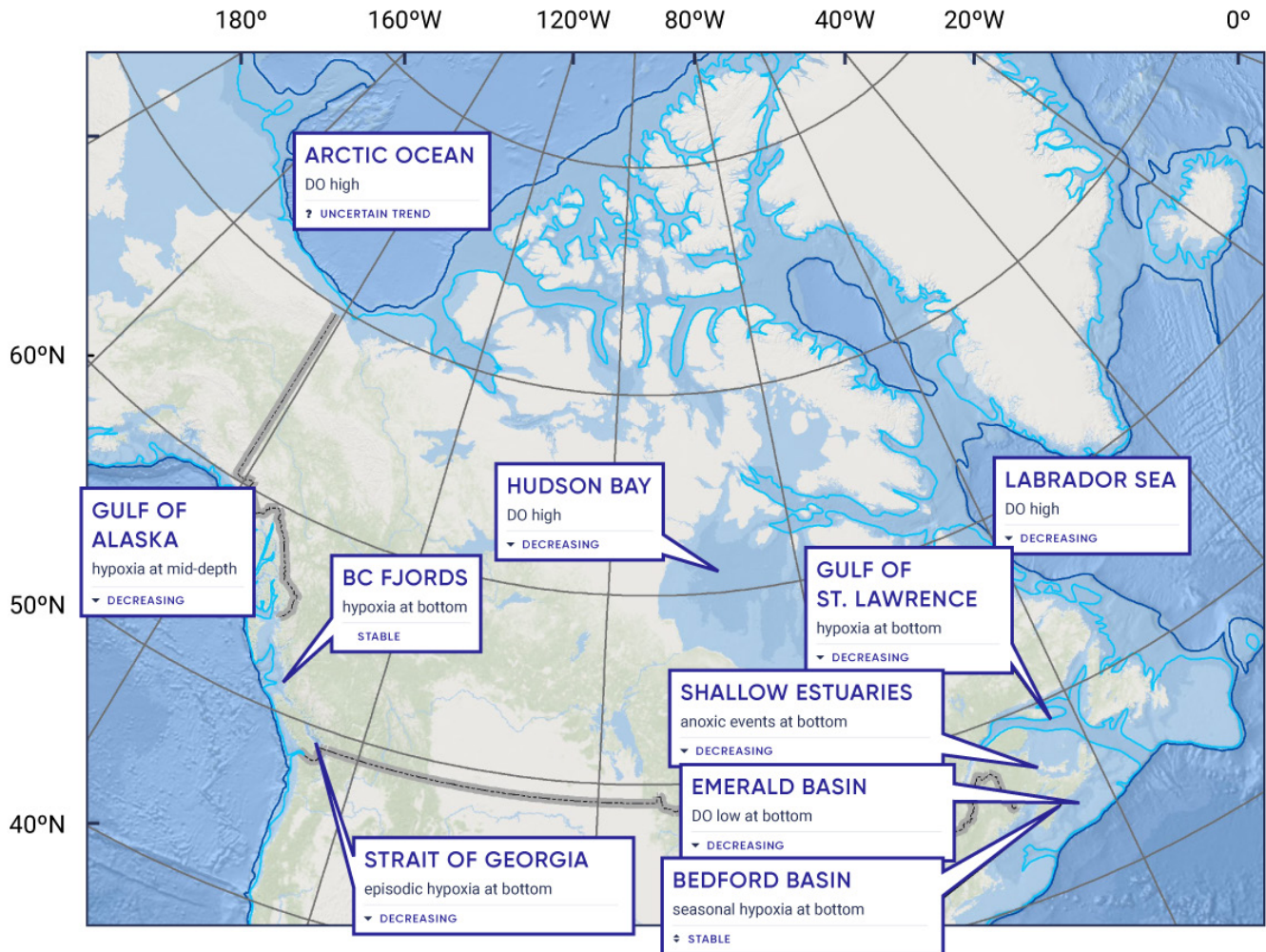


Figure 7.22: Oxygen status and trends in marine regions surrounding Canada

Figure caption: Dissolved oxygen (DO) status and trend in various regions. Most of the trends are based on short time series, which could be strongly influenced by natural (e.g., decadal) variability. However, long-term time series do exist for the Northeast Pacific (Station P) and in the Gulf of St. Lawrence, and these show statistically significant declining trends in DO. The 200 m and 1000 m depth contours are indicated by the light and dark blue lines.

FIGURE SOURCE: DATA FROM DFO MONITORING PROGRAMS (GALBRAITH ET AL., 2017; YASHAYAEV ET AL., 2014; CHANDLER ET AL., 2017).

Observations off both Pacific and Atlantic coasts of Canada indicate a general decline in the concentration of dissolved oxygen in subsurface (150–400 m) waters below the more continually ventilated surface layer (see Figure 7.23). In the Lower St. Lawrence Estuary, the oxygen decrease has been attributed mainly to an increased inflow of oxygen-poor waters from the North Atlantic’s subtropical gyre (see Box 7.2) entering the mouth of the Laurentian Channel at depth (Gilbert et al., 2005). However, excess nutrient loading from human activity likely plays a role as well (Hudon et al., 2017). The time series from the Labrador Sea indicates a rate of oxygen decline similar to that of the St. Lawrence Estuary, but the record extends back only to 1990 (Yashayaev et al., 2014). While some estuaries in Prince Edward Island, New Brunswick, and Nova Scotia occasionally become hypoxic (Price et al. 2017; Burt et al. 2013), the role of ocean-climate change remains unclear.

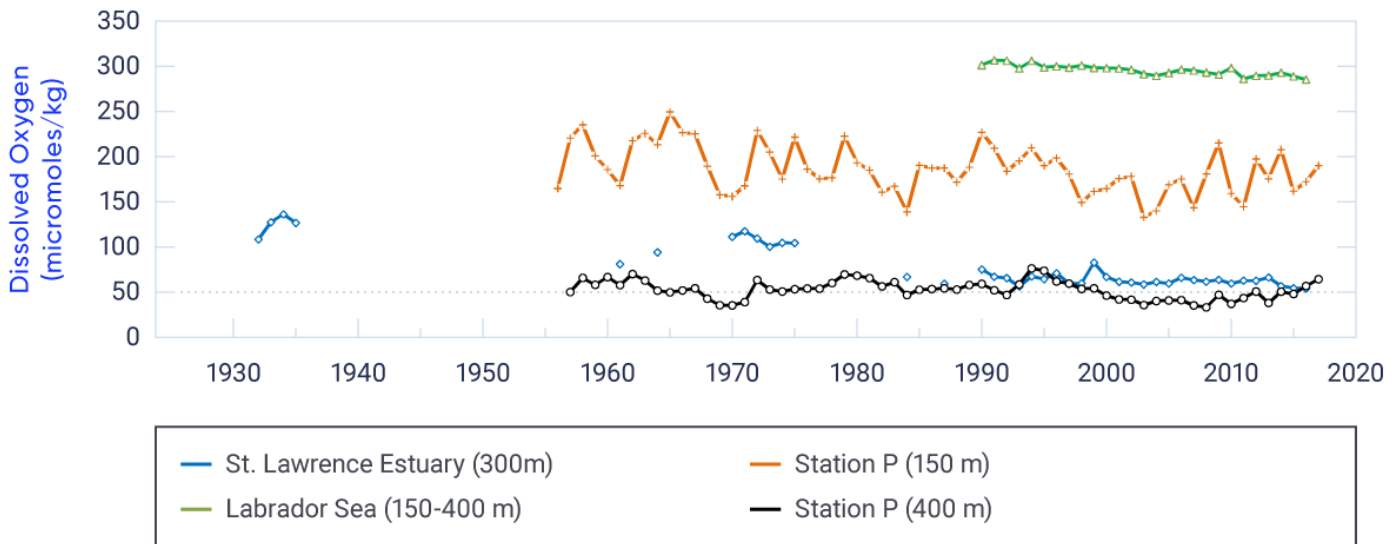


Figure 7.23: Annual mean dissolved oxygen for Northwest Atlantic and Northeast Pacific Ocean

Figure caption: Dissolved oxygen concentration at 300 m depth in the Lower St. Lawrence Estuary (1932–2016, declining trend of 0.89 $\mu\text{mol/kg}$ per decade, significant at 1% level [there is only a 1% possibility that such changes are due to chance]); depth-averaged dissolved oxygen concentration in the Labrador Sea (150–400 m, 1990–2011, declining trend of 0.75 $\mu\text{mol/kg}$ per decade, significant at 1% level); Station P dissolved oxygen concentration at 150 m depth (1956–2017, declining trend 0.61 $\mu\text{mol/kg}$ per decade, significant at 1% level) and at 400 m depth (1957–2017, declining trend 0.19 $\mu\text{mol/kg}$ per decade, significant at 1% level).

FIGURE SOURCE: DATA FROM DFO MONITORING PROGRAMS (GALBRAITH ET AL., 2017; YASHAYAEV ET AL., 2014; CHANDLER ET AL., 2017).

Hypoxia and anoxia have occurred naturally for thousands of years in some inland fjords on the British Columbia coast (Zaikova et al. 2010). Measurements at Station P dating back to 1956 indicate that ocean oxygen concentrations in the offshore Northeast Pacific have been declining for several decades (Whitney et al. 2007; Crawford and Peña, 2016; see Figure 7.23). A combination of physical and biological drivers are likely responsible for the observed changes in oxygen concentration at Station P; however, the oxygen variability in the lower ventilated thermocline is a useful tracer of physical climate change (Deutsch et al., 2006). In contrast to the long-term dissolved oxygen decline at Station P, the subsurface waters adjacent to the continental slope of British Columbia demonstrate no clear trend from the 1950s to present (Crawford and Peña, 2016). This highlights that natural decadal variability in the Northeast Pacific Ocean needs to be considered in assessing long-term changes in dissolved oxygen in this region.

Long-term observations in the Arctic are limited, and dissolved oxygen trends are thus uncertain. The Arctic Ocean has shown little evidence of hypoxia and, in fact, primary production within the so-called subsurface temperature maximum (the layer where temperature is highest) raises oxygen levels in the underlying pycnocline (an ocean layer where water density increases rapidly with depth) to levels of supersaturation (Carmack et al., 2010).

Global models project that the total amount of dissolved oxygen loss (averaged over 200-600 m) will be a few percent by the end of the 21st century (Bopp et al., 2013). However, differences in the spatial patterns of dissolved oxygen among models limit confidence in regional projections. Subsurface oxygen concentrations off Canada's Atlantic and Pacific coasts are expected to continue to decline with increasing CO₂ and heat in the atmosphere and with increasing upper-ocean stratification in most areas (Collins et al., 2013).

7.6.3: Ocean nutrients

Nutrients, the fundamental building blocks of life, are necessary to fuel the algal biomass (e.g., phytoplankton) that sustains marine food webs and the ocean's production of harvestable resources. Algae growth relies on inputs of inorganic nitrogen, phosphorus, silicon, and other nutrients into the sunlit layer near the surface where photosynthesis takes place. These nutrient inputs reach this layer through vertical mixing and transport such as upwelling. Nitrogen is the primary growth-limiting nutrient in the oceans surrounding Canada and is affected by microbial processes that can result in a gain (nitrogen fixation) or loss (e.g., denitrification, nitrous oxide emission). These microbial processes are sensitive to the availability of dissolved oxygen (Gruber, 2011; see Section 7.6.2) and the level of ocean acidification (Das and Mangwani, 2015; see Section 7.6.1).

Climate changes, such as surface warming and decreasing surface salinity, affect nutrients by increasing vertical stratification in the oceans surrounding Canada (see Box 7.4). This increased stratification reduces the nutrient supply transported from deep waters to the surface layer. Such a reduction is important because it can result in chronically low nutrient concentrations in the sunlit layer during the biologically productive spring-to-fall stratification season. While long-term changes in nutrient concentrations can be an indicator of climate change and variability, there are additional factors in the coastal ocean resulting from human activities (e.g., agricultural runoff) that affect local trends.

Nutrient variations in the North Pacific Ocean reflect influences of the Pacific Decadal Oscillation and North Pacific Gyre Oscillation (Di Lorenzo et al., 2009; see Chapter 2, Box 2.5). When the transient effects of these modes of climate variability are removed from the time series of upper-ocean nutrients available in the North Pacific (at less than 20 m depth), decreasing trends over the period 1961–2012 are evident for phosphate and silicate, while concentrations of nitrate remained stable (Yasunaka et al., 2016). This pattern is consistent with reduced vertical mixing as a result of increasing stratification and, for nitrate, a compensating nitrogen input via atmospheric deposition to the ocean (Duce et al., 2008; Kim et al., 2014). It is important to note that the linear trends in nutrient concentrations are only robust when averaged over the entire North Pacific Ocean, and regional trends are not statistically significant.

In the Northwest Atlantic Ocean adjacent to Canada, no consistent pattern of long-term trends in nutrient concentrations has been observed that could be attributed to climate change (Pepin et al., 2013). While the eastern Labrador Sea and central Scotian Shelf show significant long-term declines in nitrate, silicate, and phosphate since the 1960s (Yeats et al., 2010; Pepin et al., 2013; Hátún et al., 2017), trends in the western Labrador Sea have shown increased silicate concentrations coupled with notable declines in nitrate and, to a lesser extent, phosphate. The opposite pattern has been observed in most parts of the Gulf of Maine and Bay of Fundy (Pepin et al., 2013). Most parts of the Gulf of St. Lawrence have had notable increases in nutrient concentrations since the early 1970s, but trends in this area are affected by inputs from human activities (see Section 7.6.2). Other areas of the ocean around Atlantic Canada generally have had weak trends that were variable among nutrients.

In the Arctic, there are no long-term records of nutrient concentrations. However, the surface ocean circulation patterns around Canada (see Section 7.1) result in a nutrient connectivity of the Pacific, Arctic, and Atlantic Oceans (Woodgate et al., 2012; Tremblay et al., 2015, 2018), and this may help future research to understand changes in nutrient inventory in the Arctic. There is some evidence that declining sea ice on the Canadian Beaufort Shelf (see Chapter 5, Section 5.3) has led to episodic increases in upward nutrient supply and biological production (Tremblay et al., 2011). A decline in the nutrient concentration in the central Beaufort Sea has been observed (Li et al., 2009) and modelled (Vancoppenolle et al., 2013), but evidence of long-term freshening or increased stratification is limited (Peralta-Ferriz and Woodgate, 2015).

Section Summary

In summary, the available long-term time series of key chemical properties in the oceans surrounding Canada indicate trends that are consistent with global analyses. The increases observed in ocean acidification have been directly linked to human emissions of CO₂ and their subsequent transfer from the atmosphere to the upper ocean. Under all future emission scenarios, global ocean acidity is expected to continue to increase in the upper ocean, with pH stabilizing by 2100 only under a low emission scenario (RCP2.6). A high emission scenario (RCP8.5) would result in the Arctic surface waters becoming undersaturated by mid-century. Overall, **high confidence** has been assigned to the key message concerning ocean acidification because of the strong mechanistic understanding of the physical and chemical processes controlling these changes.

Deoxygenation of the subsurface oceans surrounding Canada is evident from high-quality time series over the last five decades in the Northeast Pacific (Station P) and Gulf of St. Lawrence. These trends are consistent with the expectations that surface warming, and in some cases freshening, will increase ocean stratification and thereby reduce vertical mixing and ventilation of the ocean interior. This conclusion has **high confidence** because of the consistency and quality of the oxygen time series in Canadian waters. In some high-population coastal areas, oxygen depletion is also affected by nutrients from runoff (e.g., agricultural activities). Deoxygenation of the global ocean is expected to continue; however, regional differences in model projections limit us to **medium confidence** in the expectation that these trends will continue in the subsurface oceans surrounding Canada.

The supply of nutrients to the upper ocean, where photosynthesis takes place, may also be affected by increased stratification as a result of climate change. Nutrient supply to the ocean-surface layer has generally decreased in the North Pacific Ocean, consistent with increasing upper-ocean stratification (**medium confidence**). No consistent pattern of nutrient change has been observed for the Northwest Atlantic Ocean off Canada. There are no long-term nutrient data available for the Canadian Arctic. The confidence statement in this finding reflects limited data availability, lack of statistical significance of regional trends, and, in some cases, differing trends in a region.

References

Allard, M., Michaud, Y., Ruz, M.H. and Héquette, A. (1998): Ice foot, freeze-thaw of sediments, and platform erosion in a subarctic microtidal environment, Manitousuk Strait, northern Quebec, Canada; *Canadian Journal of Earth Sciences*, v. 35, p. 965–979.

Atkinson, D.E., Forbes, D.L. and James, T.S. (2016): Dynamic coasts in a changing climate; in *Canada's Marine Coasts in a Changing Climate*, (ed.) D.S. Lemmen, F.J. Warren, T.S. James and C.S.L. Mercer Clarke; Government of Canada, Ottawa, Ontario, p. 27–68.

Azetsu-Scott, K., Clarke, A., Falkner, K., Hamilton, J., Jones, E.P., Lee, C., Petrie, B., Prinsenberg, S., Starr M. and Yeats, P. (2010): Calcium carbonate saturation states in the waters of the Canadian Arctic Archipelago and the Labrador Sea; *Journal of Geophysical Research*, v. 115, C11021. doi:10.1029/2009JC005917

Azetsu-Scott, K., Starr, M., Mei, Z.-P. and Granskog, M. (2014): Low calcium carbonate saturation state in an Arctic inland sea having large and varying fluvial inputs: The Hudson Bay system; *Journal of Geophysical Research: Oceans*, v. 119, p. 6210–6220. doi:10.1002/2014JC009948

Bernier, N.B. and Thompson, K.R. (2006): Predicting the frequency of storm surges and extreme sea levels in the northwest Atlantic; *Journal of Geophysical Research: Oceans*, v. 111, C10009. doi:10.1029/2005JC003168

Bopp, L., Resplandy, L., Orr, J.C., Doney, S.C., Dunne, J.P., Gehlen, M., Halloran, P., Heinze, C., Ilyina, T., Séférian, R., Tjiputra, J. and Vichi, M. (2013): Multiple stressors of ocean ecosystems in the 21st century: projections with CMIP5 models; *Biogeosciences*, v. 10, p. 6225–6245, doi:10.5194/bg-10-6225-2013

Breitburg, D., Levin, L.A., Oschlies, A., Grégoire, M., Chavez, F.P., Conley, D.J., Garçon, V., Gilbert, D., Gutiérrez, D., Isensee, K., Jacinto, G.S., Limburg, K.E., Montes, I., Naqvi, S.W.A., Pitcher, G.C., Rabalais, N.N., Roman, M.R., Rose, K.A., Seibel, B.A., Telszewski, M., Yasuhara, M., and Zhang, J. (2018): Declining oxygen in the global ocean and coastal waters; *Science*, v. 359. doi: 10.1126/science.aam7240

Bromirski, P.D., and Cayan, D.R. (2015): Wave power variability and trends across the North Atlantic influenced by decadal climate patterns; *Journal of Geophysical Research: Oceans*, v. 120, p. 3419–3443. doi:10.1002/2014JC010440

Burt, W.J., Thomas, H., Fennel, K., and Horne, E. (2013): Sediment-water column fluxes of carbon, oxygen and nutrients in Bedford Basin, Nova Scotia, inferred from 224Ra measurements; *Biogeosciences*, v. 10, p. 53–66. doi:10.5194/bg-10-53-2013

Cai, W., Borlace, S., Lengaigne, M., Rensch, P., Collins, M., Vecchi, G., Timmermann, A., Santoso, A., McPhanden, M.J., Wu, L., England, M.H., Wang, G., Guilyardi, E. and Jin, F. (2014): Increasing frequency of extreme El Niño events due to greenhouse warming; *Nature Climate Change*, v. 4, p. 111–116. doi:10.1038/NCLIMATE2100



Carmack, E.C., McLaughlin, F.A., Vagle, S., Melling, H., and Williams, W.J. (2010): Structures and property distributions in the three oceans surrounding Canada in 2007: a basis for a long-term ocean climate monitoring strategy; *Atmosphere-Ocean*, v. 48, p. 211–224.

Casas-Prat, M., Wang, X.L. and Swart, N. (2018): CMIP5-based global wave climate projections including the entire Arctic Ocean; *Ocean Modelling*, v. 123, p. 66–85. doi:10.1016/j.ocemod.2017.12.003

Chandler, P.C., King, S.A., and Boldt, J. (eds.) (2017): State of the physical, biological and selected fishery resources of Pacific Canadian marine ecosystems in 2016; Canadian Technical Report of Fisheries and Aquatic Science 3225, 243 p.

Cheng, L., Trenberth, K.E., Fasullo, J., Boyer, T., Abraham, J. and Zhu, J. (2017): Improved estimates of ocean heat content from 1960 to 2015; *Science Advances*, v. 3. doi:10.1126/sciadv.1601545

Chierici, M. and Fransson, A. (2009): Calcium carbonate saturation in the surface water of the Arctic Ocean: Undersaturation in freshwater influenced shelves; *Biogeosciences*, v. 6, p. 2421–2432. <<http://www.biogeosciences.net/6/2421/2009/>>.

Christian, J.R. and Foreman, M.G.G. (eds.) (2013): Climate trends and projections for the Pacific Large Aquatic Basin; Canadian Technical Report of Fisheries and Aquatic Science 3032, 113 p.

Christian, J.R. and Holmes, J. (2016): Changes in albacore tuna habitat in the northeast Pacific Ocean under anthropogenic warming; *Fisheries Oceanography*, v. 25, p. 544–554. doi:10.1111/fog.12171

Church, J.A., Clark, P.U., Cazenave, A., Gregory, J.M., Jevrejeva, S., Levermann, A., Merrifield, M.A., Milne, G.A., Nerem, R.S., Nunn, P.D., Payne, A.J., Pfeffer, W.T., Stammer, D. and Unnikrishnan, A.S. (2013): Sea level change; in *Climate Change 2013: The Physical Science Basis; Contribution of Working Group I to the Fifth Assessment Report of the Intergovernmental Panel on Climate Change (IPCC)*, (ed.) T.F. Stocker, D. Qin, G.-K. Plattner, M. Tignor, S.K. Allen, J. Boschung, A. Nauels, Y. Xia, V. Bex and P.M. Midgley; Cambridge University Press, Cambridge, United Kingdom and New York, NY, USA, p. 1137–1216, <https://www.ipcc.ch/site/assets/uploads/2018/02/WG1AR5_Chapter13_FINAL.pdf>.

Colbourne, E., Holden, J., Snook, S., Han, G., Lewis, S., Senciall, D., Bailey, W., Higdon, J. and Chen, N. (2017): Physical oceanographic conditions on the Newfoundland and Labrador Shelf during 2016; Fisheries and Oceans Canada, Canadian Science Advisory Secretariat, Research Document 079, 50 p.

Collins, M., Knutti, R., Arblaster, J., Dufresne, J.-L., Fichet, T., Friedlingstein, P., Wehner, M. (2013): Long-term climate change: Projections, commitments and irreversibility; in *Climate change 2013: The physical science basis; Contribution of Working Group I to the Fifth Assessment Report of the Intergovernmental Panel on Climate Change*, (ed.) T. F. Stocker, D. Qin, G.-K. Plattner, M. Tignor, S. K. Allen, J. Boschung, A. Nauels, Y. Xia, V. Bex and P. M. Midgley; Cambridge University Press, Cambridge, United Kingdom and New York, NY, USA, p. 1029–1136.



Cornford, S.L., Martin, D.F., Payne, A.J., Ng, E.G., Le Brocq, A.M., Gladstone, R.M., Edwards, T.L., Shannon, S.R., Agosta, C., van den Broeke, M.R., Hellmer, H.H., Krinner, G., Ligtenberg, S.R.M., Timmermann, R. and Vaughan, D.G. (2015): Century-scale simulations of the response of the West Antarctic Ice Sheet to a warming climate; *The Cryosphere*, v. 9, p. 1579–1600. doi:10.5194/tcd-9-1887-2015

Crawford, W. R., and Peña, M. A. (2016): Decadal trends in oxygen concentration in subsurface waters of the Northeast Pacific Ocean; *Atmosphere-Ocean*, v. 54, p. 171–192.

Crawford, W.R., Galbraith, J. and Bolingbroke, N. (2007): Line P ocean temperature and salinity, 1956–2005; *Progress in Oceanography*, v. 75, p. 161–178.

Craymer, M. and Robin, C. (2016): A national crustal velocity model for Canada; US National Geodetic Survey Brown Bag Lecture, Silver Spring, Maryland, 18 p. <https://mcraymer.github.io/geodesy/pubs/crustalmotion_ngs2016.pdf>.

Dangendorf, S., Marcos, M., Wöppelmann, G., Conrad, C.P., Frederikse, T. and Rive, R. (2017): Reassessment of 20th century global mean sea level rise; *Proceedings of the National Academy of Science*, v. 114, p. 5946–5951. doi:10.1073/pnas.1616007114

Das, S. and Mangwani, N. (2015): Ocean acidification and marine microorganisms: responses and consequences; *Oceanologia*, v. 57, p. 349–361. doi:10.1016/j.oceano.2015.07.003.

DeConto, R.M. and Pollard, D. (2016): Contribution of Antarctica to past and future sea-level rise; *Nature*, v. 531, p. 591–597. doi:10.1038/nature17145

Delworth, T. and Zeng, F. (2016): The impact of the North Atlantic Oscillation on climate through its influence on the Atlantic Meridional Overturning Circulation; *Journal of Climate*, v. 29, p. 941–962. doi:10.1175/JCLI-D-15-0396.1

Deutsch, C., Emerson, S. and Thompson, L. (2006): Physical-biological interactions in North Pacific oxygen variability; *Journal of Geophysical Research*, v. 111. doi:10.1029/2005JC003179

Dickson, A.G., Sabine, C.L. and Christian, J.R. (eds.) (2007): Guide to best practices for ocean CO₂ measurement; PICES Special Publication 3, IOC-CP Report 8, North Pacific Marine Science Organization, Sidney, British Columbia, 191 p.

Di Lorenzo, E., Fiechter, J., Schneider, N., Bracco, A., Miller, J., Franks, P.J.S., Bograd S.J., Moore, A.M., Thomas, A.C., Crawford, W., A. Peña, A. and Hermann, A.J. (2009): Nutrient and salinity decadal variations in the central and eastern North Pacific; *Geophysical Research Letter*, v. 36. doi:10.1029/2009GL038261

Drijfhout, S., van Oldenborgh, G. J., and Cimadoribus, A. (2012): Is a decline of AMOC causing the warming hole above the North Atlantic in observed and modeled warming patterns?; *Journal of Climate*, v. 25, p. 8373–8379. doi:10.1175/JCLI-D-12-00490.1



Duce, R.A., LaRoche, J., Altieri, K., Arrigo, K.R., Baker, A.R., Capone, D.G., Cornell, S., Dentener, F., Galloway, J., Ganeshram, R.S., Geider, R.J., Jickells, T., Kuypers, M.M., Langlois, R., Liss, P.S., Liu, S.M., Middelburg, J.J., Moore, C.M., Nickovic, S., Oschlies, A., Pedersen, T., Prospero, J., Schlitzer, R., Seitzinger, S., Sorensen, L.L., Uematsu, M., Ulloa, O., Voss, M., Ward, B. and Zamora, L. (2008): Impacts of atmospheric anthropogenic nitrogen on the open ocean; *Science*, v. 320, p. 893–897.

Durack, P.J. and Wijffels, S.E. (2010): Fifty-year trends in global ocean salinities and their relationship to broad-scale warming; *Journal of Climate*, v. 23, p. 4342–4362.

Durack, P. J., Wijffels, S. E., and Matear, R. J. (2012): Ocean salinities reveal strong global water cycle intensification during 1950 to 2000. *Science*, v. 336, 455–458. doi:10.1126/science.1212222

Erikson, L.H., Hegermiller, C.A., Barnard, P.L., Ruggiero, P. and van Ormondt, M. (2015): Projected wave conditions in the Eastern North Pacific under the influence of two CMIP5 climate scenarios; *Ocean Modelling*, v. 96, p. 171–185. doi: 10.1016/j.ocemod.2015.07.004

Farrell, W.E. and Clark, J.A. (1976): On postglacial sea level; *Geophysical Journal International*, v. 46, p. 647–667.

Feely, R.A., Doney, S. C., and Cooley, S. R. (2009): Ocean acidification: Present conditions and future changes in a high-CO₂ world. *Oceanography*, v. 22, p. 36–47. doi: 10.5670/oceanog.2009.95

Feely, R.A., Sabine, C.L., Hernandez-Ayon, J.M., Ianson, D. and Hales, B. (2008): Evidence for upwelling of corrosive “acidified” water onto the continental shelf; *Science*, v. 320, p. 1490–1492.

Feely, R.A., Sabine, C.L., Lee, K., Berelson, W., Kleypas J., Fabry, V.K. and Millero, F.J. (2004): Impact of anthropogenic CO₂ on the CaCO₃ system in the oceans; *Science*, v. 305, p. 362–366. doi: 10.1126/science.1097329

Forbes, D.L. and Taylor, R.B. (1994): Ice in the shore zone and the geomorphology of cold coasts. *Progress in Physical Geography*, v. 18, p. 59–89. doi: 10.1177/030913339401800104

Francis, O.P., Planteleev, G.G. and Atkinson, V.E. (2011): Ocean wave conditions in the Chukchi Sea from satellite and in situ observations; *Geophysical Research Letters*, v. 38. doi:10.1029/2011GL049839

Freeland, H.J. (2013): Evidence of change in the winter mixed layer in the Northeast Pacific Ocean: a problem revisited; *Atmosphere-Ocean*, v. 51, p. 126–133. doi: 10.1080/07055900.2012.754330

Galbraith, P.S. and Larouche, P. (2013): Trends and variability in eastern Canada sea-surface temperatures; in *Aspects of climate change in the Northwest Atlantic off Canada*, (ed.) J.W. Loder, G. Han, P.S. Galbraith, J. Chassé and A. van der Baaren; Canadian Technical Report of Fisheries and Aquatic Sciences 3045, p. 1–18.

Galbraith, P.S., Chassé, J., Caverhill, C., Nicot, P., Gilbert, D., Pettigrew, B., Lefaiivre, D., Brickman, D., Devine, L. and Lafleur, C. (2017): Physical oceanographic conditions in the Gulf of St. Lawrence in 2016; DFO Canadian Science Advisory Secretariat, Research Document 044, 91 p.



Galbraith, P.S., Larouche, P., Chasse, J. and Petrie, B. (2012): Sea-surface temperature in relation to air temperature in the Gulf of St. Lawrence: interdecadal variability and long term trends; *Deep Sea Research Part II: Topical Studies in Oceanography*, v. 77–80, p. 10–20, doi:10.1016/j.dsr2.2012.04.001

Gemmrich, J., Thomas, B., and Bouchard, R. (2011): Observational changes and trends in northeast Pacific wave records. *Geophysical Research Letters*, v. 38, L22601. doi: 10.1029/2011GL049518

Gilbert, D., Rabalais, N.N., Díaz, R.J. and Zhang, J. (2010): Evidence for greater oxygen decline rates in the coastal ocean than in the open ocean; *Biogeosciences*, v. 7, p. 2283–2296.

Gilbert, D., Sundby, B., Gobeil, C., Mucci, A. and Tremblay, G.-H. (2005): A seventy-two year record of diminishing deep-water oxygen levels in the St. Lawrence estuary: The northwest Atlantic connection; *Limnology and Oceanography*, v. 50, p. 1654–1666.

Gledhill, D.K., White, M.M., Salisbury, J., Thomas, H., Mlsna, I., Liebman, M., Mook, B., Gear, J., Candelmo, A.C., Chambers, R.C., Gobler, C.J., Hunt, C.W., King, A.L., Price, N.N., Signorini, S.R., Stancioff, E., Stymiest, C., Wahle, R.A., Waller, J.D., Rebeck, N.D., Wang, Z.A., Capson, T.L., Morrison, J.R., Cooley, S.R. and Doney, S.C. (2015): Ocean and coastal acidification off New England and Nova Scotia; *Oceanography*, v. 28, p. 182–197. doi:10.5670/oceanog.2015.41

Golledge, N., Kowalewski, D., Naish, T., Levy, R., Fogwill, C. and Gasson, E. (2015): The multi-millennial Antarctic commitment to future sea-level rise; *Nature*, v. 526, p. 421–425. doi:10.1038/nature15706

Gruber, N. (2011): Warming up, turning sour, losing breath: ocean biogeochemistry under global change; *Philosophical Transactions of the Royal Society A*, v. 369, p. 1980–1996. doi: 10.1098/rsta.2011.0003

Gulev, S.K. and Grigorjeva, V. (2006): Variability of the Winter Wind Waves and Swell in the North Atlantic and North Pacific as Revealed by the Voluntary Observing Ship Data; *Journal of Climate*, v. 19, p. 5667–5685. doi: 10.1175/JCLI3936.1

Guo, L.L., Perrie, W., Long, Z.X., Toulany, B. and Sheng, J.Y. (2015): The impacts of climate change on the north Atlantic wave climate; *Atmosphere-Ocean*, v. 53, p. 491–509. doi:10.1080/07055900.2015.1103697

Haigh, R., Ianson, D., Holt, C.A., Neate, H.E. and Edwards, A.M. (2015): Effects of ocean acidification on temperate coastal marine ecosystems and fisheries in the northeast Pacific; *PLoS One*, v. 10, e0117533, doi:10.1371/journal.pone.0117533

Haine, T.W.N., Curry, B., Rüdiger Gerdes, R., Edmond Hansen, E., Karcher, M., Lee, C., Bert Rudels, B., Spreen, G., de Steur, L., Stewart, K.D., and Woodgate, R. (2015): Arctic freshwater export: Status, mechanisms, and prospects. *Global and Planetary Change*, v. 125, p. 13–35. doi:10.1016/j.gloplacha.2014.11.013

Hamilton, J.M. and Wu, Y. (2013): Synopsis and trends in the physical environment of Baffin Bay and Davis Strait; *Canadian Technical Report of Hydrography and Ocean Science* 282, 39 p.



Han, G., Colbourne, E., Pierre, P. and Xie, Y. (2015a): Statistical projections of ocean climate indices off Newfoundland and Labrador; *Atmosphere-Ocean*, v. 53, p. 556–570. doi:10.1080/07055900.2015.1047732

Han, G., Ma, Z., Chen, D., deYoung, B. and Chen N. (2012): Observing storm surges from space: Hurricane Igor off Newfoundland; *Scientific Reports*, v. 2. doi:10.1038/srep01010

Han, G., Ma, Z., Chen, N., Thomson, R. and Slangen, A. (2015b): Changes in mean relative sea level around Canada in the twentieth and twenty-first centuries; *Atmosphere-Ocean*, v. 53, p. 452–463. doi:10.1080/07055900.2015.1057100

Han, G., Ma, Z., Chen, N., Yang, J. and Chen, N. (2015c): Coastal sea level projections with improved accounting for vertical land motion; *Scientific Reports*, v. 5. doi:10.1038/srep16085

Hartmann, D.L., Klein Tank, A.M.G., Rusticucci, M., Alexander, L.V., Brönnimann, S., Charabi, Y., Dentener, F.J., Dlugokencky, E.J., Easterling, D.R., Kaplan, A., Soden, B.J., Thorne, P.W., Wild M. and Zhai, P.M. (2013): Observations: Atmosphere and surface; in *Climate Change 2013: The Physical Science Basis; Contribution of Working Group I to the Fifth Assessment Report of the Intergovernmental Panel on Climate Change*, (ed.) T.F. Stocker, D. Qin, G.-K. Plattner, M. Tignor, S.K. Allen, J. Boschung, A. Nauels, Y. Xia, V. Bex and P.M. Midgley; Cambridge University Press, Cambridge, United Kingdom and New York, NY, USA, p. 159–254.

Hátún, H., Azetsu-Scott, K., Somavilla, R., Rey, F., Johnson, C., Mathis, M., Mikolajewicz, U., Coupel, P., Tremblay, J.-É., Hartman, S., Pacariz, S. V., Salter, I. and Ólafsson, J. (2017): The subpolar gyre regulates silicate concentrations in the North Atlantic; *Nature Scientific Reports*, v. 7. doi: 10.1038/s41598-017-14837-4

Hay, C.C., Morrow, E., Kopp, R.E. and Mitrovica, J.X. (2015): Probabilistic reanalysis of twentieth-century sea-level rise; *Nature*, v. 517, p. 481–484. doi:10.1038/nature14093

Hebert, D. (2013): Trends of temperature, salinity and stratification in the upper ocean for different regions of the Atlantic Canadian shelf; in *Aspects of Climate Change in the Northwest Atlantic off Canada*, (ed.) J.W. Loder, G. Han, P.S. Galbraith, J. Chassé and A. van der Baaren; Canadian Technical Report of Fisheries and Aquatic Science 3045, p. 33–42.

Hebert, D., Pettipas, R., Brickman, D. and Dever, M. (2016): Meteorological, sea ice and physical oceanographic conditions on the Scotian Shelf and in the Gulf of Maine during 2015; DFO Canadian Science Advisory Secretariat, Research Document 083, 49 p.

Hegerl, G.C., Zwiers, F.W., Braconnot, P., Gillet, N.P., Luo, Y., Marengo, J.A. and Stott, P.A. (2007): Understanding and attributing climate change; in *Climate Change 2007: The Physical Science Basis; Contribution of Working Group I to the Fourth Assessment Report of the Intergovernmental Panel on Climate Change*, (ed.) S. Solomon, D. Qin, M. Manning, Z. Chen, M. Marquis, K.B. Averyt, H.L. Miller; Cambridge University Press, Cambridge, United Kingdom, New York, NY, USA, p. 663–745.

Helm, K.P., Bindoff, N.L. and Church, J.A. (2010): Changes in the global hydrological-cycle inferred from ocean salinity, *Geophysical Research Letters*, v. 37. doi:10.1029/2010GL044222



Hönisch, B., Ridgwell, A., Schmidt, D.N., Thomas, E., Gibbs, S.J., Sluijs, A., Zeebe, R.E., Kump, L., Martindale, R.C., Greene, S.E., Kiessling, W., Ries, J., Zachos, J., Royer, D.L., Barker, S., Marchitto Jr., T.M., Moyer, R., Pelejero, C., Ziveri, P., Foster, G.L. and Williams, B. (2012): The geological record of ocean acidification; *Science*, v. 335, p. 1058–1063. doi:10.1126/science.1208277

Hu, X. and Myers, P.G. (2014): Changes to the Canadian Arctic Archipelago sea ice and freshwater fluxes in the twenty-first century under the Intergovernmental Panel on Climate Change A1B climate scenario; *Atmosphere-Ocean*, v. 52, p. 331–350. doi:10.1080/07055900.2014.942592

Huang, B., Kennedy, J., Xue, Y. and Zhang, H.-M. (2017): Sea surface temperatures; in *State of the Climate in 2016*; Bulletin of the American Meteorological Society, v. 98, p. S93–S98. doi:10.1175/2017BAMSStateoftheClimate.1

Hudon, C., Gagnon, P., Rondeau, M., Hébert, M.-P., Gilbert, D., Hill, B., Patoine, M. and Starr, M. (2017): Hydrological and biological processes modulate carbon, nitrogen and phosphorus flux from the St. Lawrence River to its estuary (Quebec, Canada); *Biogeochemistry*, v. 135, p. 251–276. doi:10.1007/s10533-017-0371-4

Ianson, D., Allen, S.E., Harris, S., Orians, K.J., Varela, D.E. and Wong, C.S. (2003): The inorganic carbon system in the coastal upwelling region west of Vancouver Island, Canada; *Deep Sea Research I*, v. 50, p. 1023–1042. doi:10.1016/S0967-0637(03)00114-6

Ianson, D., Allen, S.E., Moore-Maley, B.L., Johannessen, S.C. and Macdonald, R.W. (2016): Vulnerability of a semi-enclosed estuarine sea to ocean acidification in contrast with hypoxia; *Geophysical Research Letter*, v. 43, p. 5793–5801. doi:10.1002/2016GL068996

Ianson, D., Feely, R.A., Sabine, C.L. and Juraneck, L. (2009): Features of coastal upwelling regions that determine net air-sea CO₂ flux; *Journal of Oceanography*, v. 65, p. 677–687. doi: 10.1007/s10872-009-0059-z

IPCC [Intergovernmental Panel on Climate Change] (2013): Summary for policymakers; in *Climate Change 2013: The Physical Science Basis; Contribution of Working Group I to the Fifth Assessment Report of the Intergovernmental Panel on Climate Change*, (ed.) T.F. Stocker, D. Qin, G.-K. Plattner, M. Tignor, S.K. Allen, J. Boschung, A. Nauels, Y. Xia, V. Bex and P.M. Midgley; Cambridge University Press, Cambridge, United Kingdom and New York, NY, p. 3–29, <https://www.ipcc.ch/site/assets/uploads/2018/02/WG1AR5_SPM_FINAL.pdf>.

Ito, T., Minobe, S., Long, M.C. and Deutsch, C. (2017): Upper ocean O₂ trends: 1958–2015; *Geophysical Research Letter*, v. 44, p. 4214–4223. doi:10.1002/2017GL073613

James, T.S., Henton, J.A., Leonard, L.J., Darlington, A., Forbes, D.L. and Craymer, M. (2014): Relative sea level rise projections for Canada and the adjacent mainland United States; Geological Survey of Canada, Open File 7737, 67 p., <http://publications.gc.ca/collections/collection_2016/rncan-nrcan/M183-2-7737-eng.pdf>.

James, T.S., Henton, J.A., Leonard, L.J., Darlington, A., Forbes, D.L. and Craymer, M. (2015): Tabulated values of relative sea-level projections in Canada and the adjacent mainland United States; Geological Survey of Canada, Open File 7942, 81 p., doi:10.4095/297048



Jewett, L. and Romanou, A. (2017): Ocean acidification and other ocean changes; in *Climate Science Special Report: Fourth National Climate Assessment, Volume I*, (ed.) D.J. Wuebbles, D.W. Fahey, K.A. Hibbard, D.J. Dokken, B.C. Stewart, and T.K. Maycock; US Global Change Research Program, Washington, District of Columbia, p. 364–392. doi:10.7930/JOQV3JQB

Jiang, J. and Perrie, W. (2007): The impacts of climate change on autumn North Atlantic midlatitude cyclones; *Journal of Climate*, v. 20, p. 1174–1187. doi:10.1175/JCLI4058.1

Jiang, J. and Perrie, W. (2008): Climate change effects on North Atlantic cyclones; *Journal of Geophysical Research*, v. 113. doi:10.1029/2007JD008749

Joughin, I., Smith, B. and Medley, B. (2014): Marine ice sheet collapse potentially under way for the Thwaites Glacier Basin, West Antarctica; *Science*, v. 344, p. 735–738. doi:10.1126/science.1249055

Kim, I.N., Lee, K., Gruber, N., Karl, D.M., Bullister, J.L., Yang, S. and Kim, T.W. (2014): Increasing anthropogenic nitrogen in the North Pacific Ocean; *Science*, v. 346, p. 1102–1106. doi:10.1126/science.1258396

Kossin, J.P., Hall, T., Knutson, T., Kunkel, K.E., Trapp, R.J., Waliser, D.E. and Wehner, M.F. (2017): Extreme storms; in *Climate Science Special Report: Fourth National Climate Assessment, Volume I*, (ed.) D.J. Wuebbles, D.W. Fahey, K.A. Hibbard, D.J. Dokken, B.C. Stewart, and T.K. Maycock; US Global Change Research Program, Washington, District of Columbia, p. 257–276. doi: 10.7930/JO7S7KXX

Larouche, P. and Galbraith, P.S. (2016): Canadian coastal seas and Great Lakes Sea surface temperature climatology and recent trends; *Canadian Journal of Remote Sensing*, v. 42, p. 243–258. doi:10.1080/07038992.2016.1166041

Lemmen, D.S., Warren, F.J., James, T.S. and Mercer Clarke, C.S.L. (eds.) (2016): *Canada's Marine Coasts in a Changing Climate*; Government of Canada, Ottawa, Ontario, 274 p. <https://www.nrcan.gc.ca/sites/www.nrcan.gc.ca/files/earthsciences/pdf/assess/2016/Coastal_Assessment_FullReport.pdf>.

Levermann, A., Winkelmann, R., Nowicki, S., Fastook, J.L., Frieler, K., Greve, R., Hellmer, H.H., Martin, M.A., Meinshausen, M., Mengel, M., Payne, A.J., Pollard, D., Sato, T., Timmermann, R., Wang, W.L. and Bind-schadle, R.A. (2014): Projecting Antarctic ice discharge using response functions from SeaRISE ice-sheet models; *Earth System Dynamics*, v. 5, p. 271–293. doi: 10.5194/esd-5-271-2014

Li, W.K.W., McLaughlin, F.A., Lovejoy, C. and Carmack, E.C. (2009): Small-est algae thrive as the Arctic Ocean freshens; *Science*, v. 326, p. 539. doi:10.1126/science.1179798

Lintern, D.G., MacDonald, R.W., Solomon, S.M., and Jakes, H. (2011): Beaufort Sea storm and resuspension modeling, *Journal of Marine Systems*, v. 127, p. 14–25. doi:10.1016/j.jmarsys.2011.11.015

Liu, Q., Babanin, A.V., Zieger, S., Young, I.R. and Guan, C. (2016): Wind and wave climate in the Arctic Ocean as observed by altimeters; *Journal of Climate*, v. 29, p. 7957–7975. doi:10.1175/JCLI-D-16-0219.1



Loder, J.W. and van der Baaren, A. (2013): Climate change projections for the Northwest Atlantic from six CMIP5 Earth system models; Canadian Technical Report of Hydrogeology and Ocean Science 286, 112 p.

Loder, J.W. and Wang, Z. (2015): Trends and variability of sea surface temperature in the Northwest Atlantic from three historical gridded datasets; *Atmosphere-Ocean*, v. 53, p. 510–528. doi:10.1080/07055900.2015.1071237

Loder, J.W., van der Baaren, A. and Yashayaev, I. (2015): Climate comparisons and change projections for the Northwest Atlantic from six CMIP5 models; *Atmosphere-Ocean*, v. 53, p. 529–555. doi:10.1080/07055900.2015.1087836

Long, Z., Perrie, W., Chassé, J., Brickman, D., Guo, L., Drozdowski, A. and Hu, H. (2015): Impacts of Climate Change in the Gulf of St. Lawrence; *Atmosphere-Ocean*, v. 54, p. 337–351. doi:10.1080/07055900.2015.1029869

Long, Z., Perrie, W., Chassé, J., Brickman, D., Guo, L., Drozdowski, A. and Hu, H. (2016): Impacts of Climate Change in the Gulf of St. Lawrence, *Atmosphere-Ocean*, v. 54, p. 337–351, doi:10.1080/07055900.2015.1029869

Lozier, M.S., Leadbetter, S., Williams, R.G., Roussenov, V., Reed, M.S.C. and Moore, N.J. (2008): The spatial pattern and mechanisms of heat-content change in the North Atlantic; *Science*, v. 319, p. 800–803. doi:10.1126/science.1146436

Ma, Z., Han, G. and de Young, B. (2015): Oceanic responses to Hurricane Igor over the Grand Banks: A modelling study; *Journal of Geophysical Research: Oceans*, v. 120, p. 1276–1295. doi:10.1002/2014JC010322

Manson, G.K. and Solomon, S.M. (2007): Past and future forcing of Beaufort Sea coastal change; *Atmosphere-Ocean*, v. 45, p. 107–122.

Markovic, M., de Elía, R., Frigon, A. and Matthews, H.D. (2013): A transition from CMIP3 to CMIP5 for climate information providers: the case of surface temperature over eastern North America; *Climatic Change*, v. 120, p. 197–210. doi:10.1007/s10584-013-0782-8

Mazzotti, S., Lambert, A., van der Kooij, M. and Mainville, A. (2009): Impact of anthropogenic subsidence on relative sea-level rise in the Fraser River delta; *Geology*, v. 37, p. 771–774. doi:10.1130/G25640A.1

Mercer Clarke, C.S.L., Manuel, P. and Warren, F.J. (2016): The coastal challenge; in *Canada's Marine Coasts in a Changing Climate*, (ed.) D.S. Lemmen, F.J. Warren, T.S. James and C.S.L. Mercer Clarke; Government of Canada, Ottawa, Ontario, p. 69–98, <https://www.nrcan.gc.ca/sites/www.nrcan.gc.ca/files/earthsciences/pdf/assess/2016/Coastal_Assessment_Chapter3_CoastalChallenge.pdf>.

Mitrovica, J.X., Gomez, N., Morrow, E., Hay, C. and Tamisiea, M.E. (2011): On the robustness of predictions of sea level fingerprints; *Geophysical Journal International*, v. 187, p. 729–742. doi:10.1111/j.1365-246X.2011.05090.x

Mitrovica, J.X., Tamisiea, M.E., Davis, J.L. and Milne, G.A. (2001): Recent mass balance of polar ice sheets inferred from patterns of global sea-level change; *Nature*, v. 409, p. 1026–1029.



Moore-Maley, B.L., Allen, S.E. and Ianson, D. (2016): Locally driven interannual variability of near-surface pH and Ω_A in the Strait of Georgia; *Journal of Geophysical Research: Oceans*, v. 121, p. 1600–1625. doi:10.1002/2015JC011118

Moss, R.H., Edmonds, J.A., Hibbard, K.A., Manning, M.R., Rose, S.K., van Vuuren, D.P., Carter, T.R., Emori, S., Kainuma, M., Kram, T., Meehl, G.A., Mitchell, J.F.B., Nakicenovic, N., Riahi, K., Smith, S.J., Stouffer, R.J., Thomson, A.M., Weyant, J.P. and Wilbanks, T.J. (2010): The next generation of scenarios for climate change research and assessment; *Nature*, v. 463, p. 747–756.

Mucci, A., Starr, M., Gilbert, D. and Sundby, B. (2011): Acidification of lower St. Lawrence Estuary bottom waters, *Atmosphere-Ocean*; v. 49, p. 206–218. doi: 10.1080/07055900.2011.599265

Mullan, B., Salinger, J., Thompson, C., Ramsay, D. and Wild, M. (2005): Chatham Islands Climate Change, National Institute of Water & Atmospheric Research Ltd.; NIWA Client Report WLG2005-35, Wellington, New Zealand, <<http://www.mfe.govt.nz/sites/default/files/chatham-islands-climate-change-jun05.pdf>>.

Nicholls, R.J., Hanson, S.E., Lowe, J.A., Warrick, R.A., Lu, X., Long, A.J. and Carter, T.A. (2011): Constructing sea-level scenarios for impact and adaptation assessment of coastal areas: a guidance document; Intergovernmental Panel on Climate Change (IPCC), Task Group on Data and Scenario Support for Impact and Climate Analysis, Geneva, Switzerland, 47 p., <http://www.ipcc-data.org/docs/Sea_Level_Scenario_Guidance_Oct2011.pdf>.

Oschlies, A., Shulz, K. G., Riebesell, U. and Schmittner, A. (2008): Simulated 21st century's increase in oceanic suboxia by CO₂-enhanced biotic carbon export; *Global Biogeochemical Cycles*, v. 22, GB4008. doi:10.1029/2007GB003147

Ouellet, M., Petrie, B., Chassé, J. and Gilbert, D. (2011): Temporal and spatial scales of temperature, salinity and current velocity on the Newfoundland Grand Banks and in the Gulf of St. Lawrence; *Canadian Technical Report of Hydrogeology and Ocean Sciences* 272, 78 p.

Parris, A., Bromirski, P., Burkett, V., Cayan, D., Culver, M., Hall, J., Horton, R., Knuuti, K., Moss, R., Obeysekera, J., Sallenger, A. and Weiss, J. (2012): Global sea level rise scenarios for the US National Climate Assessment; NOAA Technical Memo OAR CPO-1, 37 p.

Peralta-Ferriz, C. and Woodgate, R.A. (2015): Seasonal and interannual variability of pan-Arctic surface mixed layer properties from 1979 to 2012 from hydrographic data, and the dominance of stratification for multiyear mixed layer depth shoaling; *Progress in Oceanography*, v. 134, p. 19–53.

Pepin, P., Maillet, G.L., Lavoie D. and Johnson, C. (2013): Temporal trends in nutrient concentrations in the northwest Atlantic basin; in *Aspects of climate change in the Northwest Atlantic off Canada*, (ed.) J.W. Loder, G. Han, P.S. Galbraith, J. Chassé and A. van der Baaren; *Canadian Technical Report on Fisheries and Aquatic Science* 3045, p. 127–150.

Perrie, W., Long, Z., Chassé, J., Blokhina, M., Guo, L., and Hu, H. (2015): Projected Changes in Surface Air Temperature and Surface Wind in

the Gulf of St. Lawrence, *Atmosphere-Ocean*, v. 53, p. 571–581. doi: 10.1080/07055900.2015.1086295

Perrie, W., Yao, Y. and Zhang, W. (2010): On the impacts of climate change and the upper ocean on midlatitude northwest Atlantic landfalling cyclones; *Journal of Geophysical Research*, v. 115, 14 p. doi:10.1029/2009JD013535

Peters, G.P., Andrew, R.M., Boden, T., Canadell, J.G., Ciais, P., Le Quéré, C., Marland, G., Raupach, M.R. and Wilson, C. (2013): The challenge to keep global warming below 2 °C; *Nature Climate Change*, v. 3, p. 4–6. doi:10.1038/nclimate1783

Peters, G.P., Le Quéré, C., Andrew, R.M., Canadell, J.G., Friedlingstein, P., Ilyina, T., Jackson, R. B., Joos, F., Korsbakken, J.I., McKinley, G.A., Sitch, S. and Tans, P. (2017): Towards real-time verification of CO₂ emissions; *Nature Climate Change*, v. 7, p. 848–850. doi:10.1038/s41558-017-0013-9

Petrie, B. and Dean-Moore, J. (1996): Temporal and spatial scales of temperature and salinity on the Scotian Shelf. *Canadian Technical Report of Hydrography and Ocean Sciences* 177, 45 p.

Polyakov, I.V., Pnyushkov, A.V., and Timokhov, L.A. (2012): Warming of the intermediate Atlantic water of the Arctic Ocean in the 2000s; *Journal of Climate*, v. 25, p. 8362–8370, doi:10.1175/JCLI-D-12-00266.1

Price, A. M., Coffin, M. R., Pospelova, V., Latimer, J. S. and Chmura, G. L. (2017): Effect of nutrient pollution on dinoflagellate cyst assemblages across estuaries of the NW Atlantic; *Marine Pollution Bulletin*, v. 121, p. 339–351.

Rahmstorf, S., Box, J.E., Feulner, G., Mann, M.E., Robinson, A., Rutherford, S. and Schaffernicht, E.J. (2015): Exceptional twentieth-century slow-down in Atlantic Ocean overturning circulation; *Nature Climate Change*, v. 5, p. 475–480. Doi:10.1038/nclimate2554

Raven, J. A., and Falkowski, P. G. (1999): Oceanic sinks for atmospheric CO₂. *plant cell and environment*, v. 22, p. 741–755. doi:10.1046/j.1365-3040.1999.00419.x

Rhein, M., Rintoul, S.R., Aoki, S., Campos, E., Chambers, D., Feely, R.A., Gulev, S., Johnson, G.C, Josey, S.A., Kostianoy, A., Mauritzen, C., Roemmich, D., Talley, L.D. and Wang, F. (2013): Observations: Ocean; in *Climate Change 2013: The Physical Science Basis; Contribution of Working Group I to the Fifth Assessment Report of the Intergovernmental Panel on Climate Change*, (ed.) T.F. Stocker, D. Qin, G.-K. Plattner, M. Tignor, S.K. Allen, J. Boschung, A. Nauels, Y. Xia, V. Bex and P.M. Midgley; Cambridge University Press, Cambridge, United Kingdom and New York, NY, USA, p. 255–315.

Riser, S.C., Freeland, H.J., Roemmich, D., Wijffels, S., Troisi, A., Belbeoch, M., Gilbert, D., Xu, J., Pouliquen, S., Thresher, A., Le Traon, P.-Y., Maze, G., Klein, B., Ravichandran, M., Grant, F., Poulain, P.-M., Suga, T., Lim, B., Sterl, A., Sutton, P., Mork, K.-A., Vélez-Belchí, P. J., Ansorge, I., King, B., Turton, J., Baringer, M. and Jayne, S.R. (2016): Fifteen years of ocean observations with the global Argo array; *Nature Climate Change*, v. 6, p. 145–153. doi:10.1038/nclimate2872



Ritz, C., Edwards, T., Durand, G., Payne, A., Peyaud V. and Hindmarsh, R. (2015): Potential sea-level rise from Antarctic ice-sheet instability constrained by observations; *Nature*, v. 528, p. 115–118. doi:10.1038/nature16147

Saba, V.S., Griffies, S.M., Anderson, W.G., Winton, M., Alexander, M.A., Delworth, T.L., Hare, J.A., Harrison, M.J., Rosati, A., Vecchi, G.A. and Zhang, R. (2016): Enhanced warming of the Northwest Atlantic Ocean under climate change, *Journal of Geophysical Research: Oceans*, v. 121, p. 118–132. doi:10.1002/2015JC011346

Sabine, C.L., Feely, R.A., Gruber, N., Key, R.M., Lee, K., Bullister, J.L., Wanninkhof, R., Wong, C.S., Wallace, D.W.R., Tilbrook, B., Millero, F.J., Peng, T.-H., Kozyr, A., Ono, T. and Rios, A.F. (2004): The oceanic sink for anthropogenic CO₂; *Science*, v. 305, p. 367–371.

Sanford, T., Frumhoff, P. C., Luers, A. and Gullede, J. (2014): The climate policy narrative for a dangerously warming world; *Nature Climate Change*, v. 4, p. 164–166. doi:10.1038/nclimate2148

Schmidtko, S., Stramma, L. and Visbeck, M. (2017): Decline in global oceanic oxygen content during the past five decades; *Nature*, v. 542, p. 335–339.

Sgubin, G., Swingdeouw, D., Drijfhout, S., Mary, Y. and Bennabi, A. (2017): Abrupt cooling over the North Atlantic in modern climate models; *Nature Communications*, v. 8, 12 p. doi:10.1038/ncomms14375

Shadwick, E.H., Thomas, H., Azetsu-Scott, K., Greenan, B.J.W., Head, E. and Horne, E. (2011): Seasonal variability of dissolved inorganic carbon and surface water pCO₂ in the Scotian Shelf region of the North-western Atlantic; *Marine Chemistry*, v. 124, p. 23–37, doi:10.1016/j.marchem.2010.11.004

Shepherd, T. (2014): Atmospheric circulation as a source of uncertainty in climate change projections; *Nature Geosciences*, v. 7, p. 703–708. doi:10.1038/NGE02253

Smith, M., Stammerjohn, S., Persson, O., Rainville, L., Liu, G., Perrie, W., Robertson, R., Jackson, J. and Thomson, J. (2018): Episodic reversal of autumn ice advance caused by release of ocean heat in the Beaufort Sea. *Journal of Geophysical Research: Oceans*, v. 123, p. 3164–3185. doi:10.1002/2018JC013764

Sou, T. and Flato, G. (2009): Sea Ice in the Canadian Arctic Archipelago: modeling the past (1950–2004) and the future (2041–60); *Journal of Climate*, v. 22, p. 2181–2198. doi:10.1175/2008JCLI2335.1

Squire, V.A. (2007): Of ocean waves and sea-ice revisited; *Cold Regions Science and Technology*, v. 49, p. 110–133.

Steiner, N., Azetsu-Scott, K., Hamilton, J., Hedges, K., Hu, X., Janjua, M.Y., Lavoie, D., Loder, J., Melling, H., Merzouk, A., Perrie, W., Peterson, I., Scarratt, M., Sou, T. and Tallmann, R. (2015): Observed trends and climate projections affecting marine ecosystems in the Canadian Arctic; *Environmental Reviews*, v. 23, p. 191–239. doi:10.1139/er-2014-0066

Sweet, W.V., Kopp, R.E., Weaver, C.P., Obeysekera, J., Horton, R.M., Thieler, E.R. and Zervas, C. (2017): Global and regional sea level rise scenarios



for the United States; NOAA Technical Report NOS CO-OPS 083, Silver Spring, Maryland.

Thomas, A.C., Pershing, A.J., Friedland, K.D., Nye, J.A., Mills, K.E., Alexander, M.A., Record, N.R., Weatherbee, R. and Henderson, M.E. (2017): Seasonal trends and phenology shifts in sea surface temperature on the North American northeastern continental shelf; *Elementa Science of the Anthropocene*, v. 5. Doi:10.1525/elementa.240

Thomson, J. and Rogers, W.E. (2014): Swell and sea in the emerging Arctic Ocean; *Geophysical Research Letters*, v. 41, p. 3136–3140. doi:10.1002/2014GL05998

Thomson, R.E., Bornhold, B.D. and Mazzotti, S. (2008): An examination of the factors affecting relative and absolute sea level in coastal British Columbia; Canadian Technical Report of Hydrography and Ocean Sciences 260, 49 p. <<http://www.dfo-mpo.gc.ca/Library/335209.pdf>>.

Timmermans, M.-L., Ladd, C., and Wood, K. (2018): Sea surface temperature. *Bulletin of the American Meteorological Society*, v. 99, p. S150–S152. doi: 10.1175/2018BAMSStateoftheClimate.1

Tremblay, J.-É., Anderson, L.G., Matrai, P., Bélanger, S., Michel, C., Coupel, P. and Reigstad, M. (2015): Global and regional drivers of nutrient supply, primary production and CO₂ drawdown in the changing Arctic Ocean; *Progress in Oceanography*, v. 139, p. 171–196. doi:10.1016/j.pocean.2015.08.009

Tremblay, J.-É., Bélanger, S., Barber, D.G., Asplin, M., Martin, J., Gagnon, J., Fortier, L., Darnis, G., Gratton, Y., Williams, W.J., Link, H., Archambault, P., Philippe, B. and Gosselin, M. (2011): Climate forcing multiplies biological productivity in the coastal Arctic Ocean; *Geophysical Research Letters*, v. 38. doi:10.1029/2011GL048825

Tremblay, J.-É., Sejr, M., Bélanger, S., Devred., E., Archambault, P., Arendt, K. and Merkel, F. R. (2018): Marine ecosystems; in *Adaptation Actions for a Changing Arctic: Perspectives from the Baffin Bay/Davis Strait Region*; Arctic Monitoring and Assessment Programme (AMAP), Oslo, Norway, p. 139–152.

UNEP (2017). *The Emissions Gap Report 2017*. United Nations Environment Programme (UNEP), Nairobi.

Vancoppenolle, M., Meiners, K.M., Michel, C., Bopp, L., Brabant, F., Carnat, G., Delille, B., Lannuzel, D., Madec, G., Moreau, S., Tison, J.L. and van der Merwe, P. (2013): Role of sea ice in global biogeochemical cycles: emerging views and challenges; *Quaternary Science Reviews*, v. 79, p. 207–230.

Wadhams, P., Squire, V.A., Goodman, D.J., Cowan, A.M. and Moore, S.C. (1988): The attenuation rates of ocean waves in the marginal ice zone; *Journal of Geophysical Research: Oceans*, v. 93, p. 6799–6818.

Wang, L., Perrie, W., Blokhina, M., Long, Z., Toulany, B., and Zhang, M. (2018): The impact of climate change on the wave climate in the Gulf of St. Lawrence. *Ocean Modelling*. v. 128, p. 87–101. doi.org/10.1016/j.ocemod.2018.06.003



Wang, X., and Swail, V. (2001): Changes of extreme wave heights in Northern Hemisphere oceans and related atmospheric circulation regimes. *Journal of Climate*, v. 14, p. 2204–2221, doi:10.1175/1520-0442(2001)014<2204:COEWHI>2.0.CO;2

Wang, X., and Swail, V. (2002): Trends of Atlantic wave extremes as simulated in a 40-yr wave hindcast using kinematically reanalyzed wind fields. *Journal of Climate*, v. 15, p. 1020–1035, doi:10.1175/1520-0442(2002)015<1020:TOAWEA>2.0.CO;2

Wang, X.L., Feng, Y., Chan, R. and Isaac, V. (2016): Inter-comparison of extratropical cyclone activity in nine reanalysis datasets; *Atmospheric Research*, v. 181, p. 133–153. doi:10.1016/j.atmosres.2016.06.010

Wang, X.L., Feng, Y. and Swail, V.R. (2012): North Atlantic wave height trends as reconstructed from the 20th century reanalysis; *Geophysical Research Letters*, v. 39, 6 p. doi:10.1029/2012GL053381

Wang, X.L., Feng, Y. and Swail, V.R. (2014): Changes in global ocean wave heights as projected using multimodel CMIP5 simulations; *Geophysical Research Letters*, v. 41, p. 1026–1034. doi:10.1002/2013GL058650

Wang, X.L., Feng, Y., Swail, V.R. and Cox, A. (2015): Historical Changes in the Beaufort–Chukchi–Bering Seas Surface Winds and Waves, 1971–2013; *Journal of Climate*, v. 28, p. 7457–7469. doi:10.1175/JCLI-D-15-0190.1

Wang, X.L., Swail, V.R. and Zwiers, F.W. (2006): Climatology and changes of extra-tropical cyclone activity: Comparison of ERA-40 with NCEP/NCAR Reanalysis for 1958–2001; *Journal of Climate*, v. 19, p. 3145–3166. doi:10.1175/JCLI3781.1

Whitney, F.A., Freeland, H.J. and Robert, M. (2007): Persistently declining oxygen levels in the interior waters of the eastern subarctic Pacific; *Progress in Oceanography*, v. 75, p. 179–199.

Woodgate, R.A., Weingartner, T.J. and Lindsay, R. (2012): Observed increases in Bering Strait oceanic fluxes from the Pacific to the Arctic from 2001 to 2011 and their impacts on the Arctic Ocean water column; *Geophysical Research Letters*, v. 39. doi:10.1029/2012gl054092

Wu, L., Cai, W., Zhang, L., Nakamura, H., Timmermann, A., Joyce, T., McPhaden, M.J., Alexander, M., Qiu, B., Visbeck, M., Chang, P. and Giese, B. (2012): Enhanced warming over the global subtropical western boundary currents; *Nature Climate Change*, v. 2, p. 161–166. doi:10.1038/nclimate1353

Yamamoto-Kawai, M., McLaughlin, F.A., Carmack, E.C., Nishino, S. and Shimada, K. (2009): Aragonite undersaturation in the Arctic Ocean: effects of ocean acidification and sea ice melt; *Science*, v. 326, p. 1098–1100. doi:10.1126/science.1174190

Yashayaev, I., Head, E.J.H., Azetsu-Scott, K., Wang, Z., Li, W.K.W., Greenan, B.J.W., Anning, J. and Punshon, S. (2014): Oceanographic and environmental conditions in the Labrador Sea during 2012; DFO Canadian Science Advisory Secretariat, Research Document 046, 24 p.

Yashayaev, I. and Loder, J.W. (2016): Recurring replenishment of Labrador Sea Water and associated decadal-scale variability; *Journal of Geophysical Research: Oceans*, v. 121, p. 8095–8114. doi:10.1002/2016JC012046



Yashayaev, I. and Loder, J.W. (2017): Further intensification of deep convection in the Labrador Sea in 2016; *Geophysical Research Letters*, v. 44, p. 1429–1438. doi: 10.1002/2016GL071668

Yasunaka, S., Ono, T., Nojiri, Y., Whitney, F.A., Wada, C., Murata, A., Nakaoaka, S. and Hosoda, S. (2016): Long-term variability of surface nutrient concentrations in the North Pacific; *Geophysical Research Letters*, v. 43, p. 3389–3397. doi:10.1002/2016GL068097

Yeats, P., Ryan, S. and Harrison, W.G. (2010): Temporal trends in nutrient and oxygen concentrations in the Labrador Sea and on the Scotian Shelf; *Atlantic Zone Monitoring Program Bulletin*, v. 9, p. 23–27. <<http://waves-vagues.dfo-mpo.gc.ca/Library/365688.pdf>>.

Yin, J. (2012): Century to multi-century sea level rise projections from CMIP5 models; *Geophysical Research Letters*, v. 39. doi:10.1029/2012GL052947

Yin, J., Griffies, S.M. and Stouffer, R.J. (2010): Spatial variability of sea level rise in twenty-first century projections; *Journal of Climate*, v. 23, p. 4585–4607.

Zaikova, E., Walsh, D.A., Stilwell, C.P., Mohn, W.W., Tortell, P.D. and Hallam, S.J. (2010): Microbial community dynamics in a seasonally anoxic fjord: Saanich Inlet, British Columbia; *Environmental Microbiology*, v. 12, p. 172–191. doi:10.1111/j.1462-2920.2009.02058.x

Zhai, L., Greenan, B.J.W., Hunter J., James, T.S., Han, G., MacAulay, P. and Henton, J.A. (2015): Estimating sea-level allowances for Atlantic Canada using the Fifth Assessment Report of the IPCC; *Atmosphere-Ocean*, v. 53, p. 476–490. doi:10.1080/07055900.2015.1106401

Zhai, L., Greenan, B., Hunter, J., James, T.S., Han, G., Thomson, R. and MacAulay, P. (2014): Estimating sea-level allowances for the coasts of Canada and the adjacent United States using the Fifth Assessment Report of the IPCC; *Canadian Technical Report of Hydrography and Ocean Science* 300, 146 p.

Zweng, M.M., and Münchow, A. (2006): Warming and freshening of Baffin Bay, 1916–2003. *Journal of Geophysical Research: Oceans*, v. 111, C07016. doi:10.1029/2005JC003093.





CHAPTER 8

Changes in
Canada's
Regions in a
National and
Global Context

CANADA'S CHANGING CLIMATE REPORT



Government
of Canada

Gouvernement
du Canada

Canada



Authors

Stewart Cohen, Environment and Climate Change Canada

Elizabeth Bush, Environment and Climate Change Canada

Xuebin Zhang, Environment and Climate Change Canada

Nathan Gillett, Environment and Climate Change Canada

Barrie Bonsal, Environment and Climate Change Canada

Chris Derksen, Environment and Climate Change Canada

Greg Flato, Environment and Climate Change Canada

Blair Greenan, Fisheries and Ocean Canada

Emma Watson, Environment and Climate Change Canada

Recommended citation: Cohen, S., Bush, E., Zhang, X., Gillett, N., Bonsal, B., Derksen, C., Flato, G., Greenan, B., Watson, E (2019): Synthesis of Findings for Canada's Regions; Chapter 8 in Canada's Changing Climate Report, (ed.) E. Bush and D.S. Lemmen; Government of Canada, Ottawa, Ontario, p. 424–443.



Chapter Table Of Contents

8.1: Introduction

8.2: Global context

8.3: Changes across Canada

8.4: Changes in Canada's regions

Box 8.1: Uncertainty associated with changes in climate at regional and local scales

8.4.1: Changes in northern Canada

8.4.2: Changes in southern Canada

8.4.2.1: Atlantic region

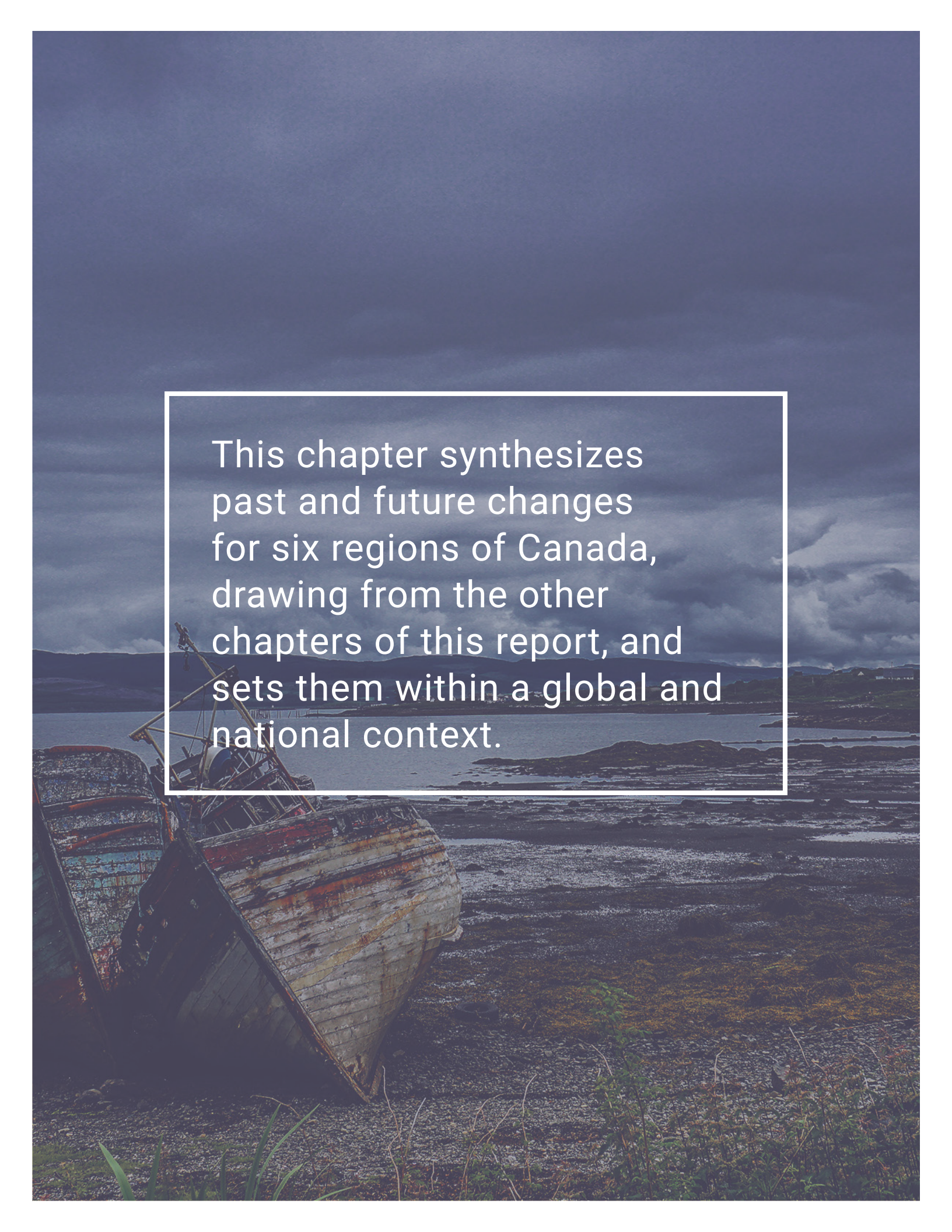
8.4.2.2: Quebec region

8.4.2.3: Ontario region

8.4.2.4: Prairies region

8.4.2.5: British Columbia region

8.5: Conclusions

A photograph of a rocky coastline. In the foreground, a large, rusted metal structure, possibly a ship's hull or a piece of industrial equipment, is partially visible. The ground is covered in dark rocks and some sparse vegetation. In the middle ground, a body of water stretches across the frame, with a small island or peninsula visible in the distance. The sky is dark and filled with heavy, grey clouds, suggesting an approaching storm or late evening. The overall mood is somber and dramatic.

This chapter synthesizes past and future changes for six regions of Canada, drawing from the other chapters of this report, and sets them within a global and national context.

8.1: Introduction

Changes in climate have consequences for Canadians, their health, well-being, and livelihoods, as well as for natural ecosystems of Canada. *Canada's Changing Climate Report* is the first report of the most recent national assessment process, *Canada in a Changing Climate: Advancing our Knowledge for Action*. This report assesses how Canada's climate has changed, why, and what changes are projected for the future. It provides a physical science foundation for the other national assessment reports to be released in the coming years, which will assess recent knowledge on climate change impacts and progress in adaptation across regions and sectors in Canada (see Chapter 1, Section 1.1).

Given the large geographic expanse of Canada, historical changes in climate have varied across the country, and projected future changes will vary as well. Chapters 4, 5, 6, and 7 of this report provide assessments of changes in several aspects of physical climate for the country as a whole, including variations across the country. This chapter synthesizes information on historical climate trends and projected future climate changes for regions of Canada using information from these chapters. References to underlying sections in previous chapters are provided to link directly to the supporting evidence, along with detailed discussions of associated uncertainties, for the results presented here. This chapter begins, however, with an overview of global-scale climate change, which is the essential context for understanding changes in Canada.

8.2: Global context

There is overwhelming evidence that the Earth has warmed during the Industrial Era and that the main cause of this warming is human influence (see Chapter 2, Sections 2.2 and 2.3). This evidence includes increases in near-surface and lower-atmosphere air temperature, sea surface temperature, and ocean heat content. Widespread warming is consistent with the observed increase in atmospheric water vapour and with declines in snow and ice. Global sea level has risen from the expansion of ocean waters caused by warming and from added water previously stored in land-based ice in glaciers and ice sheets. The observed warming and other climate changes cannot be explained by natural factors, either internal variations within the climate system or natural external factors such as changes in solar irradiance or volcanic eruptions. Only when human influences on climate are accounted for — changes in greenhouse gases, aerosols, and the land surface — can these observed changes in climate be explained. Of these human factors, the build-up of atmospheric greenhouse gases has been dominant, and carbon dioxide has been the dominant greenhouse gas emitted by human activity. Attribution studies provide quantitative assessments of the contribution of various climate drivers to observed warming over specified time periods. On the basis of such studies, it is *extremely likely*³⁰ that

30 This report uses the same calibrated uncertainty language as in the IPCC's Fifth Assessment Report. The following five terms are used to express assessed levels of confidence in findings based on the availability, quality and level of agreement of the evidence: very low, low, medium, high, very high. The following terms are used to express assessed likelihoods of results: virtually certain (99%–100% probability), extremely likely (95%–100% probability), very likely (90%–100% probability), likely (66%–100% probability), about as likely as not (33%–66% probability), unlikely (0%–33% probability), very unlikely (0%–10% probability), extremely unlikely (0%–5% probability), exceptionally unlikely (0%–1% probability). These terms are typeset in italics in the text. See chapter 1 for additional explanation.

human influences, especially emissions of greenhouse gases, have been the dominant cause of the observed global warming since the mid-20th century.

Further warming is unavoidable under all plausible future emission scenarios, as some additional greenhouse gas emissions are inevitable. However, the extent to which future emissions of greenhouse gases, particularly carbon dioxide, grow or decline will largely determine how much future climate will change (see Chapter 3, Sections 3.2, 3.3, and 3.4). Canada and the world face very different futures, depending on the level and speed at which measures to reduce greenhouse gas emissions are implemented. If and when net emissions of carbon dioxide and other long-lived greenhouse gases reach zero, global average temperature will remain approximately constant for centuries at about the peak temperature attained. Other aspects of the climate system will continue to change even after emissions cease; for example, sea level will continue to rise (see Chapter 7, Section 7.5).

Warming globally and for Canada will be similar under all plausible emission pathways over the next two decades. However, efforts to reduce greenhouse gas emissions, beginning in the next two decades and continuing thereafter, will have an increasing impact on the amount of additional warming beyond this time frame. Available estimates indicate that, by the late 21st century, the global climate will warm by a further 1°C for a low emission scenario (RCP2.6) compared to a further 3.7°C for a business-as-usual high emission scenario (RCP8.5) (relative to the reference period of 1986–2005, with a 5%–95% range of about 1°C above and below the multi-model average; see Chapter 3, Sections 3.2 and 3.3).³¹ These two scenarios reflect two very different global futures, as climate-related impacts and risks grow with increasing amounts of global warming. Only the low emission scenario (RCP2.6) is consistent with holding the increase in the global average temperature to below 2°C above pre-industrial levels, in line with Article 2 of the Paris Agreement. This scenario requires global emissions to peak almost immediately, with rapid and deep reductions thereafter (see Chapter 3, Section 3.2).

8.3: Changes across Canada

Because air in the Earth's atmosphere and water in the global oceans flow freely, Canada's climate is intimately linked to the global climate. Thus, changes in Canada's climate are a manifestation of changes in the global system, modulated by the effects of Canada's mountains, coastlines, and other geographical features. For example, a robust feature of both observed and projected global-scale climate change is the amplification of warming at high northern latitudes (so-called Arctic amplification), which means Canada's climate is expected to warm more than the global average (see Chapter 2, Section 2.2 and Chapter 3, Section 3.3). Canadian temperature has increased, and is projected to increase further, at almost double the rate of global mean temperature (see Chapter 2, Section 2.2 and Chapter 4, Section 4.2). Precipitation changes in Canada are also closely linked to global-scale changes, such as the overall intensification of the global water cycle, the increase in high-latitude precipitation, and the intensification of precipitation extremes that are projected as a result of greenhouse gas increases. Precipitation has increased in Canada since mid-century, particular-

31 These changes are over and above the roughly 0.6°C increase in global average temperature that has already occurred between 1850–1900 and the reference period of 1986–2005.

ly in northern parts of the country. Many other aspects of climate that are important to Canadians are also changing as a consequence of global-scale climate change. These changes include the extent and duration of snow and ice cover, permafrost temperatures, freshwater availability, fire weather, other extremes of weather and climate, sea level, and other properties of the oceans surrounding Canada (Chapters 4 to 7). Locations of places in Canada referred to in this chapter are shown in Figure 8.1.

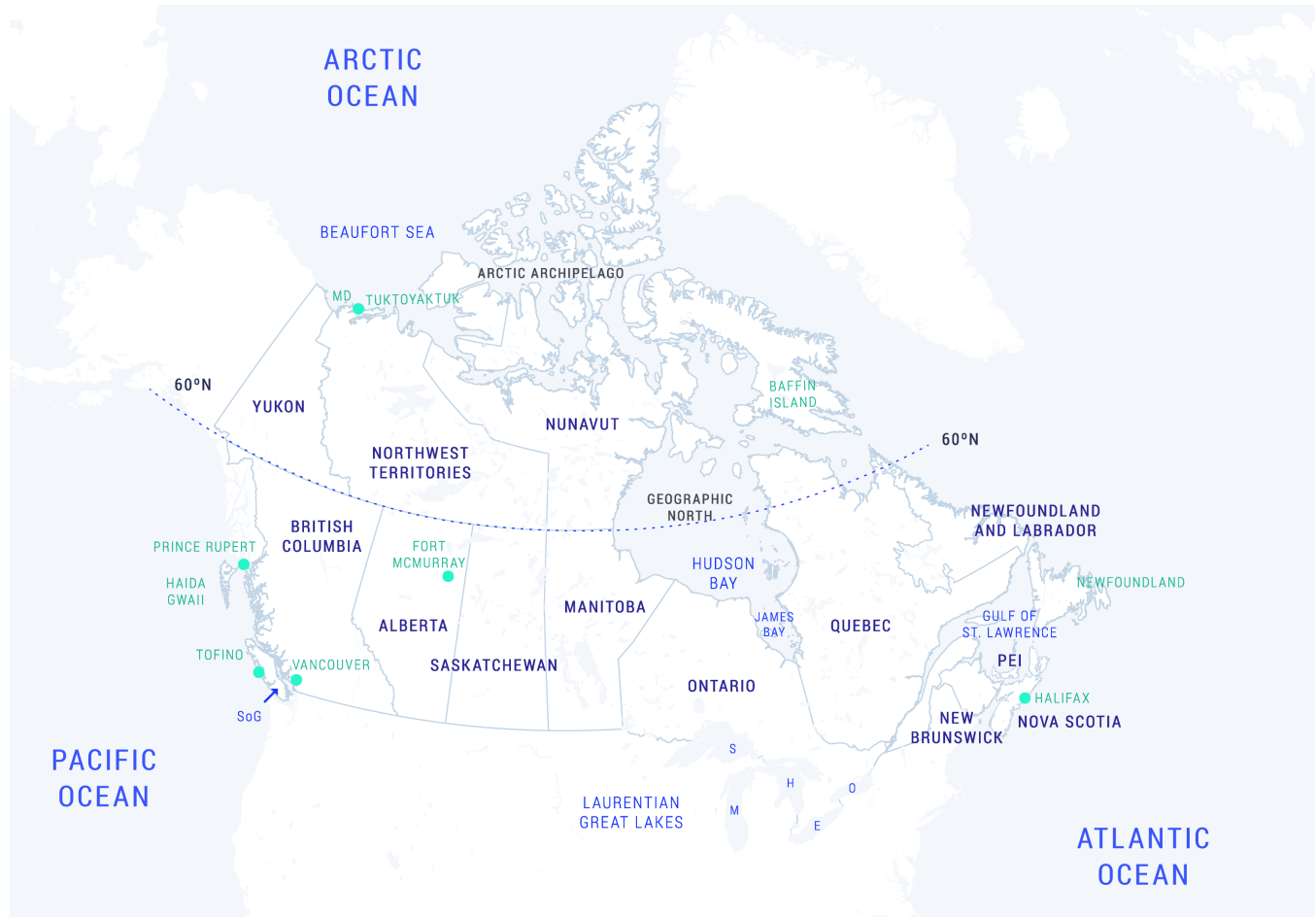


Figure 8.1: Map of Canada with place names referred to in this chapter

Figure caption: Map of Canada showing selected places mentioned in the text. PEI is Prince Edward Island, SoG is Strait of Georgia, MD is Mackenzie Delta, S is Lake Superior, H is Lake Huron, M is Lake Michigan, E is Lake Erie, and O is Lake Ontario.

There is no doubt that Canada's climate has warmed. Temperature has increased in all regions of the country and in the surrounding oceans. Since 1948, Canada's annual average surface air temperature over land has warmed by 1.7°C (best estimate), with higher temperature increases observed in the North, the Prairies, and northern British Columbia (see Chapter 4, Section 4.2.1). The greatest warming has occurred in winter. Human influence is *likely* the main cause of the observed increase in Canada's temperature, as more than half of the observed warming in annual temperature in Canada can be attributed to human influence (Chapter 4,

Section 4.2.1). Temperature extremes are also changing, consistent with the increase in mean temperature. Extreme warm temperatures have become hotter, while extreme cold temperatures have become less cold (see Chapter 4, Section 4.2.2). Overall, there is **high confidence** that most of the observed increase in the coldest and warmest daily temperatures in Canada (1948–2012) can be attributed to anthropogenic influence. Warming has also been demonstrated to have led to an increased risk of extreme fire weather in parts of western Canada (see Chapter 4, Section 4.3 and Box 4.2).

Observed changes in snow and ice features across Canada provide a coherent picture of a warming climate: fall and spring snow cover and summer sea ice extent are decreasing; glaciers are losing extent and mass; and permafrost is warming (see Chapter 5, Sections 5.2.1, 5.3.1, 5.4.1, and 5.6.1). Changes in relative (or local) sea level at locations along Canadian coastlines are driven primarily by the observed rise in average global sea level – a response to global-scale warming – and by vertical land motion (i.e., land uplift or subsidence). As a result, some coastal regions have experienced a larger relative sea-level rise compared to average global sea level, while others have experienced more modest increases or even decreases in relative sea level (see Chapter 7, Section 7.5).

Canada's climate will warm further, with warming projected in all seasons. Projected warming for Canada as a whole is almost double that of the global average, regardless of the emission scenario (see Chapter 3, Section 3.3.3, and Chapter 4, Section 4.2.1.3). Country-wide annual average temperature projections for the late century (2081–2100) range from an increase of 1.8°C³² (1.1, 2.5) for a low emission scenario (RCP2.6) to 6.3°C (5.6, 7.7) for a high emission scenario (RCP8.5), compared to the base period 1986–2005.³³ Further warming of extreme warm and cold temperatures is projected to be substantial (see Chapter 4, Section 4.2.2.3). In the future, higher temperatures will contribute to an increased risk of extreme fire weather across much of Canada. It is **very likely** that snow cover duration will decline to mid-century across Canada due to increases in temperature under all emission scenarios. Projections with a high emission scenario show continued snow loss after mid-century (**high confidence**) (see Chapter 5, Section 5.2.2). Oceans surrounding Canada are projected to continue to warm over the 21st century, in response to past and future emissions of greenhouse gases, with the size of the increase depending on the emission scenario. The warming in summer will be greatest in the ice-free areas of the Arctic and off southern Atlantic Canada, where subtropical water is projected to shift further north (**medium confidence**). Atlantic Canada will be the region of Canada's oceans that will warm the most during winter (**medium confidence**) (see Chapter 7, Section 7.2.2).

Canada's annual precipitation has increased in all regions since 1948, with relatively larger percentage increases in northern Canada and parts of Manitoba, Ontario, northern Quebec, and Atlantic Canada, although there is **low confidence** in observed regional precipitation trends. Mean precipitation has also increased in all seasons, except during winter in British Columbia and the western Prairies (see Chapter 4, Section 4.3.1). As a result of warming, snowfall has been reduced as a proportion of total precipitation in southern Canada. Seasonal snow accumulation has declined over the period of record (1981–2015) on a country-wide basis (**medium confidence**) (see Chapter 5, Section 5.2.1). The most significant observed changes in freshwater

32 Values provided are the median projection based on multiple climate models. Values in brackets represent the 25th and 75th percentile values from the fifth phase of the Coupled Model Intercomparison Project (CMIP5) multi-model ensemble. See Chapter 4, Table 4.2.

33 The linear warming trend from 1948 (start date for climate trend analysis for Canada as a whole based on observations) to 1996 (mid-point of 1986–2005) is calculated to be 1.2°C.



availability are in the seasonal distribution of streamflow in many snow-fed catchments: winter flows have become higher the timing of spring peak flows has become earlier, and there has been an overall reduction in summer flows (*high confidence*) (see Chapter 6, Sections 6.2.1, 6.2.2, and 6.2.3). However, many other indicators —annual streamflow magnitudes, surface and shallow groundwater water levels, soil moisture content and droughts — have, for the most part, been variable, with no clear increasing or decreasing trends (see Chapter 6, Sections 6.2.1, 6.3, 6.4, and 6.5). This variability corresponds to observed year-to-year and multi-year variations in precipitation, which are influenced by naturally occurring large-scale climate variability (see Chapter 2, Box 2.5).

In the future, annual and winter precipitation is projected to increase in all regions, with larger relative changes for the North. Summer precipitation shows relatively smaller changes and is projected to decrease in southern regions of Canada by the end of the century under a high emission scenario (see Chapter 4, Section 4.3.1). Daily extreme precipitation (that is, changes in extreme precipitation amounts accumulated over a day or less) is projected to increase; thus, there is potential for a higher incidence of rain-generated local flooding, including in urban areas (*high confidence*) (see Chapter 6, Section 6.2.4). Significant reductions in seasonal snow accumulation are projected through to mid-century for much of southern Canada due to warming surface temperatures, while only small changes are projected for northern Canada because winter temperatures will remain sufficiently cold despite overall warming (see Chapter 5, Section 5.2.2). In association with warmer temperatures, seasonal changes in streamflow are expected to continue, including shifts from more snowmelt-dominated regimes toward rainfall-dominated regimes. Shifts toward earlier snowmelt-related floods, including those associated with spring snowmelt, ice jams, and rain-on-snow events, are also anticipated. However, changes to the frequency and magnitude of future snowmelt-related floods are uncertain (see Chapter 6, Section 6.2.1, 6.2.3, and 6.2.4). Freshening of the ocean surface is projected in most Canadian waters over the rest of this century due to increases in precipitation and melting of land and sea ice. However, salinity is expected to increase in waters off the continental shelf south of Atlantic Canada as a result of a northward shift of subtropical water. The freshening in the upper layers of the ocean, along with warming, is expected to increase the “vertical stratification” (changes in density of ocean water at greater depths), which will affect the oceans’ ability to sequester greenhouse gases, dissolved oxygen levels, and marine ecosystems (see Chapter 7, Section 7.3.2).

8.4: Changes in Canada's regions

The assessments of changes in climate provided in the key messages of Chapters 4 to 7 are associated with a level of confidence or a statement of likelihood, when possible. This assessment of uncertainty is based on the quantity, quality, and agreement of supporting evidence for changes assessed at the national scale. Uncertainty assessments are not always included in the regional summaries that follow, because uncertainties in regional-scale changes were not formally assessed within the previous chapters of this report. However, in general, for assessments at regional and local scales, the level of confidence in changes is lower and the uncertainty is larger, especially when assessing the magnitude (rather than the direction) of change (see Box 8.1).

Box 8.1: Uncertainty associated with changes in climate at regional and local scales

For the most part, regional studies are fewer and the data more limited compared with Canada-wide or global analyses. Regional information can be extracted or derived from national-wide studies when dedicated studies for specific regions are lacking. However, at the regional scale, climate variability is fundamentally larger than at the Canada-wide or global scale. This means that the contrast between the “noise” of the natural range of climate variability and the “signal” of climate changes related to human emissions is smaller at the regional level (i.e., the climate change signal is harder to see at smaller scales). Therefore, quantifying the magnitude of change at smaller scales is subject to larger uncertainties than is the case for large-scale patterns of change.

There are also variations in observed and projected climate change on even smaller scales. Proximity to the coast or to lakes, elevation, and land cover all affect local climate and, to a lesser extent, changes to local climate. For the most part, local conditions play a rather modest role in altering local climate change, and so changes projected for a larger region are generally representative of projected changes at the local level, especially for temperature. However, urbanization, in particular, can have a substantial effect on local climate because of the widespread changes to land cover that are a feature of the urban landscape. Examples include the conversion of natural landscapes to roadways and rooftops, which typically absorb more solar radiation and hence increase local temperature. This effect does not bias estimates of regional warming in areas that have been urbanized for a long time, as they have long been recorded as warmer than their surroundings. However, it does introduce an additional warming trend at locations that are transitioning from rural to urban. In addition to a local warming effect, impermeable roadways, parking lots, and rooftops alter how much rainfall can be absorbed, leading to more runoff and the potential for increased local flooding. Other land cover changes, such as deforestation and wetland drainage, can also affect climate and hydrology on local to regional scales. Those concerned with making decisions about adapting to future climate change need to consider whether future urbanization and other land cover changes will be a factor.

To demonstrate regional differences and similarities, mean quantities for temperature and precipitation for six regions of Canada are provided below. For details about other temperature and precipitation quantities, including temperature and precipitation extremes for regions of Canada, readers are referred to the tables and figures in Chapter 4, Section 4.2.2, specifically Table 4.3, Figures 4.10, 4.11, 4.13 and 4.14 (temperature extremes and indices) and Section 4.3.2, specifically Table 4.6 (precipitation extremes). In all cases, values represent averages for the whole of the region and do not capture the significant variability between locations in every region. Information on climate trends and projected changes at the subregional and local scale are available from the Canadian Centre for Climate Services (<https://www.canada.ca/en/environment-climate-change/services/climate-change/canadian-centre-climate-services/about.html>). For further information on regional changes to sea level and other coastal issues, readers are referred to the recent report on Canada's Marine Coasts in a Changing Climate (<https://www.nrcan.gc.ca/environment/resources/publications/impacts-adaptation/reports/assessments/2016/18388>; see Chapter 1, Section 1.1).

8.4.1: Changes in northern Canada³⁴

Northern Canada is defined as the geographical region north of 60° north latitude, encompassing Yukon, Northwest Territories, most of Nunavut, and parts of Nunavik (northern Quebec) and Nunatsiavut (northernmost Newfoundland and Labrador). In this region as a whole, annual mean temperature has increased by 2.3°C from 1948 to 2016, roughly three times the warming rate of global mean temperature (see Chapter 2, Section 2.2.1, and Chapter 4, Section 4.2.1). This increase has been strongest during winter (4.3°C), and weakest during summer (1.6°C), over the same time period.

The observed temperature increase is associated with changes in other temperature-sensitive variables. Snow cover extent during spring (April–June) and fall (October–December) has been significantly reduced in northern Canada, with a commensurate reduction in annual snow cover duration (see Chapter 5, Section 5.2.1). As well, freshwater ice cover duration has decreased for most Arctic lakes (see Chapter 5, Section 5.5.1). Canada's northernmost lake, Ward Hunt Lake, had previously maintained ice cover throughout the year, but the ice melted completely in 2011 and 2012. There has been a reduction in glaciers and ice caps in the Canadian Arctic, which has accelerated in the last decade (see Chapter 5, Section 5.4.1). Permafrost temperatures have increased throughout northern Canada, and this warming of the frozen ground has led to increases in active layer thickness, melting of ground ice, and the formation of thermokarst landforms (see Chapter 5, Section 5.6.1). There is also evidence that these processes have affected lake levels in northwestern Canada (see Chapter 5, Section 5.6.1), including a higher incidence of rapid lake drainage (see Chapter 6, Section 6.3.2). The extent of sea ice cover, including areas with multi-year ice, has diminished across the Canadian Arctic (see Chapter 5, Section 5.3.1). The rate of decline for both multi-year sea ice and summer sea ice in the Beaufort Sea and the Canadian Arctic Archipelago has accelerated since 2008. Acidification of the Arctic Ocean, resulting from human emissions of carbon dioxide, has been augmented by rapid increases in freshwater input from accelerated ice melt and increased river input (Chapter 7, Section 7.6.1).

34 In this section, where changes have been estimated for the Territories, based on political boundaries, results are identified as being for Canada's North.

At coastal locations, the sea-level change that is experienced relative to land is known as “relative” sea-level change. Relative sea level has risen along the Beaufort Sea coastline (including Tuktoyaktuk) at a rate higher than that for global sea-level rise but has fallen along much of the eastern Arctic and Hudson Bay coastal regions. This variability in sea-level changes reflects regional land uplift and subsidence that is still occurring following the retreat of the ice sheet that covered the region during the last ice age (see Chapter 7, Section 7.5.1). Changes in sea ice in the Beaufort region have resulted in increased wave heights and duration of the wave season (see Chapter 7, Sections 7.4.1 and 7.4.2).

Annual mean temperature for Canada's North is projected to increase by approximately 1.8°C³⁵ (1.2, 2.5) for a low emission scenario (RCP2.6) to 2.7°C (2.0, 3.5) for a high emission scenario (RCP8.5) for 2031–2050, and by 2.1°C (1.3, 2.5) (RCP2.6) to 7.8°C (6.2, 8.4) (RCP8.5) for 2081–2100; all values are relative to the 1986–2005 mean value (see Chapter 4, Section 4.2.1). Changes in winter (January–March) snow cover and in the amount of snow (measured as pre-melt maximum snow water equivalent) are projected to be minimal across northern Canada because increased snowfall at high latitudes is expected to be offset by increasing temperatures that will shorten the snow-accumulation season (see Chapter 5, Section 5.2.2). Glaciers and ice caps will continue to shrink. Based on observed changes in recent decades, many small ice caps and ice shelves will disappear completely by 2100 (see Chapter 5, Section 5.4.2). Future warming of permafrost will be greater near the surface than in deeper layers of the ground, but the area of Canada underlain by deep permafrost is projected to decline by 16 to 20% by 2090, relative to 1990 (see Chapter 5, Section 5.6.2). This increase in permafrost thaw could lead to increases in thermokarst and affect levels of northern lakes (see Chapter 5, Section 5.6.2, and Chapter 6, Section 6.3.2). With respect to sea ice, there is a greater than 50% probability that, by 2050 under a high emission scenario, extensive regions in the Canadian Arctic will be free of sea ice in September, with additional ice-free months possible in some regions (see Chapter 5, Section 5.3.2). Hudson Bay, which is currently ice-free in August and September, has a high probability of becoming ice-free for four consecutive months (August through November). This reduction in ice cover is expected to lead to an increase in sea surface temperature of up to 4°C during these months (see Chapter 7, Section 7.2.2). With projected reductions in sea ice in the Arctic Ocean, wave heights and the duration of the summer wave season are expected to increase (see Chapter 7, Section 7.4.2). Relative sea-level is projected to rise in the Beaufort Sea coastal area, while most regions in Nunavut will experience little change or declining relative sea level due to continued land uplift (see Chapter 7, Section 7.5.2, and Figure 7.16). Under a high emission scenario, relative sea level in the Beaufort Sea coastal area, including the Mackenzie Delta region (Northwest Territories), is projected to rise between 50 and 75 cm by 2100 (median projection). In contrast, relative sea level is projected to fall substantially, by up to 90 cm, under the same scenario for Hudson Bay (Nunavut) and the Arctic Archipelago, including Baffin Island (Nunavut), as land uplift more than offsets global sea-level rise. All emission scenarios result in similar sea-level change by mid-century, with the higher emission scenarios leading to larger sea-level rise or smaller sea-level fall after 2050 (see Chapter 7, Section 7.5.2).

35 Values provided are the median projection based on multiple climate models. Values in brackets represent the 25th and 75th percentile values from the CMIP5 multi-model ensemble. See Chapter 4, Table 4.2 for temperature projections, and Table 4.5 for precipitation projection.

Long-term changes in total precipitation over northern Canada are difficult to accurately quantify because of the sparse observing network. However, all available sites in the region reveal large percentage increases in precipitation (see Chapter 4, Section 4.3.1), both annual and seasonal, with precipitation having increased in every season. During the summer, snowfall has decreased and is being replaced by rain (see Chapter 4, Section 4.3.1). However, on an annual basis, snowfall has increased, since total precipitation has increased and temperatures during the cold part of the year are still low enough for precipitation to fall as snow. In association with warming temperatures and resulting changes to snow and permafrost (see Chapter 5, Sections 5.2.1 and 5.6.1), winter streamflows have increased (see Chapter 6, Section 6.2.1), and the timing of spring freshet has shifted earlier (see Chapter 6, Section 6.2.2).

Annual mean precipitation for the North is projected to increase, by 8.2% (2.1, 14.6) for a low emission scenario (RCP2.6) to 11.3% (5.4, 18.1) for a high emission scenario (RCP8.5) for 2031–2050, and by 9.4% (2.8, 16.7) (RCP2.6) to 33.3% (22.1, 46.4) (RCP8.5) for 2081–2100; all values are relative to the 1986–2005 base period. Precipitation is projected to increase in all seasons, and daily extreme precipitation is also projected to increase (see Chapter 4, Section 4.3.2). There is **high confidence** in these projected precipitation increases, as this is a robust feature of multiple generations of climate models and can be explained by the expected increase in atmospheric moisture induced by warming (see Chapter 4, Section 4.3.1). In association with these increases, annual streamflow in the North is also projected to increase, along with continuing earlier spring freshets due to rising temperatures (see Chapter 6, Sections 6.2.1 and 6.2.2).

8.4.2: Changes in southern Canada

Southern Canada encompasses the provinces of Canada, with the exception of northernmost Quebec and Newfoundland and Labrador, which are included in the geographic definition of northern Canada. Some observed and projected changes in southern Canada were included in Section 8.2 on changes across Canada. This section characterizes broad spatial patterns in changes across southern Canada, with regional differences and similarities highlighted in the subsections below for the five regions of southern Canada.

Long-term climate observations for southern Canada extend back to 1900. Between 1900 and 2016, annual mean temperature increased by 1.9°C for southern Canada as a whole (see Chapter 4, Section 4.2.1). Projected warming under both low (RCP2.6) and high (RCP8.5) emission scenarios show a general pattern of change in winter, consistent across scenarios, with the smallest changes observed in southernmost Canada and the largest changes in Hudson Bay (and the Arctic, covered in the previous section) (see Chapter 4, Section 4.2.1). Projected warming in the summer season is more uniform across Canada, with less differentiation between southern and northern Canada. Warming is projected to continue, with larger increases in interior continental areas than in both eastern and western coastal regions.

Fall snow cover has decreased across all of southern Canada over the 35-year record, whereas spring snow cover has increased in the southwestern regions and decreased elsewhere during the same period (see Chapter 5, Section 5.2.1). Earlier spring freshet, along with an increase in winter streamflow, is a robust feature

across southern Canada. Snow cover and maximum snow water equivalent are projected to decrease across southern Canada (see Chapter 5, Section 5.2.2). The extent and duration of ice cover on rivers and lakes are also projected to decrease. There is **high confidence** that streamflow regimes will shift from primarily snow-driven, snowmelt-dominated regimes, with one pronounced spring peak, toward more rainfall-dominated regimes, with smaller and earlier spring snowmelt peaks and several rainfall-dominated warm-season peaks (see Chapter 6, Sections 6.2.2 and 6.2.3).

An increase in average precipitation was observed over the five regions of southern Canada since 1900 (**low confidence**), and the proportion of precipitation falling as snow has steadily decreased (see Chapter 4, Section 4.3.1). Projected changes in precipitation show both increases and decreases, depending on location and season. This pattern is therefore different than that for temperature, which is projected to increase everywhere and in all seasons. In the near term, a small (generally less than 10%) increase in precipitation is projected in all seasons. Increases in precipitation are projected for southern Canada in all seasons and scenarios, with the exception of the southernmost latitudes in summer, where precipitation is projected to decrease toward the late century under a high emission scenario (RCP8.5) (see Chapter 4, Section 4.3.1), which could affect surface water levels and risk of drought in these regions (see Chapter 6, Sections 6.3 and 6.4). This southernmost area of Canada is at the northern edge of a general area where climate models project a decrease in summer precipitation.

8.4.2.1: Atlantic region

In this region, annual mean temperature has increased at a modest rate, by 0.7°C from 1948 to 2016, which is below the average increase for Canada (see Chapter 4, Section 4.2.1). The trend is largest in summer, with an increase of 1.3°C, and smallest in winter, at 0.5°C. This is also in contrast with larger winter warming for most regions of Canada. Natural internal variability of the climate system may have played a role in this difference between Eastern Canada and other regions over this period. Small mountain glaciers in Labrador have contracted in area and thickness (see Chapter 5, Section 5.4.1). Sea ice in the Atlantic Ocean has declined in winter by 7.5% per decade since 1969. This is consistent with observed upper-ocean warming, which varies in magnitude across the Atlantic region (see Chapter 7, Section 7.2.1). The seawater pH of this region has been declining in response to human emissions of CO₂. Oxygen content has also decreased steadily over the last three decades (Chapter 7, Section 7.6.1, 7.6.2).

In future, annual mean temperature for 2031–2050 is projected to increase by 1.3°C³⁶ (0.9, 1.8) for a low emission scenario (RCP2.6) to 1.9°C (1.5, 2.4) for a high emission scenario (RCP8.5), and by 1.5°C (0.9, 2.0) (RCP2.6) to 5.2°C (4.5, 6.1) (RCP8.5) for 2081–2100, compared with a baseline of 1986–2005 (see Chapter 4, Section 4.2.1). Wave heights and the duration of the wave season are expected to increase in the Newfoundland/Labrador coastal area during winter because of reduced sea ice extent (Chapter 5 Section 5.3.2, Chapter 7 Section 7.4.2).

36 Values provided are the median projection based on multiple climate models. Values in brackets represent the 25th and 75th percentile values from the CMIP5 multi-model ensemble. See Chapter 4, Table 4.2 for temperature projections, and Table 4.5 for precipitation projection.

The coast of southern Atlantic Canada is sinking because of the retreat of the last ice sheet, and this will contribute to relative sea-level rise, which will be larger than the projected global sea-level rise. This region will experience the largest relative sea-level rise in Canada, reaching 75 to 100 cm for a high emission scenario by 2100 (see Chapter 7, Section 7.5.2). This combination of sea ice and sea-level changes, and continued sinking of coastlines, will lead to an increase in frequency and magnitude of extreme high water levels. For example, a 20 cm rise in relative sea level in Halifax (projected to occur within two to three decades under all emission scenarios) will increase the frequency of flooding by a factor of four (see Chapter 7, Section 7.5.3). Further north, in Labrador, a smaller relative sea-level rise is projected under a high emission scenario, primarily as a result of crustal (land) uplift following the retreat of the ice sheet (see Chapter 7, Section 7.5.2).

Annual mean precipitation has increased by 11% from 1948 to 2012, with seasonal trends ranging from 5.1% in winter to 18.2% in fall (see Chapter 4, Section 4.2.1), although there is *low confidence* in these trends. Annual precipitation for 2031–2050 is projected to increase by 3.8% (–0.8, 9.1) for a low emission scenario (RCP2.6) to 5.0% (0.6, 9.9) for a high emission scenario (RCP8.5), and by 4.7% (0.3, 9.0) (RCP2.6) to 12.0% (5.7, 19.3) (RCP8.5) for 2081–2100 (see Chapter 4, Section 4.3.1).

8.4.2.2: Quebec region

Annual mean temperature in Quebec has increased by 1.1°C over the period 1948–2016, a rate lower than for Canada as a whole. The trend is largest in summer and autumn, with an increase of 1.5°C, and smallest in spring, at 0.7°C. There has been earlier ice break-up and later freeze-up in small lakes in southern Quebec (see Chapter 5, Section 5.5.1). Permafrost in northern Quebec has warmed by 0.7°C or more since the 1990s, resulting in landscape changes throughout the region (see Chapter 5, Section 5.6.1). Sea ice cover in the Gulf of St. Lawrence and in eastern Hudson Bay and James Bay has declined (see Chapter 5, Section 5.3.1), resulting in impacts for marine ecosystems and coastal infrastructure. The deep waters of the Gulf of St. Lawrence have warmed by 0.25°C per decade during 1915–2017 (see Chapter 7, Section 7.2.1). In addition, recent satellite observations for May to November indicate a sea surface warming trend of 0.46°C per decade during 1985–2017 (see Chapter 7, Section 7.2.1). The pH of waters in the Gulf of St. Lawrence has been declining in response to increases in atmospheric carbon dioxide, and oxygen content has decreased (see Chapter 7, Sections 7.6.1 and 7.6.2).

Annual mean air temperature is projected to increase for 2031–2050 by 1.5°C³⁷ (1.0, 2.1) for a low emission scenario (RCP2.6) to 2.3°C (1.7, 2.9) for a high emission scenario (RCP8.5), and by 1.7°C (1.0, 2.2) (RCP2.6) to 6.3°C (5.3, 6.9) (RCP8.5) for 2081–2100, compared with a baseline of 1986–2005 (see Chapter 4, Section 4.2.1).

37 Values provided are the median projection based on multiple climate models. Values in brackets represent the 25th and 75th percentile values from the CMIP5 multi-model ensemble. See Chapter 4, Table 4.2 for temperature projections, and Table 4.5 for precipitation projection.

Relative sea-level is expected to rise in the range of 25 to 75 cm this century for the Gulf of St. Lawrence under a high emission scenario (see Chapter 7, Section 7.5.2). Wave heights and the duration of the wave season are expected to increase in the Gulf of St. Lawrence during winter because of reduced sea ice extent, similar to what is expected in Newfoundland/Labrador (see Chapter 5 Section 5.3.2, Chapter 7 Section 7.4.2). But relative sea level is projected to fall for James Bay and Hudson Bay (northwestern Quebec), which is similar to what is expected in Nunavut (see Chapter 7, Section 7.5.2).

Annual precipitation has increased by 10.5% during 1948–2012, with seasonal trends ranging from 5.3% in winter to 20.9% in spring, although there is *low confidence* in the magnitude of these trends (see Chapter 4, Section 4.3.1). Corresponding projected changes in annual mean precipitation for 2031–2050 are increases of 7.1% (2.0, 12.2) for a low emission scenario (RCP2.6) to 9.4% (4.5, 14.7) for a high emission scenario (RCP8.5), and of 7.2% (2.2, 13.0) (RCP2.6) to 22.5% (14.8, 32.0) (RCP8.5) for 2081–2100 (see Chapter 4, Section 4.3.1). Projections of future streamflow reveal an earlier freshet, by as much as 20 days in southern Quebec rivers by the mid-century (RCP8.5) (see Chapter 6, Section 6.2).

8.4.2.3: Ontario region

Annual mean temperature has increased 1.3°C for the Ontario region over the period 1948–2016. The trend is largest in winter, with an increase of 2.0°C, and smallest in autumn, at 1.0°C (see Chapter 4, Section 4.2.1). Laurentian Great Lakes ice cover has varied considerably from year to year since 1971 (see Chapter 5, Section 5.5.1). Sea ice cover in southern Hudson Bay and western James Bay (northern Ontario) has also declined (see Chapter 5, Section 5.3.1).

Annual mean temperature for 2031–2050 is projected to increase by 1.5°C³⁸ (1.1, 2.1) for a low emission scenario (RCP2.6) to 2.3°C (1.7, 2.9) for a high emission scenario (RCP8.5), and by 1.7°C (1.0, 2.1) (RCP2.6) to 6.3°C (5.3, 6.9) (RCP8.5) for 2081–2100, compared with a baseline of 1986–2005. Relative sea level is projected to fall along the James Bay and Hudson Bay coastlines (see Chapter 7, Section 7.4.2).

Annual precipitation has increased by 9.7% during 1948–2012, with seasonal trends ranging from 5.2% in winter to 17.8% in fall, although there is *low confidence* in the magnitude of these trends (see Chapter 4, Section 4.3.1). Lake levels in the Laurentian Great Lakes have exhibited large variability, including a rapid rise from below-average levels, with record lows for Lakes Michigan/Huron in 2012/2013, to above-average levels in 2014. However, no discernible long-term trend has been observed in the last 100 years (see Chapter 6, Section 6.2.1). There is satellite-based evidence that groundwater storage declined in the Laurentian Great Lakes region during 2002–2010, but, due to the short record, this is not necessarily indicative of a long-term trend (see Chapter 6, Section 6.4).

38 Values provided are the median projection based on multiple climate models. Values in brackets represent the 25th and 75th percentile values from the CMIP5 multi-model ensemble. See Chapter 4, Table 4.2 for temperature projections, and Table 4.5 for precipitation projection.

Annual mean precipitation for 2031–2050 is projected to increase by 5.5% (0.4, 11.1) for a low emission scenario (RCP2.6) to 6.6% (1.8, 12.4) for a high emission scenario (RCP8.5), and by 5.3% (–0.1, 10.8) (RCP2.6) to 17.3% (8.5, 26.1) (RCP8.5) for 2081–2100 (see Chapter 4, Section 4.3.1). In the future, overall lake levels in the Laurentian Great Lakes may decline as a result of higher evaporation in a projected warmer climate, exceeding projected increases in precipitation. However, there is considerable uncertainty in this projection (see Chapter 6, Section 6.3.1).

8.4.2.4: Prairies region

For the Prairie provinces, annual mean temperature has increased by 1.9°C over the period 1948–2016, at a rate above that for Canada as a whole. The trend is largest in winter, with an increase of 3.1°C, and smallest in fall, at 1.1°C (see Chapter 4, Section 4.2.1). Unlike in other southern regions, snow cover in spring increased during 1981–2015, probably as a result of natural variability (see Chapter 5, Section 5.2.1). Warming has led to an increased probability of extreme fire weather conditions in parts of western Canada, which are associated with wildfire occurrence, such as the 2016 Fort McMurray wildfire (see Chapter 4, Box 4.2 and Section 4.4).

Annual mean temperature for 2031–2050 is projected to increase by 1.5°C³⁹ (1.1, 2.1) for a low emission scenario (RCP2.6) to 2.3°C (1.7, 3.0) for a high emission scenario (RCP8.5), and by 1.9°C (1.2, 2.2) (RCP2.6) to 6.5°C (5.2, 7.0) (RCP8.5) for 2081–2100, compared with a baseline of 1986–2005 (see Chapter 4, Section 4.3.1). Relative sea level is projected to fall along the Hudson Bay coastline of Manitoba, similar to what is expected in Nunavut, Quebec, and in Ontario (see Chapter 7, Section 7.4.2).

During 1948–2012, annual precipitation increased by 7.0%, with seasonal trends ranging from a decrease of 5.9% in winter to an increase of 13.6% in spring, although there is *low confidence* in the magnitude of these trends (see Chapter 4, Section 4.3.1). Exceptionally high precipitation from the late 2000s through 2016 has resulted in a dramatic increase in levels in some closed-basin lakes after a prolonged period of decline, illustrating their high hydro-climatic variability and sensitivity to excess precipitation (see Chapter 6, Section 6.3.2). Periodic droughts are a common occurrence in the Canadian Prairies, but no long-term changes are evident during the last century (see Chapter 6, Section 6.4.2).

Annual mean precipitation for 2031–2050 is projected to increase by 5.0% (–0.7, 10.8) for a low emission scenario (RCP2.6) to 6.5% (0.4, 13.1) for a high emission scenario (RCP8.5), and by 5.9% (–0.2, 12.1) (RCP2.6) to 15.3% (6.3, 24.9) (RCP8.5) for 2081–2100 (see Chapter 4, Section 4.3.1). Future droughts and soil moisture deficits are expected to be more frequent and intense over the southern Prairies during summer, when evaporation and transpiration due to increased temperatures exceed precipitation (see Chapter 6, Sections 6.4.1 and 6.4.2). Since many Prairie rivers have their headwaters in the western mountains, summer streamflow is projected to decrease in association with decreasing snow and ice (see Chapter 6, Section 6.2.1).

39 Values provided are the median projection based on multiple climate models. Values in brackets represent the 25th and 75th percentile values from the CMIP5 multi-model ensemble. See Chapter 4, Table 4.2 for temperature projections, and Table 4.5 for precipitation projection.

8.4.2.5: British Columbia region

The annual mean warming trend for British Columbia has been 1.9°C over the period 1948–2016. The trend is largest in winter, at 3.7°C, and smallest in fall, at 0.7°C (see Chapter 4, Section 4.2.1). Upper-ocean warming trends of 0.08°C per decade have been observed over the last century off the west coast of Vancouver Island and of 0.15°C per decade in the Strait of Georgia (see Chapter 7, Section 7.2.1). Ice thickness of the Place Glacier and Helm Glacier in southern British Columbia has declined by 30 to 50 m water equivalent since the early 1980s (see Chapter 5, Section 5.4.1). Changes in ice and snow have affected annual water cycles in snowmelt-dominated catchments (e.g., Peace, Fraser, Columbia basins), including earlier spring streamflow peaks, increased winter flows, and decreased summer flows (see Chapter 6, Sections 6.2.1 and 6.2.2). Relative sea level has risen along the British Columbia coast, except in certain areas experiencing land uplift, such as Tofino.

Annual mean temperature for 2031–2050 is projected to increase by 1.3°C⁴⁰ (0.8, 1.9) for a low emission scenario (RCP2.6) to 1.9°C (1.4, 2.5) for a high emission scenario (RCP8.5), and by 1.6°C (1.1, 2.1) (RCP2.6) to 5.2°C (4.3, 6.2) (RCP8.5) for 2081–2100, compared with a baseline of 1986–2005 (see Chapter 4, Section 4.3.1).

The northeast Pacific Ocean sea surface temperature is projected to warm roughly 2°C in winter and 3°C in summer by the 2046–2065 period (see Chapter 7, Section 7.2.2) under a high emission scenario (RCP8.5), relative to 1986–2005. Wave heights off British Columbia have decreased significantly over the past three to four decades in summer and increased slightly in winter, with small decreasing annual mean trends (see Chapter 7, Section 7.4.2). Relative sea-level rise under a high emission scenario is projected to exceed 50 cm by 2100 for Prince Rupert, Haida Gwaii, and the Vancouver area (see Chapter 7, Sections 7.5.1 and 7.5.2). Oxygen content in the northeast Pacific has decreased, and ocean waters along the coast are expected to become more acidic (Chapter 7, Sections 7.6.1 and 7.6.2).

Annual mean precipitation has increased by 5% during 1948–2012, with seasonal trends ranging from a decrease of 9.0% in winter to an increase of 18.2% in spring, although there is *low confidence* in the magnitude of these trends (see Chapter 4, Section 4.3.1). The decrease in winter precipitation differs from observed seasonal precipitation change in other parts of Canada. Such regional differences arise from natural climate variability. Annual mean precipitation for 2031–2050 is projected to increase by from 4.3% (–0.4, 9.8) for a low emission scenario (RCP2.6) to 5.7% (0.0, 11.4) for a high emission scenario (RCP8.5), and by from 5.8% (0.4, 11.9) (RCP2.6) to 13.8% (5.7, 22.4) (RCP8.5) for 2081–2100 (see Chapter 4, Section 4.3.1). As in the southern Canadian Prairies, summer droughts in the interior region of British Columbia are expected to increase in frequency and intensity as a result of increased evapotranspiration due to higher temperatures (see Chapter 6, Section 6.4.2). Watersheds in British Columbia are projected to have continued increases in winter runoff, earlier spring freshets, and declines in summer flow (see Chapter 6, Sections 6.2.1 and 6.2.2).

40 Values provided are the median projection based on multiple climate models. Values in brackets represent the 25th and 75th percentile values from the CMIP5 multi-model ensemble. See Chapter 4, Table 4.2 for temperature projections, and Table 4.5 for precipitation projection.



8.5: Conclusions

Canada's Changing Climate Report describes a Canada that has warmed and will warm further. Historical warming has led to changes in rain and snow, rivers and lakes, ice, and coastal zones, and these changes are challenging our sense of what a "normal" climate is. The world's climate, including Canada's climate, is changing because of human emissions of greenhouse gases, particularly carbon dioxide (see Chapters 2 and 4). Beyond the next few decades, the largest uncertainty about the magnitude of future climate change is rooted in uncertainty about human behaviour, that is, whether the world will follow a pathway of low, medium or high emissions (see Chapter 3, Sections 3.2 and 3.3). Until climate is stabilized, there will not be a new "normal" climate.

Attribution studies have shown that anthropogenic climate change has influenced some recent extreme events, as well as long-term regional-scale trends (see Chapters 4, 5, 6, and 7). In the future, anthropogenic climate change will continue to affect aspects of climate important for agriculture, forestry, engineering, urban planning, public health, and water management, and the preparation of guidance and standards. The challenge for users of climate information is to determine how best to incorporate climate change information into the various methods and tools used for assessment and planning across these sectors. The information brought together in this report is intended to guide this process, informing the preparation of new standards, the assessment and management of climate-related risks, and the design and implementation of climate adaptation plans.

The Canada in a Changing Climate series of reports, led by Natural Resources Canada, will assess available knowledge on climate change impacts and adaptation across regions and sectors. Canada's Changing Climate Report is the first publication of this series, and it has established a foundation of knowledge about how Canada's climate is changing and why, as context for assessing impacts and adaptation responses.

